PB81-187197

Effectiveness of Activated Carbon for Removal of Toxic and/or Carcinogenic Compounds from Water Supplies

Michigan Univ.
Ann Arbor

Prepared for

Municipal Environmental Research Lab.
Cincinnati, OH

Apr 81

U.S. Department of Commerce
National Technical Information Service
NTIS

PB81-187197

EPA 600/2-81-057
April 1981

EFFECTIVENESS OF ACTIVATED CARBON FOR REMOVAL OF TOXIC AND/OR CARCINOGENIC COMPOUNDS FROM WATER SUPPLIES

by

Walter J. Weber Jr. and Massoud Pirbazari
Environmental and Water Resources Engineering
The University of Michigan
Ann Arbor, Michigan 48109

Grant No. R 804369

Project Officer

Alan A. Stevens
Drinking Water Research Division
Municipal Environmental Research Laboratory
Cincinnati, Ohio 45268

MUNICIPAL ENVIRONMENTAL RESEARCH LABORATORY
OFFICE OF RESEARCH AND DEVELOPMENT
U.S. ENVIRONMENTAL PROTECTION AGENCY
CINCINNATI, OHIO 45268

REPRODUCED BY
NATIONAL TECHNICAL
INFORMATION SERVICE
U.S. DEPARTMENT OF COMMERCE
SPRINGFIELD, VA 22161

NOTICE

THIS DOCUMENT HAS BEEN REPRODUCED FROM THE BEST COPY FURNISHED US BY THE SPONSORING AGENCY. ALTHOUGH IT IS RECOGNIZED THAT CERTAIN PORTIONS ARE ILLEGIBLE, IT IS BEING RELEASED IN THE INTEREST OF MAKING AVAILABLE AS MUCH INFORMATION AS POSSIBLE.

TECHNICAL REPORT DATA

(Please read Instructions on the reverse before completing)

1. REPORT NO. EPA-600/2-81-057

2. ORD Report

3. RECIPIENT'S ACCESSION NO. PB81 187197

4. TITLE AND SUBTITLE
Effectiveness of Activated Carbon for Removal of Toxic and/or Carcinogenic Compounds from Water Supplies

5. REPORT DATE April 1981

6. PERFORMING ORGANIZATION CODE

7. AUTHOR(S)
W. J. Weber, Jr. & M. Pirbazari

8. PERFORMING ORGANIZATION REPORT NO.

9. PERFORMING ORGANIZATION NAME AND ADDRESS
Department of Environmental and Water Resources
Engineering
University of Michigan
Ann Arbor, MI 48109

10. PROGRAM ELEMENT NO. BNC1A

11. CONTRACT/GRANT NO. R-804369

12. SPONSORING AGENCY NAME AND ADDRESS
Municipal Environmental Research Laboratory - Cin., OH
Office of Research and Development
U.S. Environmental Protection Agency
Cincinnati, OH 45268

13. TYPE OF REPORT AND PERIOD COVERED Final 4/76 - 3/80

14. SPONSORING AGENCY CODE EPA/600/14

15. SUPPLEMENTARY NOTES

Project Officer: Alan A. Stevens (513)684-7342

16. ABSTRACT

This research addressed quantification of the performance of fixed-bed granular activated carbon processes for treatment of public water supplies. It included evaluation of the adsorption of selected toxic and/or carcinogenic trace compounds of man-related origin, including carbon tetrachloride, benzene, two commerical mixtures of PCB's dieldrin, and p-dichlorobenzene. The adsorption behavior of the predominant class of natural organic matter and trihalomethane (THM) precursor, humic substances, was also characterized.

The Michigan Adsorption Design and Applications Model (MADAM) was tested and found generally able to simulate and predict the performance of fixed-bed adsorbers for removal of the compounds investigated, with the exception of humic acids.

17. KEY WORDS AND DOCUMENT ANALYSIS

a. DESCRIPTORS	b. IDENTIFIERS/OPEN ENDED TERMS	c. COSATI Field/Group

18. DISTRIBUTION STATEMENT
Release to public

19. SECURITY CLASS (This Report) Unclassified

20. SECURITY CLASS (This page) Unclassified

21. NO. OF PAGES 391

22. PRICE

EPA Form 2220-1 (9-73)

DISCLAIMER

This report has been reviewed by the Municipal Environmental Research Laboratory, U.S. Environmental Protection Agency, and approved for publication. Approval does not signify that the contents necessarily reflect the views and policies of the U.S. Environmental Protection Agency, nor does mention of trade names or commercial products constitute endorsement or recommendation for use.

EPA Form 2350-4 (4-80)

TYPING GUIDE SHEET

FOREWORD

The Environmental Protection Agency was created because of increasing public and government concern about the dangers of pollution to the health and welfare of the American people. Noxious air, foul water, and spoiled land are tragic testimony to the deterioration of our natural environment. The complexity of that environment and the interplay between its components require a concentrated and integrated attack on the problem.

Research and development is that necessary first step in problem solution and it involves defining the problem, measuring its impact, and searching for solutions. The Municipal Environmental Research Laboratory develops new and improved technology and systems for the prevention, treatment, and management of wastewater and solid and hazardous waste pollutant discharges from municipal and community sources, for the preservation and treatment of public drinking water supplies, and to minimize the adverse economic, social, health, and aesthetic effects of pollution. This publication is one of the products of that research; a most vital communications link between the researcher and the user community.

This study pertains to the effectiveness of activated carbon for removal of selected toxic and carcinogenic compounds at the μg/l level from water in the presence of background humic acids. Emphasis has been placed on the performance predictions of fixed-bed adsorber systems designed to treat the compounds of interest.

Francis T. Mayo, Director
Municipal Environmental Research
Laboratory

TYPING GUIDE SHEET

PREFACE

The ubiquitous character of trace organic compounds in public raw water sources is generally acknowledged. Urban and sub-urban developments along major water courses have affected both implicit and explicit multiple reuse of water. Successive reuse, in turn, is a primary factor for accumulation of industrial and agricultural persistent organic compounds to concentration levels which may pose threats to human health and well being. Further, a variety of natural organic substances can be transformed to potentially harmful compounds in the course of water treatment with chlorine.

Treatment with granular activated carbon is a technically and economically viable technology for removal of a broad spectrum of compounds of concern from public water supplies. The efficiency and cost effectiveness of the design and operation of this process, however, are markedly dependent upon optimum utilization of the adsorption capacity of the carbon, consistent with treatment objectives.

To accomplish efficiency and cost effectiveness, it is necessary to develop appropriate data regarding system dynamics, and to synthesize the body of these data in such a manner as to render it incorporable in actual plant design and operation. Mathematical modeling and simulation of the dynamics of granular carbon systems can be a particularly effective means for synthesis of data regarding adsorption dynamics, and resultant models can be employed to good advantage in prediction of system performance under a variety of conditions. Models of this type can thus function both as vehicles for design, and as algorithmic elements for feed-back and/or feed-forward control and operation of adsorption systems.

The research described herein has focused on development of rate and equilibrium data relative to the adsorption of several representative compounds of natural, industrial, and agricultural origin from water by activated carbon. Further, the Michigan Adsorption Design and Applications Model (MADAM) - which has indicated substantial potential for use in the design and operation of granular carbon systems for wastewater treatment, has been used for simulation and prediction of the dynamic performance of carbon beds for removal of trace quantities of these compounds under conditions approximating those encountered in water treatment practice.

ABSTRACT

This research addressed quantification of the performance of fixed-bed granular activated carbon processes for treatment of public water supplies. It included evaluation of the adsorption of selected toxic and/or carcinogenic trace compounds of man-related origin. The adsorption behavior of the predominant class of natural organic matter and trihalomethane (THM) precursor, humic substances, was also characterized.

Adsorption efficiency tests and cost effectiveness evaluations were performed initially for a number of commercial activated carbons. A bituminous-base carbon was then selected for further use throughout the research program.

Equilibrium, rate, and continuous long-term adsorption column studies were conducted to evaluate the adsorption dynamics of humic acids, carbon tetrachloride, benzene, two commercial mixtures of PCB's, dieldrin, and p-dichlorobenzene.

Experimental breakthrough profiles were developed for each trace compound separately and in the presence of background humic acid solutions to investigate competitive and/or chromatographic effects. The results indicate that the removal of trace compounds is generally affected adversely by background organic matter.

It was found that the adsorption capacity of activated carbon for humic substances is markedly enhanced by the presence and concentration of several common constituents of water supplies, including Mg^{2+} and Ca^{2+} ions. There was evidence from the work that enhanced removal of humic substances might also provide for more effective removal of associated organic molecules -- such as PCB's and dieldrin -- in water treatment operations.

The Michigan Adsorption Design and Applications Model (MADAM) was tested and found generally able to simulate and predict the performance of fixed-bed adsorbers for removal of the compounds investigated, with the exception of humic acids. Prolific biological growth in the adsorbers which received humic acids rendered reliable prediction of the removal of this substance difficult with the strictly adsorption version of MADAM. For such cases it appears necessary to incorporate

EPA Form 2350-4 (4-80)
TYPING GUIDE SHEET

biological degradation dynamics in the model.

Fixed-bed adsorber studies in water containing background humic acids were hindered by extensive biological growth and resulting headloss. Because of these operational problems, it was not always possible to test the strictly adsorption version of MADAM for dynamic performance prediction. The single-solute version of MADAM was able, however, to simulate-predict independent pilot data provided by the EPA relative to the adsorption of 1,2-dichloroethane in the presence of naturally occurring background organics in Ohio River water.

EPA Form 2350-4 (4-80)

TYPING GUIDE SHEET

BEGIN FIRST LINE OF TEXT HERE

CENTER OF PAGE

TOP OF IMAGE AREA

DROPPED HEAD BEGIN SECTIONS HERE

CONTENTS

Foreword iii
Preface iv
Abstract v
Figures x
Tables xxviii
Abbreviations and Symbols xxxi
Acknowledgment xxxiv

1. Introduction 1
2. Conclusions 5
3. Recommendations 7
4. Activated Carbon Adsorption 9
    Basic Properties and Characteristics 9
    Mechanisms and Dynamics of Adsorption 11
    Selection of Activated Carbon for This Study 13
5. Predictive Modeling of Adsorber Systems 28
    General 28
    Adsorption Equilibrium Consideration 29
    Adsorption Rate Consideration 30
    Adsorption Columns or Beds 33
6. Adsorption of Humic Acids 37
    General 37
    Analytical Methods 39
    Adsorption Equilibrium Studies 43
    Adsorption Rate Studies 55
    Adsorption Column Studies 66
    Mechanisms of Removal 86
    Summary and Conclusions 90
7. Adsorption of Carbon Tetrachloride 92
    Background 92
    Analytical Procedures 95
    Adsorption Methodologies 98
    Results and Discussion 104
    Summary and Conclusions 140
8. Adsorption of Benzene 145
    General 145
    Analytical Techniques 148
    Adsorption Methodologies 150
    Results and Discussion 151
    Summary and Conclusions 173

BEGIN LAST LINE OF TEXT

BOTTOM OF IMAGE AREA OUTSIDE DIMENSIONS OF TABLES AND ILLUSTRATIONS

3/8"

PAGE NUMBER

EPA Form 2250-1 (4-80)
(PREVIOUSLY EN. EPA FORM 2877)

U.S. GOVERNMENT PRINTING OFFICE

TYPING GUIDE SHEET

CONTENTS (Continued)

9. Adsorption of Polychlorinated Biphenyls (PCB's) . 178
    General 178
    Analytical Procedures 184
    Adsorption Methodologies 190
    Results and Discussion 198
    Summary and Conclusions 218
10. Adsorption of Dieldrin 221
    General 221
    Analytical Procedure 225
    Adsorption Methodology 226
    Results and Discussion 228
    Summary and Conclusions 249
11. Adsorption of p-Dichlorobenzene (PDB)........ 251
    General 251
    Analytical Procedures 253
    Adsorption Methodology 253
    Results and Discussion 254
    Summary and Conclusions 272
12. A Case Study: Pilot-Plant Investigations of the Adsorption of 1,2-Dichloroethane (DCE) 277
    Introduction 277
    Adsorption Procedures 277
    Adsorption Equilibrium 278
    Adsorption Rates 278
    Adsorption Columns 285
    Conclusions 285

References 296
Appendices 311

A. Physical Properties of Filtrasorb 400 Activated Carbon 311
B. Computer Program Used to Estimate Equilibrium Constants for the Three Parameter Isotherm Model 312
C. Computer Program Used to Estimate Film Transfer and Surface Diffusion Coefficients from Finite-Bath CMB Rate Data 314
D. Computer Program Used to Simulate Breakthrough Behavior for Single-Component Systems 319
E. CHN Analysis 326
F. Preparation of Humic Acid Standards 328
G. Humic Acid Fractionation 330
H. Preparation of Biogrowth on Activated Carbon for Examination by Scanning Electron Microscopy 331

EPA Form 2350-4 (1-80)

TYPING GUIDE SHEET

CONTENTS (Concluded)

J. Biological Inhibition in Bench-Scale Activated Carbon Columns 334
K. CCl_4 Standard Curve Preparation 342
L. Benzene Standard Curve Preparation 345
M. PCB Standard Curve Preparation 348
N. Dieldrin Standard Curve Preparation 351
P. Para-Dichlorobenzene (PDB) Standard Curve Preparation 354

BEGIN FIRST LINE OF TEXT HERE
TYPING GUIDE SHEET
CENTER OF PAGE
TOP OF IMAGE AREA
DROPPED HEAD: BEGIN SECTIONS HERE

FIGURES

Figure **Page**

1 A typical scanning electorn micrograph of granular activated carbon 10

2 Adsorption isotherms for humic acids (C_o=8.95 mg/l, 30/40 US sieve size carbon, buffered at pH 7) 17

3 Adsorption isotherms for carbon tetrachloride (C_o=200 μg/l, 30/40 US sieve size carbon, pH 7) 18

4 Adsorption isotherms for benzene (C_o=500 μg/l, 50/60 US sieve size carbon, pH 7) 19

5 Adsorption isotherms for PCB's (Aroclor 1016) (C_o=100 μg/l, 50/60 US sieve size carbon, pH 7) 20

6 Rates of adsorption of humic acids in CMB reactors (C_o=5 mg/l, 1 g/l of 30/40 US sieve size carbon, buffered at pH 7).... 21

7 Rates of adsorption of CCl_4 in CMB reactors (C_o=200 μg/l, 0.38 g/l of 16/20 US sieve size carbon, pH 7) 22

8 Rates of adsorption of benzene in CMB reactors (0.38 g/l of 16/20 US sieve size carbon, pH 7) 23

9 Rates of adsorption of PCB's (Aroclor 1016) in CMB reactors (0.38 g/l of 30/40 US sieve size carbon, pH 7) 24

10 Adsorption rate data and least squares fits of initial rate data (4 hours) for humic acid 25

BEGIN LAST LINE OF TEXT
BOTTOM OF IMAGE AREA; OUTSIDE DIMENSION FOR TABLES AND ILLUSTRATIONS
3/8"

PAGE NUMBER
EPA-287 (Cin.)
(4-76)

BEGIN FIRST LINE OF TEXT HERE
TYPING GUIDE SHEET
CENTER OF PAGE
TOP OF IMAGE AREA
DROPPED HEAD: BEGIN SECTIONS HERE

FIGURES (Continued)

Figure Page

11 Proposed structure of color macromolecule (after Christman and Ghassemi, 1966) 38

12 Ultraviolet absorption spectra for humic acids solutions brought to equilibrium with different amounts of granular activated carbon 41

13 Correlation between TOC and UV absorption for humic acids analysis 42

14 Adsorption isotherms for humic acids; effect of carbon particle size on adsorption capacity 46

15 Adsorption isotherms for humic acid and fulvic acid fractions of "humic acids" 47

16 Adsorption isotherms for humic acids; effect of pH on adsorption capacity ... 48

17 Adsorption isotherms for humic acids; dependence of extent of adsorption on initial concentration 49

18 Adsorption isotherms for humic acids; comparison of adsorption capacity for "sieved" and "crushed and sieved" carbons 50

19 Adsorption isotherms for humic acids; effect of background solution on adsorption capacity 52

20 Adsorption isotherms for humic acids; effect of selected inorganic species on adsorption capacity (C_o=4.9 mg/l) .. 53

21 CMB reactor rate study for humic acids; effect of carbon particle size on rate of adsorption 56

22 Effect of carbon particle size on rate of adsorption of humic acids; 1 g/l of 30/40 US standard sieve size carbon .. 57

BOTTOM OF IMAGE AREA; OUTSIDE DIMENSION FOR TABLES AND ILLUSTRATIONS
BEGIN LAST LINE OF TEXT
3/8"

PAGE NUMBER
EPA-287 (Cin.)
(4-76)

BEGIN FIRST LINE OF TEXT HERE
TYPING GUIDE SHEET
CENTER OF PAGE
TOP OF IMAGE AREA
DROPPED HEAD; BEGIN SECTIONS HERE

FIGURES (Continued)

Figure | Page

23 Effect of initial concentration on reciprocal of rate of adsorption of humic acids; 1 g/l of 30/40 US standard sieve size 58

24 CMB reactor rate study for humic acid in DDW - sensitivity of predicted profile to variation in mass transfer coefficient, K_f ± 25% 60

25 CMB reactor rate study for humic acid in DDW - sensitivity of predicted profile to variation in surface diffusion coefficient, D_s ± 25% 61

26 CMB reactor rate study for humic acid in tap water - sensitivity of predicted profile to variation in mass transfer coefficient, k_f ± 25% 62

27 CMB reactor rate study for humic acid in tap water - sensitivity of predicted profile to variation in surface diffusion coefficient, D_s ± 25% 63

28 Effect of intraparticle diffusion on the initial adsorption rate of humic acid in DDW 64

29 Effect of intraparticle diffusion on the initial adsorption rate of humic acid in tap water 65

30 Schematic diagram and experimental arrangement for humic acids column studies 68

31 Column breakthrough profiles for humic acids in buffered DDW, C_o=5 ppm, flow rate=4.85 gpm/ft^2, 250 grams of 16/20 US sieve size carbon per column.. 69

32 Column breakthrough profiles for humic acids in buffered DDW, C_o=5 ppm, flow rate=1.94 gpm/ft^2, 250 grams of 16/20 US sieve size carbon per column 70

6-1/2"
9-1/8"
BOTTOM OF IMAGE AREA; OUTSIDE DIMENSION FOR TABLES AND ILLUSTRATIONS
BEGIN LAST LINE OF TEXT
3/8"

PAGE NUMBER
EPA-287 (Cin.)
(4-76)

TYPING GUIDE SHEET
BEGIN FIRST LINE OF TEXT HERE
CENTER OF PAGE
TOP OF IMAGE AREA
DROPPED HEAD; BEGIN SECTIONS HERE

FIGURES (Continued)

Figure — Page

33 Column breakthrough profiles for humic acid in buffered DDW, C_o=5 ppm, flow rate=1.94 gpm/ft^2, expanded bed, 250 grams of 30/40 US sieve size carbon per column 71

34 Column breakthrough profiles for humic acids in tap water, C_o=5 ppm, flow rate= 1.94 gpm/ft^2, 250 grams of 16/20 US sieve size carbon per column 72

35 Column breakthrough profiles for humic acids in different background solution, C_o=5 ppm, flow=1.94 gpm/ft^2, 250 grams of 16/20 US sieve size carbon 73

36 Effect of different background solutions on cumulative adsorption of humic acids in carbon adsorption columns........... 74

37 Electron micrograph of biological growth on activated carbon exposed to humic acids. Note that the carbon surface is sparsely covered with biogrowth 76

38 Electron micrograph of biological growth on activated carbon exposed to humic acids. Note that the biofilm coverage is nonuniform 77

39 Effluent and influent concentration profiles for humic acids in DDW, C_o= 5 ppm, empty bed contact time (EBCT) = 15.6 min. 79

40 Effluent and influent concentration profiles for humic acid in DDW, C_o= 5 ppm, EBCT = 62.4 min 80

41 Effluent and influent concentration profiles for humic acids in tap water, C_o=5 ppm, EBCT = 15.6 min 81

42 Effluent and influent concentration profiles for humic acids in tap water, C_o=5 ppm, EBCT = 31.2 min 82

BEGIN LAST LINE OF TEXT
BOTTOM OF IMAGE AREA, OUTSIDE DIMENSION FOR TABLES AND ILLUSTRATIONS
9-1/8"
3/8"

EPA-287 (Cin.)
(4-76)

BEGIN FIRST LINE OF TEXT HERE
TYPING GUIDE SHEET
CENTER OF PAGE
TOP OF IMAGE AREA
DROPPED HEAD; BEGIN SECTIONS HERE

FIGURES (Continued)

Figure		Page
43	Sensitivity analyses of breakthrough profiles relative to the film transfer coefficient, $k_f \pm 25\%$, for humic acids in DDW	84
44	Sensitivity analyses of breakthrough profiles relative to the film transfer coefficient, $D_s \pm 8\%$, for humic acids in DDW	85
45	Potentiometric titration curves for Ag^+ ($C_o = 1.48 \times 10^{-3}\underline{M}$)	
46	Potentiometric titration curves for Cu^{2+} ($C_o = 1 \times 10^{-2}\underline{M}$)	88
47	Experimental apparatus for mini-column adsorber studies	89
48	Schematic illustration of the CMB reactor	100
49	Experimental apparatus for fixed-bed adsorber study	103
50	Experimental data and Freundlich isotherms for CCl_4 - a comparison of results from bottle-point and mini-column equilibrium measurements	105
51	Experimental data and Freundlich isotherms for CCl_4 - the effects of pH on equilibrium capactiies	106
52	Experimental and Freundlich isotherms for CCl_4 - the effects of particle size on equilibrium capacities	107
53	Experimental data and Freundlich isotherms for CCl_4 - the effects of initial concentration	108

BOTTOM OF IMAGE AREA; OUTSIDE DIMENSION FOR TABLES AND ILLUSTRATIONS
BEGIN LAST LINE OF TEXT
3/8"

PAGE NUMBER
EPA-287 (Cin.)
(4-76)

BEGIN FIRST LINE OF TEXT HERE
TYPING GUIDE SHEET
CENTER OF PAGE
TOP OF IMAGE AREA
DROPPED HEAD; BEGIN SECTIONS

FIGURES (Continued)

Figure		Page
54	Experimental data and Freundlich isotherms for CCl_4 - the effects of different background solutions on equilibrium capacities	109
55	Experimental data and Freundlich isotherms for CCl_4 - the effects of different background solutions on equilibrium capacities	110
56	Experimental data and Freundlich isotherms for virgin and pre-saturated (humic acid) carbons	111
57	CMB rate studies for CCl_4 - the effects of carbon particle size (0.19 g/l carbon)	114
58	Variation of adsorption rate as a function of carbon particle diameter	115
59	CMB rate study for CCl_4 - effect of interrupted stirring (0.19 g/l of 16/20 US sieve size carbon)	116
60	Experimental data and model profiles for rate of adsorption of CCl_4 from OFW in a CMB reactor (0.19 g/l of 16/20 US sieve size carbon)	117
61	Analysis of the sensitivity of model profiles to the film transfer coefficient, k_f	118
62	Analysis of the sensitivity of model to the surface diffusion coefficient, D_s	119
63	Experimental data and model profile for rate of adsorption of CCl_4 from humic acid background solution in CMB reactor, (0.19 g/l of 16/20 US sieve size carbon).	121

BEGIN LAST LINE OF TEXT
BOTTOM OF IMAGE AREA; OUTSIDE DIMENSION FOR TABLES AND ILLUSTRATIONS
3/8"

PAGE NUMBER
EPA-287 (Cin.)
(4-76)

TYPING GUIDE SHEET
BEGIN FIRST LINE OF TEXT HERE
CENTER OF PAGE
TOP OF IMAGE AREA
DROPPED HEAD; BEGIN SECTIONS HERE

FIGURES (Continued)

Figure		Page
64	Breakthrough profiles for CCl_4 in mini-column adsorbers for different influent concentrations, (2 grams of 50/60 US sieve size carbon, flow rate = 5 ml/min, EBCT = 1.1 min)	122
65	Typical breakthrough profiles for CCl_4 in large adsorbers for different flow rates ($\bar{C}_{in}$ = 250 µg/l, 250 grams of 16/20 US sieve size carobn)	123
66	Influent and effluent concentration history profiles for CCl_4 in fixed-bed Run I (mini-column), (2 grams of 50/60 US sieve size carbon, $\bar{C}_{in}$ = 177 µg/l, EBCT = 1.1 min)	126
67	Influent and effluent concentration profiles for CCl_4 in fixed-bed Run II (250 grams of 16/20 US sieve size carbon, $\bar{C}_{in}$ = 570 µg/l, EBCT = 6.0 min)..	127
68	Influent and effluent concentration history profiles for CCl_4 in fixed-bed Run III (250 grams of 16/20 US sieve size carbon, $\bar{C}_{in}$ = 267 µg/l, EBCT = 4.0 min)	128
69	Sensitivity analysis of breakthrough profiles relative to the film transfer coefficient, $k_f \pm 25\%$, for CCl_4 (fixed-bed Run I)	129
70	Sensitivity analysis of breakthrough profiles relative to the surface diffusion coefficient, $D_s \pm 25\%$, for CCl_4 (fixed-bed Run I)	130
71	Sensitivity analysis of breakthrough profiles relative to the film transfer coefficient, $k_f \pm 25\%$, for CCl_4 (fixed-bed Run II)	131
72	Sensitivity analysis of breakthrough profiles relative to the surface diffusion coefficient, $D_s \pm 25\%$, for CCl_4 (fixed-bed Run II)	132

BEGIN LAST LINE OF TEXT
BOTTOM OF IMAGE AREA; OUTSIDE DIMENSION FOR TABLES AND ILLUSTRATIONS
3/8''

PAGE NUMBER
EPA-287 (Cin.)
(4-76)

BEGIN FIRST LINE OF TEXT HERE
TYPING GUIDE SHEET
CENTER OF PAGE
TOP OF IMAGE AREA
DROPPED HEAD, BEGIN SECTIONS HERE

FIGURES (Continued)

Figure — Page

73 Sensitivity analysis of breakthrough profiles relative to the film transfer coefficient, $k_f \pm 25\%$, for CCl_4 (fixed-bed Run III) 133

74 Sensitivity analysis of breakthrough profiles relative to the surface diffusion coefficient, $D_s \pm 25\%$, for CCl_4 (fixed-bed Run III) 134

75 Equilibrium adsorption and desorption data for CCl_4 (C_o = 168 μg/l, 16/20 US sieve size carbon) 136

76 CMB reactor desorption rate study for CCl_4, (per adsorption experiments presented in Figure 59) 137

77 Experimental breakthrough and desorption profiles for CCl_4 in a fixed-bed adsorber (flow rate = 5.2 gpm/ft^2, 250 grams of 16/20 US sieve size carbon). 138

78 Experimental breakthrough and displacement profiles for CCl_4 in a fixed-bed adsorber (flow rate = 3.5 gpm/ft^2, 250 grams of 16/20 US sieve size carbon)... 139

79 Influent and effluent profiles for CCl_4 in the presence of 5 mg/l humic acids in a fixed-bed adsorber 141

80 Experimental breakthrough and displacement profiles for CCl_4 in a fixed-bed adsorber (flow rate = 3.5 gpm/ft^2, 250 grams of 16/20 US sieve size carbon).. 142

81 Experimental breakthrough profiles for CCl_4 in mini-column adsorbers; effect of pre-saturation on the capacity (flow rate = 5 ml/min, 2 grams of 50/60 US seive size carbon) 143

82 Adsorption isotherm for benzene in OFW (C_o = 490 μg/l)..................... 153

BOTTOM OF IMAGE AREA, OUTSIDE DIMENSION FOR TABLES AND ILLUSTRATIONS
BEGIN LAST LINE OF TEXT
3/8"

PAGE NUMBER
EPA-287 (Cin.)
(4-76)

TYPING GUIDE SHEET
BEGIN FIRST LINE OF TEXT HERE
CENTER OF PAGE
TOP OF IMAGE AREA
DROPPED HEAD: BEGIN SECTIONS HERE

FIGURES (Continued)

Figure		Page
83	Adsorption isotherm for benzene in humic acids background solution (C_o = 457 μg/l)	154
84	Experimental data and model profile for rate of adsorption of benzene from OFW in a CMB-reactor (C_o = 450 μg/l, 0.38 g/l of 16/20 US sieve size carbon)	156
85	Analysis of the sensitivity of model profiles to film transfer coefficient, k_f.	157
86	Analysis of the sensitivity of model profiles to surface diffusion coefficient, D_s	158
87	Experimental data and model profile for rate of adsorption of benzene from humic acids background solution in a CMB-reactor (C_o = 507 μg/l, 0.38 g/l of 16/20 US sieve size carbon)	160
88	Experimental breakthrough profiles for benzene in mini-column adsorbers	161
89	Experimental breakthrough profile for benzene in a large adsorber	162
90	Effluent and influent concentration profiles for benzene in OFW - fixed-bed adsorber Run I ($\overline{C}_{in}$ = 264 μg/l, 1 gram of 50/60 carbon, flow rate = 10 ml/min, EBCT = 0.24 min)	163
91	Effluent and influent concentration profiles for benzene in OFW - fixed-bed adsorber Run II ($\overline{C}_{in}$ = 200 μg/l, 2 grams of 50/60 carbon, flow rate = 5 ml/min, EBCT = 0.95 min)	166
92	Effluent and influent concentration profiles for benzene in OFW - fixed-bed adsorber Run III ($\overline{C}_{in}$ = 519 μg/l, 100 grams of 16/20 carbon, flow rate = 100 ml/min, EBCT = 2.5 min)	167

BEGIN LAST LINE OF TEXT
BOTTOM OF IMAGE AREA OUTSIDE DIMENSION FOR TABLES AND ILLUSTRATIONS
3/8"

PAGE NUMBER
EPA-287 (Cin.)
(4-76)

BEGIN FIRST LINE OF TEXT HERE
TYPING GUIDE SHEET
CENTER OF PAGE
TOP OF IMAGE AREA
DROPPED HEAD: BEGIN SECTIONS HERE

FIGURES (Continued)

Figure | Page

93 Sensitivity analysis of breakthrough profiles relative to the film transfer coefficient, $k_f \pm 25\%$, for benzene in OFW, (fixed-bed adsorber Run I) 168

94 Sensitivity analysis of breakthrough profiles relative to the surface diffusion coefficient, $D_s \pm 25\%$, for benzene in OFW, (fixed-bed adsorber Run I) 169

95 Sensitivity analysis of breakthrough profiles relative to the film transfer coefficient, $k_f \pm 25\%$, for benzene in OFW, (fixed-bed adsorber Run III) 170

96 Sensitivity analysis of breakthrough profiles relative to the surface diffusion coefficient, $D_s \pm 25\%$, for benzene in OFW, (fixed-bed adsorber Run III) 171

97 Adsorption-desorption studies for benzene in OFW (C_o = 442 µg/l) 172

98 Effluent and influent concentration profiles for adsorption-desorption study for benzene in OFW (100 grams of 16/20 carbon and hydraulic loading of 3.5 gpm/ft^2) 174

99 Effluent and influent concentration profiles for benzene in 5 mg/l humic acids background solution (100 grams of 16/20 carbon and hydraulic loading of 3.5 gpm/ft^2, col. dia. = 3 cm ID) 175

100 Effluent and influent profiles for adsorption of benzene on virgin carbon and pre-saturated carbon (1 gram of 50/60 carbon, flow rate = 10 ml/min column diameter = 1.2 cm ID) 176

101 Quantitative mean-percent-weight analysis of different isomer groups for Aroclor-1242 (after Webb and McCall, 1973) 186

BEGIN LAST LINE OF TEXT
BOTTOM OF IMAGE AREA OUTSIDE DIMENSION FOR TABLES AND ILLUSTRATIONS
3/8"

PAGE NUMBER
EPA-287 (Cin.)
(4-76)

TYPING GUIDE SHEET
BEGIN FIRST LINE OF TEXT HERE
CENTER OF PAGE
TOP OF IMAGE AREA
DROPPED HEAD BEGIN SECTIONS HERE

FIGURES (Continued)

Figure		Page
102	Quantitative mean-percent-weight analysis of different isomer groups for Aroclor-1254 (after Webb and McCall, 1973)	187
103	Typical packed-column chromatograms for A-1254 (3% Silicone OV-1 on 80/100 Gas Chrom Q; Ni_{63} ECD)	188
104	Typical packed-column chromatograms for A-1254	189
105	Typical packed column chromatograms for A-1016 (3% Silicone OV-1 on 80/100 Gas Chrom Q; Ni_{63} ECD)	191
106	Rate of loss of A-1254 to the air-tight Pyrex glass reactor used for CMB rate experiments	192
107	Rate and extent of volatilization of A-1254	194
108	Isotherms for adsorption of A-1254 on bacterial cells........................	195
109	Rate and extent of adsorption of acetone carrier-solvent on granular carbon in a CMB reactor (C_o = 30 mg/l, 0.66 g/l of 16/20 US sieve size carbon)	197
110	Experimental apparatus and arrangement .	199
111	Adsorption isotherm for A-1016 in OFW (spiked twice at C_o = 45 μg/l, 100/200 carbon)	200
112	Adsorption isotherm for A-1016 in solution of humic acids (C_o = 63.6 μg/l, 100/200 carbon)	201
113	Adsorption isotherm for A-1254 in OFW (C_o = 25 μg/l, 100/200 carbon)	202
114	Adsorption isotherm for A-1254 in solution of humic acids (C_o = 46.5 μg/l, 100/200 carbon)	203

BEGIN LAST LINE OF TEXT
BOTTOM OF IMAGE AREA; OUTSIDE DIMENSION FOR TABLES AND ILLUSTRATIONS
3/8"

PAGE NUMBER
EPA-287 (Cin.)
(4-76)

BEGIN FIRST LINE OF TEXT HERE
TYPING GUIDE SHEET
CENTER OF PAGE
TOP OF IMAGE AREA
DROPPED HEAD: BEGIN SECTIONS HERE

FIGURES (Continued)

Figure **Page**

115 Differential adsorption rate behavior on individual peaks for A-1254 in OFW (C_o = 38.6 μg/l, 0.115 g/l of 50/60 carbon) 206

116 Differential adsorption rate behavior of individual peaks for A-1254 in a solution of humic acids (C_o = 36.9 μg/l, 0.115 g/l of 50/60 carbon) 207

117 Experimental data and model profile for rate of adsorption of A-1016 from OFW in a CMB reactor (C_o = 40.5 μg/l, 0.114 g/l of 50/60 US sieve size carbon). 208

118 Experimental data and model profile for rate of adsorption of A-1254 from OFW in a CMB reactor (C_o = 38.6 μg/l, 0.114 g/l of 50/60 US sieve size carbon). 209

119 Experimental data and model profile for rate of adsorption of A-1016 from solution of humic acids in a CMB reactor (C_o = 51.1 μg/l, 0.114 g/l of 50/60 US sieve size carbon) 210

120 Experimental data and model profile for rate of adsorption of A-1254 form a solution of humic acids in a CMB reactor (C_o = 36.9 μg/l, 0.114 g/l of 50/60 US sieve size carbon).......... 211

121 Influent and effluent concentration data for A-1016 in fixed-bed adsorbers (flow = 20 ml/min, 5 grams of 50/60 US sieve size carbon, EBCT = 0.52 min). 214

122 Scanning electron micrograph of biological growth on activated carbon exposed to a solution of Aroclor 1016 215

123 Equilibrium adsorption and desorption data for A-1254 in OFW (C_o = 25 μg/l, 50/60 US sieve size carbon) 217

BOTTOM OF IMAGE AREA OUTSIDE DIMENSION FOR TABLES AND ILLUSTRATIONS
BEGIN LAST LINE OF TEXT
3/8"

PAGE NUMBER
EPA-287 (Cin.)
(4-76)

TYPING GUIDE SHEET
BEGIN FIRST LINE OF TEXT HERE
CENTER OF PAGE
TOP OF IMAGE AREA
DROPPED HEAD BEGIN SECTIONS HERE

FIGURES (Continued)

Figure | Page

124 Influent and effluent concentration data for A-1254 in fixed-bed adsorbers (flow = 10 ml/min), 1 gram of 50/60 US sieve size carbon) 219

125 Rate of loss of dieldrin to the Pyrex glass reactor used for CMB rate experiments 227

126 Experimental apparatus 229

127 Adsorption isotherm for dieldrin in OFW (C_o = 50 μg/l, 16/20 carbon) 230

128 Adsorption isotherm for dieldrin in solution of humic acids (C_o = 50 μg/l, 16/20 carbon) 231

129 CMB rate studies for dieldrin - effects of carbon particle size (0.17 g/l carbon) 234

130 Variation of adsorption rate as a function of carbon particle diameter... 235

131 Experimental data and model profile for rate of adsorption of dieldrin from OFW in a CMB reactor (C_o = 115.8 μg/l, 0.19 g/l of 50/60 carbon) 236

132 Analysis of the sensitivity of model profiles to the film transfer coefficient, k_f, for dieldrin 237

133 Experimental data and model profile for rate of adsorption of dieldrin from a solution of humic acids in a CMB reactor (C_o = 108 μg/l, 0.19 g/l of 50/60 carbon) 238

134 Influent and effluent concentration data for dieldrin in large fixed-bed adsorbers (flow = 40 ml/min., 250 grams 16/20 carbon, EBCT = 15 min) 242

BEGIN LAST LINE OF TEXT
BOTTOM OF IMAGE AREA: OUTSIDE DIMENSION FOR TABLES AND ILLUSTRATIONS
3/8"

PAGE NUMBER
EPA-287 (Cin.)
(4-76)

FIGURES (Continued)

Figure		Page
135	Influent and effluent concentration data for dieldrin in mini fixed-bed adsorbers (flow = 20 ml/min), 5 grams of 50/60 carbon, EBCT = 0.52 min)	243
136	Influent and effluent concentration data for dieldrin in mini fixed-bed adsorbers (flow = 15 ml/min, 2 grams of 50/60 carbon, EBCT = 0.31 min)	245
137	Influent and effluent concentration profiles for mini expanded-bed adsorbers (flow = 15 ml/min, 2 grams of 50/60 carbon)	246
138	Experimental apparatus for dieldrin (comparison of virgin and "humic acid presaturated" carbon)	247
139	Effluent concentration data for dieldrin in fixed-bed adsorbers; effect of presaturation (flow = 10 ml/min, 1 gram of 50/60 carbon)	248
140	Adsorption isotherm for PDB in OFW (C_o = 25 mg/l)	255
141	Adsorption isotherm for PDB in 5 mg/l humic acid background solution (C_o = 25 mg/l)	256
142	CMB rate studies for PDB - effects of carbon particle size (0.083 g/l carbon).	259
143	Variation of adsorption rate as a function of carbon particle diameter	260
144	Experimental data and model profile for rate of adsorption of PDB from OFW in a CMB reactor (C_o = 157 μg/l, 0.076 g/l of 50/60 carbon)	261
145	Analysis of the sensitivity of model profiles to the film transfer cceefficient, k_f	262

TYPING GUIDE SHEET

FIGURES (Continued)

Figure		Page
146	Experimental data and model profile for rate of adsorption of PDB from humic acid background solution in a CMB reactor (C_o = 167 μg/l, 0.076 g/l of 50/60 carbon)	263
147	CMB reactor rate study for adsorption of PDB on virgin and pre-saturated carbon (0.076 g/l of 50/60 carbon)	264
148	Experimental breakthrough profiles for PDB in mini fixed-bed adsorbers	267
149	Effluent and influent concentration profiles for PDB in OFW - fixed-bed adsorber Run I ($\overline{C}_{in}$ = 185 μg/l, 1 gram of 50/60 carbon, flow rate = 15 ml/min, EBCT = 0.17 min)	269
150	Effluent and influent concentration profiles for PDB in OFW - fixed-bed adsorber Run II ($\overline{C}_{in}$ = 2.53 mg/l, 5 grams of 50/60 carbon, flow rate = 20 ml/min, EBCT = 0.59 min)	270
151	Sensitivity analysis of breakthrough profiles relative to the film transfer coefficient, $k_f \pm 25\%$, for PDB in OFW (fixed-bed adsorber Run I)	271
152	Effluent and influent concentration profiles for adsorption-desorption study for PDB (5 grams of 50/60 carbon, flow rate = 20 ml/min)	273
153	Effluent and influent profiles for PDB in OFW and 5 mg/l humic acid solution (expanded-bed systems)	274
154	Effluent profiles for adsorption of PDB on virgin carbon and pre-saturated carbon ($\overline{C}_{in}$ = 185 μg/l, 1 gram of 50/60 carbon, flow rate = 15 ml/min)...	275
155	Adsorption isotherm for 1,2-dichloroethane in settled river water (Data provided by MERL, USEPA)	279

EPA-287 (Cin.)
(4-78)

FIGURES (Continued)

Figure		Page
156	CMB rate study for DCE; estimation of film transfer coefficient, k_f, from the initial stages fo rate curve (5.0 g/l of 12/40 carbon). (Data provided by MERL, USEPA)	281
157	Experimental data and model profile for rate of adsorption of DCE from SRW in a CMB reactor (C_o = 124 μg/l, 0.118 g/l of 12/40 carbon). (Data provided by MERL, USEPA)	282
158	Analysis of the sensitivity of model profiles to the film transfer coefficient, k_f, for DCE. (Data provided by MERL, USEPA)	283
159	Analysis of the sensitivity of model to the surface diffusion coefficient, D_s, for DCE. (Data provided by MERL, USEPA)	284
160	Effluent concentration profiles for DCE in SRW (fixed-bed adsorber Run I) (Data provided by MERL, USEPA)	287
161	Effluent concentration profiles for DCE in SRW (fixed-bed adsorber Run II) (Data provided by MERL, USEPA)	288
162	Effluent concentration profiles for DCE in SRW (fixed-bed adsorber Run III) (Data provided by MERL, USEPA)	289
163	Sensitivity analysis of breakthrough profiles relative to the film transfer coefficient, $k_f \pm 25\%$, for DCE (fixed-bed adsorber Run I) (Data provided by MERL, USEPA)	290
164	Sensitivity analysis of breakthrough profiles relative to the surface diffusion coefficient, $D_s \pm 25\%$, for DCE (fixed-bed adsorber Run I) (Data provided by MERL, USEPA)	291

TYPING GUIDE SHEET
BEGIN FIRST LINE OF TEXT HERE
CENTER OF PAGE
TOP OF IMAGE AREA
DROPPED HEAD BEGIN SECTIONS HERE
BEGIN LAST LINE OF TEXT
BOTTOM OF IMAGE AREA; OUTSIDE DIMENSION FOR TABLES AND ILLUSTRATIONS
3/6"
PAGE NUMBER
EPA-287 (Cin.)
(4-76)

BEGIN FIRST LINE OF TEXT HERE
TYPING GUIDE SHEET
CENTER OF PAGE
TOP OF IMAGE AREA
DROPPED HEAD BEGIN SECTIONS HERE

FIGURES (Continued)

Figure		Page
165	Sensitivity analysis of breakthrough profiles relative to the film diffusion coefficient, $k_f \pm 25\%$, for DCE (fixed-bed adsorber Run II) (Data provided by MERL, USEPA)	292
166	Sensitivity analysis of breakthrough profiles relative to the surface diffusion coefficient, $D_s \pm 25\%$, for DCE (fixed-bed adsorber Run II) (Data provided by MERL, USEPA)	293
167	Sensitivity analysis of breakthrough profiles relative to the film diffuison coefficient, $k_f \pm 25\%$, for DCE (fixed-bed adsorber Run III). (Data provided by MERL, USEPA)	294
168	Sensitivity analysis of breakthrough profiles relative to the surface diffusion coefficient, $D_s \pm 25\%$, for DCE (fixed-bed adsorber Run III) (Data provided by MERL, USEPA)	295
E-1	Calibration curve for carbon analysis using a CHN analyzer	327
F-1	Calibration curve for humic acid analysis using ultraviolet spectroscopy.	329
J-1	Rate and extent of adsorption of Cu^{+2} from DDW by granular activated carbon in a CMB reactor (0.166 g/l of 16/20 US sieve size carbon)	335
J-2	Ultraviolet Spectra for Cu^{2+} individually and in the presence of humic acids	336
J-3	Rate and extent of adsorption of Hg^{2+} from DDW by granular activated carbon in a CMB reactor (0.166 g/l of 16/20 US sieve size carbon)	337

BOTTOM OF IMAGE AREA OUTSIDE DIMENSION FOR TABLES AND ILLUSTRATIONS
BEGIN LAST LINE OF TEXT
3/8"

PAGE NUMBER
EPA-287 (Cin.)
(4-76)

FIGURES (Concluded)

Figure		Page
J-4	Rate and extent of adsorption of Ag^+ from DDW by granular activated carbon in a CMB reactor (0.167 g/l of 16/20 US sieve size carbon)	338
J-5	Ultraviolet spectra for Ag^+ individually and in the presence of humic acids	339
K-1	Calibration curve for CCl_4 using a Sc^3H ECD	343
K-2	Chromatograms for CCl_4 using: a) an electrolytic conductivity detector; and, b) a Sc^3H ECD	344
L-1	Calibration curve for benzene (dynamic headspace GC analysis)	346
L-2	Chromatogram for benzene using FID (dynamic headspace GC analysis)	347
M-1	Calibration curve for A-1254 using ^{63}Ni ECD	349
M-2	Chromatograms for PCB using ^{63}Ni ECD: a) A-1016; and, b) A-1254	350
N-1	Calibration curve for dieldrin using ^{63}Ni ECD	352
N-2	Typical chromatograms for dieldrin using: a) 3% SE-30 on Gas Chrom Q (Sc^3H ECD) b) 3% OV-1 on 100/200 Varaport 30 (^{63}Ni ECD)	353
P-1	Calibration curve for PDB using a ^{63}Ni ECD	355
P-2	Chromatograms for PDB using: a) an electrolytic conductivity detector; and, b) a ^{63}Ni ECD	356

TABLES

Table		Page
1	General Properties of Selected Commercial Activated Carbons	14
2	Freudlich Parameters for Adsorption of Selected Organic Compounds on Different Carbons.	16
3	Rate Parameters for Adsorption of Selected Organic Compounds on Different Carbons	26
4	Formulae for Predictive Model Calibration and Verification	36
5	Summary of Adsorption Equilibrium Studies for Humic Acids	45
6	Effects of Ca^{2+}, Mg^{2+}, and OCl^- On Aqueous Concentrations of Humic Acids in the Absence of Activated Carbon.....	54
7	Mass Transport Coefficients for Adsorption of Humic Acids in Different Background Solutions	59
8	Mass Transfer Coefficients for Selected Compounds of Known Adsorption Characteristics	66
9	Parameters Used for Fixed-Bed Adsorber Predictive Breakthrough Profiles for Humic Acids	83
10	Physical and Chemical Properties of Carbon Tetrachloride	93
11	Summary of Adsorption Equilibrium Studies for Carbon Tetrachloride	113
12	Estimated Adsorption Rate Mass Transfer Coefficients for CCl_4.................	120

TYPING GUIDE SHEET

TABLES (Continued)

Table		Page
13	Parameters Used For Fixed-Bed Adsorber Predictive Breakthrough Profiles for CCl_4..	125
14	Physical and Chemical Properties of Benzene	146
15	Summary of Benzene Uses	147
16	Adsorption Equilibrium Studies for Benzene	152
17	Estimated Adsorption Rate Mass Transfer Coefficients for Benzene	159
18	Fixed-Bed Adsorber Parameters for Benzene.	164
19	Summary of PCB Uses and Fate	179
20	Solubilities of Chlorobiphenyls in Water (after Hutzinger *et al*, 1974)....	181
21	Chemical and Physical Properties of Aroclors 1016 and 1254 (after Hutzinger *et al*, 1974)	183
22	Molecular Composition of Aroclors 1016 and 1254 (after Hutzinger *et al*, 1974)	183
23	Summary of Adsorption Equilibrium Parameters for A-1016 and A-1254	204
24	Summary of Adsorption Rate Parameters for Aroclor 1016 and 1254	213
25	Physical and Chemical Properties of Technical Dieldrin	222
26	Adsorption Equilibrium Parameters for Dieldrin	232
27	Estimated Adsorption Rate Mass Coefficients for Dieldrin	240
28	Physical and Chemical Properties of *p*-Dichlorobenzene	252

TABLES (Concluded)

Table		Page
29	Adsorption Equilibrium Parameters for PDB	257
30	Adsorption Rate Parameters for PDB	265
31	Fixed-Bed Adsorber Parameters for PDB	268
32	Adsorption Equilibrium Studies for 1,2-Dichloroethane in Coagulated River Water (Data provided by MERL, USEPA)	280
33	Parameters Used for Fixed-Bed Adsorber Predictive Breakthrough Profiles for DCE	286

TYPING GUIDE SHEET

LIST OF ABBREVIATIONS AND SYMBOLS

ABBREVIATIONS

DDW	-- deionized-distilled water
gm/l	-- gram per liter
gpm/ft^2	-- gallon per min per square foot
μg/l	-- microgram per liter
mg/l	-- milligram per liter
ml/min	-- milliliter per min
ng/l	-- nanogram per liter
OFW	-- organic free water

SYMBOLS

Ca^{2+}	-- calcium ion
Mg^{2+}	-- magnesium ion
OCl^-	-- hypochlorite ion
CCl_4	-- carbon tetrachloride
DCB	-- *p*-dichlorobenzene
DCE	--1,2-dichloroethane
PCB's	-- polychlorinated biphenyls

A	Three parameter isotherm constant, $q_e(1+BC_e^{\beta})/C_e$
A_a	Cross sectional area of absorber bed, cm^2
a_p	Particle surface area to volume ratio, cm^2/cm^3
b	Langmuir isotherm parameter, l/mg
B	Three parameter isotherm constant, $(AC_e-q_e)/q_eC_e^{\beta}$
C	Solution concentration, mg/l
C_e	Equilibrium solution concentration, mg/l
C_i	Solution concentration of species i, mg/l
C_o	Initial concentration, mg/l
$\bar{C}$	Reduced solution concentration, dimensionless
$\bar{C}_o$	Reduced influent concentration as a function of throughput, dimensionless
C_s	Liquid phase concentration near solid particle, mg/l
D_d	Dispersion Coefficient, cm^2/sec
D_g	Solute Distribution parameter, dimensionless

EPA Form 2350-4 (4-80)
TYPING GUIDE SHEET

LIST OF ABBREVIATIONS AND SYMBOLS (Continued)

D_l	Free liquid phase diffusivity, cm^2/sec
D_s	Intraparticle surface diffusivity, cm^2/sec
d_p	Particle diameter, cm
K_f	Freundlich isotherm parameter, $q/C^{1/n}$
k_f	Film transfer coefficient, cm/sec
L	Length of absorber bed, cm
N_{pe}	Peclet number, dimensionless
N_s	Intraparticle pore solid phase diffusion flux, mg/cm^2-sec
1/n	Freundlich isotherm parameter, dimensionless
Q	Volumetric flow rate, l/min
q	Solid phase (adsorbed phase) concentration, mg/gm
q_e	Solid phase concentration in equilibrium with C_e, mg/gm
q_i	Intraparticle solid phase concentration in Equation 5, and solid phase concentration of species i in Equation 18, mg/gm.
q_o	Solid phase concentration in equilibrium with C_o, mg/gm
q_s	Solid phase concentration in equilibrium with C_s, mg/gm
R	Radius of particle, cm
r	Radial coordinate
$\bar{r}$	Reduced radial coordinate
R_e	Reynolds number, dimensionless
R_e'	Modified Reynolds number, dimensionless
S_c	Schmidt number, dimensionless
Sh	Sherwood number, dimensionless
St_m	Modified Staton number, $t/(TD_g)$, dimensionless
t	Time, min
T	Absolute temperature, °K
$\bar{T}$	Throughput parameter, dimensionless
v	Interstitial fluid velocity in the adsorber bed, cm/sec
V	Reactor volume, l
V_c	Volume of carbon in adsorber bed, cm^3
V_s	Superficial velocity, cm/sec
v_z	Axial velocity in adsorber bed, cm/sec
V_o	Molar volume, cm^3/mol
W	Weight of carbon, gm
X	Association parameter for solvent, dimensionless
z	Longitudinal coordinate

LIST OF ABBREVIATIONS AND SYMBOLS (Concluded)

$\bar{z}$	Reduced longitudinal coordinate
β	Three parameter isotherm constant, dimensionless
ϵ_p	Porosity of carbon particle, dimensionless
γ	Liquid fraction in carbon bed, dimensionless
δ_p	Carbon density, gm/l of bed
σ_l	Liquid density, gm/cm^3
σ_p	Dry carbon density, gm/cm^3
μ	Viscosity, gm/cm-sec
T	Hydraulic residence time, min

TYPING GUIDE SHEET

ACKNOWLEDGEMENT

The cooperation of the Municipal Environmental Research Laboratory (MERL) of the U.S. Environmental Protection Agency, Cincinnati, Ohio, especially Mr. Alan Stevens, is gratefully acknowledged.

Sincere thanks are extended to several graduate students in the Environmental and Water Resources Engineering Program at the University of Michigan: Doug Barton, Bruce Bawkon, Dave Cooper, Dave Fischer, Mark Herbert, Gary Hunt, Jim Long, Gail Melson, Alan Moore, Bob Stevenson, and Tom Voice for their faithful and diligent laboratory work in connection with this project. The efforts of Afshan Afshar for excellent graphic design and illustrations, and Penelope Frey for skillful manuscript preparation are duly recognized.

Appreciation is expressed to Mr. Leown Moore of MERL, USEPA, for providing the experimental data for 1,2-dichloroethane.

EPA Form 2350-1 (6-80)

TYPING GUIDE SHEET

BEGIN FIRST LINE OF TEXT HERE
TYPING GUIDE SHEET
CENTER OF PAGE
TOP OF IMAGE AREA
DROPPED HEAD; BEGIN SECTIONS HERE

SECTION 1

INTRODUCTION

Organic contaminants of major concern in water supplies can be broadly divided into two classes: (1) naturally-occurring substances, such as humic acids, which can impart color, taste, and/or odor to water and which may also be transformed to trihalomethanes in the course of water treatment with chlorine; and, (2) potentially toxic and/or carcinogenic organic compounds of agricultural, industrial or other anthropic origin. Both classes of organic contaminants include compounds which are persistent in receiving waters and raw water sources. Further, many of these compounds may undergo interactions to yield species which may be more harmful than their precursors (Schnitzer and Khan, 1972).

A comprehensive nationwide survey (National Organic Reconnaissance Survey - NORS) was conducted in 1975 by the Environmental Protection Agency to determine the presence, concentrations, and potential effects of certain organic chemicals in drinking water. The NORS program provided for analysis of eighty water supplies representing a wide variety of raw water sources, treatment techniques, and geographical locations. Because it had been postulated that trihalomethanes were ubiquitous to chlorinated drinking waters -- indeed, that they resulted largely from chlorination practice (USEPA, 1975) -- chloroform, bromoform, bromodichloromethane, and dibromochloromethane, along with two other volatile halogenated hydrocarbons, carbon tetrachloride and 1,2-dichloroethane, were of particular interest and focus for the NORS investigation.

Rook (1974) had earlier reported the formation of such compounds during chlorination of Rhine River water, and, in a later investigation (1976), discussed the probable role of the fulvic fraction of humic substances as precursors in the production of trihalomethanes. He elaborated on the reactivity of meta-dihydroxy aromatic compounds, the basic building blocks of humic substances, with chlorine. In a more recent report, Rook (1977) presented possible reaction pathways leading to haloforms and other chlorinated by-products. Coleman et al (1975), in a five-city survey, also documented the "apparent" formation of halogenated organics (aliphatic and aromatic) during chlorination of drinking water.

BEGIN LAST LINE OF TEXT
BOTTOM OF IMAGE AREA; OUTSIDE DIMENSION FOR TABLES AND ILLUSTRATIONS
3/8"

PAGE NUMBER
EPA-287 (Cin.)
(4-76)

TYPING GUIDE SHEET
BEGIN FIRST LINE OF TEXT HERE
CENTER OF PAGE
TOP OF IMAGE AREA
DROPPED HEAD, BEGIN SECTIONS HERE

With respect to the second group of organic contaminants, 34 compounds of industrial and agricultural origin were identified in lower Mississippi River water (Miller, 1973). An investigation by Kloepfer and Fairless (1972) of chloroform extracts of municipal drinking water from the Ohio River revealed over 40 detectable synthetic organic compounds. Other studies conducted by a number of investigators throughout the country similarly indicated the probability of widespread contamination of water supplies.

There is little concrete evidence to link organic compounds in water supplies directly to cancer, birth defects, cardiovascular disease, or other physiologic anamolies (Tardiff and Deinzer, 1973). The etiologies of such diseases are complex, and not sufficiently defined. Although acute or chronic toxicity may be measured for animals, extrapolations of such measurements for prediction of effects on human beings are difficult and uncertain. Evaluations of possible teratogenicity and/or mutagenicity are even more difficult and uncertain. Nonetheless, in the absence of more definitive procedures, such bioassays may be the best available means of assessing the potential toxicity of compounds present in water supplies (Ongerth *et al*, 1973).

In this light, it is worth noting that such bioassays have indicated luekemic reactions and bladder papilloma in laboratory mice injected cutaneously and subcutaneously with carbon-chloroform extracts of water (Heuper and Payne, 1963). Further, studies by Dowty *et al* (1975) have revealed the existence of five halogenated compounds in the blood plasma of persons living in New Orleans. The concentration of carbon tetrachloride in the blood plasma was found to be substantially higher than that in the drinking water, and the authors postulated that bioaccumulation effects might be operative in humans. Most recently, the National Cancer Institute has presented evidence that chloroform may be carcinogenic (N.C.I., 1976).

It is clear that potentially toxic and/or carcinogenic organic compounds of municipal, industrial, and agricultural origin, coupled with naturally-occurring organics which may be transformed into hazardous substances in the course of water chlorination, constitute a matter of substantial public health concern for the water works industry. It is incumbent upon this industry to ensure the safety of water supplies by developing, refining and employing treatment technologies which will minimize the formation of harmful organic compounds during treatment and which will remove trace compounds present in raw water supplies.

Treatment of water with granular activated carbon is one potential means for accomplishing removal of both precursor compounds and trace synthetic organic species present in

BEGIN LAST LINE OF TEXT
BOTTOM OF IMAGE AREA OUTSIDE DIMENSION FOR TABLES AND ILLUSTRATIONS
3/8"

PAGE NUMBER
EPA-287 (Cin.)
(4-76)

raw waters. A substantial amount of information is available regarding the efficiency of carbon for removing taste and odor substances from drinking waters and a variety of organic compounds from industrial and municipal wastewaters (Weber, 1974-a, 1974-b; Birkmeier et al, 1978). However, insignificant information exists regarding the effectiveness of carbon for providing required levels of removal of organic substances at the extremely low initial concentrations typically present in drinking waters.

Thus, while adsorption on activated carbon provides a potential solution, the complexities associated with the extremely low-level concentrations of trace compounds of concern in the presence of higher background concentrations of naturally-occurring organics must be fully evaluated. The technology of granular activated carbon applications in water treatment is relatively sophisticated; much of this sophistication relates to the complex dynamics of adsorption processes. The adsorption dynamics of low-level concentrations of trace compounds must be better understood to facilitate efficient and cost-effective design of water treatment systems using granular activated carbon. This necessitates development of appropriate data regarding system dynamics, and synthesis of this data to render it incorporable in actual plant design and operation.

The overall objectives of the research described in this report were to investigate removal of trace organic contaminants of industrial and/or agricultural origin at the microgram per liter level; to evaluate the competitive effects of naturally-occurring organics on the effectiveness of carbon for removal of the trace compounds on a long-term continuous basis; and to quantify the associated adsorption dynamics to facilitate optimum design and application methodology. Specific studies were designed to:

(1) determine the behavior of different commercial activated carbons to compare the selectivities and capacities for removal of selected organic contaminents;

(2) determine fundamental kinetic and thermodynamic adsorption parameters for model trace organic compounds (benzene, carbon tetrachloride, dieldrin, PCB's and para-dichlorobenzene) and naturally-occurring organics (water-soluble compounds present in peat consisting of humic and fulvic materials) separately and in combination;

(3) conduct continuous long-term column studies to evaluate associated adsorption phenomena for each compound and appropriate combination, thereof including

competitive and/or chromatographic effects in dynamic systems; and,

(4) test and evaluate the capability of predictive design models for describing the dynamic behavior of model trace compounds individually and in the presence of naturally-occurring organics in fixed-bed adsorbers.

SECTION 2

CONCLUSIONS

1. Carbon tetrachloride, benzene, polychlorinated biphenyls (PCB's), dieldrin, and *p*-dichlorobenzene (PDB) all generally manifest adsorption isotherms of energetically favorable type; that is, of the type indicating amenability to effective removal from water by activated carbon.

2. Humic acids exhibited adsorption isotherm characteristics ranging from energetically favorable to unfavorable, depending on background ionic constituents.

3. Adsorption capacities of activated carbon for humic acids are markedly enhanced by the presence of several common ionic constituents of water, including Ca^{2+}, Mg^{2+}, and OCl^-.

4. The effectiveness of activated carbon for removal of PCB's and dieldrin from water is adversely affected by the association of these compounds with background humic substances. Introduction of certain inorganic species such as Mg^{2+} and Ca^{2+} for more effective removal of humic substances might also provide for more effective removal of associated organic molecules--such as PCB's and dieldrin--in water treatment operations.

5. Experimental data suggest that although a carbon is presaturated with background organics it may continue to remove trace quantities of materials with strong adsorption potential, such as PCB's and dieldrin.

6. The Michigan Adsorption Design and Applications Model (MADAM) was generally able to simulate and predict the performance of fixed-bed adsorbers for removal of carbon tetrachloride, benzene, and *p*-dichlorobenzene in organic-free-water background solution. Because it was not possible to obtain experimental breakthrough profiles for PCB's and dieldrin (no breakthrough occurred in 7-8 months of operation), no attempt was made to model the behavior of these substances in fixed-bed adsorber systems.

TYPING GUIDE SHEET

7. Fixed-bed adsorber studies in water containing background humic acids were hindered by extensive biological growth and resulting headloss. Because of these operational problems, it was not possible to test adequately the strictly adsorption version of MADAM for forecasting the dynamic performance of adsorber beds under such circumstances. It would appear desirable, when modeling adsorbers which exhibit or have a tendency toward prolific biological growth, to use a version of MADAM which incorporates biological degradation terms. The single-solute, strictly adsorption version of the MADAM model, however, was used successfully to simulate-predict independent USEPA pilot-plant data on the adsorption of 1,2-dichloroethane in the presence of naturally occurring background organics in Ohio River water.

8. A notable characteristic of the column data for humic acid is the establishment of a near steady-state breakthrough plateau, the precise level of which varies with system particulars and operating conditions. Mechanisms responsible for this phenomenon likely include--at a minimum--biological degradation and hindered diffusion of these large macromolecules within the carbon micropores.

9 The results of long term column studies with the trace compounds--including PCB's, dieldrin, and 1,2-dichloroethane--suggest the development of specific micro-organisms that may be capable of biodegrading these relatively resistant compounds in activated carbon adsorbers.

10. The results indicate that granular activated carbon provides an effective filtration/adsorption media for compounds such as PCB's and dieldrin in water treatment operations.

SECTION 3

RECOMMENDATIONS

1. Properly designed laboratory mini-column adsorbers, fed with the actual water to be treated, and subjected to periodic air scouring and backwashing, should be further evaluated as a means for determining feasibility and associated design data for adsorption operations for specific water treatment applications. The use of such mini-columns, coupled with the application of modeling programs such as MADAM, appears to have significant potential for reduction of the costs and time normally associated with large-scale pilot-plant testing programs.

2. The studies reported herein have been limited to virgin carbons. This work should be extended to include reactivated carbon. The mini-column adsorbers are of sufficiently small size that the carbon may be regenerated on a laboratory scale after breakthrough to pre-established limits, and its removal efficiency re-evaluated. The adsorption-regeneration cycle may be repeated as many times as it is necessary to simulate a "real" treatment situation. Such studies would yield additional valuable information regarding the adsorption efficiency and cost effectiveness of carbon for a variety of specific uses.

3. Because of the endemic characteristics and partial biodegradability of typical raw water background organic matter such as humic substances, coupled with the usual qualitative and quantitative seasonal variations therein, mini-column studies of the type described above should be of sufficient duration--usually several months--to ensure that all major anticipated influent variables for a particular application are properly accounted for in the assessment of treatment efficiency and cost effectiveness.

4. Because the application of strictly physicochemical predictive models to waters with a large fraction of biodegradable compounds is not rigorous, further work should be done on adaptation of such models to incorporate biological dynamics, in a manner similar to that suggested by Ying and Weber (1978) for waste treatment applications.

5. High pressure mini-column techniques, similar to that described by Rosene et al (1980) for chloroform and benzene, should be evaluated as potential replacements for the standard adsorption isotherm test for determination of the adsorption capacities and isotherm parameters for trace quantities of compounds with extremely low solubility, such as PCB's and dieldrin. The rapidity of such tests might well provide the advantage of ensuring isolation of adsorptive effects from biological degradation effects.

6. Further testing and development work relating specifically to water treatment conditions should be done on the recently developed micro-column procedure of Weber and Liu (1980). This technique has already been demonstrated, under waste treatment conditions, to yield more accurate and reliable estimates for both the film transfer coefficient, k_f, and intraparticle diffusion coefficient, D_s, used in modeling predictions.

TYPING GUIDE SHEET

SECTION 4

ACTIVATED CARBON ADSORPTION

BASIC PROPERTIES AND CHARACTERISTICS

Activated carbon is a generic term for a rather broad family of amorphous carbonaceous materials so prepared as to exhibit a high degree of porosity and an extensive associated surface area. The effectiveness of activated carbon for removal of a wide spectrum of organic compounds from waters and wastewaters is attributable to its dual properties of large specific surface area and its high degree of surface activity (Weber and van Vliet, 1980).

Surface areas usually range between 450 and 1500 m^2/g and are normally determined by measuring the amount of nitrogen gas adsorbed at liquid nitrogen temperature (-196°C). The monolayer surface coverage can then be calculated using the Brunauer, Emmett, Teller (BET) equation (Weber, 1972). The actual area available for adsorption of a specific compound from water, however, can be considerably less than the total surface area determined by adsorption of nitrogen gas. Further, total surface area is not by itself a satisfactory measure of available surface. Rather, it is the distribution of surface area as a function of pore size which is important.

A variety of substances have been found to be suitable raw materials for production of activated carbon, including: coal, wood, lignite, lime, sawdust, pulp, peat, oil shale, anthracite coal, lignin, and sugar (Hassler, 1963; Mattson and Mark, 1971). The manufacturing process involves formation of a char from the raw material by heating and driving off volatile fractions. Carbonization is then accomplished by elevating the temperature to as high as 600°C (Hassler, 1963). The carbonaceous char thus produced is generally activated under controlled conditions in the presence of oxidizing gases (such as carbon dioxide, steam, and air), resulting in the development of: 1) macropores with effective radii of 5,000 - 20,000 Å (angstroms); 2) transitional pores with effective radii of 40-200 Å, and; 3) micropores with effective radii of 10-30 Å (Dubinin et al, 1964). A typical scanning electron micrograph of an activated carbon illustrating the macropores is presented in Figure 1.

BEGIN
FIRST
TYPING GUIDE SHEET
CENTER
TOP OF

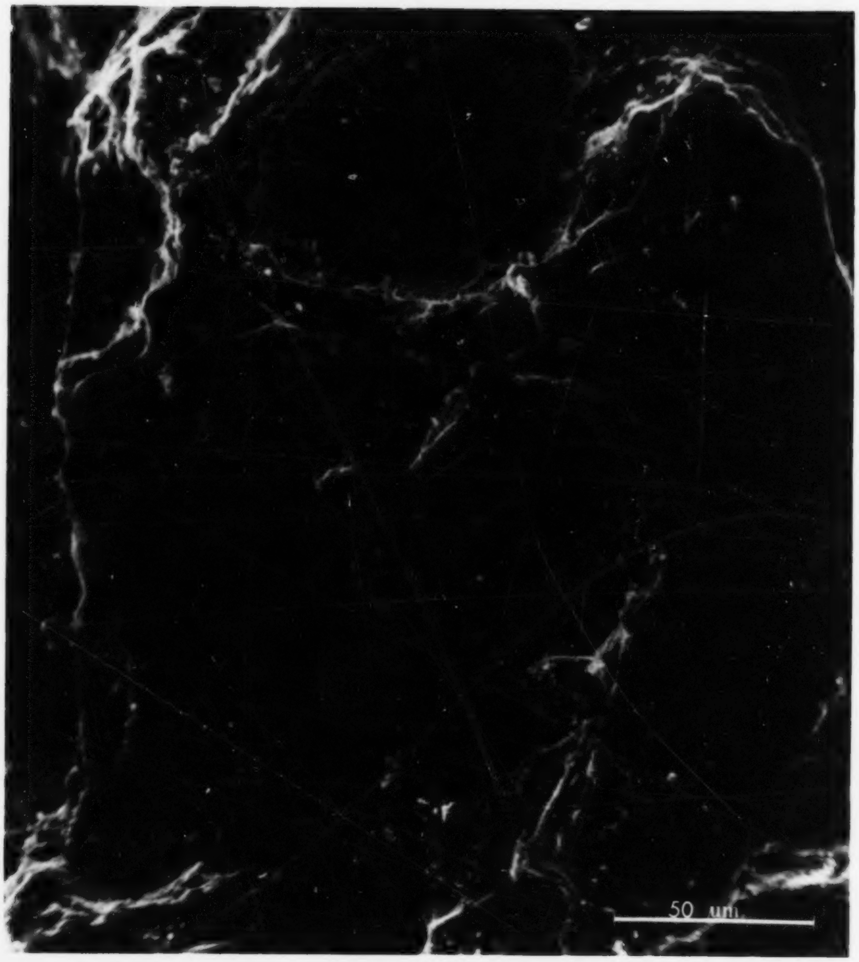

Figure 1. A typical scanning electron micrograph of granular activated carbon.

Reproduced from best available copy.

The structure of activated carbon consists of microcrystallite layers stacked parallel to each other in packets of 3 to 30 layers about 10 to 100 Å thick. These layers are held together by relatively weak van der Waals forces with an interlayer spacing of 3.6 Å. Each microcrystallite layer is comprised of an infinite number of layers of fused hexagonal rings; this structure is analogous to a very large polynuclear aromatic molecule with each carbon atom joined by σ bonds to three neighboring carbon atoms (Coughlin and Ezra, 1968).

Macropores are formed by the burnout of hydrocarbon radicals attached to the carbon atom on the edge of the microcrystallite plane, whereas micropores are formed mainly by burnout of microcrystallite planes (Wolff, 1958). Because the majority of the internal surface area is attributed to micropore walls, the larger percentage of the total surface area is likely to be of the microcrystallite plane type.

The microcrystallite surfaces are relatively uniform in nature; no attached functional groups are present because adjacent carbon atoms form covalent bonds with each other. Thus, adsorption occurring on this type of surface is predominantly due to van der Waals forces. However, the sides of the microcrystallite planes are more heterogeneous and contain carbon-oxygen functional groups that participate in electron sharing reactions and thus exhibit selectivity for adsorbing species (Zettlemoyer, 1959; Snoeyink and Weber, 1967). The most frequently-occurring functional groups include carboxyl; phenolic hydroxyl, and quinone-type carbonyl; groups with slightly less occurrence include fluorescein-like lactones, carboxylic acid anhydrides, and cyclic peroxides (Mattson and Mark, 1971).

As might be expected, many active carbons have high percentages of oxygen, hydrogen, and inorganic ash. Oxygen may constitute from 2 to 25% by weight of the carbon; the exact percentage depends upon the temperature and activation method. Hydrogen exists either in the form of terminal groups on the microcrystallite planes or as part of the hydrocarbon functional groups attached to these planes. Inorganic constituents are present both in the starting materials and in various inorganic salts that may be added to catalyze the carbonization and activation processes or to impart special sorptive properties to the active carbon (Wolff, 1958; 1959).

MECHANISMS AND DYNAMICS OF ADSORPTION

Nature and Types of Adsorption

The adsorption of organic compounds from water by activated carbon may result from solute hydrophobicity, or may be caused by a high affinity of the solute for the carbon. For most systems encountered in water treatment, adsorption results from a combination of these factors.

The solubility of a substance in water (i.e., the extent of chemical compatibility between the water and the solute) is highly significant in determining the intensity of adsorption. The more hydrophobic a substance is, the more likely it is to be adsorbed; conversely, a hydrophilic substance is less likely to be adsorbed (Weber, 1972).

In the context of solute affinity for the carbon, two major types of binding forces are commonly distinguished. The affinity may be predominantly due to either physical adsorption or chemisorption. Physical adsorption is a relatively weak adsorptive interaction resulting from the action of van der Waals forces. It is generally assumed that physical adsorption proceeds at a very rapid rate and is (completely) thermodynamically reversible. In contrast, chemisorption results from chemical interactions between the solute and solid surface and may or may not proceed rapidly. It has been proposed that some "chemisorption" reaction may involve a thermodynamically reversible step (Mattson and Mark, 1971).

Many adsorptions of organic substances by activated carbon result from specific interactions between functional groups on the sorbate and on the surface of the sorbent. These specific interactions may exhibit a large range of binding energies, from values commonly associated with physical adsorption to higher energies associated with chemisorption (Weber, 1974).

Factors Influencing Adsorption

A variety of parameters influence the kinetics and equilibrium level of adsorption of contaminants from water by activated carbon. The most significant parameters relative to the adsorbent were discussed above. Relative to the solute, contributing factors include polarity, molecular size, molecular structure, molecular weight, molecular stereochemistry, and concentration. Ionization potential, pH, and temperature can also markedly affect the adsorption characteristics of many organic compounds (Weber, 1972).

Competitive Adsorption

Organic compounds in water may interfere with the adsorption of one another, undergo mutual enhancement of adsorption, or act relatively independently. Adsorption column effluent concentration profiles for individual species in multi-component systems may differ markedly from those for single-solute solutions of the same species. This is partly due to adsorption site selectivity for a given component. Further, it has been postulated that kinetic interactions between solutes depend, to some extent, on relative effective diffusivities and, consequently, on respective sizes and configurations of adsorbate molecules (Weber, 1964).

Weber and Usinowicz (1973) demonstrated and discussed cases for binary mixtures (components A and B) that resulted in kinetically-induced chromatographic effects in fixed-bed adsorbers. They explained the effect in the following way: component A might be adsorbed more rapidly than component B, and therefore during initial periods of operation, component A is completely removed by a fraction of the bed while component B is adsorbed throughout a greater depth. After a period of operation, the fraction of the bed which is saturated with solute A may still adsorb B while the rest of the bed adsorbs both A and B. It is, of course, also possible that component B is not co-adsorbed and is instead replaced by A as the saturated front moves down the column. The intensity of the competitive effect of one adsorbate on another is a function of relative, as well as absolute, concentrations of the two, and of their relative energies of adsorption (Weber, 1964).

SELECTION OF ACTIVATED CARBONS FOR THIS STUDY

A number of different commercial activated carbons were investigated in the selection of a suitable carbon for this research. A brief summary of the basic properties of these carbons is given in Table 1.

Two of the most significant factors determining the suitability of a carbon for a particular application are its adsorptive performance in that application and its cost effectiveness (Weber, 1977). A dynamic test that gives some indication of adsorptive efficiency with respect to the organic substances in the water to be treated is useful in assessing performance characteristics. As far as the cost effectiveness characteristics is concerned, initial cost and resistance to attrition during air scour, backwash, and regeneration are important.

Completely-mixed batch (CMB) reactor isotherm and rate tests were conducted to obtain essential information regarding the relative effectiveness of each of the activated carbons. Each carbon was sieved using a set of United States Standard Sieves, and then selected size fractions were washed with deionized-distilled water (DDW) to remove leachable materials and carbon fines. The carbons were then dried to constant weight at 105°C for 12 hours and immediately dessicated. After reaching room temperature, the carbons were

TABLE 1. GENERAL PROPERTIES OF SELECTED COMMERCIAL ACTIVATED CARBONS

Carbon type	Raw material	Total surface area (N_2 - BET) m^2/g	Pore size distribution	Primary application
NORIT (American Norit Co.)	Peat	700 - 800	Large transitional pore structure	Water Treatment
FILTRASORB-400 (Calgon Corp.)	Bituminous Coal	1050 - 1200	Most of adsorption area available in pores between 6 and 100Å	Municipal and Industrial Wastewater Treatment
NUCHAR WV-G (Westvaco)	Bituminous Coal	1100	Broad spectrum of pore sizes with predominant volume in micro and transitional range	Water Treatment
HYDRODARCO-1030 (ICI United States)	Lignite	650	Mean pore radius of 29Å	Water Treatment

stored in airtight glass bottles.

Equilibrium and kinetic tests were conducted for four representative compounds, including: humic acids, representing a high molecular weight compound; carbon tetrachloride, a low molecular weight volatile chlorinated hydrocarbon; benzene, an aromatic hydrocarbon; and polychlorinated biphenyls (PCB's), hydrophobic chlorinated hydrocarbons with extremely low solubility. Methodologies for the isotherm and rate tests are discussed in ensuing sections.

Several theoretical and empirical equations, including the Freundlich, Langmuir and the three-parameter isotherms, were investigated for suitability for mathematical description and quantification of the adsorption equilibrium data. The Freudlich and three-parameter isotherms were found to provide the best description of the experimental data. The Freudlich equation was chosen because of its relative simplicity and common use.

Figures 2 through 5 demonstrate typical equilibrium adsorption data and associated Freudlich isotherms for adsorption of selected compounds on the several carbons tested. The Freundlich isotherm parameters are tabulated in Table 2.

It may be observed that Filtrasorb 400 exhibits the highest capacities for humic acids, carbon tetrachloride and benzene and an intermediate capacity for PCB's (Aroclor 1016) relative to the other three carbons.

CMB reactor rate data for adsorption of the test compounds on the commercial activated carbons are presented in Figures 6 through 9. Rates of adsorption of organic solutes from dilute aqueous solutions by activated carbon in CMB reactors are frequently controlled by intraparticle transport of solute in the pores and capillaries of the adsorbent (Weber and Morris, 1963 and 1964; Crittenden and Weber, 1978a, b, and c). For systems in which intraparticle transport is the rate limiting step, data for uptake of solutes from solution by the adsorbent generally follows an initially linear relationship when plotted as a function of the square root of time (Crank, 1956). The rate data were plotted in this manner, and good linearization of the data for at least the initial part of the rate study was observed. A typical plot for humic acids is demonstrated in Figure 10. The slope of the least-squares regression line from such a plot is indicative of the overall relative rate of uptake, and can function as an empirical "rate parameter" for comparison of the several carbons. Values for the rate parameters and correlation coefficients for the least-square regression fits to the rate data are tabulated in Table 3. The softer lignite and peat-base carbons

TABLE 2. FREUNDLICH PARAMETERS FOR ADSORPTION OF SELECTED ORGANIC COMPOUNDS ON DIFFERENT CARBONS*

Compound / Carbon	Humic Acids**			Carbon† Tetrachloride			Benzene†			Polychlorinated Biphenyls, PCB's (Aroclor 1016)		
	K_F	1/n	r††	K_F	1/n	r	K_F	1/n	r	K_F	1/n	r
Norit	12.44	0.437	0.980	0.16	0.75	0.994	0.73	0.61	0.972	13.72	0.27	0.866
Filtrasorb 400	13.42	0.42	0.931	0.23	0.74	0.987	1.12	0.39	0.983	6.65	0.36	0.872
Nuchar WV-G	6.85	0.617	0.976	0.22	0.69	0.984	1.07	0.48	0.969	15.41	0.25	0.912
Hudrodarco 1030	9.84	0.486	0.945	0.13	0.68	0.991	1.18	0.36	0.964	4.06	0.46	0.964

*Freundlich equation $q_e = K_F C_e^{1/n}$ (discussed in Chapter III)

**Calculated based on C_e in mg/l and q_e in mg/gm

† Calculated based on C_e in μg/l and q_e in mg/gm

††r= Correlation coefficient for fit of the isotherm to the experimental data

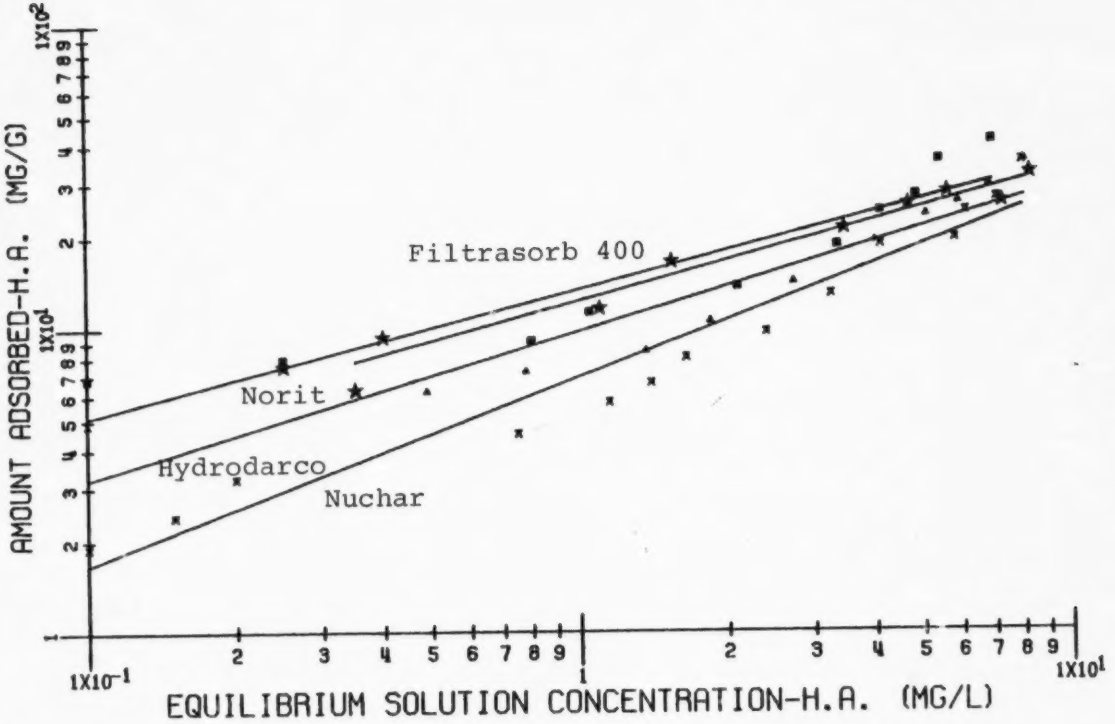

Figure 2. Adsorption isotherms for humic acids (C_o=8.95 mg/ℓ, 30/40 US sieve size carbon, buffered at pH 7).

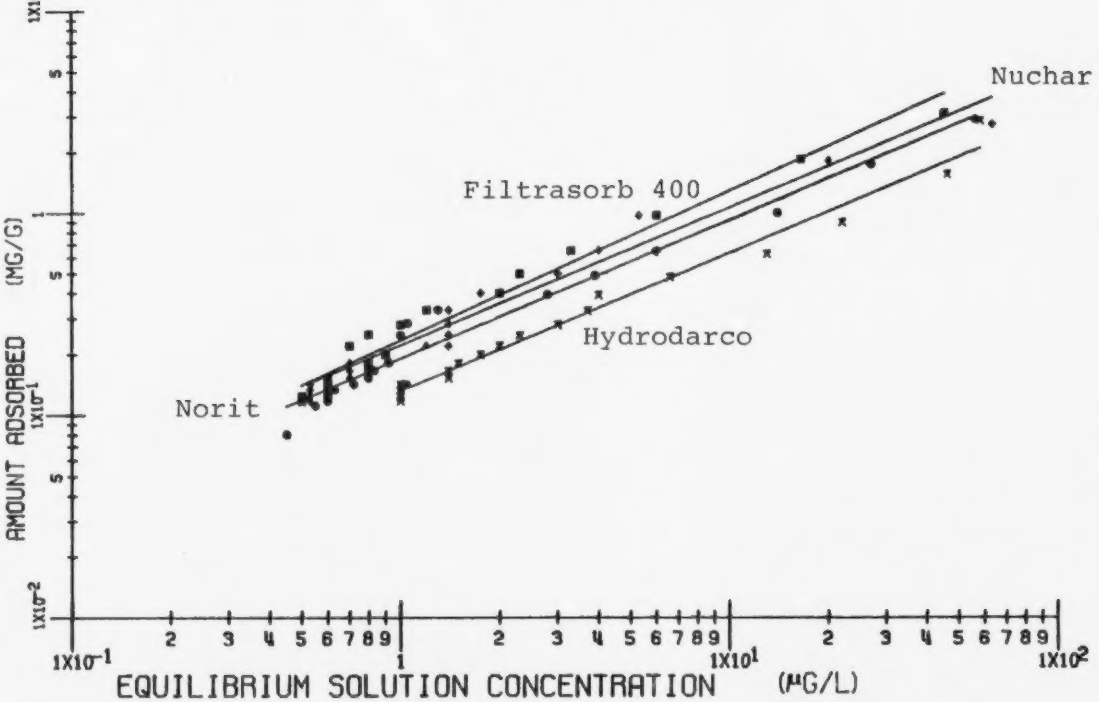

Figure 3. Adsorption isotherms for carbon tetrachloride (C_o=200 µg/ℓ, 30/40 US sieve size carbon, pH 7).

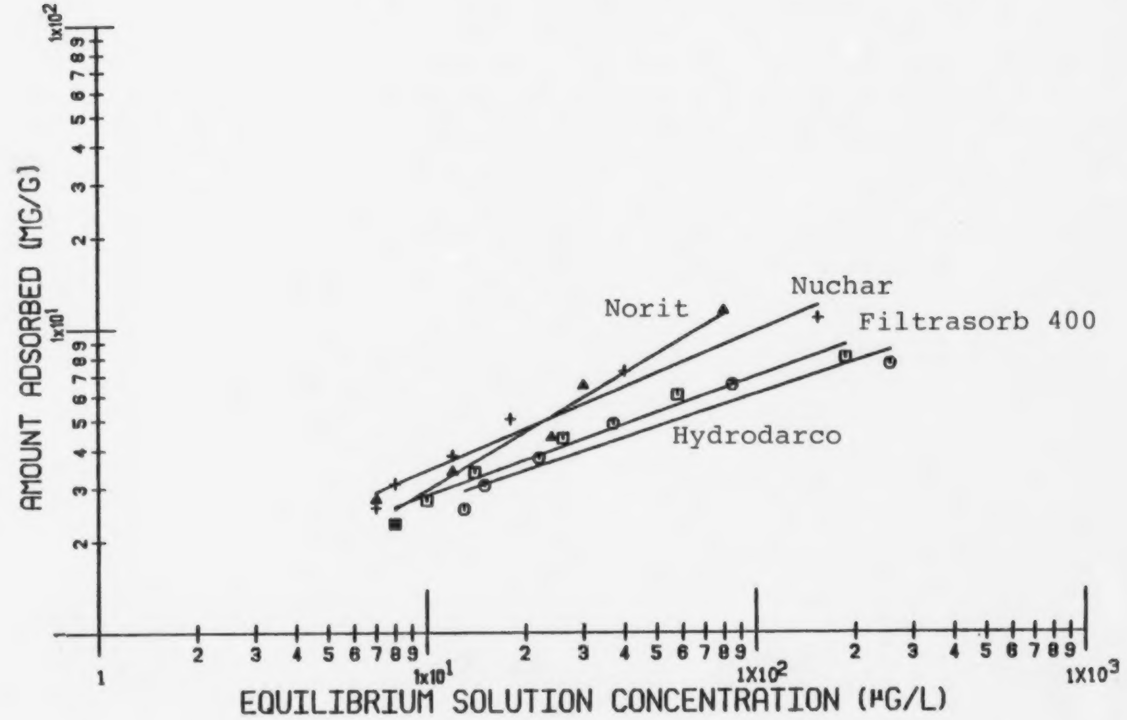

Figure 4. Adsorption isotherms for benzene (C_o=500 µg/ℓ, 50/60 US sieve size carbon, pH 7).

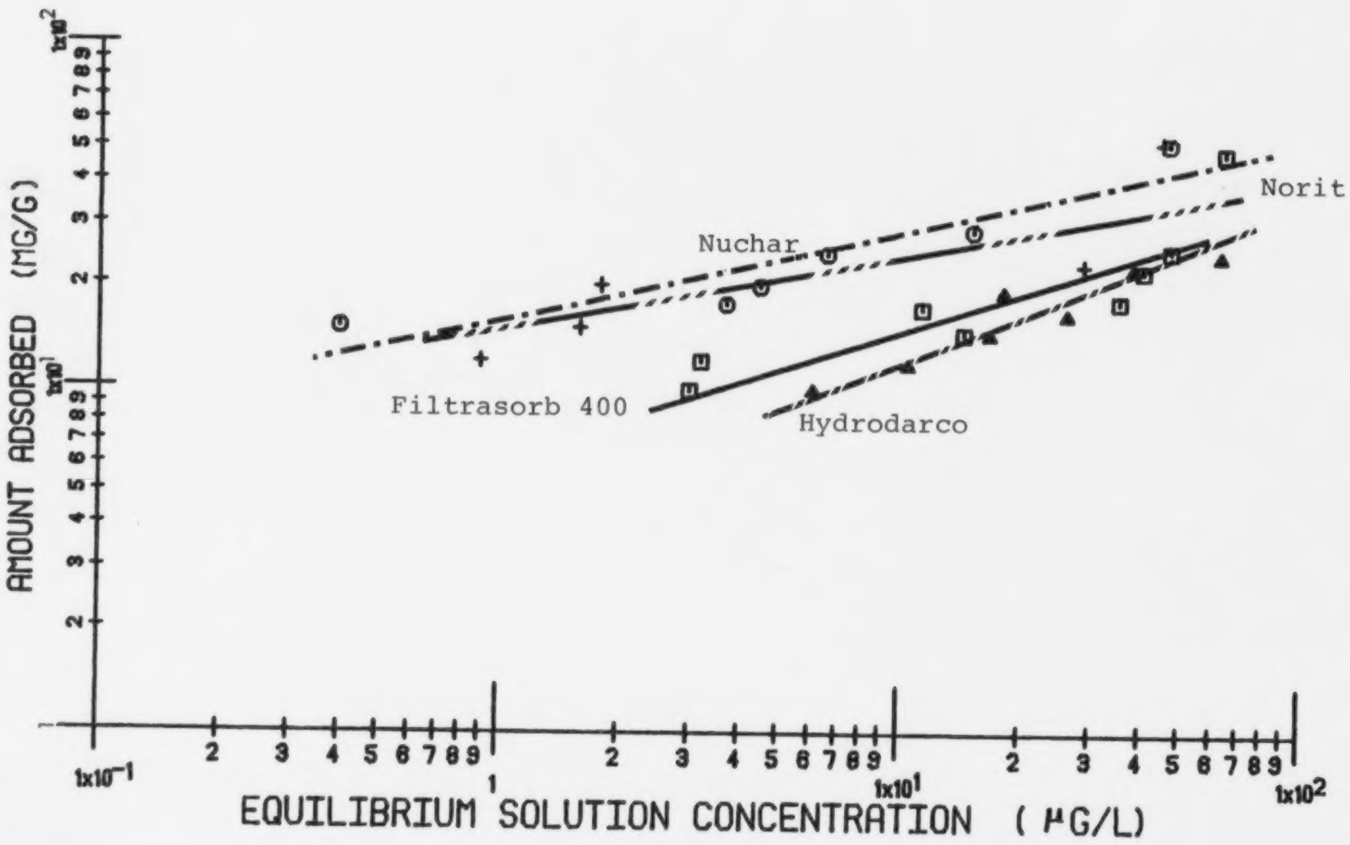

Figure 5. Adsorption isotherms for PCB's (Aroclor 1016) (C_o=100 μg/ℓ, 50/60 US sieve size carbon, pH 7).

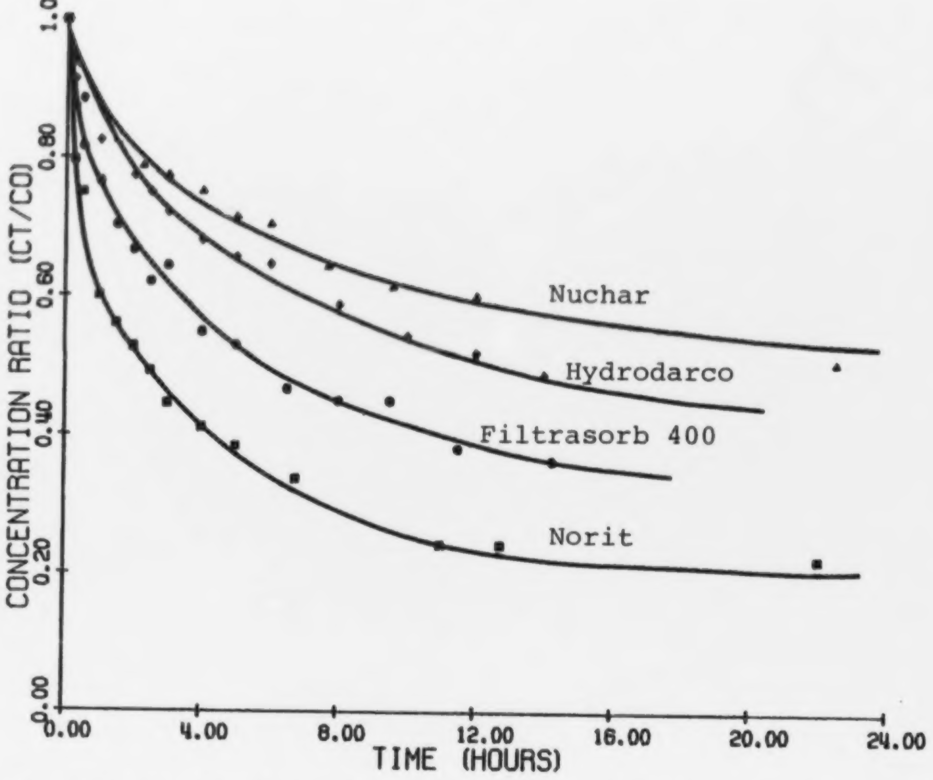

Figure 6. Rates of adsorption of humic acids in CMB reactors (C_o=5 mg/ℓ, 1.0 g/ℓ of 30/40 US sieve size carbon, buffered at pH 7).

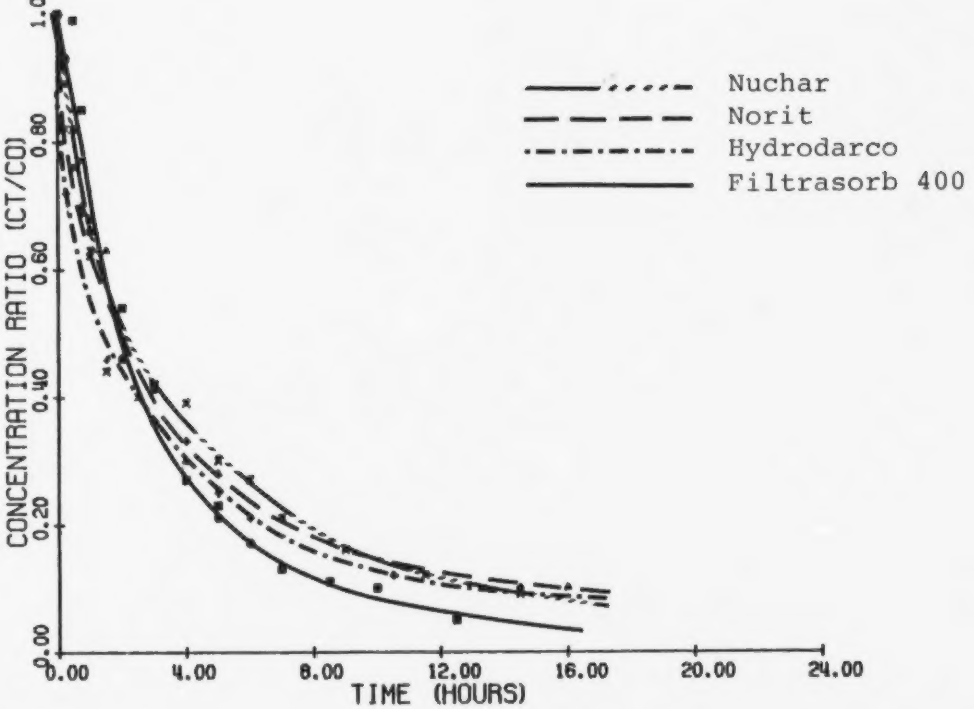

Figure 7. Rates of adsorption of CCl_4 in CMB reactors (C_O=200 µg/ℓ, 0.38 g/ℓ of 16/20 US sieve size carbon, pH 7).

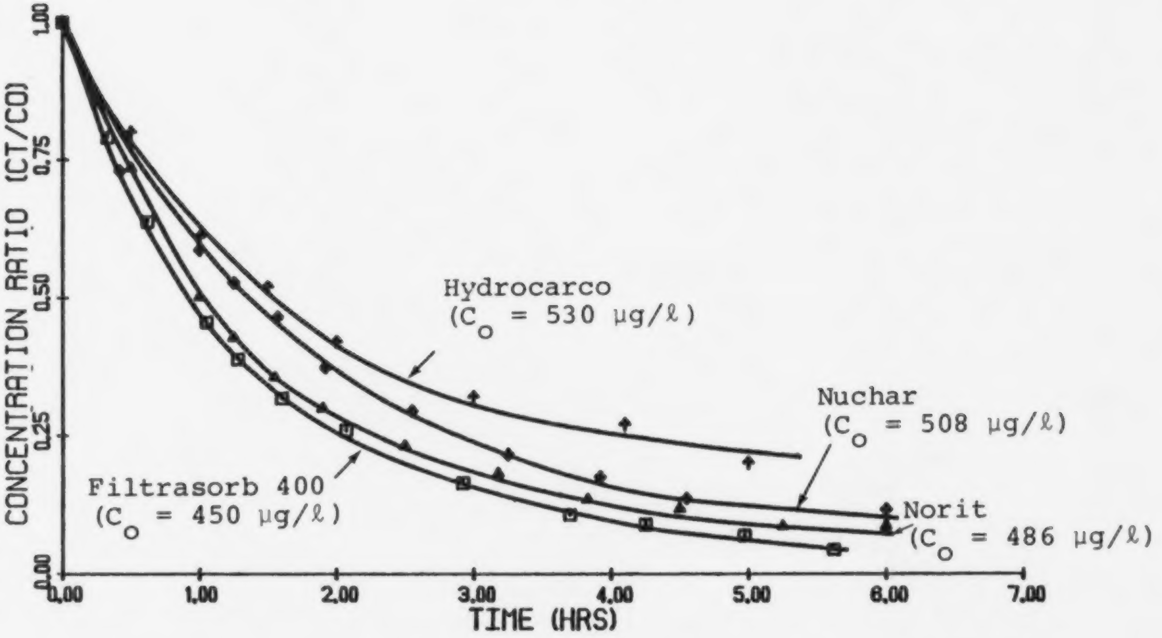

Figure 8. Rates of adsorption of benzene in CMB reactors (0.38 g/ℓ of 16/20 US sieve size carbon, pH 7).

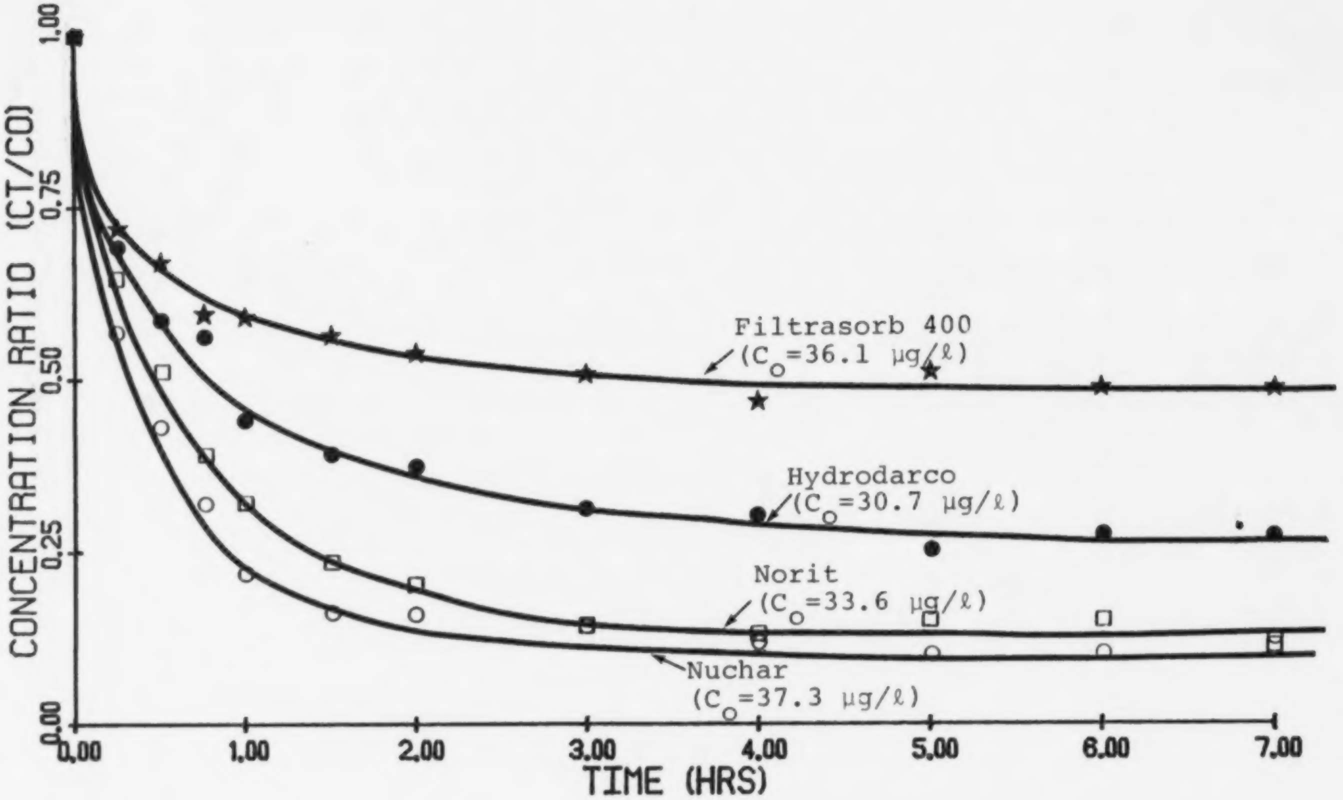

Figure 9. Rates of adsorption of PCB's (Aroclor 1016) in CMB reactors (0.38 g/ℓ of 30/40 US sieve size carbon, pH 7).

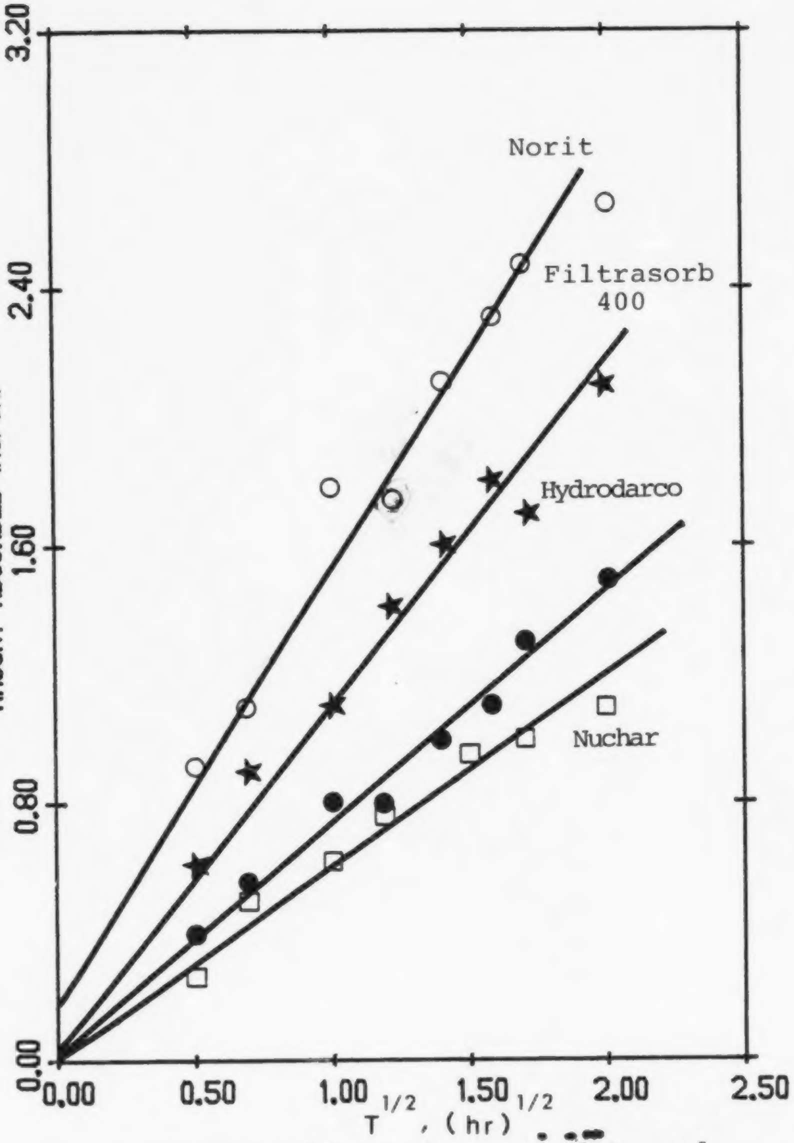

Figure 10. Adsorption rate data and least squares fits of initial rate data (4 hours) for humic acid.

TABLE 3. RATE PARAMETERS FOR ADSORPTION OF SELECTED ORGANIC COMPOUNDS ON DIFFERENT CARBONS

Compound / Carbon	Humic Acids		Carbon Tetrachloride		Benzene		PCB's (Aroclor 1016)	
	k*	r**	k	r	k	r	k	r
Norit	1.18	0.981	0.19	0.927	0.84	0.992	0.052	0.984
Filtrasorb 400	0.99	0.987	0.24	0.982	0.75	0.991	0.027	0.932
Nuchar WV- G	0.56	0.482	0.21	0.945	0.68	0.995	0.057	0.992
Hydrocarco 1030	0.71	0.994	0.22	0.966	0.74	0.996	0.034	0.981

*k= Rate Parameter = $q/t^{0.5}$; $(mg/gm)/(hr)^{0.5}$

**r = Correlation coefficient for fit of the rate parameter to the experimental data

(Hydrodarco 1030 and Norit, respectively), tend to degrade in particle size during mixing in the CMB reactor, and, the resulting decreased particle sizes tend to exhibit higher apparent rates of adsorption than the original particle size.

Repetitive air scour tests were run to evaluate the capability of each carbon to function in routine use without excessive attrition. This is essential for both packed- and expanded-bed adsorption applications to avoid carbon loss, high head loss due to reduction of particle size, effluent deterioration and increased disinfectant demand due to carry-over of carbon fines. As a result of these tests, the generally higher capacities and adsorption rates of the Filtrasorb 400 activated carbon, coupled with the superior attrition resistance of the bituminous carbons, led to the selection of Filtrasorb 400 for the remainder of the studies. The physical properties of Filtrasorb 400 is presented in Appendix A.

TYPING GUIDE SHEET

SECTION 5

PREDICTIVE MODELING OF ADSORBER SYSTEMS

GENERAL

The manner of achieving the most effective contact between a carbon and a water to be treated is of particular significance for large-scale activated carbon adsorption operations. Weber and Morris (1963) suggested that the optimum use of granular activated carbon for water treatment is achieved by column-type or fixed-bed operations. Packed-bed adsorbers are conventionally used in water treatment applications. However, upflow-expanded fixed-beds have been demonstrated to have advantages over packed-bed adsorbers for certain applications (Weber, 1972).

Successful design of a fixed-bed activated carbon adsorption process requires reliable prediction of concentration-time profiles for the effluent. If such a prediction can be made on the basis of easily-determined laboratory experiments, pilot-plant scale studies can be minimized and considerable savings in time and money realized.

Different conceptual models with various degrees of sophistication have been developed to predict breakthrough profiles for adsorber systems. For simplicity of analytic solution, many of these models deal with description of only single component systems, relatively simple rate expressions such as first or second order rate equations, and/or linear or irreversible isotherm models to describe equilibrium conditions. Keinath and Weber (1968) developed a predictive model which successfully describes breakthrough curves for some single component systems. Weber and Usinowicz (1973) applied this model for description of breakthrough profiles for mixtures of components treated in terms of a single lumped-parameter concentration term, i.e., TOC (Total Organic Carbon). The model could reliably predict the first 50-75% of the breakthrough profile.

To overcome the shortcomings of these earlier models, Weber and Crittenden (1975, 1978a, 1978b, 1978c) developed a numeric based model (MADAM: Michigan Adsorption Design and Application Model) which permits inclusion of multicomponent

EPA-287 (Cin.)
(4-76)

TYPING GUIDE SHEET
BEGIN FIRST LINE OF TEXT HERE
CENTER OF PAGE
TOP OF IMAGE AREA
DROPPED HEAD BEGIN SECTIONS HERE

interactions, biological activity, solid mixing, dispersion, and milticomponent equilibrium hysteresis.

The model incorporates algorithms for coupled mass transfer resistances and for non-linear adsorption equilibria. In addition to reactor configuration evaluations, this modeling technique is based on information obtained from two basic sets of "parameter determination" experiments to develop equilibrium data for characterization of the adsorption isotherm and rate data for characterization of the mass transfer resistances. Evaluation of most of these parameters can be performed by measurements in flow-through column-type systems. Nonetheless, due to the elaborate nature of such tests, it is more advantageous to evaluate these parameters in simple agitated non-flow systems (Keinath and Weber, 1968), or CMB reactors.

It is essential to be able to generate concentration-time profiles associated with column operations for successful predictions and simulations. In this research, attempts were made to generate such concentration history profiles for each compound of interest individually and for combinations of each trace organic with humic acids, and to then experimentally verify the model predictions and simulations.

ADSORPTION EQUILIBRIUM CONSIDERATIONS

The adsorption isotherm is useful for representing the capacity of an activated carbon for adsorbing organics from water, and for describing the functional dependence of capacity on solute concentration (Weber, 1972).

Several theoretical and empirical equations are available to describe the functional character of adsorption equilibria. The Langmuir and Freundlich equations are two nonlinear isotherms that have been widely and successfully used to represent equilibrium data over relatively narrow ranges of solute concentration. These two equations provide means for mathematical description of experimentally observed dependencies of capacity, q_e, on solution concentration, C_e. The langmuir isotherm has the form:

$$q_e = QbC_e/(1+bC_e) \qquad (1)$$

where Q is the ultimate adsorption capacity and b is related to the energy of adsorption (Weber, 1972).

The Freundlich equation has the form:

$$q_e = K_F C_e^{1/n} \qquad (2)$$

BOTTOM OF IMAGE AREA OUTSIDE DIMENSION FOR TABLES AND ILLUSTRATIONS
BEGIN LAST LINE OF TEXT
3/8"
PAGE NUMBER
EPA-287 (Cin.)
(4-76)

where K_f and $1/n$ are empirical constants relating to adsorption capacity and intensity, respectively (Weber, 1972). To determine the adsorption isotherm parameters for a specific system, Equations 1 and 2 are linearized and fit to experimental data. A plot of $1/q_e$ vs. $1/C_e$ for the linearized form of the Langmuir equation yields a straight line with a slope of $1/bQ$ and an intercept of $1/Q$. Similarly, a plot of log q_e vs. log C_e for the Freundlich equation yields a straight line with slope $1/n$ and an intercept of log K_F. The Freundlich isotherm generally agrees well with the Langmuir equation over moderate ranges of concentration.

The applicability of the Langmuir and the Freundlich isotherms has thus far been demonstrated for only a limited concentration range (Crittenden, 1976). An empirical three-parameter equation that can describe equilibrium behavior over a wider concentration range has been proposed by Radke and Prausnitz (1972). This equation has the form:

$$q_e = AC_e/1+BC_e^{\beta} \qquad (3)$$

where A, B, and β are empirical constants. If BC_e is significantly greater than 1, Equation 3 reduces to the Freundlich equation. When β is equal to 1, Equation 3 becomes the Langmuir isotherm. The three-parameter equation cannot be linearized, and the corresponding isotherm constants must be estimated by a least-square analysis of the experimental data. A computer program (Appendix B) has been developed by Mathews (1975) for estimation of the isotherm parameters by the best statistical representation of the experimental data.

ADSORPTION RATE CONSIDERATIONS

CMB Reactors

Overall rates of adsorption of organic compounds from aqueous solution by porous activated carbon are governed essentially by three consecutive transport stages: (1) diffusion of adsorbate to the external surface of the particle through the hydrodynamic boundary layer, (2) diffusion through the pore of the adsorbent or along the surface of the pore, (3) attainment of local equilibrium at the surface of the carbon particle (Weber and Morris, 1963). The third stage may be assumed to be rapid with respect to the first two stages, and its contribution to the overall adsorption rate thus neglected (Weber, 1972; Furusawa and Smith, 1973 and 1974).

Formulations involved in representing a single component adsorption process in a batch reactor are (Mathews and Weber, 1975, and 1977; Mathews, 1975):

1) Rate of mass transfer of solute through the hydrodynamic boundary layer:

$$dq/dt = [(k_f a_p 1000)/V_p \sigma_p](C-C_s) \qquad (4)$$

C and q are concentrations in the liquid and solid phases, respectively, and C_s is the liquid phase concentration near the particle's exterior surface. k_f is the mass transfer coefficient and a_p, V_p, σ_p are surface, volume and density respectively of the particle.

2) Variation of solid phase concentration along the radial dimension of a spherical particle:

$$\partial q_i/\partial t = D_s[(\partial^2 q_i/\partial r^2)+(2/r)(\partial q_i/\partial r)] \qquad (5)$$

q_i is the intraparticle solid phase concentration and D_s is the intraparticle surface diffusivity. r is the radial coordinate.

3) Average concentration over the volume of the particle:

$$q = (3/R^3)\int_0^R q_i r^2 dr \qquad (6)$$

4) Adsorption equilibrium at the surface of the particle based on the Freundlich isotherm:

$$q_s = K_f C_s^{1/n} \qquad (7)$$

C_s and q_s are equilibrium concentrations at the particle surface in the fluid and solid phases, respectively, and k_f and 1/n are isotherm constants.

5) Material balance for the solute in the batch reactor:

$$V(dc/dt) = -W(dq/dt) \qquad (8)$$

V is the volume of fluid in the reactor and W is the total amount of carbon.

6) The initial and boundary conditions are:

$$q_i(r,0) = 0 \qquad (9)$$

$$q(0) = C_s(0) = 0 \qquad (10)$$

$$C(0) = C_o \qquad (11)$$

$$q_i(R,t) = q_s(t) \qquad (12)$$

$$\partial q_i/\partial t \;|_{r=0} = 0 \qquad (13)$$

The system of equations (4) to (13) must be solved numerically to obtain values for the mass transfer coefficient, k_f, and the surface diffusion coefficient, D_s, for a specific application. Mathews and Weber (1975) have developed a numerical solution using the implicit finite difference method of Crank-Nicholson (Appendix C).

In the technique described by Mathews and Weber (1975), a direct parameter search and estimation procedure, PRAXIS (NAAS: LIT), is used. PRAXIS is a minimization procedure that does not require computation of derivatives for variables over which the objective function is minimized, resulting in substantial savings in computation time. The objective function used in this program is the sum of the squares of percentage deviations between experimental and calculated data for liquid phase concentrations. The program searches for best values of the variables k_f and D_s within certain specified constraints given by initial estimates for these variables. To minimize the program search it is possible to estimate a close control value of k_f by conducting a separate CMB rate experiment in which a large amount of carbon is employed to nearly deplete the solute within the first few minutes of the experiment. The change in C with respect to time is related to the fluid-particle mass transfer coefficient by the equation (Furusawa and Smith, 1974):

$$dC/dt = -k_f S_s (C - C_s) \qquad (14)$$

S_s is the carbon particle exterior surface area per unit volume. The value of C_s can be approximated to zero as t approaches zero, the Equation 14 then takes the form:

$$[d(C/C_o)/dt] \;|_{t=0} = -k_f S_s \qquad (15)$$

The slope at t=0 of a plot C/C_o vs. t is equal to $-k_f S_s$. The value of S_s can be obtained from the following equation:

$$S_s = 6w/d_p \sigma_p (1-\varepsilon_p) \qquad (16)$$

w is the mass of the carbon particle per unit volume of particle-free solution and d_p and ε_p are the diameter and porosity of the carbon particle, respectively.

ADSORPTION COLUMNS OR BEDS

As noted previously, Weber and Crittenden (1975, 1978a, 1978b, 1978c) developed a numeric-based adsorption model MADAM, for predicting single solute and multi-component breakthrough curves for fixed-bed adsorbers. The following system of partial differential equations (PDE's), which constitute MADAM and describe the dynamic behavior of fixed-bed adsorber systems, were derived from material balance relationships for each solute in the liquid and solid phases, respectively:

$$-D_d(\partial^2 C_i/\partial z^2)+v_z(\partial C_i/\partial x)+\gamma(\partial C_i/\partial t)+r_i = 0 \qquad (17)$$

$$r_i = \sigma_p(1-\gamma)(\partial q_i/\partial t) \qquad (18)$$

C_i is the concentration of species i and D_d is the dispersion coefficient. r_i is the solid-phase uptake rate for species i on a total volume basis of the adsorber and z is the longitudinal distance along the adsorber.

The generalized, dimensionless forms of these equations for a single solute using a two-step rate transport system are:

$$(1/N_{pe}\gamma)(\partial^2\bar{C}/\partial\bar{z}^2)+(\partial\bar{C}/\partial\bar{z})+(1/D_g)(\partial\bar{C}/\partial\bar{T})+3(\partial/\partial\bar{T})$$

$${}_0\int^1 \overline{q}\overline{r}^2 d\bar{r} = 0 \qquad (19)$$

$$(N_s/\bar{r}^2)(\partial/\partial\bar{r})[\bar{r}^2(\partial\bar{q}/\partial\bar{r})] = \partial\bar{q}/\partial\bar{T} \qquad (20)$$

$\bar{C}$ and $\bar{q}$ are the reduced liquid and solid phase concentrations. N_{pe} and D_g are the Peclet number and solute distribution parameter, respectively. $\bar{T}$ is the throughput parameter and N_s is the surface diffusion modulus. $\bar{r}$ and $\bar{z}$ are the reduced radial and longitudinal coordinates, respectively.

The final form of the system of equations with the approximate initial and boundary conditions (assumption of negligible dispersion) are:

$$(\partial\bar{C}/\partial\bar{z})+(1/D_g)(\partial\bar{C}/\partial\bar{T})+(\partial/\partial\bar{T})\,3\,{}_0\int^1 \overline{q}\overline{r}^2 d\bar{r} = 0 \qquad (21)$$

$$(N_s/\bar{r}^2)(\partial/\partial\bar{r})[\bar{r}^2(\partial q/\partial\bar{r})] = \partial\bar{q}/\partial\bar{T} \tag{22}$$

The boundary conditions are:

$$Sh(\bar{C}-\bar{C}_s) = \partial\bar{q}/\partial\bar{r}\,\big|_{\bar{r}=1} \tag{23}$$

$$St_m(\bar{C}-\bar{C}_s) = \partial/\partial\bar{T}\,\int_0^1 \bar{q}\bar{r}^2 d\bar{r} \tag{24}$$

$$(\partial\bar{q}/\partial\bar{r})\big|_{\bar{r}=0} = 0 \tag{25}$$

St_m is the modified Staton number and Sh is the Sherwood number based on the surface diffusion coefficient.

The initial conditions are:

$$\bar{q}(\bar{z},\ \bar{r},\ \bar{T} = 0) = 0 \tag{26}$$

$$\bar{C}_o(\bar{z},\ \bar{T} = 0) = 0 \tag{27}$$

Finally, the three-parameter isotherm describing the equilibrium adsorption behavior at the particle surface is:

$$\bar{q}_s = A\bar{C}_s/(1+B\bar{C}_s^{\beta}) \tag{28}$$

It is to be noted that both the three parameter equation and Freundlich equation describe equally well the experimental equilibrium data reported in this research. The three parameter isotherm, however, is used for the ease of extending an isotherm describing a single-component system to a multi-component system.

The MADAM model of Weber and Crittenden assumes: 1) dilute solution conditions prevail; 2) diffusion coefficients are not concentration-dependent; 3) longitudinal dispersion in the fixed-bed reactors is negligible; and 4) the adsorbent is in a fixed position in the reactor. To solve the associated liquid-phase and solid-phase material balance PDE's (Equations 21 and 22), the implicit finite backward difference method and the Crank-Nicholson numeric analyses were employed, respectively (Appendix D).

The numeric solution requires specification of equilibrium and kinetic coefficients. Equilibrium constants are determined from the best statistical representation of batch experimental data. The internal surface diffusion, D_s, is determined from the two-step resistance rate model described earlier. The fixed-bed mass transfer coefficients, k_f, which relates to the hydrodynamic characteristics of the fluid-particle system, can be obtained by choosing the most suitable correlation method amongst the available techniques, for example: 1) Williamson et al (1963); 2) Ergun, 1952; 3) Thoenes and Kramers, (1958); 4) Resnick and White, (1949); and Pieffer and Happel, (1964). Alternatively, the newly developed method of Weber and Liu (1980) can be employed to give more representative values for k_f.

Other parameters which might be specified to permit solution of the breakthrough equations include: the volumetric flow rate, Q; influent concentration, C_o; adsorber bed density, δ_p; bed porosity, γ; and the free liquid diffusivity, D_l. The necessary formulae and parameters for predictive model calibration and verification are tabulated in Table 4.

TABLE 4. FORMULAE FOR PREDICTIVE MODEL CALIBRATION AND VERIFICATION

$D_1 = 7.4 \times 10^{-8} [T(\chi M)^{1/2}/\mu V_o^{0.6}]$ (Wilke and Chang, 1955)

$V_s = Q/A_a$

$\gamma = (V-V_c)/V; \ V_c = W/(1000\sigma_p)$

$\delta_p = W/V = 1000\sigma_p(1-\gamma)$

$R_e = \sigma_1 d_p V_s/\mu$

$D_g = \delta_p q_o/C_o \gamma$

$q_o = AC_o/1+BC_o^{\beta}$

$S_c = \mu/\sigma_1 D_1$

$(k_f/V_s)(S_c^{0.58}) = 2.40R_{e'}^{-0.66}$ (Williamson *et al*, 1963)

$R_{e'} = R_e/\gamma$

$\chi = 2.6; \ M = 18 \text{ gm/mol}; \ \sigma_p = 0.68 \text{ gm/cm}^3;$

$\sigma_1 = 0.998 \text{ gm/cm}^3; \ \mu = 1.005 \times 10^{-2} \text{ gm/cm - sec}$

SECTION 6

ADSORPTION OF HUMIC ACIDS

GENERAL

Humic acids are operationally defined as the base-soluble fraction of humus (Schnitzer and Khan, 1972). They are distinguished from fulvic acids, which are soluble in both acid and base, and from humin, the non-extractable fraction of humus. The ambiguity of this definition reflects not only the amorphous nature of the substance, but also its indistinct formative processes and imprecise structure. Humic acid macromolecules are complex products of carbohydrates, protein decomposition substances, and aromatic compounds (Kononova, 1961). They may be formed in soils in a number of ways, including lignin degradation to polyphenols followed by complexation with amino acids, or as the products of different molds (Steelnik, 1963). Average molecular weights are estimated to be in the range of 20,000 to 50,000, but values as low as 1,000 and as high as 1,000,000 have been reported (Schnitzer and Khan, 1972; Kononova, 1961). Elemental composition ranges from 45% - 63% carbon, 3% - 6% hydrogen, 0.5% - 5% nitrogen, and 35% - 45% oxygen (Gjessing, 1976). Carboxyl, phenolic and aliphatic hydroxyl functional groups have been identified as components of the humic core. There is also evidence that a number of alkali metals are in some way connected to humic molecules. The following metal ion binding gradation has been suggested for soil humus (Gjessing 1976):

$$Fe^{2+} < Cu^{2+} < (UO_2)^{2+} < Fe^{3+} < V^{3+} < La^{3+} < Th^{3+} < Zn^{2+}$$

$$Ca^{2+} < Sr^{2+} < Ba^{2+} < Ra^{2+}$$

$$Li^{+} < Na^{+} < K^{+} < Rb^{+} < Cs^{+}$$

Considering the multitude of fragments, functional groups, and elements that are associated with humic acids, it is not surprising that a large number of different chemical structures have been proposed. One such structure is illustrated in Figure 11 to demonstrate the complexity of the diverse humic

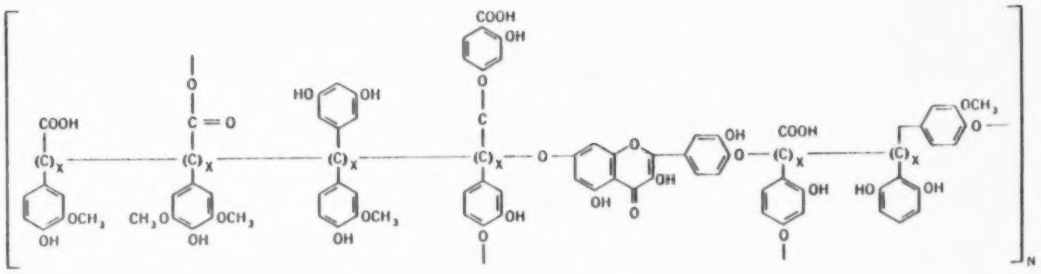
COOH
(C)x
OCH,
OH
O
C = O
CH,O
HO
OH
C
O
OH
N

Figure 11. Proposed structure of color macromolecule (after Christman and Ghassemi, 1966).

acid macromolecule (Christman and Ghassemi, 1966).

Several prospective haloform precursor groups are also believed to be structurally associated with humic acid macromolecules. Acetyl (Rook, 1974; Stevens et al, 1975), metadihydroxybenzene (Rook, 1974), and pyrolic and 1,3-dicarbonyl compounds (Morris and Baum, 1977) have been identified as likely precursor structures. Although a variety of possible pathways have been proposed, there is yet no general agreement on mechanisms for haloform production.

To provide a reasonably reproducible reference point and to ensure experimental consistence, Aldrich Chemical technical grade dried humic acid was used for the present study. Carbon, hydrogen, and nitrogen (CHN) analyses of this material, using a Hewlett-Packard CHN Analyzer Model 185B, indicated an average elemental composition of 45% carbon, 4.3% hydrogen, and 1% nitrogen, by weight (Appendix E). It should be noted that the natural variability of humic compounds imposes limits on the validity of quantitative extrapolation. Also, data obtained for one type of material may not be applicable to other systems. Nonetheless, observations made relative to a typical reference compound can be used for qualitatively interpreting the behavior of other humic substances, and for qualitatively comparing related investigations.

ANALYTICAL METHODS

There is no direct and specific analytical method for the determination of humic acids in water. Extraction and isolation procedures are tedious and lack the accuracy and precision required for the present investigations. Surrogate procedures which measure organic content include: biochemical oxygen demand (BOD), chemical oxygen demand (COD), total organic carbon (TOC), and ultraviolet spectrophotometry (UV). Limit of detection, sensitivity, reproducibility, and speed of analysis were primary considerations in the selection of an analytical technique for routine humic acid analysis in the present research.

Since humic acids are refractory compounds (Gjessing, 1976), BOD was ruled out as a method for quantitative analysis. Humic acids are also resistant to quantitative oxidation using standard COD techniques. Gjessing reported 85-95% oxidation with potassium dichromate using the standard COD procedure, and only 30-35% oxidation with permanganate under milder reaction conditions.

TOC is a proven and reliable means for measurement of the organic content of water. The suitability of this analysis for routine determination of humic acid concentrations was evaluated using two different but comparable instruments, the Oceanography International TOC Analyzer and the Beckman Model 915 TOC Analyzer. The ampule technique employed with the former provides a sufficiently low detection limit, but involves a relatively large sample volume and substantial effort and time for each analysis. Conversely, the direct injection technique employed with the Beckman 915 uses a small sample volume and is rapid and reproducible, but the detection limit is too high. Instrumentation with lower detection limits would likely have made TOC a satisfactory analysis, but these were not available for this study.

Ultraviolet spectrophotometry has been used for quantification of natural organic matter in water (Dobbs *et al*, 1972). To evaluate the suitability and sensitivity of this technique for routine analysis of humic acids in this work, spectra of humic acid solutions before and after treatment with activated carbon were generated using a Perkin Elmer 202 scanning spectrophotometer. These spectra, obtained in the absence of other organic materials which might interfere with UV analysis, are presented in Figure 12.

The degree of correlation between UV absorbance (250 nm wavelength) and TOC analysis was then determined by analyzing a series of humic acid standards by each of the two methods and comparing the data; the results are plotted in Figure 13. The trace of the data in Figure 13 indicates good linear correlation and the slope of 0.44 reasonably confirms the earlier determination of CHN analysis that approximately 45% of the humic acid is comprised of organic carbon.

The possibility of differential adsorption of ultraviolet irradiation of various humic acid fractions was viewed as a potential drawback of UV spectrophotometry. If activated carbon selectively adsorbs different humic acid fractions, analytic artifacts would then be a possible problem. To investigate this possibility, several aliquots of a solution of humic acids with an initial concentration of 60 mg/l were contacted with different amounts of activated carbon until equilibrium was obtained. Samples were then withdrawn and analyzed both for UV adsorption at 250 nm and for TOC. The relationship between these two sets of data was found to be linear, with a correlation coefficient of 0.98, suggesting no significant preferential adsorption of ultraviolet irradiation by different humic acid fractions.

Ultraviolet spectrophotometry at 250 nm was therefore adopted for routine quantitative analysis of humic acid concentrations. The method was rapid, reproducible, and provided a detection limit of approximately 0.1 mg/l using a 1-cm quartz cell. An Hitachi 181 spectrophotometer was employed.

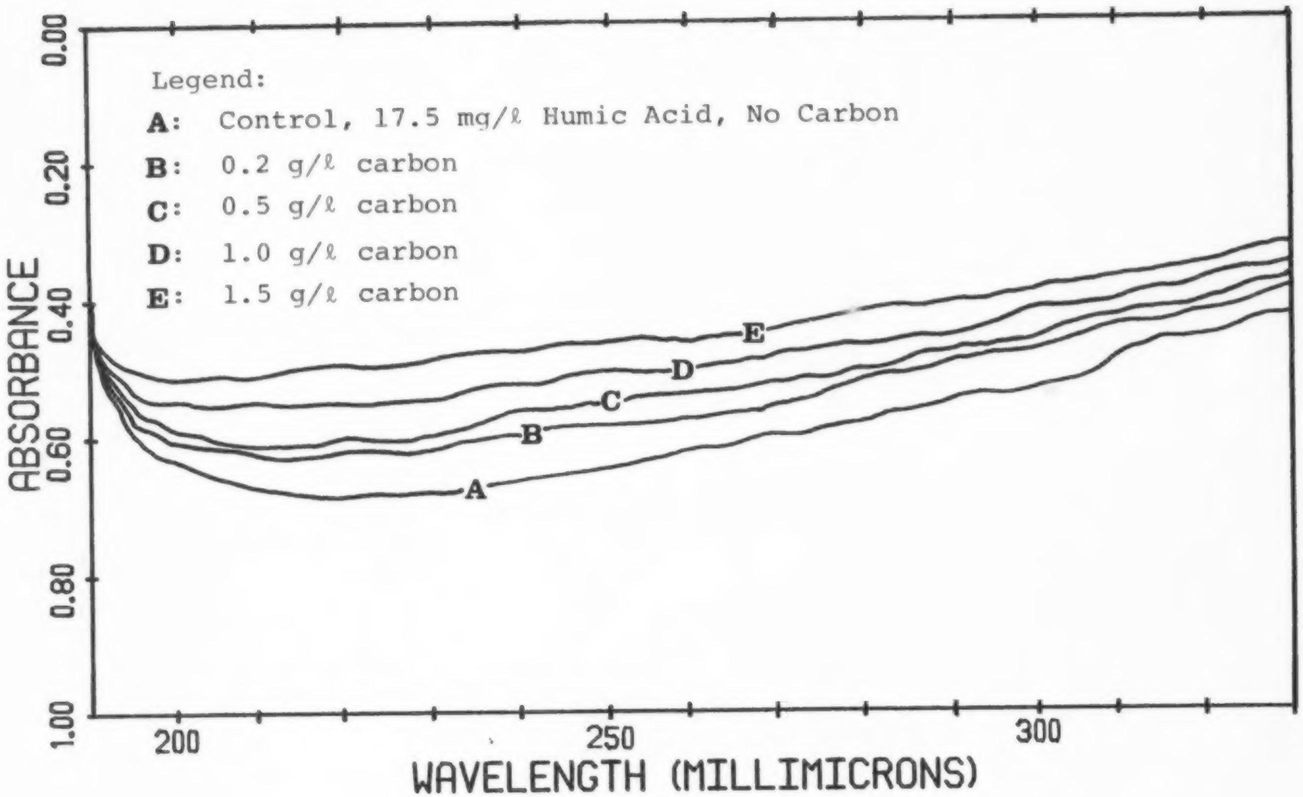

Figure 12. Ultraviolet absorption spectra for humic acids solutions brought to equilibrium with different amounts of granular activated carbon.

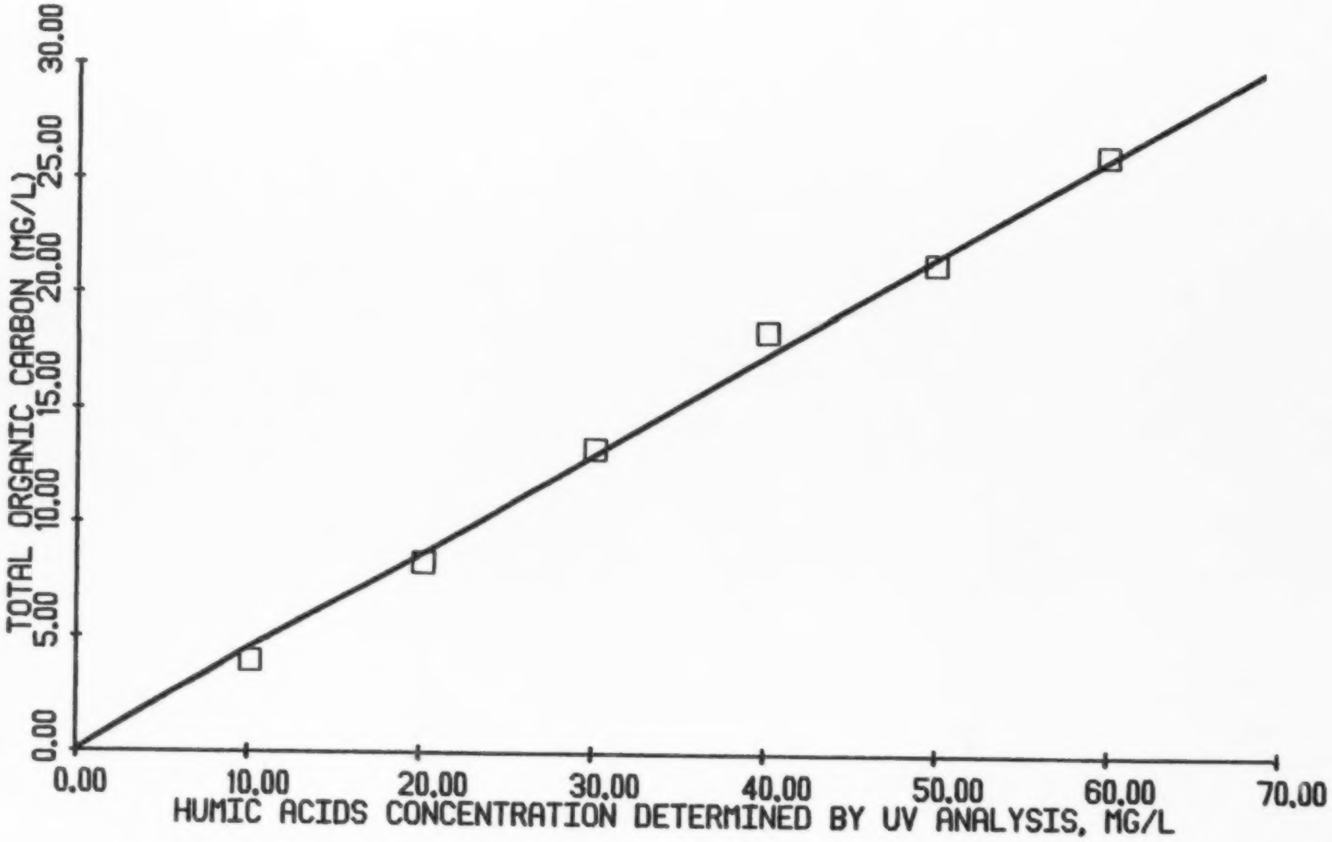

Figure 13. Correlation between TOC and UV absorption for humic acids analysis.

ADSORPTION EQUILIBRIUM STUDIES

Experimental Methodology

All humic acid solutions used in this research were prepared by adding appropriate amounts of humic acid to deionized-distilled water (DDW). The pH was adjusted to 11.0 by the addition of 1.0 N NaOH. The mixture was then agitated vigorously until no further dissolution was observed. The pH of the mixture was adjusted to 7± 0.2 with 1.0 N HCl and the solution was filtered through a 11.0 cm Reeve Angel glass fiber filter, using a ceramic Buchner funnel and a four-liter suction flask, to remove any colloidal and/or nonsoluble portions. The preparation of humic acids standards is discussed in Appendix F.

Adsorption equilibrium studies with humic acids were conducted using carefully weighed amount of sieved, washed, and dried granular carbon together with 100 ml aliquots of humic acid in 125-ml tightly sealed glass bottles fitted with polyethylene-lined plastic caps. The bottles were agitated until equilibrium between the liquid phase and the activated carbon was reached. Control samples containing no carbon were run with each experimental set to check losses due to biodegradation and/or glass adsorption.

The equilibrium concentraiton of the humic acids, C_e, was determined by comparing the amount of UV light absorbed at 250 nm by each sample with the amount of UV light absorbed by a standard humic acids solution. The amount of humic acids adsorbed on W grams of carbon for each bottle containing V liters of solution, was then calculated using the following equation:

$$q_e = (C_o - C_e)V/W$$

where $(C_o - C_e)$ indicates the decrease in concentration.

Isotherm Parameter Evaluation

Several theoretical and empirical equations, including the Freundlich, Langmuir, and three-parameter isotherms, were investigated for their mathematical description and quantification of the humic acid adsorption equilibrium data. The experimental data correlated best with the Freundlich and three-parameter isotherms. However, the Freundlich isotherm was found to be superior to the three-parameter model because of simpler and more efficient parameter estimation. Also, the Freundlich isotherm computation yields a unique set of parameters, making it advantageous for comparison and evaluation of the adsorption characteristics of different isotherms.

Results and Discussion

To investigate the effectiveness of activated carbon for adsorption of humic acids and to further evaluate associated adsorption characteristics under different conditions, a number of experimental equilibrium studies were performed. Because of the heterogeneous nature of humic acids, these investigations yielded several interesting results which require close consideration. A summary of the experimental system conditions and adsorption equilibrium parameters is tabulated in Table 5.

Figure 14 illustrates the effects of carbon particle size on equilibrium capacity for humic acids. A definite enhancement of capacity with decreased particle size was observed. This phenomenon may relate to the very large size of humic acid molecules relative to pore constrictions within the carbon particles, rendering certain internal areas of larger particles unavailable to these molecules. It may also relate to higher activities of the smaller particles resulting either from the activation process or from selective fractionation of the carbon during the sizing process.

Figure 15 demonstrates the adsorption of different fractions of commercial humic acids (the fractionation procedure is discussed in Appendix G). It was noted that the extent of adsorption of humic acids is larger than that of the fulvic acids. This may partly be due to the lower solubility of the former.

Figure 16 illustrates the effects of pH on adsorption equilibrium of humic acids. It may be observed that the amount of humic acids adsorbed generally increases at lower pH; the intensity of adsorption however, is slightly lowered. It may be postulated that at a lower pH the molecules are more completely protonated and are thus less negatively charged, resulting in the adsorption of a larger fraction of humic acids.

Figure 17 shows the dependence of extent of adsorption on the initial concentration of humic acids. It may be observed that lower initial concentrations yield higher capacities; however, the intensities are relatively similar. This dependence may be of significance in estimating the fraction of available active surface that can be considered useful over a practical concentration range.

Figure 18 compares the equilibrium data for adsorption of humic acids on "sieved" and "crushed and sieved" carbons. The former carbon was sieved to size (30/40 mesh) from the commercial batch. The latter carbon was crushed and then sieved to size (30/40 mesh) from a previously sieved larger

TABLE 5. SUMMARY OF ADSORPTION EQUILIBRIUM STUDIES FOR HUMIC ACIDS*

Figure No.	Background Solution	Carbon Size, US Standard Mesh Size	Initial Concentration C_o, (mg/l)	Buffer, KH_2PO_4	Freundlich Isotherm Constants† K_f	1/n	r††	Remarks
14	DDW	200/325	3.15	-	19.312	1.286	0.886	particle size effect
14	DDW	80/100	3.15	-	9.429	0.848	0.957	
14	DDW	35/50	3.15	-	7.274	0.843	0.938	
15	DDW	30/35	5.98	-	9.431	0.639	0.978	humic acid frac.
15	DDW	30/35	7.1	-	1.808	2.002	0.795	fulvic acid frac.
16	DDW (pH 8.5)	30/40	8.89	5×10^{-3} M	10.330	0.448	0.955	pH effect
16	DDW (pH 7)	30/40	8.95	5×10^{-3} M	13.408	0.420	0.932	
16	DDW (pH 5)	30/40	7.39	5×10^{-3} M	14.488	0.332	0.941	
17	DDW	16/20	1.64	5×10^{-3} M	6.507	0.523	0.963	initial concentration effect
17	DDW	16/20	4.21	5×10^{-3} M	6.020	0.495	0.962	
17	DDW	16/20	8.84	5×10^{-3} M	4.726	0.604	0.955	
18	DDW	30/35	5.0	-	7.970	0.734	0.866	"sieved" carbon
18	DDW	30/35	5.0	-	5.089	0.687	0.993	"crushed and sieved" carbon
19 & 20	DDW	16/20	4.82	-	1.213	1.019	0.910	background solution effect
19	Tap water	16/20	4.68	-	6.543	1.593	0.993	
20	DDW + 10 mg/l Ca^{2+}	16/20	3.75	-	3.123	0.411	0.655	inorganic species effect
20	DDW + 10 mg/l Mg^{2+}	16/20	4.02	-	5.125	0.774	0.940	
20	DDW + 3.5 mg/l OCl^{-1}	16/20	4.69	-	1.420	1.579	0.890	
20	DDW + 0.05 mg/l Fe^{3+}	16/20	4.75	-	1.110	1.054	0.814	

*All studies were conducted at pH 7 unless otherwise noted

†Based on C_e and q_e expressed in mg/l and mg/gm, respectively

††r = correlation coefficient for fit of the isotherm to the experimental data

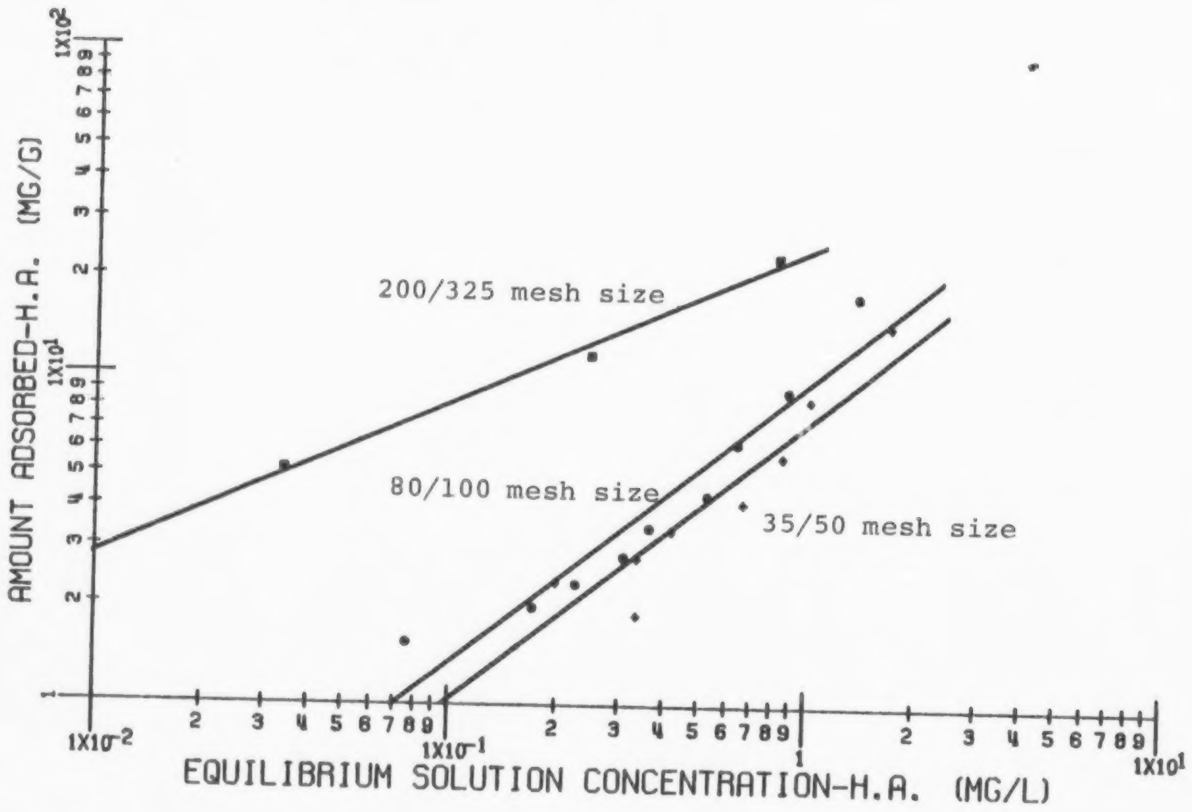

Figure 14. Adsorption isotherms for humic acids; effect of carbon particle size on adsorption capacity.

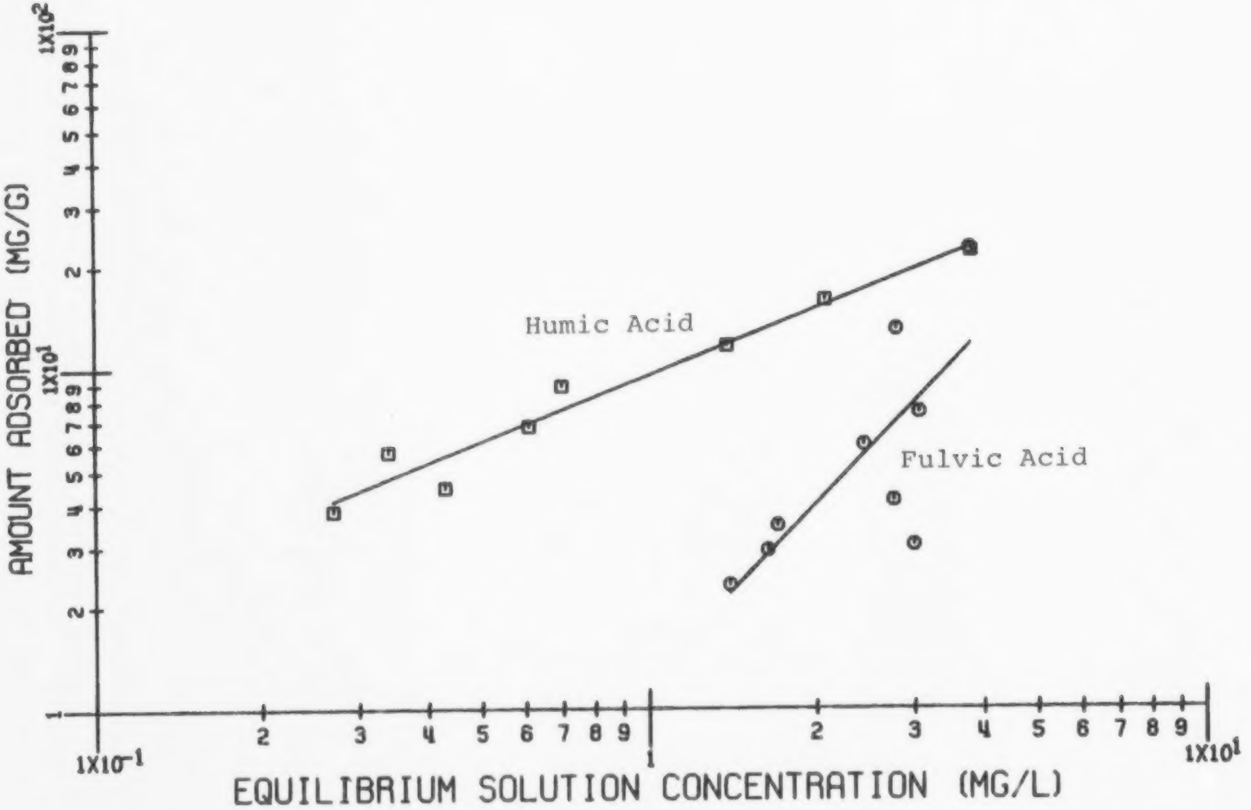

Figure 15. Adsorption isotherms for humic acid and fulvic acid fractions of "humic acids".

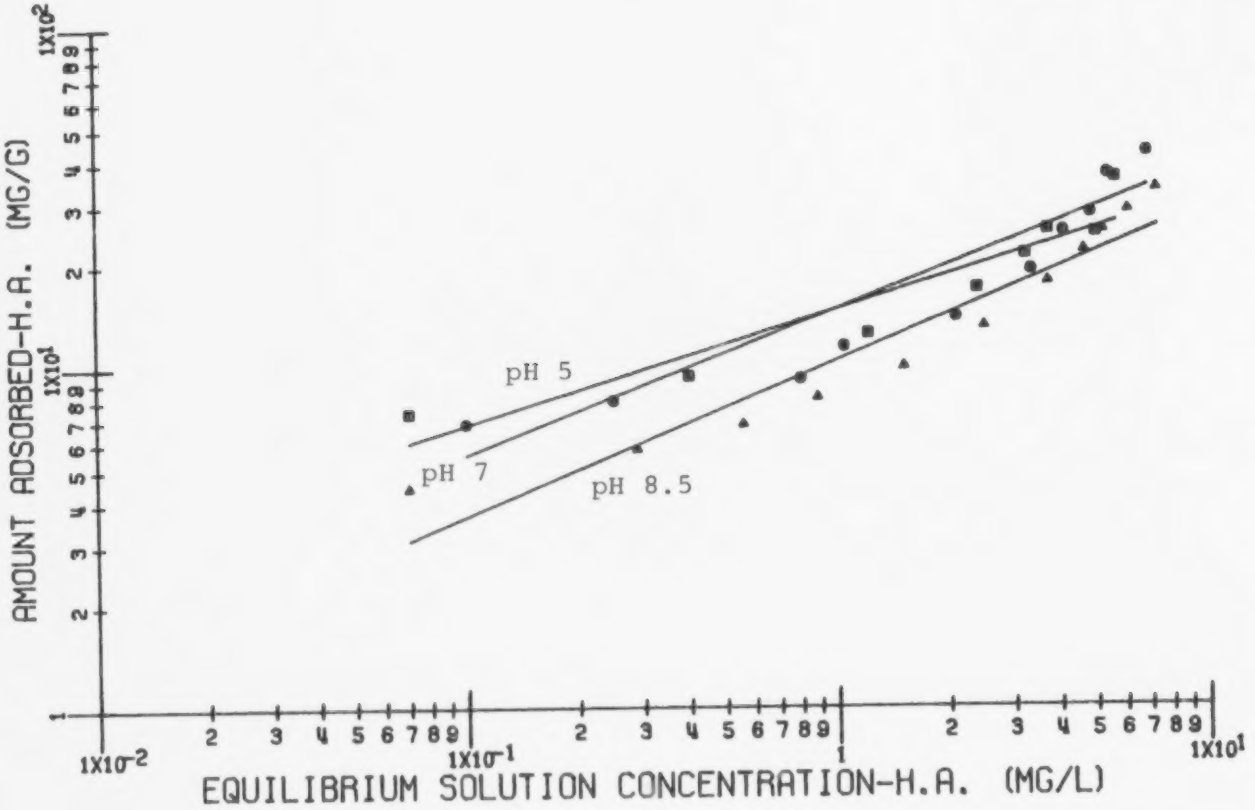

Figure 16. Adsorption isotherms for humic acids; effect of pH on adsorption capacity.

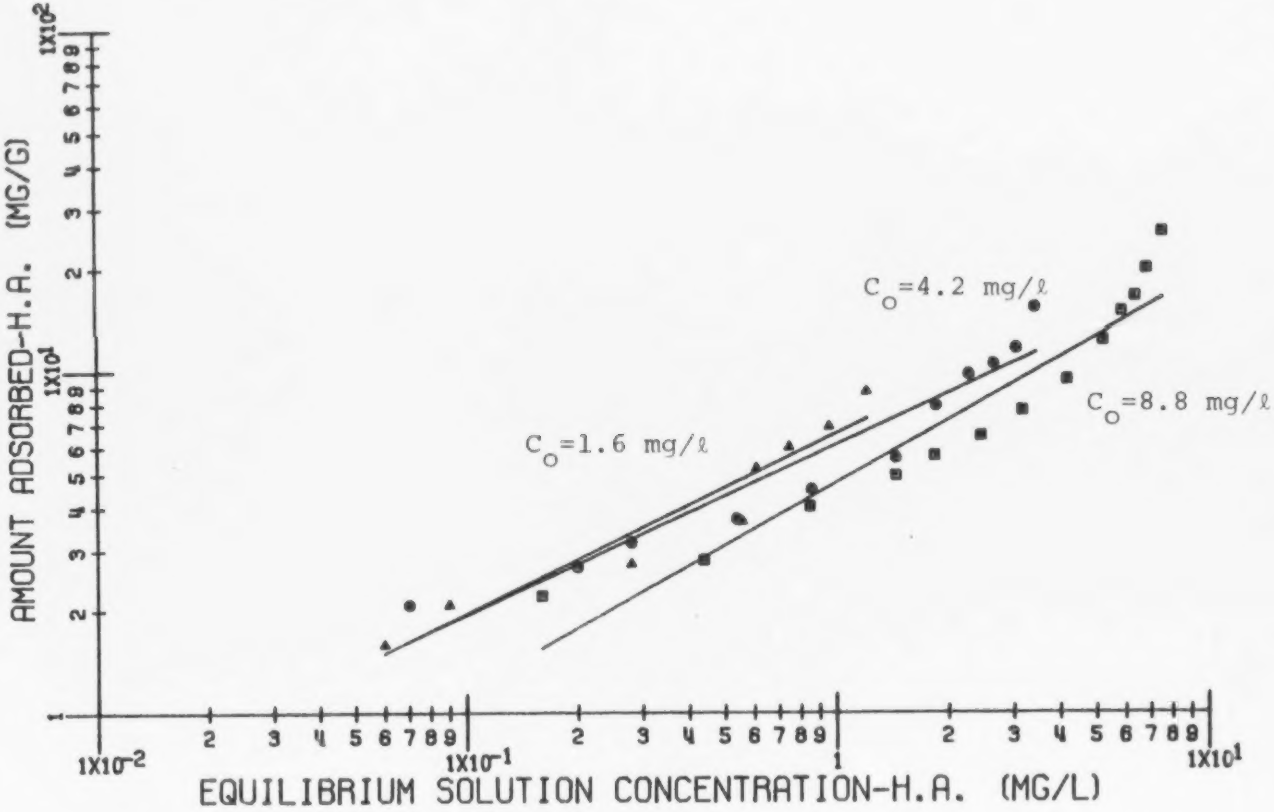

Figure 17. Adsorption isotherms for humic acids; dependence of extent of adsorption on initial concentration.

carbon particle (16/20 mesh). It may be observed that the "sieved" carbon demonstrates a larger capacity for humic acid than the "crushed and sieved" carbon. It may be speculated that the enhanced capacity is due to the larger activated surface and/or larger number of macropores of the original fine particles of the "sieved" carbon.

Figure 19 presents experimental data and Freundlich isotherms for humic acids adsorption from tap water and from DDW. The pronounced difference in the isotherms and in the corresponding parameters given in Table 5 indicate that certain constituents in Ann Arbor tap water enhanced the uptake of humic acids by the carbon. Concentrations of major individual ions present in the tap water were determined and the effect of certain species (Ca^{2+}, Mg^{2+}, Fe^{3+}, and OCl^-) on humic acids adsorption were examined in batch equilibrium experiments.

Figure 20 illustrates equilibrium data and Freundlich isotherms for adsorption of humic acids from DDW and from a DDW solution containing Ca^{2+}, Mg^{2+}, Fe^{3+}, and OCl^-. The ion concentrations specified in Figure 20 closely correspond to those in Ann Arbor tap water. (Ca^{2+} and Mg^{2+} were added as sulfate salts, Fe^{3+} as a chloride salt, and OCl^- as a sodium salt). The effects of these species on the apparent equilibrium capacities of the carbon for humic acids are evident. Magnesium exhibits the greatest effect; calcium and chlorine also substantially increase apparent adsorption. That the ferric iron did not significantly alter adsorption capacity is likely due to its relatively low concentration in the systems studied. Kavanagh and Weber (1978) have shown that iron can markedly impact the adsorption of organic chelating compounds on activated carbon.

To determine whether the enhanced removals were possible artifacts of destabilization, precipitation, and/or oxidation reactions, a series of tests were run in the absence of activated carbon. Varying concentrations of Ca^{2+}, Mg^{2+}, and OCl^- were added to DDW solutions of humic acids in stirred reactors. The solutions were allowed to stand for 15 hours after initial mixing. Samples of supernatent were then withdrawn and analyzed for residual humic acids concentration. There was a small but noticeable amount of settleable floc formed in the reactors containing Ca^{2+} and Mg^{2+}, and some reduction in color in the reactors containing OCl^-. The results of these tests are presented in Table 6.

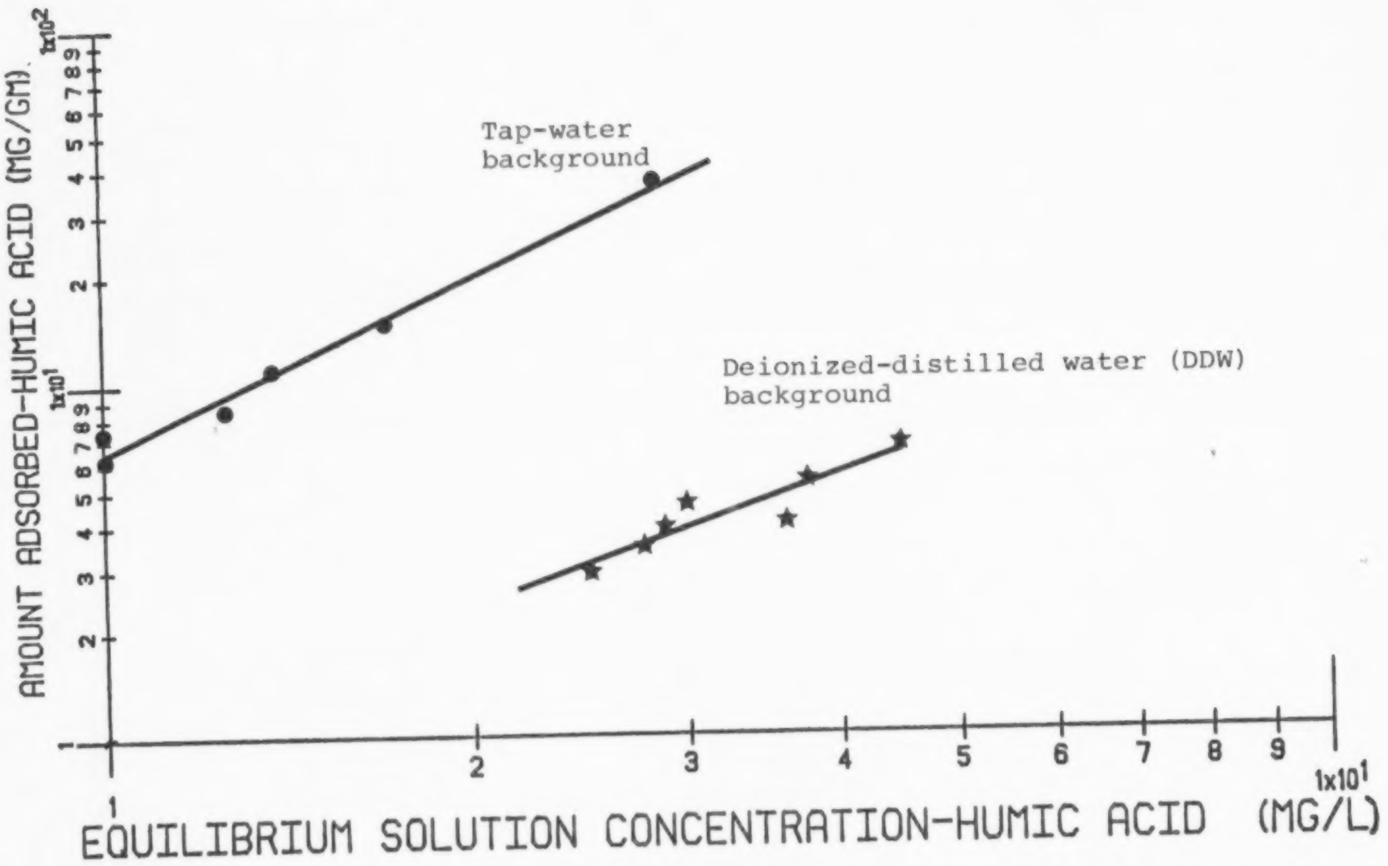

Figure 19. Adsorption isotherms for humic acids; effect of background solution on adsorption capacity.

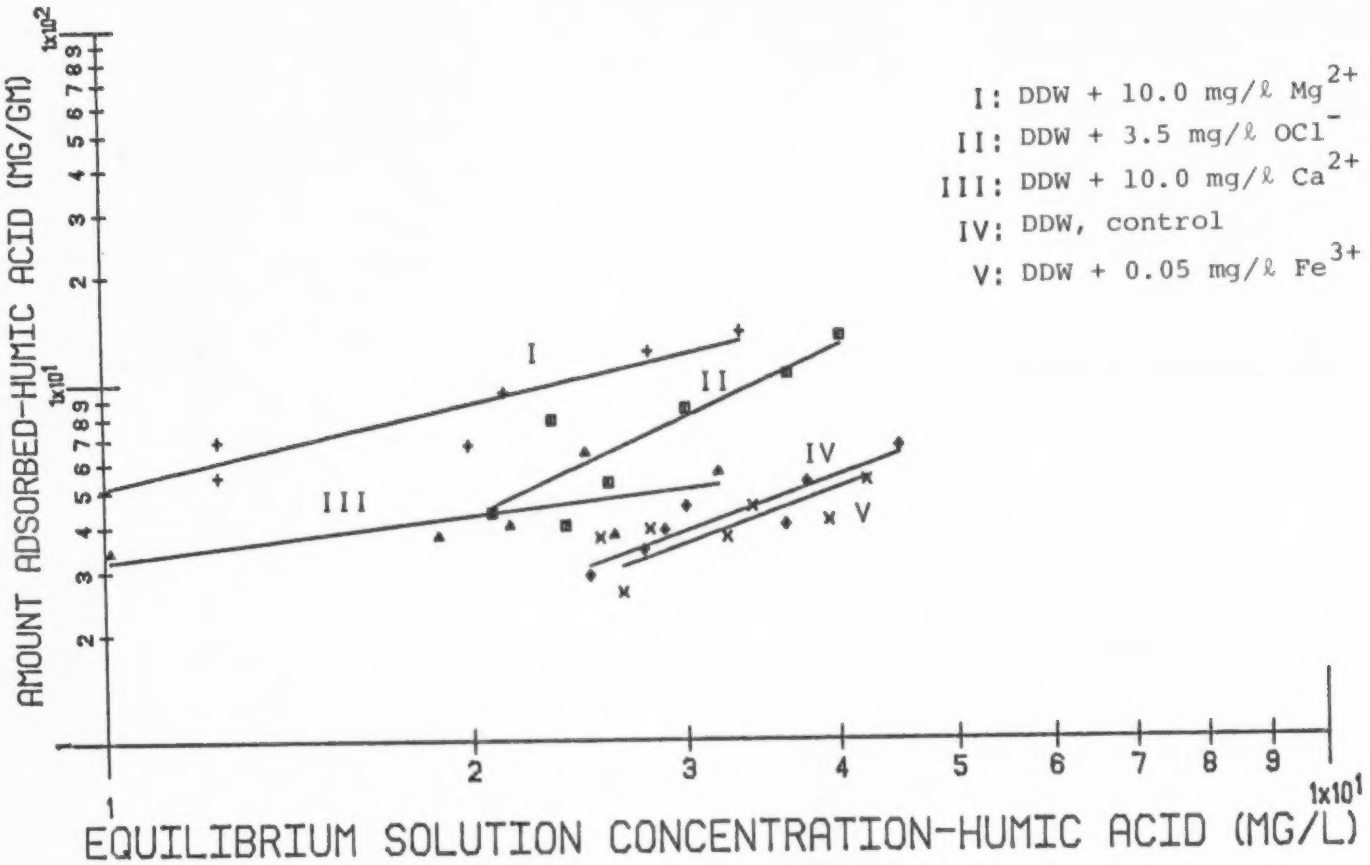

Figure 20. Adsorption isotherms for humic acids; effect of selected inorganic species on adsorption capacity (C_o = 4.9 mg/ℓ).

TABLE 6. EFFECTS OF Ca^{2+}, Mg^{2+}, AND OCl^- ON AQUEOUS CONCENTRATIONS OF HUMIC ACIDS IN THE ABSENCE OF ACTIVATED CARBON.

Initial humic acids concentration, mg/l	Species added	Species concentration, mg/l	Residual humic acids concentrations, mg/l
5.0	Mg^{2+}	1.0	4.9
		5.0	4.9
		10.0	4.8
4.7	Ca^{2+}	5.0	4.3
		10.0	4.1
		30.0	3.7
5.7	OCl^-	0.1	5.5
		0.7	5.3
		3.5	5.2

It is evident from the data given in Table 6 that the effects of the added species on removal of humic acids by possible destabilization, precipitation, and/or oxidation reactions are minor compared to their effects on apparent adsorption capacity. It may therefore be concluded that Ca^{2+}, Mg^{2+}, and OCl^- function to enhance humic acids removal in systems containing activated carbon primarily by alteration of adsorption affinity.

Gjessing (1976) reported eighteen different elements believed to be associated with humus, including calcium and chlorine. That magnesium is able to bind to the humic molecule is distinctly likely. Kononova (1961) suggested that humic substances (humic acids and fulvic acids) interact with cations of alkali and alkaline earth metals via exchange reactions between these cations and the hydrogen ions associated with carboxyl and phenolic hydroxyl groups on the humic substances. Carboxyl and phenolic functional groups are also associated with activated carbon surfaces (Weber, 1972). Moreover, the ability of chlorine, in a +1 oxidation state, to replace hydrogen in organic compounds via oxidative substitution is well recognized (Weber, 1972). It is conceivable that the enhanced adsorption observed in the presence of Ca^{2+}, Mg^{2+}, and OCl^- is attributable to modification of humic acids through coordinate covalent bonding and/or substitutive oxidation to render the macromolecules more amenable to attachment at functional group sites on the carbon. In the case of complex-bound Ca^{2+}, and Mg^{2+}, the interaction of humic acid macromolecules with functional surface groups on the carbon may further result from coordination of the bound metals by the basic oxygen molecules of surface functional groups.

ADSORPTION RATE STUDIES

Rate studies were conducted in complete mixed batch (CMB) glass reactors of normal 3.5 liter capacity. Three liters of humic acid solution and an appropriate quantity of granular activated carbon were agitated in the reactors using stainless steel stirrers driven by T-line Model #105 electric motors. The stirrer speed was controlled, using a powerstat speed controller (Superior Electric Co.), and adjusted by a type 1200D Dawe Strobescope. Ten-ml samples were withdrawn periodically using a 10-ml automatic pipette, and were stored in small glass vials and capped with polyethylene tops. Analysis of residual sorbate concentration as a function of time yielded data for determination of adsorption rates. Figure 21 illustrates typical experimental concentration-time profiles for different carbon particle sizes.

Rates of adsorption from solution by a porous adsorbent such as activated carbon are generally controlled by microtransport processes, involving both external and internal mass transport. Mathematical considerations indicate that if the rate varies approximately with the reciprocal of the square of the diameter of the carbon particle, the limiting rate mechanism is likely to be intraparticle transport (Weber and Morris, 1963).

To test this effect, the raw data was approximated by an empirical second-order equation, and the derivative rate constant evaluated with respect to particle size. Figure 22 illustrates this relationship. The effect of the initial concentration of adsorbate on the rate of adsorption was also investigated. Figure 23 demonstrates a linear relationship between initial concentration of humic acids and the reciprocal of the rate constant.

Rate Parameter Evaluation

The MADAM model (Weber and Crittenden, 1975, 1978a, 1978b) was used for the estimation of mass transfer coefficients simultaneously from the CMB rate data. To minimize the program search for the appropriate values of the film transfer coefficient, k_f, and the intraparticle coefficient,

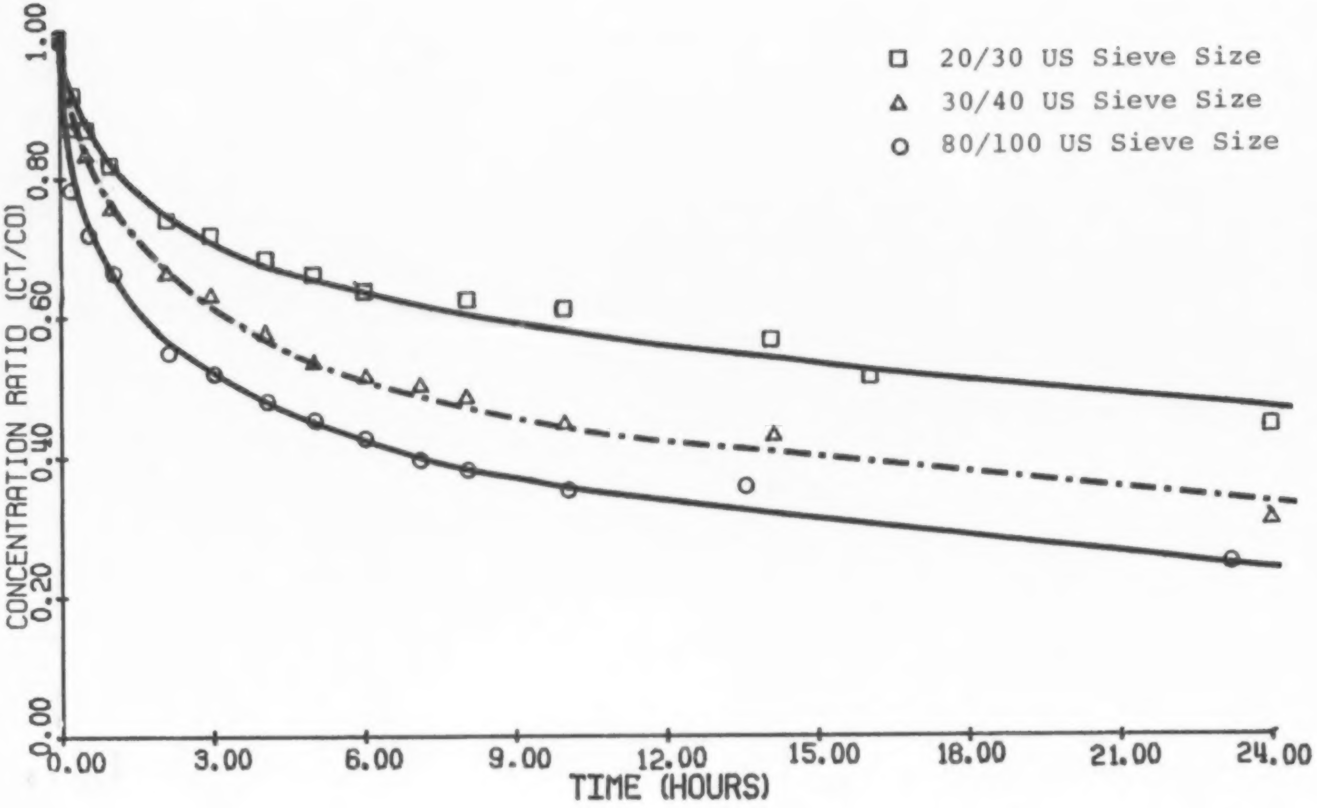

Figure 21. CMB reactor rate study for humic acids; effect of carbon particle size on rate of adsorption.

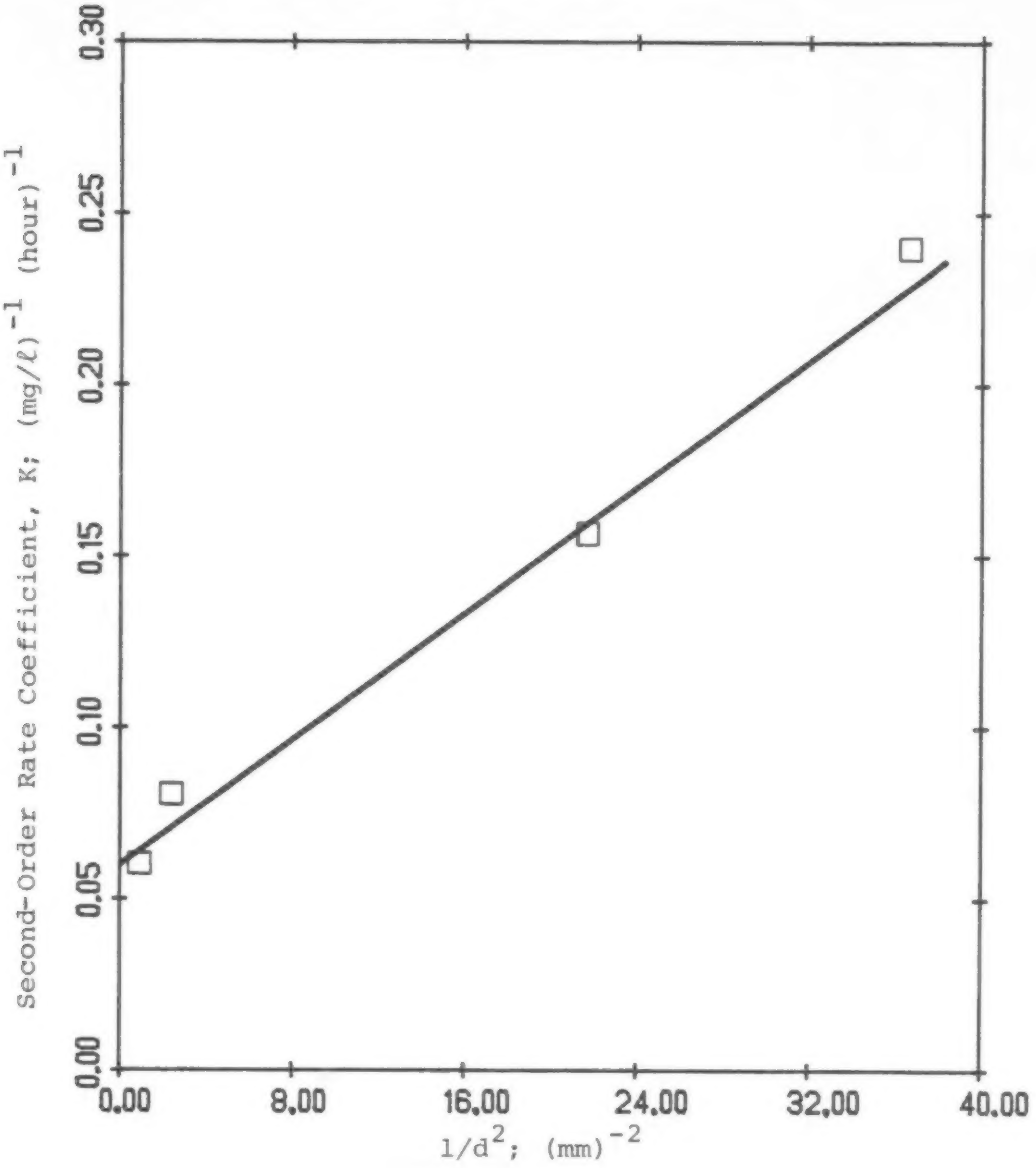

Figure 22. Effect of carbon particle size on rate of adsorption of humic acids; 1 g/ℓ of 30/40 US standard sieve size carbon.

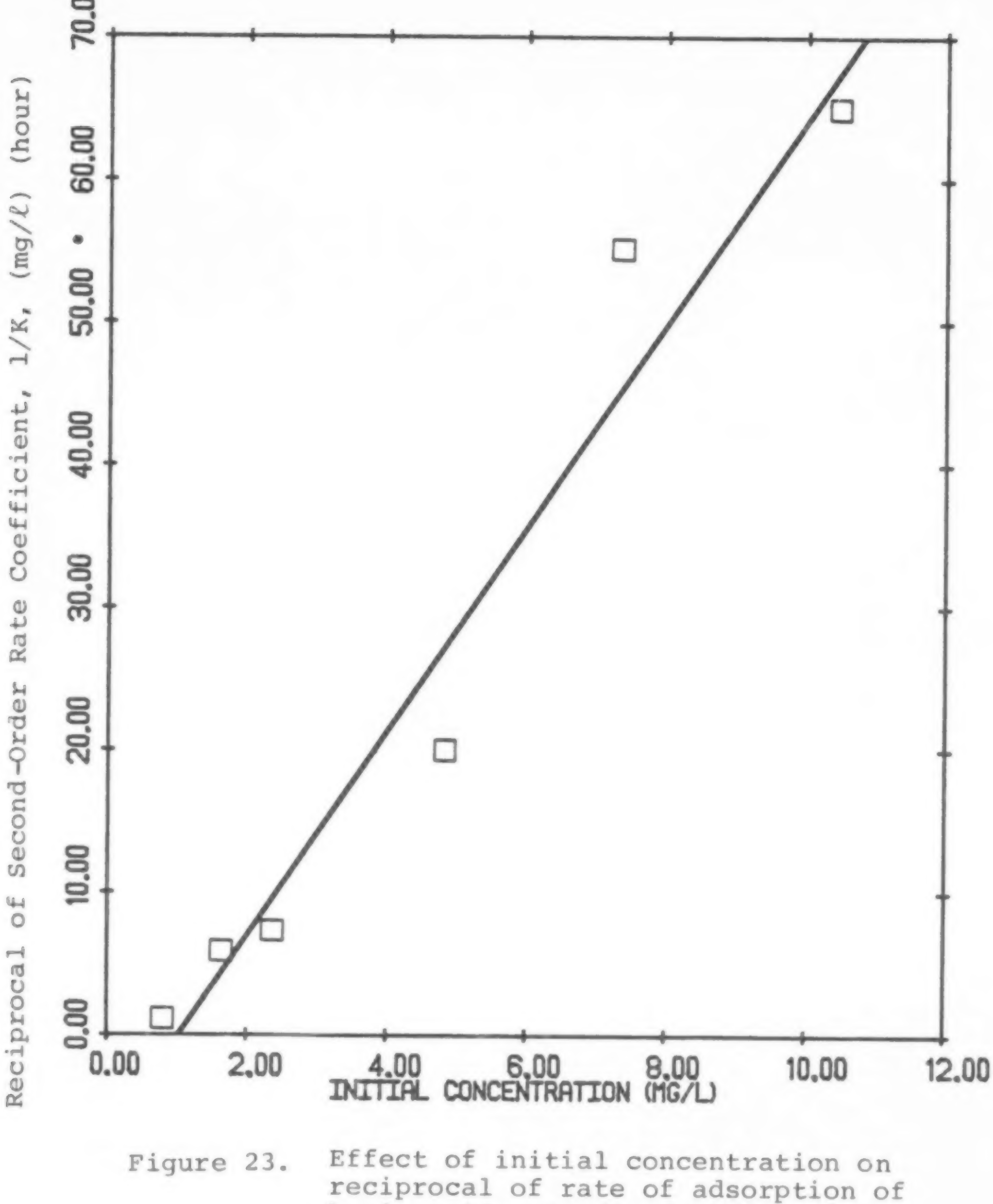

Figure 23. Effect of initial concentration on reciprocal of rate of adsorption of humic acids; 1 g/ℓ of 30/40 US standard sieve size.

D_s, a close control value for k_f was estimated by conducting a CMB rate experiment using a large amount of carbon to nearly deplete the solute within the first few minutes of the experiment. (The mathematical interpretation has already been discussed in Section 5).

Figures 24 and 25 illustrate experimental CMB rate data and the results of a MADAM simulation for humic acids in DDW solutions in which sensitivity analyses were conducted for different values of k_f and D_s. Figures 26 and 27 exhibit similar simulation runs for humic acids in Ann Arbor tap water. As is evident, a variation of $\pm$ 25% in the external mass transfer resistance affects substantial deviations in the concentration-time profiles.

The effect of intraparticle diffusion on the initial adsorption rate of humic acids in DDW and Ann Arbor tap water is illustrated in Figures 28 and 29. These predicted profiles were obtained by allowing $D \rightarrow \infty$ in the two-resistance model. It is apparent that with such an assumption the initial rates are affected significantly by diffusion within the particle.

Table 7 presents the estimated values of k_f and D_s obtained from the best fit to the experimental data.

TABLE 7. MASS TRANSPORT COEFFICIENTS FOR ADSORPTION OF HUMIC ACIDS IN DIFFERENT BACKGROUND SOLUTIONS

Background solution	Film transfer coefficient, k_f (cm/sec)	Surface diffusion coefficient, D_s (cm^2/sec)
Deionized-distilled water	1.44×10^{-4}	1.64×10^{-10}
Tap water	7.04×10^{-4}	1.36×10^{-10}

For comparison, reported values of k_f and D_s for several compounds for which activated carbon is commonly used as a removal technique are tabulated in Table 8 (Crittenden and Weber, 1978a). It appears that humic acids exhibit substantially lower film transfer and surface diffusion coefficients than compounds shown in Table 8. This may partly be due to the large size of humic acid molecules.

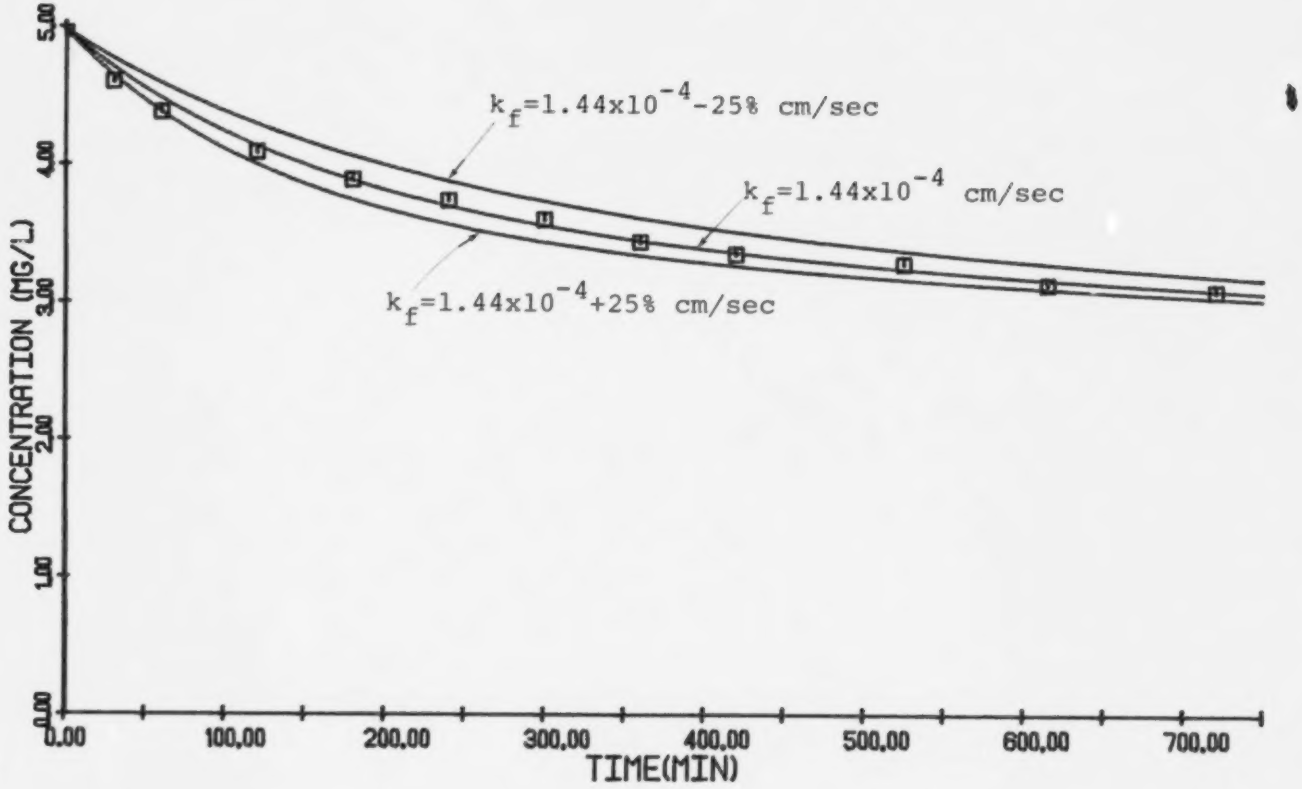

Figure 24. CMB reactor rate study for humic acid in DDW - sensitivity of predicted profile to variation in mass transfer coefficient, $K_f \pm$ 25%.

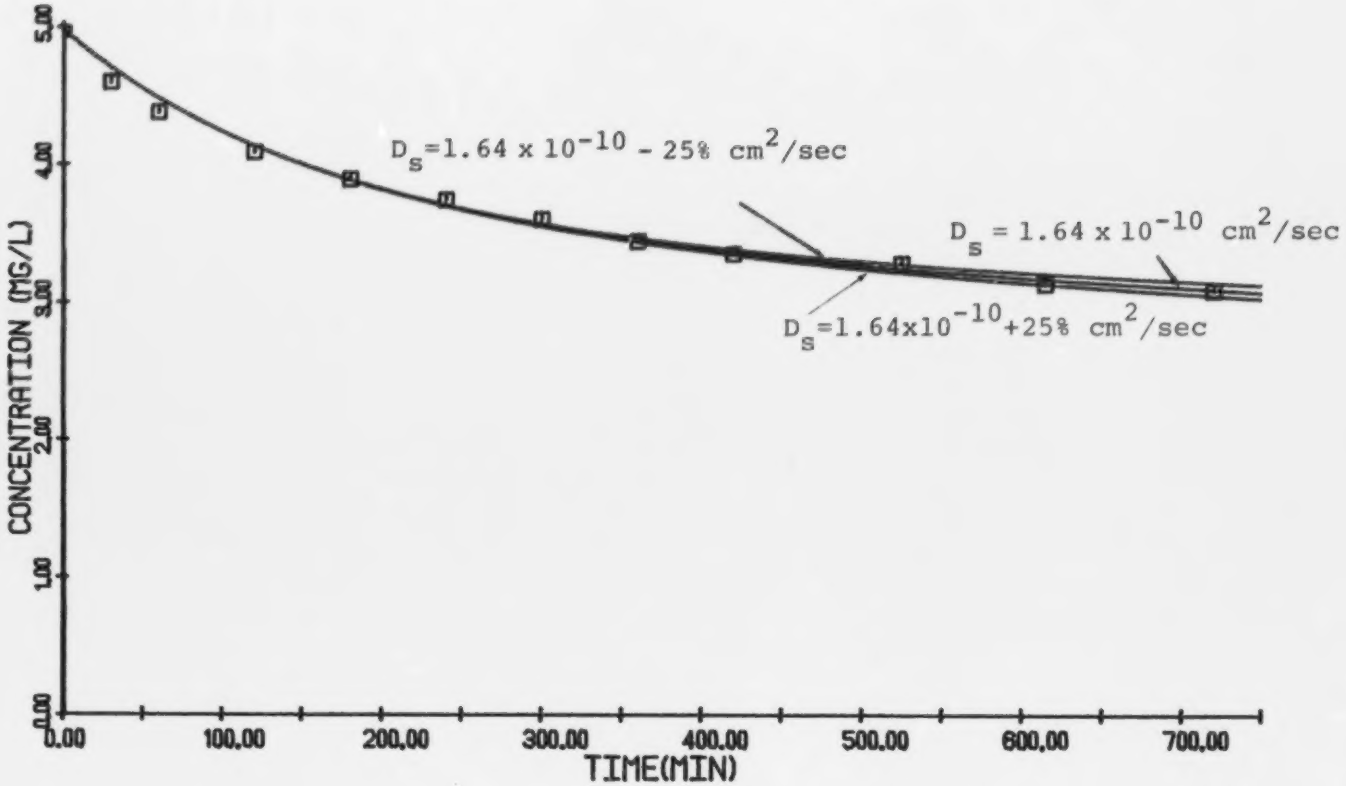

Figure 25. CMB reactor rate study for humic acid in DDW - sensitivity of predicted profile to variation in surface diffusion coefficient, $D_s \pm 25\%$.

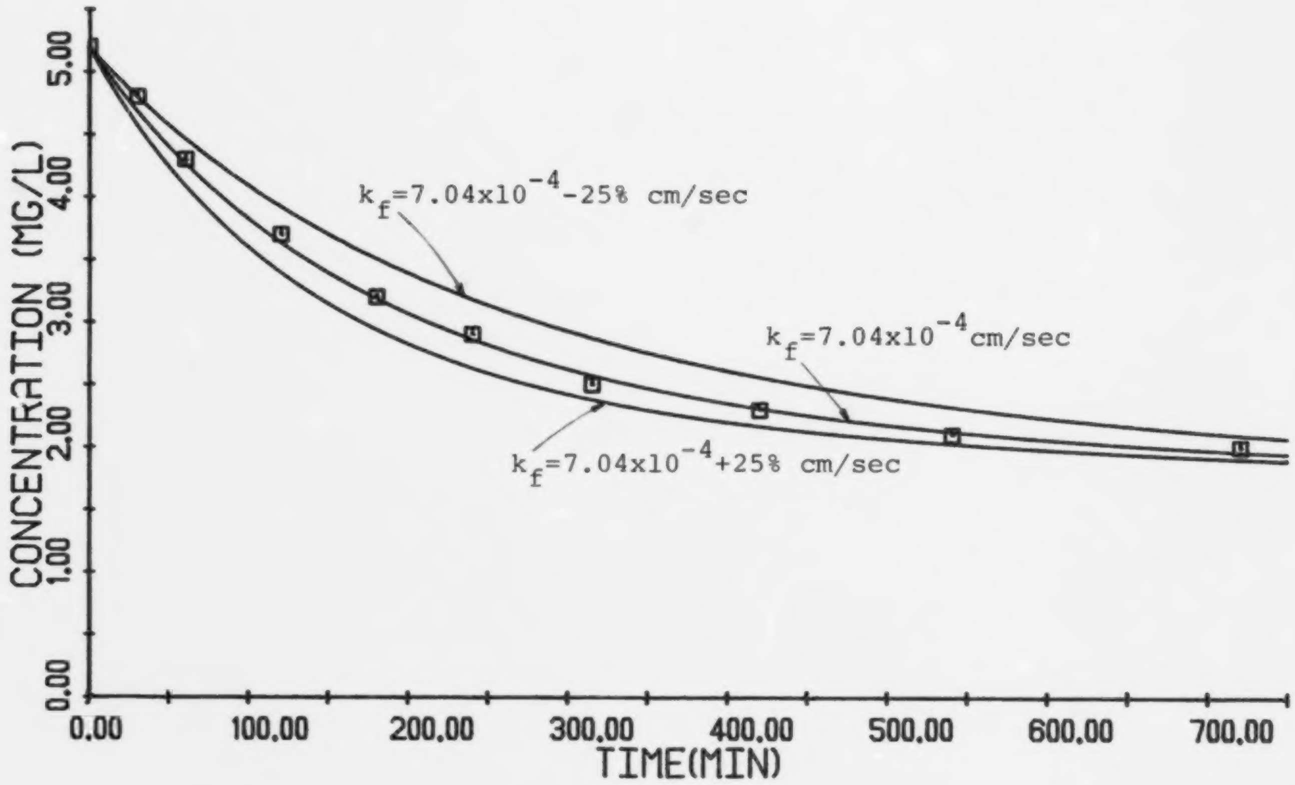

Figure 26. CMB reactor rate study for humic acid in tap water - sensitivity of predicted profile to variation in mass transfer coefficient, $k_f \pm 25\%$.

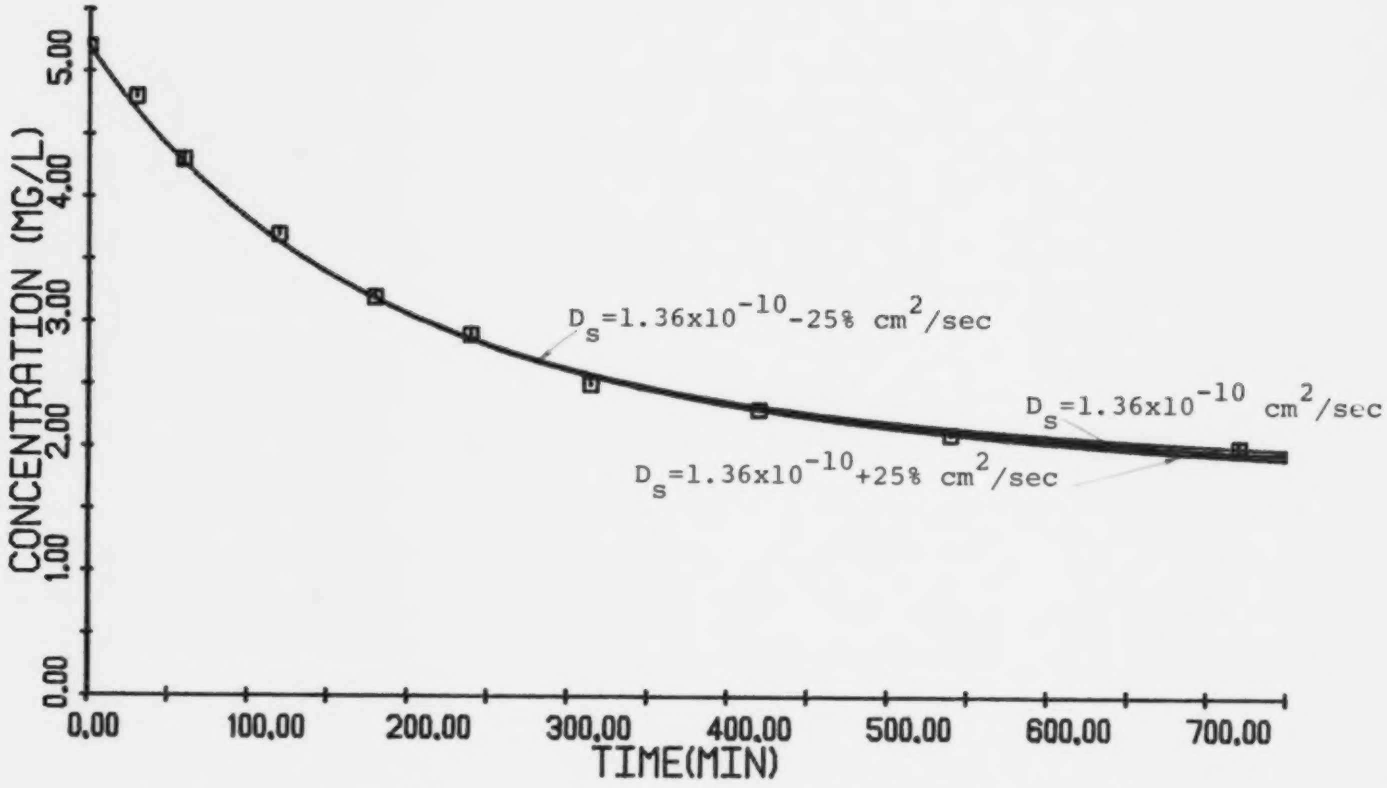

Figure 27. CMB reactor rate study for humic acid in tap water - sensitivity of predicted profile to variation in surface diffusion coefficient, $D_s \pm 25\%$.

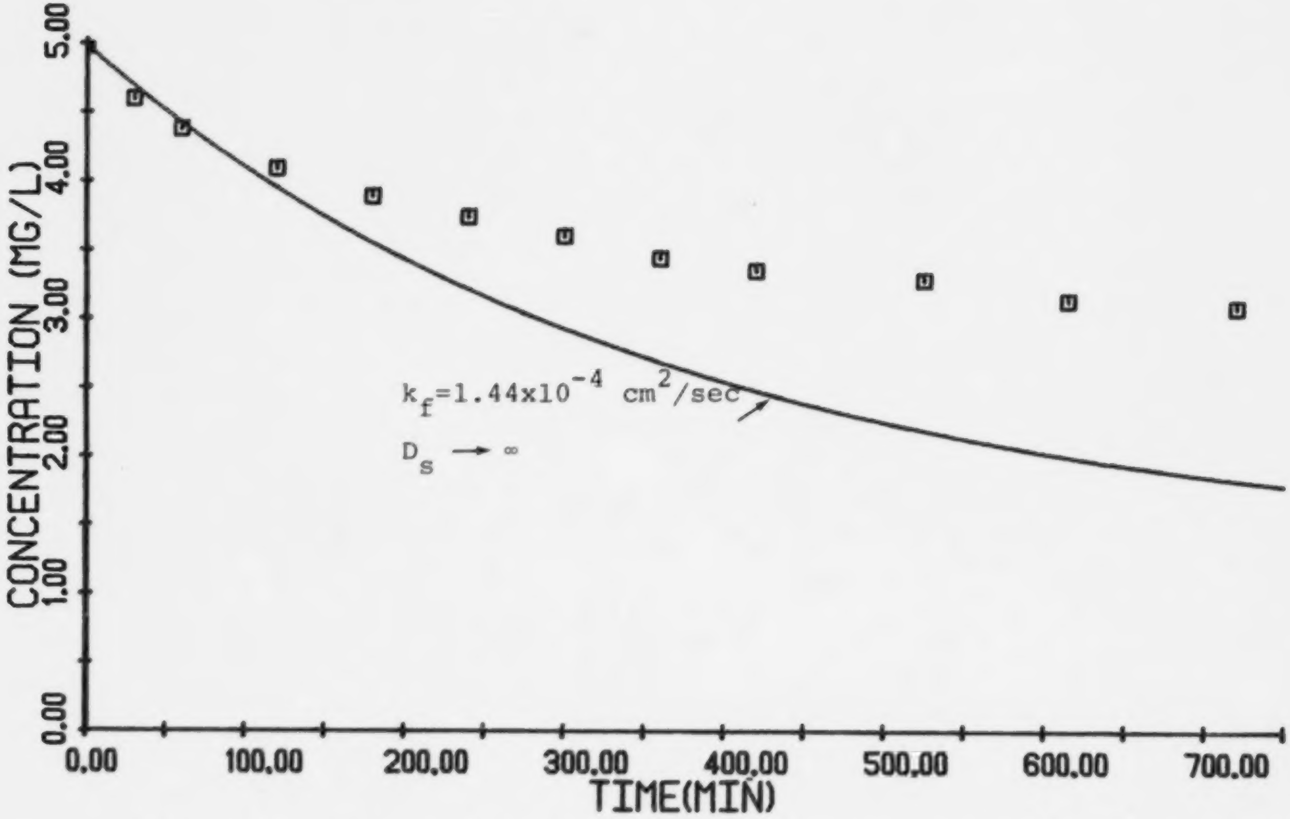

Figure 28. Effect of intraparticle diffusion on the initial adsorption rate of humic acid in DDW.

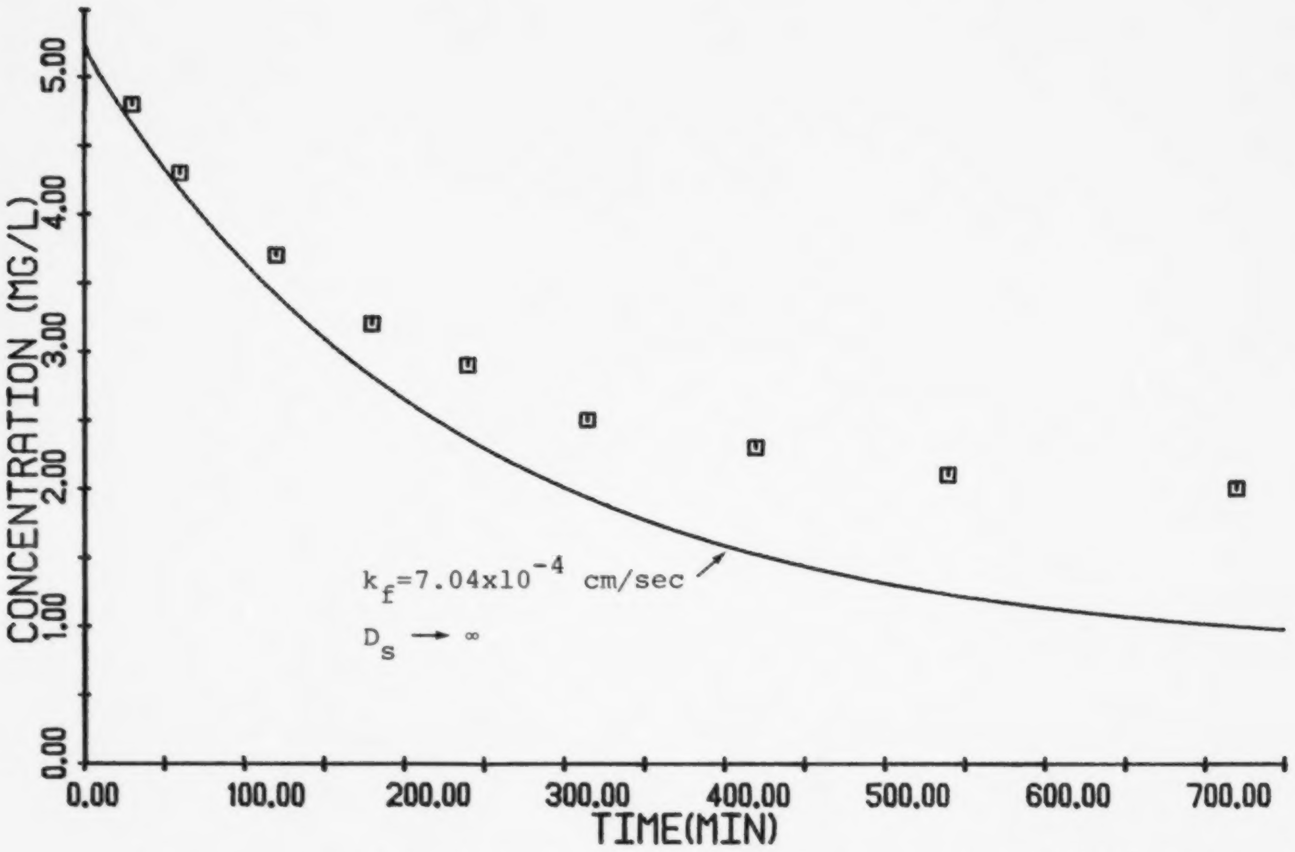

Figure 29. Effect of intraparticle diffusion on the initial adsorption rate of humic acid in tap water.

TYPING GUIDE SHEET

It is of further interest to note the effect of background solution on the film transfer coefficients given in Table 7. It is obvious that background solution species such as Ca^{2+}, Mg^{2+}, and OCl^{-} are responsible for this difference. The data, however, do not permit rigorous interpretation of the mechanistic effects of the background species.

TABLE 8. MASS TRANSFER COEFFICIENTS FOR SELECTED COMPOUNDS OF KNOWN ADSORPTION CHARACTERISTICS

Solute	k_f, (cm/sec)	D_s, (cm^2/sec)
Phenol	2.10×10^{-2}	3.53×10^{-8}
p-Bromophenol	1.35×10^{-2}	8.56×10^{-8}
p-Toluene Sulfonate	1.45×10^{-2}	1.9×10^{-8}
Dodecyl Benzene Sulfonate	6.07×10^{-3}	4.69×10^{-9}

ADSORPTION COLUMN STUDIES

Initial column studies for characterization of humic acid breakthrough phenomena were conducted in 6-ft., 1-in internal diameter (ID) plexiglass columns. The adsorbers contained 200 grams of sieved and washed Filtrasorb 400 carbon, 16/20 U.S. Standard mesh size. Influent humic acids concentration was maintained at 5 ppm, and flow rate was kept at 4.85 gpm/ft^2. The feed solution was buffered at pH 7. An immediate breakthrough was observed; and within just ten hours the effluent concentration reached 65% of the influent concentration. After 160 hours of operation, the effluent concentration reached 90% of the influent concentration and was relatively constant until the experiment was terminated after a total operation time of 405 hours.

Based on these observations, a study with four identical packed-bed columns in series, each containing 250 grams of 16/20 U.S. Standard mesh Calgon Filtrasorb 400, was conducted with the objective of containing and quantitatively defining the breakthrough curves for the humic acid. The background solution consisted of deionized-distilled water (DDW) passed through an activated carbon column for further purification. Humic acids feed solution was made up in 50-gallon polypropylene tanks and pumped to the carbon adsorbers. All tubing was

EPA-287 (Cin.)
(4-76)

TYPING GUIDE SHEET

Tygon with a 3/8 inch (1 cm) I.D.

A schematic diagram of the experimental apparatus is presented in Figure 30. Figure 31 illustrates effluent-concentration profiles for an influent concentration of 5 ppm humic acids buffered at pH 7 for a flow rate of 4.85 gpm/ft^2. Figures 32 and 33 illustrate effluent concentration profiles for two different particle sizes for a flow rate of 1.94 gpm/ft^2. The significant effect of particle size is evident from comparison of the breakthrough curves given in these figures.

Breakthrough curves for the adsorption of humic acids in the Ann Arbor tap water are presented in Figure 34. Also, single column studies for adsorption of humic acids in different background solutions are demonstrated in Figure 35 and in the cumulative adsorption curves shown in Figure 36. The difference in the dynamic adsorption characteristics of humic acids in the two different background solution are pronounced. There was virtually immediate breakthrough of humic acids in the DDW, while no significant breakthrough occurred for the tap water during the first 60 hours of column operation. Moreover, after approximately 200 hours of operation the latter system exhibited an instantaneous removal efficiency that was nearly three-times that of the former. Thus, the findings of the batch studies relative to the background solution effects were verified for dynamic adsorption systems.

Biological Growth in Carbon Columns

All column experiments conducted with humic acids and granular activated carbon in this study exhibited biological activity. Biological growth was invariably visible in the columns within 100 hours from the onset of operation. To verify the presence and nature of the growth, carbon particles taken from the columns were examined using scanning electron microscopy. It is essential that great care be exercised in handling, fixing, dehydration, drying, and coating the samples, since fragile biological materials are easily damaged, and artifacts or unrecognizable features may result (Weber *et al*, 1978).

Preparations were fixed by modification of the method suggested by Karnovsky (1965). The carbon particles were immersed for 2 hours in a paraformaldehyde/glutaraldehyde solution in 0.2 *M* sodium phosphate buffer at pH 7.3. A 3-hour post-fixation followed, using 1% OsO_4 in 0.1 *M* sodium phosphate buffer at pH 7.3 (Parducz, 1967). Subsequently, dehydration was accomplished by rinsing the particles in graded ethanol (50%, 70%, 80%, 90% and 100%). Samples were prepared for critical-point drying in a 1:1 100% ethanol/amylacetate solution, and stored overnight in amylacetate.

EPA-287 (Cin.)
(4-76)

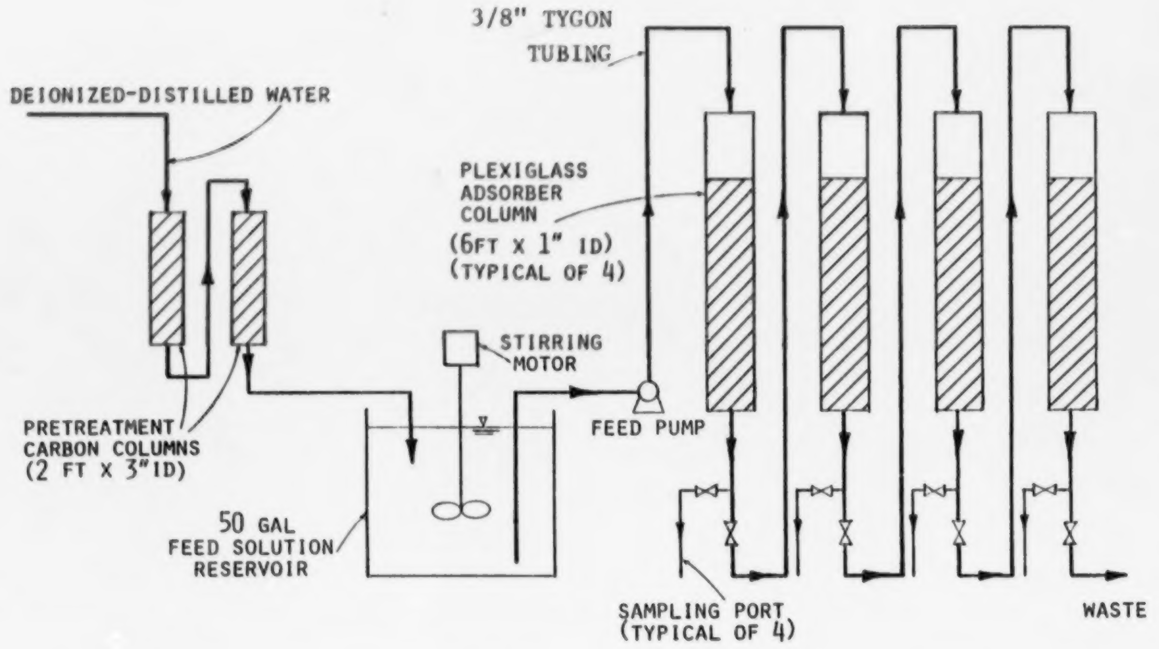
3/8" TYGON
TUBING
DEIONIZED-DISTILLED WATER
PLEXIGLASS
ADSORBER
COLUMN
(6FT x 1" ID)
(TYPICAL OF 4)
STIRRING
MOTOR
PRETREATMENT
CARBON COLUMNS
(2 FT x 3"ID)
FEED PUMP
50 GAL
FEED SOLUTION
RESERVOIR
SAMPLING PORT
(TYPICAL OF 4)
WASTE

Figure 30. Schematic diagram and experimental arrangement for humic acids column studies.

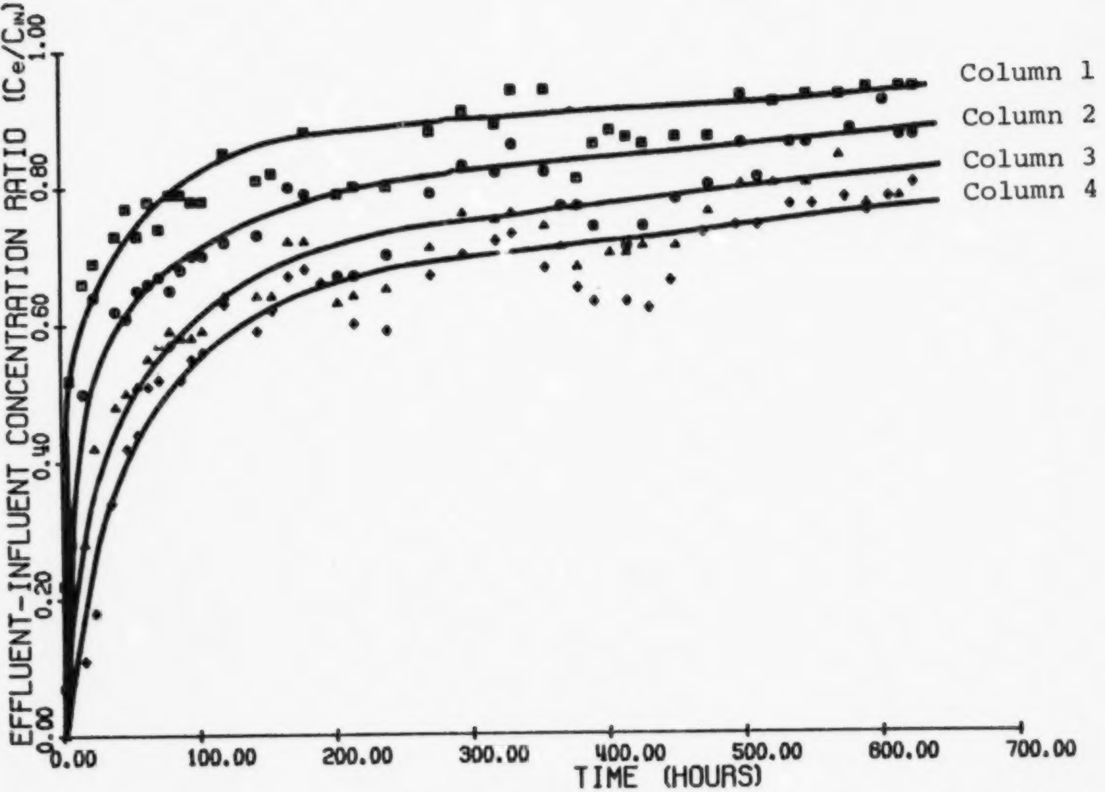

Figure 31. Column breakthrough profiles for humic acids in buffered DDW, C_o = 5ppm, flow rate = 4.85 gpm/ft^2, 250 grams of 16/20 US sieve size carbon per column.

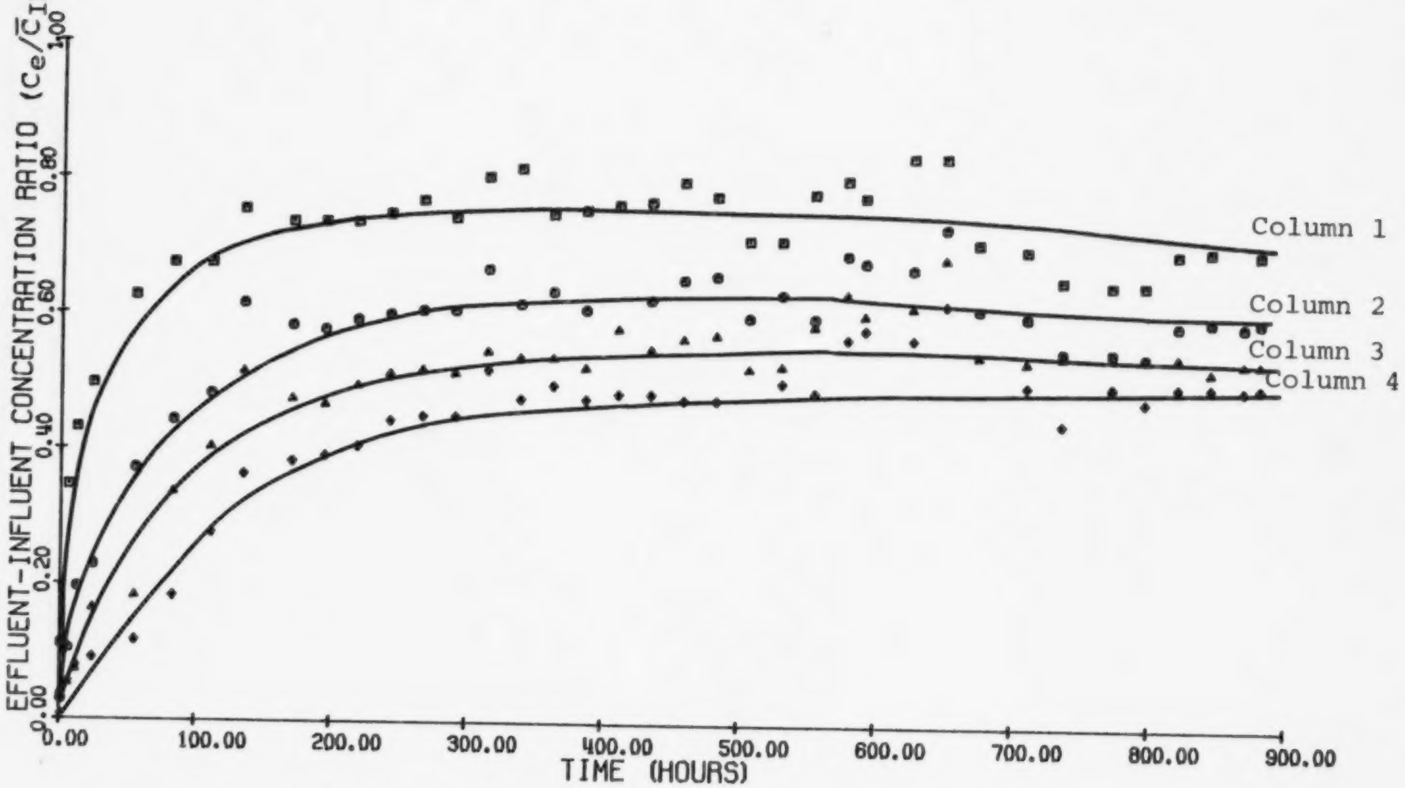

Figure 32. Column breakthrough profiles for humic acids in buffered DDW, C_o=5ppm, flow rate=1.94 gpm/ft^2, 250 grams of 16/20 US sieve size carbon per column.

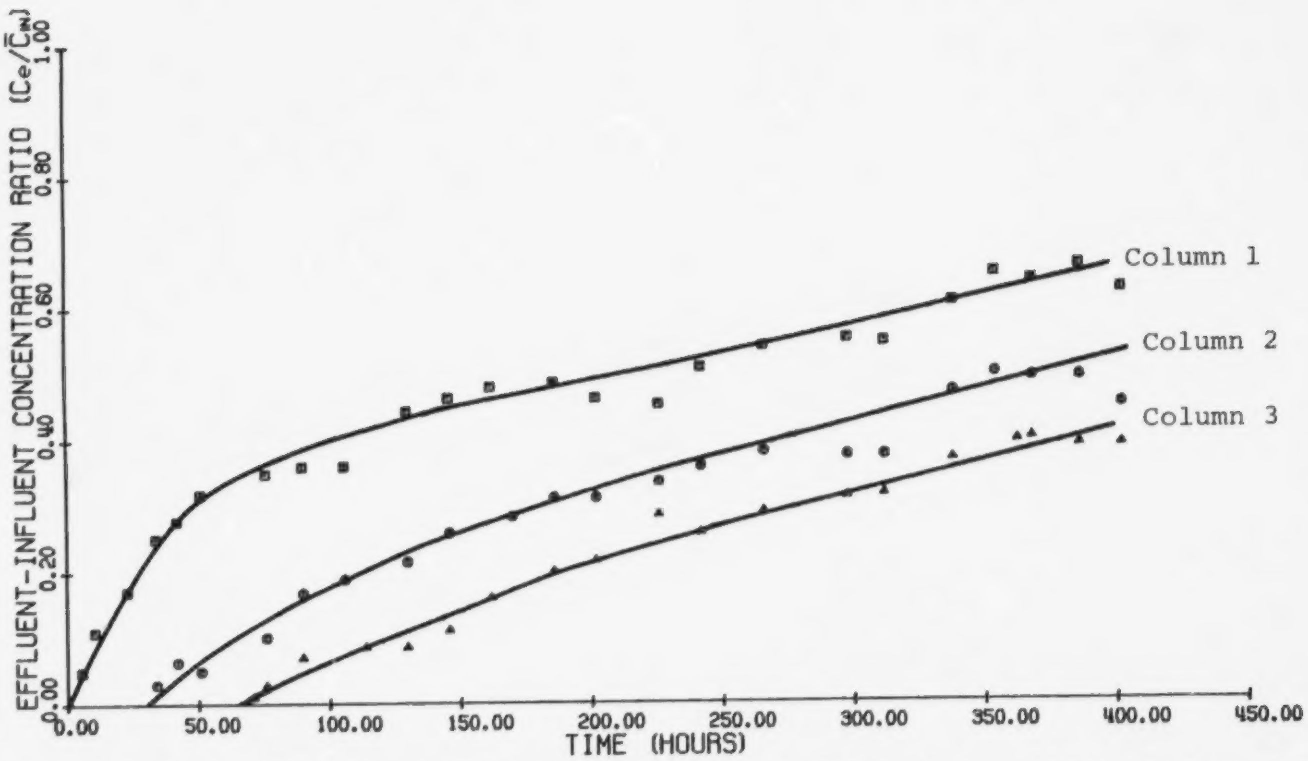

Figure 33. Column breakthrough profiles for humic acid in buffered DDW, C_o=5ppm, flow rate=1.94 gpm/ft^2, expanded bed, 250 grams of 30/40 US sieve size carbon per column.

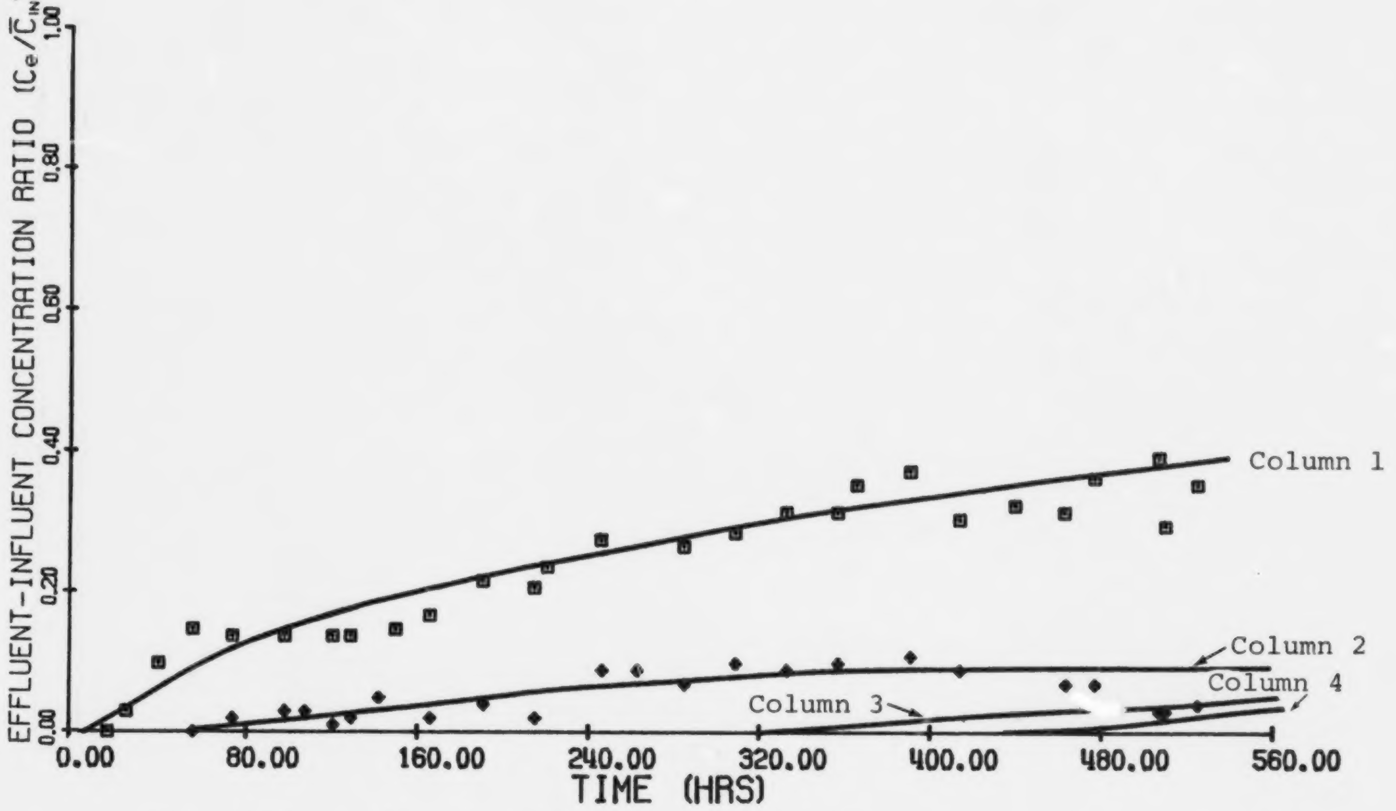

Figure 34. Column breakthrough profiles for humic acids in tap water, C_o=5ppm, flow rate=1.94 gpm/ft^2, 250 grams of 16/20 US sieve size carbon per column.

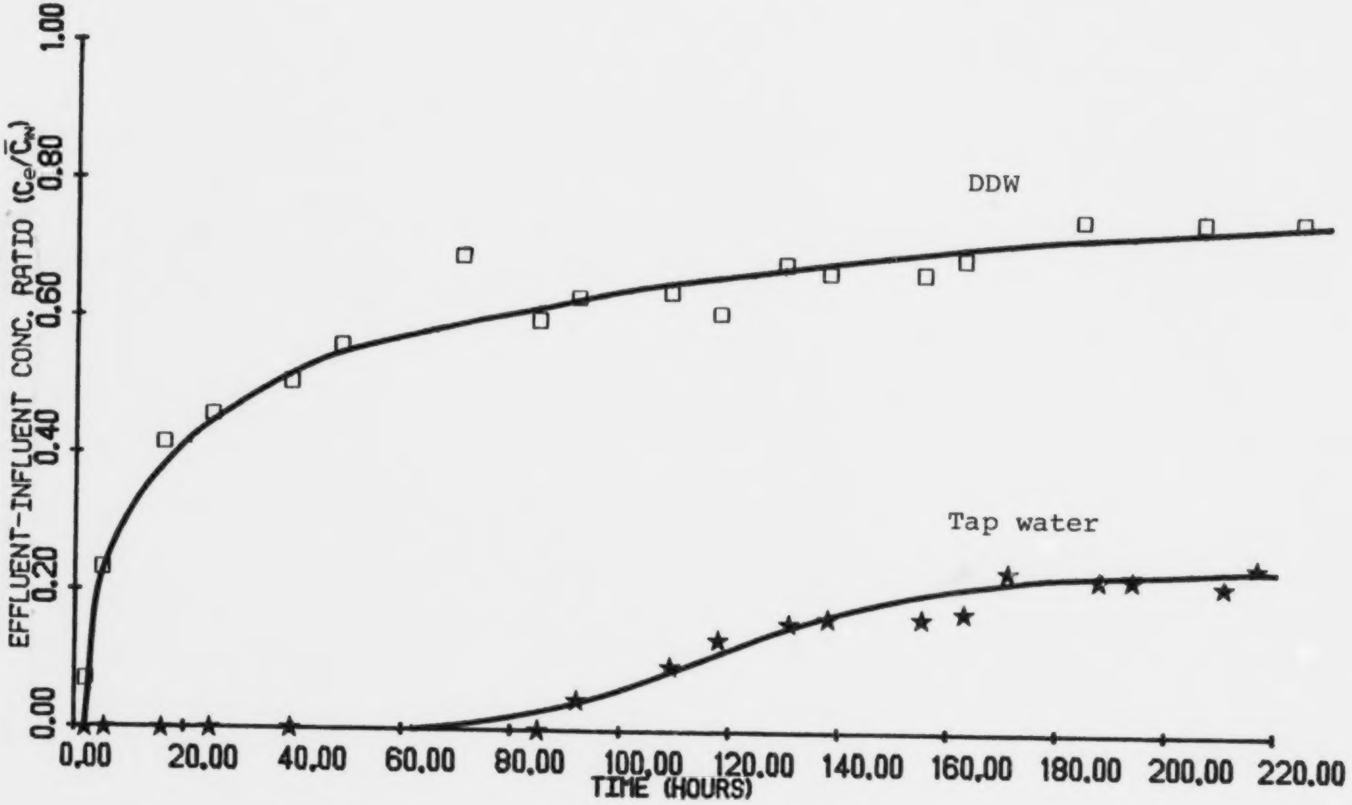

Figure 35. Column breakthrough profiles for humic acids in different background solution, C_o = 5ppm, flow = 1.94 gpm/ft^2, 250 grams of 16/20 US sieve size carbon.

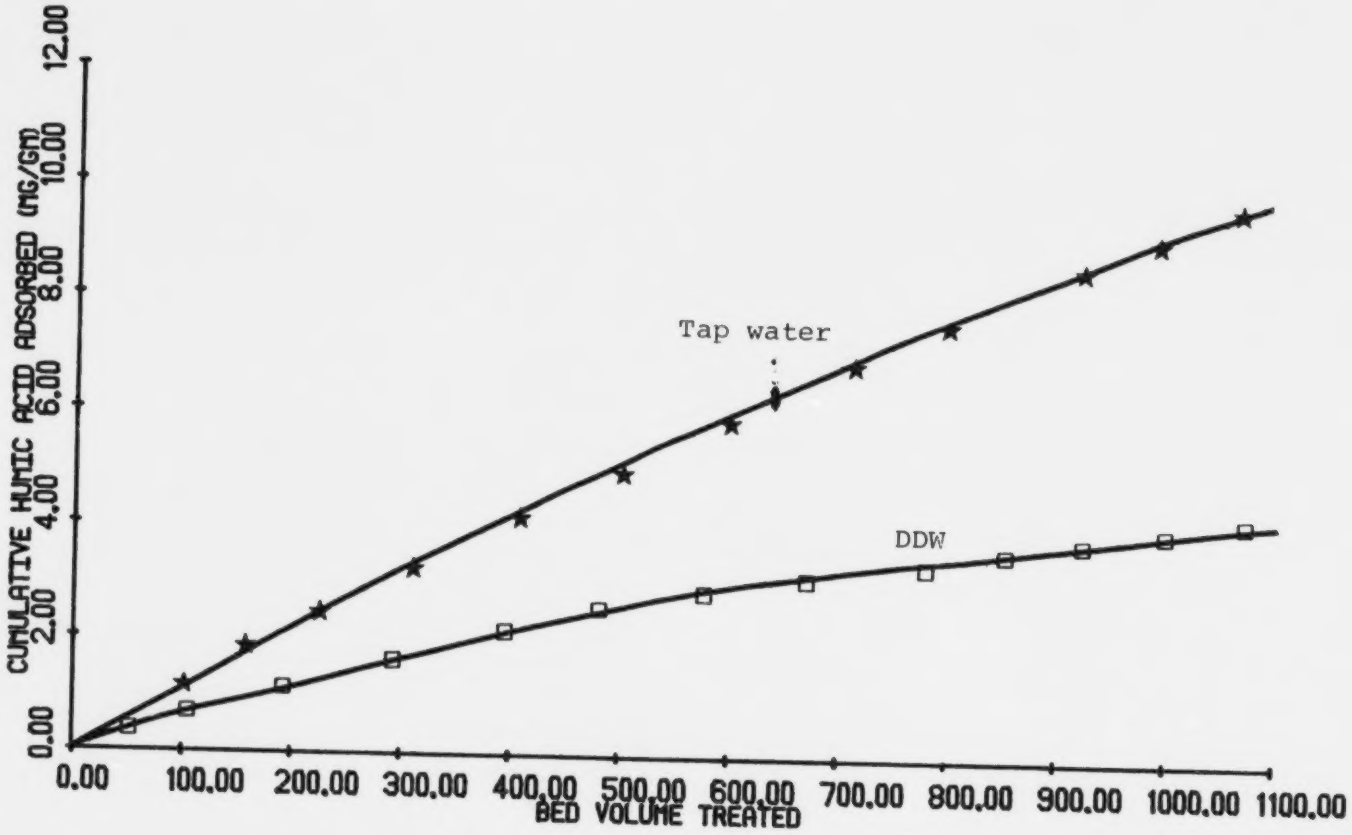

Figure 36. Effect of different background solutions on cumulative adsorption of humic acids in carbon adsorption columns.

TYPING GUIDE SHEET

A DCP-1 critical point dryer was used for drying the fixed particles (Bartlett and Burstyn, 1975). The particles were then mounted on aluminum stubs and coated with 100 Å gold in a low-discharge coater to minimize charging and increase the conductivity of the biological material. The last two steps were carried out as precisely as possible after critical point drying to avoid rehydration and consequent damage to the fixed biological growth. A JOEL JSM-U3 Scanning Electron Microscope operated at an accelerating voltage of 15-25 KeV was used for observing the specimens. A detailed description of materials and methods for preparation of biogrowth for examination by scanning electron microscopy is presented in Appendix H.

Figures 37 and 38 are representative micrographs demonstrating the nonhomogeneous nature of the coverage by bacteria. This nonhomogeneity suggests that precise straightforward quantification may not be possible for the attached biological growth and the diffusional transport processes associated with adsorption.

In examining the biofilm, another interesting phenomenon was the appearance of stalked protozoa; this indicated a more advanced biological colonization of the carbon surface. The establishment of an ecosystem including bacteria and bacteriovorous protozoa is evidence of improving mineralization of organics, as well as nutrient regeneration. These types of processes, which are basic to trickling filter wastewater treatment systems, could be quite advantageous to the performance of activated carbon systems, and could provide an additional means for removal of biodegradable organic substances in water treatment applications.

Predicted Breakthrough Profiles

Parameter values used for adsorption column performance predictions for humic acids were estimated based on the following parameters:

1) isotherm constants calculated from a three-parameter isotherm;

2) surface diffusion coefficients predicted from finite-bath batch reactor experiments;

3) the adsorber column external mass transfer coefficient, k_f [for single-solute systems k_f may be estimated from correlation techniques such as those given by Williamson et al, (1963), Ergun (1952), Thoenes and Kramers (1958), and Resnick and White (1949). This coefficient, however, is a function of the free liquid diffusivity of the solute. Because no

EPA-287 (Cin.)
(4-76)

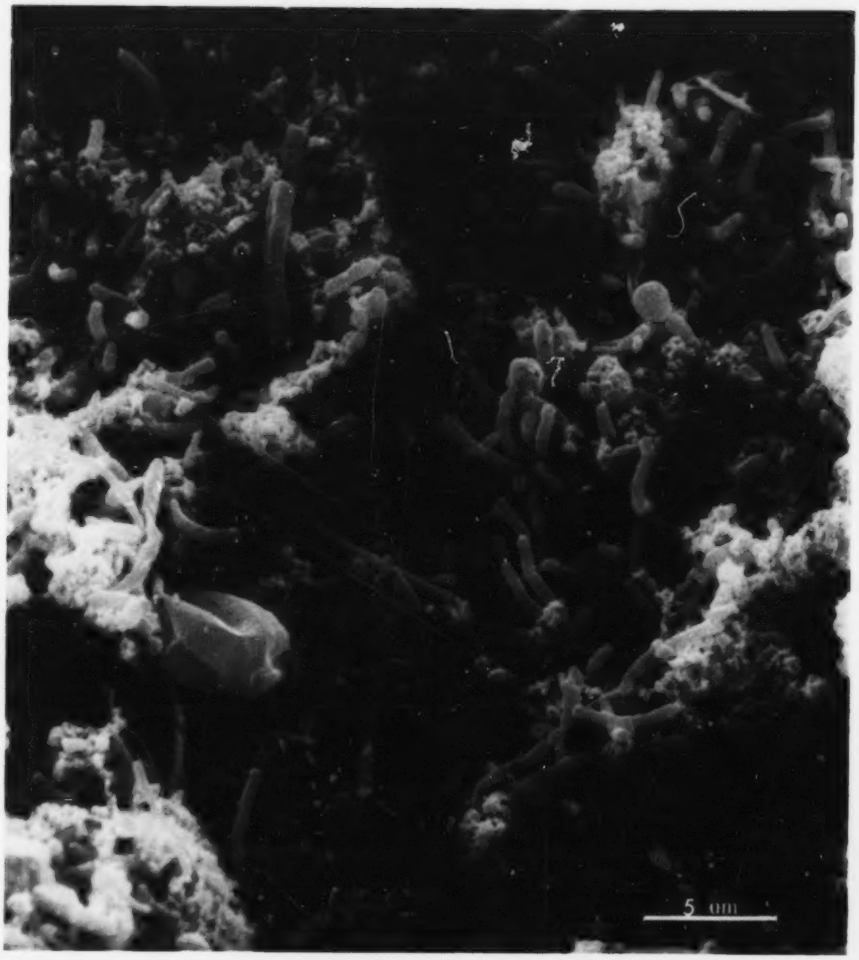

Figure 37. Electron micrograph of biological growth on activated carbon exposed to humic acids. Note that the carbon surface is sparsely covered with biogrowth.

Reproduced from
best available copy.

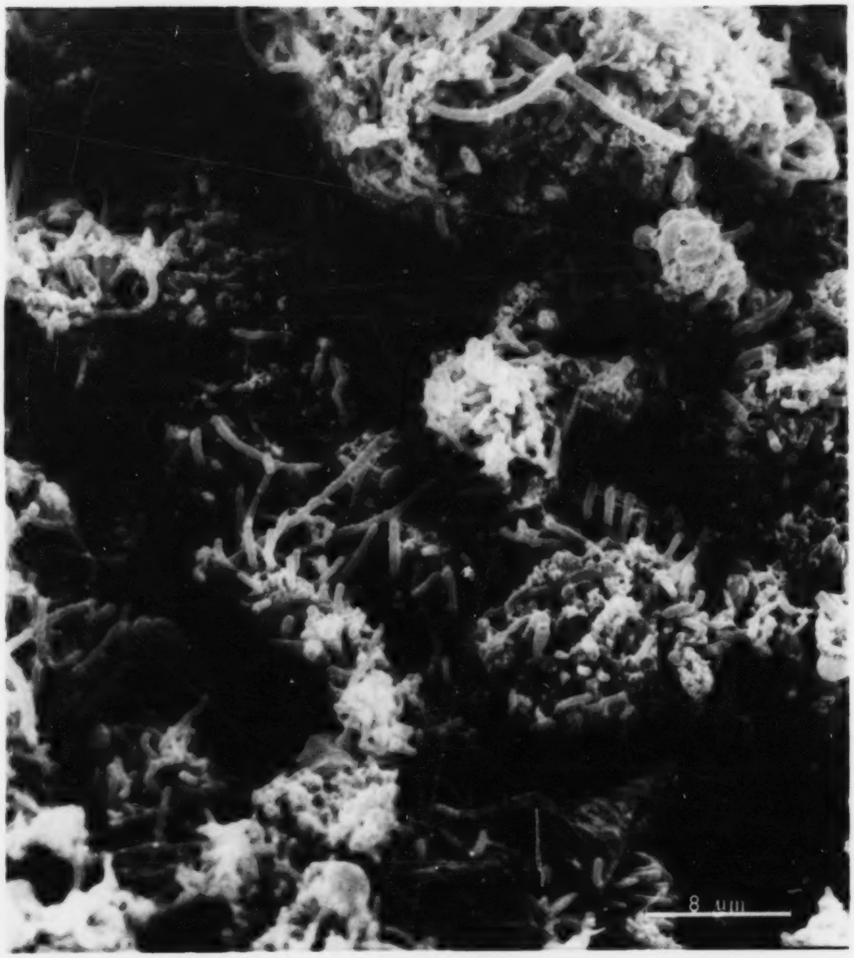

Figure 38. Electron micrograph of biological growth on activated carbon exposed to humic acids. Note that the biofilm coverage is nonuniform.

Reproduced from best available copy.

reported free luquid diffusivity value was available in the literature for the type of humic acid used in this study, k_f values were estimated from column simulation].

4) the solute distribution papameter, D_g, based on equilibrium capacity measured in equilibrium bottle point studies.

Model Calibration and Verification--

Simulation analyses were conducted for humic acids in DDW for a bed length of 123 cm using the D_s value obtained from CMB-reactor rate studies. It was found that the initial stages of the breakthrough curve is dominated by external "film" transport. Therefore, values of k_f were estimated from this initial portion. The model was then verified for a bed length of 492 cm. Because the final stage of the breakthrough curve was dominated by surface diffusion, the value of D_s was determined by regression analysis of the data for the entire breakthrough curve. The values of k_f and D_s thus obtained were used to predict the profiles demonstrated in Figures 39 and 40. Similar results for humic acids in Ann Arbor tap water are presented in Figures 41 and 42.

Table 9 summarizes values for the parameters used for different column runs, including: influent concentration, $\overline{C}_{in}$, adsorber bed void fraction, γ, interstitial velocity, v, bed length, L, column film transfer coefficient, k_f, and surface diffusion coefficient, D_s.

Model Sensitivity--

Model sensitivity analyses were performed to investigate the effects of variations in k_f and D_s on model behavior. By way of example, Figure 43 illustrates model sensitivity to the film transfer coefficient for a typical column study. The breakthrough profile demonstrates sensitivity to changes in k_f in the initial stages of throughput, indicating that film diffusion is rate controlling in this region. Figure 44 illustrates the sensitivity of model predictions to the surface diffusion coefficient for the same system. It may be noted from this figure that the model sensitivity to D_s increases as throughput increases, indicating that surface diffusion is the principal controlling mechanism.

It may be observed that the values estimated for the intraparticle diffusivity predicated on the CMB reactor rate data are different from those obtained from the parameter search for the best simulation of the column breakthrough profiles. It is likely that removal of humic acid fractions by biological activity adversely affects the

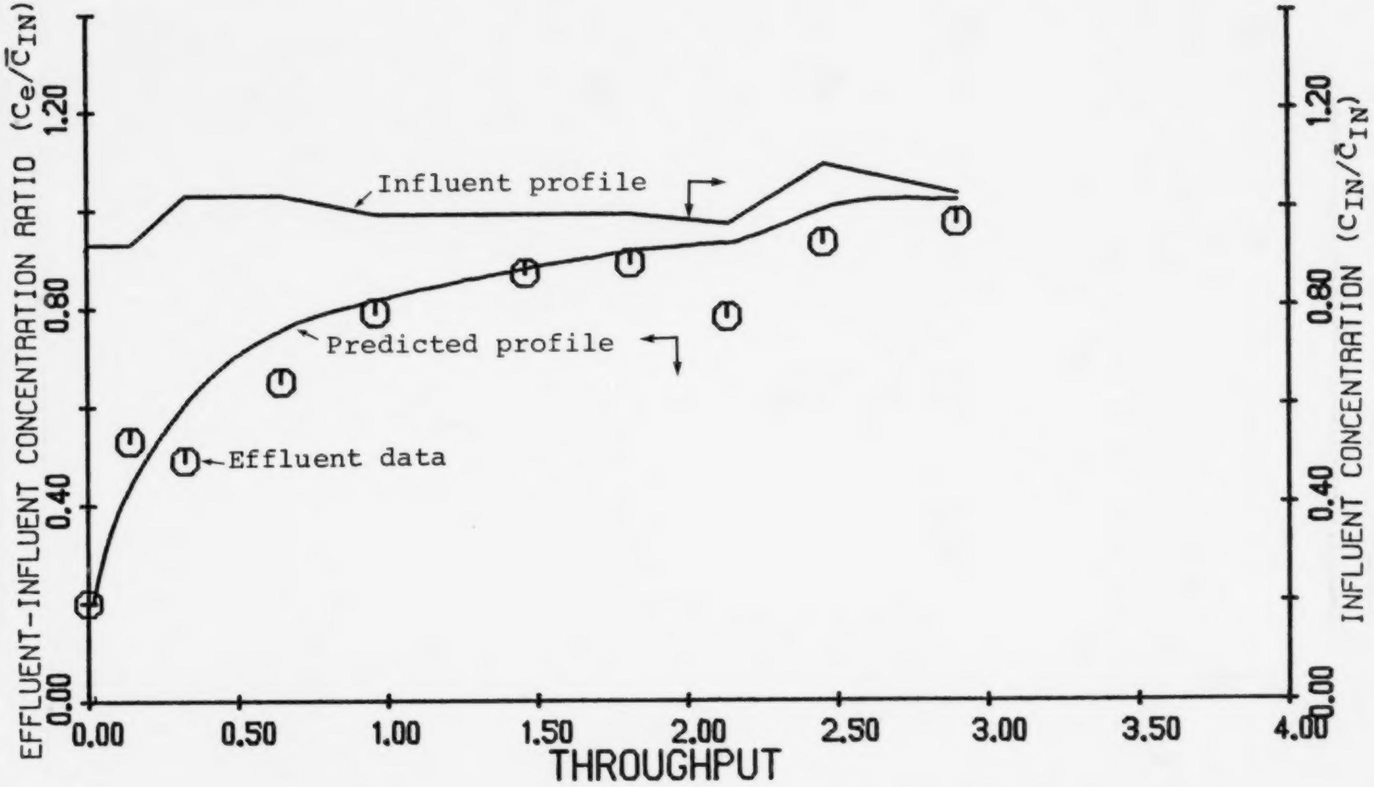

Figure 39. Effluent and influent concentration profiles for humic acids in DDW,
C_o=5ppm, empty bed contact time (EBCT) = 15.6 min.

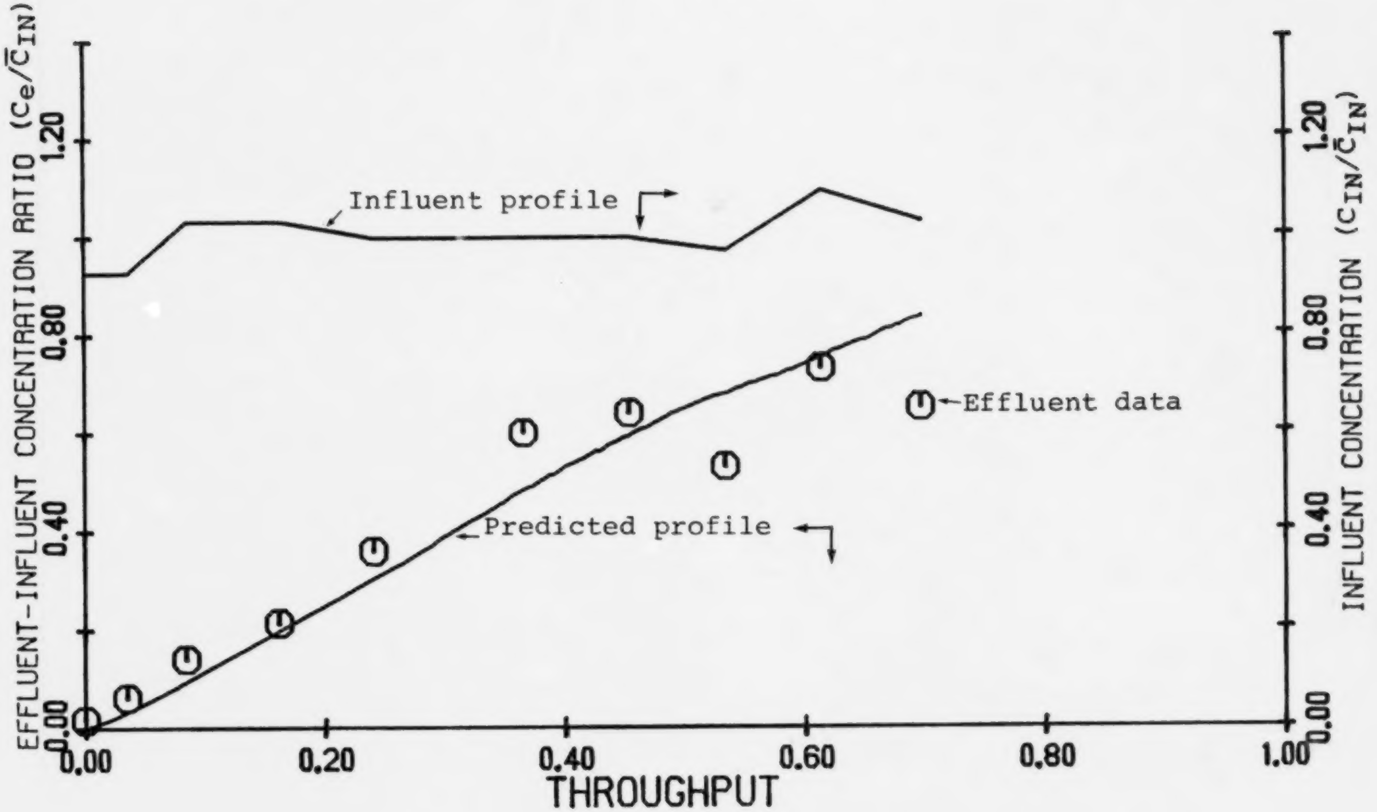

Figure 40. Effluent and influent concentration profiles for humic acid in DDW, C_o=5ppm, EBCT = 62.4 min.

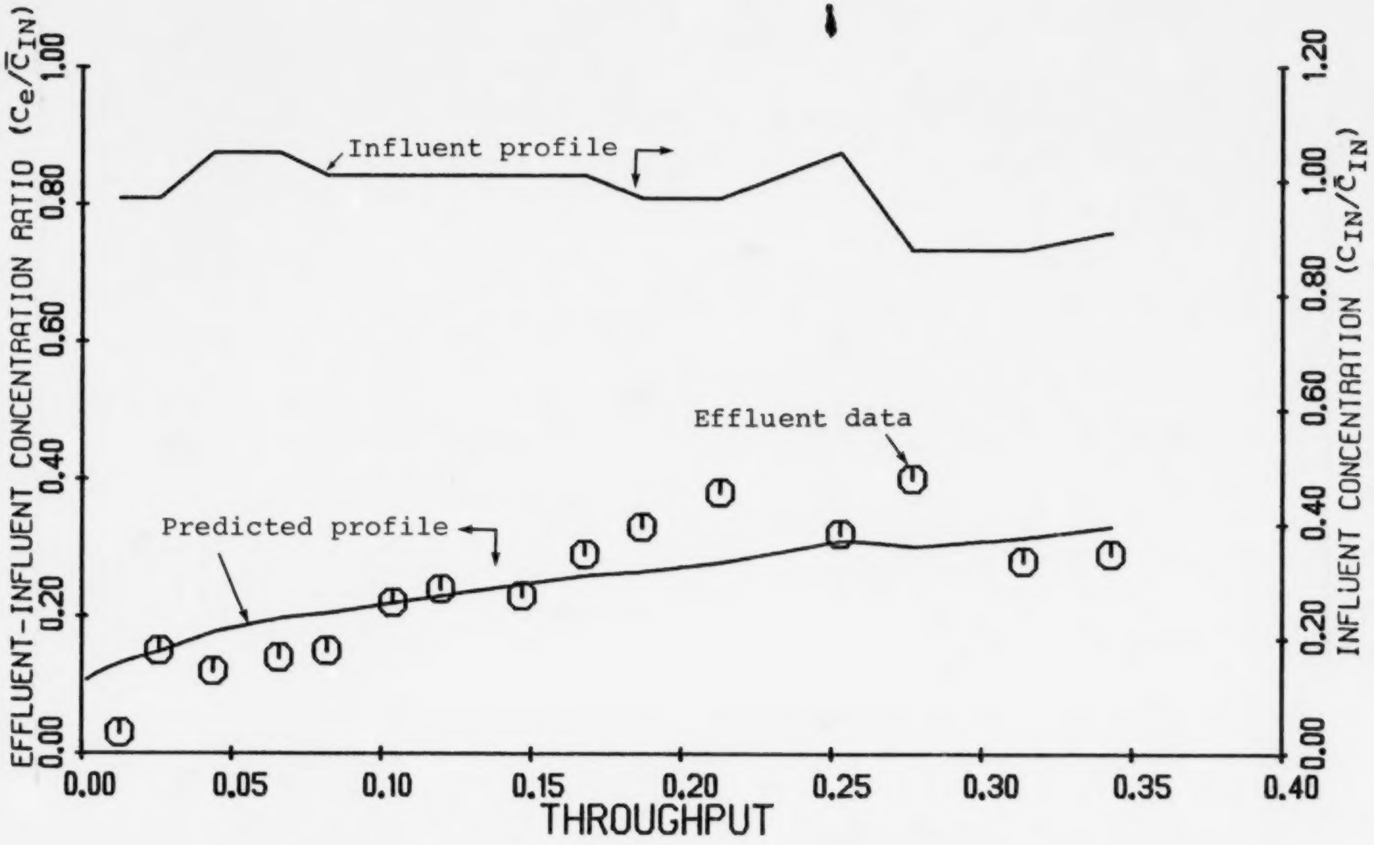

Figure 41. Effluent and influent concentration profiles for humic acids in tap water,
C_o=5ppm, EBCT = 15.6 min.

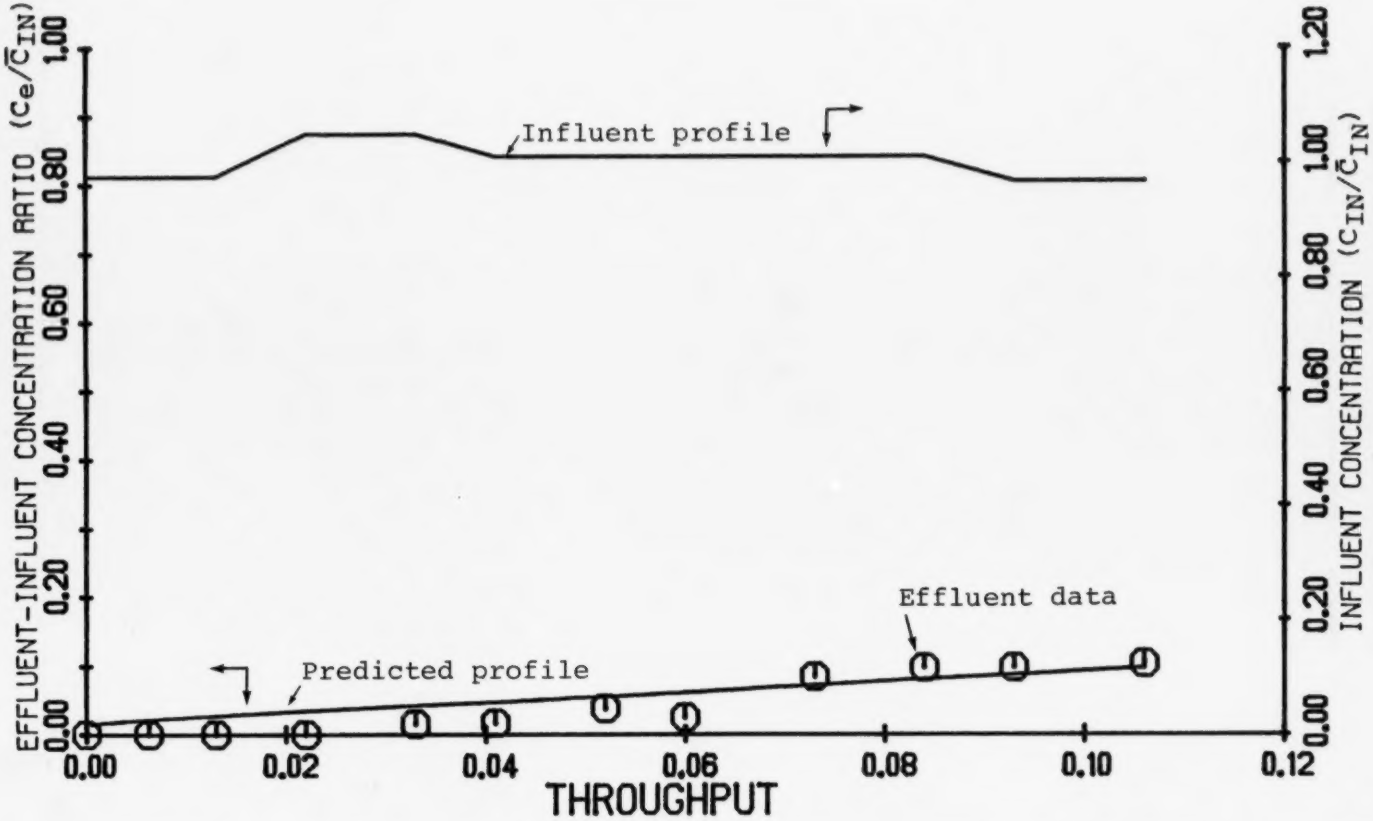

Figure 42. Effluent and influent concentration profiles for humic acids in tap water, C_o=5ppm, EBCT = 31.2 min.

TYPING GUIDE SHEET

TABLE 9. PARAMETERS USED FOR FIXED-BED ADSORBER PREDICTIVE BREAKTHROUGH PROFILES FOR HUMIC ACIDS

Number	Background Solution	$\overline{C}_{in}$ (mg/l)	L (cm)	γ	v, (cm/sec)	k_f (cm/sec)	D_s' (cm^2/sec)
1	DDW	5	123	0.4	0.33	5.0×10^{-5}	2.0×10^{-10}
2	DDW	5	492	0.4	0.33	5.0×10^{-5}	2.0×10^{-10}
3	Tap Water	5	123	0.4	0.33	7.0×10^{-5}	2.0×10^{-10}
4	Tap Water	5	246	0.4	0.33	7.0×10^{-5}	2.0×10^{-10}

$\overline{C}_{in}$: Average influent concentration;

L: Bed length;

γ: Bed porosity, dimensionless;

v: Interstitial fluid velocity;

k_f: Film transfer coefficient; and,

D_s: Surface diffusion coefficient.

EPA-287 (Cin.)
(4-76)

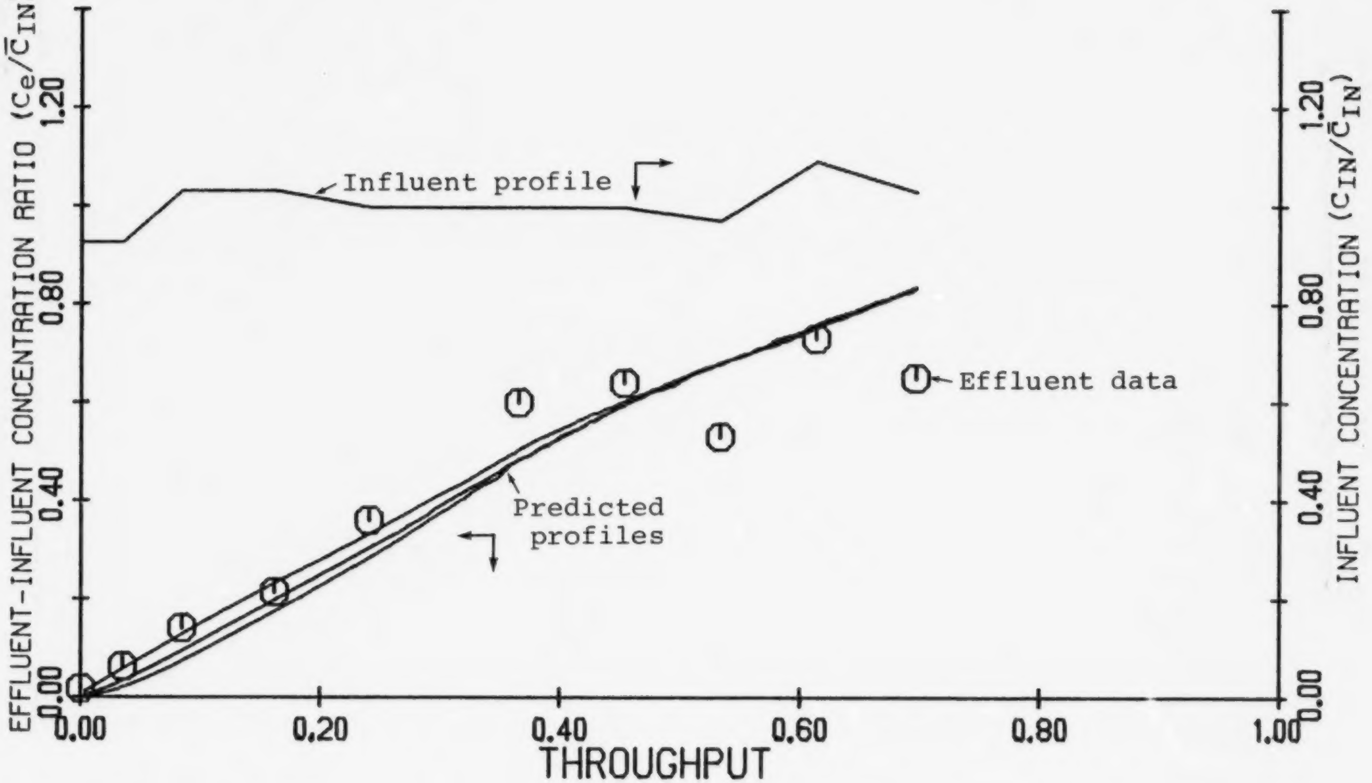

Figure 43. Sensitivity analyses of breakthrough profiles relative to the film transfer coefficient, $k_f \pm 25\%$, for humic acids in DDW.

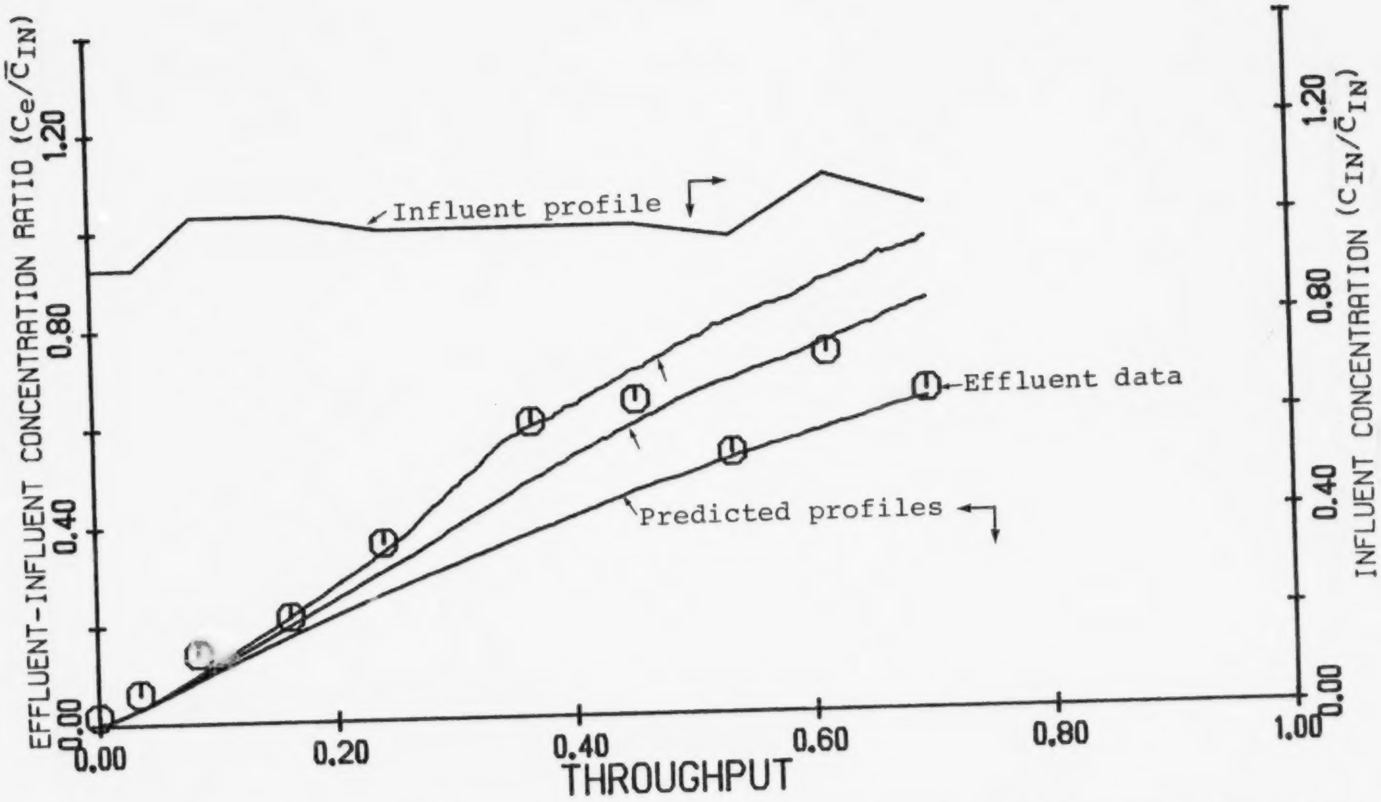

Figure 44. Sensitivity analyses of breakthrough profiles relative to the film transfer coefficient, $D_s \pm 8\%$, for humic acids in DDW.

validity of a strictly physicochemical model in such cases, and resort must be made to a model which incorporates biological dynamics, such as the biophysicochemical version of MADAM developed by Ying and Weber (1979).

MECHANISMS OF REMOVAL

A notable characteristic of the column data presented in Figures 31 and 32 is the relatively rapid approach of the breakthrough profile to an apparent plateau. This is true to all adsorption column experiments conducted with humic acids for this investigation, and has likewise been observed in other studies. This rapid partial breakthrough followed by an extensive plateau is not characteristic of simple adsorption processes. In columns that have been run for close to 1,000 hours (well beyond the carbon's adsorptive capacity for humic acids), the effluent concentration commonly fails to rise above a maximum breakthrough corresponding to a plateau (Weber _et al_, 1978). As evidenced by the data in Figure 45, the precise level of the plateau varies with system particulars and operating conditions. Various mechanisms have been proposed for the near steady-state removal observed at the breakthrough plateaus; the two most prominent mechanisms are catalytic oxidation and biological degradation of the humic substances, although secondary micropore diffusion is another possibility.

Biological growth on granular activated carbon in water treatment applications results from a favorable environment characterized by abundant attachment sites, areas sheltered from fluid shear forces, and substrate and oxygen enrichment (Weber _et al_, 1973; Weber and Ying, 1978). The resulting biofilm may affect the adsorption characteristics of the carbon by acting as a physical barrier and by altering mass transport rates. The microorganisms also oxidize certain organic compounds in the outer biolayer, thus effectively lowering the organic loading imposed on the carbon (Weber _et al_, 1973; Weber and Ying, 1978).

Materials and methods used to suppress biological activity in experimental adsorption systems must be carefully selected if the results are to be interpreted quantitatively. The inhibitor must be toxic to microorganisms at low concentrations and in the required pH ranges. At the same time it must be neither reacted with, nor adsorbed by, either the carbon or the sorbate. Commonly used inhibitors include oligodynamic heavy metals and chlorine; in view of the findings reported earlier in this section difficulty was anticipated in the use of these materials in the humic acids-activated carbon column systems. In this research, attempts were made to quantify the effects of the bio-oxidation by conducting comparative column experiments in the presence and absence of biological growth. These experiments were unsuccessful because a suitable method could not be developed to inhibit growth without affecting the adsorptive properties of either the carbon or of the humic acids. A detailed presentation of the biological inhibition experiments is presented in Appendix J.

Cupric, mercuric and silver ions are known biological inhibitors, and silver has been used successfully in some studies for inhibition of biogrowth in activated carbon columns treating systems containing no humic acids (Ying, 1978). These metals were all tested for adsorption on carbon and for reactivity with humic acids. Mercuric ions were strongly adsorbed by the carbon. Cupric and silver ions were not appreciably adsorbed, but potentiometric titrations of solutions of humic acids containing these ions demonstrated a high degree of complexation, as illustrated in Figures 45 and 46 for Ag^+ and Cu^{2+} respectively. In addition to eliminating these substances as inhibitors, these experiments also reinforced some of the earlier postulates regarding metal ion-humic acids complexes.

In the absence of a suitable inhibitor for continuous-flow dynamic column systems, further attempts to use such systems for characterization of the relative role of bio-activity in humic acids removal in adsorbers were abandoned. Consideration was then given to the use of static equilibrium adsorption measurements to gain some insight to the magnitude of bio-oxidation effects.

Two sets of equilibrium experiments were performed. The sealed reactors of one set were autoclaved at 121°C for 20 minutes to ensure sertile conditions; the second set was run under normal non-sterile conditions. The humic acids solutions and carbon contained in these reactors were then continuously mixed over a four-week period at room temperature (20°C ± 1). Some biological growth was evident in the non-autoclaved reactors. The isotherms developed in the two sets of equilibrium experiments indicated no enhanced removal by biological activity. Indeed, the isotherm for the sterile set indicated a greater capacity for uptake of humic acids by the carbon.

Several explanations might account for these results: 1) the autoclave treatment may have caused alterations of the carbon surface, enabling greater adsorption in the sterlized systems; 2) the microbial growth observed in the non-sterile systems may have only partially degraded the humic acids into lower molecular weight fractions, some of which were not as readily adsorbed as the parent compounds; or, 3) the carbon surface acted as a catalyst in a chemical oxidation process and the lower molecular weight fractions were more easily

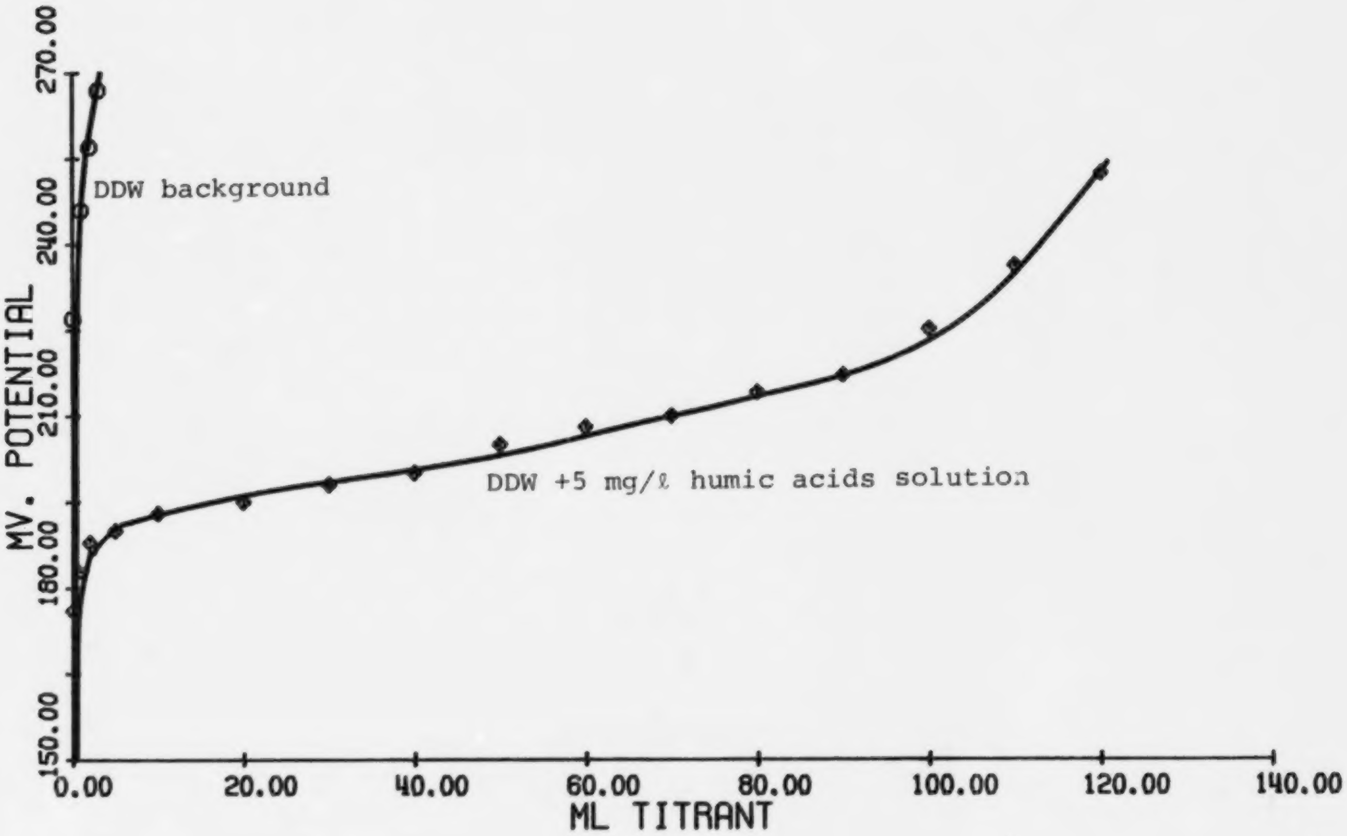

Figure 45. Potentiometric titration curves for Ag^+ (C_o=1.48x$10^{-3}$$\underline{M}$).

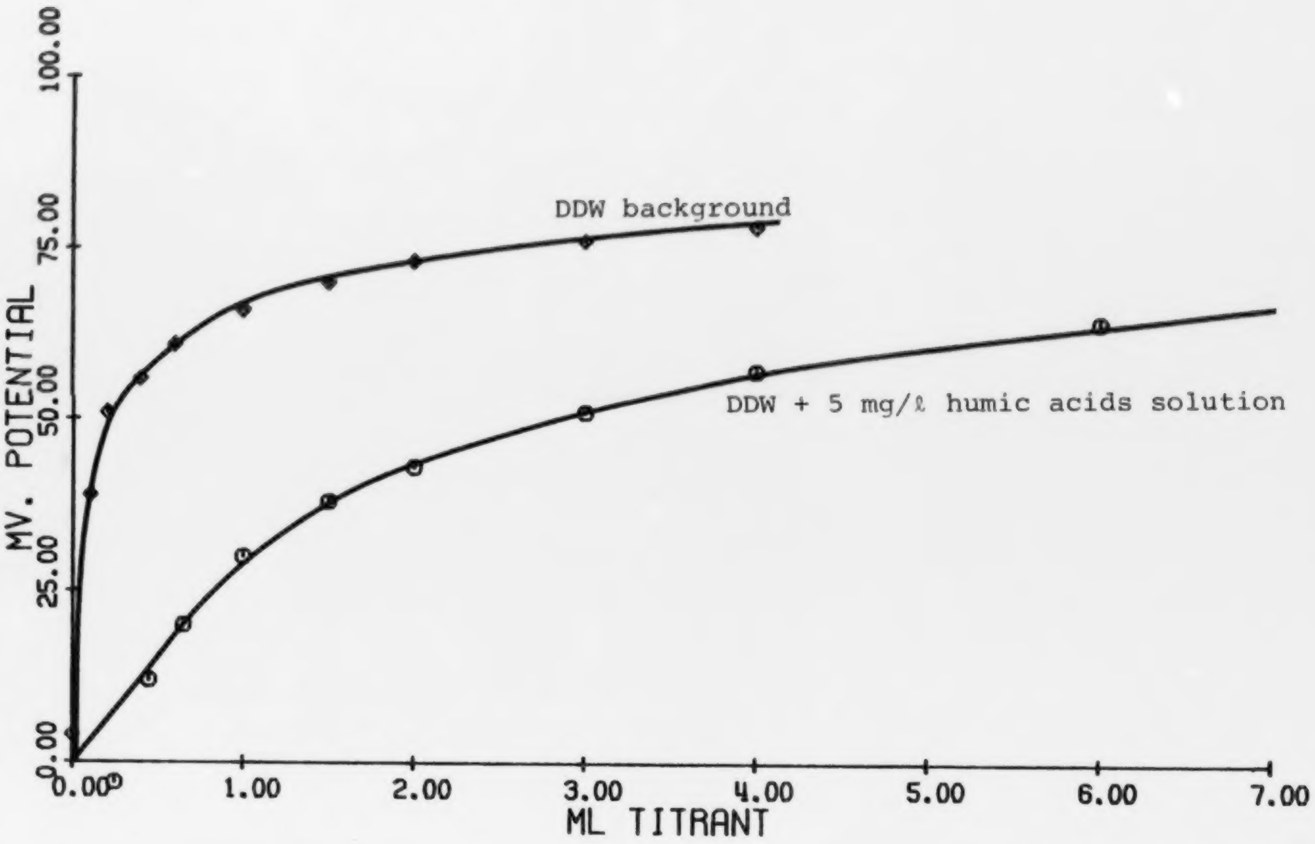

Figure 46. Potentiometric titration curves for Cu^{2+} ($C_o=1x10^{-2}\underline{M}$).

oxidized. The latter two explanations are more reasonable since it is unlikely that the relatively mild autoclaving conditions would significantly change the surface properties of a carbon that was previously activated under much more severe conditions.

These possibilities were further pursued by experiments in which 10g of carbon which had been saturated with humic acids and 10g of fresh carbon were added to separate reactors containing humic acids solution. The concentration of humic acids in each of these reactors was 27 mg/l, well below the residual concentration of the solution that had been used to saturate the one 10g quantity of activated carbon. A third reactor containing the same humic acids solution (but no activated carbon) functioned as a control. The three reactors were sealed and autoclaved at 121°C for twenty minutes. Samples were withdrawn after a 12-hour mixing period and residual concentrations were measured. The humic acids solution exposed to the presaturated carbon was reduced in concentration by 70%, while the concentration of the solution exposed to fresh carbon was reduced only slightly more, by 86%. The concentration in the control was unchanged. The conditions of the autoclaving apparently either altered the carbon surface or caused catalytic oxidation of the presorbed humic acids.

As noted earlier, it is unlikely that the carbon surface would be significantly modified by the relatively mild autoclaving conditions; rather, catalytic oxidation seems more likely. Whether such catalytic oxidation is significant for ambient conditions found in carbon applications for water and wastewater operations is open to speculation. Nonetheless the phenomenon cannot be ruled out as a possible explanation for the observed behavior of humic acids in carbon columns. Nor can partial bio-oxidation of lower molecular weight fractions be eliminated in the presence of ubiquitous growth of bacteria in humic acid-activated carbon systems. A combination of catalytic oxidation and biodegradation is most likely operative in such systems.

SUMMARY AND CONCLUSIONS

1. Ultraviolet spectrophotometry is used for quantification of humic acids. A good correlation was determined between UV absorbance at a specific wavelength of 250 nm and TOC analysis for the type of humic acids (Aldrich) used in this study.

2. Adsorption equilibrium time for humic acids isotherms on granular carbon was determined to be 4-5 weeks. Since only a minor fraction of the Aldrich humic acids is biodegradable, the effect of any biological growth

was minimal during this time period. However, it may be noted that some humic substances are comprised of large fractions of biodegradable compounds; therefore, efforts must be made to inhibit biological growth in order to avoid erroneous results. Because of complexation phenomena, oligodynamic heavy metals and chlorine may not be used. To alleviate this problem, reactors and solutions must be autoclaved prior to carbon additions.

3. Due to disparity in adsorption properties of humic substances obtained from different sources, any generalization about the effectiveness of activated carbon in removing "humic acids" would appear premature.

4. The adsorptive affinity of activated carbon for the humic acids used in this investigation is markedly dependent upon the presence and concentrations of several common constituents of water supplies, including Ca^{2+}, Mg^{2+}, and OCl^{-}. It seems likely that the adsorption mechanism involves formation of ion-humate-carbon complexes. Humic acids have been implicated as trihalomethane precursors, and their removal from water supplies by fixed-bed activated carbon adsorption systems has been recommended. Such treatment might well be rendered more efficient and cost-effective in many instances by addition of relatively simple and inexpensive reagents.

5. Column experiments conducted for humic acids in buffered DDW under different hydraulic loading conditions and a constant residence time demonstrated little difference in removal efficiencies (Figures 31 and 32). This suggests that film transfer is a minor resistance compared to surface diffusion in this system. This phenomenon was further verified by predictive model sensitivity analyses (Figures 43 and 44).

6. It was concluded that MADAM, being a strictly physicochemical model, cannot be truly predictive of adsorber performance in this study because of the existence of biogrowth in the adsorbers. However, because of the relatively small influence of biooxidation, values for the column film transfer coefficient, k_f, and the intraparticle diffusion coefficient, D_s, were determined from column simulation. These values were successfully used for model verification. Further substantiation of the validity of such an approach is necessary before definite general conclusions can be made.

SECTION 7

ADSORPTION OF CARBON TETRACHLORIDE

BACKGROUND

Carbon tetrachloride (CCl_4) is a colorless heavy liquid first observed by Regnault (~1840) as a product of the reaction between chlorine and chloroform in sunlight. Commercial manufacture of CCl_4 involves the chlorination of either carbon disulfide in the presence of an iron catalyst or the chlorination of hydrocarbons such as methane (Kirk-Othmer, Encyclopedia of Chemical Technology, 1964). The first of these methods is most widely used because of inherent temperature disadvantages associated with the exothermic reactions of the latter method.

Carbon tetrachloride is relatively stable in comparison to chloroform, trichloroethylene and other related compounds. It hydrolyzes slowly in contact with water to form hydrochloric acid. At high temperatures and in the presence of metal catalysts CCl_4 becomes much more reactive, even serving as chlorinating agent at 250°C. Table 10 summarizes the physical and chemical properties of carbon tetrachloride.

Near the turn of the 20th century, CCl_4 was widely used as a solvent, dry-cleaning agent, fire extinguisher, grain fumigant, and machinery and metal cleaner (degreaser). Use of this compound as a solvent and clothing dry-cleaner related to its ability to dissolve oils, greases, waxes, tars, and other organic compounds. By 1949, however, because of its metal corrosivity and high volatility, CCl_4 was largely displaced in this application by tetrachloroethylene, a similar chemical with comparable solvent characteristics (Kirk-Othmer, Encyclopedia of Chemical Technolgoy, 1964). CCl_4 continued in wide-spread use as a fire extinguisher, largely due to its non-flammable character and non-conducting properties. Although U.S. production of CCl_4 increased between 1940 and and 1972, its uses in the dispersive type applications cited above decreased from 84% to 7% of its total production (Singh et al, 1976). This was due in large measure to increased recognition of the acute and chronic toxicity of carbon tetrachloride and the substitution of less harmful materials for applications which would result in dispersion of such substances to the environment.

TABLE 10. PHYSICAL AND CHEMICAL PROPERTIES OF CARBON TETRACHLORIDE*

Formula Weight	153.82
Crystaline Form and Color	Colorless Liquid
Specific Gravity (at 20°C)	1.594
Melting Point	-22.96°C
Boiling Point	76.8°C
Heat of Vaporization	46.5 cal/gram
Solubility	
a) Water (at 20°C)	0.08%
b) Alcohol, ether, and benzene	∞
Viscosity (at 25°C)	0.88 centipoise
Vapor Pressure	log p=7.58248 - 1644.41/T
Dielectric Constant	2.24

* Sources: Lange's Handbook of Chemistry, 1979; CRC Handbook of Chemistry and Physics, 1976-1977; Kirk-Othmer, Encyclopedia of Chemical Technology, 1949).

The principal use of CCl_4 since 1950 has been as a primary reactant in production of refrigerants (chloroflurocarbons-Freons). These refrigerants are mixtures of fluorine and chlorine derivatives of methane, which result when anhydrous hydrofluoric acid is reacted with carbon tetrachloride in the presence of appropriate catalysts. Compounds ranging from fluorotrichloromethane to tetrafluoromethane are formed, depending on reaction intensity (Kirk-Othmer, Encyclopedia of Chemical Technology, 1964).

Sources and Sinks in the Environment

Virtually all carbon tetrachloride involved in dispersive uses is eventually released to the environment. It has been estimated that approximately 3.04 million tons of CCl_4 have been emitted to the environment to date (Singh et al, 1976). Recent losses have been decreasing due to restricted use in dispersive applications. In 1970, for example, approximately 450,000 metric tons of CCl_4 were produced but only 5% lost to the environment, compared to a loss factor of 95% during the years up to 1930 (Altshuller, 1976; Singh et al, 1976).

Because the only significant breakdown process for CCl_4 is slow reaction with -OH radicals, its long lifetime in the troposphere (longer than 330 years) allows it to diffuse to the stratosphere. The ocean is another final storage area, with an estimated aqueous solution loading of 2-3% of the biospheric loading. The half-life of carbon tetrachloride in the ocean has been reported to be 7 x 10^4 years (Singh et al, 1976).

With respect to the contamination of water supplies, the 1975 National Organic Reconnaissance Survey (NORS) study of 80 cities throughout the USA reported that carbon tetrachloride was found in 12.5 percent of the finished waters and about 4.1 percent of the raw waters (USEPA, 1975). Appearance of CCl_4 in the raw water and finished waters of the city of Zurich, Switzerland, has also been confirmed (Grob and Grob, 1974). The occurrence of CCl_4 in raw waters is frequently due to covert waste discharges (Morris and Johnson, 1976; Ward, 1977); its presence in finished waters when no traces are found in associated raw waters has been attributed to carbon tetrachloride contamination of chlorine used for water treatment (Rook, 1974; Cairo et al, 1979).

Health Effects Assessment

Carbon tetrachloride is believed to be acutely and chronically harmful to animals and humans. It is capable of being absorbed through intact skin and, like chloroform, can act as an anesthetic and narcotic. CCl_4 has induced cancer in laboratory animals, and is strongly suspected of being a human carcinogen (NCI Report, 1976). Metabolic intermediates of carbon tetrachloride have been demonstrated to cause liver damage, either by binding to critical cellular elements or by inducing peroxidation of lipid structural elements (De Ferreyra et al, 1975; Gingerich et al, 1978). Persons with impaired liver or kidney functions, or who are critically ill, are more susceptible to the harmful effects of carbon tetrachloride. Such toxicological observations have prompted Region 3 of the EPA to adopt a 2-μg/l limit on CCl_4 concentrations in finished drinking waters and to require investigations to determine source(s) of CCl_4 if this limit is exceeded (Cairo et al, 1979).

ANALYTICAL PROCEDURES

General

Precise quantitative determination of residual concentrations of trace organics in the μg/l range requires analytical procedures which are highly sensitive. Further, when such measurements are to be made in conjunction with evaluations of treatment processes such as adsorption, they must be compatible with the experimental methodologies associated with the process studies. General and specific characteristics inherent to particular analytical methods must be considered in both these regards. These characteristics include: efficiency, limits of detection, particular interferences, speed and ease of analysis, pretreatments requried on samples prior to analysis, sample size, reproducibility, and cost and availability of materials.

Three principal factors generally affect the validity of the analytical procedures: 1) type of analysis and of associated detector systems used; 2) technique employed for sample collection and concentrations; and, 3) type of system to which sample collection and analysis is applied (i.e., configureation of the system, frequency of sampling, and type of analysis necessary for evaluation).

Several different analytical procedures were evaluated for analysis of carbon tetrachloride. All of these procedures demonstrated compatibility with the methodologies employed for evaluation of the adsorption properties and characteristics of carbon tetrachloride.

Analysis

Gas chromatography was used for analysis of carbon tetrachloride. A Varian 2700 gas chromatograph equipped with a scandium tritide electron capture detector was employed for samples in which carbon tetrachloride was present in very low concentration. The chromatograph was equipped with a 6' x 1/8" stainless steel column packed with 20% SP 2100/0.1% Carbowax 1500 on 100/120 Supelcoport obtained from Supelco, Inc. Operating temperatures were: 70°C for the column; 130°C for the injector; and 240°C for the detector. Prepurified nitrogen was used as carrier gas, at a flow rate of 20 ml/min. The detector response was recorded with a Hewlett

Packard 7123A strip chart recorder. The detector was highly sensitive, but linear only over a small range of mass. The most sensitive linear response of the detector corresponded to the mass range from 0.1 to 0.7 ng of carbon tetrachloride. Injection volumes were therefore varied from 2.0 to 9.0 µl, and extraction volumes from 1.0 to 5.0 ml, to keep the of CCl_4 analyzed within this range.

To eliminate the problems associated with the characteristically small linear range of response of the scandium tritide electron capture detector, more concentrated samples were analyzed using a Varian 1700 gas chromatograph equipped with a Tracor Instruments Model 700 Hall electrolytic conductivity detector, in the chlorine detection mode. Although the limit of detection (≈10 µg/l) of the electrolytic conductivity detector was not as low as that for the electron capture detector, it exhibited a wide range of linear response for masses greater than 1.0 ng of carbon tetrachloride, in addition to being specific for detection of the chlorine atom.

The Varian 1700 gas chromatograph was equipped with a column similar to that described earlier. A 20-ml/min flow rate of nitrogen carrier gas was used, and the following temperature conditions employed: 70°C for the column; 130°C for the injector, 150°C from the column to the pyrolysis oven, and 850°C for the pyrolysis oven. The detector response was recorded with a Heath Schlumberger Model SR 255B strip chart recorder. A discussion of the preparation of carbon tetrachloride standards is presented in Appendix K.

Sample Collection and Concentration

Dynamic Headspace--

The stripping and pre-adsorption technique developed by Bellar and Lichtenberg (1974) for volatile halogenated compounds was investigated as a potential technique for the analysis of carbon tetrachloride at $\leq$ 1 µg/l. The method involved quantitative removal of carbon tetrachloride from water by purging with pre-purified nitrogen gas at room temperature and subsequently trapping the solute on a 60/80 U.S. Standard mesh size Tanax-GC adsorbent. The carbon tetrachloride was then desorbed at room temperature into a 6-ft., 1/8-inch stainless steel gas chromatographic column packed with 60/80 mesh Chromosorb 101. The Varian 1700 gas chromatograph, equipped with the Tracor 700 Hall electrolytic conductivity detector and programmed to the operating conditions described earlier, was used for analysis.

This technique, although highly efficient and reproducible, required special equipment for the stripping, adsorption, and desorption procedures and demanded considerable amounts of time for the large number of samples to be analyzed.

Static Headspace--

Pursuant to Henry's law for dilute solutions, the concentration of a gas dissolved in a liquid is proportional at equilibrium to the partial pressure of that gas in the vapor phase, or headspace gas. Static headspace has been reported to be a sensitive technique for halomethane detection (Morris and Johnson, 1976). For evaluation of this procedure, in which compounds of interest in a water sample are brought to equilibrium with the headspace in a closed container, water samples were spiked with carbon tetrachloride and agitated in sealed reactors for one hour at constant temperature to achieve equilibrium. A sample of the headspace gas was then removed and analyzed using the Varian 2700 gas chromatograph fitted with a 6 ft., 1/8-inch stainless steel column packed with 60/80 mesh Chromosorb 101 and equipped with a scandium tritide electron capture detector.

The procedure, as previously discussed by Weber et al, (1977), was efficient and reproducible, but highly temperature sensitive. Further, the presence of solid, liquid, and vapor phases in adsorption experiments would require a total mass balance estimation necessitating preparation of two sets of calibration curves.

Aqueous Injection--

Nicholson and Meresz (1976) developed a technique whereby aqueous samples are directly injected into the gas chromatograph using a Sc^3H electron capture detector. A detection limit of 1 μg/l was reported for target haloforms. A similar procedure using a ^{63}Ni electron capture detector was employed by Hammarstrand (1976) for chloroform; a detection limit of 1 μg/l was specified.

This technique was evaluated for analysis of carbon tetrachloride using the Varian 2700 gas chromatograph equipped with the scandium tritide electron capture detector and a 6-ft., 1/4-inch glass column packed with 60/80 mesh Chromosorb 101. It was found, however, that aqueous injection was detrimental to the detector, substantially shortening its useful life.

Liquid-Liquid Extraction--

Liquid-liquid extraction techniques have attracted considerable interest since the development of specific modifications for the analysis of haloforms (e.g., Henderson et al, 1976; Mieure, 1977). In general, these techniques involve extraction into an organic solvent followed by measurement by electron capture gas chromatography. A detection limit of less than 1 μg/l can be obtained by this method.

The liquid-liquid extraction technique was found to be the most attractive alternative for the present work, particularly with respect to compatibility with the adsorption experiments. In this procedure, 5-10 ml samples were mixed with 1-5 ml of Phillips 66 Pure Grade n-hexane and 0.5-1 g of Baker Analyzed sodium chloride in 10-20 ml vials fitted with Teflon-coated screw-on caps. The samples were shaken vigorously for 1 minute, the hexane allowed to separate, and solute analysis performed by injecting a few microliters of the extract into a gas chromatograph.

ADSORPTION METHODOLOGIES

Equilibrium Studies

Adsorption equilibrium experiments for carbon tetrachloride were conducted using both bottle-point techniques and a mini-adsorber-column procedure.

Two distinct methods of preparing and analyzing the isotherms were evaluated in the bottle-point experiments; these were the static-headspace and liquid-liquid extraction techniques described above. Each method yielded results which were easily reproduced by the other method.

The static headspace method consisted of placing different amounts of granular activated carbon in each of a series of carefully cleaned and muffled (heated in a muffle furnace at 400°C for 2 hours) 150 ml air-tight Hypo-Vials. The vials were then filled with 100 ml of background solution spiked with carbon tetrachloride. Background solutions included, for different experiments, organic-free water (OFW), deionized glass-distilled water passed through a milli-Q water purifier, Millipore, Inc., and 5 mg/l of humic acid prepared in OFW water. The vials were quickly sealed using Teflon-coated septa and crimped-on aluminum caps. The samples and the standards were agitated at constant room temperature for four days to achieve equilibrium. A series of standards containing no carbon was run under identical conditions for each experiment.

Equilibrium vapor phase concentrations were determined by injecting 0.1 to 0.5 ml of the overhead gas from each vial into the gas chromatograph and comparing detector response with a calibration curve prepared using known weights of compound dissolved in hexane solvent. The amount of compound in the vapor phase of each system containing carbon was then compared with the vapor concentrations of the standards to yield, after correction for vapor-solution equilibria, the

TYPING GUIDE SHEET

final aqueous concentration of the sample.

The amount of the compound adsorbed on the carbon was determined by subtracting the sum of the amount in the liquid phase and the amount in the vapor phase from the initial amount added to the vial.

The liquid-liquid extraction procedure was employed in adsorption experiments conducted in a manner similar to that discussed above, except that there was no vapor headspaces in the Hypo-Vials used to bring the activated carbon and CCl_4 solution to equilibrium. After equilibrium had been achieved, a 10-ml aliquot of each sample was subjected to liquid-liquid extraction with the solvent system described earlier in this section. A calibration curve of relating concentration of a standard solution to detector response was used for determination of the sample concentration.

Four sets of mini-column studies were conducted to evaluate dynamic adsorption capacities of activated carbon with respect to four different influent concentrations of carbon tetrachloride. These concentrations were chosen to cover a broad range; i.e., 50, 200, 600, and 2,000 μg/l. Feed solutions of CCl_4 were prepared in 12-gal glass carboys using OFW. A second carboy of 5-gallon capacity was used in each experiment to attenuate variations in influent concentration. A 0.5 mm-ID capillary column was pierced through the Teflon-coated stopper of the larger carboy to prevent formation of a vacuum as solution was displaced. A precision volumetric pump (Flow Metering, Inc. model #RP-SY) was employed to transfer the solution through Teflon tubing to a 1-ft long glass adsorber having an internal diameter of 1 cm and containing a 1-gram quantity of 50/60 U.S. standard sieve size activated carbon. A flow rate of 1.56 gpm/ft^2 (50 $l/m^2/min$) was maintained in all column runs. The experimental apparatus and arrangement is illustrated in Figure 47. Effluent and influent samples were collected in glass vials and subjected to liquid-liquid extraction and G.C. analysis.

Rate Studies

CMB-reactor adsorption rate experiments were conducted for carbon tetrachloride -- individually and in the presence of humic acid -- in carefully sealed 2.6-liter glass reactors of the type illustrated in Figure 48. Weighed and pre-wetted quantities of granular activated carbon were added to appropriate experimental solutions (pH 7; OFW or 5 mg/l humic acid prepared in OFW background solution) in the vapor-phase-free reactors. The carbon was dispersed by a motor-driven glass stirrer and 5-ml samples withdrawn at fixed time intervals using a 10-ml hypodermic syringe. A displacement plunger

EPA-287 (Cin.)
(4-76)

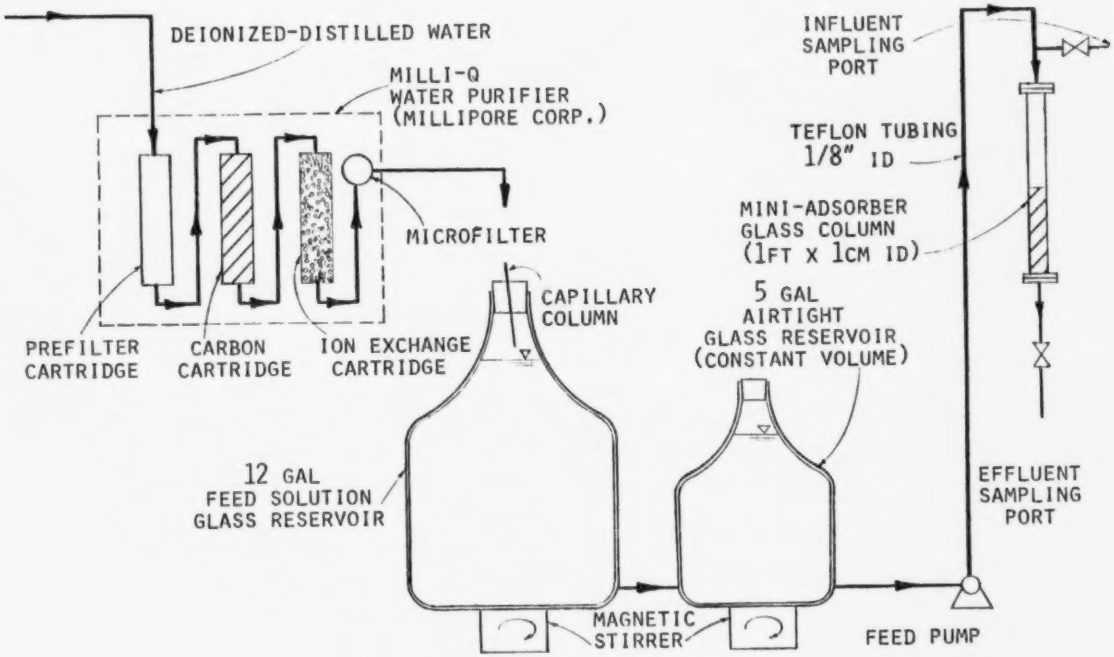
DEIONIZED-DISTILLED WATER
MILLI-Q WATER PURIFIER (MILLIPORE CORP.)
MICROFILTER
PREFILTER CARTRIDGE
CARBON CARTRIDGE
ION EXCHANGE CARTRIDGE
CAPILLARY COLUMN
12 GAL FEED SOLUTION GLASS RESERVOIR
5 GAL AIRTIGHT GLASS RESERVOIR (CONSTANT VOLUME)
MAGNETIC STIRRER
FEED PUMP
INFLUENT SAMPLING PORT
TEFLON TUBING 1/8" ID
MINI-ADSORBER GLASS COLUMN (1FT x 1CM ID)
EFFLUENT SAMPLING PORT

Figure 47. Experimental apparatus for mini-column adsorber studies.

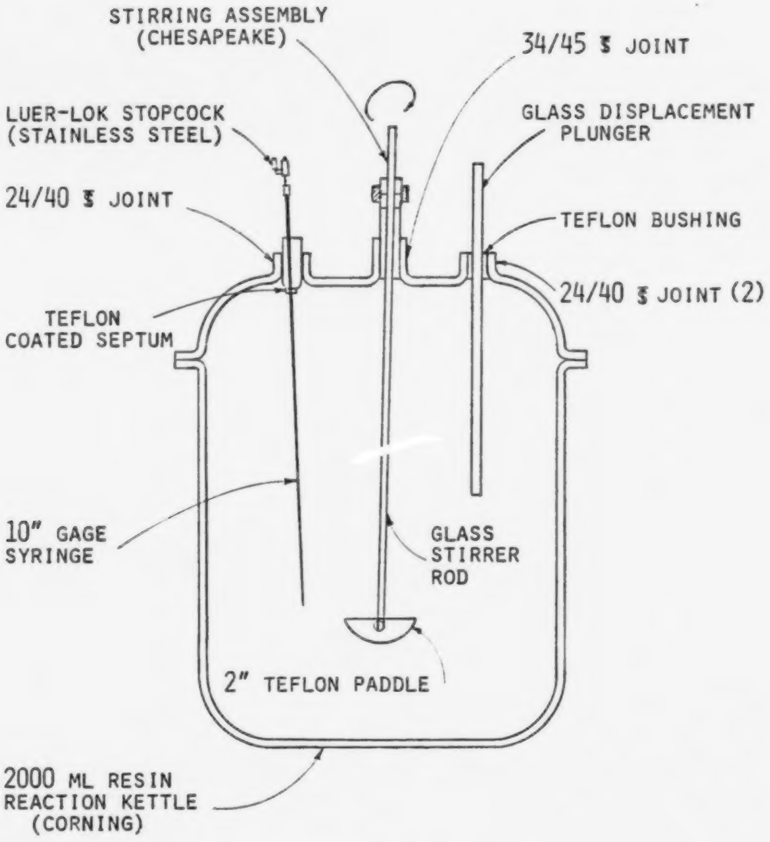
STIRRING ASSEMBLY (CHESAPEAKE)
34/45 ₮ JOINT
LUER-LOK STOPCOCK (STAINLESS STEEL)
GLASS DISPLACEMENT PLUNGER
24/40 ₮ JOINT
TEFLON BUSHING
TEFLON COATED SEPTUM
24/40 ₮ JOINT (2)
10" GAGE SYRINGE
GLASS STIRRER ROD
2" TEFLON PADDLE
2000 ML RESIN REACTION KETTLE (CORNING)

Figure 48. Schematic illustration of the CMB reactor.

built into the reactor eliminated introduction of headspace by sample volume displacement.

Both dynamic headspace and liquid-liquid extraction techniques were found to be compatible with the methods employed in the CMB adsorption rate studies with carbon tetrachloride. The liquid-liquid extraction procedure was used for most of the studies because it involved less time.

The reactor systems and experimental procedures devised for these rate studies were particularly successful. The reactor design eliminated potential solute loss by volatilization and evaporation. Further, because the solution in the CMB reactor was in contact only with glass and Teflon, no measureable sorbate loss to containing surfaces was encountered. Elimination of these losses is extremely important when rate studies are performed with very dilute solutions of volatile compounds.

Column Studies

Column studies were conducted for evaluation of breakthrough profiles for carbon tetrachloride. Saturated solutions of carbon tetrachloride were prepared in 200-liter air-tight stainless steel feed tanks. After reaching saturation, the experimental aqueous feed solutions were kept in constant contact with carbon tetrachloride vapor.

Saturated solution was withdrawn by high precision volumetric pumps, diluted to appropriate concentration with high purity water, and then passed through glass mixing chambers to the adsorbers. All transfer tubing was stainless steel and/or Teflon. Each adsorber was comprised of a 6-ft long glass column with an internal diameter of 3 cm containing a 250-gram quantity of 16/20 U.S. standard sieve size activated carbon. Influent and effluent samples were collected in 20-ml vials. Care was taken during sample transfer to minimize carbon tetrachloride loss by volatilization. The samples were then concentrated using the liquid-liquid extraction technique and analyzed by gas chromatography. Figure 49 illustrates the experimental apparatus and arrangement.

Two major problems were encountered during the course of these experiments. First, the influent concentration fluctuated considerably, perhaps due to blockage of the carbon tetrachloride solution transfer tubing. This necessitated frequent maintenance and re-adjustment. Second, biological growth on carbon particles in the adsorber generated considerable headloss, requiring periodic air-scouring and backwashing. Various inhibitors for preventing biological growth were evaluated to permit singular determination of appropriate adsorption parameters. Silver was chosen because

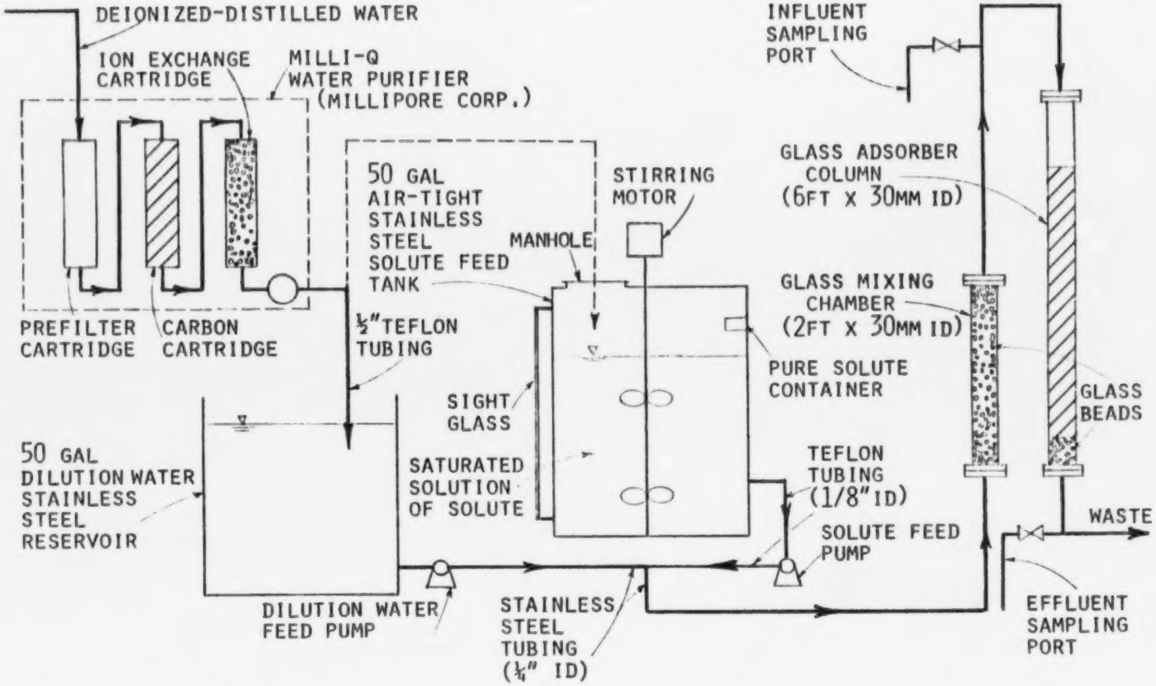
DEIONIZED-DISTILLED WATER
ION EXCHANGE CARTRIDGE
MILLI-Q WATER PURIFIER (MILLIPORE CORP.)
PREFILTER CARTRIDGE
CARBON CARTRIDGE
50 GAL AIR-TIGHT STAINLESS STEEL SOLUTE FEED TANK
MANHOLE
STIRRING MOTOR
½"TEFLON TUBING
SIGHT GLASS
SATURATED SOLUTION OF SOLUTE
PURE SOLUTE CONTAINER
50 GAL DILUTION WATER STAINLESS STEEL RESERVOIR
DILUTION WATER FEED PUMP
STAINLESS STEEL TUBING (¼" ID)
TEFLON TUBING (1/8"ID)
SOLUTE FEED PUMP
INFLUENT SAMPLING PORT
GLASS ADSORBER COLUMN (6FT X 30MM ID)
GLASS MIXING CHAMBER (2FT X 30MM ID)
GLASS BEADS
WASTE
EFFLUENT SAMPLING PORT

Figure 49. Experimental apparatus for fixed-bed adsorber study.

of its combined inhibitory effects and relatively weak adsorption; a silver dosage of 2 mg/l was employed.

RESULTS AND DISCUSSION

Adsorption Equilibria

As for humic acid, several different isotherm models were investigated for carbon tetrachloride, and the Freundlich equation was found to provide the most straightforward best fit to the experimental data.

Equilibrium data for carbon tetrachloride derived from both bottle-point and mini-column experiments are presented in Figure 50; some small differences in adsorption capacities obtained by the two methods may be observed. Figure 51 illustrates that pH has no significant effect on the equilibrium adsorption characteristics of carbon tetrachloride. No dependency of equilibrium capacity on carbon particle size was experienced, as illustrated in Figure 52. Further, Figure 53 demonstrates that initial concentration has no significant effect on the position of the isotherm.

Isotherm data from equilibrium experiments performed to characterize the adsorption behavior of carbon tetrachloride in different background solutions are presented in Figures 54 and 55. Figure 54 compares isotherm data for carbon tetrachloride in OFW background solution and in the presence of 5 mg/l humic acid in OFW. Comparative isotherm data for OFW background solutions in Ann Arbor tap water are presented in Figure 55. It is evident from these figures that the equilibrium capacities of activated carbon for CCl_4 are not markedly affected by organic and inorganic background constituents characteristics of raw water sources and finished drinking water supplies. It is important to note, however, that these data pertain only to equilibrium capacities for adsorption, and do not address potential competitive effects relating to adsorption rates. Moreover, they pertain only to systems in which initial adsorption occurs simultaneously for both carbon tetrachloride and potential competitive organics such as humic acids.

To test the possibility that the observed lack of competitive influence of the humic acids on equilibrium capacities for CCl_4 may be due to more rapid equilibration by the latter, additional equilibrium studies were conducted with carbon that was previously equilibrated with humic acids. Figure 56 presents the experimental data and the Freundlich isotherms for this system and for the control. It may be observed that the pre-saturated carbon demonstrated a significantly lower adsorption capacity for carbon tetrachloride.

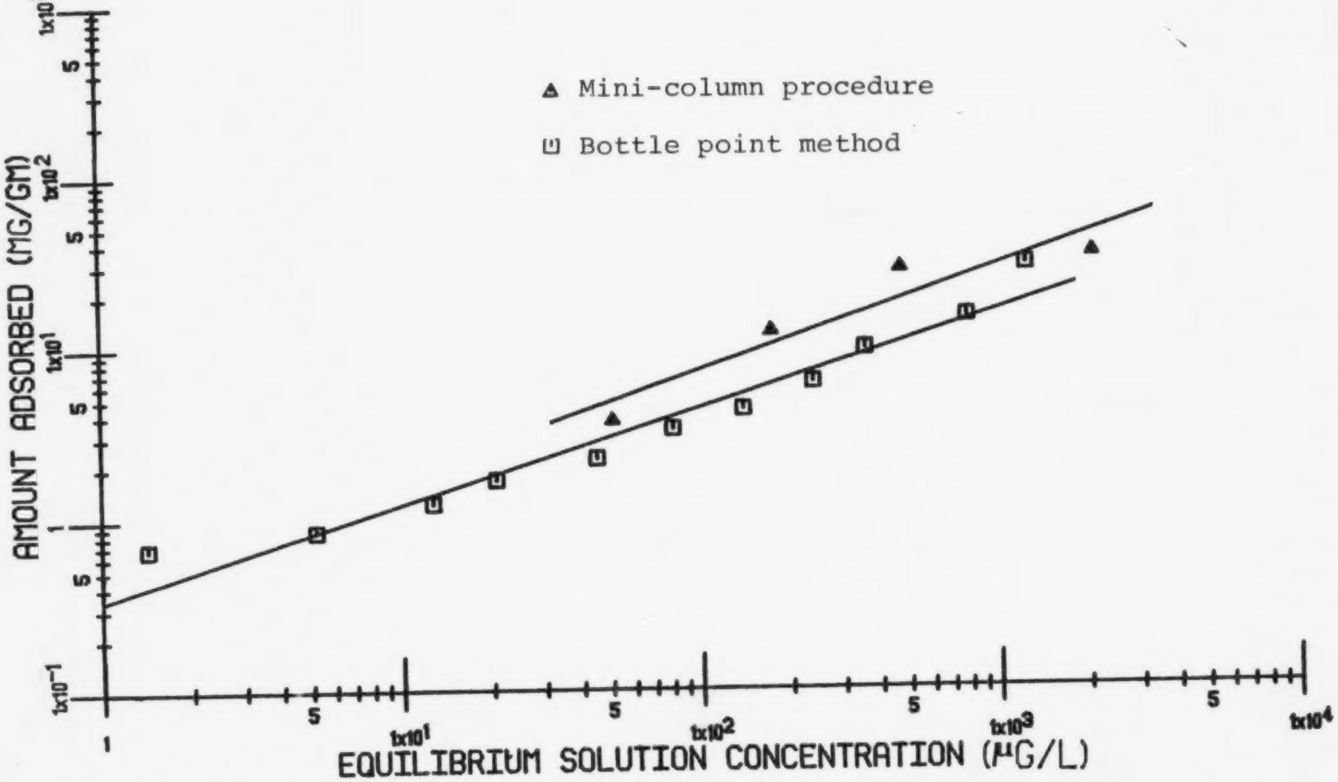

Figure 50. Experimental data and Freundlich isotherms for CCl_4 - a comparison of results from bottle-point and mini-column equilibrium measurements.

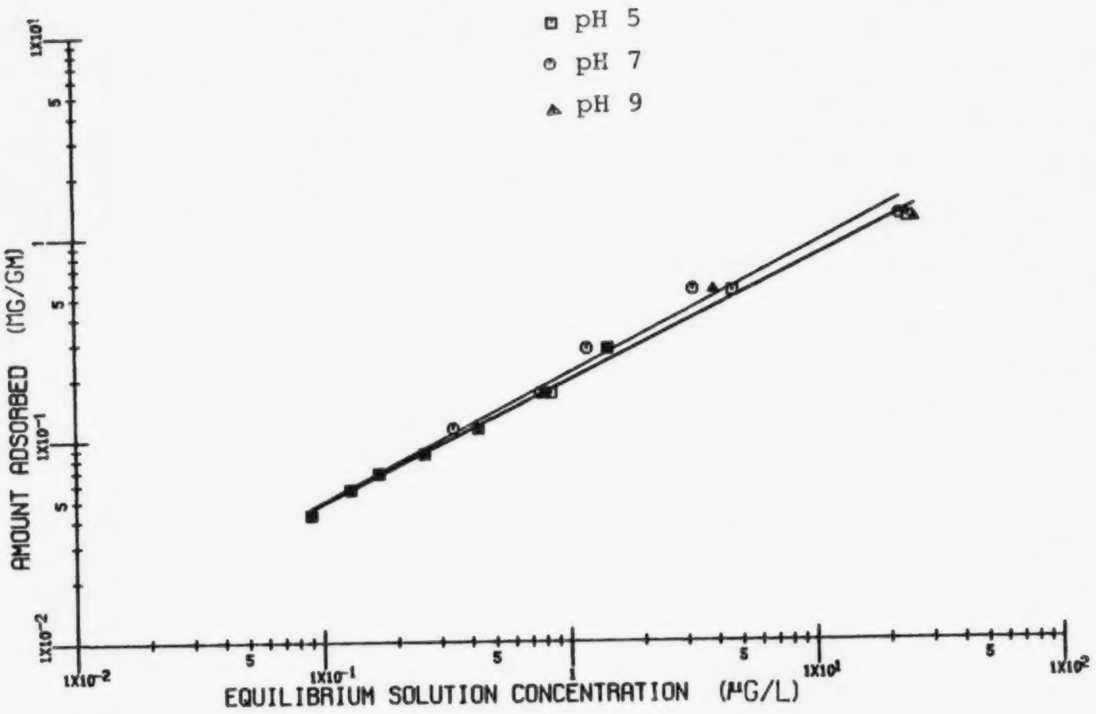

Figure 51. Experimental data and Freundlich isotherms for CCl_4 - the effects of pH on equilibrium capacities.

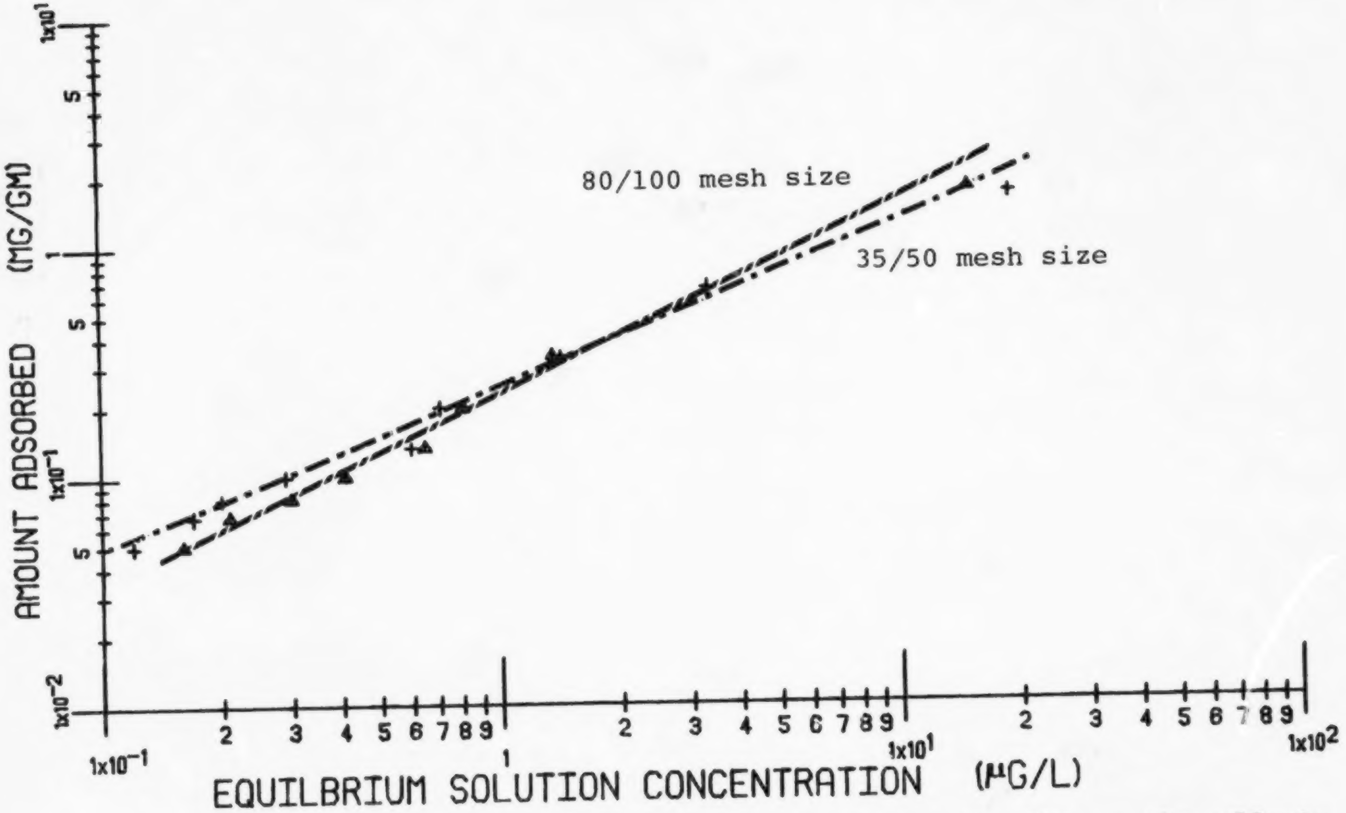

Figure 52. Experimental and Freundlich isotherms for CCl_4 - the effects of particle size on equilibrium capacities.

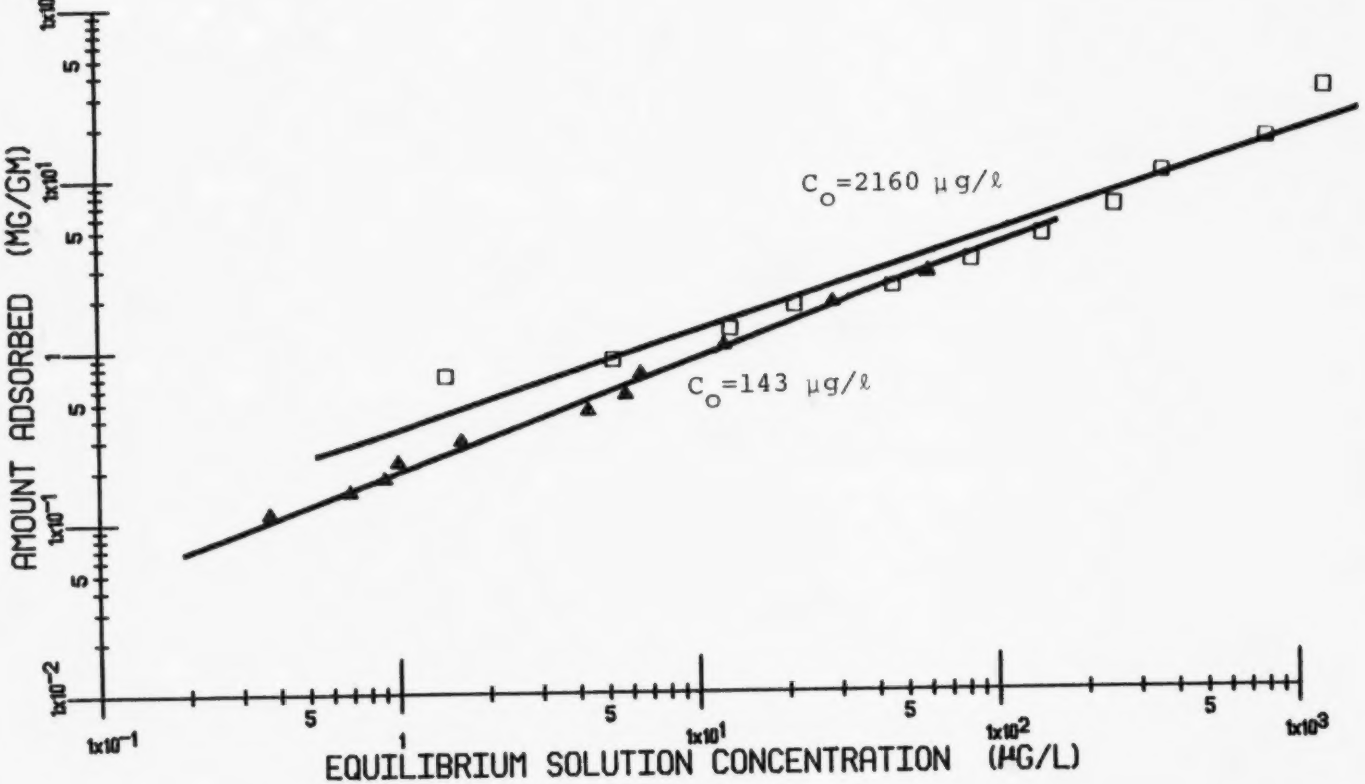

Figure 53. Experimental data and Freundlich isothemrs for CCl_4 - the effects of initial concentration.

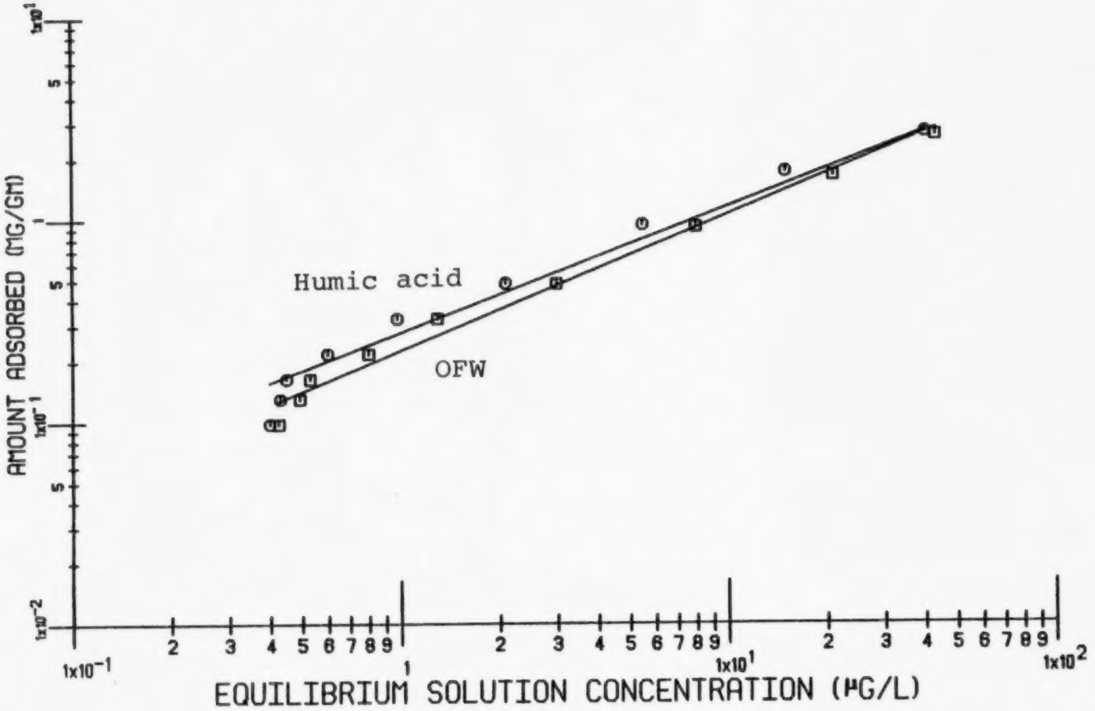

Figure 54. Experimental data and Freundlich isothemrs for CCl_4 - the effects of different background solutions on equilibrium capacities.

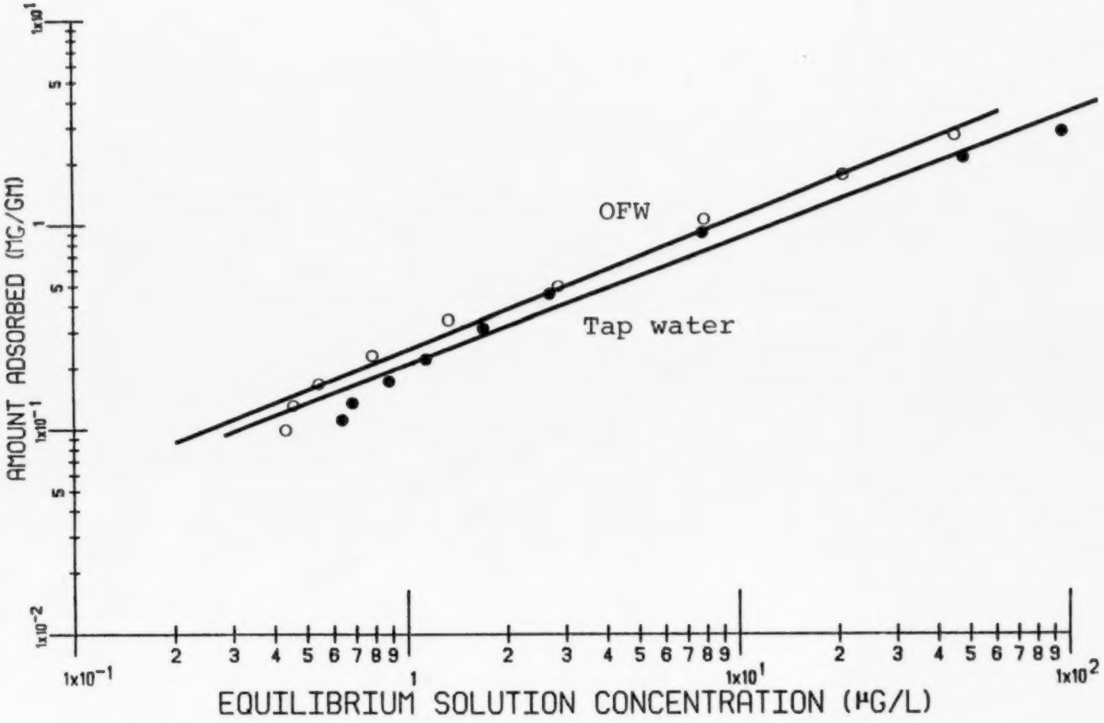

Figure 55. Experimental data and Freundlich isotherms for CCl_4 - the effects of different background solutions on equilibrium capacities.

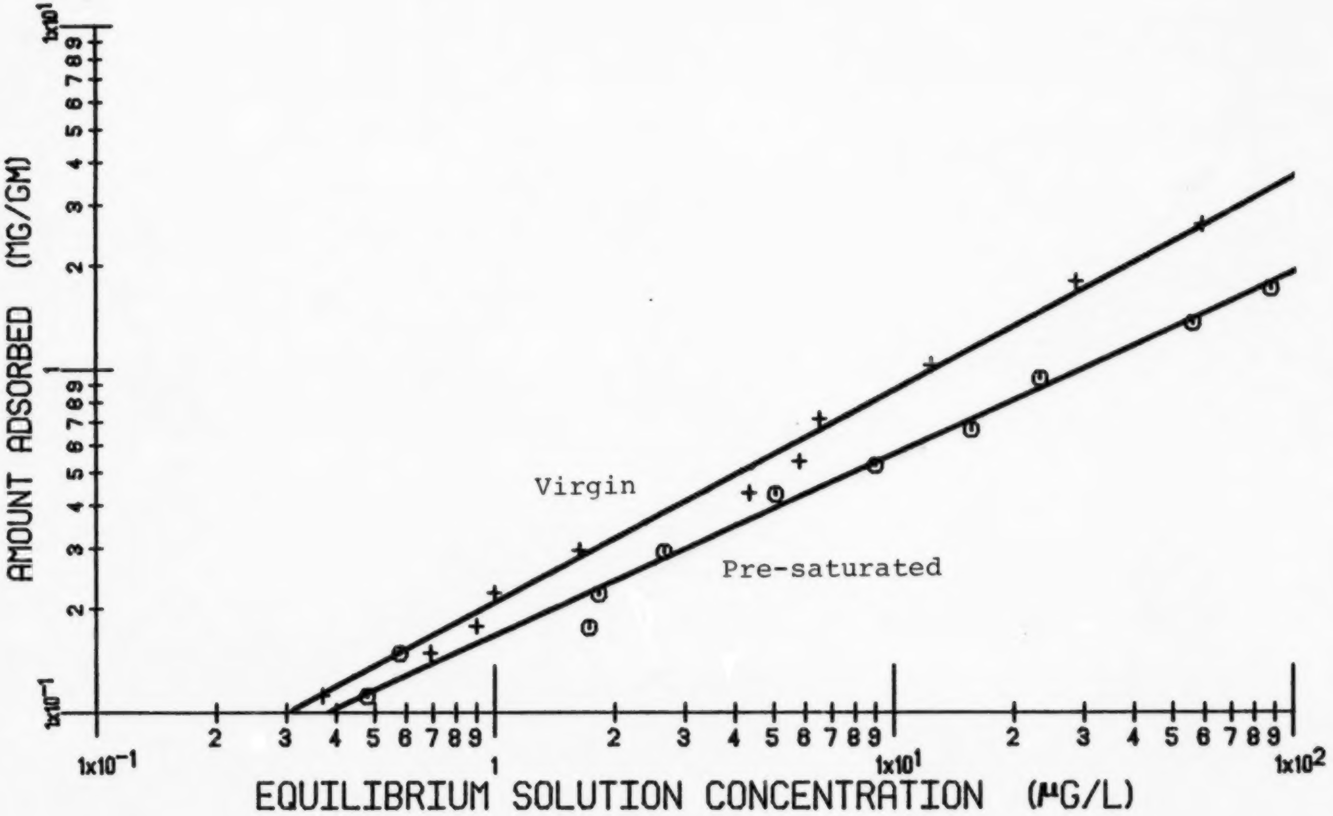

Figure 56. Experimental data and Freundlich isotherms for virgin and pre-saturated (humic acid) carbons.

TYPING GUIDE SHEET

Isotherm parameters for all equilibrium studies are summarized in Table 11.

Adsorption Rates

CMB-reactor experiments were performed to investigate the effects of carbon particle size on rates of adsorption of CCl_4. Figure 57 illustrates concentration-time profiles for different particle sizes of activated carbon and Figure 58 presents the general character of the variation of adsorption rate as a function of particle diameter. A simple second-order rate expression was used to correlate the data from these experiments to facilitate evaluation of the general character of the effect of particle size depicted in Figure 58. As will be noted shortly, adsorption rates involve complex mass transport steps which require more complete mechanistic description than provided by simple first- or second-order rate expressions. Nonetheless, the more simple expressions are useful for first-out evaluations of the type illustrated in Figure 58.

Two mass transport steps -- external and intraparticle diffusion -- are usually involved in the uptake of organic compounds from aqueous solution by activated carbon, either one of which may be rate-limiting (Weber, 1972). It has been observed for intraparticle-controlled systems that incompletely exhausted carbon can achieve some degree of enhanced rate of uptake of organic matter upon standing because of continuing diffusion of the organic matter into the capillaries of the carbon during this period, thus freeing adsorption volume for greater rate of uptake upon remixing of the carbon with the solution. The results of similar experiments with CCl_4, illustrated in Figure 59, indicate no uptake during a 16-hour quiescent period during which mixing of the reactor was suspended, and no significant change in the rate of uptake after resumption of stirring. This suggests film or external diffusion control, rather than intraparticle control, for CCl_4.

A simulation-modeling analysis was performed for adsorption of carbon tetrachloride from OFW to evaluate appropriate rate coefficients, k_f and D_s, for the two-resistance mass transport model (MADAM). A preliminary value for k_f was estimated using a method similar to that discussed for humic acid (Section 6). The estimated coefficients, $k_f = 4.07 \times 10^{-3}$ cm/sec and $D_s = 3.02 \times 10^{-10}$ cm^2/sec, were used to predict the experimental profile represented by the solid line in Figure 60. Figures 61 and 62 demonstrate the results of sensitivity analyses conducted for k_f and D_s, respectively. It may be observed from Figure 61 that variations of $\pm$ 25% in the film transfer coefficient, k_f, result in substantially different predicted profiles, while, as may be noted in Figure 62, the

EPA-287 (Cin.)
(4-76)

TABLE 11. SUMMARY OF ADSORPTION EQUILIBRIUM STUDIES FOR CARBON TETRACHLORIDE[†]

Figure No.	Background Solution	Carbon Size, US Standard Mesh Size	Initial Concentration (μg/1)	Buffer, KH_2PO_4	Freundlich Isotherm Constants* K_F	1/n	$r^{††}$	Remarks
50 & 53	OFW**	30/40	2,160	-	0.344	0.551	0.975	
50	OFW	50/60	-	-	0.497	0.585	0.942	mini-column
51	OFW (pH 5)	200/325	100	$1x10^{-3}\underline{M}$	0.209	0.603	0.998	pH effect
51	OFW (pH 7)	200/325	100	$1x10^{-3}\underline{M}$	0.224	0.630	0.993	
51	OFW (pH 9)	200/325	100	$1x10^{-3}\underline{M}$	0.208	0.601	0.995	
52	OFW	35/50	100	$1x10^{-3}\underline{M}$	0.243	0.818	0.954	particle size effect
52	OFW	80/100	100	$1x10^{-3}\underline{M}$	0.234	0.700	0.995	
54	OFW	16/20	125	-	0.209	0.678	0.965	background solution effect
54	OFW + 5ppm humic acid	16/20	125	-	0.262	0.674	0.987	
55	Tap water	30/40	178	-	0.195	0.594	0.970	
55	OFW	30/40	125	-	0.215	0.610	0.985	
56	OFW	30/40	142	-	0.169	0.517	0.992	pre-saturated carbon
56	OFW	30/40	143	-	0.202	0.633	0.996	virgin carbon

[†] All studies were conducted at pH 7 unless otherwise noted

* Based on C_e and q_e expressed in μg/ℓ and mg/gm, respectively

** Organic free water

[††] r = correlation coefficient for fit of the isotherm to the experimental data

TYPING GUIDE SHEET

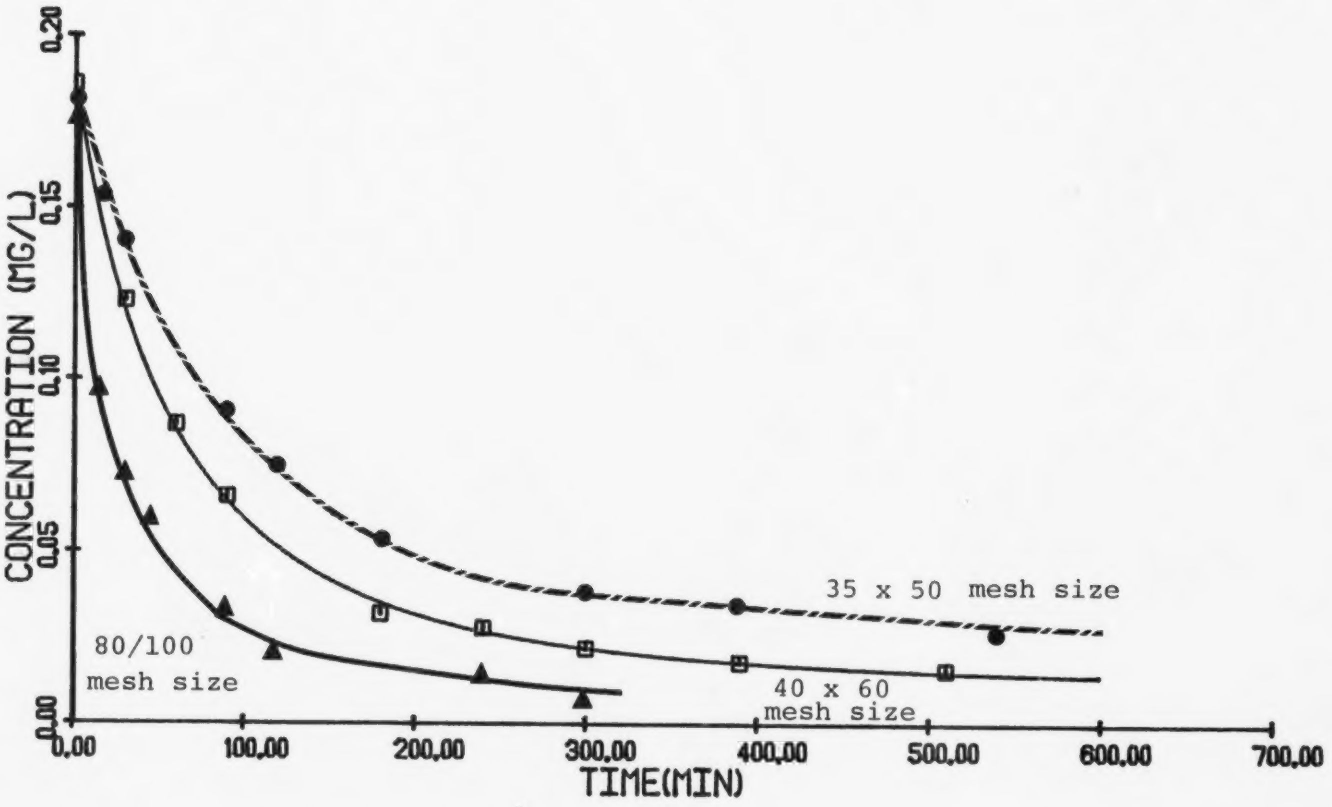

Figure 57. CMB rate studies for CCl_4 - the effects of carbon particle size (0.19 g/ℓ carbon).

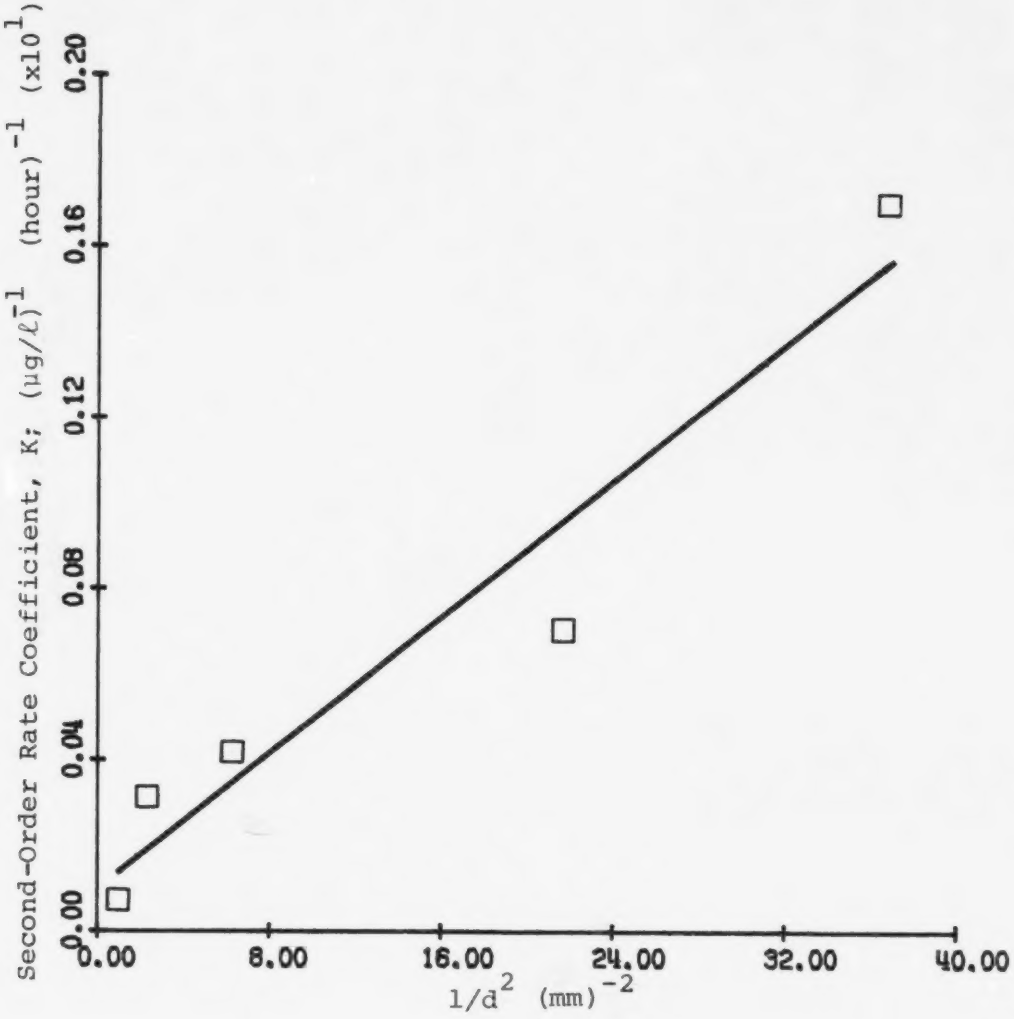

Figure 58. Variation of adsorption rate as a function of carbon particle diameter.

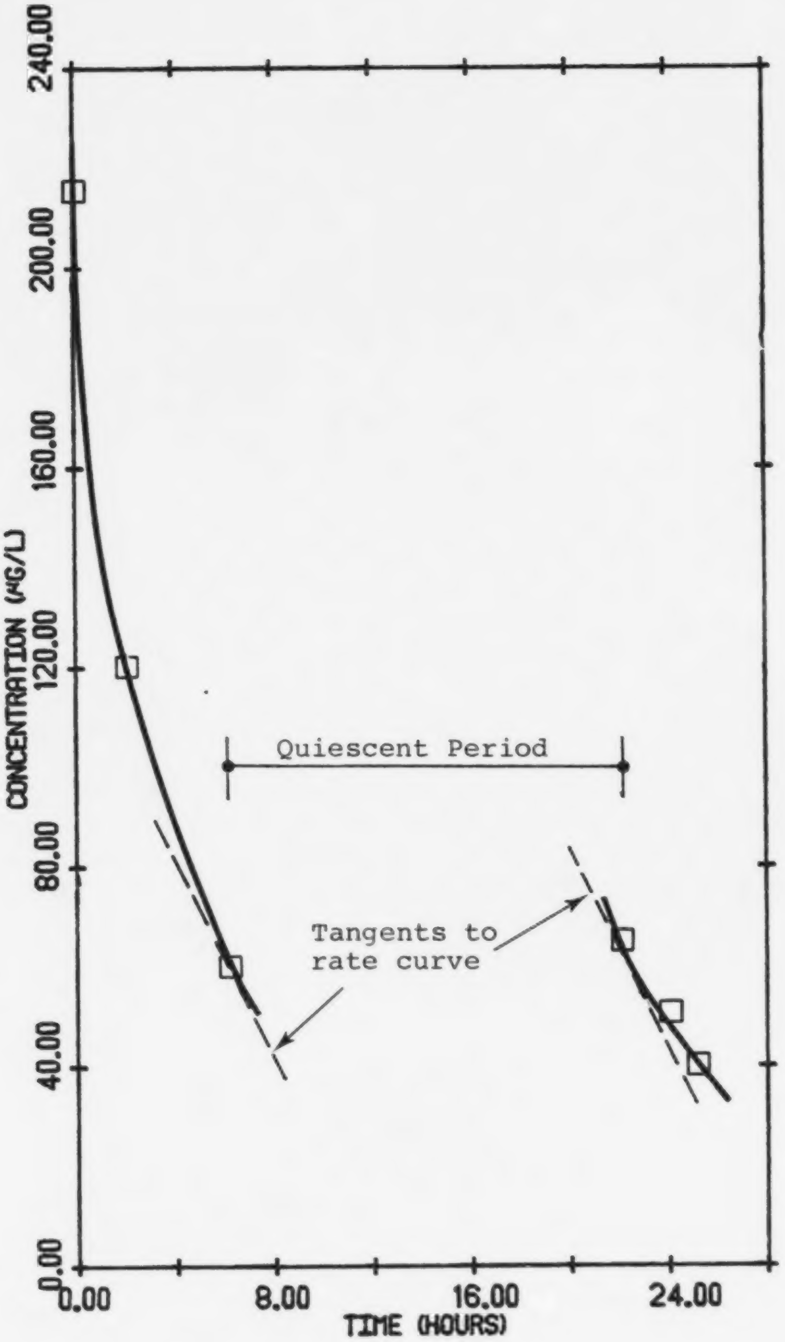

Figure 59. CMB rate study for CCl_4 - effect of interrupted stirring (0.19 g/ℓ of 16/20 US sieve size carbon).

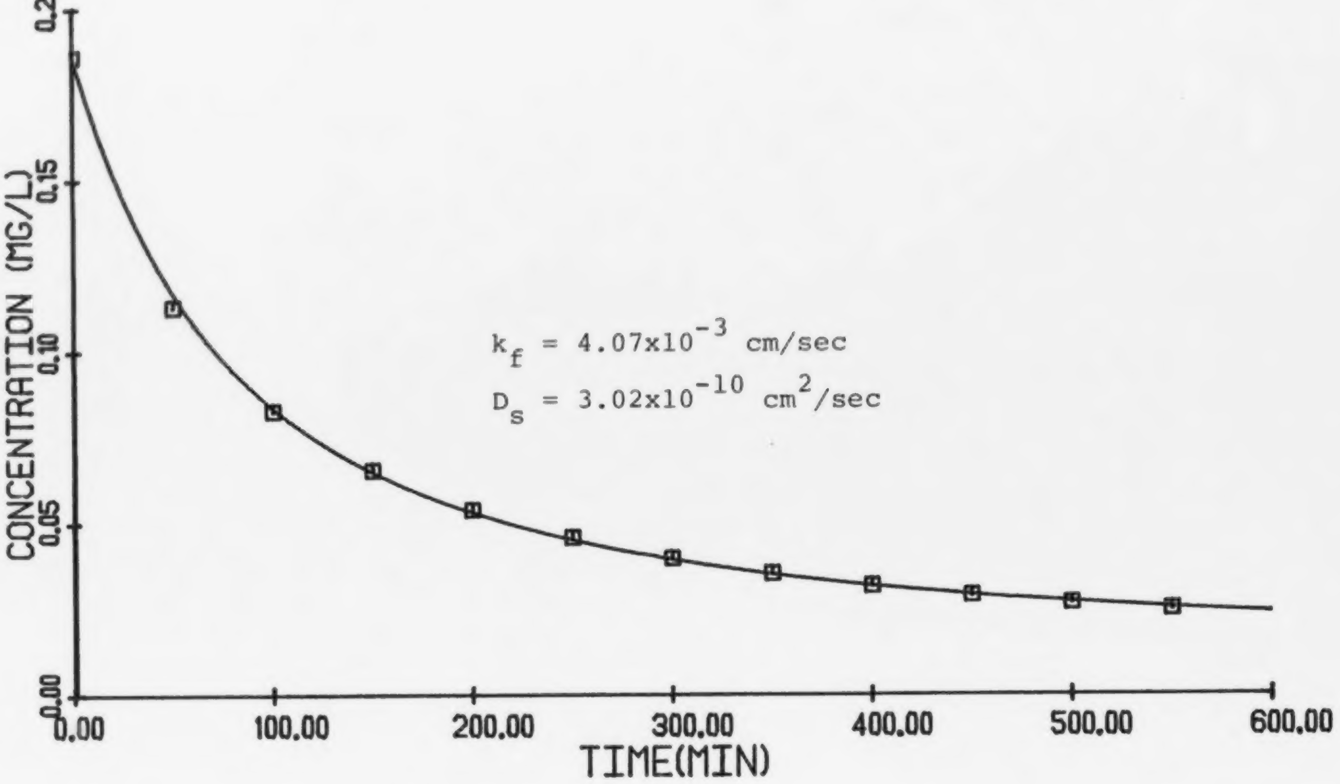

Figure 60. Experimental data and model profiles for rate of adsorption of CCl_4 from OFW in a CMB reactor (0.19 g/ℓ of 16/20 US sieve size carbon).

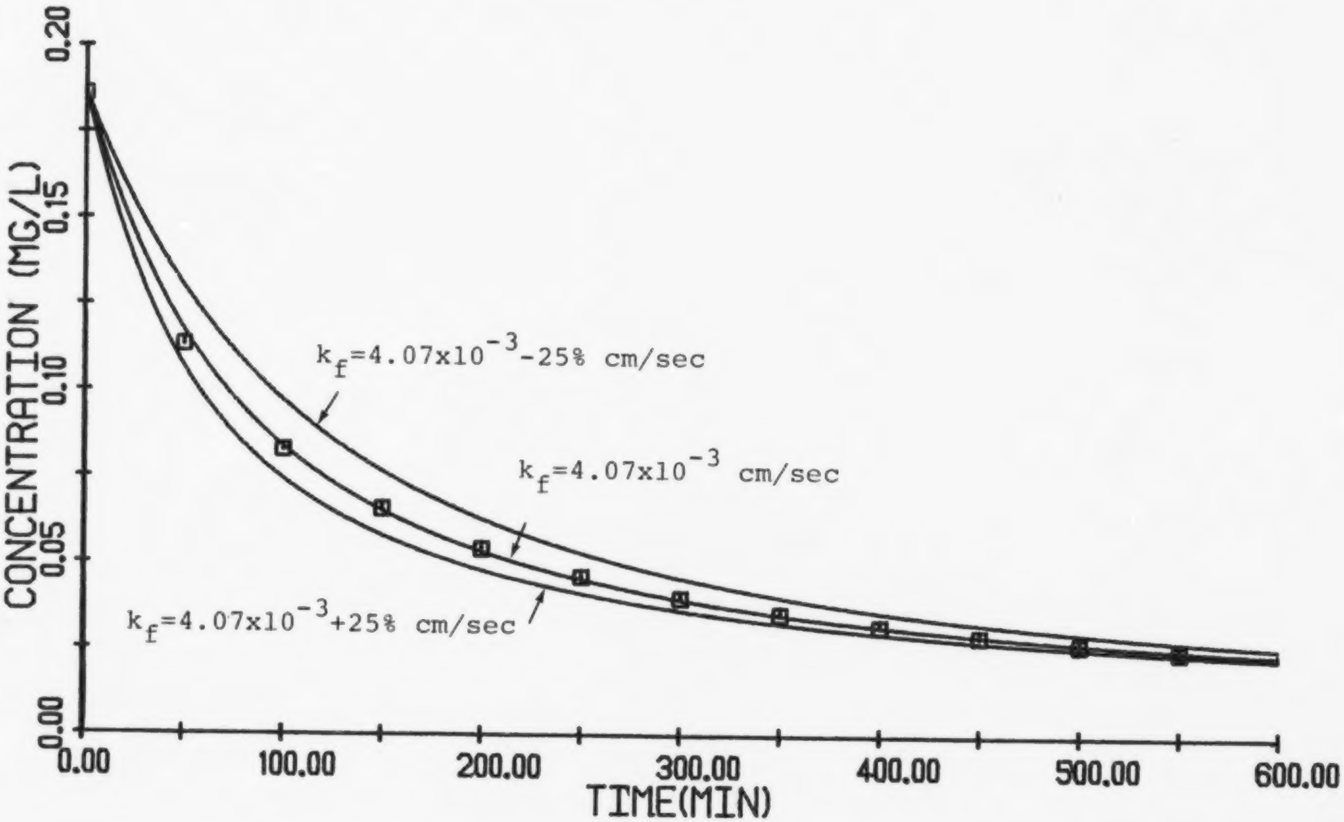

Figure 61. Analysis of the sensitivity of model profiles to the film transfer coefficient, k_f.

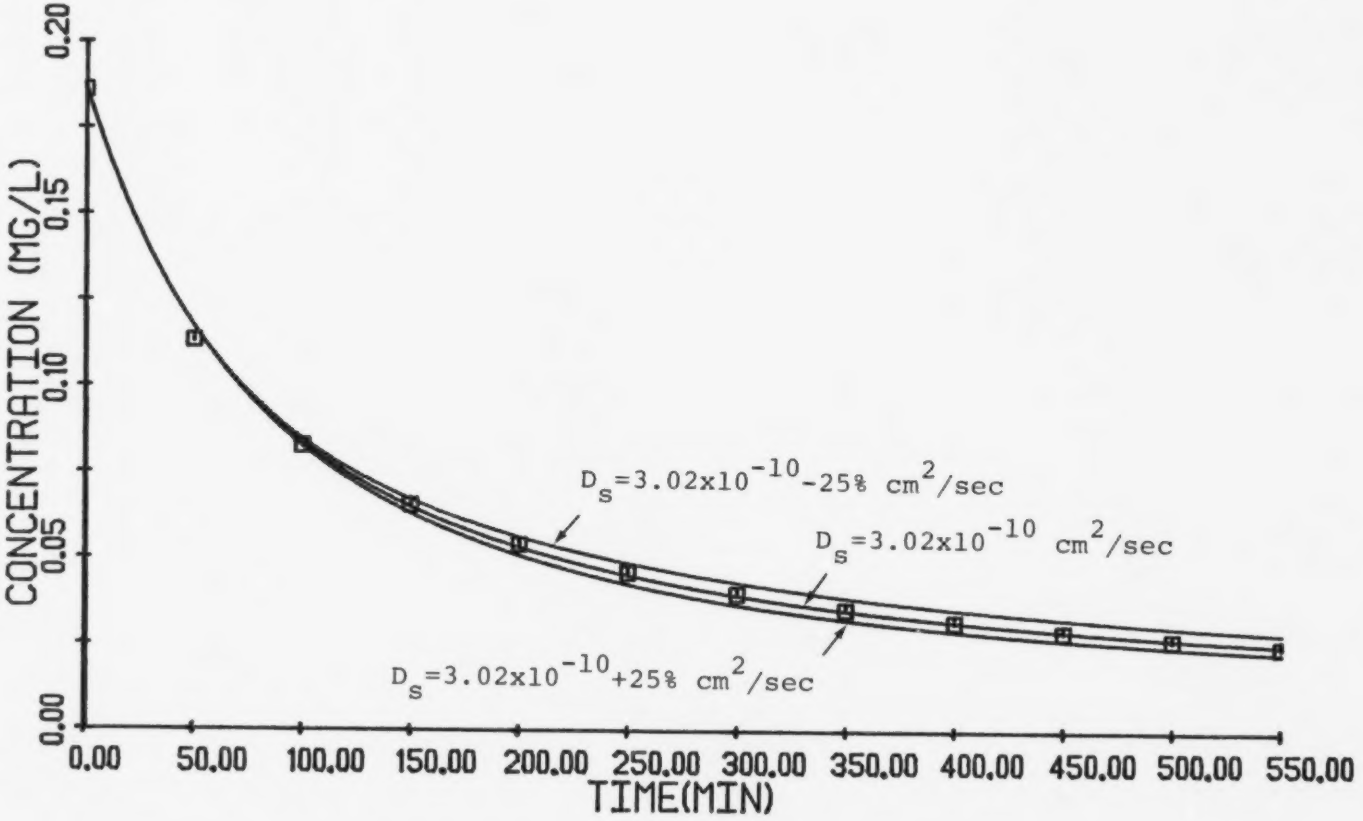

Figure 62. Analysis of the sensitivity of model to the surface diffusion coefficient, D_s.

system is relatively insensitive to changes in D_s. This accords with the earlier observations that external mass transfer most likely controls rates of adsorption of CCl_4 by activated carbon.

A similar simulation procedure was employed for analysis of data from CMB adsorption rate studies with carbon tetrachloride in the presence of 5 mg/l of humic acid. Figure 63 presents the experimental data and the predicted profile (solid line) based on the estimated values of, $k_f = 3.78 \times 10^{-3}$ cm/sec and $D_s = 1.86 \times 10^{-10}$ cm^2/sec. The intraparticle diffusion coefficient for the system containing humic acids was significantly lower than that for the organic-free system. It appears that the humic acid molecules retard the diffusion of carbon tetrachloride molecules within the carbon pores. Experimental conditions and associated mass transfer coefficients for the systems depicted in Figures 60 and 63 are summarized in Table 12.

TABLE 12. ESTIMATED ADSORPTION RATE MASS TRANSFER COEFFICIENTS FOR CCl_4

Figure No.	Background Solution	C_o, µg/l	Carbon Dosage, g/l	k_f, cm/sec (x 10^3)	D_s, cm^2/sec (x 10^{10})
60	OFW	186	0.19	4.07	3.02
63	OFW+5mg/l Humic Acids	200	0.19	3.78	1.87

Adsorption Columns

Experimental fixed-bed column studies for carbon tetrachloride were designed and executed in two phases. Phase I studies consisted of mini-column tests to obtain preliminary data for predictive model calibration. Phase II studies comprised breakthrough runs with large fixed-bed adsorbers to develop data for model verification. Examples of column data and best fit profiles are given in Figures 64 and 65 for the Phase I and Phase II studies, respectively.

It was assumed that properly designed mini-column studies would yield necessary information for predictive model calibration. Experiments with the larger adsorber columns, which were devised to simulate more realistic adsorber systems in order to more closely approximate removal efficiencies,

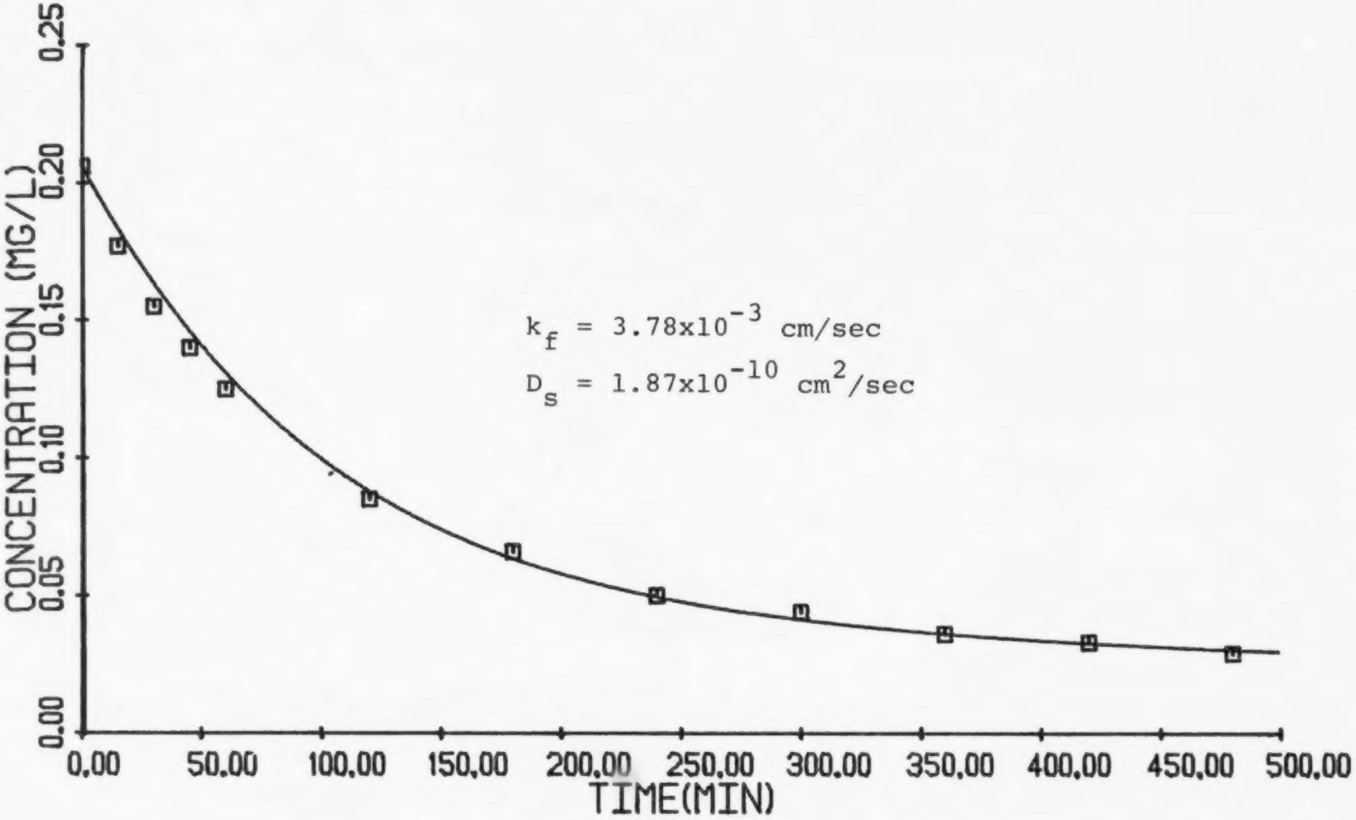

$k_f = 3.78 \times 10^{-3}$ cm/sec

$D_s = 1.87 \times 10^{-10}$ cm^2/sec

Figure 63. Experimental data and model profile for rate of adsorption of CCl_4 from humic acid background solution in CMB reactor, (0.19 g/ℓ of 16/20 US sieve size carbon).

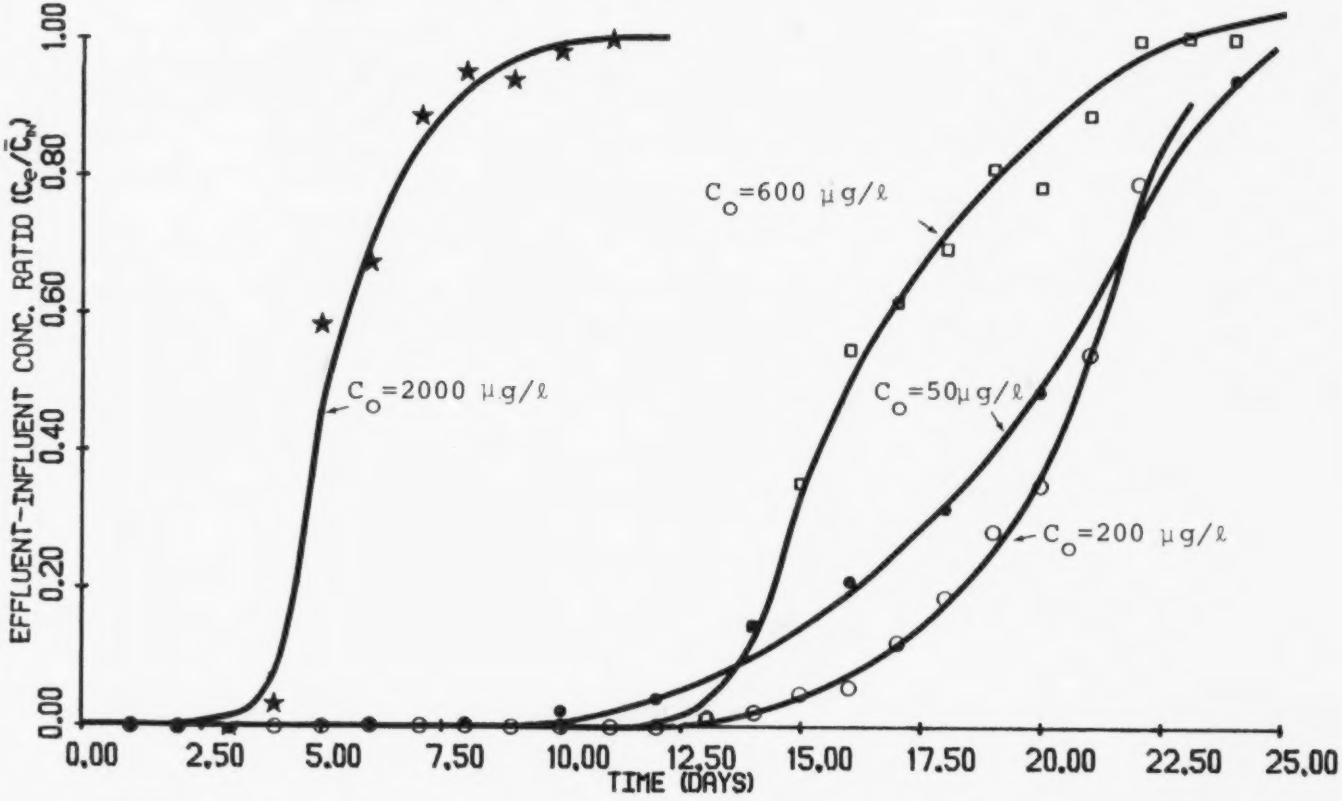

Figure 64. Breakthrough profiles for CCl_4 in mini-column adsorbers for different influent concentrations, (2 grams of 50/60 US sieve size carbon, flow rate = 5 mℓ/min, EBCT = 1.1 min)

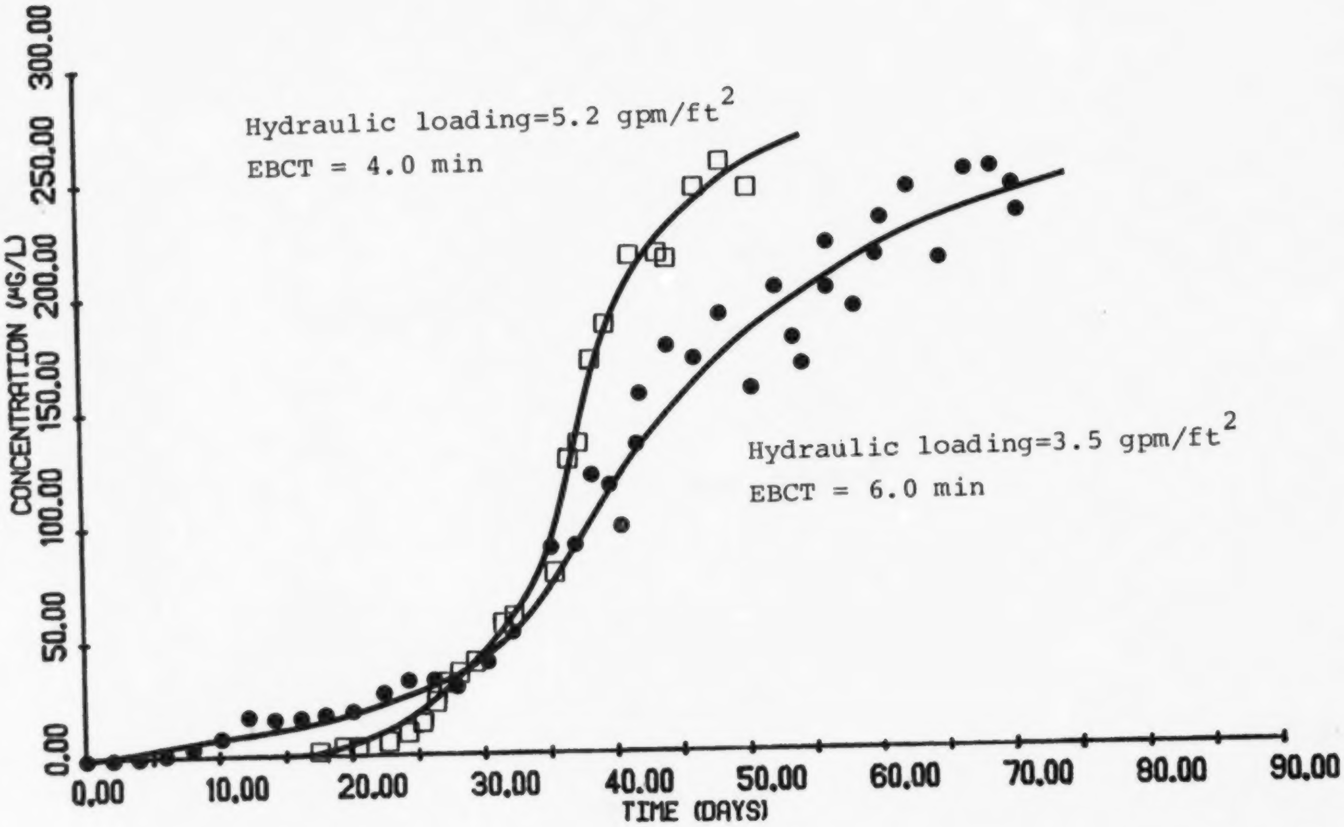

Figure 65. Typical breakthrough profiles for CCl_4 in large adsorbers for different flow rates ($\overline{C}_{in}$=250 μg/ℓ, 250 grams of 16/20 US sieve size carbon).

encountered some operational problems stemming largely from biological growth on the carbon.

Table 13 summarizes values for the physical and chemical parameters associated with selected adsorber studies, including values for the surface diffusion coefficient, D_s, and the film transfer coefficient, k_f. Surface diffusion coefficients were estimated from the CMB-reactor rate tests and film transfer coefficients by a correlation technique proposed by Williamson et al (1963). This particular correlation technique was found to best agree with the experimental column parameters and conditions.

Model Verification--

Experimental data and predictive breakthrough profiles for typical fixed-bed adsorber runs are presented in Figures 66 and 67. Good agreement between the experimental data and the predicted breakthrough profiles for Runs I and II is observed (Figures 66 and 67). The experimental data and predicted breakthrough profile associated with adsorber Run III do not agree as well (Figure 68). Two reasons can be advanced to explain this discrepancy. First, it was necessary to air-scour and backwash the column twice during the period of operation due to air entrapment within the carbon bed and/or excessive headloss caused by biological growth. Air-scouring and backwashing may have disturbed the original bed stratification and/or caused some elution or desorption. Second, the influent concentration fluctuated drastically in the course of the run, imposing marked re-equilibration phenomena in the adsorber bed.

Model Sensitivity--

Model sensitivity analyses with respect to k_f and D_s were conducted for the mini-column fixed-bed Run I. Figures 69 and 70 demonstrate deviations in breakthrough profiles for variations of $k_f \pm 25\%$ and $D_s \pm 25\%$, respectively. It may be observed that the predictive model displays similar sensitivity to k_f and D_s, suggesting that both film diffusion and intraparticle diffusion are equally important for CCl_4 in fixed-bed adsorber systems.

Figures 71 through 74 present similar sensitivity studies for the larger column fixed-bed Runs II and III. It is evident that film diffusion appears to be the principal control in the adsorber Run II while surface diffusion is the controlling mass transport in adsorber Run III.

For the large fixed-bed adsorbers (Runs II and III), increasing the interstitial fluid velocity from 0.63 cm/sec to 0.94 dm/sec appears to result in a change in the rate limiting mass transport mechanism from film diffusion to intraparticle diffusion. It was demonstrated that in the

TABLE 13. PARAMETERS USED FOR FIXED-BED ADSORBER PREDICTIVE BREAKTHROUGH PROFILES FOR CCl_4

Adsorber Runs	$\overline{C}_{in}$,μg/1	d,cm	L,cm	γ	v,cm/sec	k_f,cm/sec	D_s,cm^2/sec
I (Figure 66)	177	0.027	7.0	0.456	0.23	5.50×10^{-3}	3.04×10^{-10}
II (Figure 67)	570	0.1	84.5	0.374	0.63	2.97×10^{-3}	3.04×10^{-10}
III (Figure 68)	267	0.1	84.0	0.374	0.94	3.41×10^{-3}	3.04×10^{-10}

$\overline{C}_{in}$ = average influent concentration;

d = carbon particle diameter;

L = bed length;

γ = bed porosity, dimensionless;

v = interstitial fluid velocity;

k_f = film transfer coefficient; and,

D_s = surface diffusion coefficient

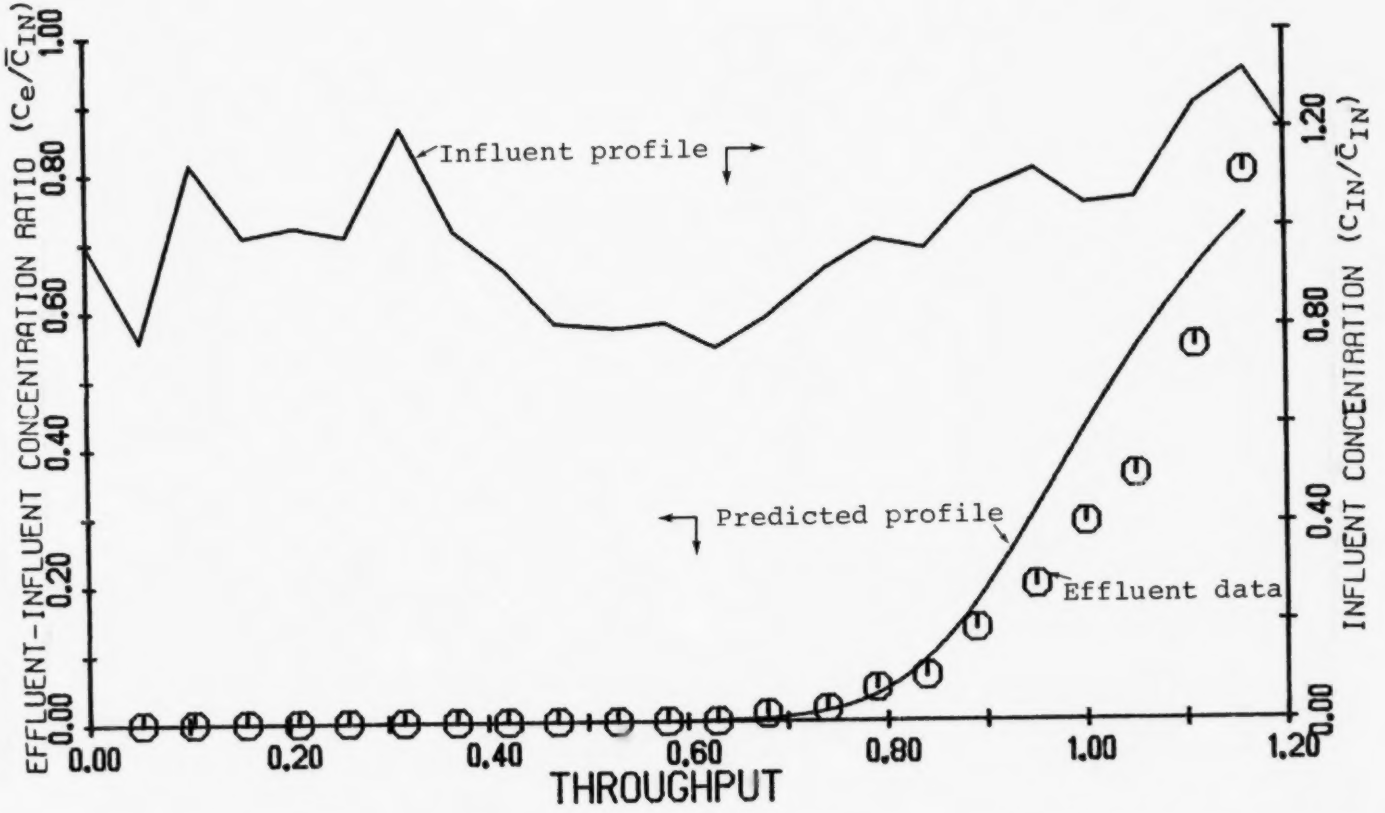

Figure 66. Influent and effluent concentration-history profiles for CCl_4 in fixed-bed Run I (mini-column), (2 grams of 50/60 US sieve size carbon, $\bar{C}_{in}$=177 μg/ℓ, EBCT = 1.1 min.).

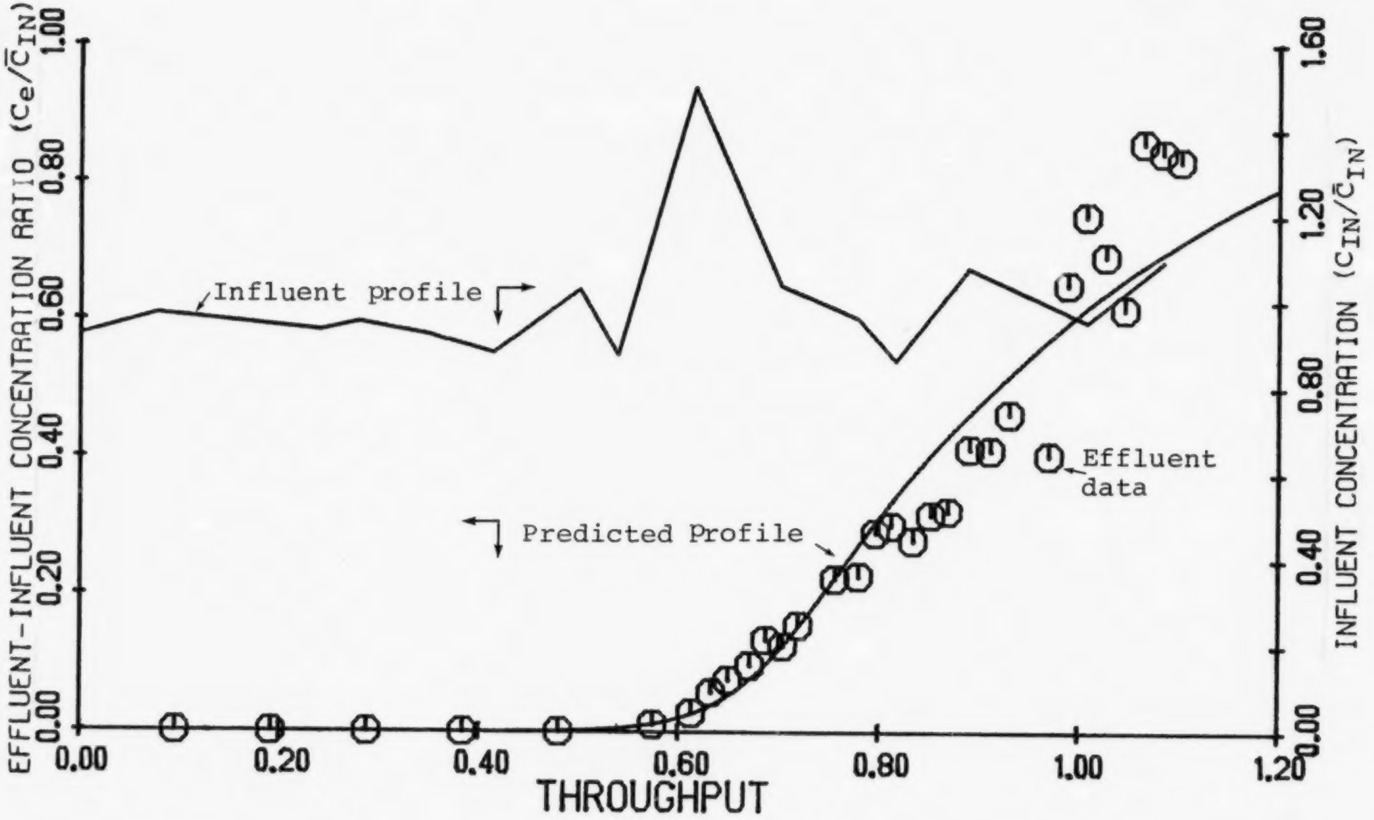

Figure 67. Influent and effluent concentration profiles for CCl_4 in fixed-bed Run II (250 grams of 16/20 US sieve size carbon, $\overline{C}_{in}$ = 570 μg/ℓ, EBCT = 6.0 min).

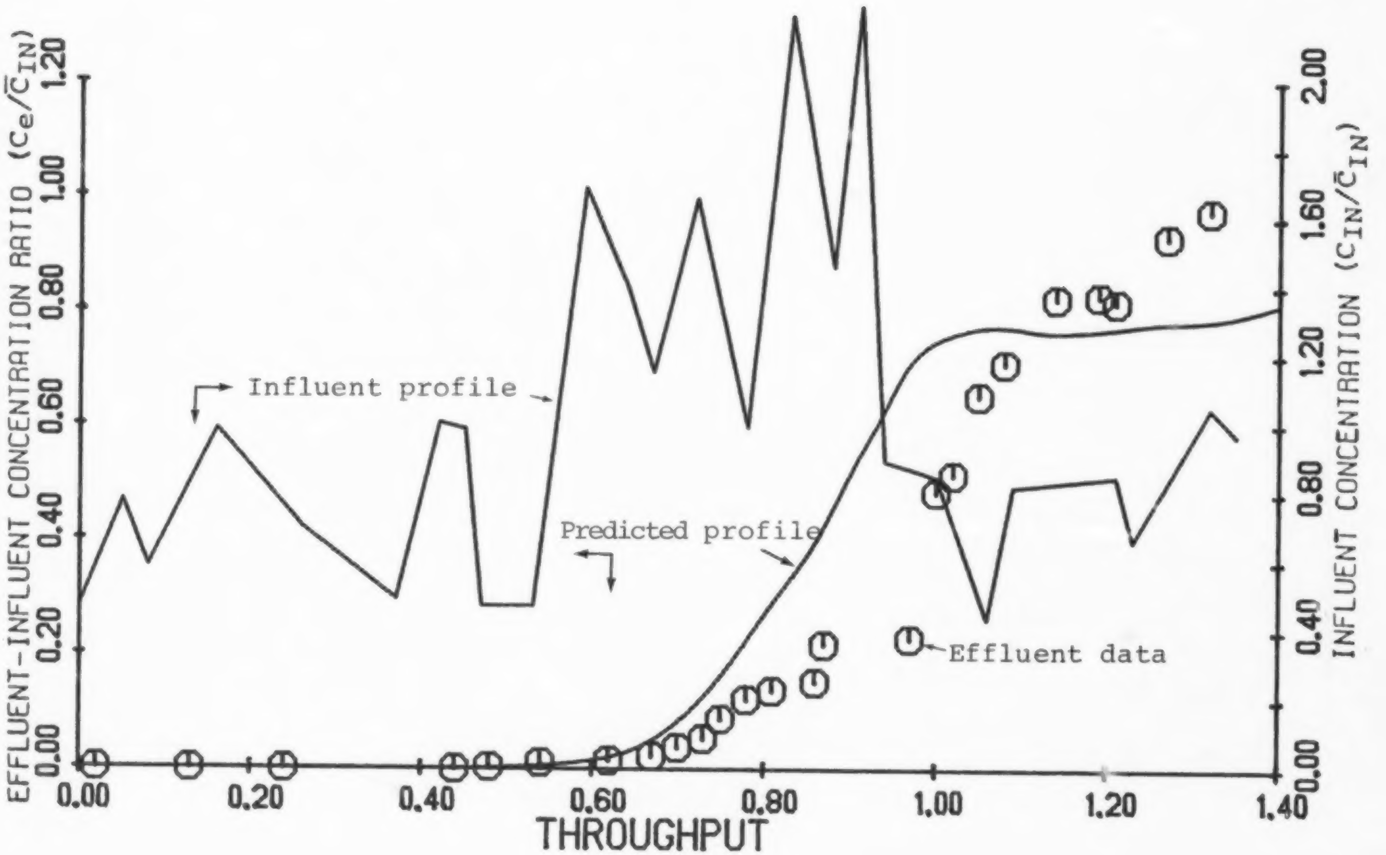

Figure 68. Influent and effluent concentration history profiles for CCl_4 in fixed-bed Run III (250 grams of 16/20 US sieve size carbon, $\bar{C}_{in}$ =267 μg/ℓ, EBCT= 4.0 min).

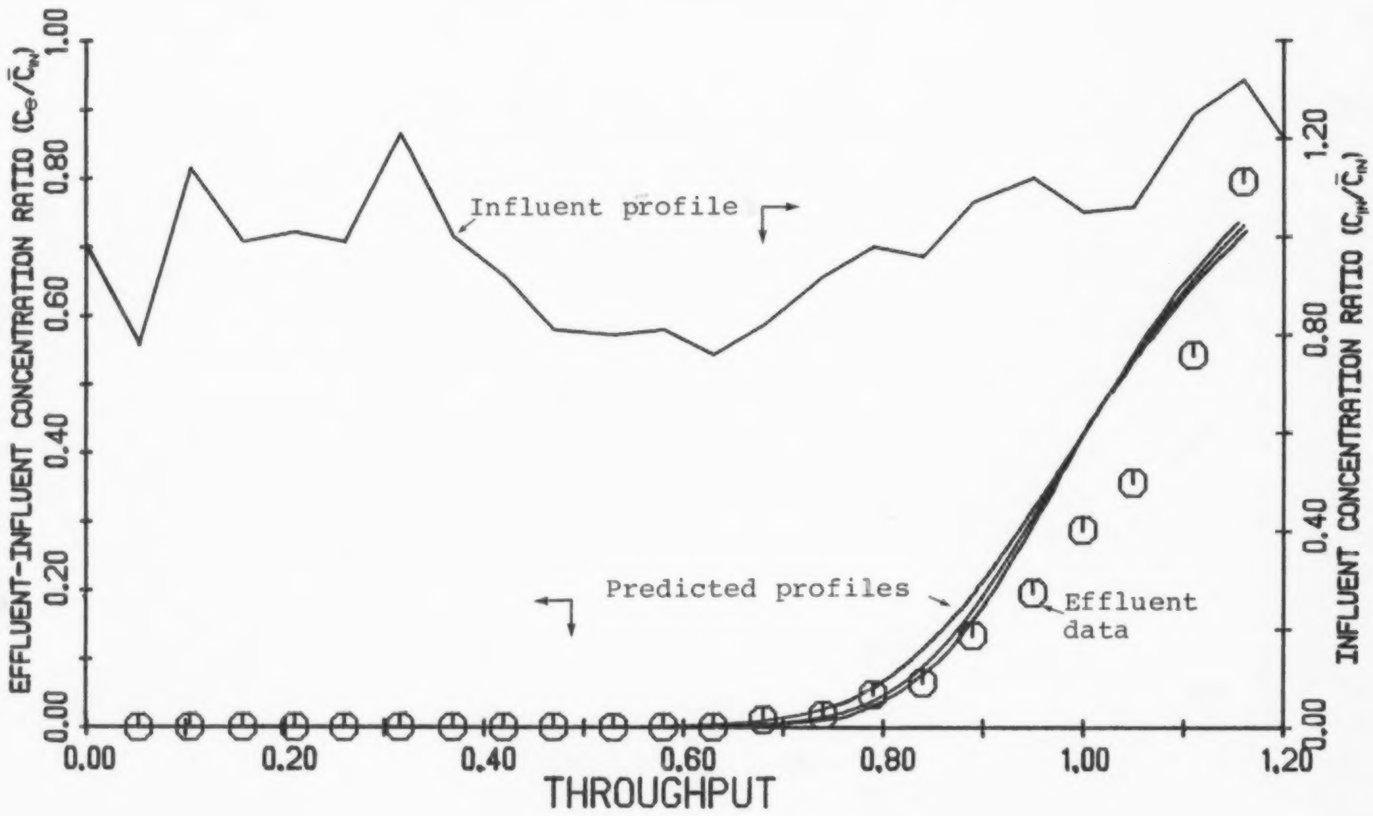

Figure 69. Sensitivity analysis of breakthrough profiles relative to the film transfer coefficient, $k_f \pm 25\%$, for CCl_4 (fixed-bed Run I).

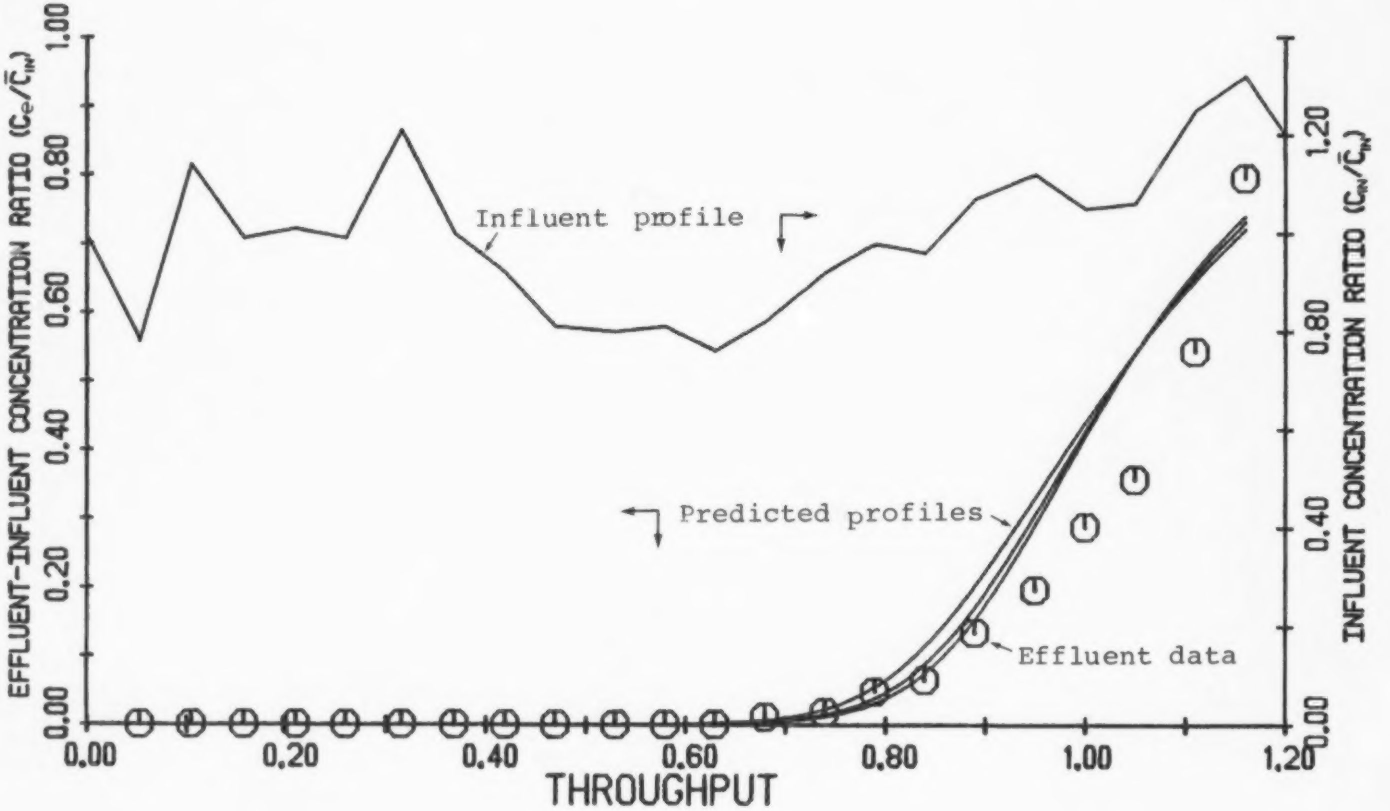

Figure 70. Sensitivity analysis of breakthrough profiles relative to the surface diffusion coefficient, $D_s \pm 25\%$, for CCl_4 (fixed-bed Run I).

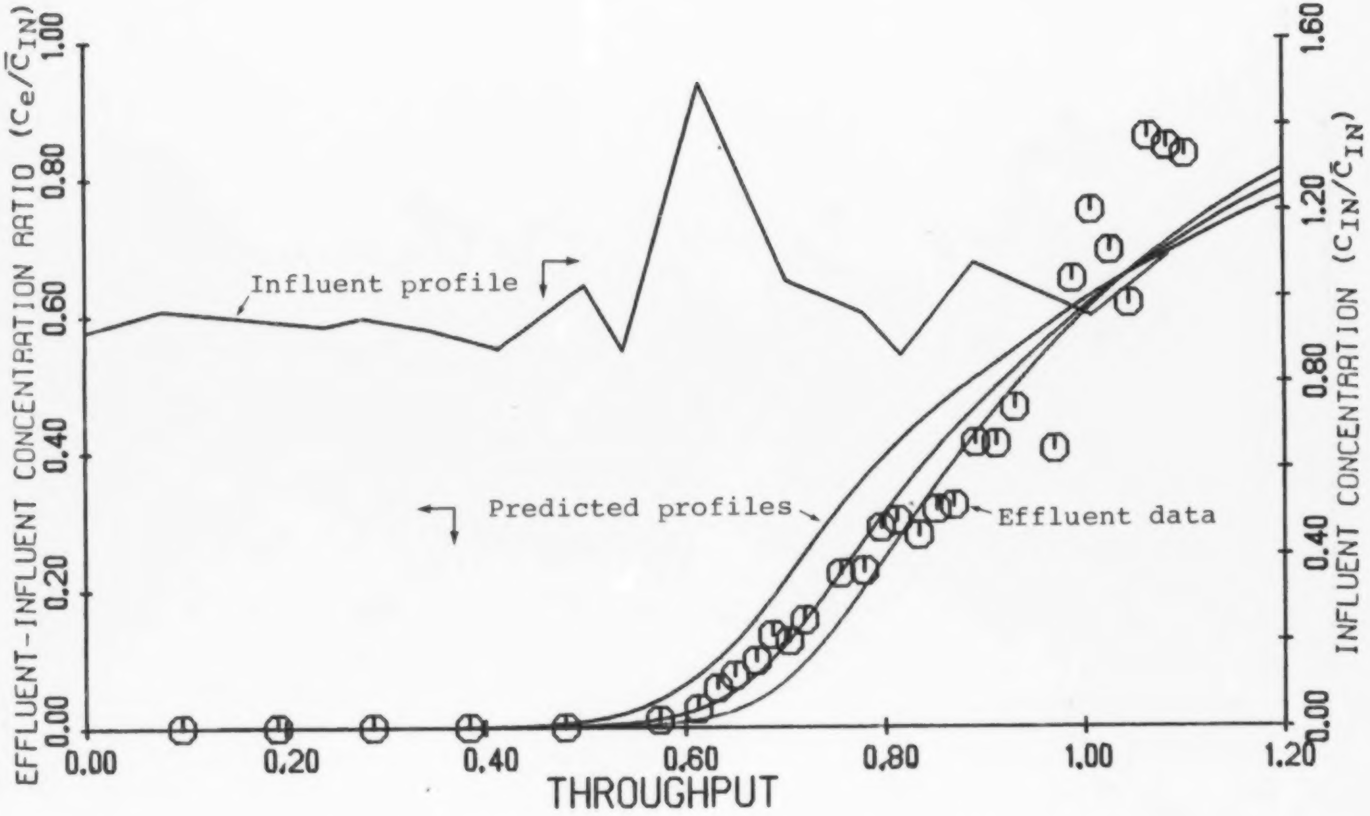

Figure 71. Sensitivity analysis of breakthrough profiles relative to the film transfer coefficient, $k_f \pm 25\%$, for CCl_4 (fixed-bed Run II).

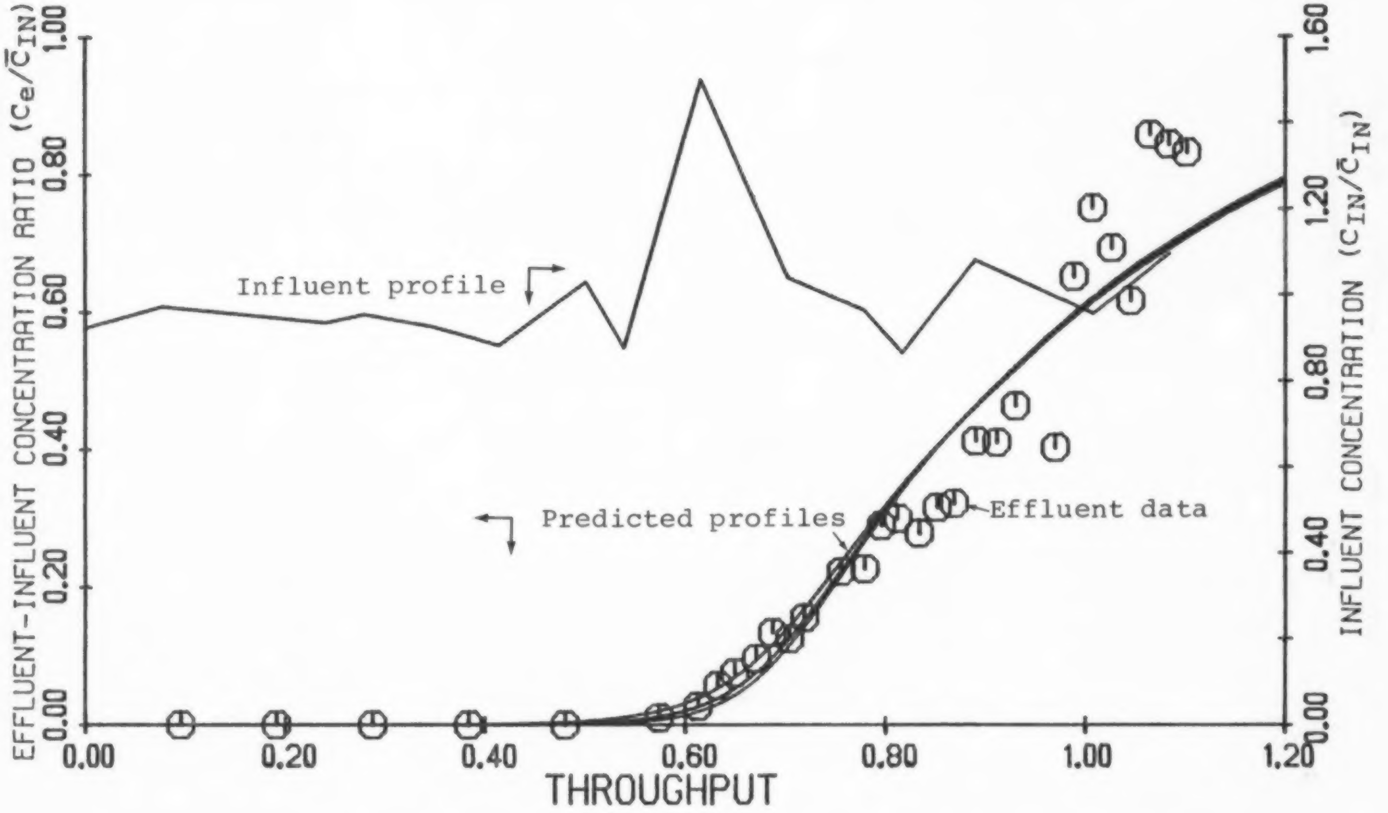

Figure 72. Sensitivity analysis of breakthrough profiles relative to the surface diffusion coefficient, $D_s \pm 25\%$, for CCl_4 (fixed-bed Run II).

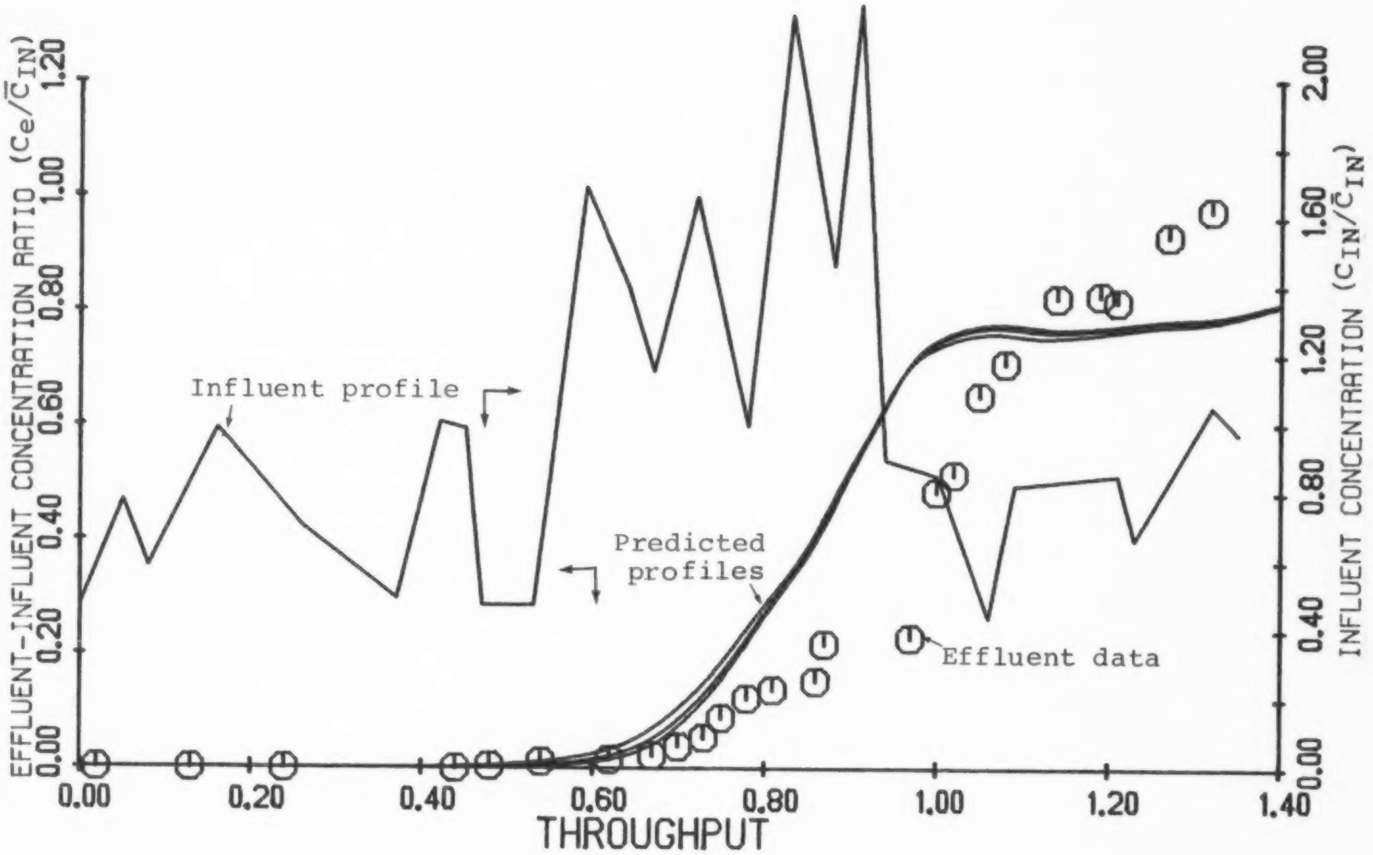

Figure 73. Sensitivity analysis of breakthrough profiles relative to the film transfer coefficient, $k_f \pm 25\%$, for CCl_4 (fixed-bed Run III).

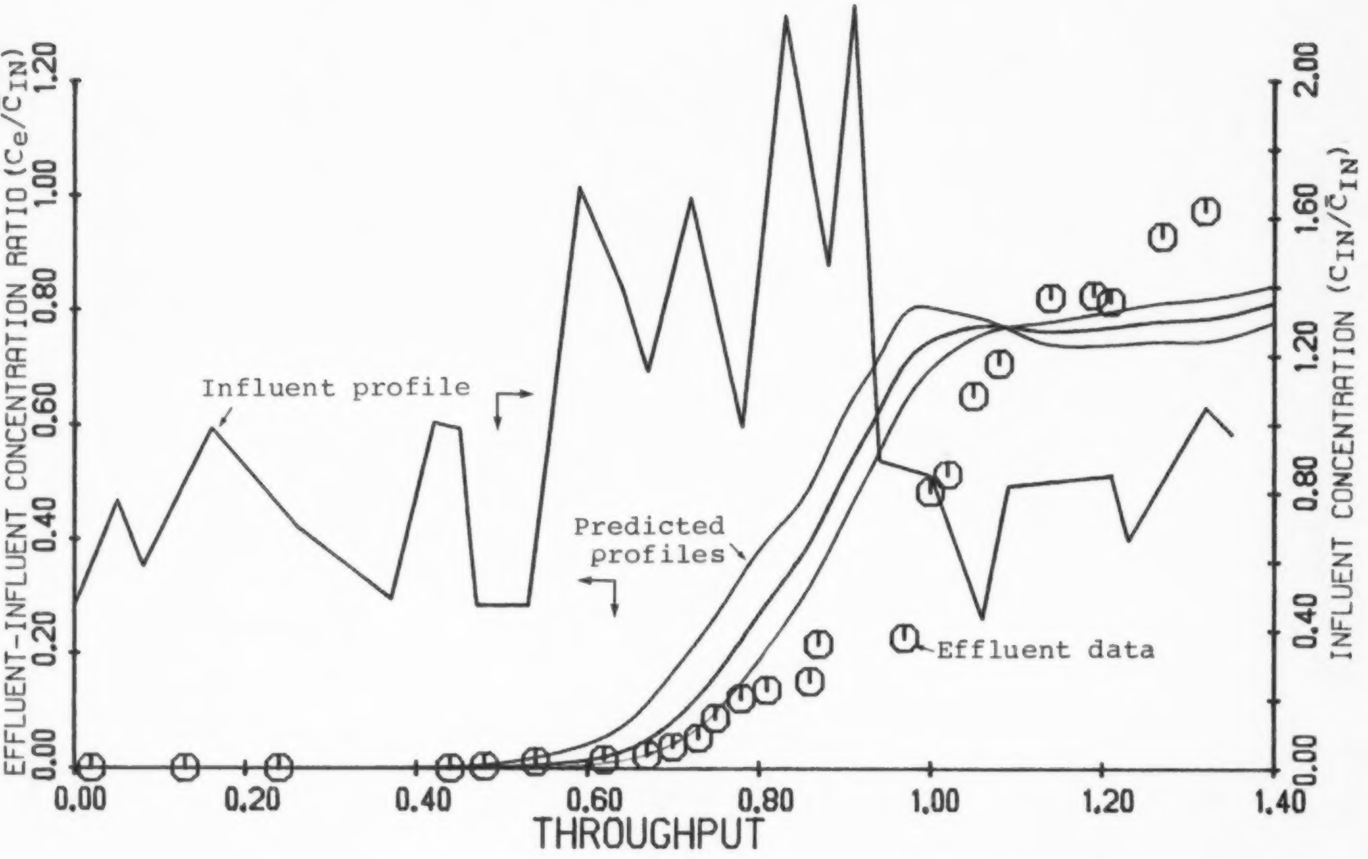

Figure 74. Sensitivity analysis of breakthrough profiles relative to the surface diffusion coefficient, $D_s \pm 25\%$, for CCl_4 (fixed-bed Run III).

mini-column study (Run I), for which lower interstitial velocity (0.23 cm/sec) and smaller carbon particle size were used, both film diffusion and intraparticle diffusion were important. The controlling mass transport mechanism for carbon tetrachloride thus appears to be particularly sensitive to the physical characteristics of the system. Further study is required to substantiate and refine this conclusion.

Desorption and Chromatographic Effects

Equilibrium adsorption-desorption experiments were performed using the bottle-point technique described earlier in this section. When equilibrium was achieved, the supernatent aqueous solution was discarded and the Hypo-Vials containing the carbon re-filled with OFW, sealed, and agitated until equilibrium was reestablished. Samples were withdrawn from each vial, subjected to concentration by liquid-liquid extraction and analyzed by electron capture gas chromatography. The experimental data for the adsorption-desorption studies, presented in Figure 75, indicate no significant equilibrium hysteresis.

Rates of desorption of carbon tetrachloride from carbon were also examined. CMB reactor adsorption rate studies were performed in the manner described earlier in this section. After equilibrium had been attained, the supernatent solution was discarded and the reactor filled with organic-free water. The rate of release of carbon tetrachloride from the carbon was then measured, using the same procedure employed for the rate of uptake experiments. The rate of approach to equilibrium in the desorption experiments was faster than that of the adsorption tests. Data for a typical desorption study are shown in Figure 76.

Desorption studies were then conducted in a fixed-bed adsorber column containing 250 grams of carbon and operated at a flow rate of 5.2 gpm/ft^2. After the column reached exhaustion, high purity water was fed to the saturated adsorber for a period of 30 days to evaluate desorption effects. A significant amount of carbon tetrachloride was desorbed, as indicated in Figure 77. To investigate the possibility of chromatographic phenomena, a 5-mg/l solution of humic acid was fed to a saturated column for a period of 15 days. The effluent profile demonstrated in Figure 78 strongly suggests displacement of carbon tetrachloride by humic acid.

Competitive Adsorption

Fixed-bed adsorption studies with carbon tetrachloride in the presence of 5 mg/l humic acid were conducted to investigate competitive adsorption phenomenon. These experiments were designed and executed in a manner similar to those

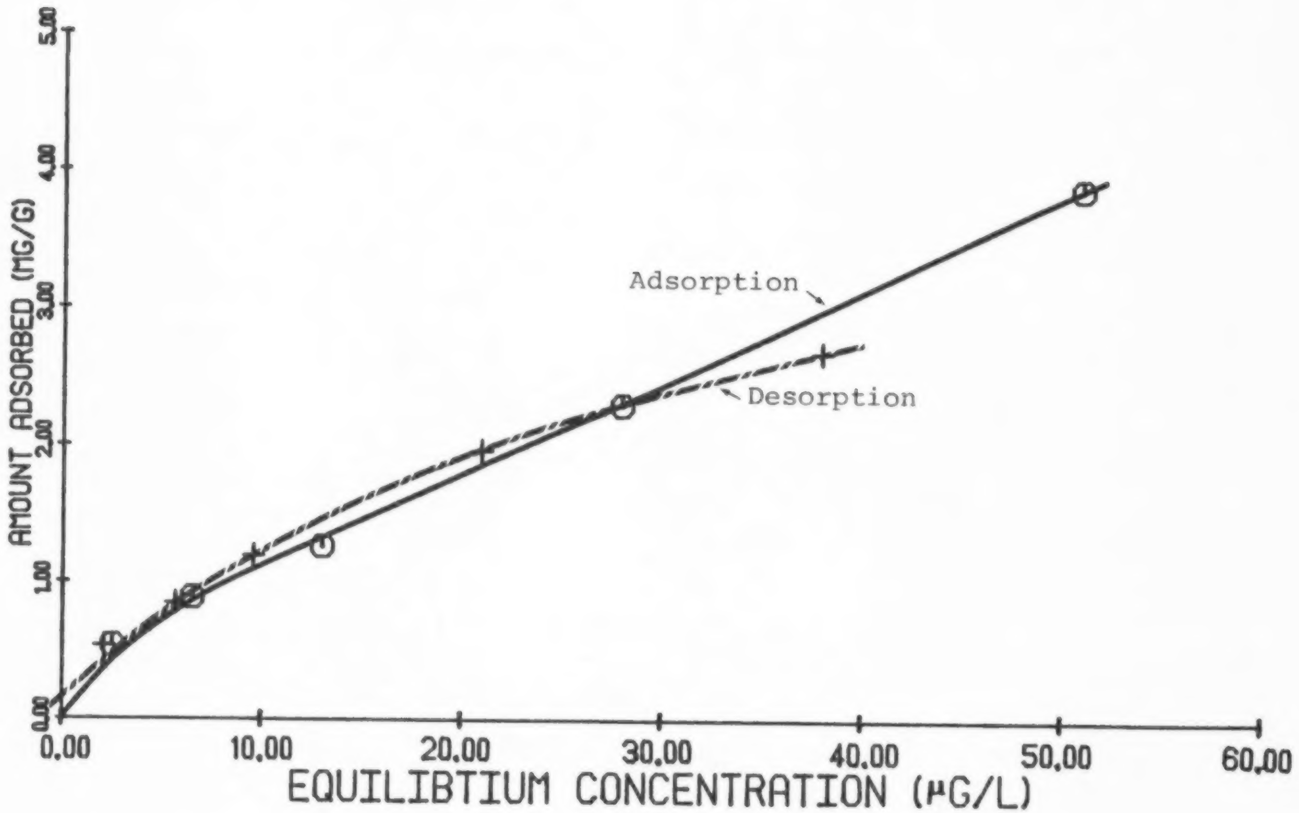

Figure 75. Equilibrium adsorption and desorption data for CCl_4 (C_o=168 μg/ℓ, 16/20 US sieve size carbon).

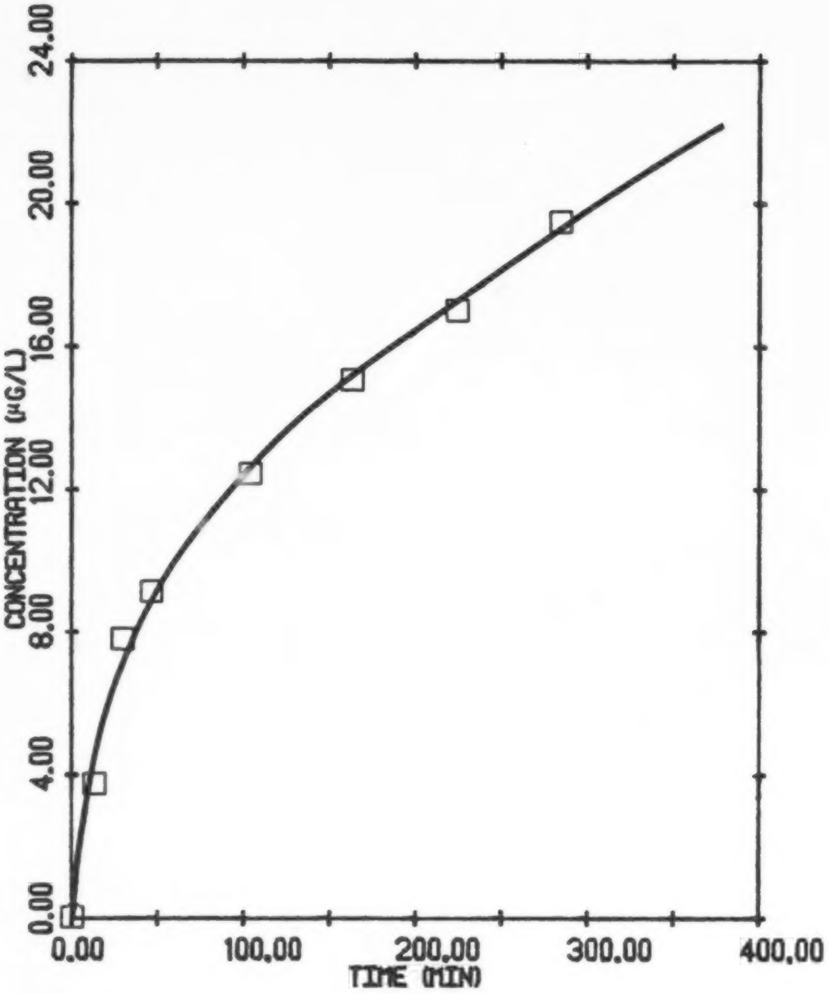

Figure 76. CMB reactor desorption rate study for CCl_4, (per adsorption experiments presented in Figure V-13).

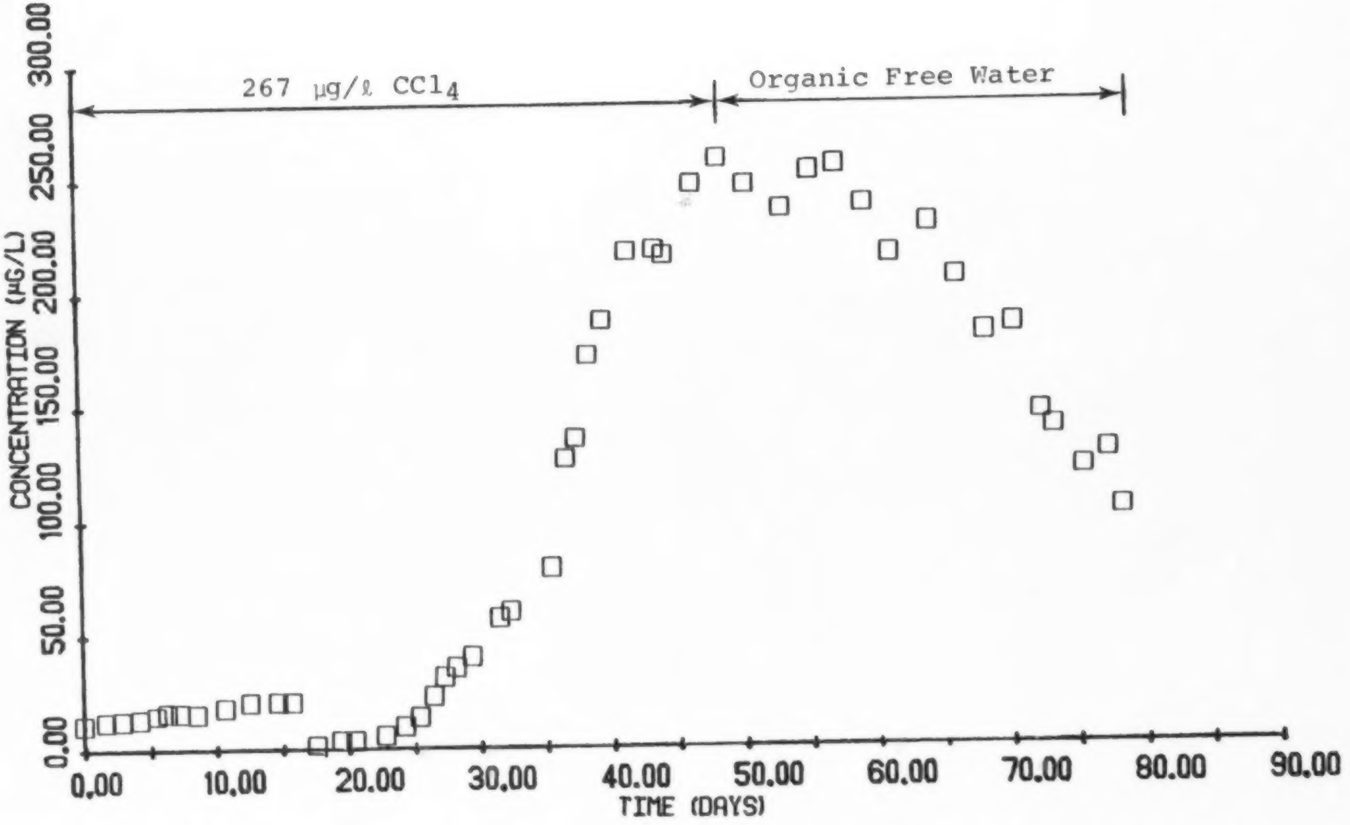

Figure 77. Experimental breakthrough and desorption profiles for CCl_4 in a fixed-bed adsorber (flow rate=5.2 gpm/ft^2, 250 grams of 16/20 US sieve size carbon).

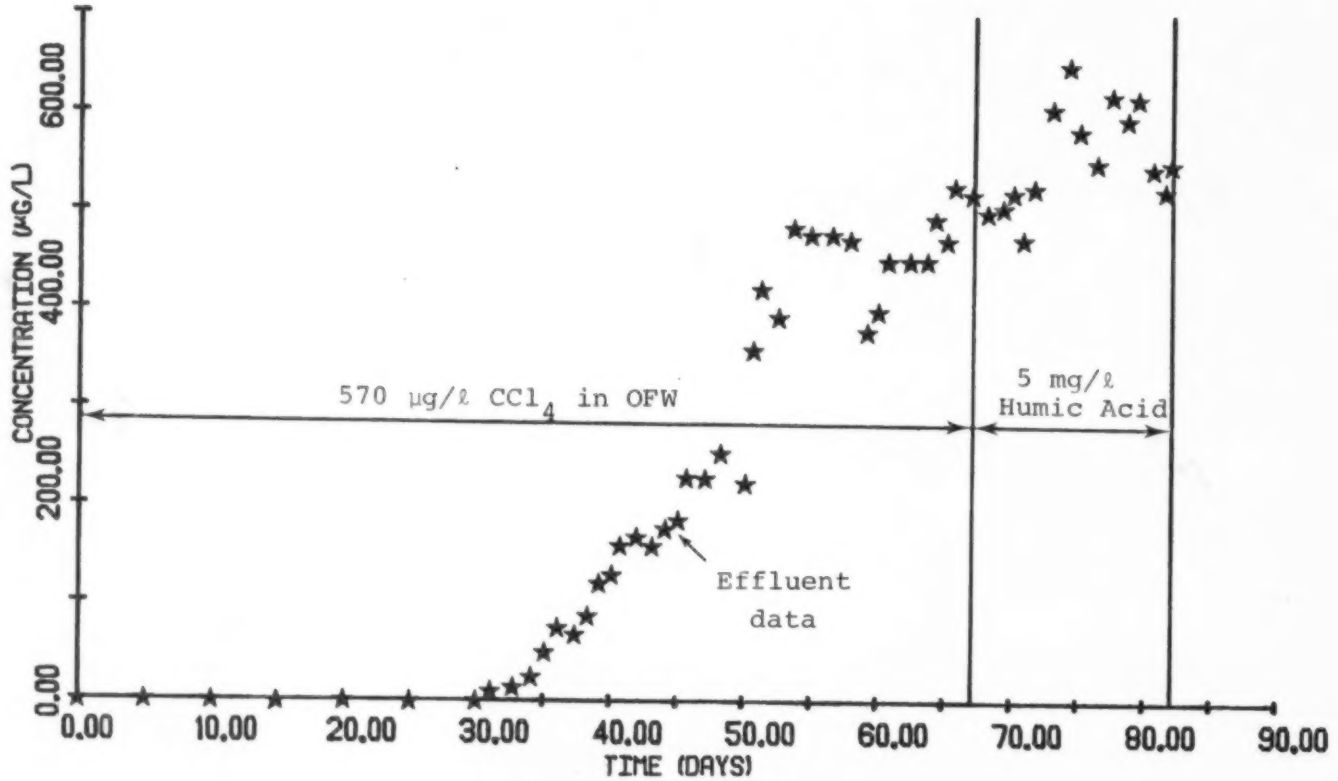

Figure 78. Experimental breakthrough and displacement profiles for CCl_4 in a fixed-bed adsorber (flow rate=3.5 gpm/ft^2, 250 grams of 16/20 US sieve size carbon).

described earlier for the OFW background solutions and utilized a 3-cm ID glass adsorber containing 100 grams of 16/20 carbon. Analogous conditions were used to facilitate comparison of model profile simulations in terms of estimated values for k_f and D_s.

All attempts to carry the fixed-bed adsorber operations to completion were hampered by extensive biological growth. Figure 79 presents typical influent and effluent data for CCl_4 in a 5-mg/l humic acid background solution for the initial part of the breakthrough profile. It is evident that the effects of the biological growth make it virtually impossible to reach any definite conclusions regarding the dynamic adsorption behavior of CCl_4 in the presence of humic acids.

Efforts were then made to inhibit biological activity. The feed solution was dosed with 2 mg/l silver nitrate. This inhibitor was subsequently deemed unsatisfactory because it complexes with humic acid and changes the adsorption characteristics of the latter (as discussed in Section 6). Earlier column investigations had indicated that tap water might have some inhibitory effect due to its residual chlorine content, but it was found in subsequent experiments that this did not completely eliminate biological growth.

Other alternatives were explored. Fixed-bed adsorbers saturated with carbon tetrachloride were fed with a solution of 5 mg/l humic acid and carbon tetrachloride for a period of 10 days, beyond which it was impossible to continue the operation because of prolific biological growth. Figure 80 presents data from this experiment.

Two mini-column adsorbers, one containing two grams of carbon saturated with humic acid and the other two grams of virgin carbon, were fed with a solution of carbon tetrachloride in further experiments. The corresponding effluent breakthrough profiles for carbon tetrachloride presented in Figure 81 indicate a substantial reduction in the capacity of the pre-saturated carbon for adsorption of CCl_4. Further analyses showed no humic acid residuals in the effluent from the pre-saturated column, indicating no humic acid displacement by carbon tetrachloride. Thus competitive adsorption appears to play a significant role in the dynamics of removal of carbon tetrachloride in typical adsorber applications.

SUMMARY AND CONCLUSIONS

1. The adsorption methodologies and associated analytical procedures described herein for carbon tetrachloride can be applied to compounds which demonstrate comparable physical and chemical characteristics; specifically,

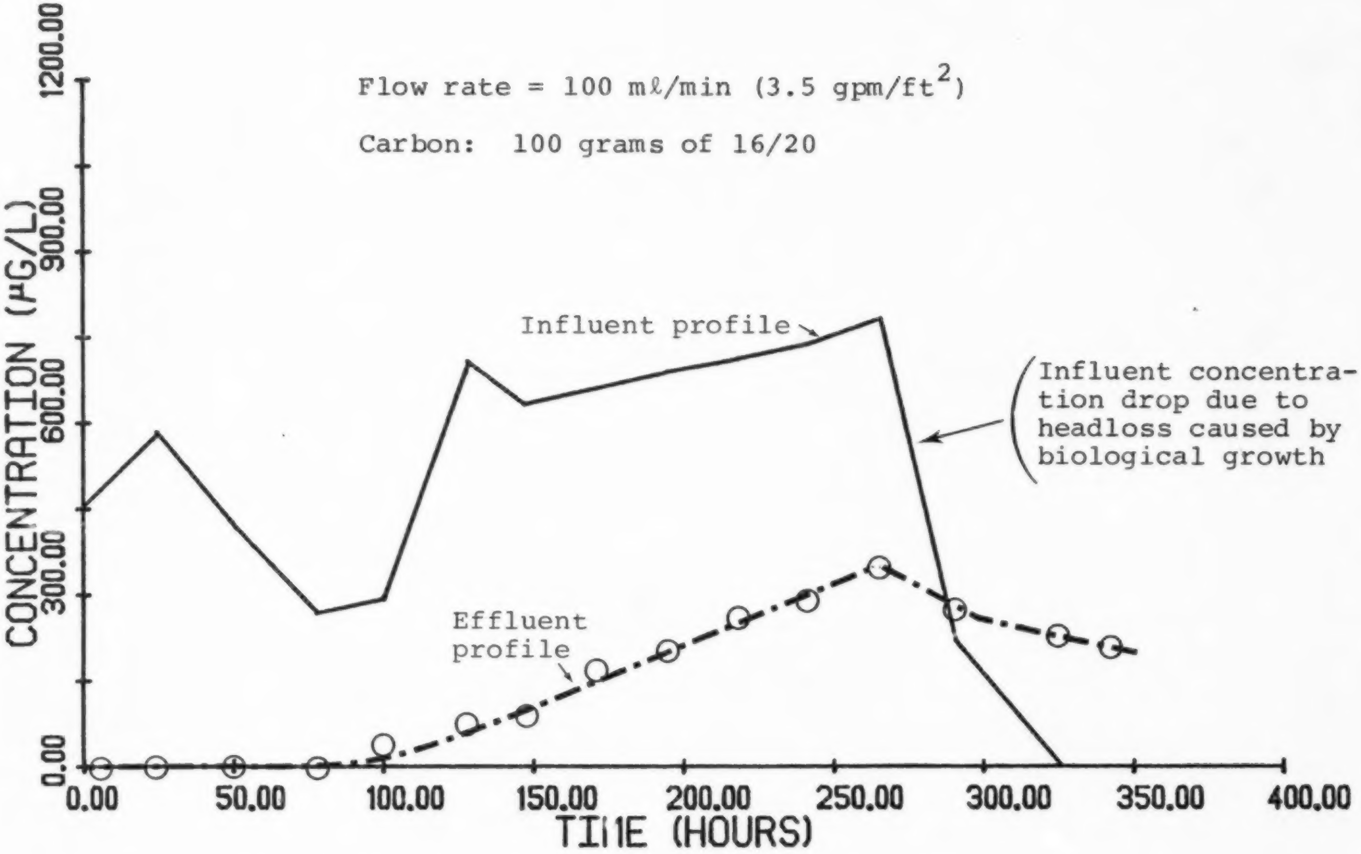

Figure 79. Influent and effluent profiles for CCl_4 in the presence of 5 mg/ℓ humic acids in a fixed-bed adsorber.

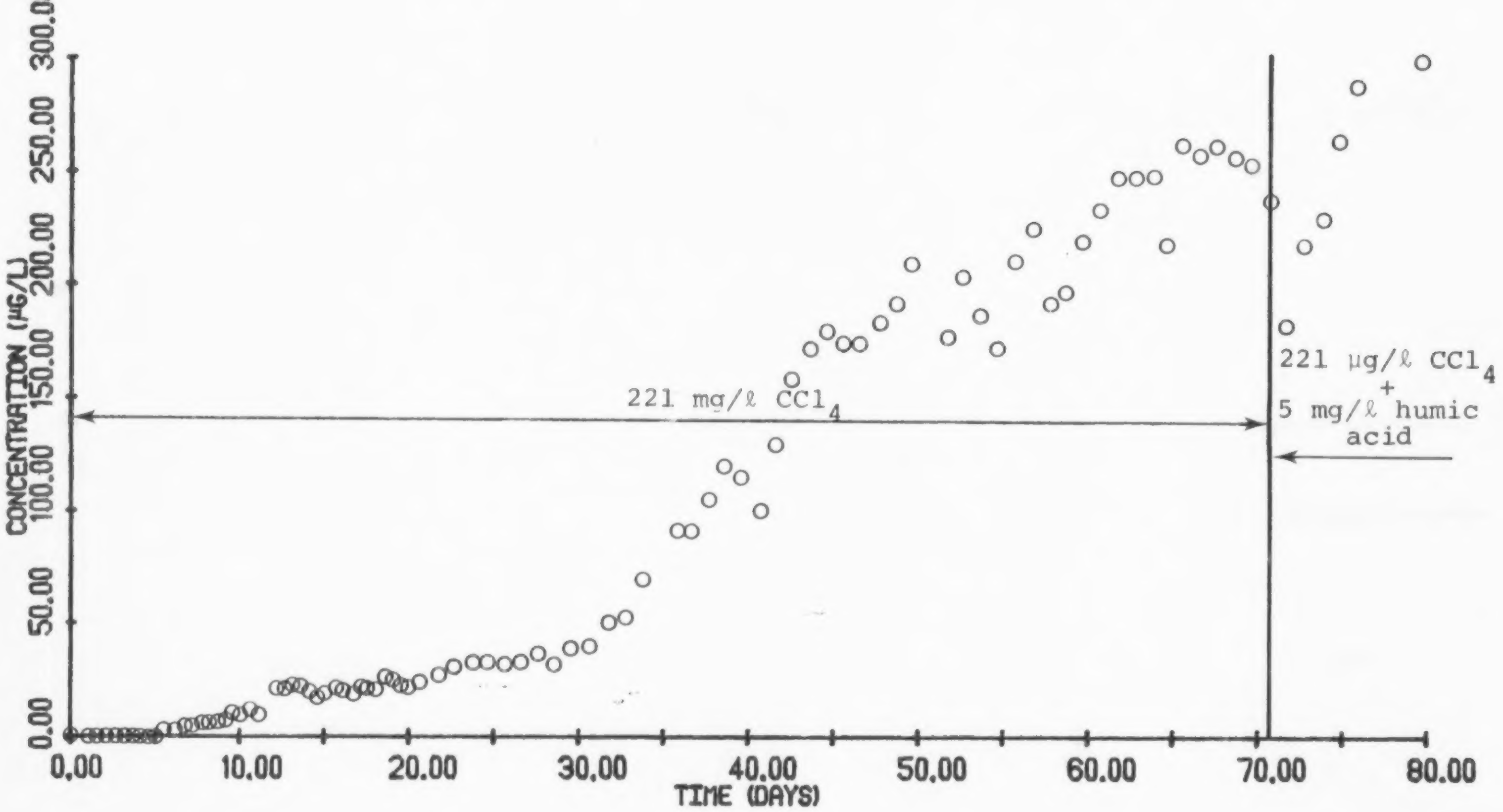

Figure 80. Experimental breakthrough and displacement profiles for CCl_4 in a fixed-bed adsorber (flow rate= 3.5 gpm/ft^2, 250 grams of 16/20 US sieve size carbon).

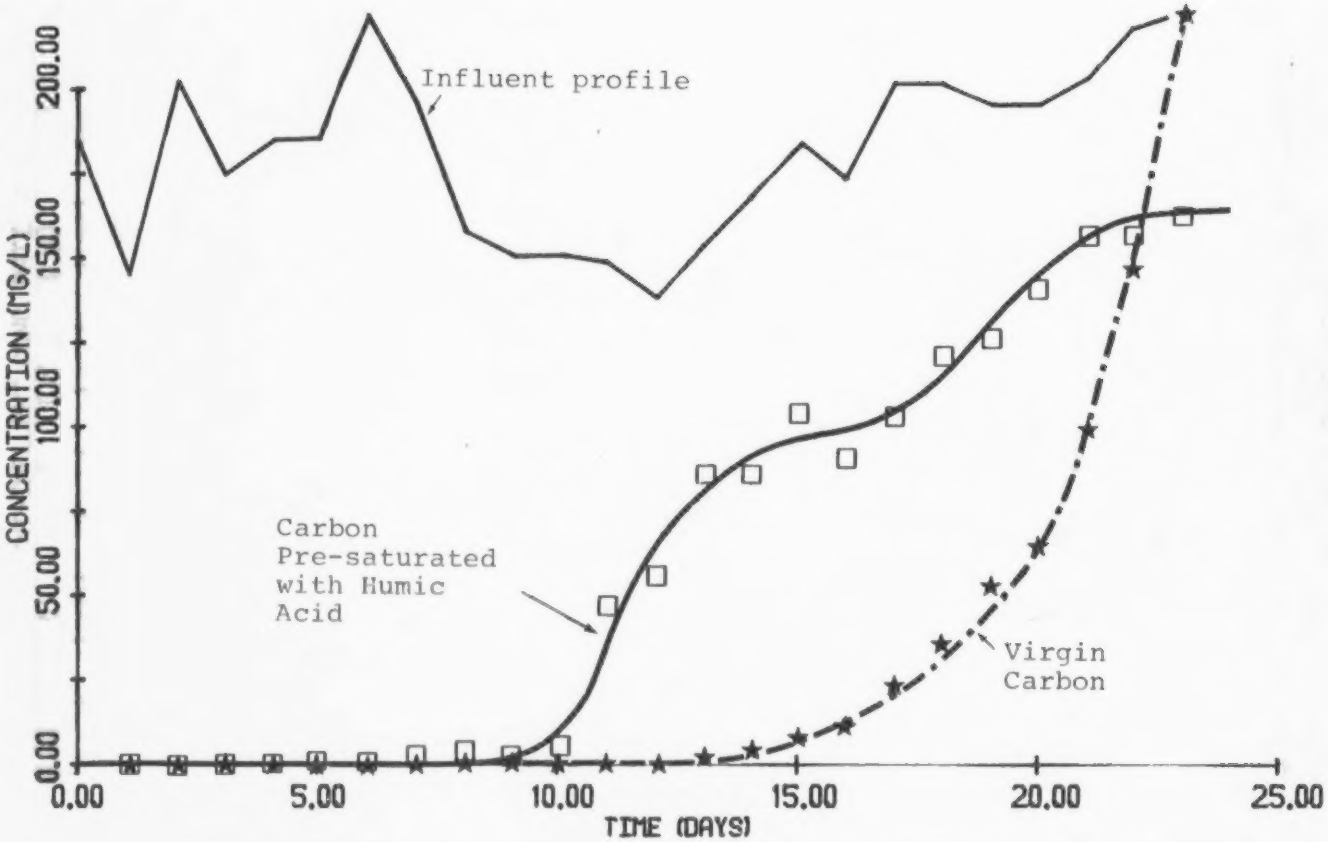

Figure 81. Experimental breakthrough profiles for CCl_4 in mini-column adsorbers; effect of pre-saturation on the capacity (flow rate=5 mℓ/min , 2 grams of 50/60 US sieve size carbon).

the trihalomethanes.

2. The results of adsorption-desorption equilibrium studies suggest that adsorption of CCl_4 is readily reversible. Further, it was demonstrated that substantial amounts of CCl_4 were released from the adsorber columns in the course of dynamic desorption studies. These facts suggest that adsorption of CCl_4 on carbon occurs predominantly as a result of van der Waals attraction forces (physical adsorption) which are generally characterized by low energies of adsorption.

3. The MADAM adsorption model was generally able to simulate and predict the performance of fixed-bed adsorbers for adsorptive removal of carbon tetrachloride. Predictions suffered, however, in cases where influent concentrations fluctuated drastically and/or where frequent air scouring and backwashing were required to control head-losses caused by excessive biological activity in the adsorbers.

4. Quantitative predictions of the performance of fixed-bed adsorbers for CCl_4 may be predicated on model calibrations performed with mini-column systems, which are generally more flexible and easier to operate and maintain than larger systems.

5. The effectiveness of activated carbon for removal of CCl_4 from water in practical applications is adversely affected by the competitive adsorption effects of background organic substances such as humic acids.

6. The observations of apparently different rate controls in the mini-column and pilot column suggest that the mass transport limiting mechanism for CCl_4 depends in large measure on the physical characteristics of the system including the column type, hydraulic regime, and carbon particle size.

7. Larger long-term fixed-bed adsorber studies with CCl_4 in waters containing background organic matter such as humic acids are hampered by extensive biological growth and resulting headloss. A number of inhibitors were examined for biogrowth suppression, but none was found entirely suitable for the reasons discussed in Appendix J.

SECTION 8

ADSORPTION OF BENZENE

GENERAL

Benzene, (C_6H_6), also variously termed benzol, benzole, cyclohexatriene and phene, was first isolated and named in 1825 by Faraday. It has since found wide-scale use in numerous industrial applications. Benzene is produced from petroleum fractions by reforming-separation processes. Reforming, which increases the benzene content of these fractions, is accomplished by hydrogenation and dealkylation of methyl and dimethyl cyclopentanes, and cyclodehydrogenation of straight chain aliphatics. Other means for producing benzene include dealkylation and transalkylation of toluene, and steam cracking of heavy naphthas or gas oils. Coal, the most important source of benzene prior to 1950, is likely to again replace petroleum as a source for hydrocarbons in general (Kirk-Othmer, Encyclopedia of Chemical Technology, 1978). Table 14 summarizes the salient physical and chemical properties of benzene.

The major use of benzene prior to World War II was in motor fuels. When appropriately mixed with heptanes and octanes, it improves the antiknock, starting ability and efficiency characteristics of high compression engines. Today, 1.8% by weight of gasoline is benzene. Since World War II, many other applications for benzene have been realized. Benzene is a significant raw material for production of other chemicals. Chlorination of benzene leads to production of certain insecticides (dichlorobenzenes), and to one precursor of phenol (monochlorobenzene). Alkylation of benzene with ethylene produces a precursor of styrene, which is a major component of synthetic rubber and numerous polystyrene compounds. Cyclohexane and nitrobenzene, used in nylon and dye manufactures, respectively, are also derived from benzene. Another important use of benzene is as a solvent in paints and coatings, and in preparation of artificial and natural leathers. A summary of benzene uses in the United States is given in Table 15 (Greene, 1978).

TABLE 14. PHYSICAL AND CHEMICAL PROPERTIES OF BENZENE*

Formula Weight	78.11
Crystalline Form and Color	liquid, colorless
Specific Gravity (20°C)	.879
Melting Point (°C)	5.5
Boiling Point (°C)	80.1
Heat of Vaporization (kcal/mol)	7.352
Solubility (%):	
Water	.07
Alcohol/ether/acetone	$\infty/\infty/\infty$
Viscosity (25°C)	0.6028 centipoise
Vapor Pressure	$\log p = 6.90565 \text{ x } 1{,}211.033/(t + 220.790)$
Dielectric Constant	2.275

*Sources: Lange's Handbook of Chemistry, 1979; CRC Handbook of Chemistry and Physics, 1976-1977; Kirk-Othmer, Encyclopedia of Chemical Technology, 1978.

TABLE 15. SUMMARY OF BENZENE USES

Application	Use, % of Total
Packaging, consumer goods, toys, disposables	25
Household goods	17
Transportation	17
Building and construction	10
Chemical intermediates	7
Apparel	6
Surfactants	5
Agricultural chemicals	3
Exports	10
Total	100

Sources and Sinks in the Environment

Because of its numerous and wide-spread applications, opportunities for benzene release to the environment are many. Evaporation from petroleum fuels, solvents and other liquids, as well as the breakdown of benzene-containing goods, are sources fo widespread water, soil and air contamination. Grob and Grob (1974) reported, for example, that evaporation of automotive fuels and subsequent atmospheric washout constitutes the major source of the organic pollutants found in Lake Zurich, Switzerland; benzene was found to be a principle component of these organics. Waste discharges from the leater, rubber, printing, paint, and dry-cleaning industries are other major sources. It has been estimated that, as of 1975, 60-90% of the drinking water supplies in the United States contained benzene (including the alkylated benzenes) in the part-per-billion (ppb) range, the highest concentration reported was 10 ppb (USEPA, Report to Congress, 1975).

Health Assessment

Concern regarding benzene in the environment relates in large measure to its toxic effects on human and animal life. Its toxic character was first recognized in 1897 by Santesson; only recently, however, has the seriousness of benzene poisoning received national attention (Cohen et al, 1978).

Chronic effects of poisoning from low benzene concentrations are manifest in the blood forming system, and result in pancytopenia - a decrease in red cells, white cells, and platelets (aplastic anemia). Benzene is most likely stored in the lipids and fat of the body where it is soluble. The liver eventually metabolizes it to benzene oxide and further to various other products including, phenol, benzene glycol, and phenylmercapturic acid (Thorpe, 1978). Based on studies of benzene poisoning of animals, some researchers speculate that one or more metabolites of benzene are responsible for pancytopenia (Cohen et al, 1978). Some evidence indicates hyperplastic or overactive marrow. In any case, the effects of benzene poisoning are long-lasting, and some experts even suggest they may lead to leukemia (Cohen et al, 1978; Thorpe, 1978). Thus, benzene is included in the EPA hazardous chemical list.

ANALYTICAL TECHNIQUES

Several important points were considered in the search to select a most suitable analytical method for the detection of benzene in dilute aqueous solution, including: specificity, sensitivity, sample size, reproducibility, detection limit of ≈ 1 μg/l, quickness and ease. The flame ionization gas chromatography technique was found most suitable from these several perspectives. Four modes of operation were investigated, including: direct aqueous injection, liquid-liquid extraction, static headspace analysis and dynamic headspace analysis.

Direct Aqueous Injection

To test the applicability of this method, a series of aqueous benzene solutions of low (μg/l) concentration was prepared. Samples up to 20 μl were withdrawn using a microsyringe and introduced into a Varian 2700 gas chromatograph equipped with a 6' x 1/8" stainless steel column packed with 80/100 Tenax-GC. The operating conditions were set at 150°C column, 220°C injector, 250°C detector with a nitrogen carrier gas flow rate of 40 ml/min. The lowest detection limit achieved was ≈ 50 μg/l and, the technique was therefore deemed unsatisfactory.

Liquid-Liquid Extraction

In this technique, 5 milliliters of aqueous solution were extracted with 1 ml of carbon disulfide (CS_2). Carbon disulfide was chosen because of its insensitivity to flame ionization detector. A 10 microliter quantity of the CS_2 extract was then injected into the gas chromatograph column at the same operating conditions described earlier for direct aqueous injection. The lower limit of detection obtained was 20 µg/l, again too high for this study.

Static Headspace Analysis

For evaluationg this procedure, 100 mls of different benzene standard solutions were placed in 150 ml Hypo-Vials. Aluminum caps with Teflon-lined septa were then crimped onto the vials to give an airtight seal. The solutions were shaken vigorously until equilibrium between the liquid and gaseous phases were reached. The vapor phase was withdrawn using a 1.0 ml gas-tight syringe and introduced into the gas chromotograph. The desired limit of detection, however, could not be achieved by this method.

Dynamic Headspace Analysis

The method employed for dynamic headspace analysis was similar to the one described by Bellar and Lichtenberg (1974) and discussed in Section 7 for carbon tetrachloride. The technique involved the use of a specialized apparatus including a glass purging device, a cold trap for collecting and concentrating the purged benzene, and a thermal desorber which was incorporated into a modified injector port mounted on a Varian 2700 gas chromatograph (GC).

In this procedure, a 5.0 ml quantity of aqueous sample is purged for 11.0 minutes with pre-purified nitrogen gas at a flow rate of 13 ml/min. The benzene contained in the aqueous sample is effectively concentrated onto a 6' x 1/8" stainless steel cold trap packed with 60/80 Chromosorb 101 held at room temperature. The adsorbed benzene is then desorbed from the cold trap at 120°C with pre-purified nitrogen for 3 minutes at a flow rate of 20 ml/min. The purged benzene is subsequently resorbed on a 6' x 1/8" stainless steel gas chromatographic column packed with 10% Tri (Cyanoethoxy) Propane on 80/100 Chrom sorb P AW (Supelco Co.) held at 40°C. The column is then heated rapidly (40°C per min) to 90°C, and benzene eluted off the column within 3 minutes after the 90°C temperature is reached.

The GC detector response for each sample was recorded by measuring the peak heights, traced by a recorder. A calibration curve based on the quantity of the benzene contained in the standard solutions versus the peak heights was used for sample concentration determination. A discussion of benzene standard solution preparation and calibration is included in Appendix L.

This method, in addition to requiring specialized apparatus and modification of the gas chromatograph, demands a considerable amount of time per analysis. Nonetheless, the technique yielded a desired limit of detection (2 μg/l), with a reproducibility of 5.6% (coefficient of variation) and extraction efficiency of 96%. The dynamic headspace analysis thus was judged to be the only feasible technique for this study.

ADSORPTION METHODOLOGIES

Equilibrium Studies

Adsorption equilibrium studies for benzene were conducted using a bottle point technique. In this procedure, carefully weighed quantities of 50/60 US standard sieve size carbon were placed in properly cleaned 150 ml Hypo-Vials containing 100 ml of OFW. An appropriate volume of benzene was transferred to each vial from a stock solution using a pipette. The vials were then filled with OFW, leaving no headspace, and sealed with Telfon-lined and crimped-on aluminum caps. The vials were subsequently placed in a specially designed tumbler box and tumbled for 5 days at room temperature until equilibrium was achieved. 5 ml samples were then withdrawn from the vials and subjected to the dynamic headspace gas chromatographic analysis, described earlier.

Equilibrium experiments for benzene in humic acid background solution (5 mg/l humic dissolved in OFW) were also performed in the manner described above.

Rate Studies

CMB-reactor rate studies for benzene were conducted in a manner analogous to the methodology described for CCl_4 (Section 7). In these experiments, 2 liters of OFW were added to a 2.6-l air-tight glass reactor. An appropriate volume of benzene stock solution was added to the reactor and the reactor filled with OFW, leaving no headspace. The solution was mixed for five minutes prior to the addition of a weighed quantity of pre-wetted carbon. The carbon was dispersed by a motor-driven glass stirrer. Samples were withdrawn at pre-determined time intervals. A positive displacement plunger was used to eliminate the headspace introduced by sample withdrawal. Samples were analyzed using the dynamic headspace GC analysis technique, described in an earlier subsection of this section.

CMB-reactor rate experiments for benzene in humic acid background solution were also performed in the manner discussed above.

Column Studies

Experimental column studies for benzene were designed and executed in the manner described for CCl_4 (Section 7). Mini-column and large adsorber column studies were performed to investigate the behavior of breakthrough profiles for benzene. The large fixed-bed adsorber columns consisted of 100-gram quantities of 16/20 US standard sieve size carbon in 3-cm ID glass adsorbers. Influent and effluent samples were collected manually in 10 ml vials. Extreme care was exercised to minimize benzene loss due to volatilization. The samples were analyzed immediately using the dynamic headspace analysis technique. The feed solution was dosed with 2 mg/l of silver to suppress biological growth. Maintaining a steady influent concentration was difficult and frequent system readjustment was necessary.

The fixed-bed mini-column adsorbers were comprised of 1- or 2-gram quantities of 50/60 carbon in 1.2-cm ID glass columns. The mini-column experimental system demonstrated ease, flexibility, and operational consistency. The experimental apparatus and arrangement for the benzene column studies was similar to the systems described for carbon tetrachloride.

RESULTS AND DISCUSSION

Adsorption Equilibria

As for humic acid and CCl_4, the Fruendlich equation was found to provide the best fit to the experimental data. The experimental data and fitted Freundlich isotherm obtained for benzene in OFW using the bottle point technique are presented in Figure 82, and for benzene in 5 mg/l humic acid background solution in Figure 83. The experimental system conditions and isotherms parameters are listed in Table 16.

As evident from Figure 82, Figure 83, and Table 16, no significant difference in the extent of the adsorption was observed between the two systems, indicating that competitive adsorption is not a major factor in this particular case.

Adsorption Rates

A simulation modeling analysis was conducted on the data from the adsorption rate studies for benzene in OFW background solution to evaluate the appropriate mass transfer coeffi-

TYPING GUIDE SHEET

TABLE 16. ADSORPTION EQUILIBRIUM STUDIES FOR BENZENE[†]

Figure No.	Background Solution	Initial Concentration (μg/l)	Freundlich Isotherm Constants*		
			K_f	1/n	r**
82	OFW	490	1.14	0.398	0.987
83	OFW + 5 mg/l humic acid	457	0.814	0.510	0.992

† All studies were conducted at pH 7 unless otherwise noted.

* Based on C_e and q_e expressed in μg/l and mg/gm, respectively.

r** Correlation coefficient for fit of the isotherm to the experimental data.

EPA-287 (Cin.)
(4-76)

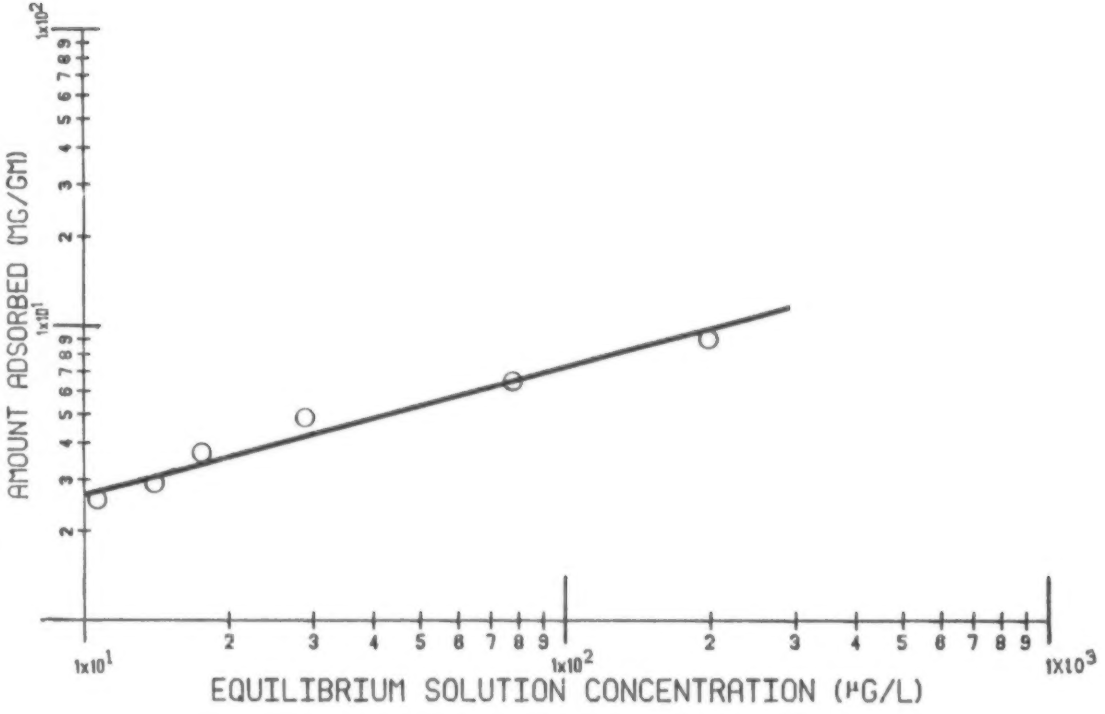

Figure 82. Adsorption isotherm for benzene in OFW (C_o = 490 μg/ℓ).

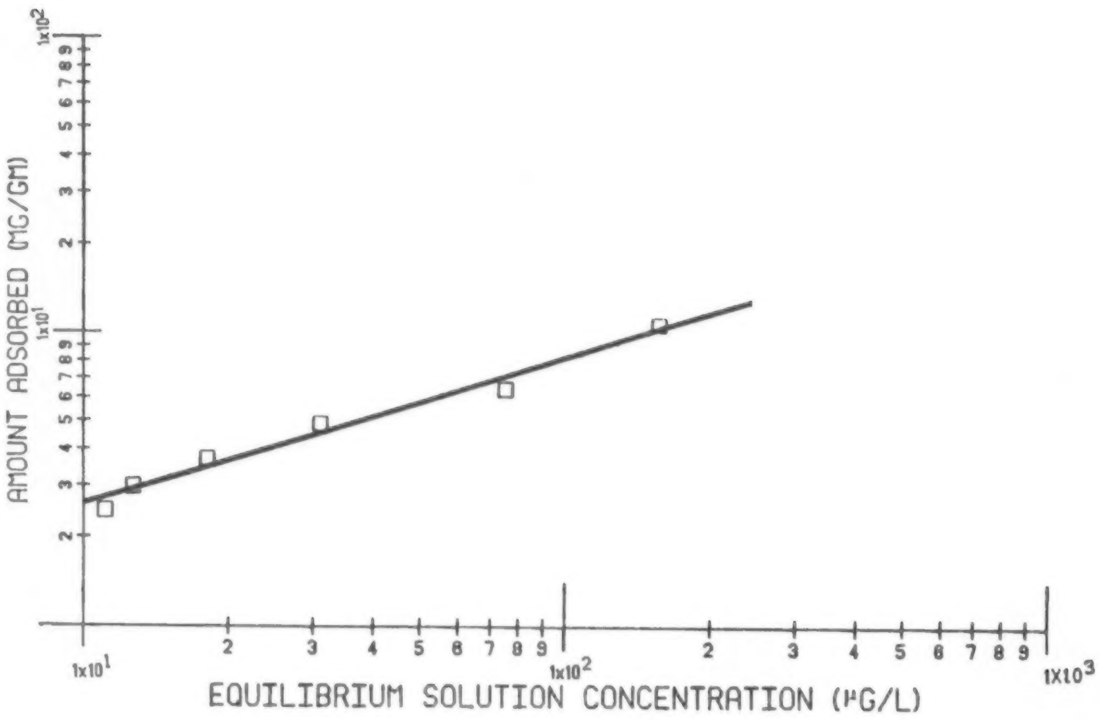

Figure 83. Adsorption isotherm for benzene in humic acids background solution (C_o = 457 µg/ℓ).

cients, k_f and D_s. Values for the coefficients of $k_f = 7.48 \times 10^{-3}$ cm/sec and $D_s = 1.3 \times 10^{-9}$ gave the concentration-history profile demonstrated by the solid line in Figure 84. Figures 85 and 86 show the results of sensitivity analyses performed for k_f and D_s, respectively. It may be observed from Figure 85 that the effect of variation in film transfer coefficient, $k_f \pm 25\%$, generates substantially different predicted profiles whereas the system is relatively insensitive to changes in D_s(Figure 86). This indicates that external mass transfer most likely controls rates of adsorption of benzene by activated carbon. Further, simulation studies were performed for benzene in 5 mg/l humic acid background solution. The solid line presented in Figure 87 is a profile predicted on estimated mass transfer coefficients of, $k_f = 6.38 \times 10^{-3}$ cm/sec and $D_s = 1.37 \times 10^{-9}$ cm^2/sec. A summary of the experimental conditions and the mass transfer coefficients are tabulated in Table 17.

The humic acid system demonstrates a slightly lower film transfer coefficient, k_f, than the OFW system, while, no significant change in surface diffusion coefficient, D_s, is observed.

Adsorption Columns

For model calibration and verification, three sets of experimental column data were collected for benzene in OFW background solution. Typical experimental data and the best fit profiles are presented in Figures 88 and 89.

Table 18 includes the physical and chemical parameters associated with selected adsorber studies, in addition to values for the corresponding mass transfer coefficients, k_f and D_s. The surface diffusion coefficient was estimated from the CMB-reactor rate experiments and the film transfer coefficient was obtained by the correlation technique suggested by Williamson et al (1963).

Figures 90 and 91 represent experimental data and predicted breakthrough profiles for typical mini-column runs conducted for different bed lengths and hydraulic loadings.

Model Calibration--

The results of model calibrations predicated on parameter values estimated independently of column experiments (Crittenden and Weber; 1978a, b, and c) for a flow rate of 10 ml/min and a bed length of 2.1 cm are illustrated in Figure 90. Good agreement is demonstrated between the experimental data and the predicted profile.

Model Verification--

To test the model for generality, it was verified for

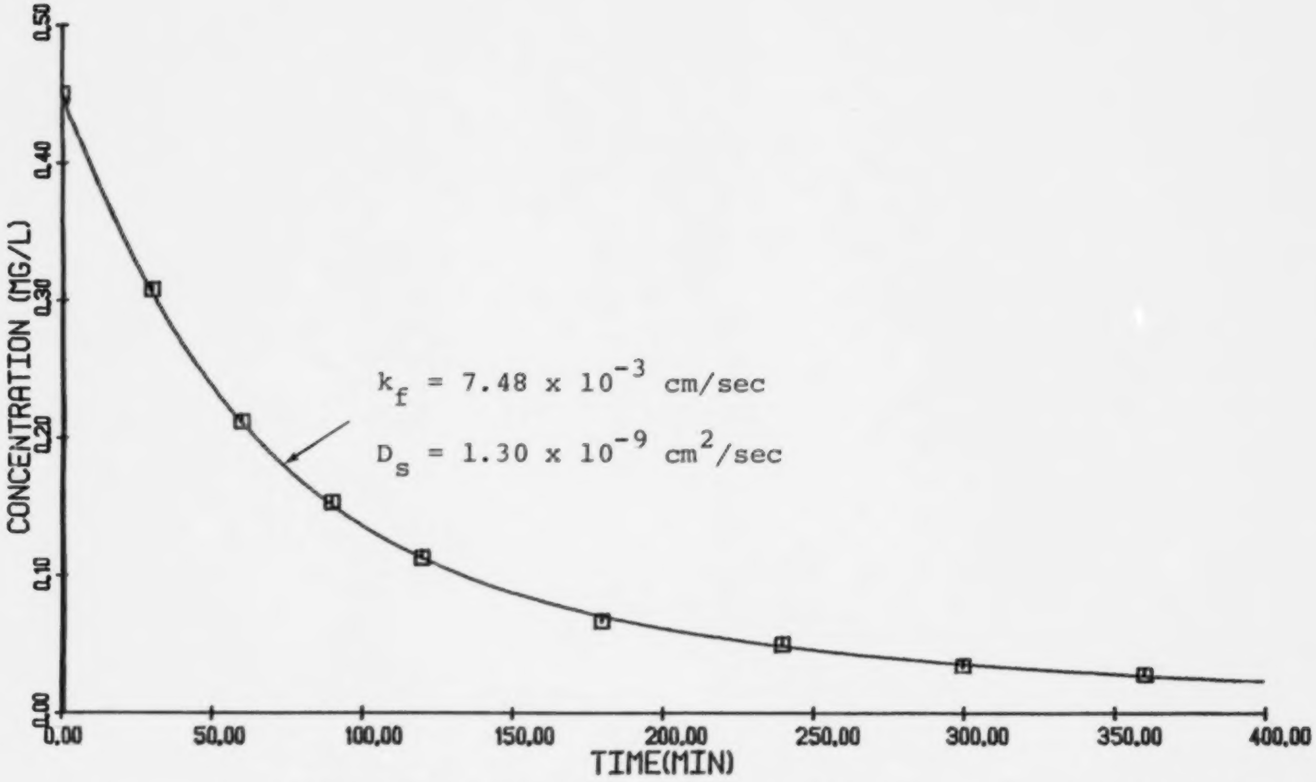

Figure 84. Experimental data and model profile for rate of adsorption of benzene from OFW in a CMB reactor (C_o = 450 μg/ℓ, 0.38 g/ℓ of 16/20 US sieve size carbon).

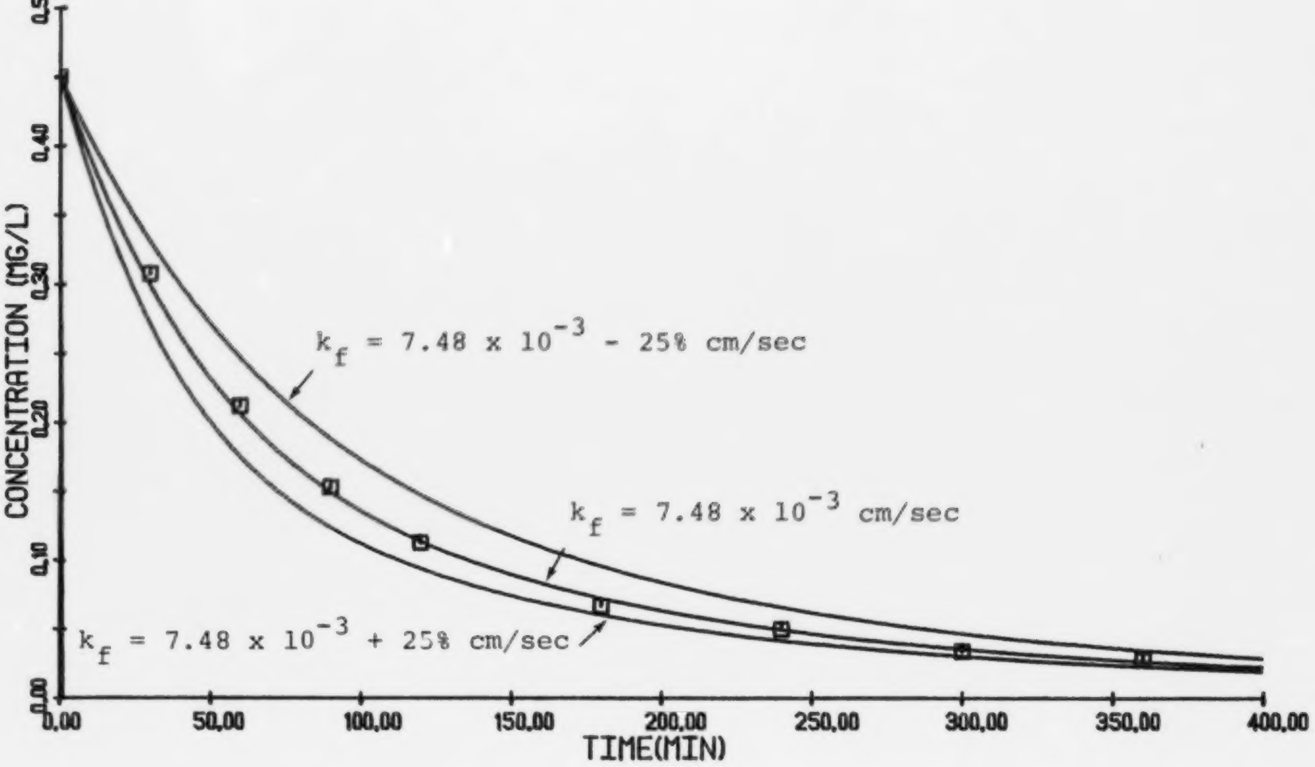

Figure 85. Analysis of the sensitivity of model profile to film transfer coefficient, k_f.

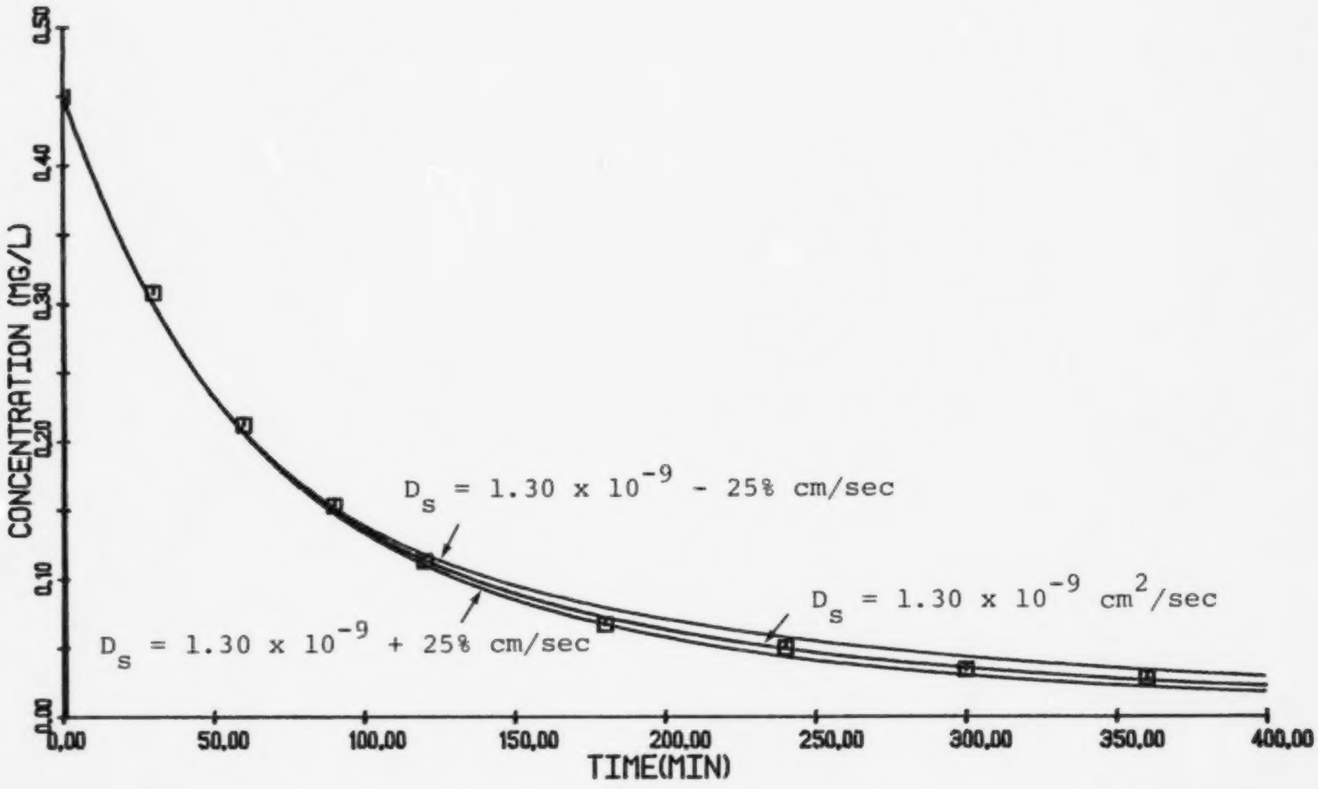

Figure 86. Analysis of the sensitivity of model profiles to surface diffusion coefficient, D_s.

TYPING GUIDE SHEET
BEGIN FIRST LINE OF TEXT HERE
DROPPED HEAD. BEGIN SECTIONS HERE
CENTER OF PAGE
TOP OF IMAGE AREA
BEGIN LAST LINE OF TEXT
BOTTOM OF IMAGE AREA; OUTSIDE DIMENSION FOR TABLES AND ILLUSTRATIONS
3/8"
6-1/2"
7/8"

TABLE 17. ESTIMATED ADSORPTION RATE MASS TRANSFER COEFFICIENTS FOR BENZENE

Figure No.	Background Solution	C_o, µg/l	Carbon Dosage, µg/l	k_f, cm/sec	D_s, cm/sec
84	OFW	450	0.38	7.48×10^{-3}	1.30×10^{-9}
87	OFW + 5 mg/l humic acid	507	0.38	6.38×10^{-3}	1.37×10^{-9}

C_o = Initial concentration;

k_f = Film transfer coefficient; and,

D_s = Surface diffusion coefficient.

PAGE NUMBER
EPA-287 (Cin.)
(4-76)

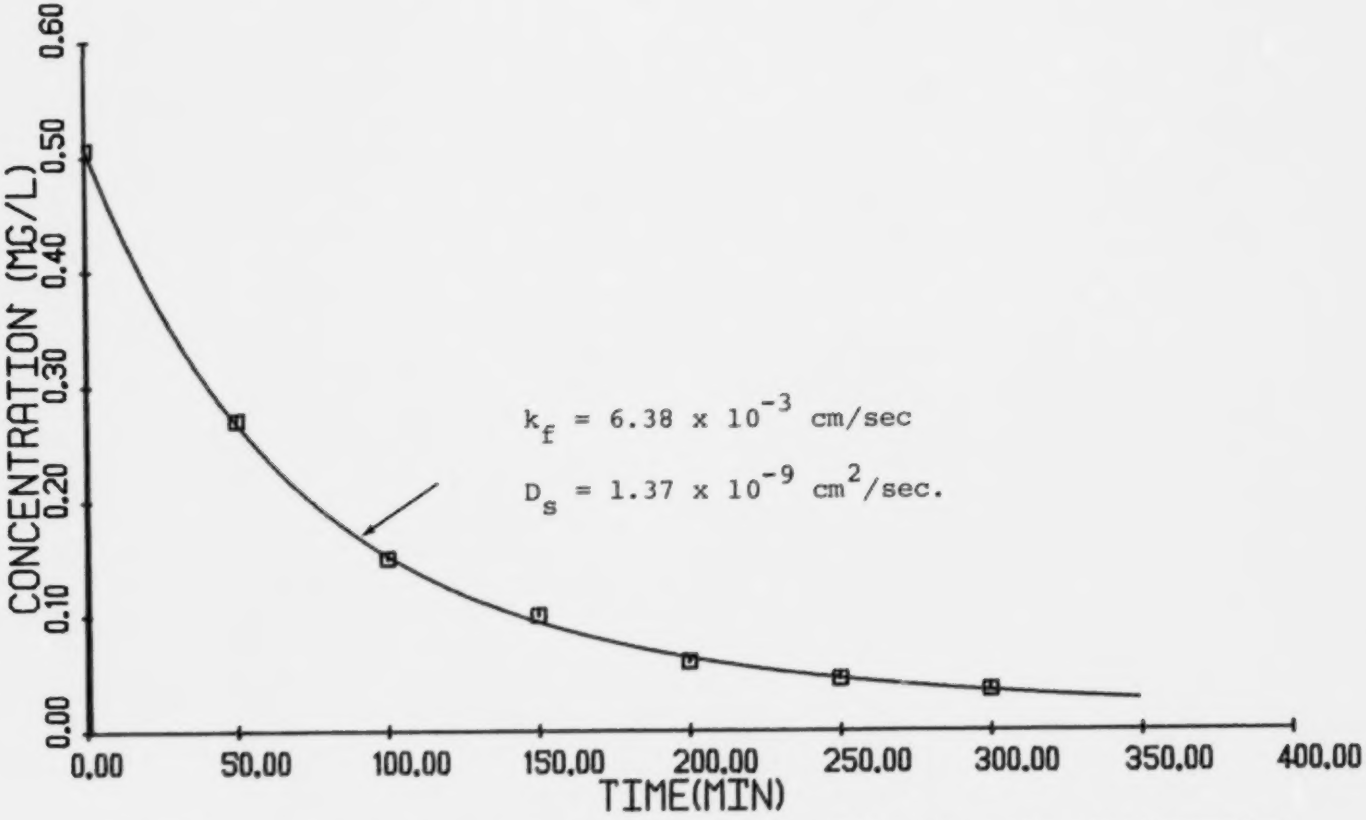

Figure 87. Experimental data and model profile for rate of adsorption of benzene from humic acids background solution in a CMB-reactor (C_o = 507 μg/ℓ, 0.38 g/ℓ of 16/20 US sieve size carbon).

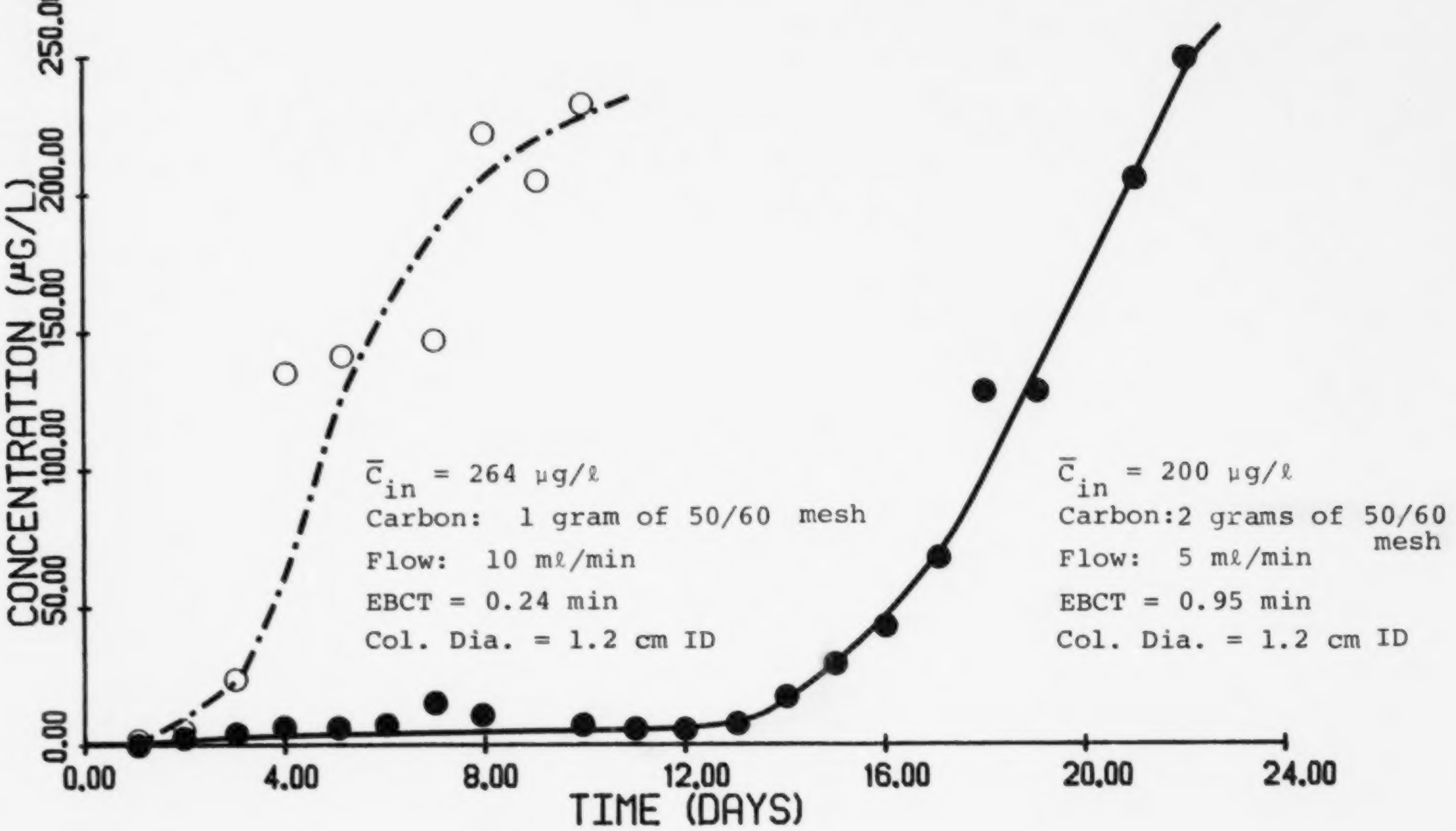

Figure 88. Experimental breakthrough profiles for benzene in mini-column adsorbers.

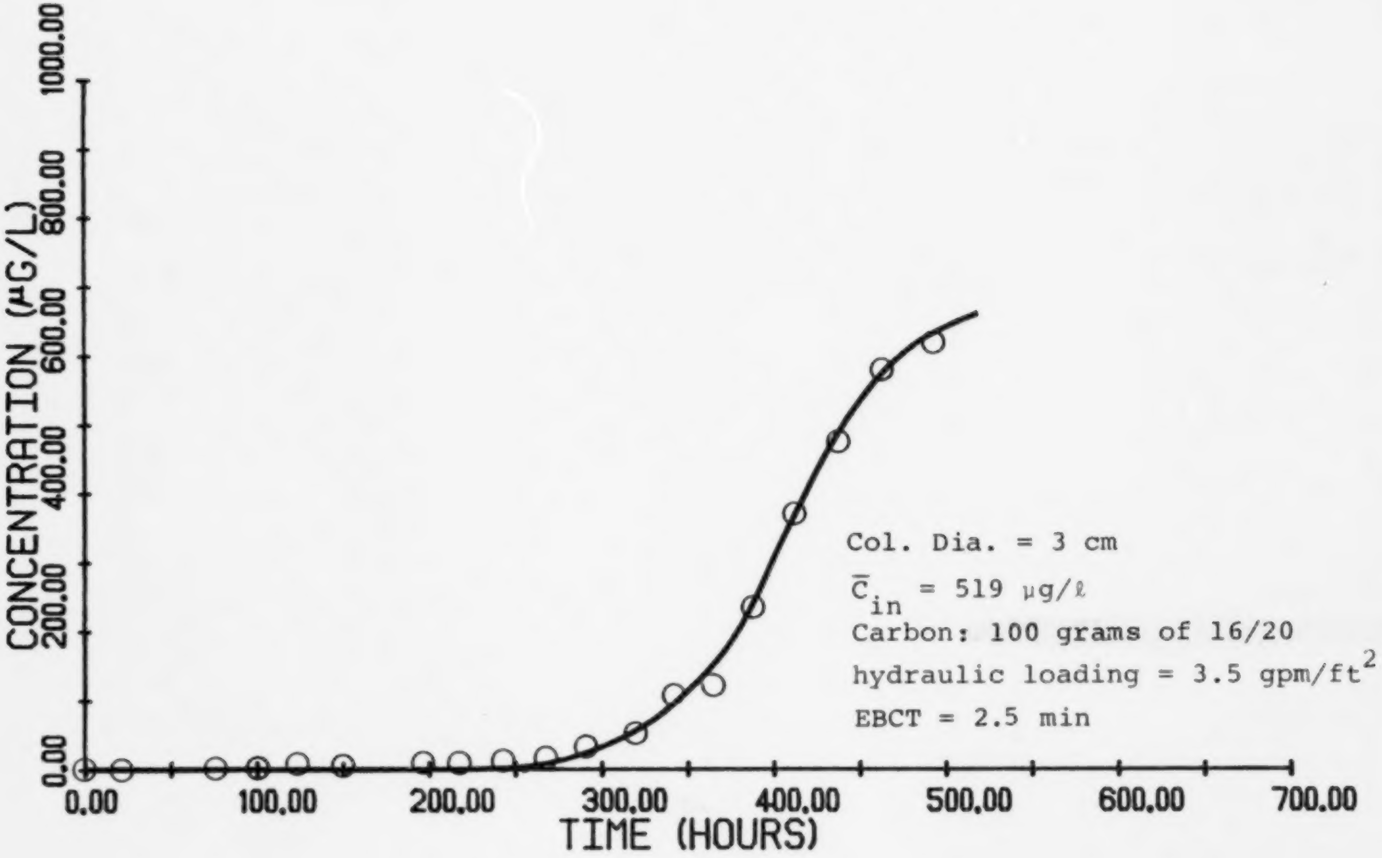

Figure 89. Experimental breakthrough profile for benzene in a large adsorber.

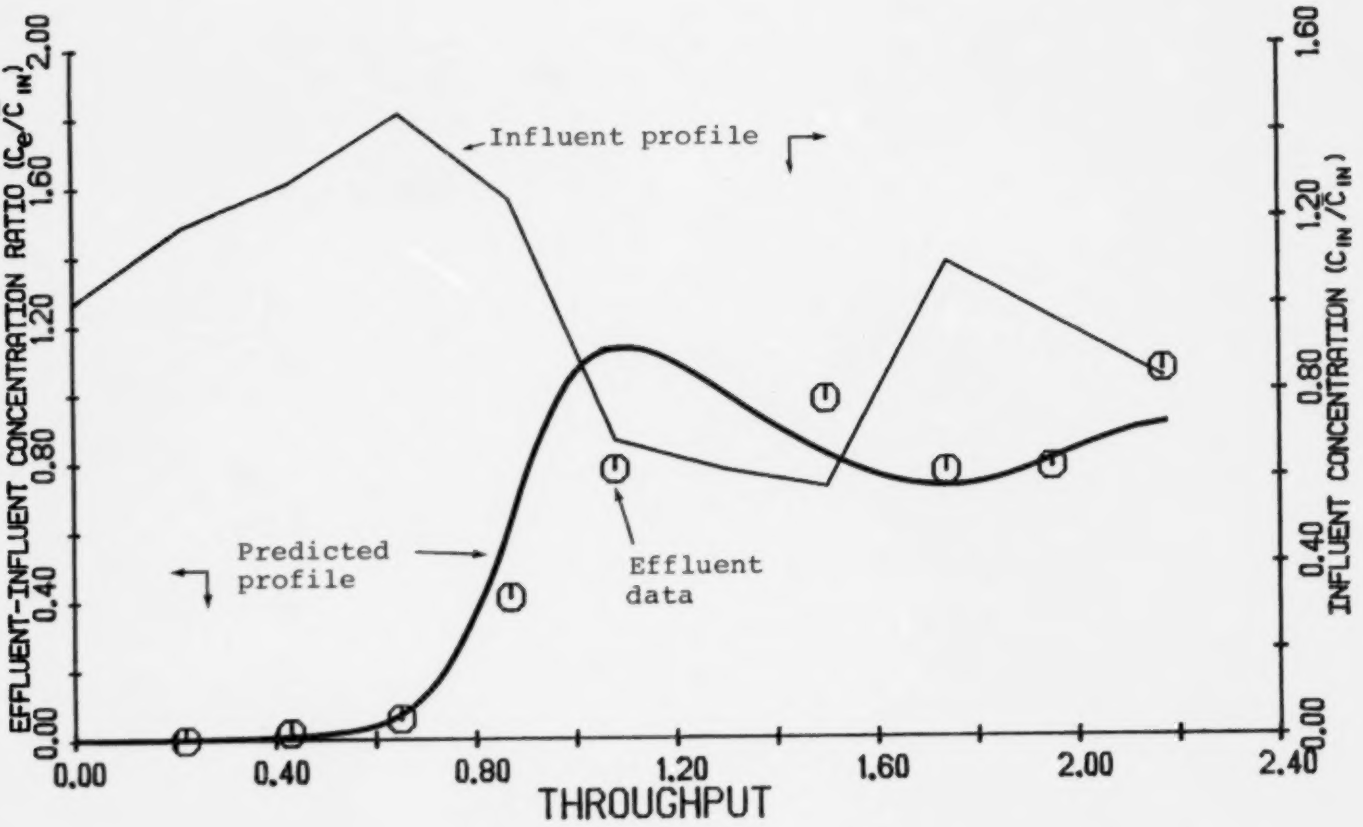

Figure 90. Effluent and influent concentration profiles for benzene in OFW - fixed-bed adsorber Run I ($\bar{C}_{in}$ = 264 µg/ℓ, 1 gram of 50/60 carbon, flow rate = 10 mℓ/min, EBCT = 0.24 min).

TABLE 18. FIXED-BED ADSORBER PARAMETERS FOR BENZENE

Adsorber Run	$\overline{C}_{in}$, µg/l	d, cm	L, cm	γ	v, cm/sec	k_f, cm/sec	D_s, cm^2/sec
I (Figure 90)	264	0.027	2.1	0.37	0.4	6.07×10^{-3}	1.3×10^{-9}
II (Figure 91)	200	0.027	4.2	0.37	0.2	4.79×10^{-3}	1.3×10^{-9}
III (Figure 92)	519	0.1	36	0.41	0.57	3.26×10^{-3}	1.3×10^{-9}

$\overline{C}_{in}$ = Average influent concentration;

d = Carbon particle diameter;

L = Bed length;

γ = Bed porosity, dimensionless;

v = interstitial fluid velocity;

k_f = Film transfer coefficient; and,

D_s = Surface diffusion coefficient.

TYPING GUIDE SHEET
EPA-287 (Cin.)
(4-76)

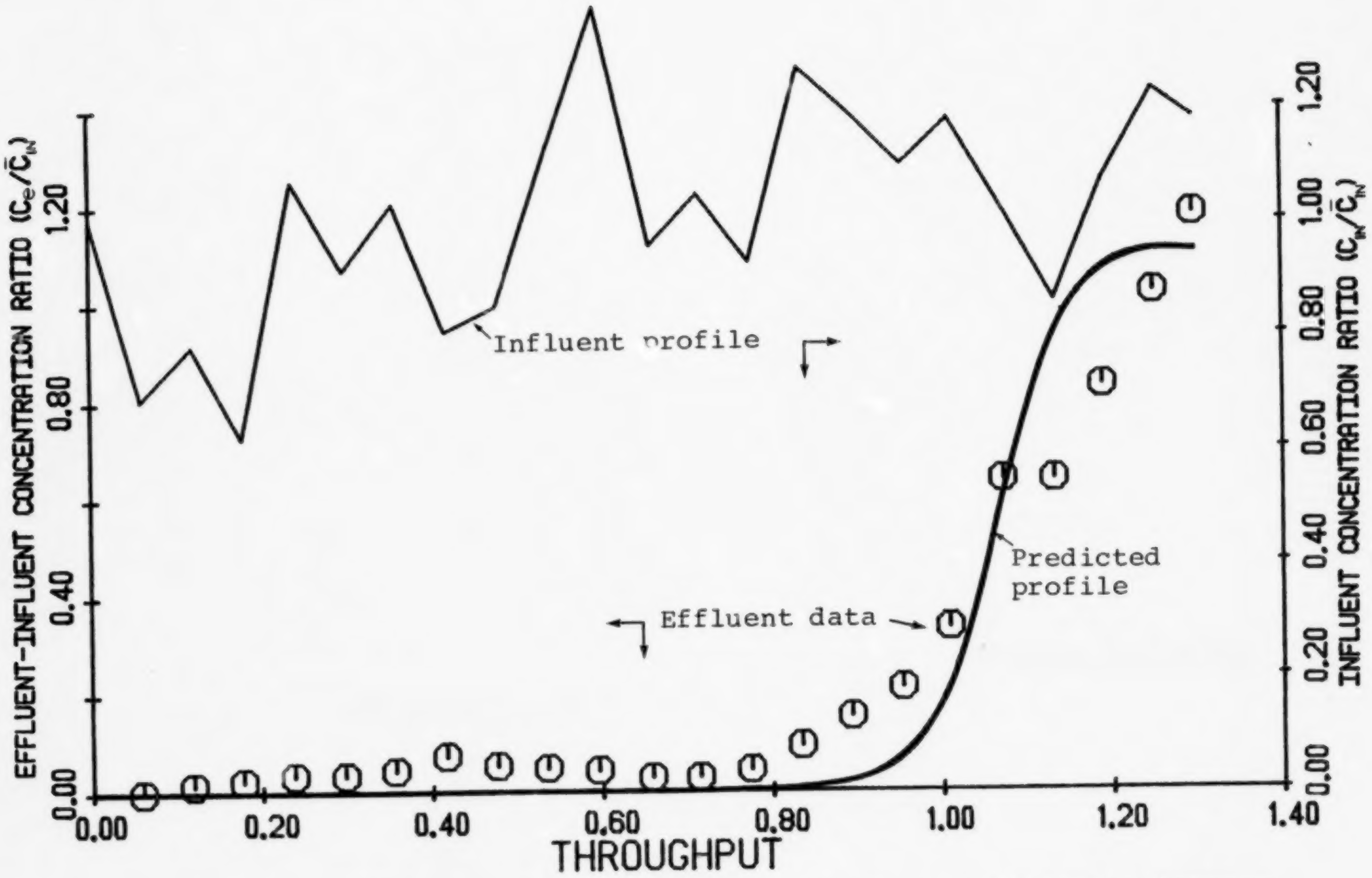

Figure 91. Effluent and influent concentration profiles for benzene in OFW - fixed-bed adsorber Run II ($\bar{C}_{in}$ = 200μg/ℓ, 2 grams of 50/60 carbon, flow rate = 5 mℓ/min, EBCT = 0.95 min).

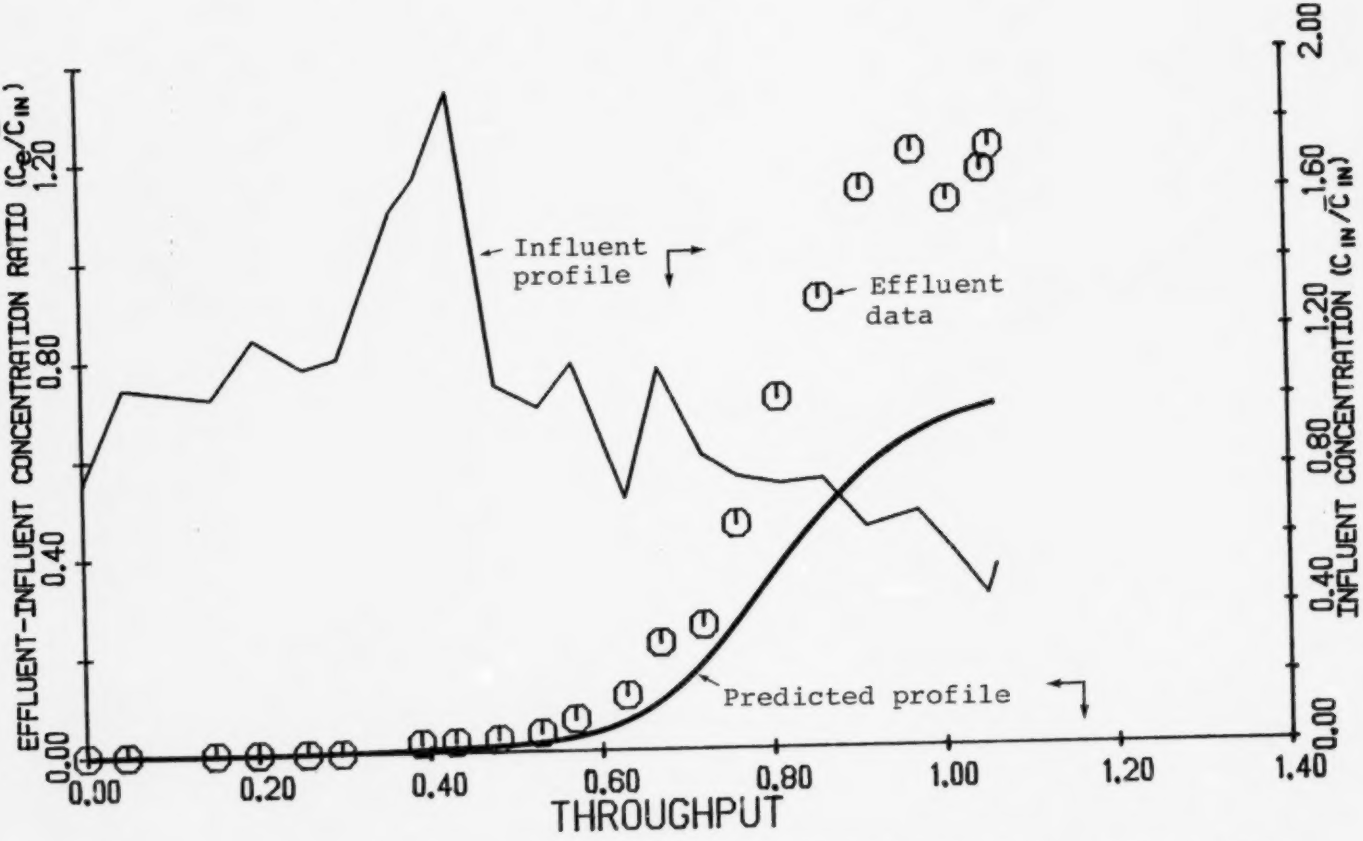

Figure 92. Effluent and influent concentration profiles for benzene in OFW - fixed-bed adsorber Run III ($\bar{C}_{in}$ = 519 µg/ℓ, 100 grams of 16/20 carbon, flow rate = 100 mℓ/min, EBCT = 2.5 min).

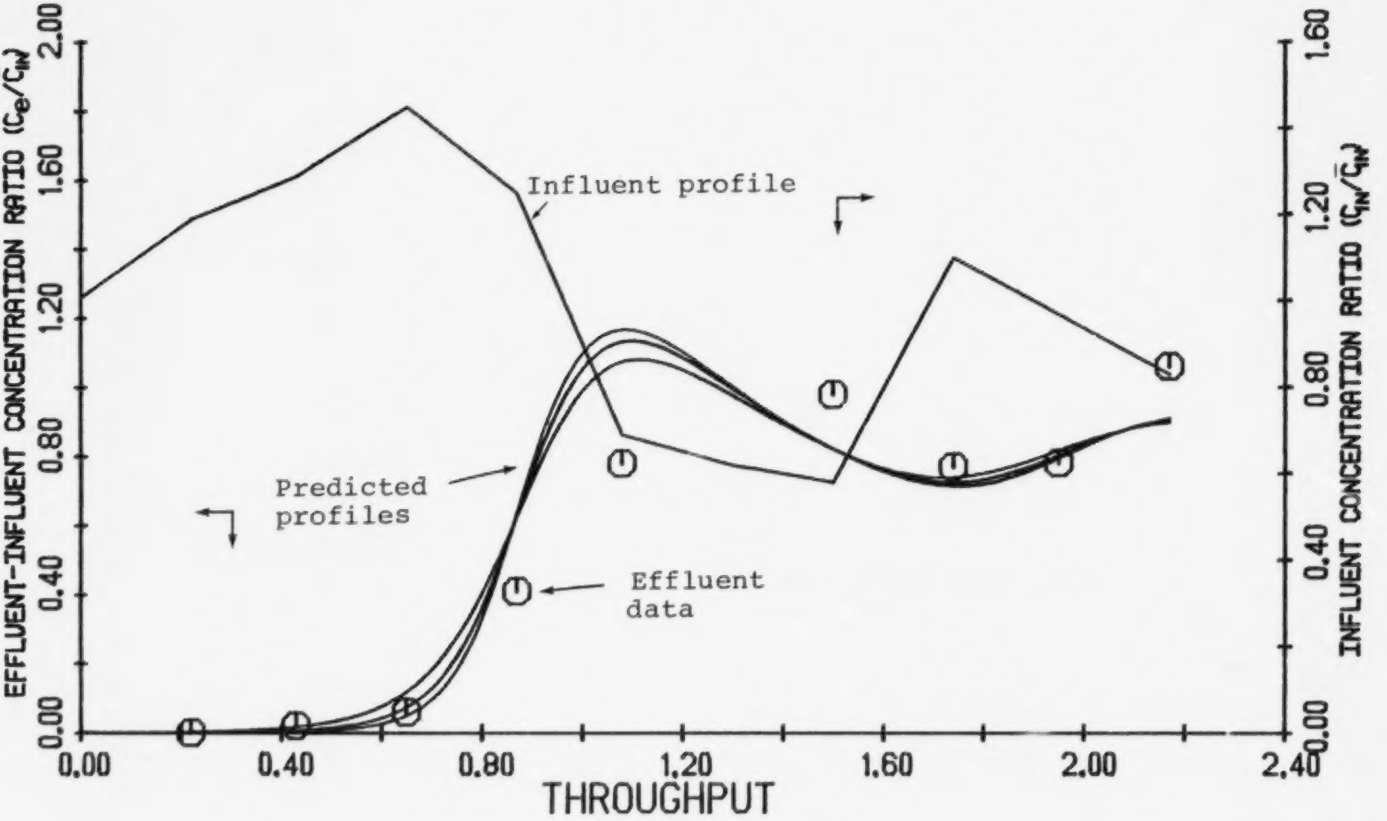

Figure 93. Sensitivity anslysis of breakthrough profiles relative to the film transfer coefficient, $k_f \pm 25\%$, for benzene in OFW, (fixed-bed adsorber Run I).

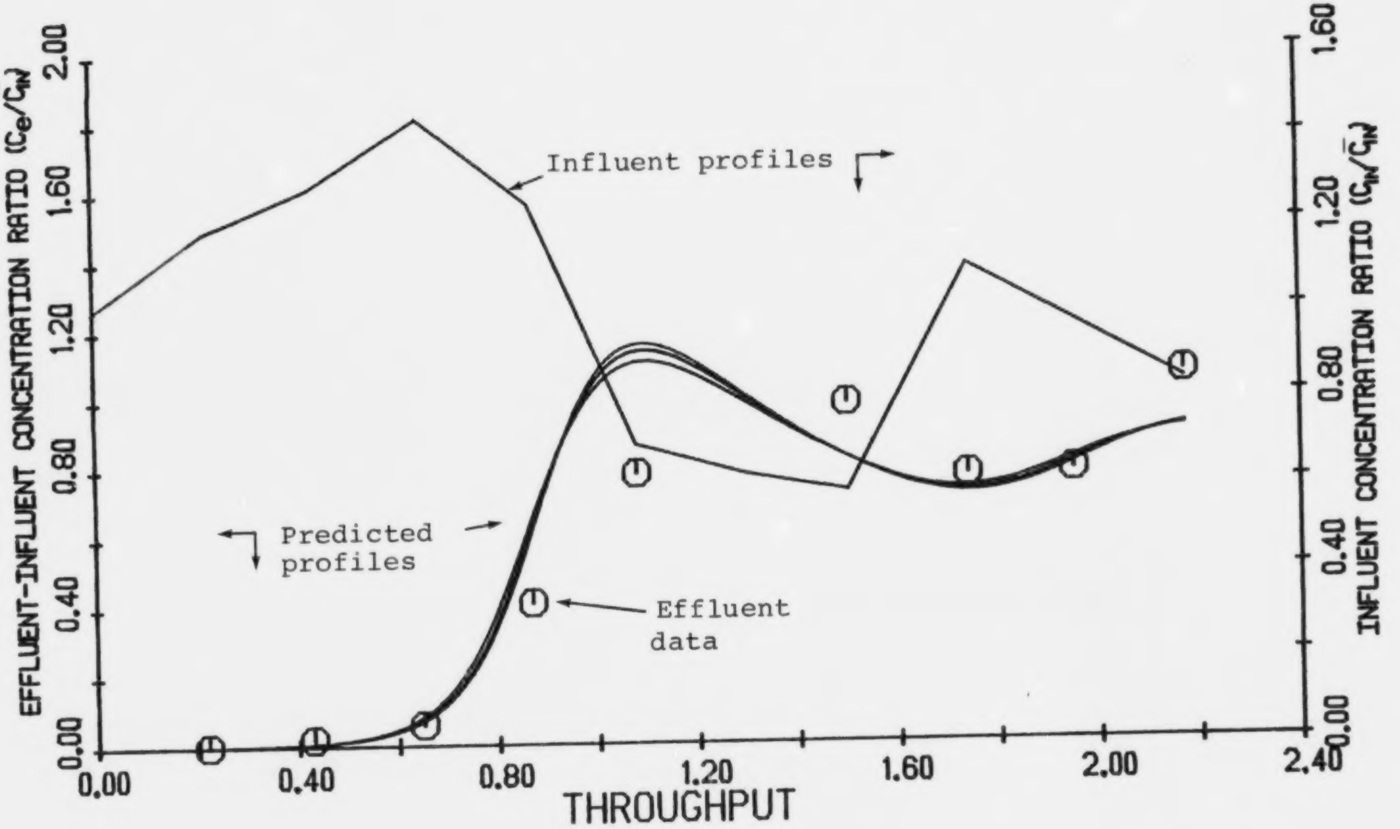

Figure 94. Sensitivity analysis of breakthrough profiles relative to the surface diffusion coefficient, $D_s \pm 25\%$, for benzene in OFW, (fixed-bed adsorber Run I).

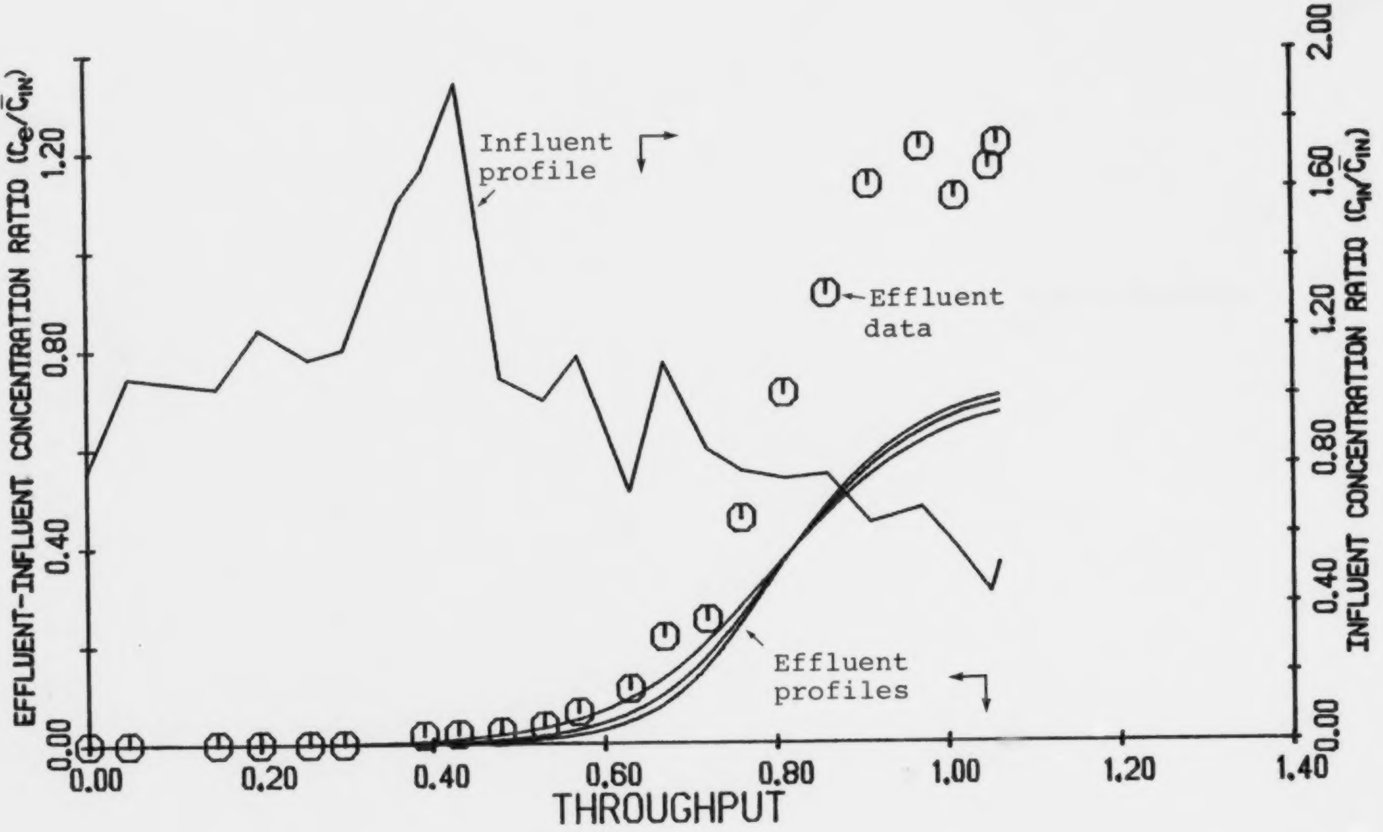

Figure 95. Sensitivity analysis of breakthrough profiles relative to the film transfer coefficient, $k_f \pm 25\%$, for benzene in OFW, (fixed-bed adsorber Run III).

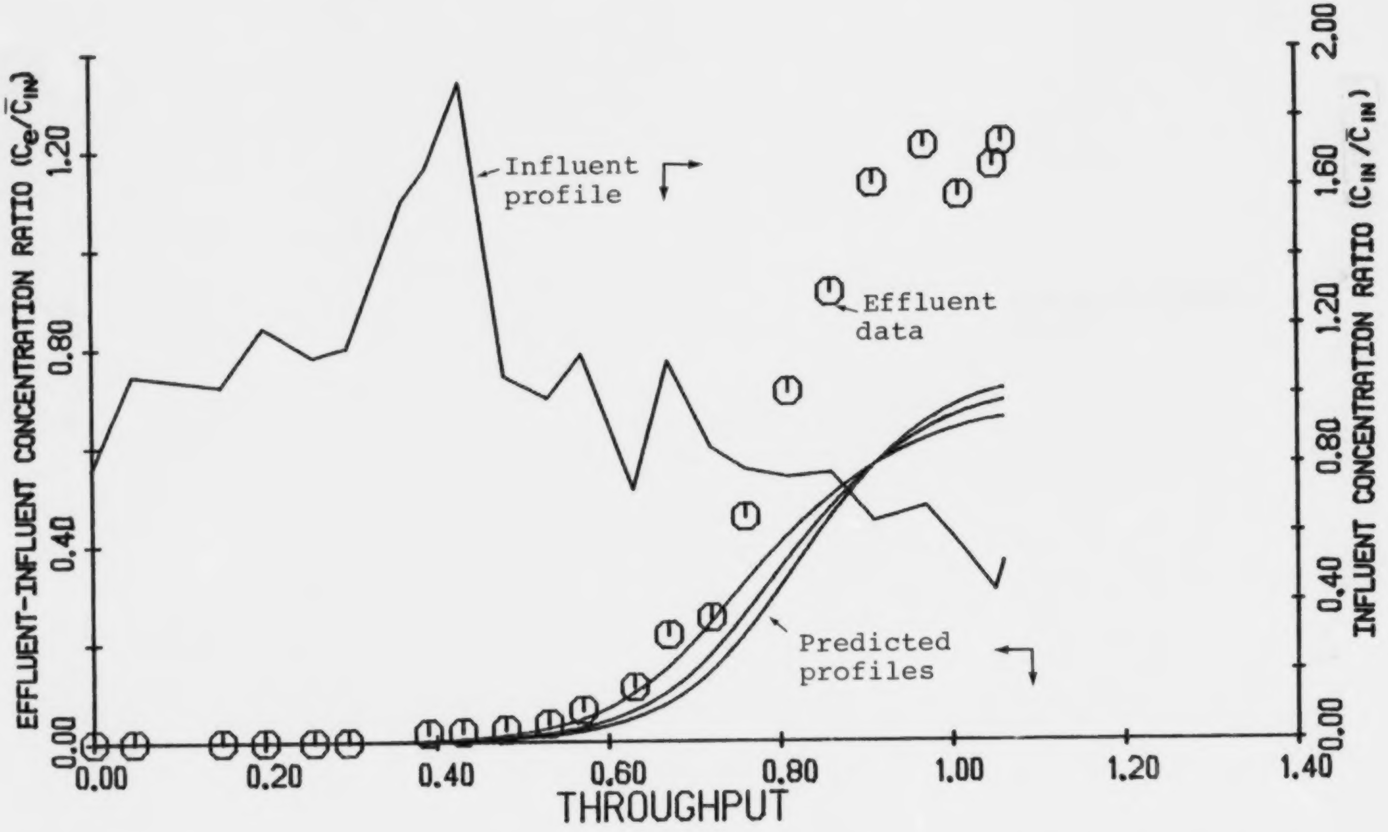

Figure 96. Sensitivity analysis of breakthrough profiles relative to the surface diffusion coefficient, $D_s \pm 25\%$, for benzene in OFW, (fixed-bed adsorber Run III).

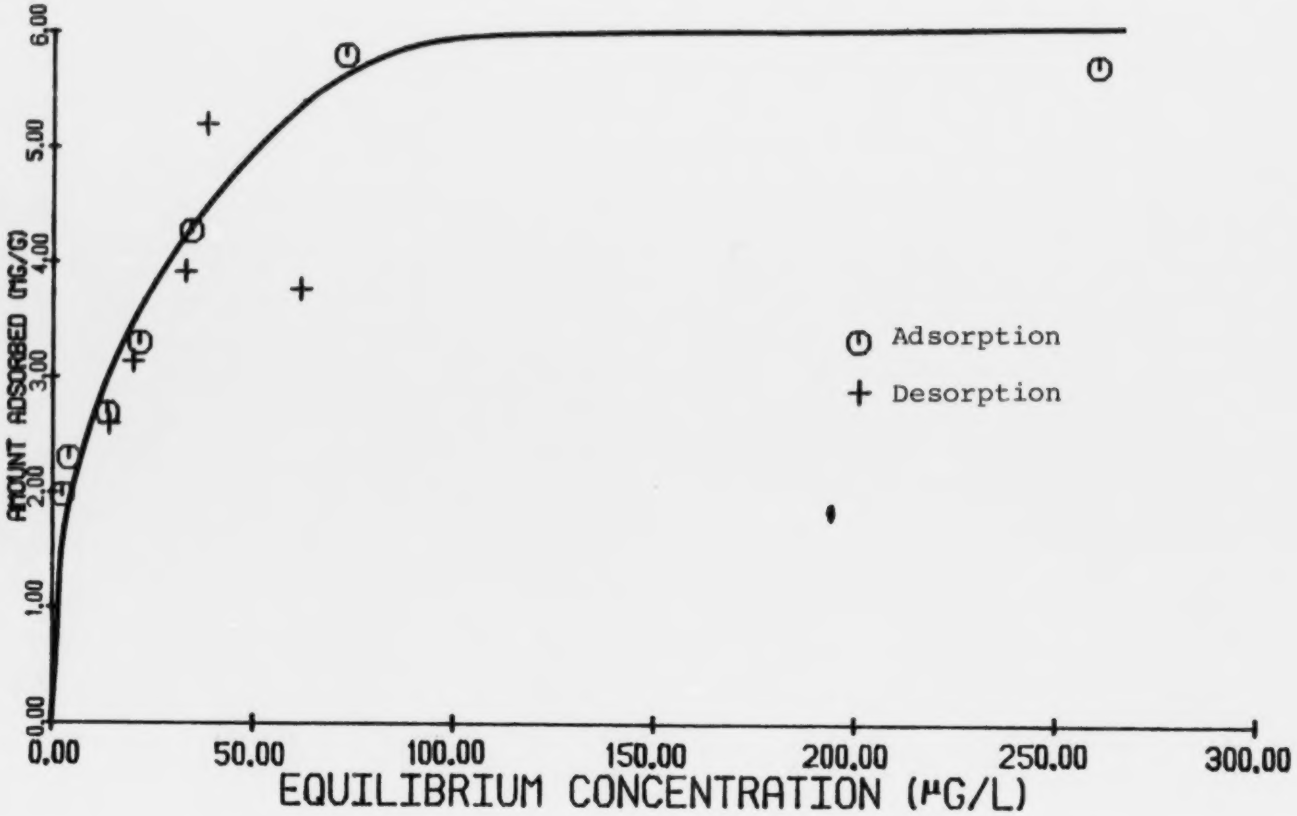

Figure 97. Adsorption-desorption studies for benzene in OFW (C_o = 442 μg/ℓ).

TYPING GUIDE SHEET

Desorption studies were conducted for benzene in a 3-cm ID adsorber column containing 100 grams of carbon and operated at 3.5 gpm/ft^2 hydraulic loading. After attaining exhaustion, the column was fed with OFW for a period of 160 hours. A substantial quantity of benzene was desorbed, as demonstrated in Figure 98.

Competitive Adsorption

To study competitive adsorption phenomena, column studies were conducted for benzene in 5 mg/l humic acid background solution. A 3-cm ID glass adsorber column containing 100 grams of 16/20 mesh carbon was employed, with a hydraulic loading of 3.5 gpm/ft^2. The experimental apparatus and arrangement are illustrated in Figure 49 (Section 7).

These experiments, as for similar studies with CCl_4, were designed to verify the predictive capabilities of MADAM relative to the adsorption dynamics of benzene in the presence of humic acids, and to investigate the behavior of the benzene breakthrough relative to possible chromatographic phenomena. It was difficult to keep the influent concentration from fluctuating drastically in these experiments because of extensive biological growth and resulting headlosss. After 350 hours of operation it was impossible to maintain any benzene residual in the column feed, and the experiment was therefore terminated. Figure 99 presents the influent and effluent data.

It is thus not possible to establish any conclusion regarding the dynamic behavior of benzene in the presence of humic acids. However, by comparing the latter part of the benzene breakthrough profiles in Figures 98 and 99 -- representing benzene in OFW and 5 mg/l humic acid solution, respectively -- it may be observed that benzene is adsorbed less in the presence of humic acids.

To further substantiate the competitive adsorption, two mini-columns, one containing one gram of 50/60 carbon saturated with humic acids and the other one gram of virgin carbon, were fed with benzene in OFW background solution. Figure 100 demonstrates the corresponding influent and effluent profiles, indicating a substantial reduction in the capacity of the pre-saturated carbon for adsorption of benzene. Further, the pre-saturated carbon effluent profile demonstrates that chromatographic phenomena are in effect.

SUMMARY AND CONCLUSIONS

1. As for CCl_4, the results of adsorption-desorption equilibrium studies and adsorber column dynamic desorption studies suggest that adsorption of benzene on carbon can

EPA-287 (Cin.)
(4-76)

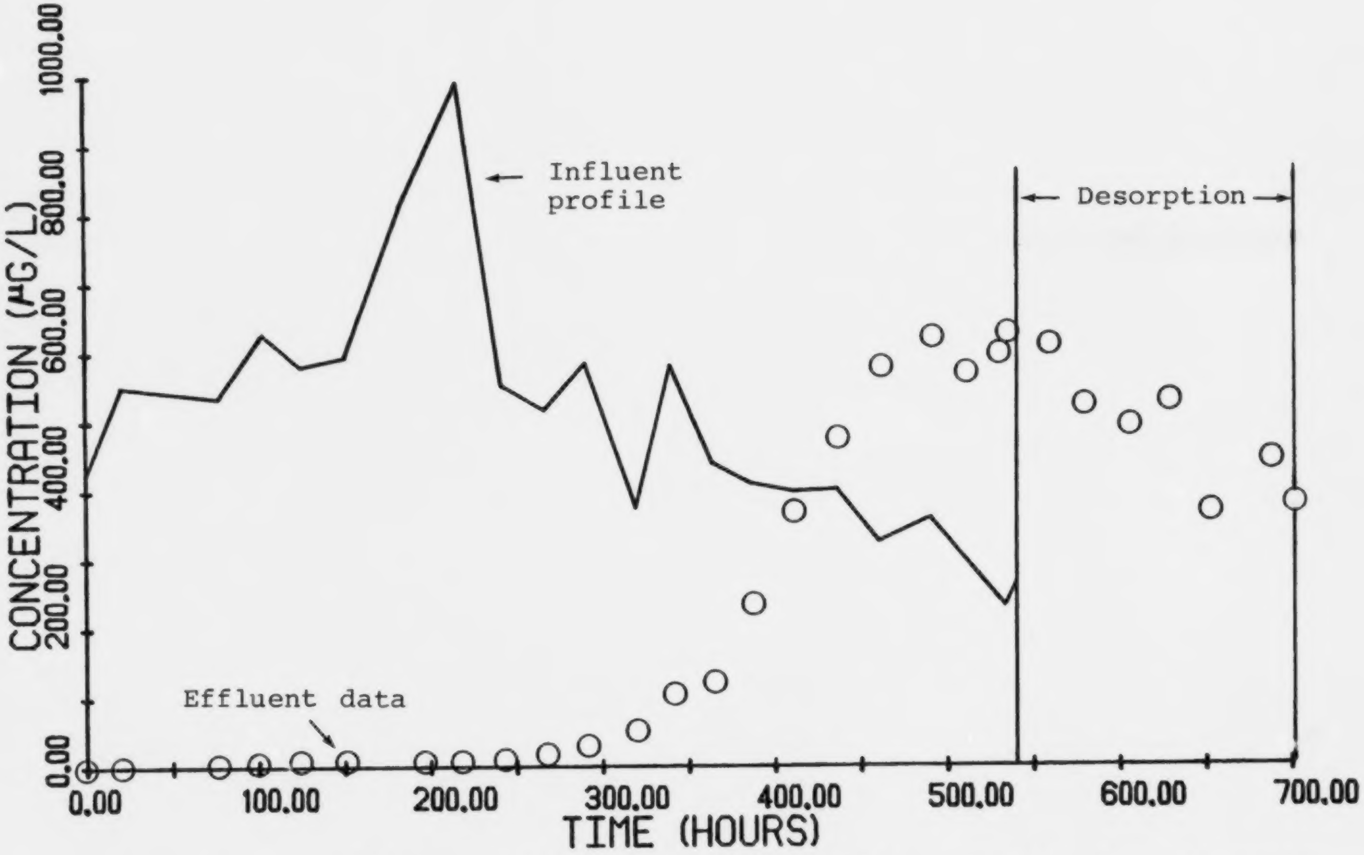

Figure 98. Effluent and influent concentration profiles for adsorption-desorption study for benzene in OFW (100 grams of 16/20 carbon and hydraulic loading of 3.5 gpm/ft^2).

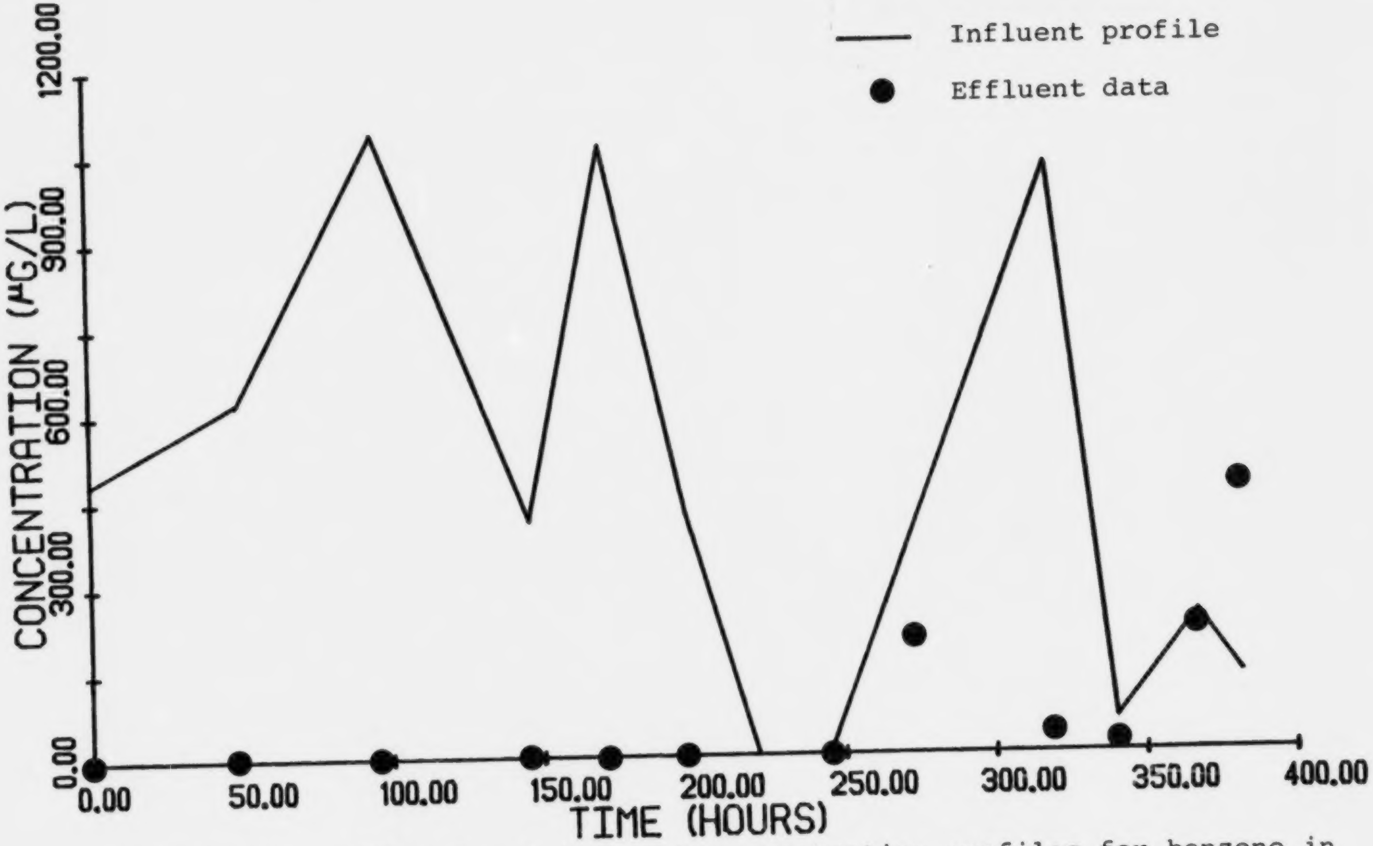

Figure 99. Effluent and influent concentration profiles for benzene in 5 mg/ℓ humic acids background solution (100 grams of 16/20 carbon and hydraulic loading of 3.5 gpm/ft^2, col dia = 3 cm).

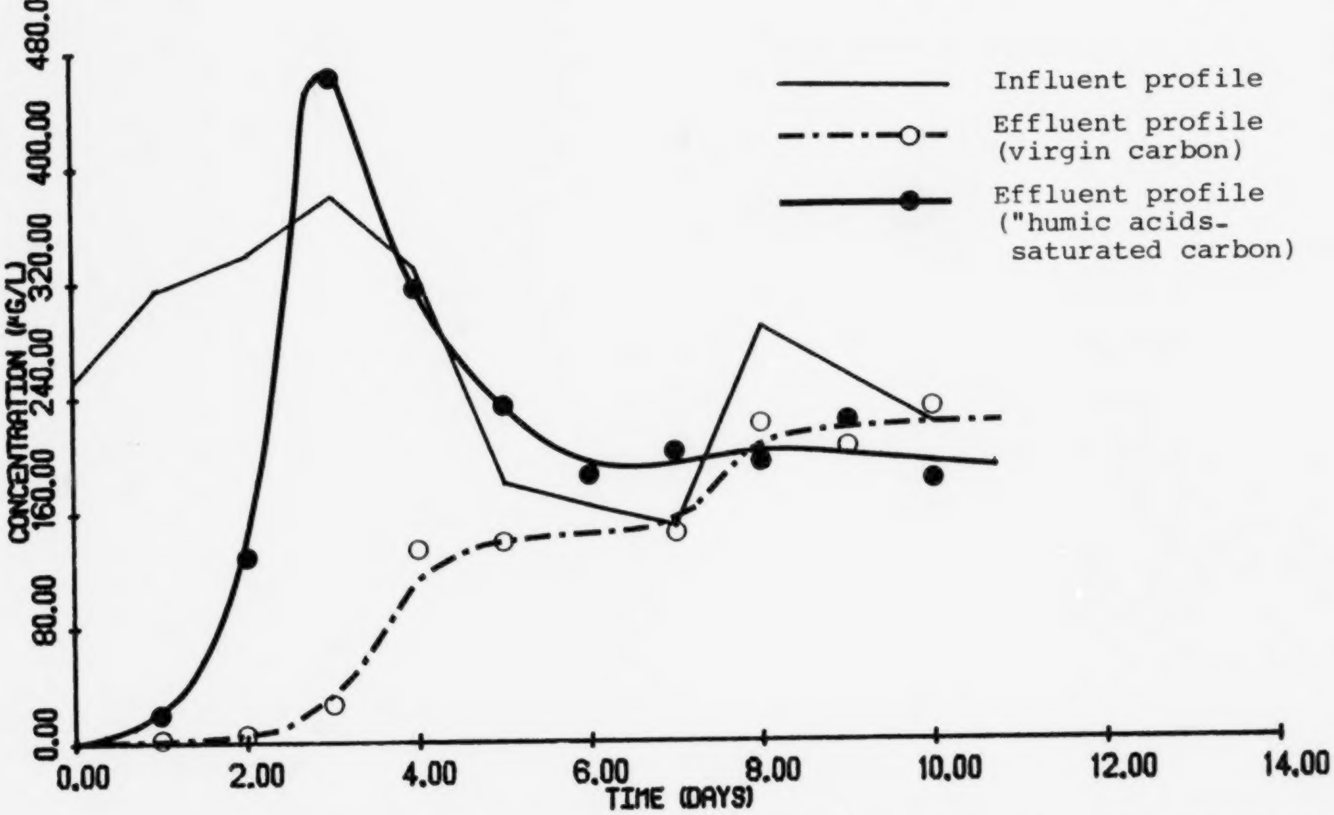

Figure 100. Effluent and influent profiles for adsorption of benzene on virgin carbon and pre-saturated carbon (1 gram of 50/60 carbon, flow rate = 10 mℓ/min column diameter = 1.2 cm).

be characterized as predominantly "physical adsorption."

2. The MADAM adsorption model was generally able to simulate and predict the performance of fixed-bed adsorbers for removal of benzene. Prediction was affected, however, in cases where influent concentration fluctuated severely, mainly due to re-equilibrium phenomena.

3. The effectiveness of activated carbon for removal of benzene from water in practical applications is adversely affected by the competitive adsorption effects of background organic substances such as humic acids.

4. The predictive performance of fixed-bed adsorbers for benzene may be based on model calibrations conducted with mini-column systems, which are generally more flexible and easier to operate and maintain than larger adsorber systems.

5. The observations of apparently different rate controls in the mini-column and pilot column indicate that the mass transport limiting mechanism for benzene depends in large measure on the physical characteristics of the system, including the column type, hydraulic regime, and carbon particle size.

BEGIN FIRST LINE OF TEXT HERE
TYPING GUIDE SHEET
CENTER OF PAGE
TOP OF IMAGE AREA
DROPPED HEAD BEGIN SECTIONS HERE

SECTION 9

ADSORPTION OF POLYCHLORINATED BIPHENYLS (PCB's)

GENERAL

Introduction

Polychlorinated biphenyls constitute a class of chlorinated aromatic compounds with distinctive physical and chemical characteristics. These properties include: thermal stability; resistance to oxidation; resistance to acids, alkalies and corrosive chemicals; and favorable dielectric constant Hutzinger *et al*, 1974). PCB's are produced industrially by chlorination of biphenyl with anhydrous chlorine in the presence of selected catalysts, most commonly ferric chloride or iron shavings (Gustafson, 1970). Depending on the extent of chlorination, as many as 209 isomers may be formed. The number of chlorine atoms per molecule and the position of these atoms around the biphenyl group determine the chemical character of each specific isomer (Hutzinger *et al*, 1974). Although as many as ten chlorine atoms may attach to one biphenyl group, the majority of PCB's contain between one and six chlorine atoms per molecule. Increased chlorination increases the density and boiling point, but decreases the vaporization rate, water solubility and biodegradability of a PCB.

PCB's were first produced commercially in 1930 as an alternative to mineral oil as a dielectric fluid for capacitors and transformers. Monsanto Chemical Company, the only U.S. manufacturer, marketed PCB's under the trade name "Aroclor" in conjunction with a 4-digit number; e.g., Aroclor 1254. The first two digits represent the parent molecule, biphenyl, and the last two digits designate the weight percentage of chlorine in the mixture. An exception is Monsanto's Aroclor 1016, which is primarily a trichlorobiphenyl similar to Aroclor 1242, but has a lower penta- and hexachlorobiphenyl content than Aroclor 1242.

The use of PCB's was widespread in the United States prior to 1972. Their inertness, fire resistance, chemical stability and excellent dielectric properties made them invaluable in capacitors, transformers, plasticisers, carbonless carbon paper, paints, inks, and hydraulic lubricating, cutting and

BEGIN LAST LINE OF TEXT
BOTTOM OF IMAGE AREA OUTSIDE DIMENSION FOR TABLES AND ILLUSTRATIONS
3/8"

PAGE NUMBER
EPA-287 (Cin.)
(4-76)

TYPING GUIDE SHEET

heat transfer fluids. In 1970, Monsanto restricted domestic sales to essentially closed-system uses (capacitors and transformer applications), and in 1977 stopped production of PCB's. A summary mass-balance account of PCB's for the 45-year period of production in the United States is presented in Table 19 (USEPA, 1976).

TABLE 19. SUMMARY OF PCB USES AND FATE

Uses and Fate	Quantity (millions of pounds)
Industrial Uses	790
Landfills and Dumps	290
Destroyed by Incineration and Degradation	55
Released to the Environment	150
TOTAL	1,285

Sources and Sinks in the Environment

Routes of introduction of PCB's to the environment have been multifaceted and extensive. They include inputs from production facilities, industrial discharges, municipal sewage treatment plants, surface runoff and ground water leachate from dumps, evaporation of plasticizers and improper incineration (Nisbet and Sarofim, 1972; Dube, *et al*, 1974; and, Stratton and Susebee, 1976). Recent evidence also indicates that chlorobiphenyls may form during chlorination of biphenyl waste (Gaffney, 1977; Smith *et al*, 1977). It is thus not surprising that PCB's have been found in the finished waters of a number of cities across the United States (USEPA, *Report to Congress*, 1975).

The major environmental sink of PCB appears to be sediments. PCB's are hydrophobic, and tend to adsorb onto suspended particulates upon entry into the aquatic environment. The extent of association depends in large measure on the nature and composition of the particulates; notably, their size and organic content (Weber *et al*, 1980; Hiraizumi *et al*, 1979). PCB's have been demonstrated to enter the food chain from the

EPA-287 (Cin.)
(4-76)

sediments and accumulate at all levels therein (Nimmo *et al*, 1971; Vieth, 1975; Ahmed, 1976). It has been reported that the amount of PCB that can concentrate in plankton and fish is proportional to the lipid content of the organisms (Linko *et al*, 1974).

Public Health Assessment

The potential threat of PCB's to the environment was realized in 1966, when their extensive presence in fish and wildlife samples was discovered (Jensen *et al*, 1969). PCB's have since been found, literally from *pole to* pole, in numerous aquatic species. The threat they constitute to aquatic life can be extrapolated to human life as well. An example is provided by the "Yusho Syndrome" which occurred in 1969 in Japan. The incident involved consumption of PCB contaminated rice oil by over 1,000 people. Symptoms included eyelid swelling, liver disorders, visual impairments, skin lesions, and neurological disorders (Kuratsune *et al*, 1972). Animal reactions to PCB's have included disrupted osmoregulatory control in fish (Kinter *et al*, 1968), microsomal enzyme activity and mitochondrial alterations in rats (Gustafson, 1970; Williams *et al*, 1977), and reproductive failure and egg calcification in birds (Risebrough *et al*, 1968). PCB has been reported to adversely affect oxygen production and chloroplastic membrane functioning in some species of marine phytoplankton (Harding *et al*, 1978). PCB's have been found also to increase the toxicity of some other chemicals. Lichtenstein (1972) reported that PCB's increase the toxicity of some insecticides. Nobuyki *et al* (1973) indicated that exposure to PCB's in the presence of some suspected carcinogens causes hepatocellular carcinomas in mice.

Regulations concerning PCB's in drinking water have not yet been promulgated. However, the U.S. Environmental Protection Agency has established a criterion of 0.1 μg/l for marine waters (*Quality Criteria for Water,* USEPA, 1976).

Water Solubility

PCB mixtures are comprised of a variety of chlorobiphenyl isomers with different physical and chemical characteristics. Most individual isomers are solids at room temperature, whereas commercial mixtures are mobile oils, viscous liquids, or sticky resins, depending on the degree of chlorination of constituent isomers (Hutzinger *et al*, 1974).

The most important physical property of PCB's from an adsorption point of view is solubility. Solubility in water is extremely low, and, in general, decreases with increasing chlorine content. Values for the solubility of individual chlorobiphenyls are listed in Table 20 (Hutzinger *et al*, 1974).

TABLE 20. SOLUBILITIES OF CHLOROBIPHENYLS IN WATER
(after Hutzinger et al, 1974)

Compound	Solubility mg/l (ppm)
Monochlorobiphenyls	5.9
2 -	3.5
3 -	1.19
4 -	
Dichlorobiphenyls	1.40
2,4 -	1.50
2,2' -	1.88
2,4' -	0.08
4,4' -	
Tichlorobiphenyls	0.085
2,4,4' -	0.078
2',3,4' -	
Tetrachlorobiphenyls	0.046
2,2',5,5' -	0.034
2,2',3,3' -	0.170
2,2',3,5' -	0.068
2,2',4,4' -	0.058
2,3',4,4' -	0.041
2,3',4,5 -	0.175
3,3',4,4' -	
Pentachlorobiphenyls	0.022
2,2',3,4,5' -	0.031
2,2',4,5,5' -	
Hexachlorobiphenyl	0.0088
2,2',4,4',5,5' -	
Octachlorobiphenyl	0.0070
2,2',3,3',4,4',5,5' -	
Decachlorobiphenyl	0.015
4,4' -Dichlorobiphenyl	5.9
+ Tween 80 0.1%	>10.0
+ Tween 80 1%	0.07
+ Humic acid extract	

TYPING GUIDE SHEET
BEGIN FIRST LINE OF TEXT HERE
CENTER OF PAGE
TOP OF IMAGE AREA
DROPPED HEAD; BEGIN SECTIONS HERE
BOTTOM OF IMAGE AREA OUTSIDE DIMENSION FOR TABLES AND ILLUSTRATIONS
BEGIN LAST LINE OF TEXT
PAGE NUMBER
EPA-287 (Cin.)
(4-76)

BEGIN FIRST LINE OF TEXT HERE
TYPING GUIDE SHEET
CENTER OF PAGE
TOP OF IMAGE AREA
DROPPED HEAD; BEGIN SECTIONS HERE

Reported values for solubility of PCB mixtures in water vary significantly. Tulp and Hutzinger (1978), in summarizing data collected by seven groups of researchers for several PCB isomers, suggested that observed discrepancies were due to such experimental factors as equilibration time, mixing characteristic, initial filtration or centrifugation and extraction techniques. Further, humic substances and surface active compounds in water may act as stabilizers or carriers of the immiscible PCB's, thus increasing apparent "soluble" concentration of PCB's.

There is, indeed, some question as to whether many hydrocarbons, or derivatives, such as PCB's, exist in aqueous solution state at all. The fact that centrifugation and filtration reduce the apparent solubility of PCB's suggest that these substances may actually take the form of colloids, micelles or stable emulsions, especially the more hydrophobic isomers (Tulp and Hutzinger, 1978).

PCB's Selected for This Research

Two commercial PCB mixtures were selected for the adsorption experiments reported herein; namely, Aroclor 1254 (A-1254) and Aroclor 1016 (A-1016). The choice of Aroclor 1254 related to its widespread industrial utilization, resistance to biodegradation, and high chlorine content. Conversely, A-1016 was chosen to represent PCB mixtures with low chlorine content. The Aroclors were obtained from Monsanto Chemical Company. Table 21 lists the physical and chemical properties of these Aroclors.

Molecular compositions of these two Aroclors are tabulated in Table 22. It may be observed that the major components of A-1016 are di-, tri-, and tetrachlorobiphenyls, whereas the predominant components of A-1254 are tetra, penta - and hexachlorobiphenyls. The differences in molecular composition, coupled with differences in solubility, can be expected to have marked effects on respective adsorption characteristics.

To determine the overall solubility (not to be confused with the solubility of individual isomers), 500 mg of the chemical (A-1016 or A-1254) was placed in a 2-l volumetric flask containing OFW and the solution agitated with a magnetic stirrer. An aliquot of the aqueous sample was withdrawn periodically and filtered through a 0.45 μm membrane filter and anlayzed for PCB's. Saturation points of ≃ 120 μg/l and ≃ 50 μg/l were reached for A-1016 and A-1254, respectively.

BEGIN LAST LINE OF TEXT
BOTTOM OF IMAGE AREA; OUTSIDE DIMENSION FOR TABLES AND ILLUSTRATIONS
3/8"

EPA-287 (Cin.)
(4-76)

TYPING GUIDE SHEET
BEGIN FIRST LINE OF TEXT HERE
CENTER OF PAGE
TOP OF IMAGE AREA
DROPPED HEAD, BEGIN SECTIONS HERE

TABLE 21. CHEMICAL AND PHYSICAL PROPERTIES OF AROCLORS 1016 AND 1254 (after Hutzinger et al, 1974)

	A-1016*	A-1254
Average molecular weight	261	327
Appearance	Clear, mobile oil	Light-yellow viscous liquid
Chlorine, percent	41	54
Specific gravity (15.5°C)	1.392	1.505
Density, lb/gal (25°C)	11.50	12.82
Viscosity, sec Saybolt Universal (37.8°C)	82-92	1800-2500

* Some data are based on Aroclor 1242

TABLE 22. MOLECULAR COMPOSITION OF AROCLORS 1016 AND 1254 (after Hutzinger et al, 1974)

Chlorobiphenyl Composition	Percent by Weight	
	A-1016	A-1254
$C_{12}H_{10}$	<0.1	<0.1
$C_{12}H_9Cl$	1	<0.1
$C_{12}H_8Cl_2$	20	0.5
$C_{12}H_7Cl_3$	57	1
$C_{12}H_6Cl_4$	21	21
$C_{12}H_5Cl_5$	1	48
$C_{12}H_4Cl_6$	<0.1	23
$C_{12}H_3Cl_7$	ND	6
$C_{12}H_2Cl_8$	ND	ND

BEGIN LAST LINE OF TEXT
BOTTOM OF IMAGE AREA; OUTSIDE DIMENSION FOR TABLES AND ILLUSTRATIONS
3/8"

EPA-287 (Cin.)
(4-76)

TYPING GUIDE SHEET

ANALYTICAL PROCEDURES

Sample Collection and Concentration

Determination of residual concentrations of PCB's in aqueous solution was accomplished by liquid-liquid extraction followed by gas chromatographic analysis. Depending on the quantity of PCB's in a given sample, one of two different methods of extraction was employed; these are detailed below.

Vial Extraction Technique--

For higher PCB concentration (1 μg/l or larger), 10 to 15 ml of sample and 2 ml of Baker Resi-Analyzed hexane were added into a 20-ml vial. This vial was then sealed with a Teflon-lined screw-cap and shaken vigorously for five minutes. The vials were subsequently stored in an incubator overnight at 4°C in an inverted position to eliminate loss of hexane due to evaporation. The samples were brought to room temperature (20°C ± 1) before gas chromatographic analysis. Extraction efficiency was estimated to be 85%.

Multiple Extraction Technique--

For lower PCB concentration (less than 1 μg/l), 300 ml of the sample and 25 ml of hexane were placed in a 1-l separatory funnel. The separatory funnel was shaken vigorously for five minutes and then left to stand in quiescent condition until complete separation between the phases had occurred. The water phase was drained from the separatory funnel into the sample bottle and the hexane phase passed through a Na_2SO_4-filled funnel into a Kuderna-Danish apparatus fitted with a 10-ml concentrator tube. The water sample was then subjected to the same extraction procedure two additional times. The Kuderna-Danish apparatus containing the composite extracts was fitted with a three-ball Snyder column and the volume of extract reduced to 8 ml. The concentrator was then placed in an Organomation N-Evap evaporation apparatus and the concentrate evaporated to 1 ml under a gentle stream of pre-purified nitrogen. The concentrate was then diluted with 1 ml hexane. A 70% extraction efficiency was achieved by this method.

Analysis

Electron capture gas chromatographic analyses of the extracts were conducted using two different detectors; a Sc^3H electron capture detector (ECD) and a ^{63}Ni ECD. The ^{63}Ni ECD demonstrated greater sensitivity and consistency, in addition to exhibiting a linear response over a larger concentration range. A Varian 2700 GC fitted with a 6-ft. x 2-mm ID glass column packed with 3% Silicone OV-1 on 80/100 Gas Chrom Q was employed for the analysis. Prepurified nitrogen was used as carrier gas at a flow rate of 40 ml/min. Tempera-

EPA-287 (Cin.)
(4-76)

TYPING GUIDE SHEET

tures for the injector and detector were 220°C and 250°C, respectively. Column temperature for analysis of A-1016 was 180°C, and for A-1254 was 210°C.

The detector response was recorded graphically using a strip chart recorder, and the areas of the peaks integrated with an Autolab Minigrator. A calibration curve of peak areas versus amount of PCB was used for concentration determination. The method for preparation of standard curves is discussed in Appendix M.

Examination of chromatograms for Aroclor mixtures reveal that the lower chlorinated isomers have shorter retention times. This is likely to be due to the greater volatility of lesser chlorinated biphenyls. Figures 101 and 102 represent GC retention time versus percent chlorine content for Aroclors 1242 and 1254 (Webb and McCall, 1973).

Differential Behavior of PCB Isomers

More than 69 isomers have been identified in Aroclor 1254 (Sisson and Welti, 1971). The water solubilities of these isomers vary nearly three orders of magnitude, as indicated in Table 20. Because the solubility of a compound or mixture of compounds has a major influence on its adsorption characteristic, several studies were conducted in this research to investigate possible differential adsorption behavior of PCB isomers.

Figures 103 and 104 show typical chromatograms for A-1254 extracted under different experimental conditions. Six major peaks, each representing a group of isomers, are demonstrated. Figure 103a is the chromatogram for an extraction of OFW spiked with A-1254 and stirred for three months. Figure 103b, the chromatogram for a standard solution of A-1254 in hexane, illustrates the actual isomer distribution in the pure product. Chromatograms for extracts of OFW and OFW plus 5 mg/l humic acid solutions spiked with A-1254 in acetone carrier solvent are presented in Figures 103c and 104a, respectively. This method of spiking, which was employed for the preparations of PCB solutions for the experimental work, is seen to yield a distribution of isomers nearly identical to that found in pure A-1254.

Further studies were performed to investigate the adsorption behavior of individual isomers. Figure 104b shows residual PCB after activated carbon adsorption equilibrium had been reached, indicating preferential adsorption of individual isomers. Figure 104c also indicates that glass containers tend to adsorb certain isomers preferentially.

Typical chromatograms for Aroclor 1016 extracted under

EPA-287 (Cin.)
(4-76)

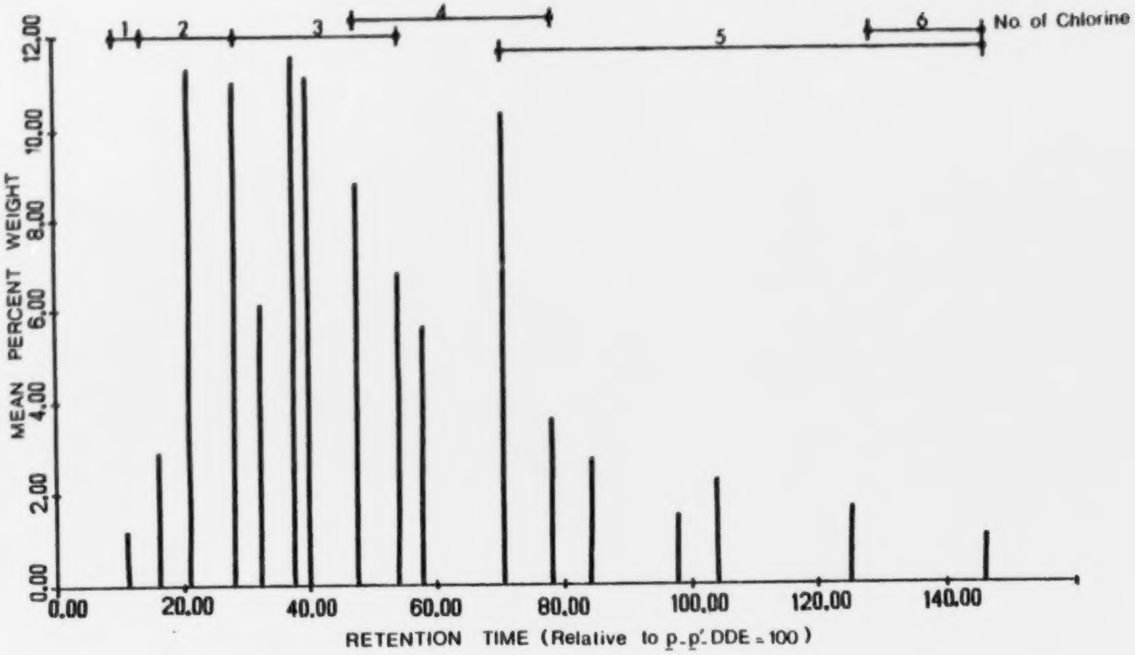

Figure 101. Quantitative mean-percent-weight analysis of different isomer groups for Aroclor-1242 (after Webb and McCall, 1973).

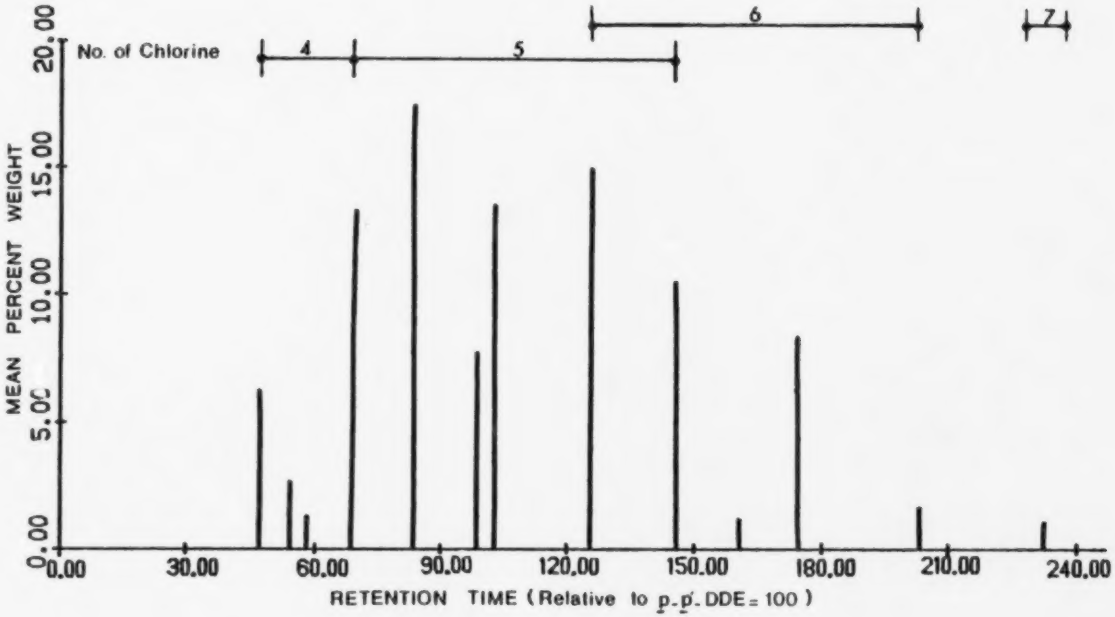

Figure 102. Quantitative mean-percent-weight analysis of different isomer group for Aroclor-1254 (after Webb and McCall, 1973).

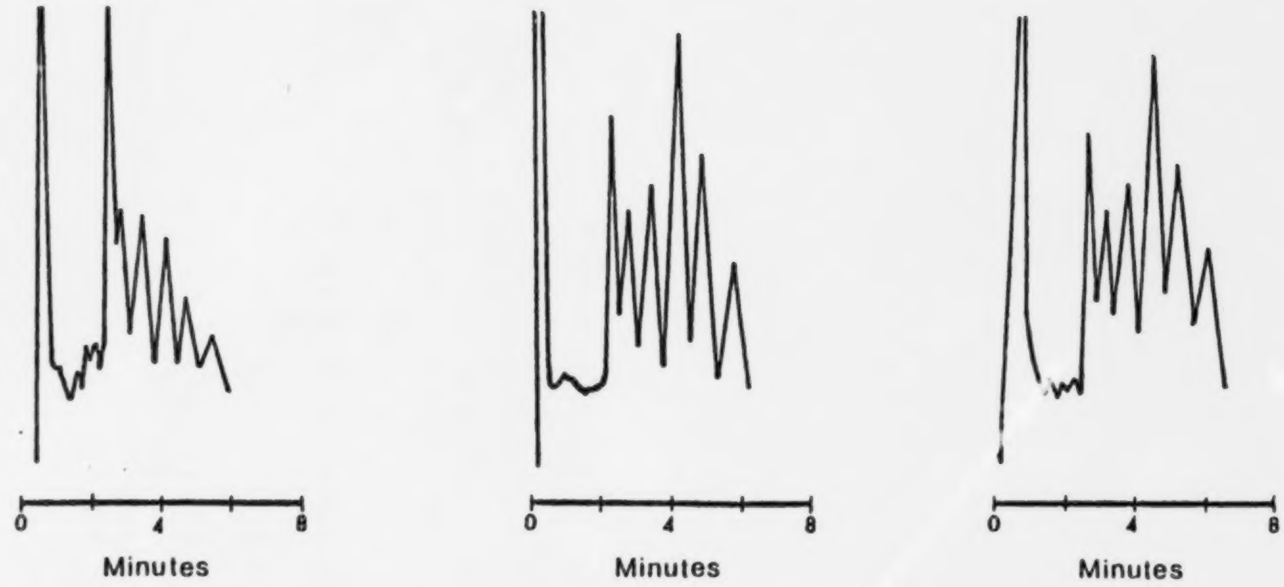

a) Aqueous Solution (stirred)

b) Standard in Hexane

c) OFW (acetone carrier)

Figure 103. Typical packed-column chromatograms for A-1254 (3% Silicone OV-1 on 80/100 Gas Chrom Q; Ni_{63} ECD).

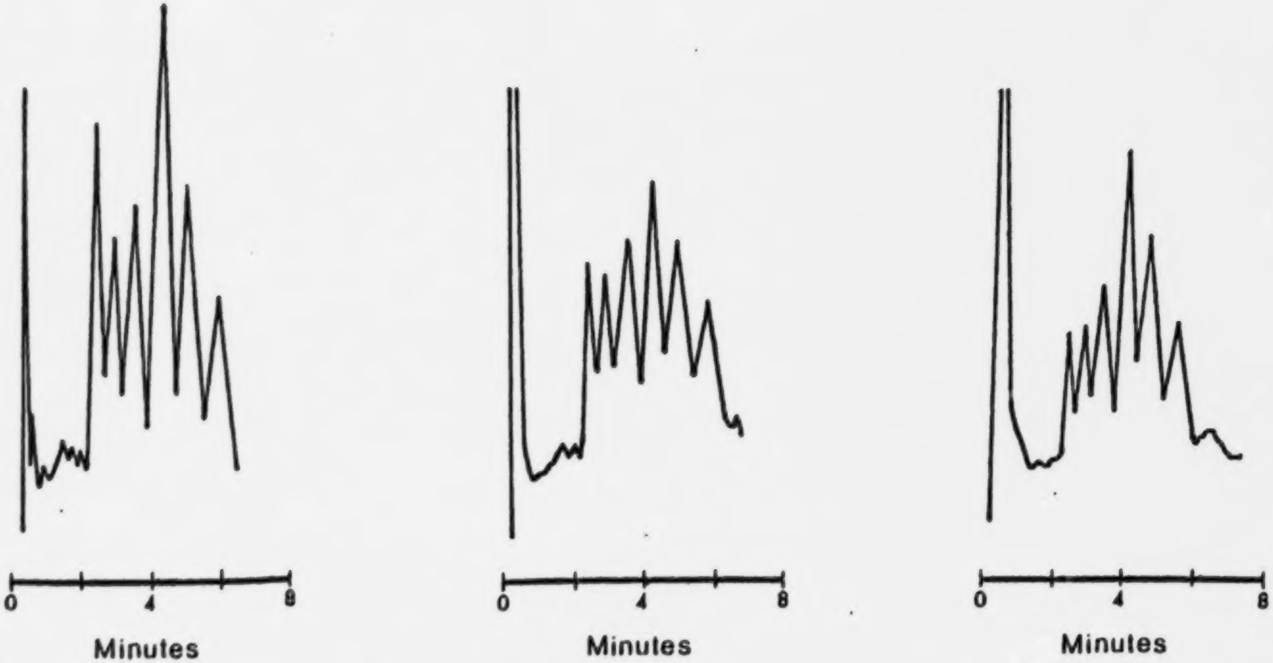

a) OFW+5mg/ℓ Humic Acid (acetone carrier)   b) Carbon Adsorption   c) Glass sorption

Figure 104. Typical packed-column chromatograms for A-1254.

different experimental conditions are shown in Figure 105. Figure 105a represents a standard of A-1016 in hexane, highlighting isomer distribution in the pure mixture. Figure 105b illustrates the chromatogram for an extraction of OFW spiked with A-1016 using hexane as carrier solvent. As was found for A-1254, the isomer distribution is nearly identical to that of the pure PCB. The chromatogram for the residual A-1016 after carbon adsorption equilibrium had been attained (Figure 105c) indicates some preferential adsorption of individual isomers.

ADSORPTION METHODOLOGIES

General

Rational design criteria for evaluation of the removal of chlorinated hydrocarbons at the extremely low levels found in water supplies require recognition of a number of factors which markedly influence the quantification of adsorption parameters. These factors include sorption on reactor walls, volatilization, biological growth, interferences and potential adsorption of carrier solvents.

Sorption on Reactor Walls--

Because they are hydrophobic, PCB's sorb to the surfaces of reactors in which adsorption studies are carried out. The extent of sorption depends in large measure on the material with which the reactor is constructed. To find a suitable reactor material, sorption studies were conducted in different types of vessels including 1-l Pyrex flasks, 100-ml Teflon bottles, and 150-ml Hypo-Vials. The reactors were spiked with 50 μg/l of A-1254 and agitated for 24 hours to ensure equilibrium between the solution and reactor walls. As noted in Figure 106, initial experiments with sealed and agitated Pyrex reactors indicated that equilibrium conditions with reactor surfaces were achieved in less than 24 hours. PCB losses to the reactor surfaces were found to be: 30 to 50% for Teflon bottles, 50 to 70% Hypo-Vials, but only 10 to 15% for the Pyrex flasks. The Pyrex reactors and Hypo-Vials were then treated with dimethyldichlorosilane, and the adsorption tests repeated. The silinized Pyrex reactors exhibited no significant improvement in PCB recovery (90%). Losses in the silinized vials were decreased to 15%, but were still higher than those for the Pyrex.

Based on these observations, Pyrex reactors were selected for the adsorption experiments reported herein. Figure 106 indicates rate and extent of PCB uptake by the surfaces of the sealed Pyrex reactors used for adsorption.

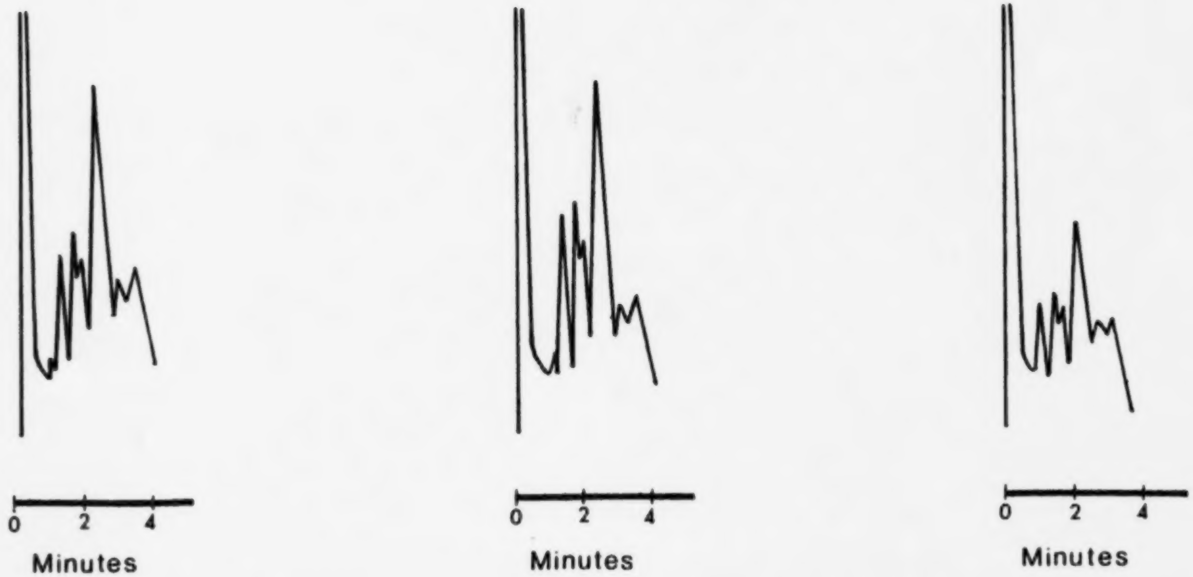

a) Standard in Hexane b) OFW (acetone carrier) c) Carbon Adsorption

Figure 105. Typical packed column chromatograms for A-1016 (3% Silicone OV-1 on 80/100 Gas Chrom Q; Ni_{63} ECD).

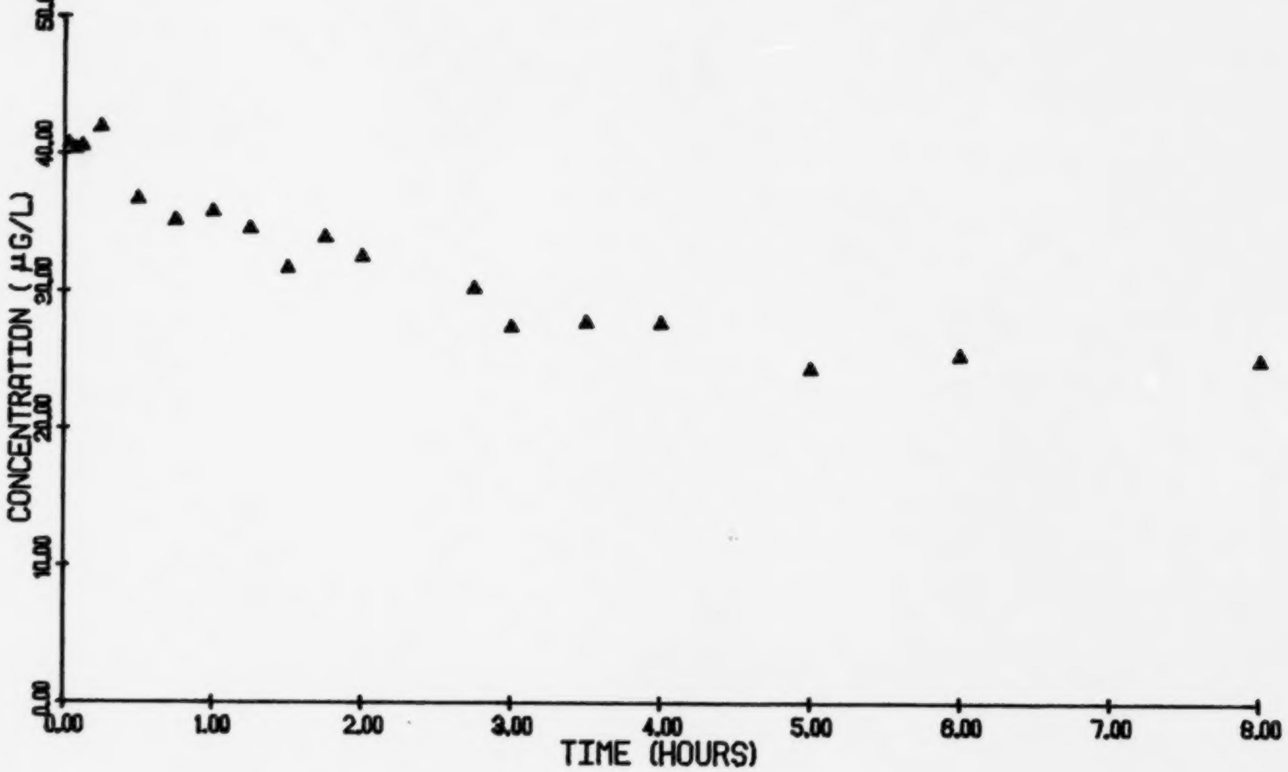

Figure 106. Rate of loss of A-1254 to the air-tight Pyrex glass reactor used for CMB rate experiments.

TYPING GUIDE SHEET
BEGIN FIRST LINE OF TEXT HERE
CENTER OF PAGE
TOP OF IMAGE AREA
DROPPED HEAD; BEGIN SECTIONS HERE

Volatilization--

The rate and extent of loss of PCB from solution by volatilization was examined. Two 3-l glass containers were filled with OFW and spiked with A-1254 to obtain an aqueous concentration of 40 µg/l. One container was stored at 4°C and the other at 20°C. Both were sampled periodically over a 20-day period. Figure 107 illustrates the concentration decay of A-1254 at these temperatures. It is evident that both rate and extent of volatilization substantially increase at higher temperature. It was further observed that lower chlorine isomers volatilize more rapidly. Airtight reactors with no headspace (rate studies) or minimum headspace (equilibrium studies to allow agitation) were utilized to eliminate these losses in the course of subsequent adsorption experiments.

Biological Growth--

Because of the high sorption affinity of PCB's for solids, it is essential that adsorption experiments be conducted in the absence of such extraneous particulates as biological solids. Ulanoff (1979) demonstrated that both viable and dead bacteria can sorb Aroclor 1254 extensively, as illustrated in Figure 108. The appearance of bacterial flocs in long-term experimental systems can thus cause errors in carbon adsorption studies. This problem may be alleviated by introducing a biological inhibitor, such as Ag^+, or by sterilizing the entire system prior to initiation of an experiment.

Interferences--

Every effort should be made to avoid interferences from experimental contamination. Major sources of contamination are: dilution water, glassware, plastic materials, and solvents. Dilution water should be free of extraneous organic constituents. A high quality water can be obtained from distillation units constructed entirely of glass and Teflon. Glassware should be cleaned scrupulously. A cleansing procedure recommended by the USEPA (Thompson, 1977) was found satisfactory. Contact with plastic caps and the cap-lining used on extraction vials and reagent bottles should be avoided. A Teflon sheet can be placed carefully on the mouth of these bottles before screwing on the caps. Solvents should be checked for purity. Commercial pesticide-grade or laboratory purified solvents should be used.

Adsorption of Carrier Solvent--

The extent and rate of adsorption of acetone (used as PCB carrier-solvent) by carbon and possible interference with adsorption of PCB's was investigated. A 2-gram quantity of 16/20 carbon was added to a 30-mg/l solution of acetone in OFW in an airtight reactor and the reactor stirred vigorously. Samples of 5-µl volume were withdrawn periodically and injected into a Varian 2700 GC equipped with a flame ionization detector and 6' x 1/8" stainless steel column packed with

BEGIN LAST LINE OF TEXT
BOTTOM OF IMAGE AREA; OUTSIDE DIMENSION FOR TABLES AND ILLUSTRATIONS
3/8"

PAGE NUMBER
EPA-287 (Cin.)
(4-76)

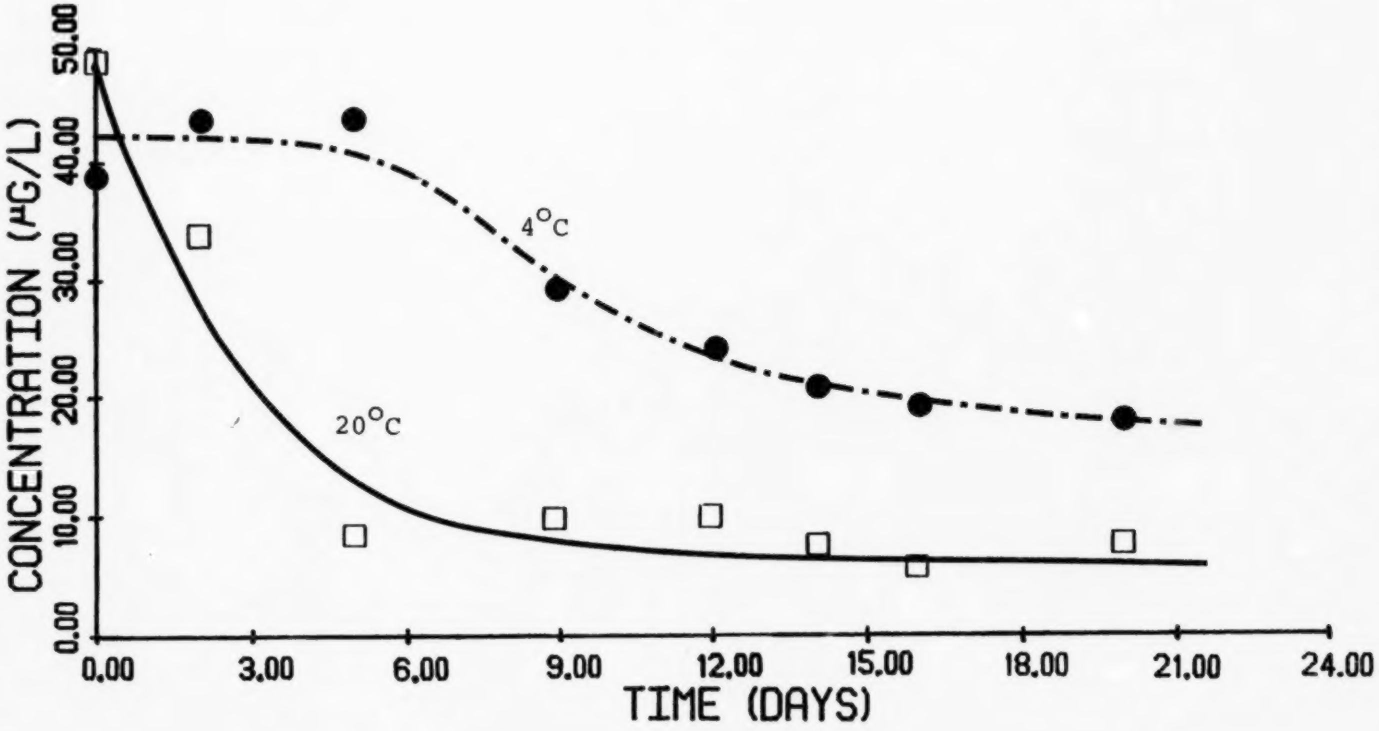

Figure 107. Rate and extent of volatilization of A-1254.

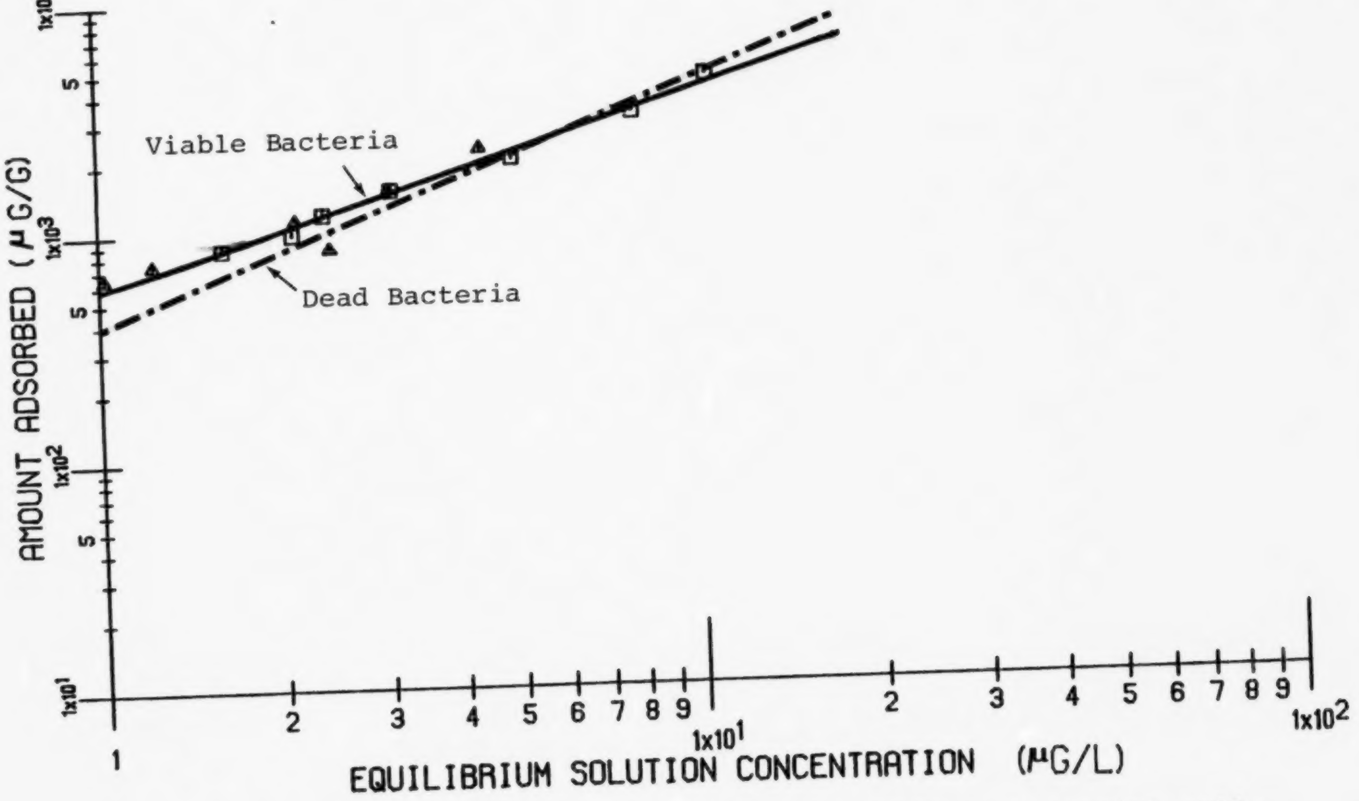

Figure 108. Isotherms for adsorption of A-1254 on bacterial cells.

60/80 Tenax-GC. Operating temperatures were: 225°C for the injector, 100°C for the column and 250°C for the detector. A flow rate of 40 ml/min was used for the nitrogen carrier gas. The concentration decay curve depicted in Figure 109 indicates that acetone is only moderately adsorbed by carbon. It was therefore concluded that acetone would present no significant interference with adsorption of PCB's on carbon.

Equilibrium Studies

Equilibrium experiments were performed in 1-l Pyrex Erlenmeyer flasks using the bottle-point technique. Carefully weighed amounts of carbon and 850 ml aliquots of OFW -- or 5 mg/l humic acid prepared in OFW background solution -- were placed in the flasks, which were then spiked with PCB in acetone carrier-solvent to achieve a desired aqueous concentration. The flasks were immediately sealed with ground-glass stoppers, placed on a shaker and agitated until equilibrium was achieved. Equilibration time ranged from 48 hours for powdered carbon to three weeks for granular carbon. For A-1016 equilibrium experiments it was found necessary to employ a step-spike procedure, whereby flasks with no detectable residual PCB were spiked periodically and allowed to reach a new equilibrium condition.

A liquid-liquid extraction technique followed by gas chromatographic analysis was used for determination of residual PCB concentrations. For isotherm studies with powdered carbon the samples were centrifuged for 30 minutes at 2600 rpm to remove the carbon prior to extraction. Depending on the residual concentration, either the simple vial extraction or the multiple extraction technique discussed previously in this section was employed.

Rate Studies

CMB-rate studies for PCB were conducted in air-tight glass reactors similar to those described for CCl_4 and benzene. The reactor surfaces were pre-equilibrated with the PCB solutions.

Weighed and pre-wetted quantities of 50/60 carbon were added to the experimental solutions (spiked OFW or 5 mg/l humic acid prepared in OFW background solution; pH 7) at the outset of each experimental run. Samples of 10-ml volume were then withdrawn periodically and placed in 20-ml vials containing 2-ml of hexane. The vials were sealed with screw-on caps lined with Teflon faced septa, and agitated vigorously. A few microliters of the extract was withdrawn and subjected to gas chromatographic analysis.

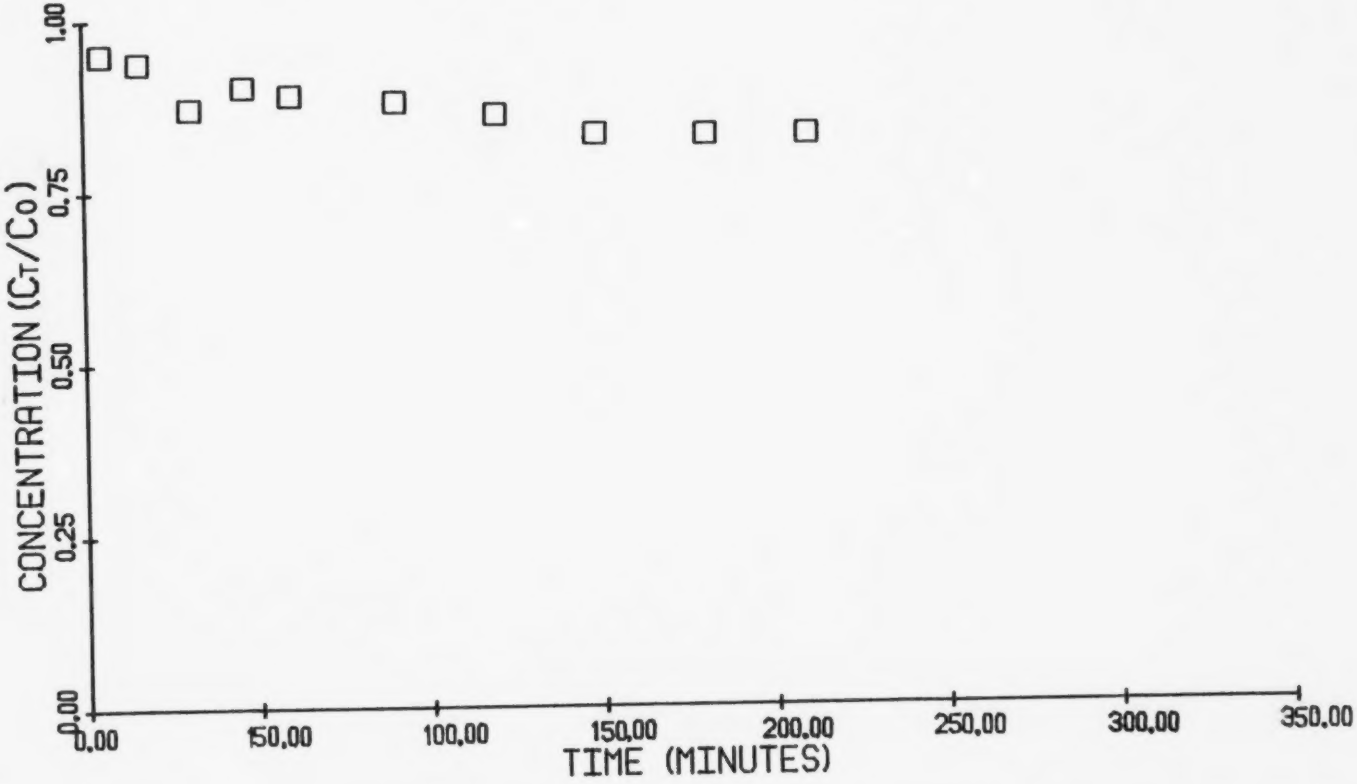

Figure 109. Rate and extent of adsorption of acetone carrier-solvent on granular carbon in a CMB reactor (C_o = 30 mg/ℓ, 0.66 g/ℓ of 16/20 US sieve size carbon).

Column Studies

Fixed-bed adsorber studies were conducted in 1-cm (ID) glass mini-columns containing a few grams of 50/60 carbon. Two 12-gallon glass reservoirs were filled with OFW and spiked with PCB in acetone. The feed solution was stirred for one hour and then pumped to the mini-columns at a flow rate of 10-20 ml/min. All tubing and connections were constructed of glass, Teflon and/or stainless steel. The reservoirs were sealed with Teflon-coated rubber stoppers to minimize loss of PCB due to volatilization. To eliminate any vacuum caused by solution displacement, a 1/2-mm (ID) capillary column was pierced through the stoppers. Samples were taken periodically and subjected to extraction and GC analysis. Figure 110 illustrates the experimental apparatus and arrangement.

RESULTS AND DISCUSSION

Adsorption Equilibrium

As for the other solutes discussed in this report, the Freundlich equation was found to provide the most straightforward best-fit to the experimental equilibrium data for the PCB's.

As noted previously in this section, a step-spike procedure was employed for equilibration of A-1016 solutions in OFW. The solutions were spiked with A-1016 and agitated until equilibrium was achieved. Analysis of the samples indicated no residual A-1016 in solutions. The bottles were respiked with A-1016 and agitated for reequilibration. Figure 111 presents equilibrium data for A-1016 in OFW. It was not necessary to respike solutions for the equilibrium studies with Aroclor 1016 in the presence of humic acids. Figure 112 indicates that Aroclor 1016 adsorption is decreased in the presence of humic acids. One possible explanation is that both the activated carbon and the humic acids macromolecules compete for adsorption of PCB's. This phenomenon advances the possibility of enhanced PCB removal via mechanisms which enhance the adsorption of humic acids by carbon, as discussed in Section 6.

Isotherm data from experiments performed to characterize the adsorption behavior of A-1254 in OFW and 5 mg/l humic acid background solutions are presented in Figures 113 and 114, respectively. Once again the decrease in PCB adsorption is observed in the presence of humic acids.

Isotherm parameters for the equilibrium studies are summarized in Table 23.

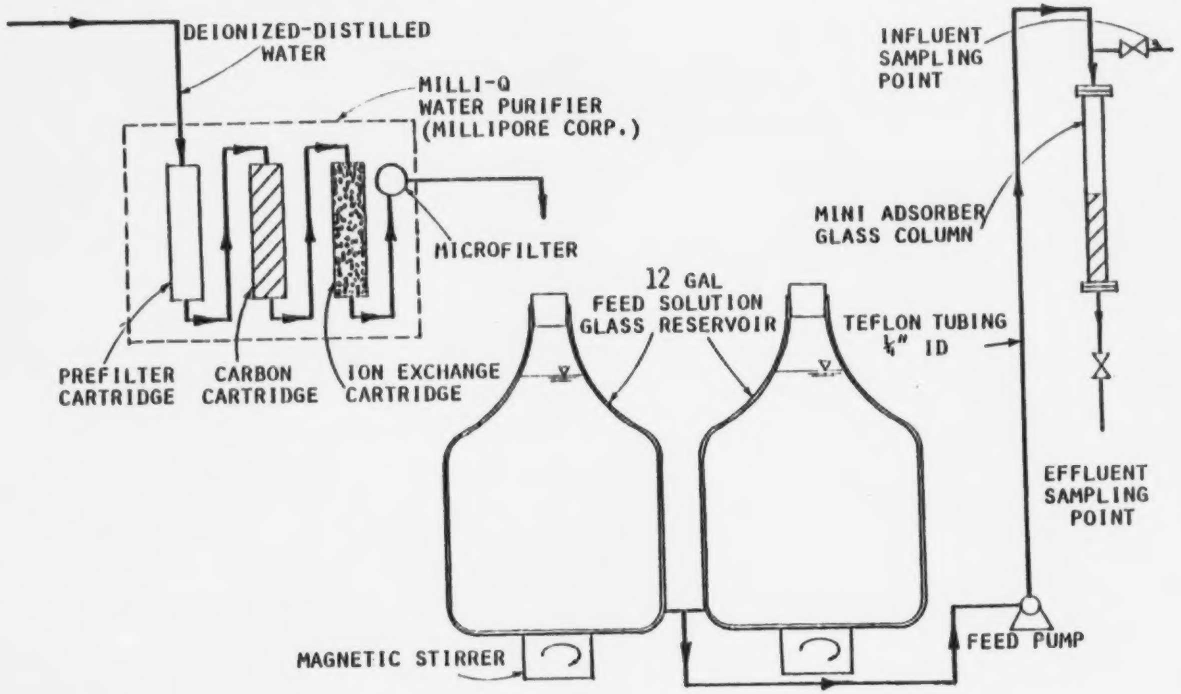
DEIONIZED-DISTILLED WATER
MILLI-Q WATER PURIFIER (MILLIPORE CORP.)
MICROFILTER
PREFILTER CARTRIDGE
CARBON CARTRIDGE
ION EXCHANGE CARTRIDGE
12 GAL FEED SOLUTION GLASS RESERVOIR
MAGNETIC STIRRER
INFLUENT SAMPLING POINT
MINI ADSORBER GLASS COLUMN
TEFLON TUBING ¼" ID
EFFLUENT SAMPLING POINT
FEED PUMP

Figure 110. Experimental apparatus and arrangement.

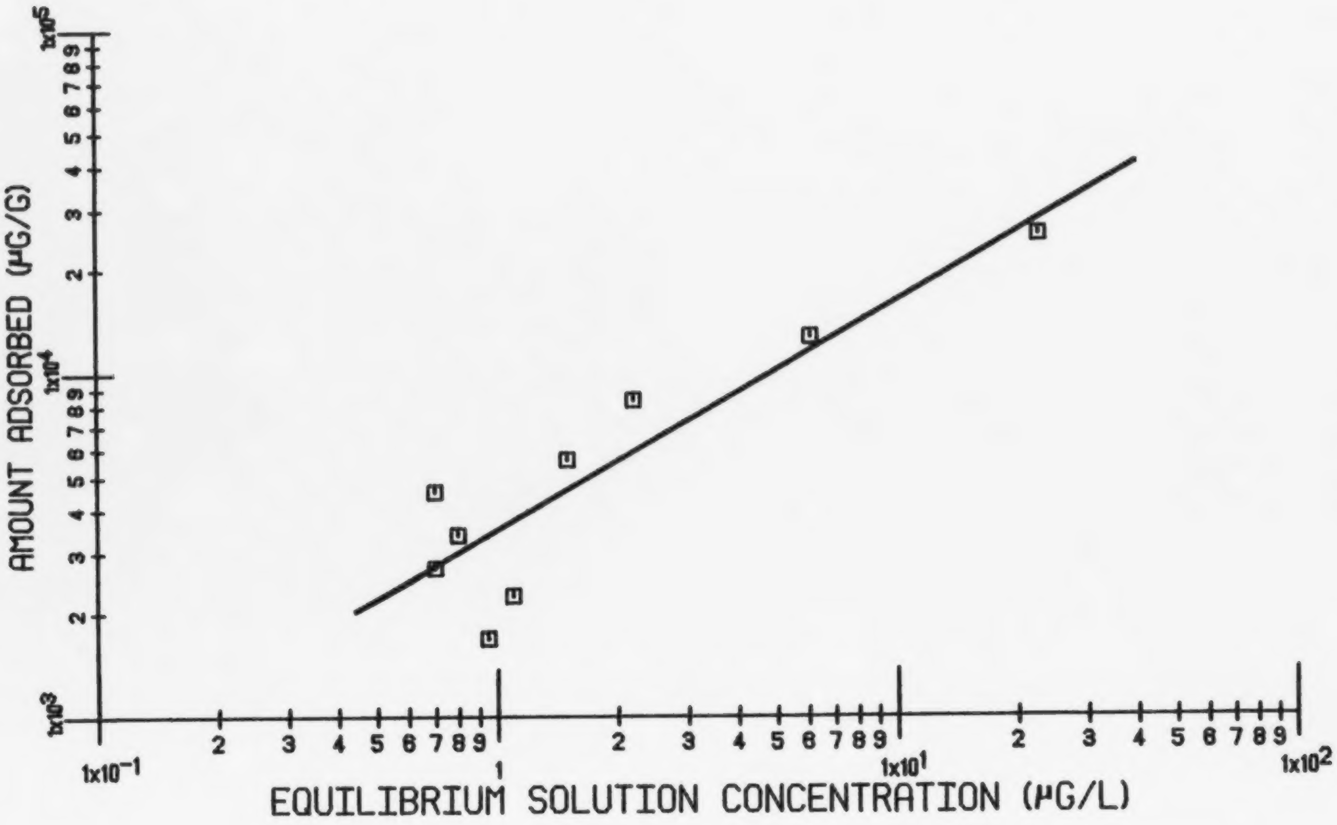

Figure 111. Adsorption isotherm for A-1016 in OFW (spiked twice at C_o = 45 µg/ℓ, 100/200 carbon).

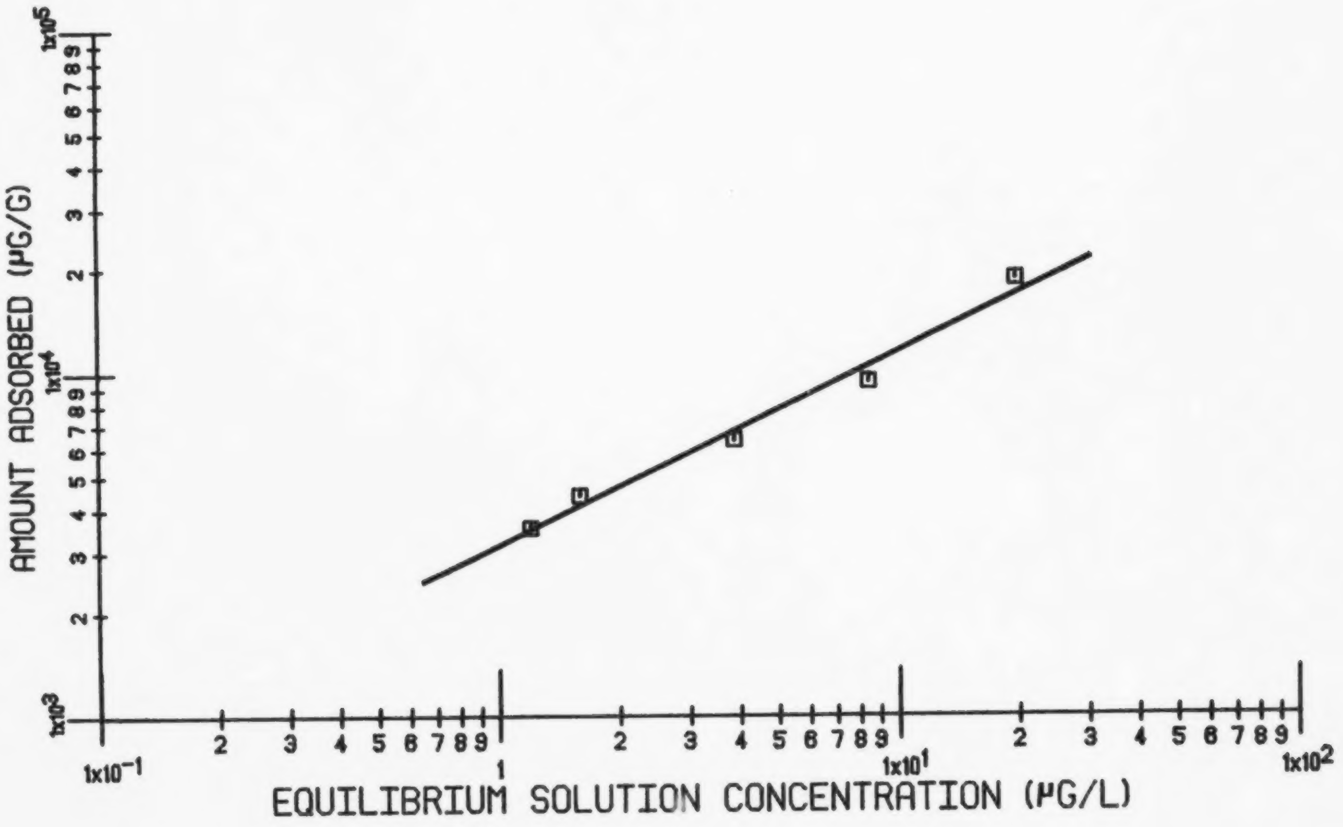

Figure 112. Adsorption isotherm for A-1016 in solution of humic acids (C_o = 63.6 µg/ℓ, 100/200 carbon).

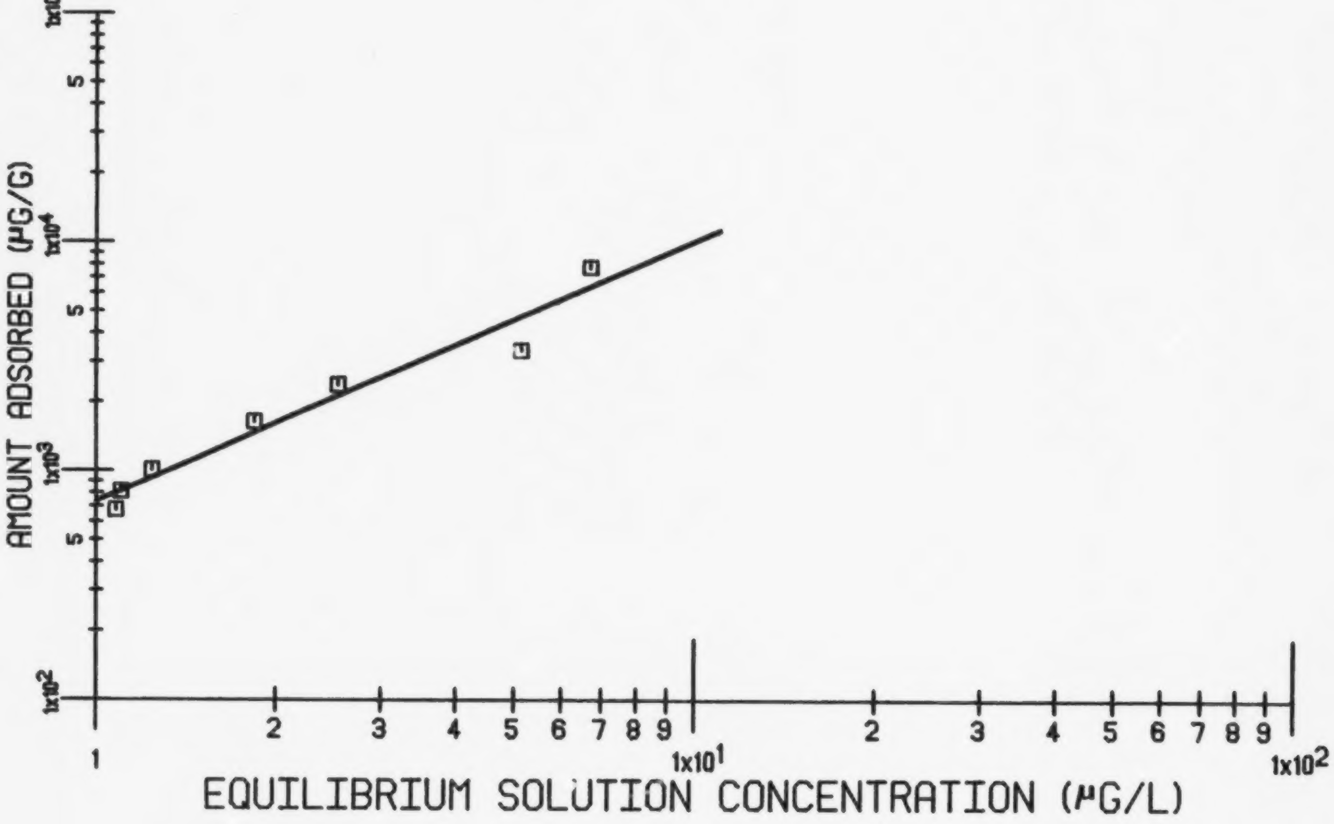

Figure 113. Adsorption isotherm for A-1254 in OFW (C_o = 25 µg/ℓ, 100/200 carbon).

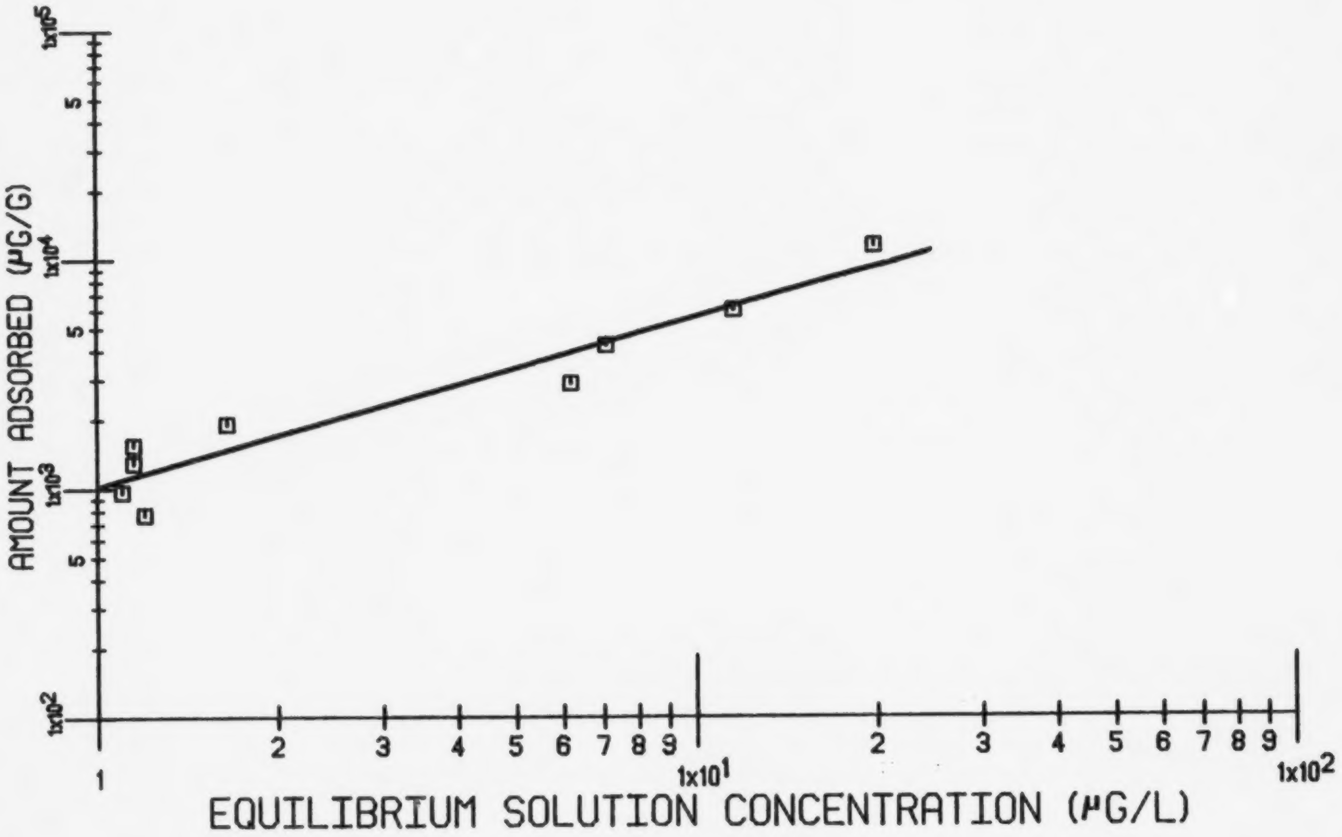

Figure 114. Adsorption isotherm for A-1254 in solution of humic acids (C_o = 46.5 μg/ℓ, 100/200 carbon).

TABLE 23. SUMMARY OF ADSORPTION EQUILIBRIUM PARAMETERS FOR A-1016 AND A-1254†

Compound	Background Solution	Carbon Size, US Standard Sieve Mesh	Co, µg/l	Freundlich Isotherm Constants*		
				K_f	1/n	$r^{\dagger\dagger}$
A-1016	OFW	100/200	85.3	3.44	0.664	0.897
A-1016	OFW + 5 mg/l humic acids	100/200	63.6	3.16	0.560	0.991
A-1254	OFW	100/200	25	0.73	1.14	0.977
A-1254	OFW + 5 mg/l humic acids	100/200	46.5	1.017	0.737	0.959

† = All studies were conducted at pH 7 unless otherwise noted.

* = Based on C_e and q_e expressed in µg/l and mg/gm, respectively.

$r^{\dagger\dagger}$ = Correlation coefficient for fit of the isotherm to the experimental data.

It may be observed from Figures 111 through 114 and the information summarized in Table 23 that A-1016 is adsorbed to a greater extent than A-1254. In that A-1016 is generally more soluble than A-1254, this appears contrary to the general observation that adsorption is inversely related to aqueous solubility. This generalization may not be particularly valid for PCB solutions in that these do not truly conform to the definition of "ideal solutions" (Schoor, 1975). Further, Aroclors are mixture of various isomers -- with different weight percentages and different physical and chemical characteristics -- that compete for adsorption sites on carbon in a multi-component milieu.

To investigate differential adsorption of PCB isomers, CMB reactor rate studies were performed for A-1254 in OFW. The concentration decay curve for the first 4 peaks on the chromatogram representing groups of isomers with similar chlorine content were measured using an integrator. A plot of the ratio of the percent of total areas represented by each peak at time = t and at time = 0 versus time is depicted in Figure 115. This plot indicates that the lower chlorine isomers are adsorbed more extensively.

Similar CMB reactor rate studies were performed with A-1254 in humic acid solution. The results are presented in Figure 116. It may be observed that the plots exhibit differential adsorption phenomena, especially the plot following peak No. 1. Further, the background solution has a marked effect on the adsorption of the isomers, as shown in a comparison of Figures 115 and 116.

To more fully investigate differential adsorption it would be necessary to obtain better separation of isomers. Capillary columns with suitable wall coatings, such as Sp-2100, may be used for this purpose.

Adsorption Rates

A simulation-modeling analysis was performed for adsorption of A-1016 and A-1254 from OFW and humic acid solutions to evaluate the mass transfer coefficients, k_f and D_s. Figures 117 through 120 present results from parameter search routines for these coefficients for A-1016 and A-1254. These figures illustrate significant disparity between experimental data and fitted rate profiles. Such disparity is to be expected in that the form of the MADAM model used to determine the mass transfer coefficient was the single-solute form. Because each PCB mixture is comprised of a large number of different isomers, deviation from single-solute behavior should be anticipated. Although the MADAM model is capable of analyzing data and predicting performance for multi-solute systems, insufficient input data exists for the variety of individual solutes

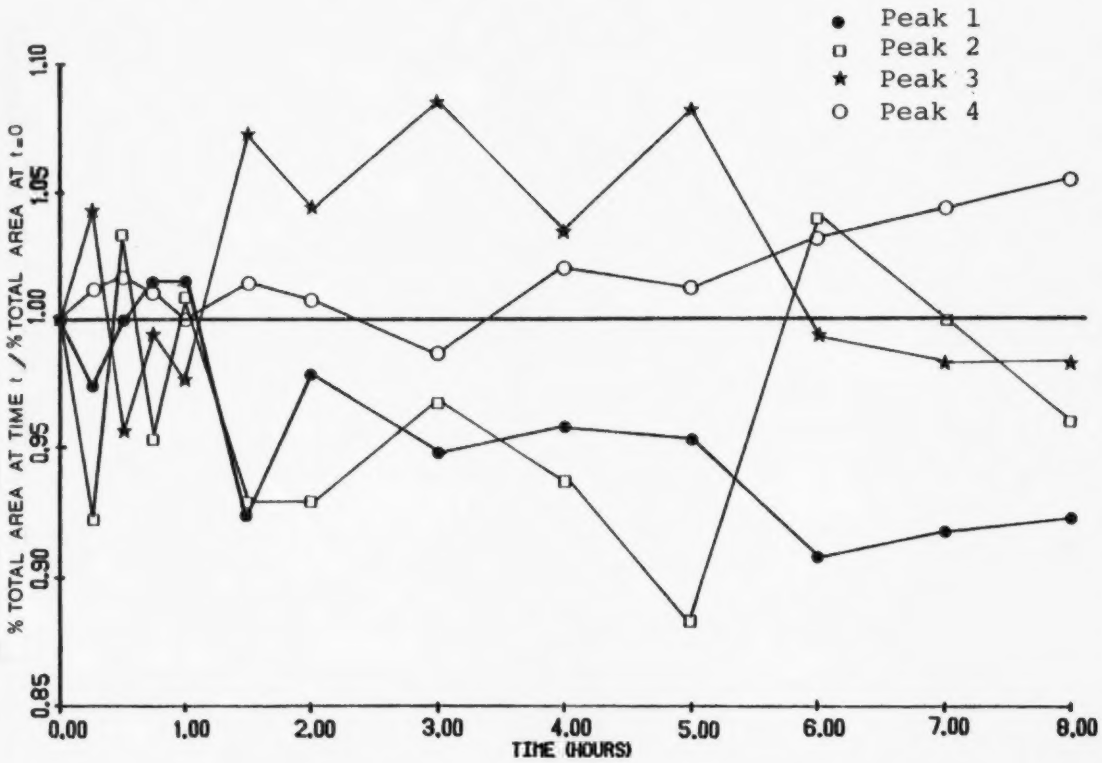

Figure 115. Differential adsorption rate behavior of individual peaks for A-1254 in OFW (C_o = 38.6 µg/ℓ, 0.115 g/ℓ of 50/60 carbon).

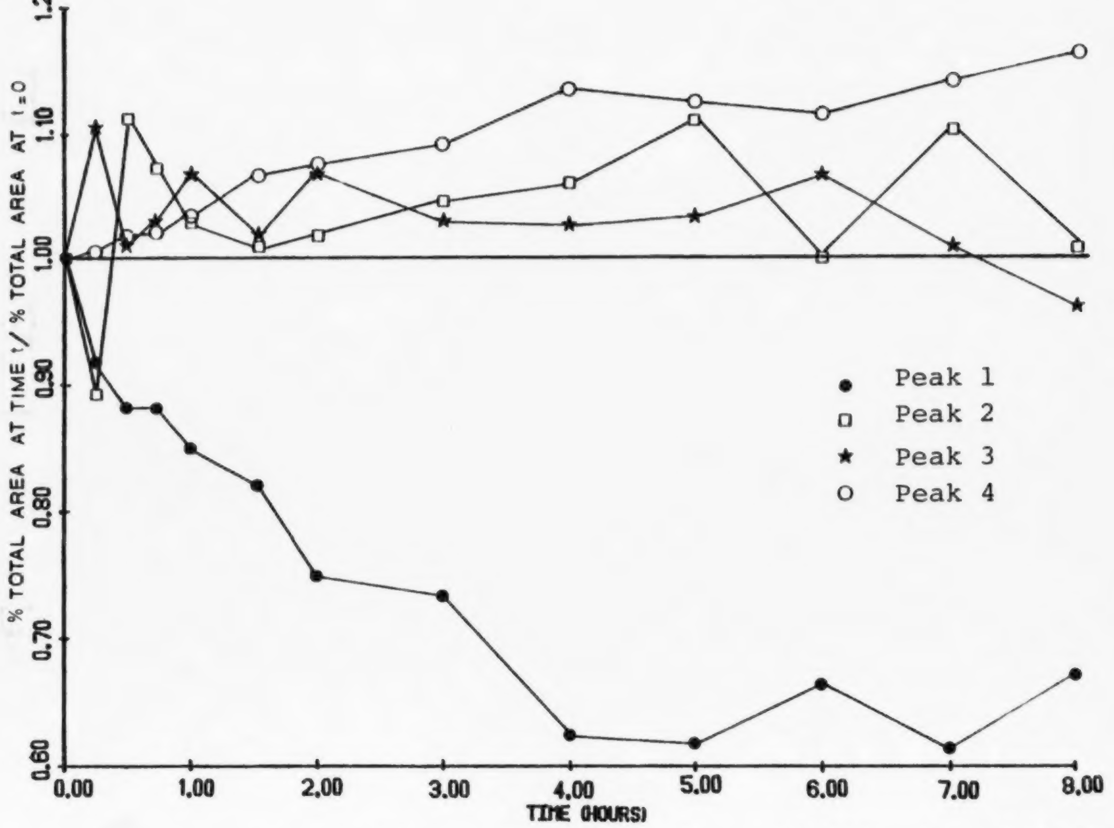

Figure 116. Differential adsorption rate behavior of individual peaks for A-1254 in a solution of humic acids (C_o = 36.9 μg/ℓ, 0.115 g/ℓ of 50/60 carbon).

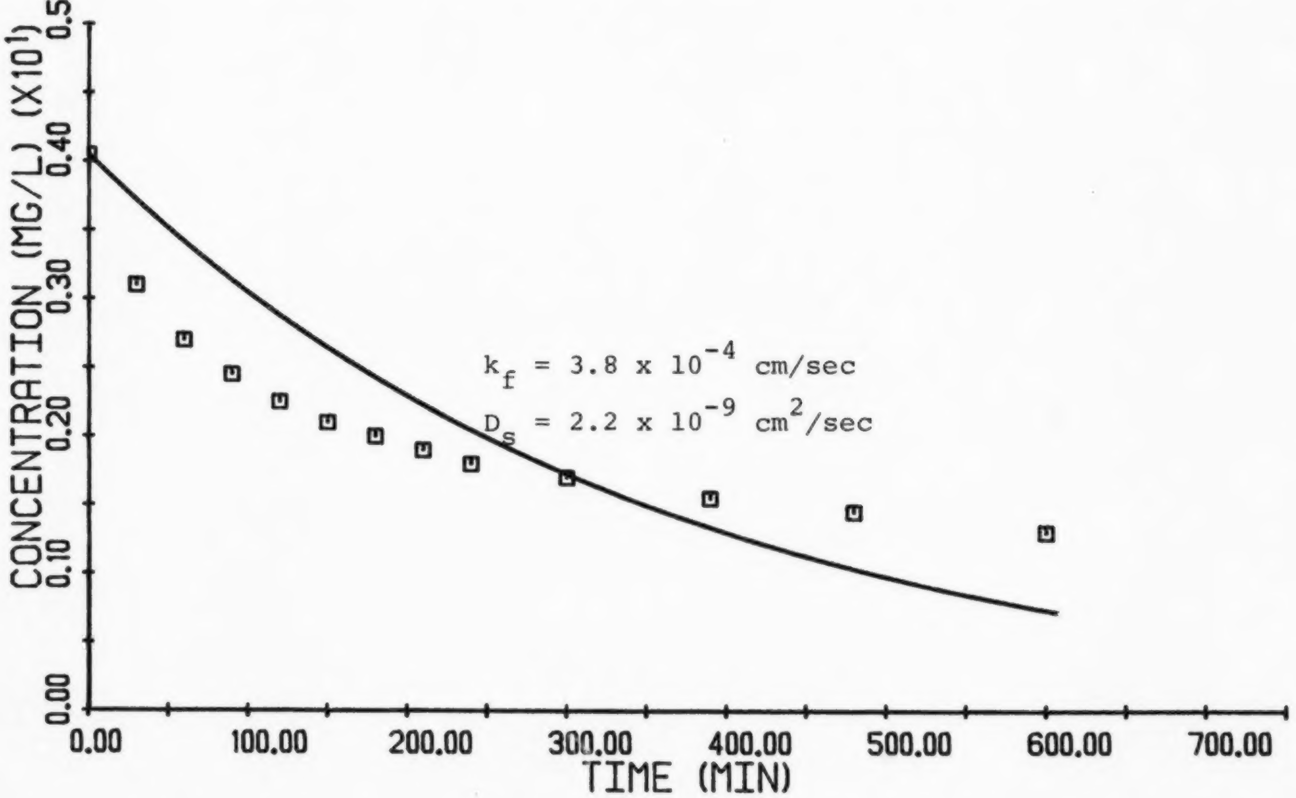

Figure 117. Experimental data and model profile for rate of adsorption of A-1016 from OFW in a CMB reactor (C_o = 40.5 μg/ℓ, 0.114 g/ℓ of 50/60 US sieve size carbon).

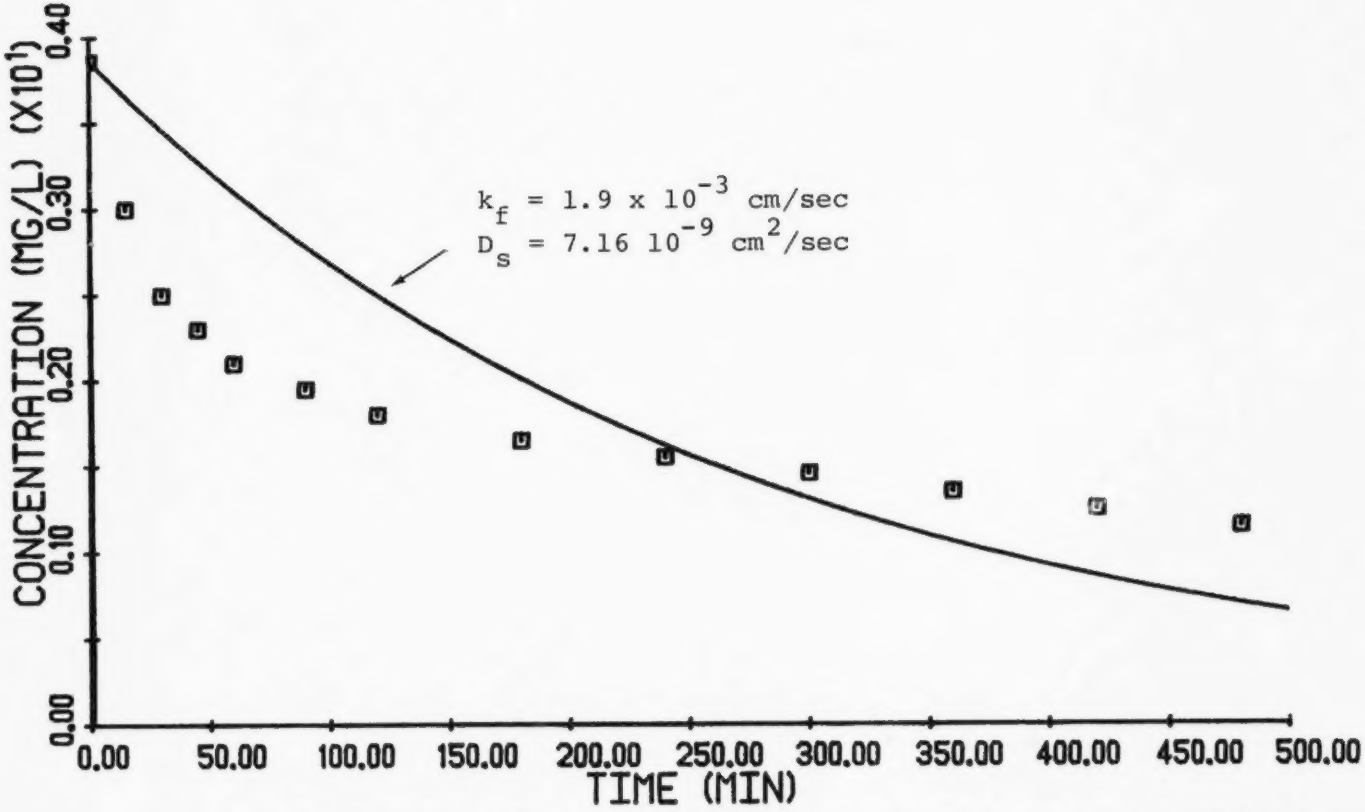

Figure 118. Experimental data and model profile for rate of adsorption of A-1254 from OFW in a CMB reactor (C_o = 38.6 μg/ℓ, 0.114 g/ℓ of 50/60 US sieve size carbon).

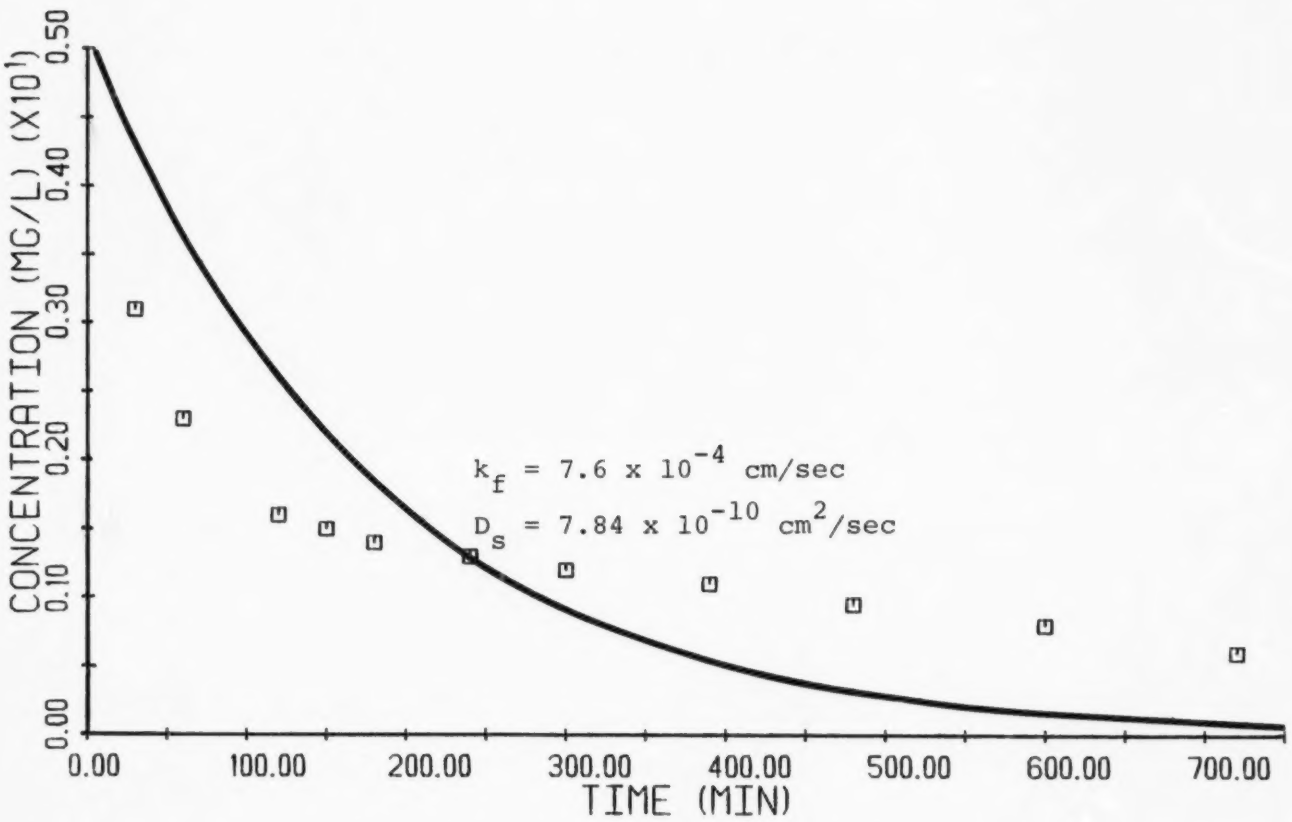

Figure 119. Experimental data and model profile for rate of adsorption of A-1016 from solution of humic acids in a CMB reactor (C_o = 51.1 μg/ℓ, 0.114 g/ℓ of 50/60 US sieve size carbon).

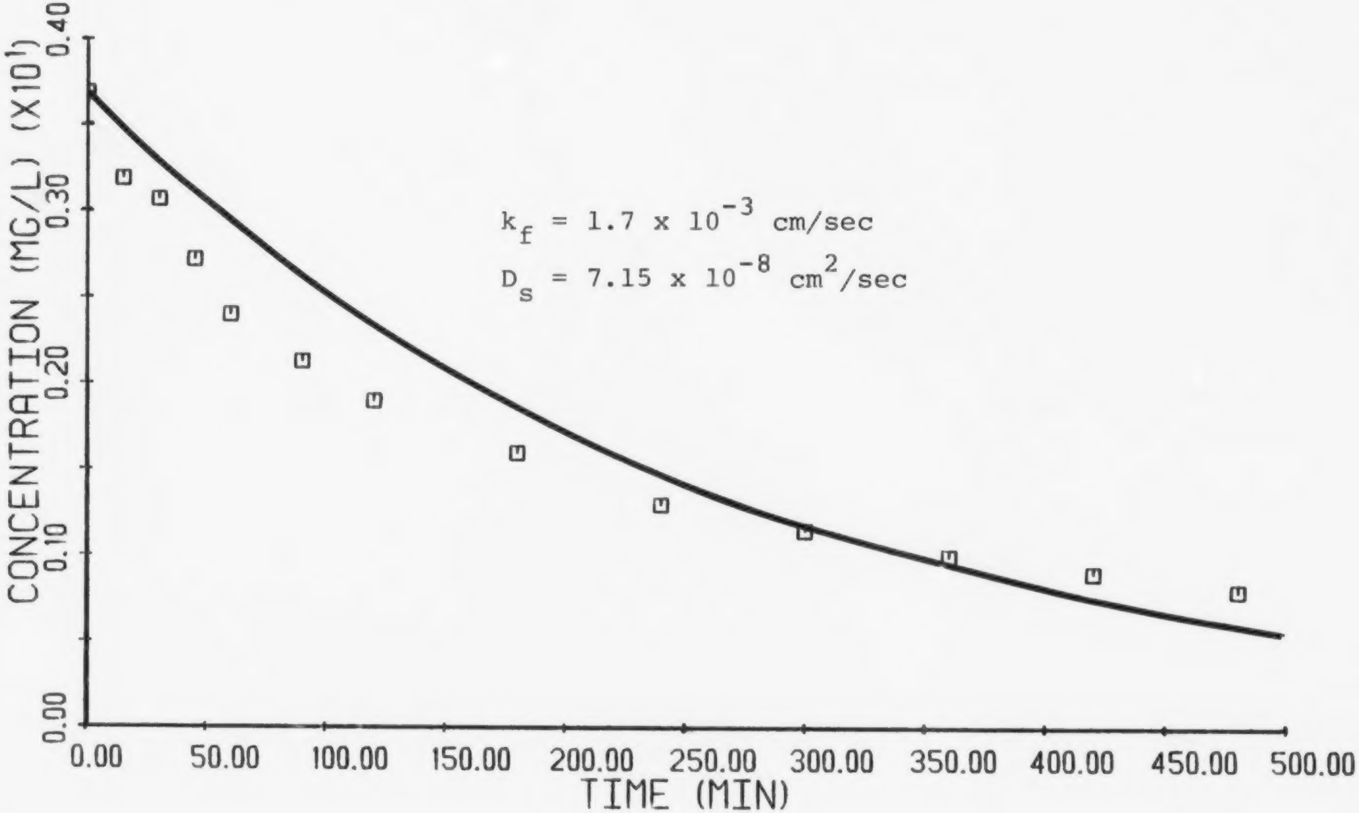

Figure 120. Experimental data and model profile for rate of adsorption of A-1254 from a solution of humic acids in a CMB reactor (C_o = 36.9 μg/ℓ, 0.114 g/ℓ of 50/60 US sieve size).

comprising the PCB mixtures.

Table 24 summarizes the experimental conditions and associated mass transfer coefficients for the systems depicted in Figures 117, 118, 119, and 120. Once again, the rate parameters given in this table are lumped parameters which can be used for inter-comparison purposes but cannot be taken as absolute values for purposes of predictive modeling.

Adsorption Columns

Mini fixed-bed experiments for A-1016 were designed and conducted with A-1016 to obtain data relative to adsorber breakthrough characteristics. A number of early difficulties, including biological growth, channeling, and interferences due to contamination were encountered and systematically resolved. For these experiments 5 grams of 50/60 carbon were used in a system similar to that described earlier in this section. The feed solution was dosed with 2 mg/l of Ag^+ and the flow rate was maintained at 20 ml/min. Influent samples were extracted using a vial-extraction technique. Effluent samples were subjected to a multiple extraction technique. The influent and effluent concentration profiles for A-1016 are presented in Figure 121. No breakthrough was reached within the 244 days of operation, which represents a duration well beyond the theoretical carbon capacity. Several plausible explanations may be advanced.

Biodegradation of PCB's--

Biological growth was visible in the carbon column as early as 50 days from onset of operation. Silver did not appear to have a thorough inhibitory effect on this particular case. To verify the presence of the growth, carbon particles from the column were examined by scanning electron microscopy. Figure 122 presents a typical micrograph illustrating the nature of the coverage by bacteria.

That bacteria degrade PCB's has been documented by a number of researchers. Ahmed and Focht (1973) demonstrated that two species of *Achromobacter*, isolated from sewage effluent, used biphenyl and p-chlorobiphenyl as sole carbon sources. Furukawa and Matsumura (1976) reported the metabolic degradation of various PCB isomers by a bacterial strain (*Alkaligenes* sp.) isolated from a lake sediment. Sayler *et al* (1977) observed that PCB's stimulated growth and oxygen uptake by *Pseudomonas* sp. and suggested bioaccumulation as a potential mechanism for removal. Furukawa *et al* (1978) concluded that bacteria were able to adsorb PCB's onto the cell surface and gradually metabolize them.

Gibson (1975) discussed possible metabolic pathways for the degradation of several aromatic compounds. Similar

TYPING GUIDE SHEET
BEGIN FIRST LINE OF TEXT HERE
CENTER OF PAGE
TOP OF IMAGE AREA
DROPPED HEAD BEGIN SECTIONS HERE
BEGIN LAST LINE OF TEXT
BOTTOM OF IMAGE AREA; OUTSIDE DIMENSION FOR TABLES AND ILLUSTRATIONS
PAGE NUMBER
EPA-287 (Cin.)
(4-76)

TYPING GUIDE SHEET
BEGIN FIRST LINE OF TEXT HERE
DROPPED HEAD: BEGIN SECTIONS HERE
CENTER OF PAGE
TOP OF IMAGE AREA
BEGIN LAST LINE OF TEXT
BOTTOM OF IMAGE AREA OUTSIDE DIMENSION FOR TABLES AND ILLUSTRATIONS
3/8"
PAGE NUMBER
EPA-287 (Cin.)
(4-76)

TABLE 24. SUMMARY OF ADSORPTION RATE PARAMETERS FOR AROCLOR 1016 AND 1254

Compound	Background Solution	Co, μg/l	Carbon Dosage, g/l	k_f, cm/sec	D_s, cm^2/sec
A-1016	OFW	40.5	0.114	3.8×10^{-4}	2.2×10^{-9}
A-1016	OFW + 5 mg/l humic acids	51.1	0.114	7.6×10^{-4}	7.84×10^{-10}
A-1254	OFW	38.6	0.114	1.9×10^{-3}	7.16×10^{-9}
A-1254	OFW + 5 mg/l humic acids	36.9	0.114	1.7×10^{-3}	7.15×10^{-8}

C_o = Initial concentration;

k_f = Film transfer coefficient; and,

D_s = Surface diffusion coefficient.

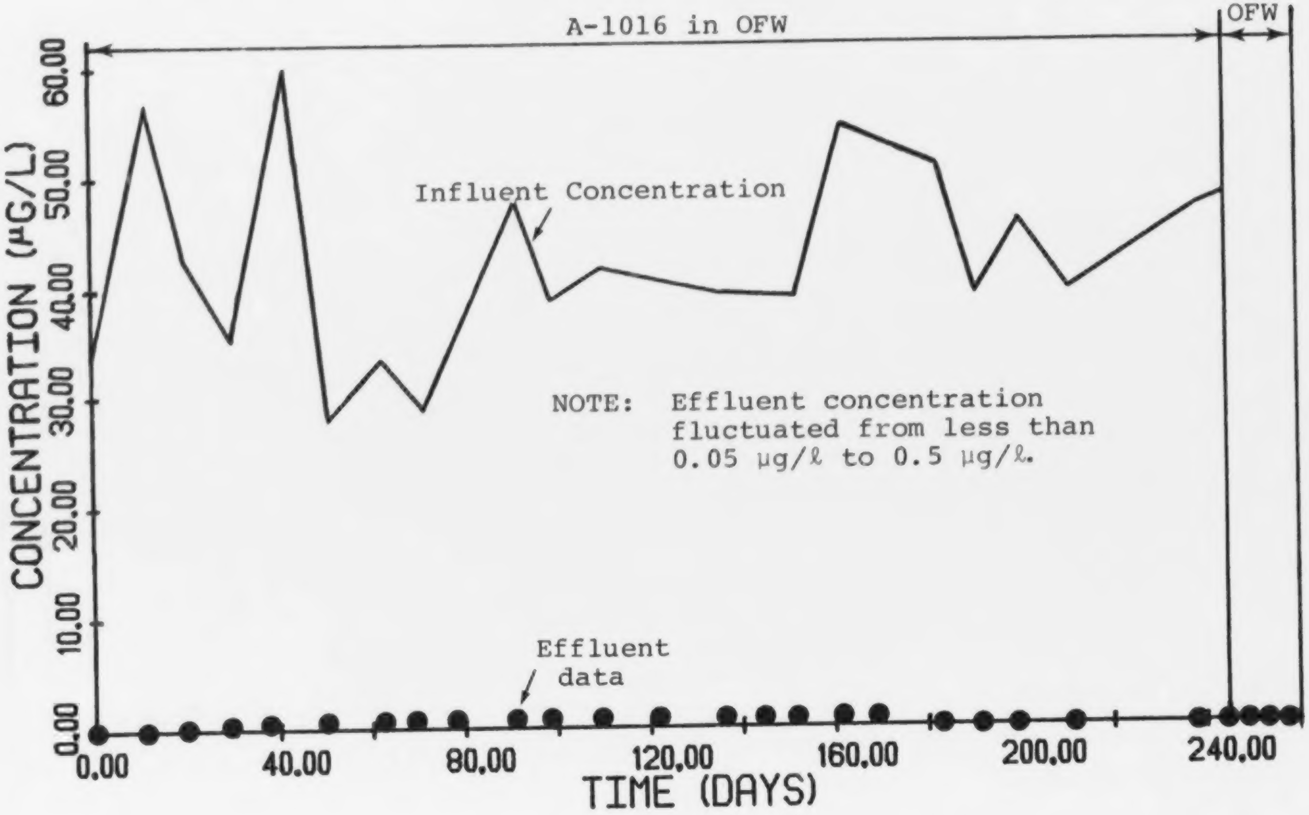

Figure 121. Influent and effluent concentration data for A-1016 in fixed-bed adsorbers (flow = 20 mℓ/min, 5 grams of 50/60 US sieve size carbon, EBCT = 0.52 min).

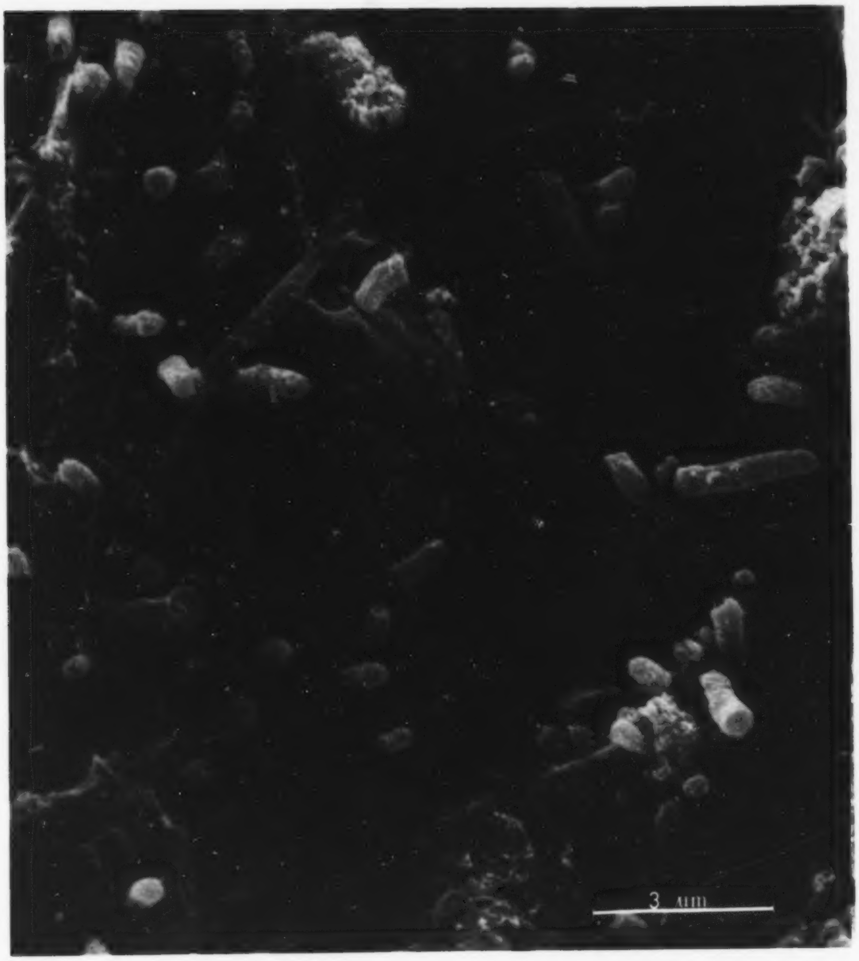

Figure 122. Scanning electron micrograph of biological growth on activated carbon exposed to a solution of Aroclor 1016.

Reproduced from best available copy.

pathways yielding different metabolites may be suggested for the PCB's. These metabolities may elude detection for one or more of these reasons: 1) if they contain no chlorine (Kaiser and Wong, 1974); 2) if they are not extractable by hexane; and, 3) if they are strongly adsorbed by carbon.

PCB Aggregates--

PCB molecules in acetone carrier may form aggregates when introduced to water (Schoor, 1975). The aggregates, depending on their size, may have been filtered out by the carbon/bacteria matrix within the carbon column. Such filtration would have been particularly efficient on the top of the column, where a dense mat of bacteria was formed. To substantiate this it would have been necessary to examine the very top portion of the carbon column for PCB concentration.

Desorption Experiments

Equilibrium adsorption-desorption experiments for A-1254 using powdered carbon were conducted in a manner similar to that described earlier in this section. After achieving equilibrium, 10-ml samples were withdrawn from each flask and subjected to centrifugation, extraction and GC analysis. The remaining supernatent was then filtered using pre-washed 0.45 μm filters and the carbon retained on each filter washed into a clean 1-l flask. The flasks were filled with 850 ml of OFW and agitated on a mechanical shaker for 48 hours until equilibrium was reestablished. Samples were then withdrawn, centrifuged, extracted, and analyzed. Figure 123, which depicts the data for the equilibrium adsorption-desorption studies, suggests equilibrium hysteresis for PCB's on carbon. Further studies in the part-per-trillion concentration range are required for a more rigorous conclusion.

Dynamic desorption studies were performed for A-1016 in the mini-column described earlier following 244 days of adsorption operation. Before the start of the desorption experiments, the entire feeding system, with the exception of the carbon column, was meticulously cleaned to eliminate any sorbed PCB. The mini-column was then fed with OFW for a period of 10 days. Figure 121 illustrates the experimental results, demonstrating that no PCB was eluted or desorbed from the column during this 10-day period of operation.

Competitive Adsorption

Two mini-adsorber columns, one containing 1 gram of 50/60 carbon saturated with humic acids, and the other 1 gram of virgin carbon, were fed with A-1254 solution, dosed with 2 mg/l Ag^+, and maintained at a flow rate of 10 ml/min. The effluent concentration data illustrated in Figure 124 indicates no significant reduction in the capacity of the

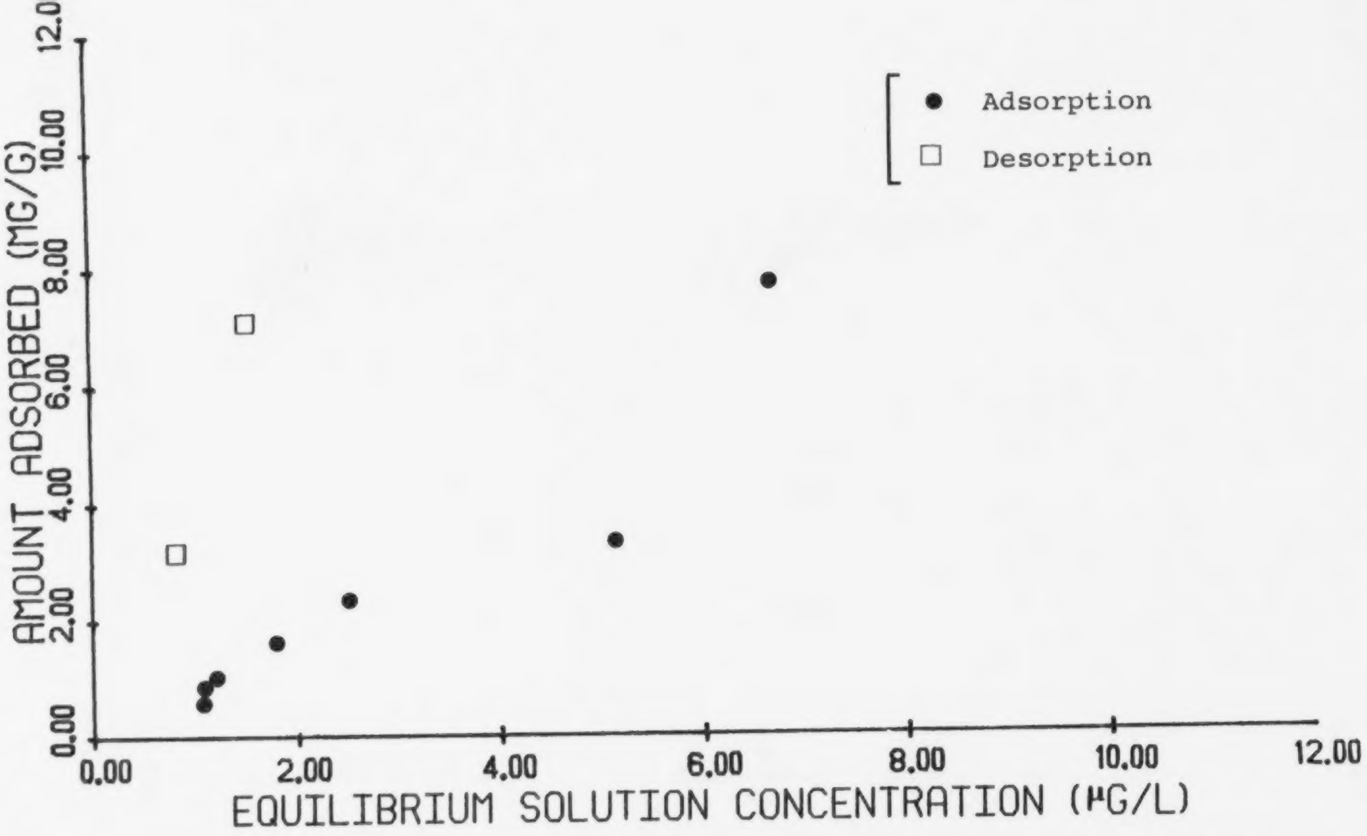

Figure 123. Equilibrium adsorption and desorption data for A-1254 in OFW (C_o = 25 µg/ℓ, 50/60 US sieve size carbon).

presaturated carbon. This may be highly significant with respect to the ability of carbon which is saturated with background organics to continue to remove trace quantities of materials with strong adsorption potential, such as PCB's. It may also suggest that removal of PCB's in adsorption columns is accomplished in large measure by filtration rather than adsorption. Further investigations are required to elucidate and more rigorously explain these observations.

After 47 days of adsorption operation a 5-mg/l humic acid solution was introduced to the column which originally contained virgin carbon. Influent and effluent data for this phase of the experiment are also depicted in Figure 124. An increase in A-1254 concentration on the effluent upon addition of humic acid to the influent may be noted, indicating that humate-PCB complexes might be leaching out of the column. Further study is required to determine whether the observed release of PCB's is due to: 1) humate-PCB complexes formed in the feed solution which eventually pass through the column unadsorbed, 2) humate-PCB complexes formed within the column; or, 3) some combination of these effects.

SUMMARY AND CONCLUSIONS

1. The adsorption methodologies described for PCB's can be applied to compounds which demonstrate comparable physical and chemical characteristics; specifically, extremely low-solubility chlorinated hydrocarbons.

2. The results of adsorption-desorption equilibrium studies suggest that adsorption of PCB is at least partially irreversible. It was further demonstrated that no PCB was released from carbon adsorber columns in the course of dynamic desorption studies. These observations suggest that adsorption of PCB's on carbon may be predominantly "chemisorption."

3. The results of equilibrium adsorption sutdies for two commerical PCB mixtures demonstrated that carbon has higher affinity for A-1016 than A-1254. The diversity of adsorption characteristics among the isomers comprising these mixtures, does not permit explicit interpretation.

4. The effectiveness of activated carbon for removal of PCB's from water may be highlighted by fixed bed adsorber mini-column studies conducted for A-1016. It was demonstrated that with a load of 40 μg/l of A-1016, an EBCT = 0.52 min, and a hydraulic loading of 6.25 gal/ft^2/min, the column was able to reduce the concentration below the detection limit (<0.05 μg/l) for an extended (≈8 months).

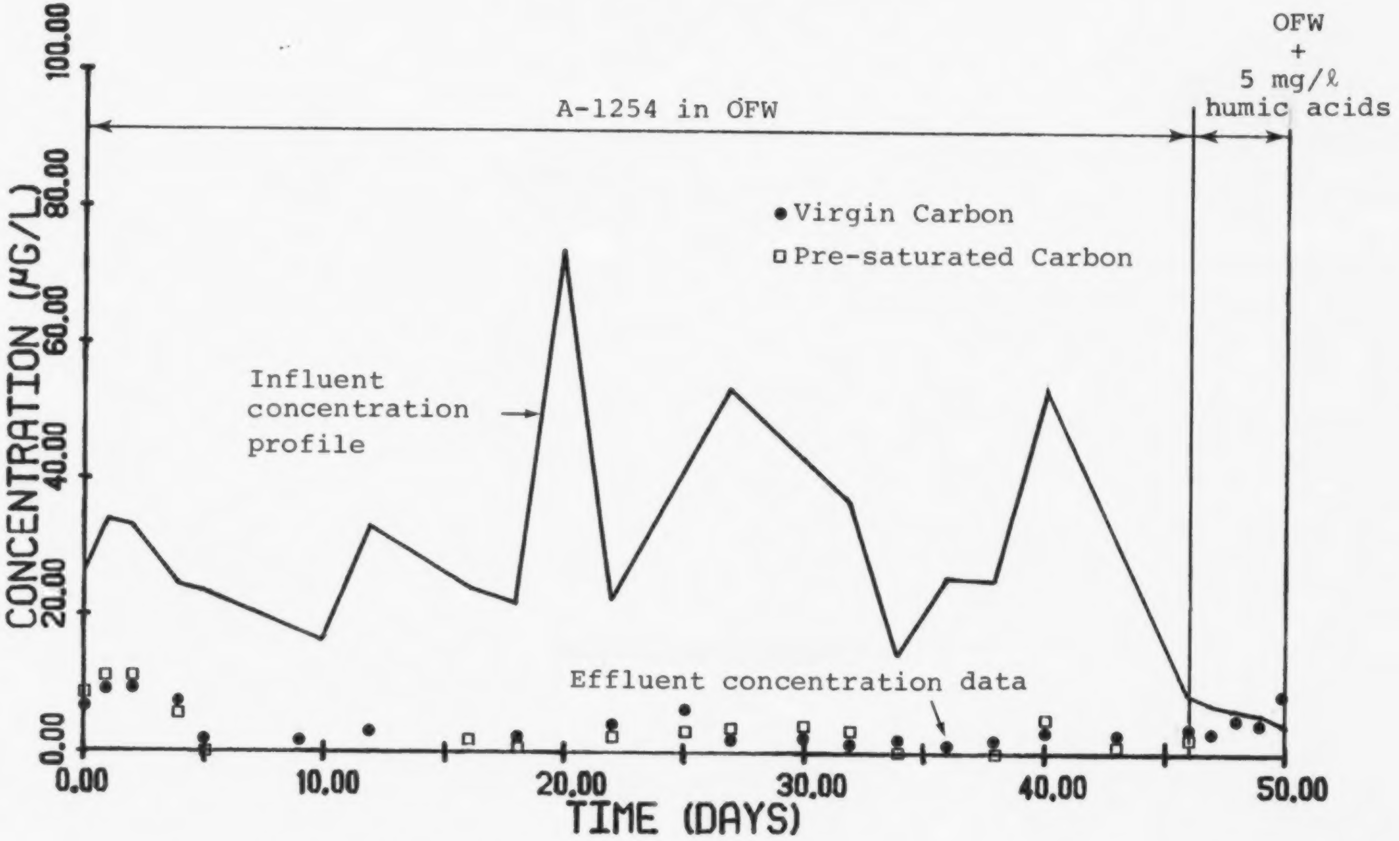

Figure 124. Influent and effluent concentration data for A-1254 in fixed-bed adsorbers (flow = 10 mℓ/min , 1 gram of 50/60 US sieve size carbon).

period of time.

5. Because of their hydrophobic character, PCB's associate with suspended materials. A well-designed sand filter may effectively remove particles in the size range of 0.5 to 20 µm, along with associated trace pollutants (Kavanaugh *et al*, 1978). It has been demonstrated, however, that sorption reactions of PCB's on natural suspended solids, including inorganic clays and silts, phytoplankton, and bacterial flocs, is substantially reversible (Weber *et al*, 1979). The possibility of leaching and release of sorbed PCB's from such particles retained in sand filters is thus significant. Activated carbon would thus seem to provide a much more effective filtration/ adsorption media for removal of such compounds in water treatment operations.

6. The effectiveness of activated carbon for removal of PCB's from water is adversely affected by their association with certain background organic substances such as humic acids. Development of methods for more effective removal of humic acids by carbon, as suggested in an earlier section of this report, might also provide for more effective removal of associated organic molecules -- such as PCB's -- in water treatment operations.

   It seems likely that introduction of certain inorganic species such as Mg^{2+}, Ca^{2+}, etc. (see Section 6) might lead to the formation of ion-humate-PCB-carbon complexes which would eventually be removed more effectively.

7. The single-solute version of the MADAM model was not able to satisfactorily simulate and predict CMB adsorption rates for PCB's. This is not unexpected because the PCB's (A-1016 and A-1254) are comprised of several isomers with different adsorption characteristics. Although the multi-solute version of the model might have been more successful, there was insufficient data regarding the adsorption characteristics of the individual isomers to permit its use. Because it was not possible to obtain experimental breakthrough profiles for the PCB's (no breakthrough occurred in approximately 8 months of operation), no attempt was made to quantitatively predict the dynamic performance of the adsorber beds.

BEGIN FIRST LINE OF TEXT HERE
TYPING GUIDE SHEET
CENTER OF PAGE
TOP OF IMAGE AREA
DROPPED HEAD. BEGIN SECTIONS HERE

SECTION 10

ADSORPTION OF DIELDRIN

GENERAL

Dieldrin, $C_{12}H_{10}OCl_6$, is the generic name for insecticide products containing not less than 85% of 1, 2, 3, 4, 10, 10-hexachloro - 6, 7, - epoxy- 1, 4, 4a, 5, 6, 7, 8, 8a - octahydro - 1, 4-endo, exo-5, 8-dimethanonaphthalene (HEOD) and not less than 15% active related compounds (The Condensed Chemical Dictionary, 1971). Dieldrin derives from a series of reactions, beginning with that between cyclopentadiene and acetylene to produce bicyclo (2, 2, 1) hepta- 2, 5-diene. The latter is then subjected to a Diels-Alder reaction with hexachlorocyclopentadiene to produce the compound aldrin, which upon epoxidation yields dieldrin (O'Brien, 1967; and, Brooks, 1977). Reactions which convert aldrin to its epoxide dieldrin occur under atmospheric conditions; light does not seem to be essential for this transformation. Photochemical reactions of dieldrin in the natural environment produce significant changes in which the chlorinated double bond breaks and a single bond is formed with the loss of a hydrogen atom giving photodieldrin, an isomer found to be more toxic than dieldrin (Crosby, 1969). The physical and chemical properties of dieldrin are summarized in Table 25.

The production of dieldrin in the United States was 1.5 million pounds in 1966, and 0.6 million pounds in 1970 (von Rumker et al, 1975). When its use was banned by the USEPA in 1977, production presumably dropped to zero, but the persistence of this insecticide renders it still of environmental concern.

Dieldrin is extremely hydrophobic, and tends to concentrate on suspended soils, sediments and other particulates in the aquatic environment. The degree of association and extent of distribution between sorbed and aqueous phase concentrations depends on a number of factors, but most investigators agree that organic matter associated with the particulates is significant (Eye, 1968; and, Huang and Liao, 1970). Dieldrin is highly toxic and extremely resistant to biological degradation (Jager, 1970; and, Eichelberger and Lichtenberg, 1971). Hence, contamination of a water resource by dieldrin poses a serious long-term threat to water quality.

BOTTOM OF IMAGE AREA OUTSIDE DIMENSION FOR TABLES AND ILLUSTRATIONS
BEGIN LAST LINE OF TEXT
3/8"

PAGE NUMBER
EPA-287 (Cin.)
(4-76)

TABLE 25. PHYSICAL AND CHEMICAL PROPERTIES OF TECHNICAL DIELDRIN*

Chemical Structure	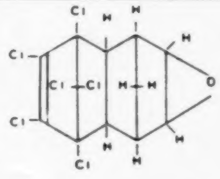
Spatial Configuration	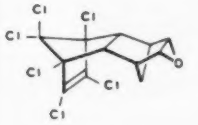
Molecule Weight	331
Physical State at 20°C	Solid, dry flakes
Color	Light tan
Specific Gravity, 20°C	1.7
Chlorine Content, % by wt.	55 - 56
Water Content, % by wt.	< 0.1
Melting Point, (°C)	175
Vapor Pressure (25°C, mm Hg)	1.8×10^{-7}
Solubility (% by wt):	
Ethyl Alcohol	5
Acetone	25
Benzene	39

*SOURCES: Condensed Chemical Dictionary, 1971; CRC Handbook of Chemistry and Physics, 1976-1977; and, Kirk-Othmer, Encyclopedia of Chemical Technology, 1964)

TYPING GUIDE SHEET
BEGIN FIRST LINE OF TEXT HERE
CENTER OF PAGE
TOP OF IMAGE AREA
DROPPED HEAD: BEGIN SECTIONS HERE
6-1/2''
9-1/8''
BEGIN LAST LINE OF TEXT
BOTTOM OF IMAGE AREA; OUTSIDE DIMENSION FOR TABLES AND ILLUSTRATIONS
3/8''
PAGE NUMBER
EPA-287 (Cin.)
(4-76)

BEGIN FIRST LINE OF TEXT HERE
TYPING GUIDE SHEET
CENTER OF PAGE
TOP OF IMAGE AREA
DROPPED HEAD; BEGIN SECTIONS HERE

Dieldrin exhibits resistance to removal by conventional water treatment techniques. Robeck et al (1965), in an investigation of the removal of selected chlorinated hydrocarbon pesticides in a pilot water treatment plant, demonstrated that lime and soda ash softening did not improve on the removal of dieldrin obtained by alum coagulation alone, which provided 55% removal. Chlorine, potassium permanganate, and ozone were found to have little oxidizing effect on dieldrin. The authors did demonstrate that activated carbon was efficient in removal of dieldrin in the system under study.

Sources and Sinks in the Environment

Dieldrin has been shown in numerous studies to be present in the environment. The half-life of dieldrin, through retention in soils, is eight to ten years (Weber, 1972). Inputs to the environment have included effluents from production facilities, aircraft spraying, careless handling during manufacture or application, accidental leakage from drums, agricultural and forest runoff, evaporation, leaching through soil, and fall-out with rainwater (Schafer et al, 1969; and, Jager, 1970). The prinicpal mode of current introduction to the aquatic environment may occur when dieldrin-containing particles are carried with runoff into streams during heavy rainfall. Runoff provides a fairly steady concentrated source, as evidenced by recorded dramatic increases in dieldrin and resulting fish kills in receiving waters after heavy rains. Increased levels may also be accounted for by elevated sediment loads (Westlake and Gunther, 1966).

Food chain concentration and bioaccumulation of dieldrin to toxic levels is known to occur (USEPA, 1972). It has been reported that trout exposed to dieldrin in water at a level of 0.0023 ppm for 17-23 days contained levels of 7.7 ppm, representing a 3,300 fold magnification in concentration (Dustman and Stickel, 1969). Dieldrin has also been detected in food consumed by humans. Of 8,775 different samples of milk, raw agricultural products, and fish, 14% were found to contain dieldrin in amounts ranging from 0.11-0.5 ppm; lower concentrations in the range 0.04 - 0.1 ppm were found in an additional 19.3% of the samples (Duggan, 1969).

The occurrence of dieldrin in water throughout the United States, from Ohio rainwater to California estuary waters, has been reported by a number of investigators. For example, in 1972 the average concentration in surface waters was reported to be 407 ng/l (Crosby, 1972). In a survey conducted by USEPA to test for chlorinated hydrocarbon insecticides in drinking water, dieldrin was found in 54 of 196 samples at concentrations in the range 1-10 μg/l (USEPA, Report to Congress, 1975). Further, of 500 grab samples of 10 municipal drinking waters obtained from the Mississippi and Missouri rivers,

BEGIN LAST LINE OF TEXT
BOTTOM OF IMAGE AREA; OUTSIDE DIMENSION FOR TABLES AND ILLUSTRATIONS
3/8"

PAGE NUMBER
EPA-287 (Cin.)
(4-76)

TYPING GUIDE SHEET

approximately 40% contained "detectable" amounts of dieldrin (Schafer et al, 1969). Dieldrin has also been found in 29 different water supplies throughout the world (Shackelford and Keith, 1976).

Public Health Assessment

Experiments on laboratory animals with dieldrin have shown immediate intestinal absorption following oral administration. Dieldrin is initially distributed widely in the body, but redistribution takes place rapidly into fat (Jager, 1970). The N.I.O.S.H. carcinogens list states that dieldrin has been found to invoke a carcinogenic and/or neoplastic response in lab animals (USEPA, March 1976). Biochemical brain changes have also been observed following dieldrin poisoning. The exact mode of action of dieldrin on the central nervous system is, however, still not fully understood. It appears that dieldrin inhibits glutamine synthesis in the brain (O'Brien, 1967; and, Jager, 1970). The effects of dieldrin on the mammalian system as demonstrated on rats, include growth reductions due to fatty acids deficiencies (Tinsley and Lowry, 1969). Rats metabolize dieldrin into several products which are excreted (Fukuto and Metcalf, 1969).

Several interesting facts concerning residues in humans have been reported by Durham (1969). In the United States population, the average storage level of dieldrin in fat tissue rose from 0.15 ppm in 1961 to 0.31 ppm in 1964. Blood dieldrin levels of 0.0014 to 0.0019 ppm were reported during 1965 with lower levels noted in females. Zavon et al (1969) found concentrations as high as 0.442 ppm dieldrin in newborn babies. Pharmacodynamic studies with human volunteers have shown a definite relationship between level of intake and storage in blood and adipose tissue (Jager, 1970).

Regulations concerning dieldrin in drinking water have not as yet been promulgated (USEPA, Quality Criteria for Water, 1976), although dieldrin is mentioned in the EPA priority pollutant list.

Water Solubility

Aqueous solubility values reported for dieldrin range from less than 100 μg/l to 180 μg/l (e.g., Kirk-Othmer, Encyclopedia of Chemical Technology, 1964; Robeck et al, 1965; and, Eye, 1968). To establish a value for use in the present research, 1 gram of dieldrin (Technical Grade, 99.5%; Shell Chemical Co.) was added to a 1-l volumetric flask containing OFW. The solution was agitated for several hours using a Teflon-coated mangetic stirrer. Aliquots of aqueous sample were withdrawn periodically and filtered through a

EPA-287 (Cin.) (4-76)

0.45 μm membrane filter and analyzed for dieldrin. A saturation point of ≃ 190 μg/l was estimated and subsequently used for the research reported herein.

ANALYTICAL PROCEDURE

Sample Collection and Concentration

Determination of residual concentrations of dieldrin in aqueous phase was accomplished by a one-step extraction technique followed by gas chromatographic analyses. Depending on the quantity of dieldrin in the sample, different sample sizes were assayed in the manners described below.

Vial Extraction Procedure--
For concentrations larger than 1 μg/l, 10-ml of sample was transferred to a 4-dram vial containing 1-ml of hexane (Baker Resi-Analyzed). The extraction procedure was similar to that described for PCB's in Section 9. The extraction efficiency for this method was estimated to be 99%.

One-Step Separatory Funnel Procedure--
For concentrations less than 1 μg/l, 250-ml of the sample together with 25-ml of hexane (10:1) were transferred to narrow-mouth, ground-glass-stoppered bottle. The bottles were closed tightly and shaken for one hour on a mechanical shaking unit to achieve complete extraction. The emulsion that occasionally formed was allowed to separate overnight. A separatory funnel was used to separate the hexane extract from the water layer. The extract was then transferred to a dry, conical, 50-ml glass stoppered centrifuge tube along with the hexane rinses of the sample bottle and the separatory funnel, and held at 4°C until assayed. Any remaining water droplets were removed with the use of a pipet. The hexane extracts were subsequently concentrated by placing the centrifuge tubes in an N-EVAP analytical evaporator (Organomation; Shrewsburg, Mass). The concentration step was carried out by heating the extracts in a 55°C water bath under a gentle flow of pre-purified nitrogen. The samples were concentrated to approximately 5-ml, transferred to a 10-ml conical centrifuge tube, and further concentrated to 1-ml. 2-8 μl volumes of the final concentrates were subjected to GC analysis. An extraction efficiency of 80% was achieved for this method.

Analysis

Electron capture gas chromatographic analysis was performed using: 1) a 2700 Varian GC equipped with a Sc^3H ECD, and a 150 cm x 2 mm ID glass column packed with 3% SE-30 on Gas Chrom Q; and, 2) a 1700 Varian GC equipped with a ^{63}Ni ECD, and a 6 ft. x 2 mm ID glass column packed with 3% OV-1 on

TYPING GUIDE SHEET

100/200 Varaport 30. Temperatures for the former GC unit were: injector 230°C, column 185°C, and detector 250°C; and for the latter: injector 225°C, column 200°C, and detector 240°C. Pre-purified nitrogen was used as a carrier gas at a flow rate of 40 ml/min. The detector response traced by a chart recorder and peak heights were used as a measure of concentration. A calibration curve was constructed by plotting peak height versus concentration in nanograms. The method for preparation of the standard curve is discussed in Appendix N.

The overall performance of the ^{63}Ni ECD for the analysis of dieldrin was more satisfactory than that of the Sc^{3}H ECD; its utilization for this research depended on the availability of the instrument.

ADSORPTION METHODOLOGY

To satisfactorily characterize the adsorption behavior of dieldrin, a number of factors which might influence quantification of adsorption parameters must be recognized and appropriately treated; these have been discussed in Section 9 with respect to PCB's.

Equilibrium Studies

Equilibrium studies for dieldrin were conducted using precisely weighed amounts of carbon together with 950 ml of OFW or 5 mg/l humic acid background solution in 1-l glass reactors. To inibit bacterial growth, the reactors and solutions were autoclaved prior to addition of carbon. The glass bottles were carefully sealed using screw-on caps with Teflon liners and placed in a specially-designed rotary tumbler until equilibrium was achieved. The equilibriation time was from 48 hours for powdered carbon to three weeks for 50/60 granular carbon. 10-ml samples were transferred to 4-dram vials and subjected to vial-extraction and GC analysis.

Rate Studies

CMB-reactor rate studies for dieldrin were performed in a manner similar to that described for PCB's in Section 9. To investigate the extent of glass sorption and volatilization, studies were conducted in closed and open reactors without carbon. The results presented in Figure 125 indicate that glass sorption was negligible but significant dieldrin was volatilized in the open reactor.

As for the PCB studies, weighed and pre-wetted quantities of carbon were added to experimental solutions (OFW or 5 mg/l humic acid background solution; pH 7), 10-ml samples were withdrawn periodically, extracted and subjected to GC analysis.

EPA-287 (Cin.)
(4-78)

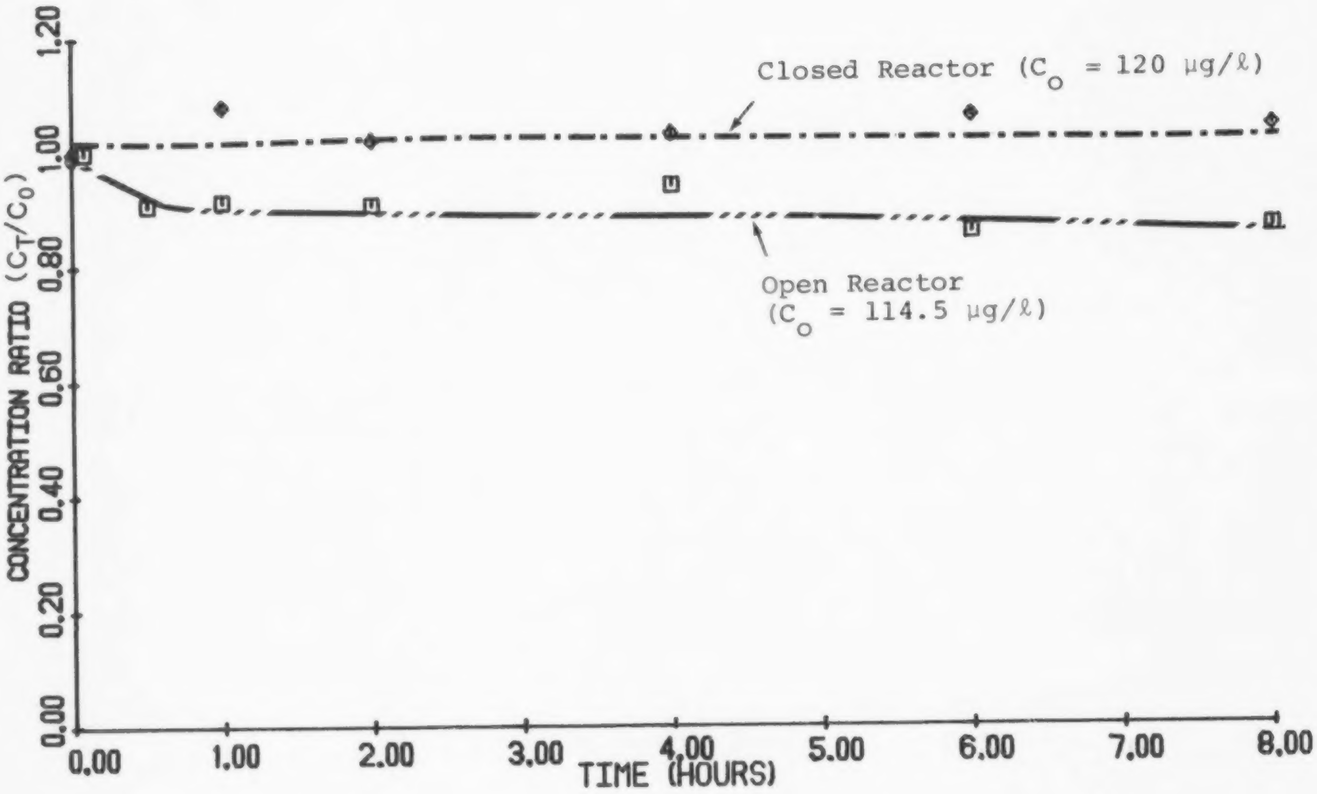

Figure 125. Rate of loss of dieldrin to the Pyrex glass reactor used for CMB rate experiments.

Column Studies

To investigate the dynamic adsorption behavior of dieldrin, fixed-bed adsorber studies were designed and executed as described below.

Large Fixed-Bed Adsorbers--

These studies were performed in 6-ft glass columns having an internal diameter of 30 mm. The feed solution was prepared by dilution of a saturated aqueous dieldrin solution to desired concentration in 200-liter stainless steel tanks containing DDW buffered at pH7. All tubings and fittings were stainless steel. The adsorber was charged with 250-gram quantity of 16/20 US mesh size carbon. Dieldrin concentration in the feed solution was adjusted to 15 μg/l and the flow rate maintained at 40 ml/min. To detect the effluent in the parts per billion range, 250 ml samples were extracted and concentrated using the one-step sep-funnel procedure, described earlier in this section, and subjected to gas chromatographic analysis.

Figure 126 schematically illustrates the experimental apparatus.

Mini Fixed-Bed Adsorbers--

Mini-column studies for dieldrin were conducted in 1-cm ID glass adsorbers containing 5 grams of 50/60 carbon. The column was fed with dieldrin in OFW background solution. The experimental apparatus, arrangement, and procedure were similar to that described for PCB's. The feed solution was dosed with 2 mg/l of Ag^+ to inhibit biological growth.

RESULTS AND DISCUSSION

Adsorption Equilibria

As for other solutes discussed in previous sections, the Freundlich isotherm model was found to provide the best statistical fit to the experimental data for dieldrin.

Figures 127 and 128 present adsorption isotherms for dieldrin in OFW and 5 mg/l humic acid background solution, respectively. The corresponding isotherm parameters are listed in Table 26. It may be observed that less dieldrin is adsorbed in the presence of humic acids. The difference may be due to a preferential association of dieldrin and humic species in solution, resulting in less dieldrin uptake by the carbon. Robeck *et al* (1965) observed similar differences in uptake of dieldrin between distilled water and river water.

That chlorinated hydrocarbon pesticides such as dieldrin

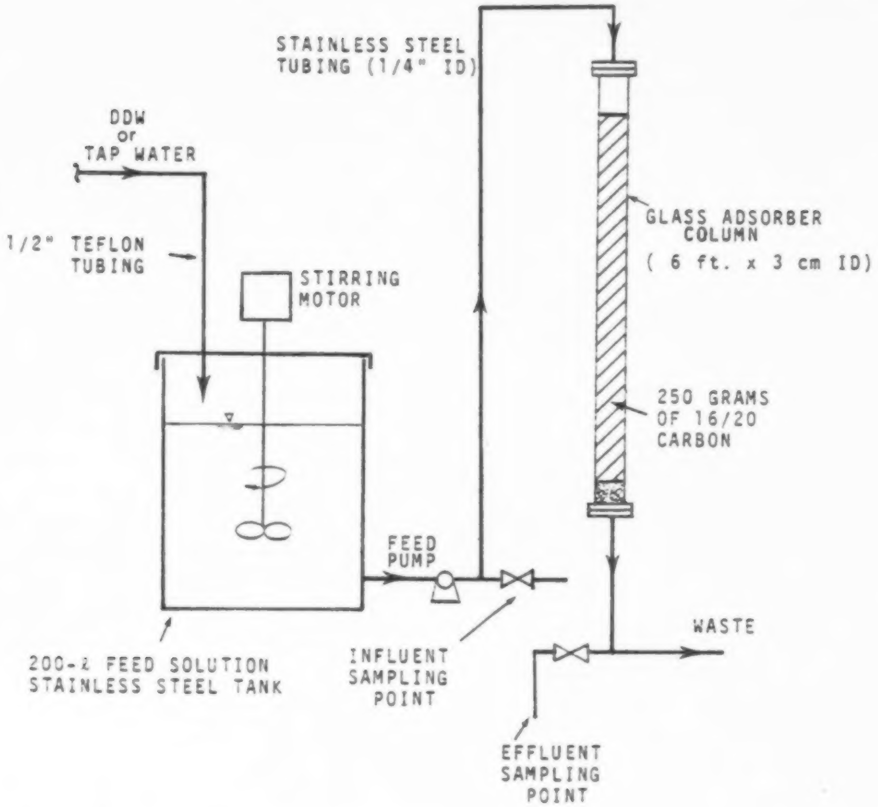
STAINLESS STEEL TUBING (1/4" ID)
DDW or TAP WATER
1/2" TEFLON TUBING
STIRRING MOTOR
GLASS ADSORBER COLUMN (6 ft. x 3 cm ID)
250 GRAMS OF 16/20 CARBON
FEED PUMP
200-ℓ FEED SOLUTION STAINLESS STEEL TANK
INFLUENT SAMPLING POINT
WASTE
EFFLUENT SAMPLING POINT

Figure 126. Experimental apparatus.

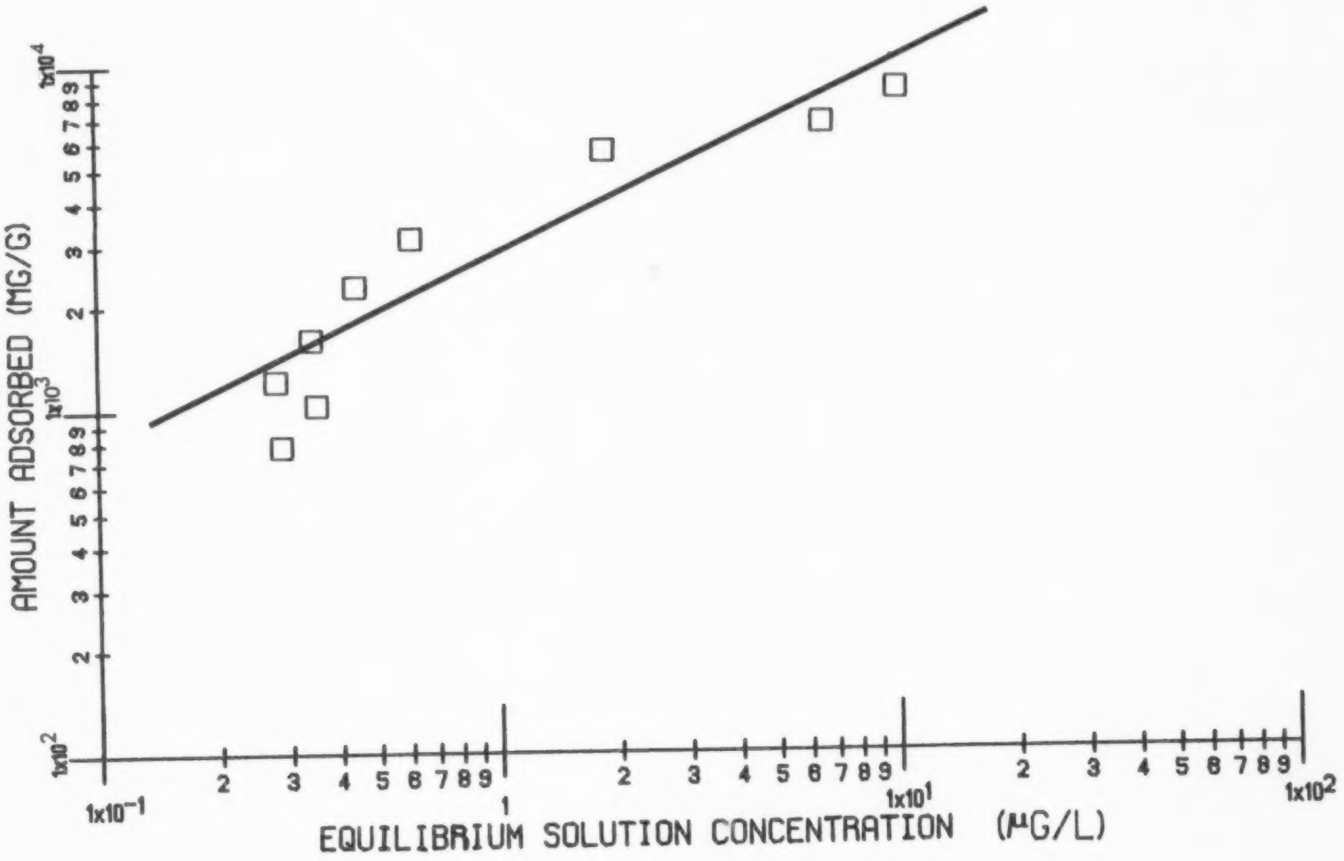

Figure 127. Adsorption isotherm for dieldrin in OFW (C_o = 50 μg/ℓ, 16/20 carbon).

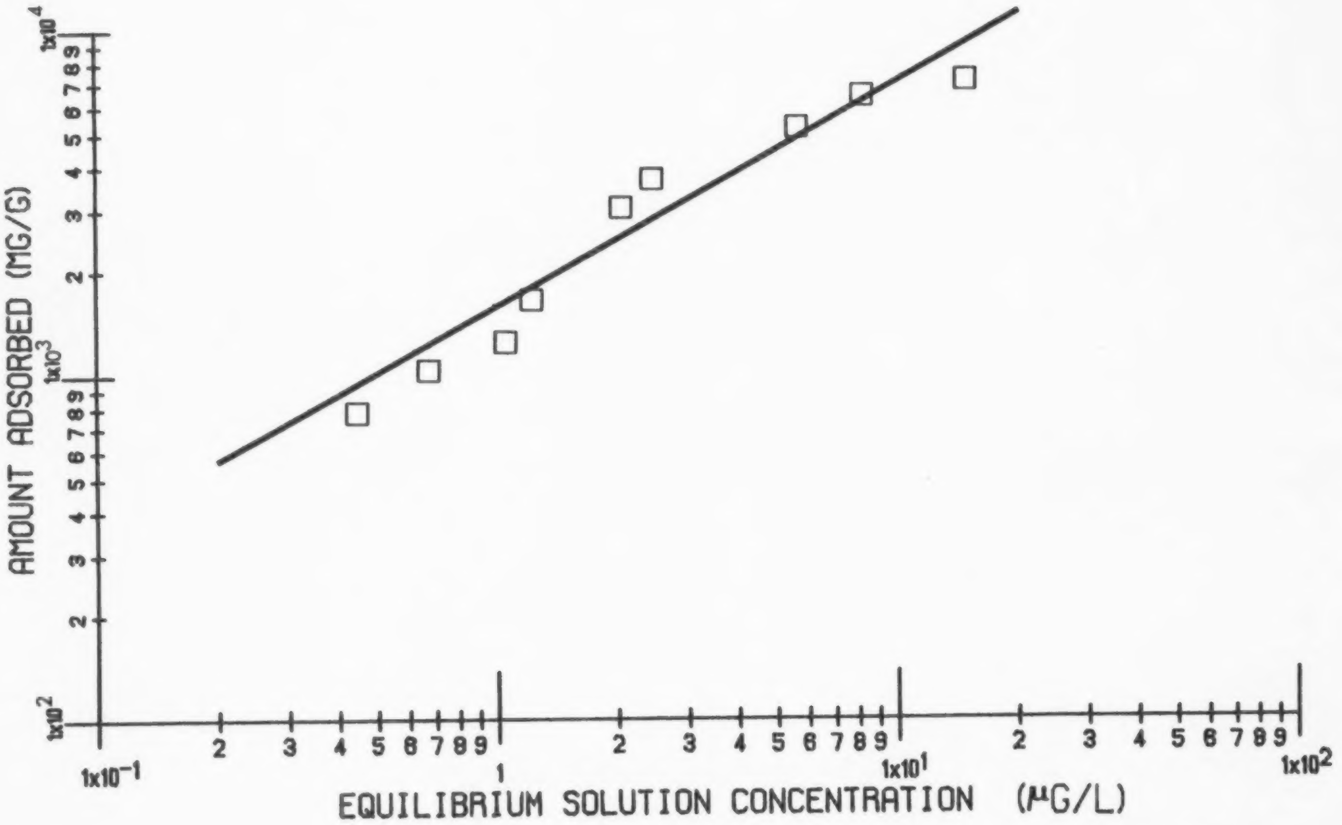

Figure 128. Adsorption isotherm for dieldrin in solution of humic acids (C_o = 50 µg/ℓ, 16/20 carbon).

TYPING GUIDE SHEET

TABLE 26. ADSORPTION EQUILIBRIUM PARAMETERS FOR DIELDRIN[†]

Background Solution	Carbon Size, US Mesh Size	C_o, µg/l	Freundlich Isotherm Constants*		
			K_f	1/n	r
OFW	16/20	50	2.74	0.56	0.917
OFW + 5 mg/l humic acids	16/20	50	1.46	0.68	0.977

† All studies were conducted at pH 7 unless otherwise noted.

* Based on C_e and q_e expressed in µg/l and mg/gm, respectively.

r = Correlation coefficient for fit of the isotherm to the experimental data.

BEGIN FIRST LINE OF TEXT HERE
DROPPED HEAD; BEGIN SECTIONS HERE
CENTER OF PAGE
TOP OF IMAGE AREA
BEGIN LAST LINE OF TEXT
BOTTOM OF IMAGE AREA, OUTSIDE DIMENSION FOR TABLES AND ILLUSTRATIONS
PAGE NUMBER
EPA-287 (Cin.)
(4-76)

associate themselves with the natural organic materials is well documented (for example: Wershal *et al*, 1969; Boucher and Lee, 1972; Khan and Schnitzer, 1972; Pierce *et al*, 1974; Chol and Chen, 1976). The extent of association, however, depends on the type and concentration of the natural organic materials. It is thus possible that in systems containing both humic substances and activated carbon, some competitive uptake of dieldrin between humate molecules and the carbon occurs.

As for PCB's, the adsorption of dieldrin on carbon in the presence of humic substances may be enhanced by development of methods which might provide for more efficient removal of humic acids (see Section 6).

Adsorption Rates

CMB reactor experiments were conducted to investigate the effect of carbon particle size on rates of adsorption of dieldrin. Figure 129 represents concentration decay curves for different particle sizes of carbon, indicating a strong dependency of rate of dieldrin adsorption on particle size. The general character of the variation of adsorption rate as a function of particle diameter is illustrated in Figure 130. To simplify preliminary assessment of the nature of the rate dependence on particle size, a simple second-order rate expression was used to develop the "overall rate coefficient" employed for this correlation. Mathematical expressions indicate that if rate varies approximately with the reciprocal of diameter of carbon particles, the limiting rate mechanism is likely to be external transport. As will be noted shortly, this appears to be the case for rate of mass transport of dieldrin in such systems.

A simulation-modeling analysis was conducted for adsorption of dieldrin from OFW to evaluate appropriate rate coefficients, k_f and D_s. The solid line given in Figure 131 is the model trace given by a coefficient set of $k_f = 1.75 \times 10^{-3}$ cm/sec and $D_s = 4.43 \times 10^{-9}$ cm^2/sec. Figure 132 illustrates the results of sensitivity analyses relative to k_f, indicating substantial sensitivity to this parameter. The results of similar sensitivity analysis for D_s indicated that the system is insensitive to changes in D_s. This agrees with the earlier observations that external mass transfer most likely controls rates of adsorption of dieldrin by activated carbon.

Simulation analyses were also performed for rate studies with dieldrin in 5 mg/l humic acid background solution. Figure 133 illustrates the model profile (solid line) predicated on estimated coefficient values of $k_f = 1.29 \times 10^{-3}$ cm/sec and $D_s = 1.33 \times 10^{-10}$ cm^2/sec. It may be noted that both the film

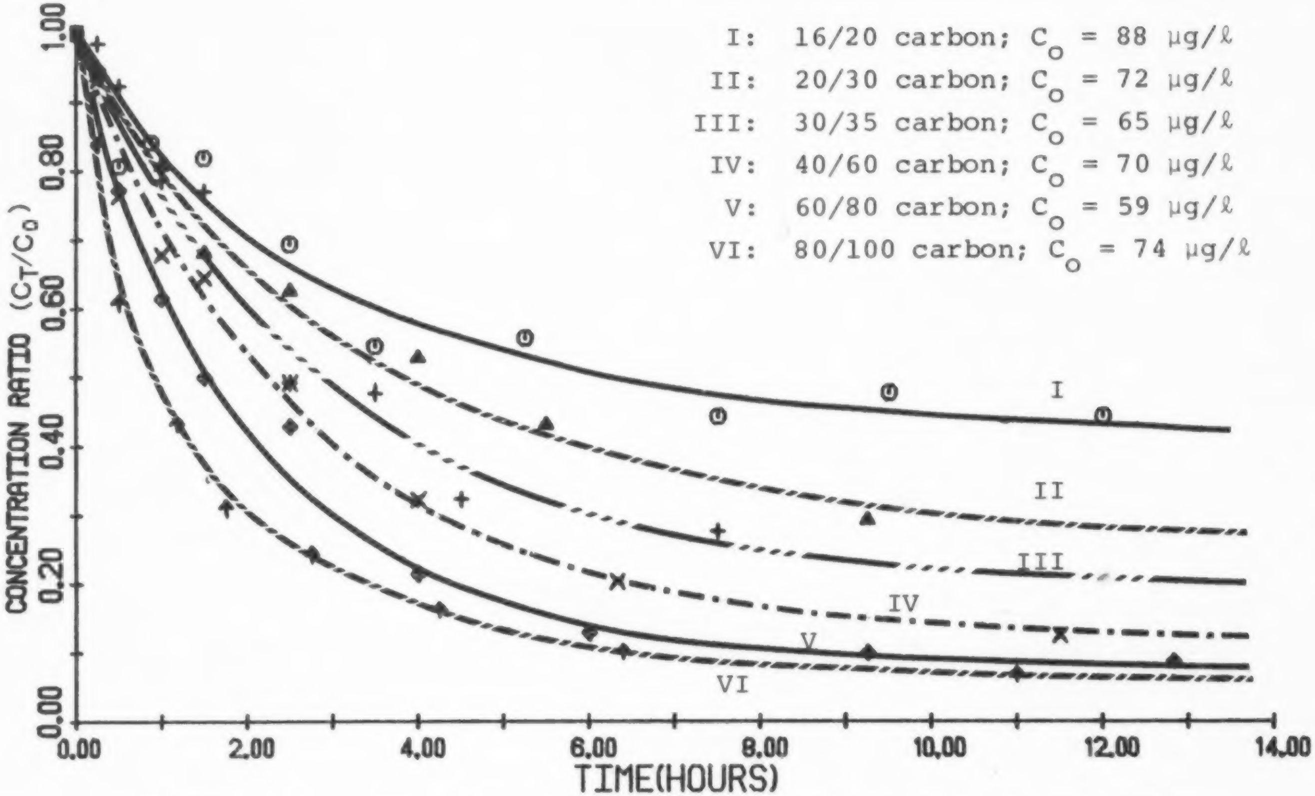

Figure 129. CMB rate studies for dieldrin - effects of carbon particle size (0.17 g/ℓ carbon).

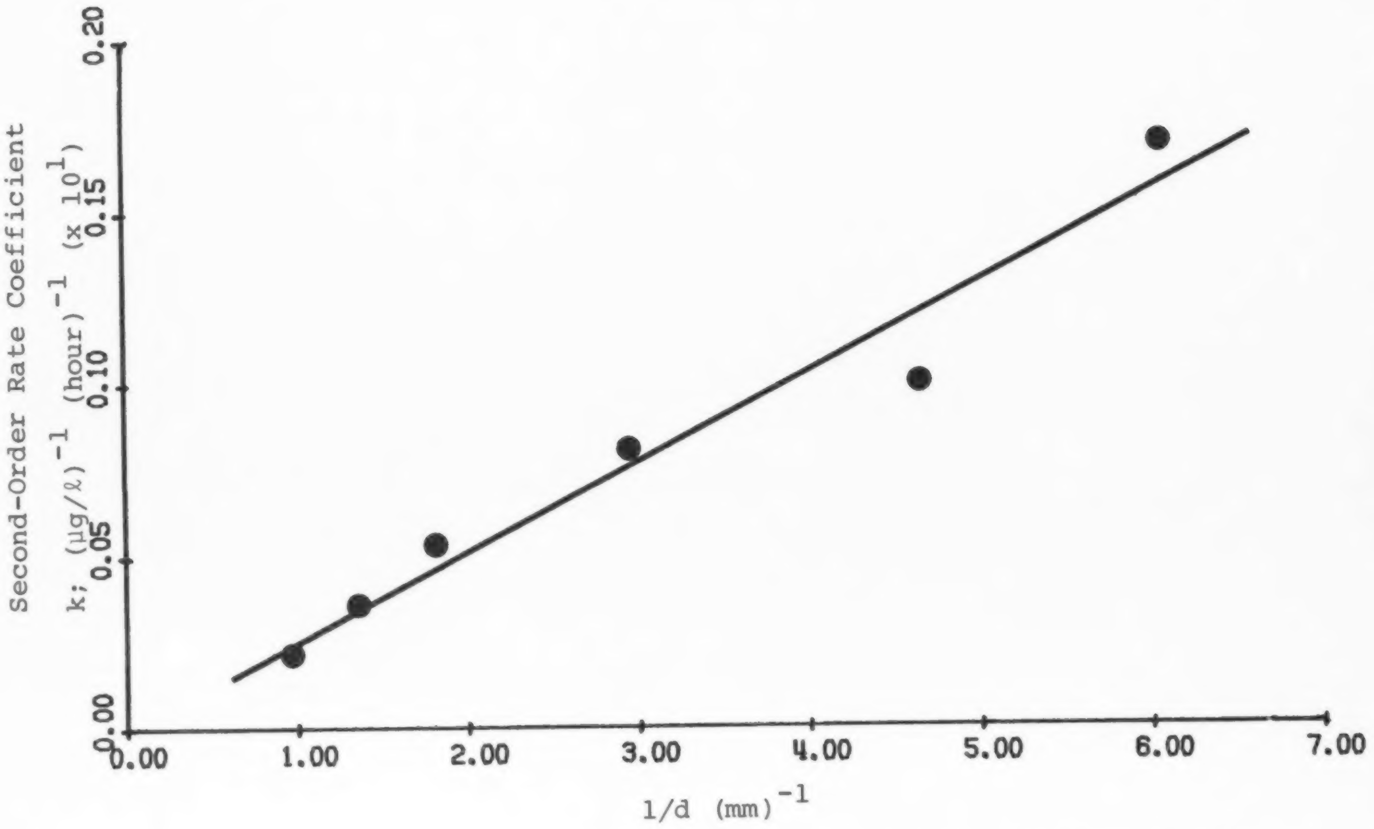

Figure 130. Variation of adsorption rate as a function of carbon particle diameter.

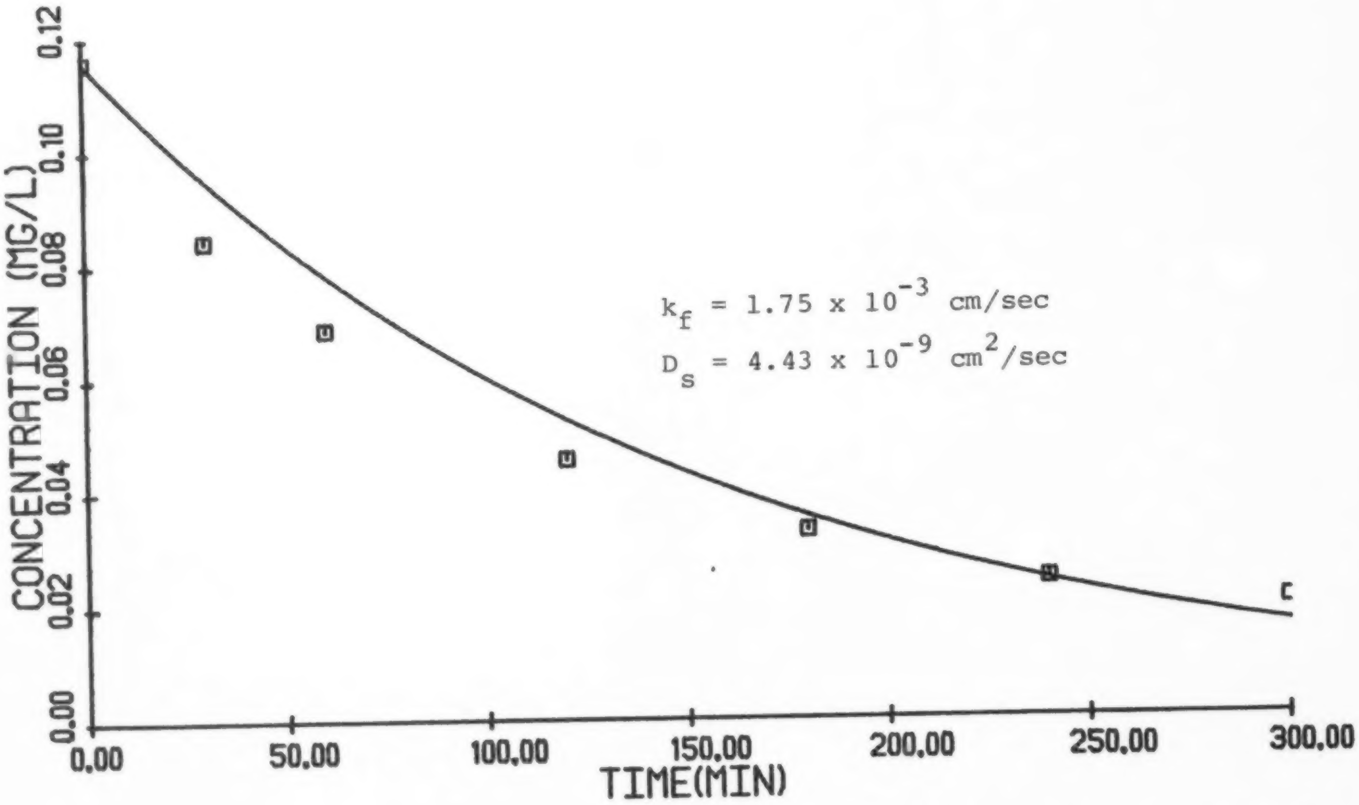

Figure 131. Experimental data and model profile for rate of adsorption of dieldrin from OFW in a CMB reactor (C_o = 115.8 μg/ℓ, 0.19 g/ℓ of 50/60 carbon).

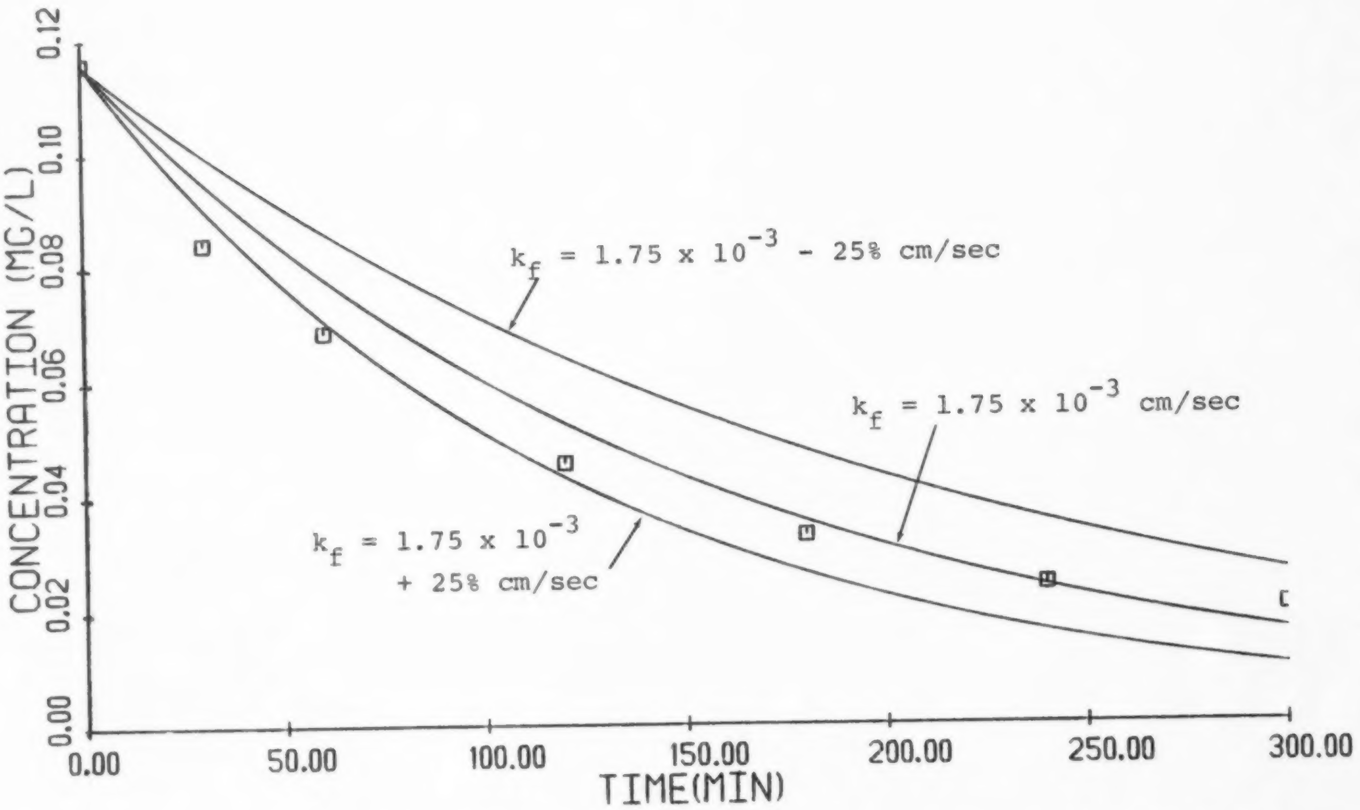

Figure 132. Analysis of the sensitivity of model profiles to the film transfer coefficient, k_f, for dieldrin.

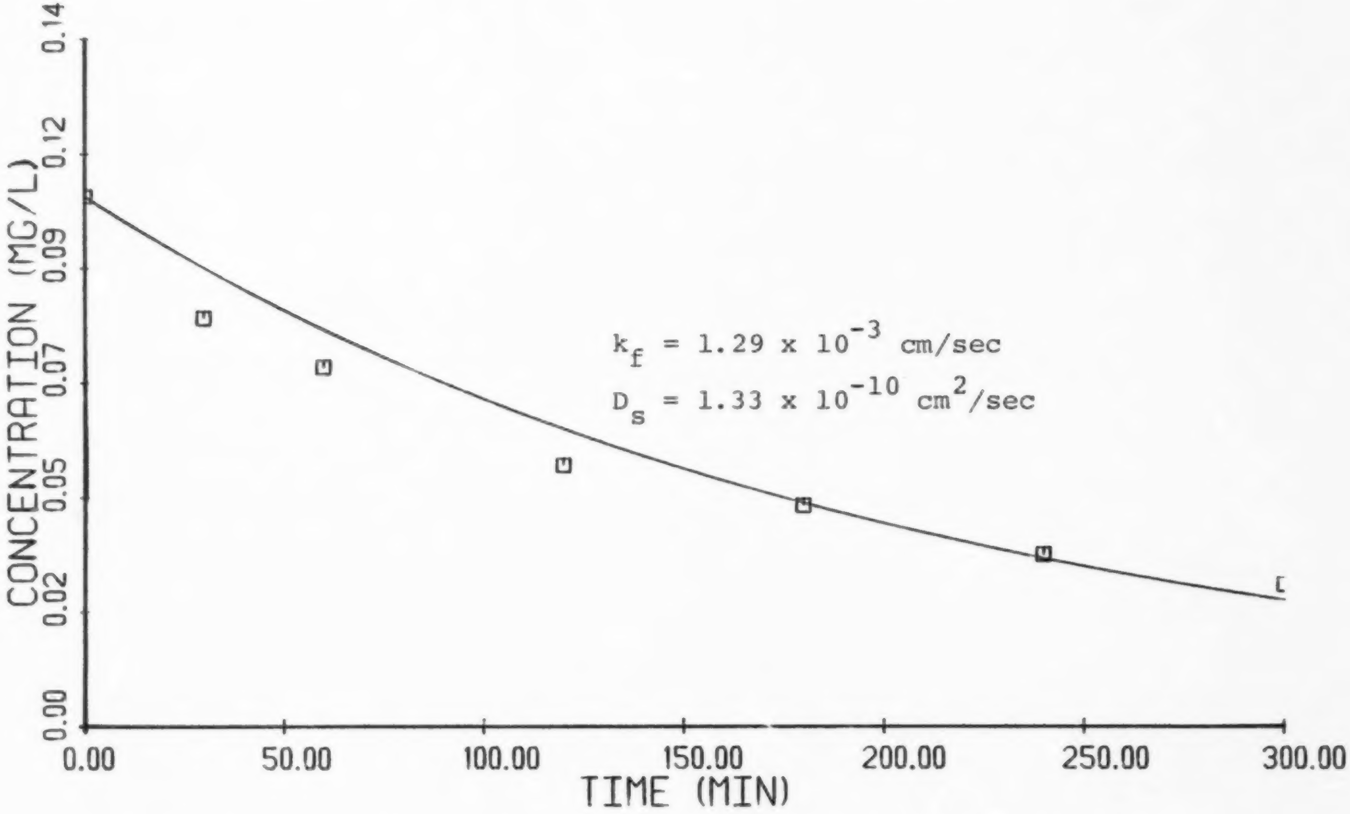

Figure 133. Experimental data and model profile for rate of adsorption of dieldrin from a solution of humic acids in a CMB reactor (C_o = 108 μg/ℓ, 0.19 g/ℓ of 50/60 carbon).

transfer coefficient and the intraparticle diffusion coefficient for the system containing humic acids are significantly lower than those for the OFW system. It thus appears that adsorption of dieldrin is retarded in the presence of humic acids. The retardation mechanism might be due to: 1) competitive adsorption of dieldrin and humic acids on the carbon surface, 2) association of dieldrin with humic acids in aqueous phase, and/or 3) a combination of these effects.

Table 27 summarizes experimental conditions and associated mass transfer coefficients for the systems illustrated in Figures 131 and 133.

Adsorption Columns

Fixed-bed adsorber experiments were designed and executed to evaluate the effectiveness of carbon for removal of dieldrin in a "close-to-real" situation. The feed solution was prepared by dilution of saturated aqueous solutions which were prepared by introducing 2 grams of dieldrin into a series of glass reactors, each containing 3-l of deionized-distilled water. The solutions were agitated for two days and then filtered through a 0.45 μm membrane filter to obtain saturated dieldrin solutions of ≈190 μg/l. The saturated solutions were subsequently diluted with DDW to approximately 15 μg/l and buffered with 1×10^{-3} $\underline{M}$ phosphate buffer.

After 2-3 weeks of operation, profuse biological growth within the columns became evident. The amount of growth depended on the room temperature. During a 3-4 day air-conditioning shut down, the room temperature reached 29°C resulting in accelerated growth. This resulted in substantial headlosses, which necessitated periodic air-scouring and backwashing. The backwashing released large amounts of biomass. Analyses showed significant amounts of dieldrin in the backwash water, probably due to release of dieldrin (desorption phenomena) by the bacteria, algae, and/or carbon.

To investigate the nature of the growth, random samples of the biofilm were taken from the column, Gram stained and observed under a light microscope. The growth appeared to consist principially of two types of bacteria: large oval shaped Gram Positive bacteria and more numerous but smaller rod-shaped Gram Negative bacteria. Further experiments using scanning electron microscopy revealed abundant growth on the carbon particles.

In view of the bioresistant nature of dieldrin, it was then hypothesized that the phosphate buffer and the organic constituents of the dilution water (DDW, 1 mg/l TOC) might have caused the biogrowth. After 144 days from onset of the

TYPING GUIDE SHEET
BEGIN FIRST LINE OF TEXT HERE
CENTER OF PAGE
TOP OF IMAGE AREA
DROPPED HEAD; BEGIN SECTIONS HERE

operation, in order to suppress biological growth, tap water was used for dilution and the phosphate buffer was omitted while keeping the pH adjusted to 7. The presence of chlorine in the tap water and the absence of the nutrient PO_4^{3-} significantly diminished the rate of growth. Thus, tap water was used for the remainder of this column study.

Figure 134 depicts the influent and effluent concentration data for dieldrin, indicating that carbon column was able to reduce influent levels of dieldrin as great as 30 μg/l to effluent levels lower than the detection limit (≈0.01 μg/l). Based on the adsorption capacities measured in the isotherm studies, it would have taken nearly 10 years for the column to reach exhaustion.

Mini-column adsorber experiments for dieldrin were designed and run to obtain data relative to adsorption breakthrough characteristics for prediction/simulation modeling investigations. For these experiments, 5 grams of 50/60 carbon were used and the flow rate was maintained at 20 ml/min. The feed solution was dosed with 2 μg/l Ag^+ to suppress biological growth. Figure 135 depicts influent and effluent concentration profiles. No breakthrough was observed in 206 days of operation, a duration well beyond the isotherm capacity (calculated from the dieldrin isotherm). As for PCB's several plausible explanations may be advanced.

Biological growth was apparent in the column as early as 30 days from onset of operation. Scanning electron microscopy exhibited significant growth on carbon particles. Adsorption of dieldrin by bacteria and algae is thus one possible expalnation. Because of its hydrophobic characteristics, dieldrin can be adsorbed onto biological cell surfaces and gradually absorbed into the cells. Wheeler (1970) demonstrated that dieldrin penetrated algal cells (Chlorella) rapidly and a maximum per cell level was reached within 6 to 24 hrs after introduction of the insecticide. Further experiments by the author revealed the absence of metabolites.

Although extremely resistant to microbial biodegradation, dieldrin was degraded in a strongly anaerobic biological system (Hill and McCarty 1967). Matsumura *et al* (1967) isolated a few bacteria that were capable of degrading dieldrin. In the present context, biodegradation may yield different metabolities which may elude detection because: 1) they contain no chlorine; 2) they are not extractable by hexane; and/or, 3) they are strongly adsorbed by carbon.

Desorption Experiments

Dynamic desorption studies were conducted for dieldrin in the large and mini fixed-bed adsorbers described earlier.

BEGIN LAST LINE OF TEXT
BOTTOM OF IMAGE AREA OUTSIDE DIMENSION FOR TABLES AND ILLUSTRATIONS
3/8"

PAGE NUMBER
EPA-287 (Cin.)
(4-78)

TYPING GUIDE SHEET

TABLE 27. ESTIMATED ADSORPTION RATE MASS COEFFICIENTS FOR DIELDRIN

Background Solution	C_o, µg/l	Carbon Dosage, g/l	k_f, cm/sec	D_s, cm^2/sec
OFW	115.8	0.19	1.75×10^{-3}	4.43×10^{-9}
OFW + 5 mg/l humic acids	108	0.19	1.29×10^{-3}	1.33×10^{-10}

k_f = film transfer coefficient; and,

D_s = surface diffusion coefficient

EPA-287 (Cin.)
(4-76)

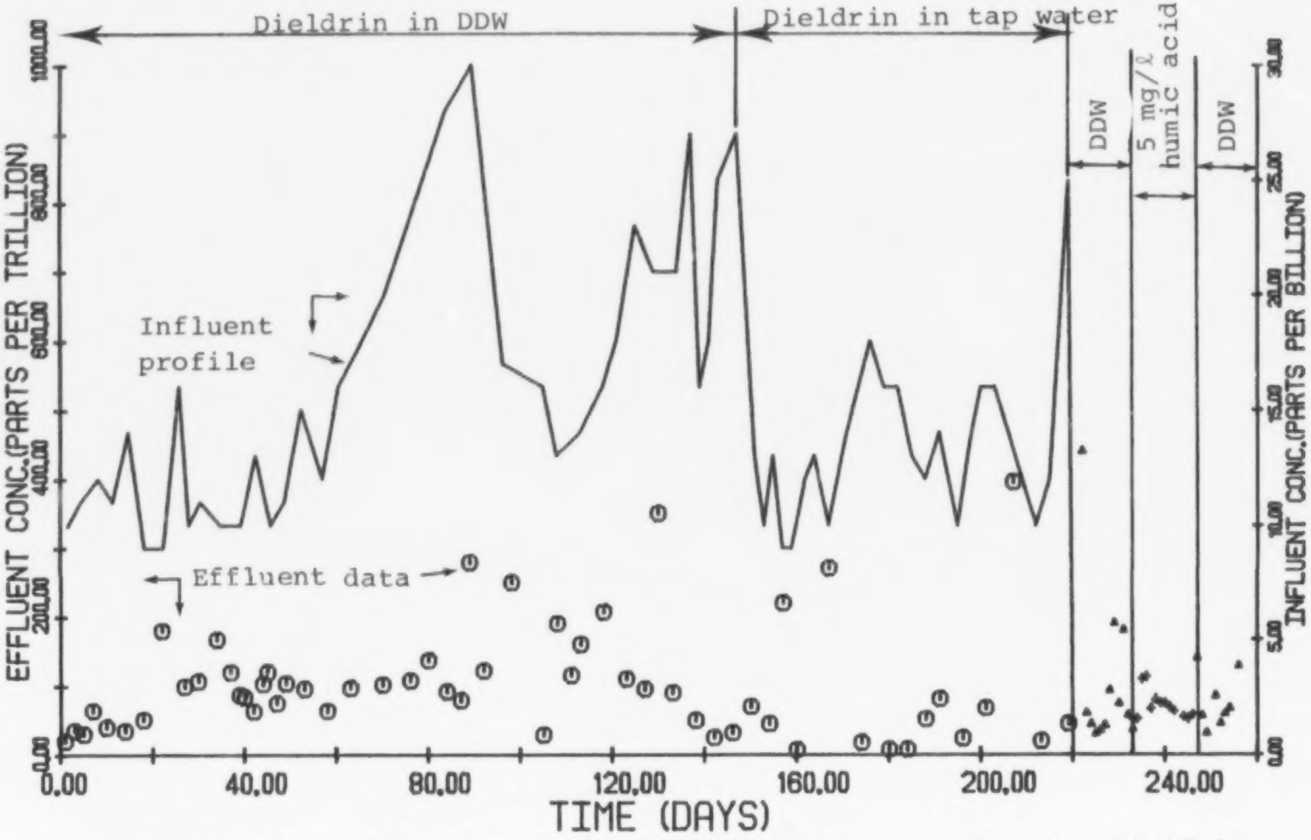

Figure 134. Influent and effluent concentration data for dieldrin in large fixed-bed adsorbers (flow = 40 mℓ/min, 250 grams of 16/20 carbon, EBCT = 15 min).

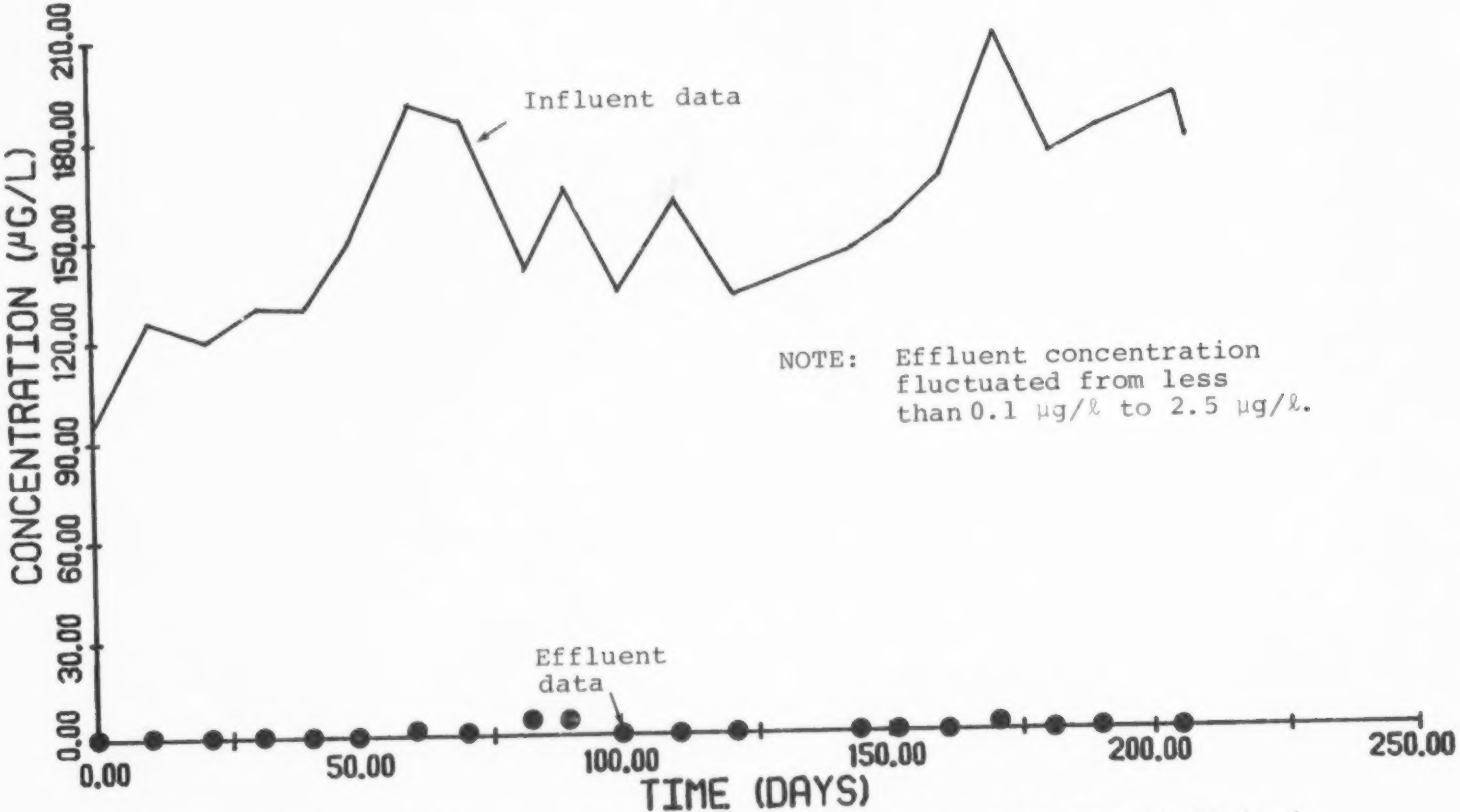

NOTE: Effluent concentration fluctuated from less than 0.1 µg/ℓ to 2.5 µg/ℓ.

Figure 135. Influent and effluent concentration data for dieldrin in mini fixed-bed adsorbers (flow = 20 mℓ/min, 5 grams of 50/60 carbon, EBCT = 0.52 min).

After 220 days from onset of operation the entire feeding system to the large column, with the exception of the carbon column, was vigorously cleaned to eliminate any sorbed dieldrin. The column was then fed with DDW alone. The results, illustrated in Figure 134 indicate that dieldrin was eluted or desorbed from the column. Experiments with the mini-column fed with OFW demonstrated similar results as depicted in Figure 136.

Competitive Adsorption

Mini fixed-bed adsorber experiments with dieldrin in 5 mg/l humic acid solution were performed in a manner similar to that described for dieldrin in OFW to investigate the dynamic behavior of dieldrin in the presence of humic acids. Because of extensive biological growth and resulting headloss, however, the operation had to be discontinued.

It was then decided to conduct mini expanded-bed experiments to alleviate the headloss problem. In these experiments two separate systems, each consisting of a 1-cm (ID) glass column containing 2-grams of 50/60 carbon, were used and the flow was maintained at 15 ml/min. The first column was fed with dieldrin in OFW and the second column with dieldrin in 2.5 mg/l humic acid solution. Efforts were made to maintain a constant dieldrin concentration feed to the columns to eliminate the concentration-history effect on the effluent profiles. Figure 137 depicts the influent and effluent concentration profiles for the two systems, indicating that competitive effects may be operative.

Further experiments were conducted with the large and mini fixed-bed adsorber columns described earlier, to investigate displacement effects. For these experiments, 5 mg/l humic acid solutions were passed through the columns. The results, presented in Figures 134 and 136 indicate some displacement in the case of the mini-column (Figure 136). Displacement in the larger column does not appear to be significantly different from the desorption caused by DDW alone.

Mini-adsorber column studies with virgin and pre-saturated carbon were conducted in two 1-cm (ID) glass columns, one containing 1-gram of 50/60 virgin carbon, and the other 1-gram of carbon saturated with humic acids. The columns were fed with solutions of dieldrin in OFW, dosed with 2 mg/l Ag^+ and maintained at a flow rate of 10 ml/min. The experimental apparatus and arrangements are illustrated schematically in Figure 138. The effluent concentration data depicted in Figure 139 indicate some reduction in the capacity of the presaturated carbon.

Based on the above observations, several possible

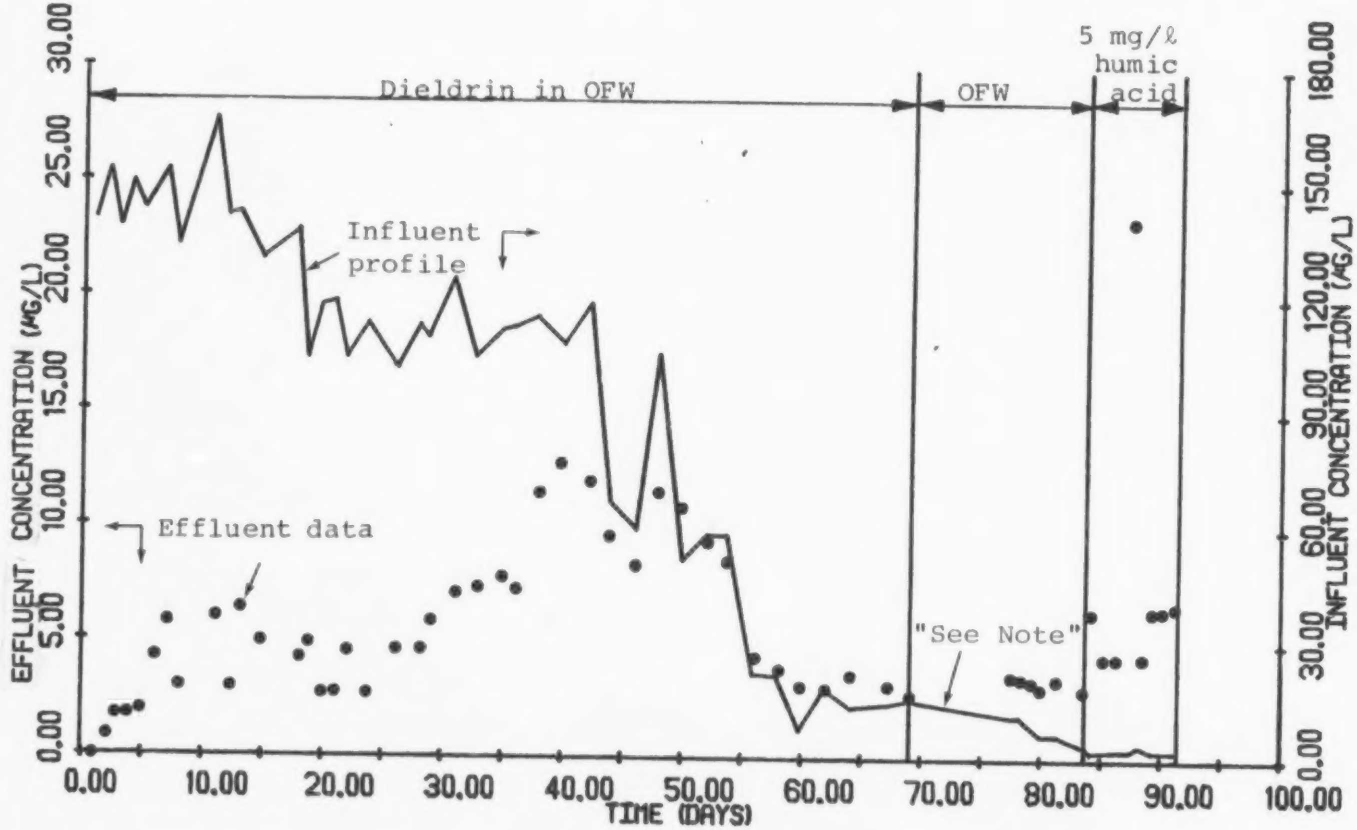

Figure 136. Influent and effluent concentration data for dieldrin in mini fixed-bed adsorbers (flow = 15 mℓ/min, 2 grams of 50/60 carbon, EBCT = 0.31 min).
Note: residual dieldrin desorbed from the feeding system.

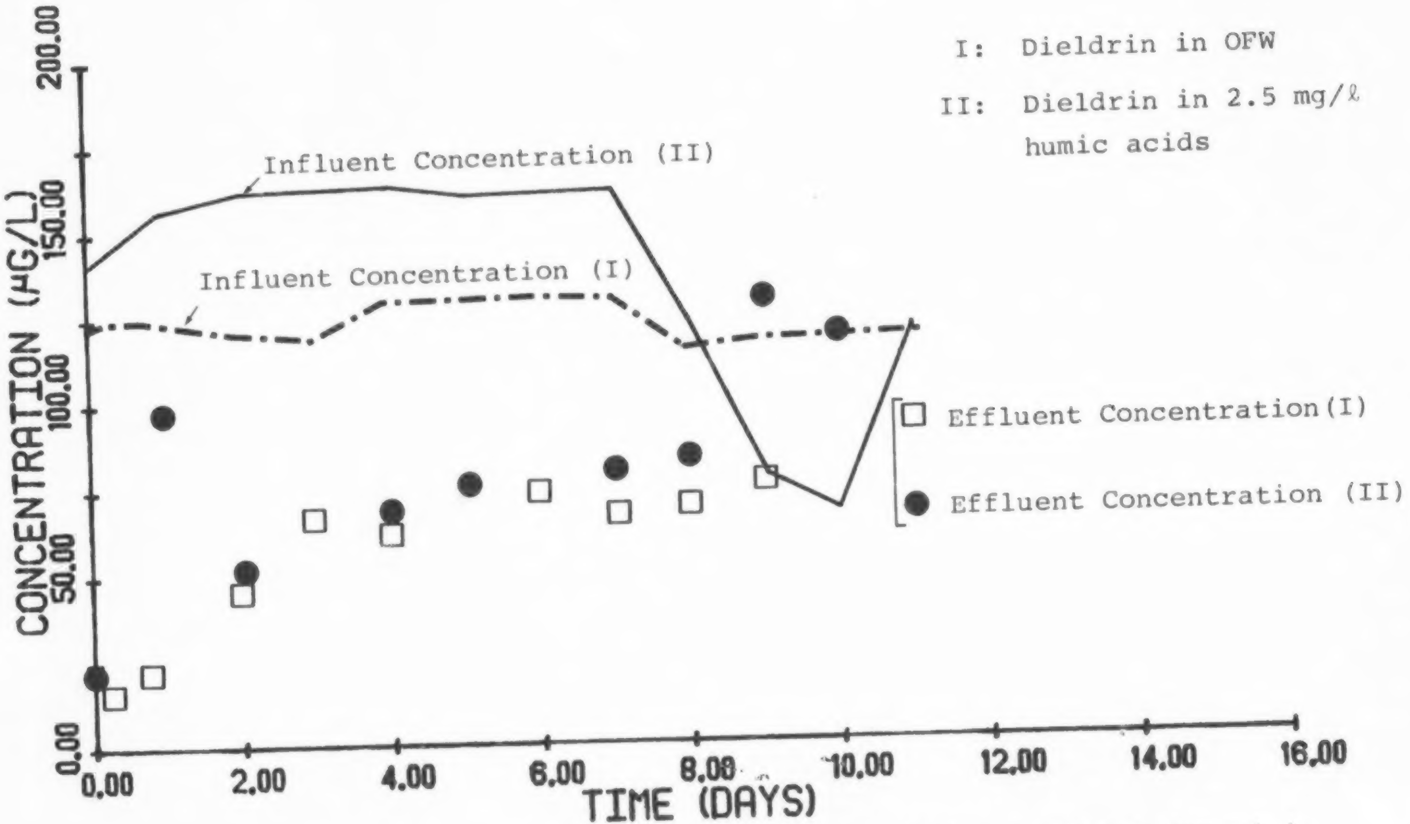

Figure 137. Influent and effluent concentration profiles for mini expanded-bed adsorbers (flow = 15 mℓ/min, 2 grams of 50/60 carbon).

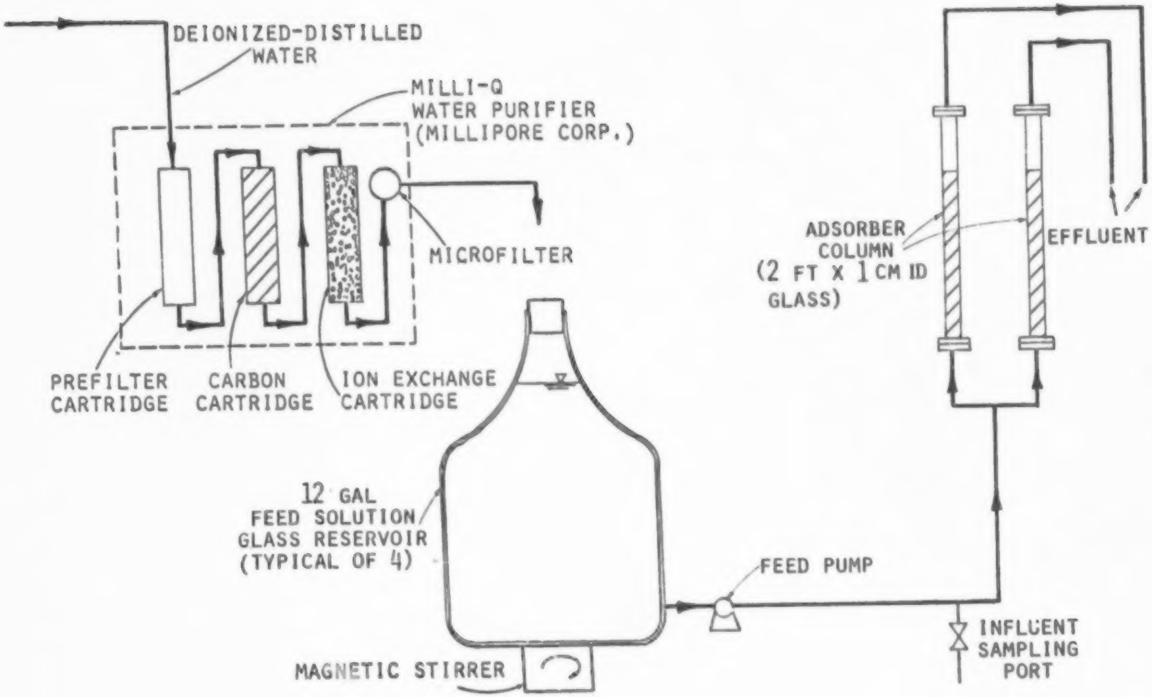
DEIONIZED-DISTILLED WATER
MILLI-Q WATER PURIFIER (MILLIPORE CORP.)
MICROFILTER
PREFILTER CARTRIDGE
CARBON CARTRIDGE
ION EXCHANGE CARTRIDGE
12 GAL FEED SOLUTION GLASS RESERVOIR (TYPICAL OF 4)
MAGNETIC STIRRER
FEED PUMP
INFLUENT SAMPLING PORT
ADSORBER COLUMN (2 FT X 1 CM ID GLASS)
EFFLUENT

Figure 138. Experimental apparatus for dieldrin (comparison of virgin and "humic acid presaturated" carbon).

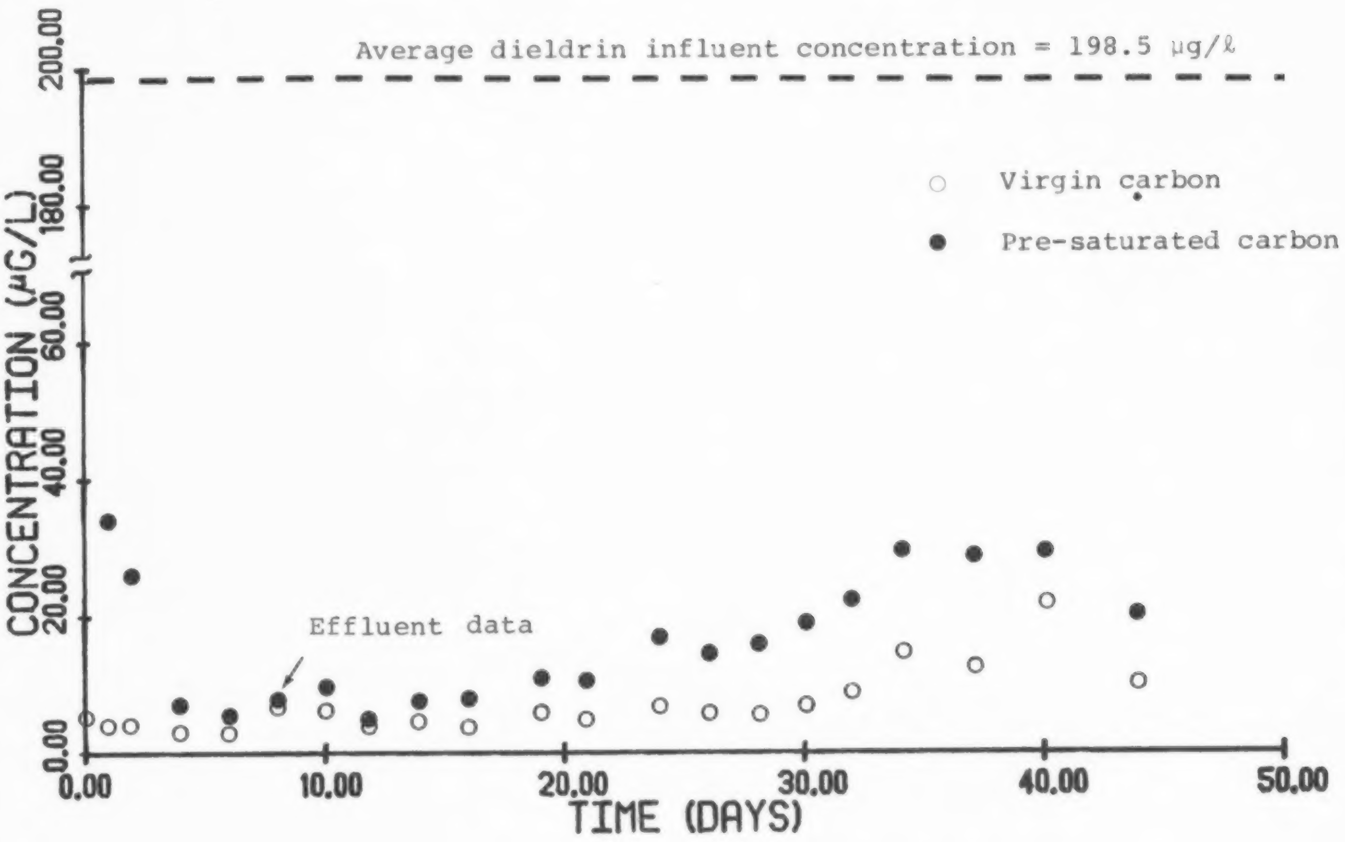

Figure 139. Effluent concentration data for dieldrin in fixed-bed adsorbers; effect of pre-saturation (flow = 10 mℓ/min, 1 gram of 50/60 carbon).

mechanisms may be advanced regarding the elution/release of dieldrin: 1) humic acids displace dieldrin from the carbon surface, 2) humic acids compete with dieldrin for available sites on the carbon surface, 3) humate-dieldrin complexes formed in the feed solution pass through the column unadsorbed, 4) humate-dieldrin complexes formed within the column elute from the column; or, 5) some combination of these effects.

SUMMARY AND CONCLUSIONS

1. The effectiveness of activated carbon in removal of dieldrin from water may be highlighted by fixed-bed adsorber studies conducted in 3-cm ID columns containing 250 grams of carbon. It was demonstrated that with a load of dieldrin as high as 30 μg/l, an EBCT = 15 min, and a hydraulic loading of 1.4 gal/ft^2/min, the column was able to reduce the concentration below the detection limit (≃0.01 μg/l) for an extended period of time (≃7.5 months).

2. The effectiveness of activated carbon for removal of dieldrin is adversely affected by its association with certain background organic substances such as humic acids. It seems likely that methods for effective removal of humic acids by carbon (see Section 6) might also provide for more effective removal of associated dieldrin molecules in water treatment operations.

3. Adsorption of dieldrin by activated carbon appears to be predominantly "chemisorption", whereby reactions occur between the highly active epoxide ring of dieldrin molecule, and the electron-rich oxygen atoms on the carbon surface. The results of dynamic desorption studies suggest, however, that some adsorption of dieldrin may occur partially due to weak van der Waals attraction forces. Because the dieldrin molecule possesses a certain dipole moment, these forces may take place principally as a result of hydrogen bonding with the carbon surface and/or other adsorbed dieldrin molecules.

4. The MADAM model was able to satisfactorily simulate CMB adsorption rates for dieldrin. It was demonstrated that external mass transport most likely controls the rates of adsorption of dieldrin on activated carbon. Because it was not possible to obtain experimental breakthrough profiles for dieldrin (no breakthrough occurred in approximately 7 months of operation - see Figure 135), no attempt was made to quantify the dynamic performance of the adsorber beds.

5. The results of the fixed-bed adsorber studies with presaturated carbon indicate substantial reduction of dieldrin concentration (see Figure 139). This may be significant with respect to the ability of a carbon which is saturated with background organics to continue to remove dieldrin.

6. Because the headloss caused by biological growth in expanded-bed (vs. packed-bed) experimental adsorbers in minimal, a properly designed and executed mini-column expanded-bed system should yield better information regarding the nature of competitive adsorption between background organics and trace compounds with physical and chemical characteristics similar to those of dieldrin.

TYPING GUIDE SHEET

SECTION 11

ADSORPTION OF *p*-DICHLOROBENZENE (PDB)

GENERAL

p-Dichlorobenzene ($C_6H_4Cl_2$; 1,4-dichlorobenzene, *p*-dichlorobenzol; PDB), a white, crystalline solid which sublimes at room temperature, is directly incorporated in a variety of consumer products and widely used as a reactive intermediate for production of a number of other chemicals. Some major applications include use as a pesticide in moth repellents, as a fungicide/bactericide and odor-suppressor in cleaning fluids, as an extreme pressure lubricant, as a component of mixtures of insecticides and germicides, and a precursor in dye manufacture (Kirk-Othmer, Encyclopedia of Chemical Technology, 1964; and, von Rumker *et al*, 1975). A summary of the physical and chemical properties of PDB is given in Table 28.

Production of PDB is accomplished by chlorination of liquid benzene in the presence of ferric chloride. Fractional distillation followed by mulitple re-crystallization is employed to separate the closely boiling isomers which result. Repeated recrystallization results in greater purity (Kirk-Othmer, Encyclopedia of Chemical Technology, 1964). The total annual production of PDB in the United States approaches 100-110 million pounds (von Rumker *et al*, 1975).

Sources and Sinks in the Environment

Domestic sewage, industrial effluents and spills and wastes from insecticide, germicide, and dye manufacturing operations are common sources of PDB in the environment. The major environmental sink appears to be the atmosphere. Schwarzenbach *et al* (1979), on the basis of mass balance determinations for PDB in the central basin of Lake Zurich, Switzerland, concluded that mass transfer to the atmosphere is the predominant eliminaton mechanism for aquatic environments. PDB is degradable by biological organisms, non-biological factors, and sunlight. The major degradation products are 2,5-dichlorophenol, dichloroquinol, and conjugates (von Rumker *et al*, 1975). PDB, which has been detected in the water supplies of several major cities in the U.S. and abroad (USEPA, *Report to Congress*, 1975; Shackelford and Keith,

EPA-287 (Cin.)
(4-76)

TABLE 28. PHYSICAL AND CHEMICAL PROPERTIES OF *p*-DICHLOROBENZENE

Formula Weight	147
Crystalline Form and Color	monoclinic, white
Specific Gravity	1.458
Melting Point (°C)	53.1
Boiling Point (°C)	174.4
Vapor Pressure (25°C, mmHg)	0.4
Heat of Fusion (cal/gram)	29.07
Heat of Vaporization (cal/gram)	72.18
Solubility:	
Water	80 mg/l
Benzene	soluble
Alcohol	∞ soluble
Ether	very soluble
Acetone	∞ soluble

Sources: CRC Handbook of Chemistry and Physics, 1976-1977; Kirk-Othmer, Encyclopedia of Chemical Technology, 1964; Lange's Handbook of Chemistry, 1979; and, von Rumker *et al*, 1975.

1976; Piet and Morra, 1979) is included in the USEPA priority pollutant list.

Public Health Assessment

PDB is relatively nontoxic to lower aquatic organisms and moderatley toxic to birds (von Rumker *et al*, 1975). Its absorption by human tissue is slow, but it can cause mild to moderate irritation upon contact with skin, irritation and possibly some transient corneal injury upon contact with the eye, and aggrevation of acute or chronic liver or kidney diseases (Kirk-Othmer, Encyclopedia of Chemical Technology, 1964; von Rumker *et al*, 1975).

ANALYTICAL PROCEDURES

Sample Collection and Concentration

Determination of residual concentrations of PDB (Analytical Grade; Dow Chemical) in solution phase was accomplished by a vial extraction technique and gas chromatographic analysis. The procedure involved transfer of 10-ml of a sample to a 4-dram vial containing 1-ml of hexane (Baker Resi-Analyzed). The vial was then sealed with a Teflon-lined screw-cap and shaken vigorously for 3 minutes. The vials were subsequently stored in a walk-in incubator overnight at 4°C in an inverted position to eliminate loss of hexane due to evaporation. The samples were brought to room temperature (20°C+ 1) before GC analysis. Extraction efficiency was estimated to be 98%.

Analysis

Gas chromatographic analysis for PDB was conducted using a 1700 Varian GC equipped with a 10' x 1/8" stainless steel column packed with 3% SE-30 on Varaport 30. Two types of detectors were employed: an electrolytic conductivity detector, and a ^{63}Ni electron capture detector. Temperatures were: injector 125°C, column 100°C, and detector 150°C. Pre-purified nitrogen was used as a carrier gas at a flow rate of 40 ml/min. The detector response was recorded graphically and peak height used as a measure of concentration. The procedure for preparation of standard curves is described in Appendix P.

ADSORPTION METHODOLOGY

Equilibrium Studies

Equilibrium studies for PDB were performed using the bottle point technique. A saturated PDB solution was prepared by introducing 0.3 gram of PDB into a glass reactor containing 3-l of OFW. The solution was stirred overnight, filtered (0.45 μm filter), and diluted to desired concentrations. Carefully weighed amounts of carbon and 100-ml aliquots of the PDB solution in OFW--or in OFW containing 5 mg/l humic acid -- were placed in 150-ml Hypo-Vials. The vials were tightly sealed with Teflon-lined septa and crimped-on aluminum caps. The Hypo-Vials were subsequently agitated in a specially-designed rotary tumbler until equilibrium was achieved. The equilibriation time was from 48 hours for powdered carbon to 4 weeks for 16/20 granular carbon. Preliminary investigations had indicated negligible quantities of PDB in the headspace gas phase. Residual concentrations in the Hypo-Vials were determined by the vial-extraction technique followed by GC analysis.

Rate Studies

CMB-rate studies for PDB were conducted in a manner similar to that described for PCB's and dieldrin. Weighed and pre-wetted quantities of granular carbon were added to the experimental solutions (spiked OFW or 5 mg/l humic acid prepared in OFW background solution; pH 7). Samples were withdrawn periodically and subjected to vial extraction and GC analysis.

Column Studies

Fixed-bed adsorber studies were conducted in mini-columns containing 1 - 5 grams of 50/60 mesh carbon. The feed solution was spiked with PDB in acetone, dosed with 2 mg/l of Ag^+, stirred for 30 min, and pumped to the mini-columns at a flow rate of 15-20 ml/min. Samples were withdrawn periodically and subjected to extraction and GC analysis. Experimental apparatus and arrangements were similar to those described for PCB (Figure 110).

RESULTS AND DISCUSSION

Adsorption Equilibria

As for the other solutes discussed earlier in this report, the Freundlich equation was found to provide the best statistical fit to the experimental equilibrium data for PDB.

The resulting data and parameter values presented in Figures 140, 141 and Table 29 indicate no significant differences in the equilibrium extent of adsorption for PDB in OFW and 5 mg/l humic acid background solution.

TYPING GUIDE SHEET
EPA-287 (Cin.)
(4-76)

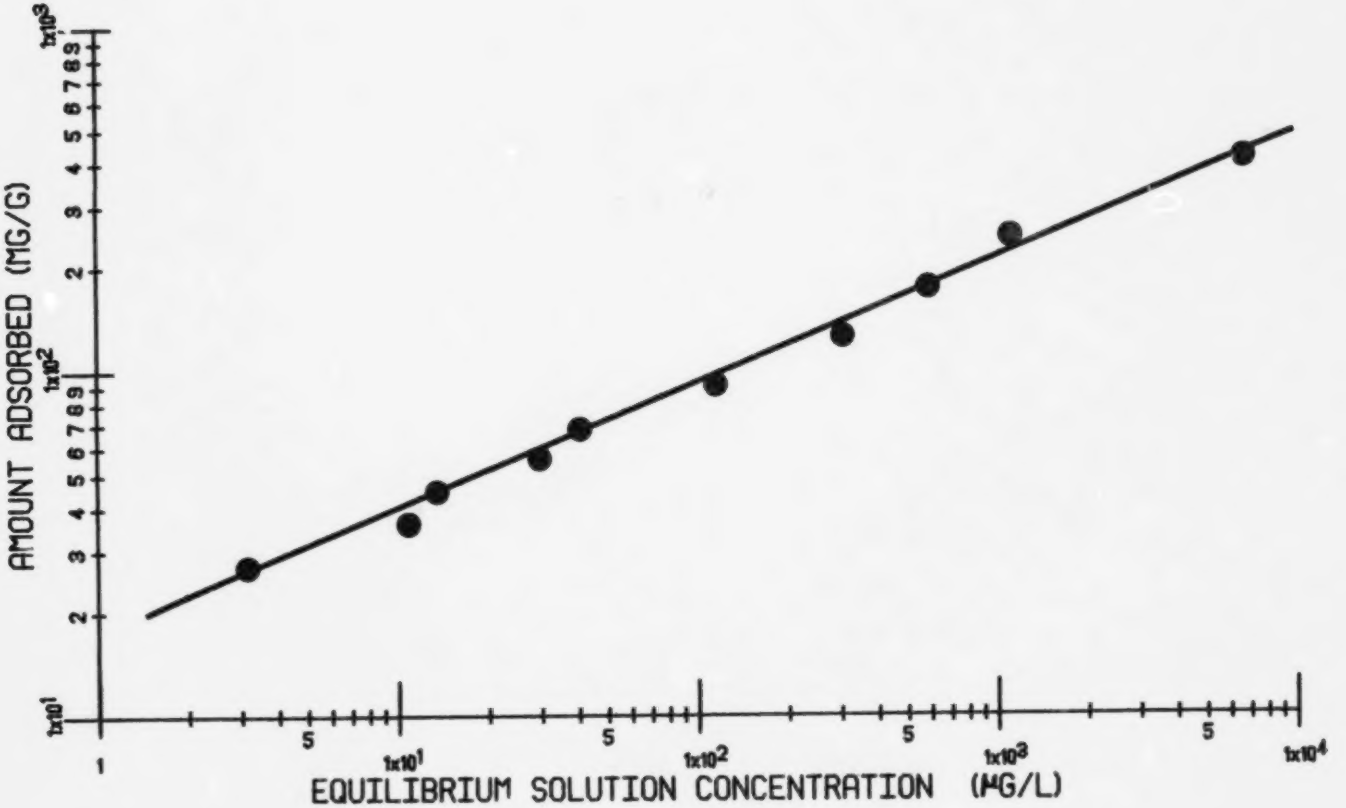

Figure 140. Adsorption isotherm for PDB in OFW (C_o = 25 mg/ℓ).

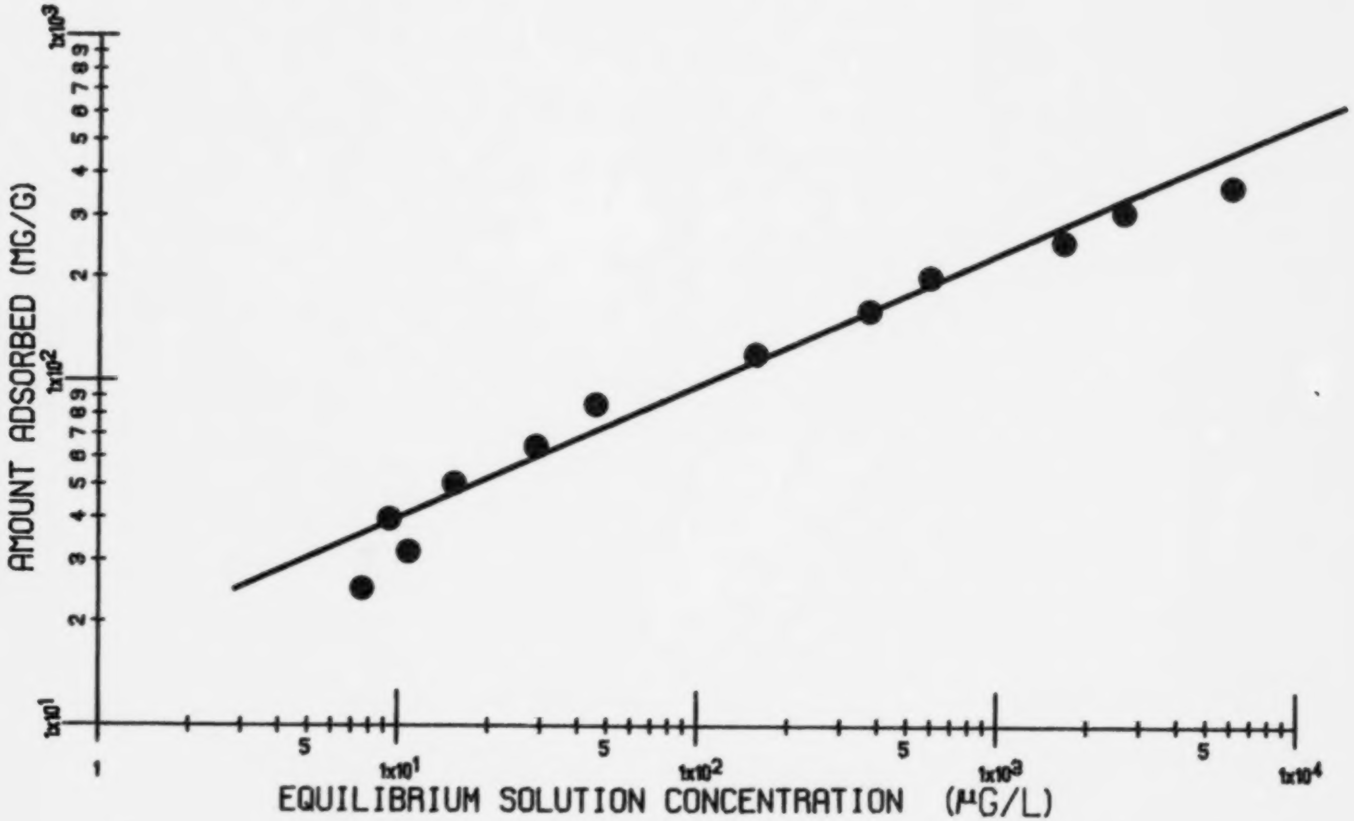

Figure 141. Adsorption isotherm for PDB in 5 mg/ℓ humic acid background solution (C_o=25 mg/ℓ).

TYPING GUIDE SHEET

TABLE 29. ADSORPTION EQUILIBRIUM PARAMETERS FOR PDB[†]

Background Solution	Carbon Mesh Size	Freundlich Isotherm Constants*			
		C_o, mg/1	k_f	1/n	r
OFW	16/20	25	17.07	0.374	0.997
OFW + 5 mg/1 humic acids	16/20	25	16.25	0.388	0.986

† All studies were conducted at pH 7 unless otherwise noted.

* Based on C_e and q_e expressed in µg/1 and mg/gm, respectively.

r = Correlation coefficient for fit of the isotherm to the experimental data.

EPA-287 (Cin.)
(4-76)

Adsorption Rates

CMB experiments were performed to investigate the effects of carbon particle size on rates of adsorption of PDB. Figure 142 illustrates concentration decay curves for different particle sizes of carbon, signifying a strong dependence of rate of PDB adsorption on particle size. As for dieldrin, the general character of variation of adsorption rate as a function of particle diameter, illustrated in Figure 143, suggests that the limiting rate mechanism is external transport.

A simulation-modeling analysis was conducted for adsorption of PDB from OFW for an initial concentration of $C_o = 157$ μg/l to evaluate appropriate rate coefficients, k_f and D_s. The estimated coefficients values $k_f = 4.3 \times 10^{-3}$ cm/sec and $D_s = 8.0 \times 10^{-8}$ cm^2/sec define the solid-line model simulation presented in Figure 144. Analyses of the sensitivity of the simulation to values of k_f and D_s were performed to investigate the nature of the mass transport rate limiting mechanism. Figure 145 illustrates substantial sensitivity to the film transfer coefficient, k_f. Similar analyses for the intraparticle diffusion coefficient showed relative insensitivity to values of D_s. This accords with the earlier observation that external mass transfer most likely controls rates of adsorption of PDB by activated carbon.

Simulations were also conducted for rate studies with PDB in 5 mg/l humic acid background solution. The model profile represented by the solid line in Figure 146 is predicated on estimated coefficient values of, $k_f = 5.3 \times 10^{-3}$ cm/sec and $D_s = 8.0 \times 10^{-8}$ cm^2/sec. Although the estimated value for the film transfer coefficient for the system containing humic acids is higher than that for the OFW system, it will be observed from Figure 146 that the model simulation for the former system does not describe the data quite as well as the simulation for the latter (Figure 144), particularly in the early stages of the profile. In reality, somewhat lower values of k_f for the humic acid system -- approaching those for the OFW system -- give a more accurate fit of the experimental data for the early stages of the adsorption. Thus, it is reasonable to conclude that the observed results indicate essentially no effect of the humic acids on the rate of adsorption of the PDB.

The relative insensitivity of PDB adsorption rate to the presence of humic acids is supported by data presented in Figure 147 comparing rates of adsorption on virgin and "humic acid saturated" carbon.

A summary of experimental conditions and associated mass transfer coefficients for the PDB adsorption rate investigations is given in Table 30.

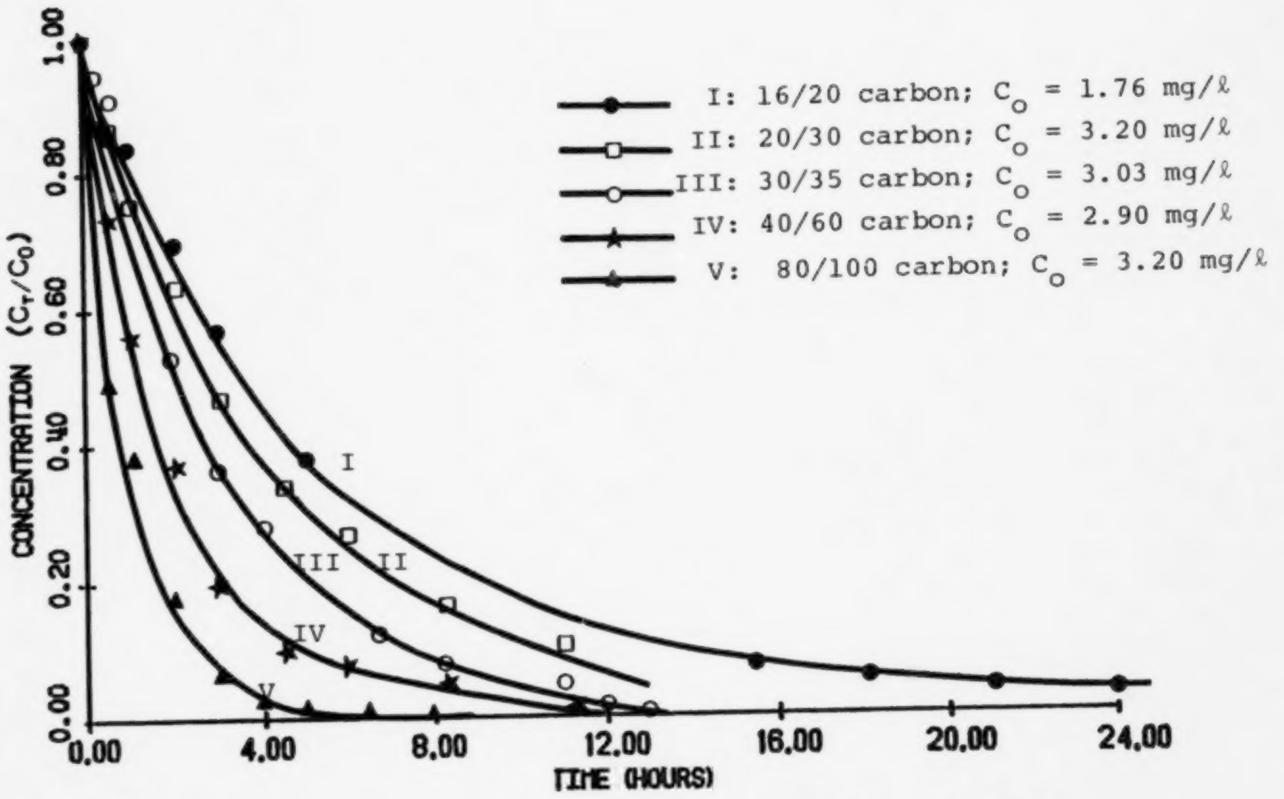

Figure 142. CMB rate studies for PDB - effects of carbon particle size (0.083 g/ℓ carbon).

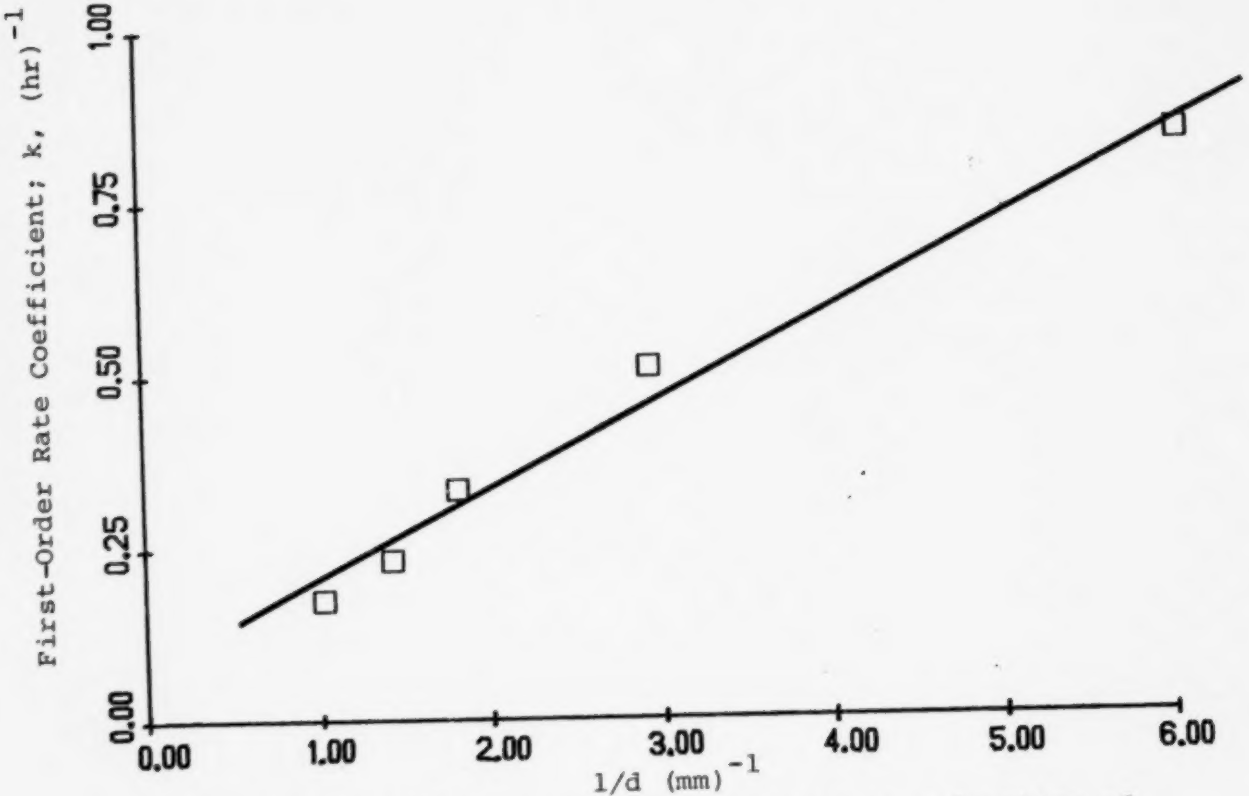

Figure 143. Variation of adsorption rate as a function of carbon particle diameter.

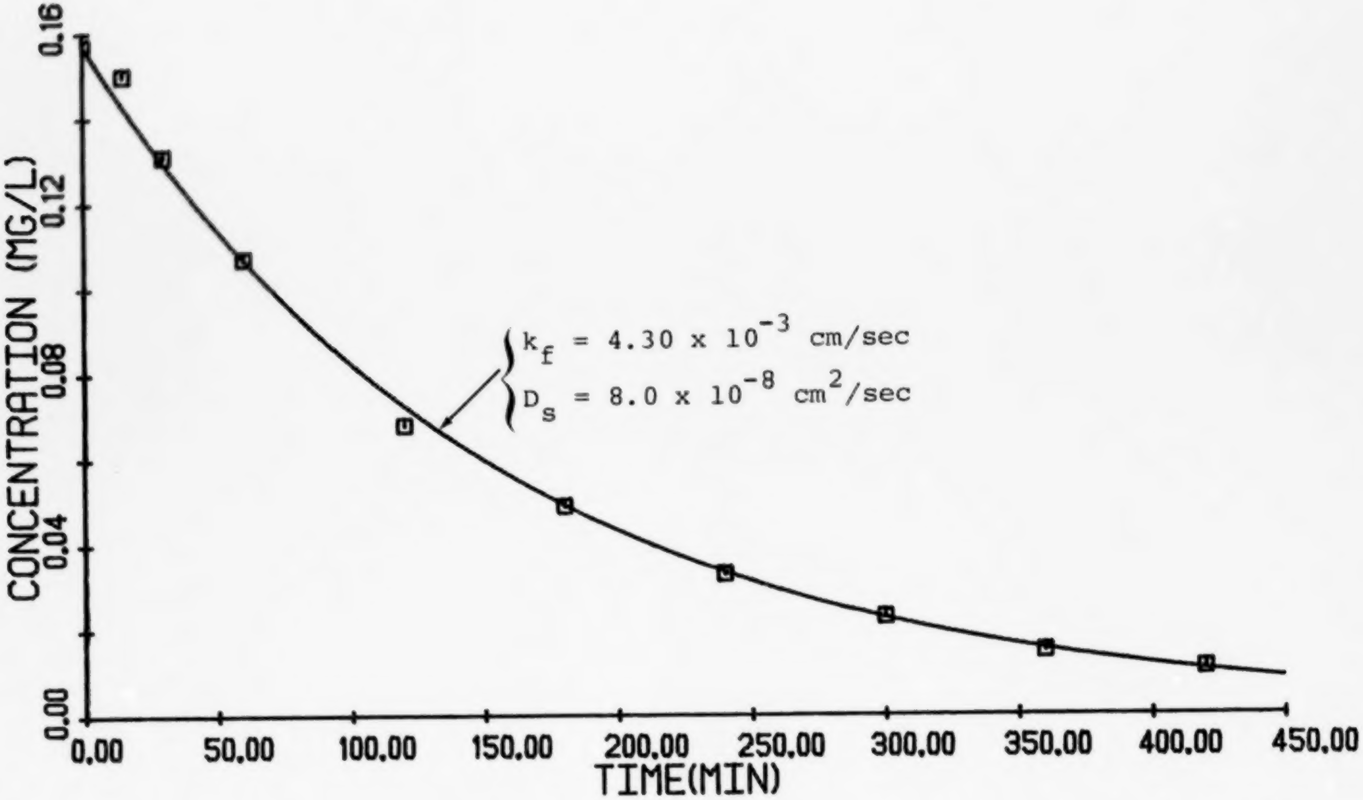

Figure 144. Experimental data and model profile for rate of adsorption of PDB from OFW in a CMB reactor (C_o = 157 μg/ℓ, 0.076 g/ℓ of 50/60 carbon).

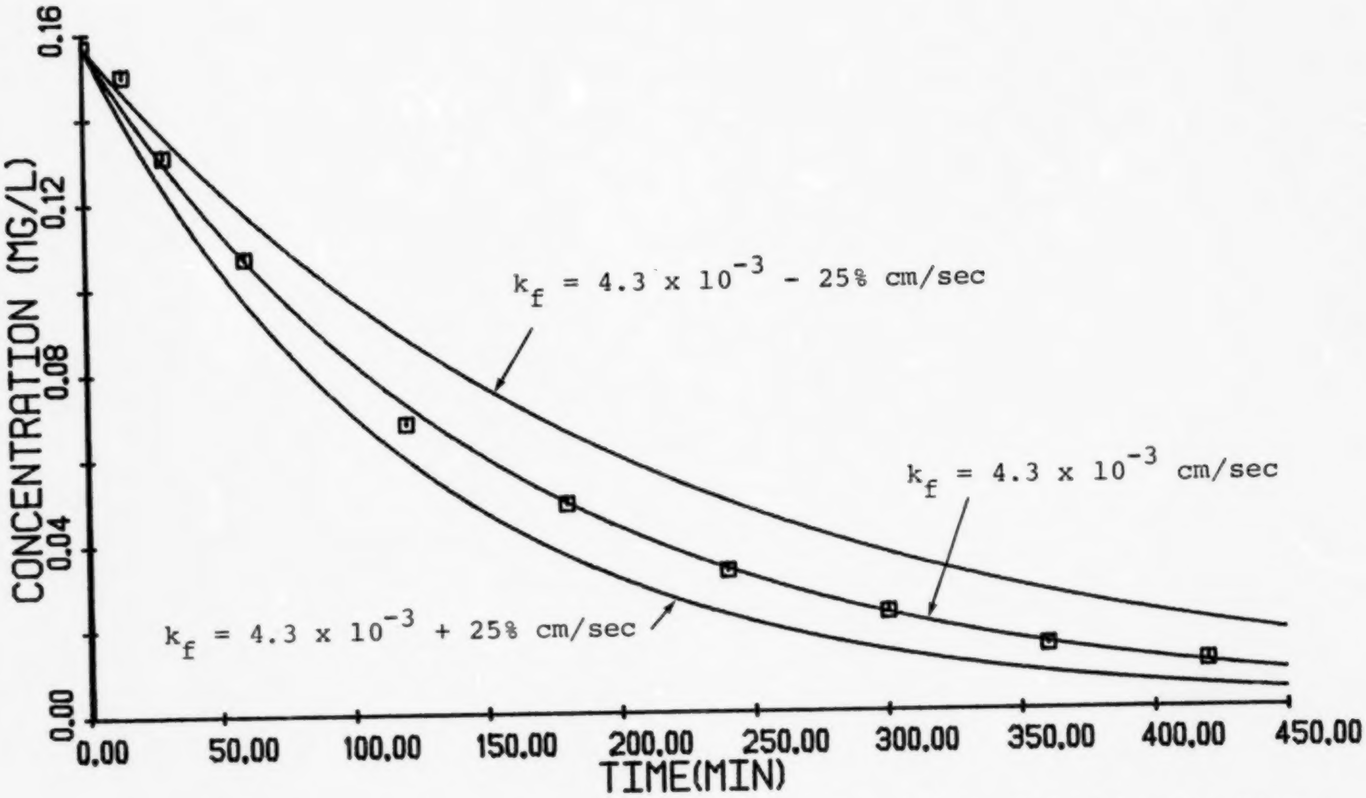

Figure 145. Analysis of the sensitivity of model profiles to the film transfer coefficient, k_f.

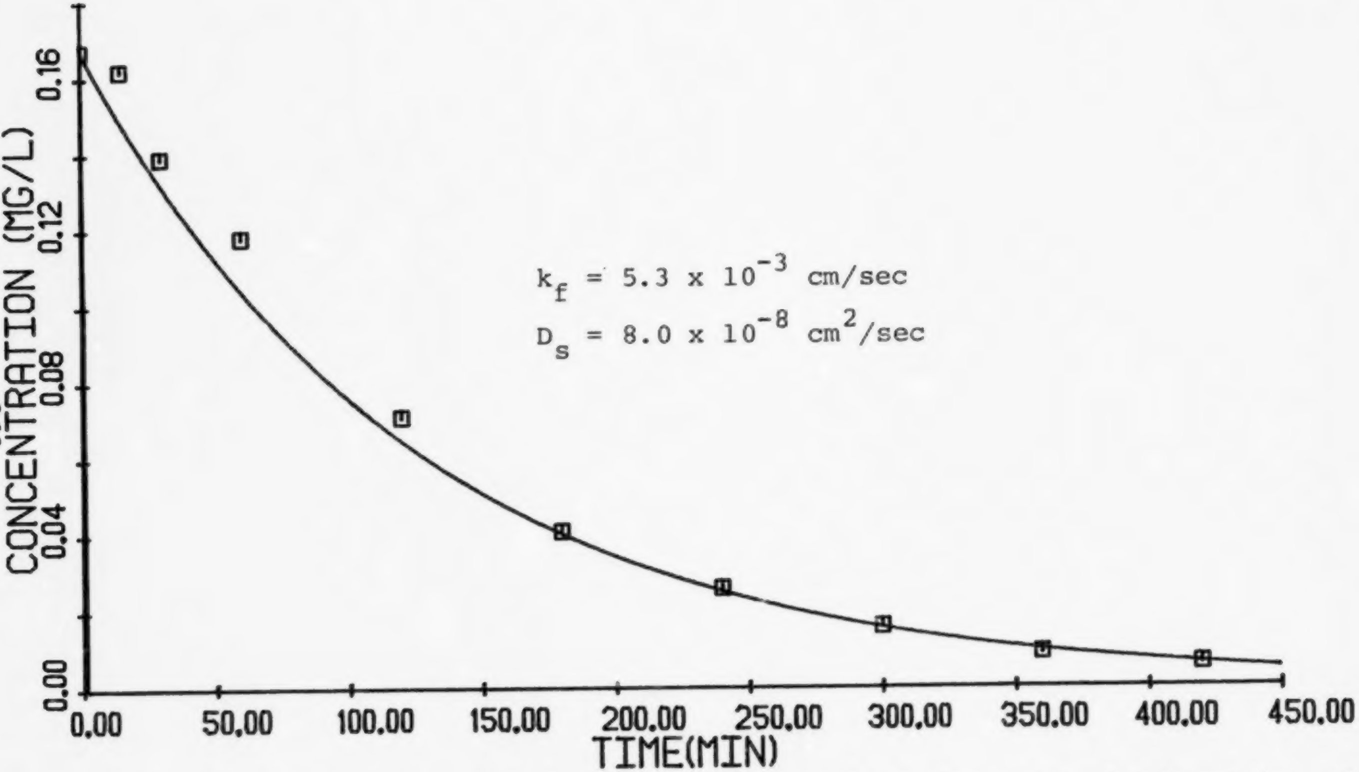

Figure 146. Experimental data and model profile for rate of adsorption of PDB from humic acid background solution in a CMB reactor (C_o = 167 μg/ℓ, 0.076 g/ℓ of 50/60 carbon).

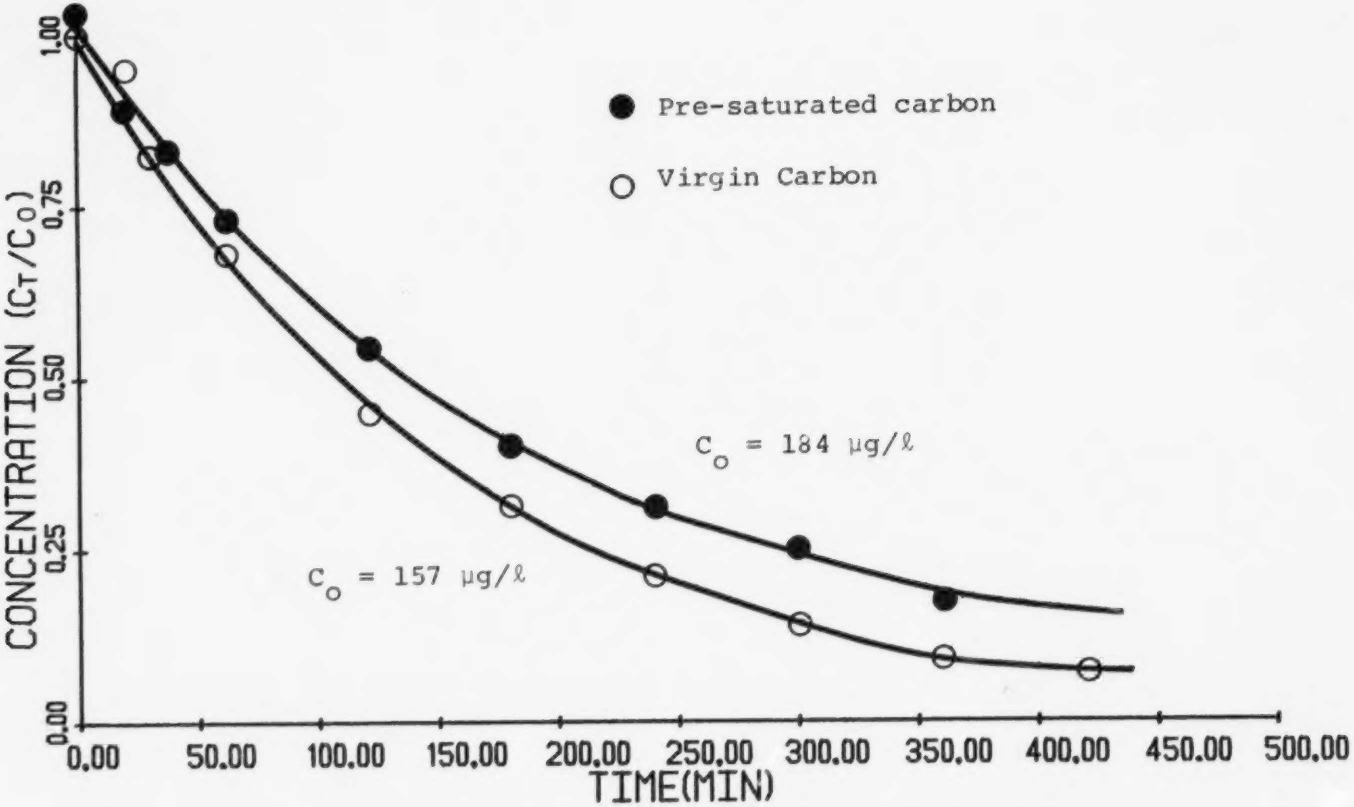

Figure 147. CMB reactor rate study for adsorption of PDB on virgin and pre-saturated carbon (0.076 g/ℓ of 50/60 carbon).

TABLE 30. ADSORPTION RATE PARAMETERS FOR PDB

Background Solution	C_o, µg/l	Carbon Dosage, g/l	k_f, cm/sec	D_s, cm^2/sec
OFW	157	0.076	4.3×10^{-3}	8.0×10^{-8}
OFW + 5 mg/l humic acids	167	0.076	5.3×10^{-3}	8.0×10^{-8}

C_o = Initial concentration;

k_f = Film transfer coefficient; and

D_s = Surface diffusion coefficient.

Adsorption Columns

Mini fixed-bed adsorber experiments were conducted for PDB to investigate its dynamic adsorption behavior and to obtain data relative to adsorption breakthrough characteristics for prediction/simulation modeling.

Typical experimental breakthrough data for different influent concentrations, carbon quantities, flow rates, and hydraulic residence times are presented in Figure 148.

The physical and chemical parameters associated with selected adsorber studies, in addition to values for corresponding mass transfer coefficients k_f and D_s are summarized in Table 31. As for CCl_4 and benzene, the surface diffusion coefficient was estimtated from the CMB-reactor rate experiments, and the film transfer coefficient was obtained by the correlation technique suggested by Williamson et al (1963).

Model Calibration--

The results of model calibration for a hydraulic loading of 3.87 gpm/ft^2, a bed length of 2.6 cm, and an average influent concentration of 185 μg/l are illustrated in Figure 149. Relatively good agreement is demonstrated between the data and the predicted profile.

Model Verification--

To test for generality, the model was verified for an influent concentration of 2.53 mg/l, a hydraulic loading of 7.4 gpm/ft^2, and a bed length of 17.6 cm. The results, presented in Figure 150, indicate only a small disparity between the experimental data and the predicted profile, the latter being quite acceptable for all practical purposes.

Based on these observations, it is thus possible to conduct column studies with a much higher initial concentration to insure attaining a breakthrough profile in a shorter time. The model can then be calibrated based on these data and verified for desired influent concentrations.

Model Sensitivity--

Model sensitivity analyses for k_f and D_s were conducted for fixed-bed adsorber Run I. Figure 151 depicts the sensitivity of breakthrough profiles for variation of ±25% in k_f. No significant sensitivity was observed for variations of ±25% D_s, indicating once more that film transfer is the principal rate controlling mechanism for adsorption of PDB on activated carbon.

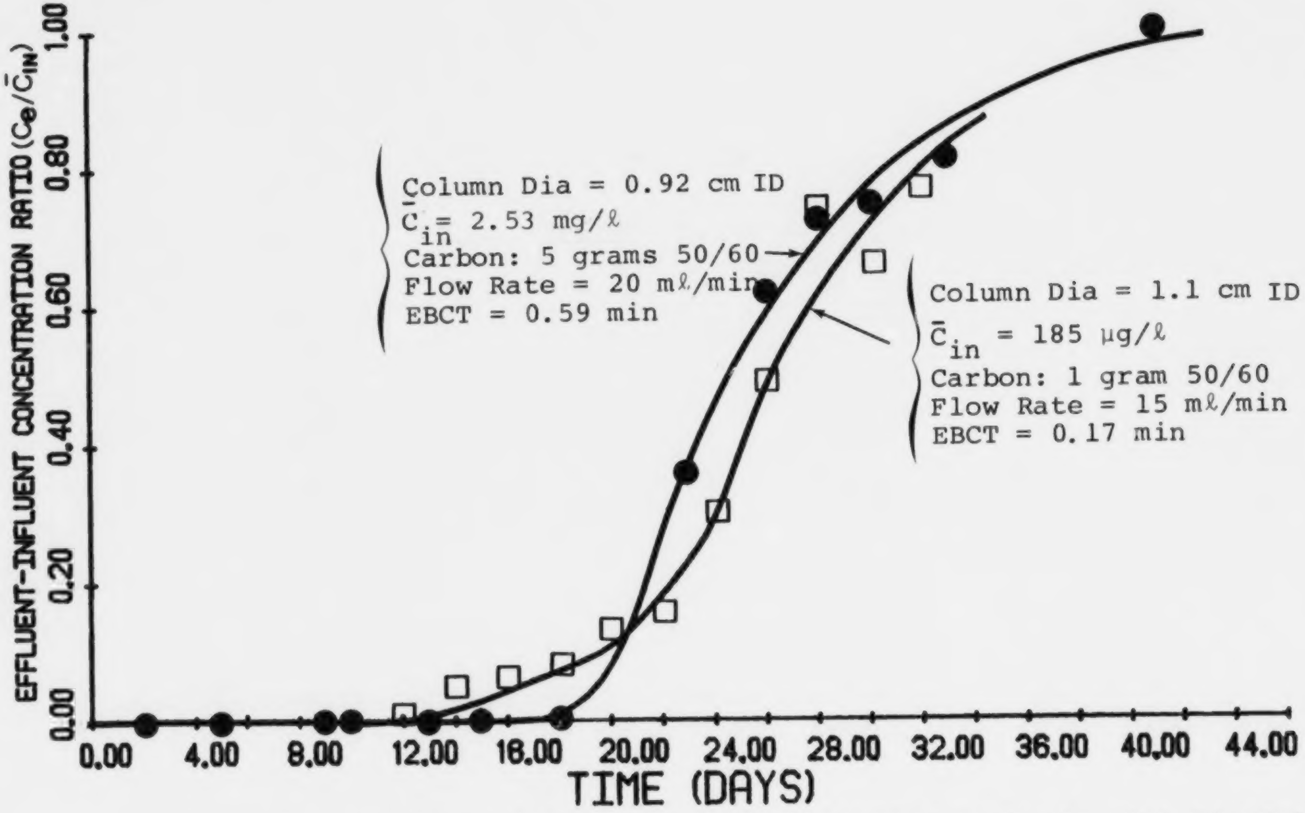

Figure 148. Experimental breakthrough profiles for PDB in mini fixed-bed adsorbers.

TYPING GUIDE SHEET

TABLE 31. FIXED-BED ADSORBER PARAMETERS FOR PDB

Adsorber Run	$\overline{C}_{in}$	d, cm	L, cm	γ	v, cm/sec	k_f, cm/sec	D_s, cm^2/sec
I (Figure 149)	185 μg/1	0.027	2.6	0.39	0.67	6.8×10^{-3}	8.0×10^{-8}
II (Figure 150)	2.53 mg/1	0.027	17.6	0.35	1.43	7.0×10^{-3}	8.0×10^{-8}

$\overline{C}_{in}$ = Average influent concentration;

d = Carbon particle diameter;

L = Bed length;

γ = Bed porosity, dimensionless;

v = Interstitial velocity;

k_f = Film transfer coefficient; and,

D_s = Surface diffusion coefficient.

EPA-287 (Cin.)
(4-76)

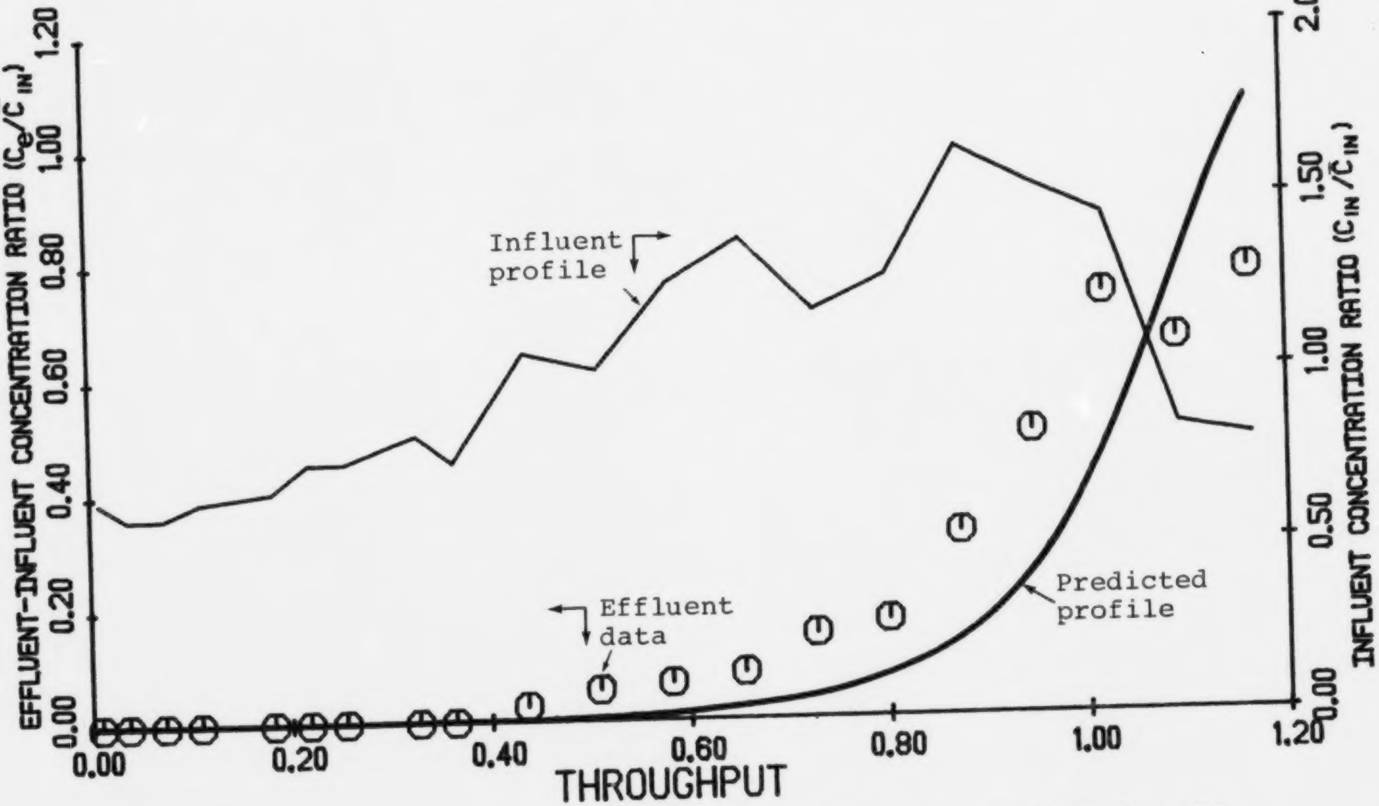

Figure 149. Effluent and influent concentration profiles for PDB in OFW - fixed-bed adsorber Run I ($\bar{C}_{in}$ = 185 μg/ℓ, 1 gram of 50/60 carbon, flow rate = 15 mℓ/min, EBCT = 0.17 min).

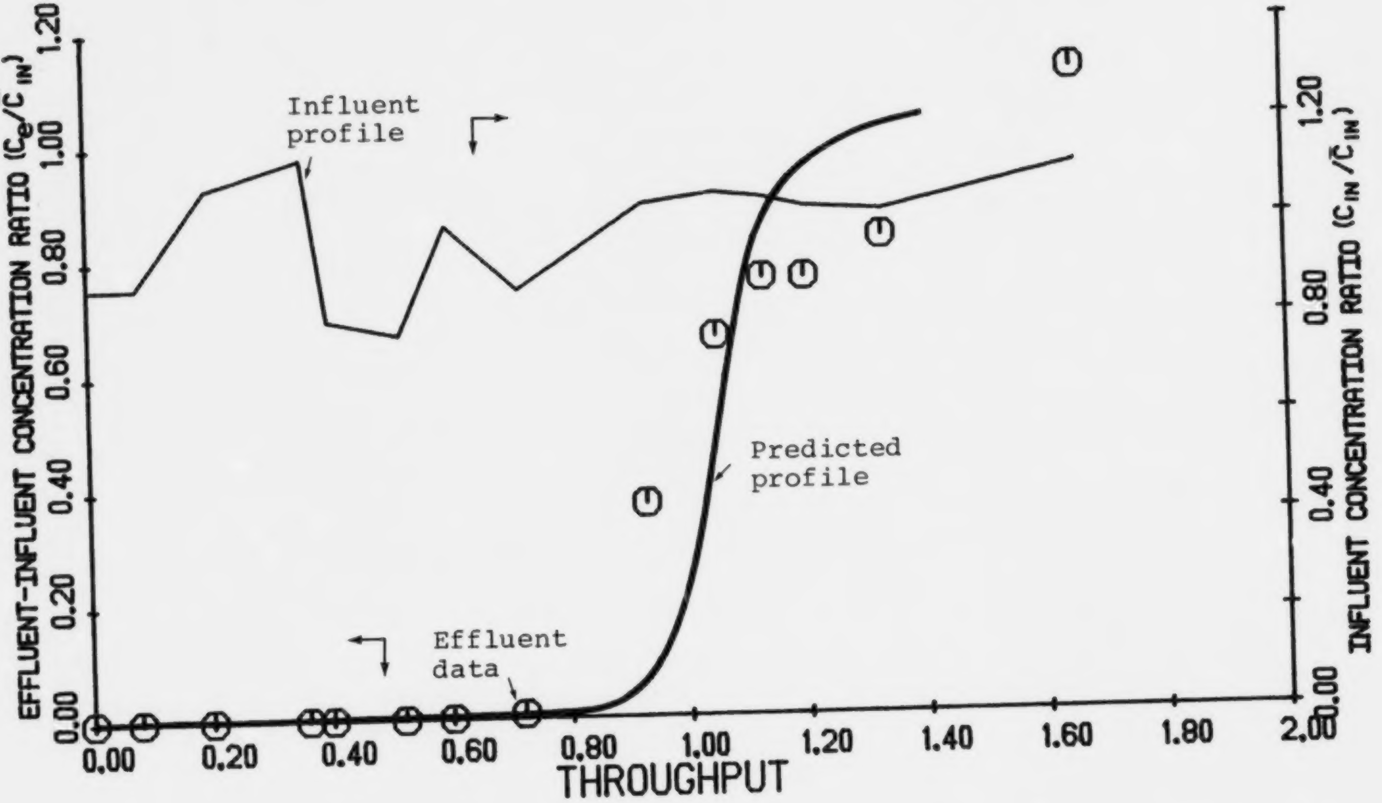

Figure 150. Effluent and influent concentration profiles for PDB in OFW - fixed-bed adsorber Run II ($\bar{C}_{in}$ = 2.53 mg/ℓ, 5 grams of 50/60 carbon, flow rate = 20 mℓ/min, EBCT = 0.59 min).

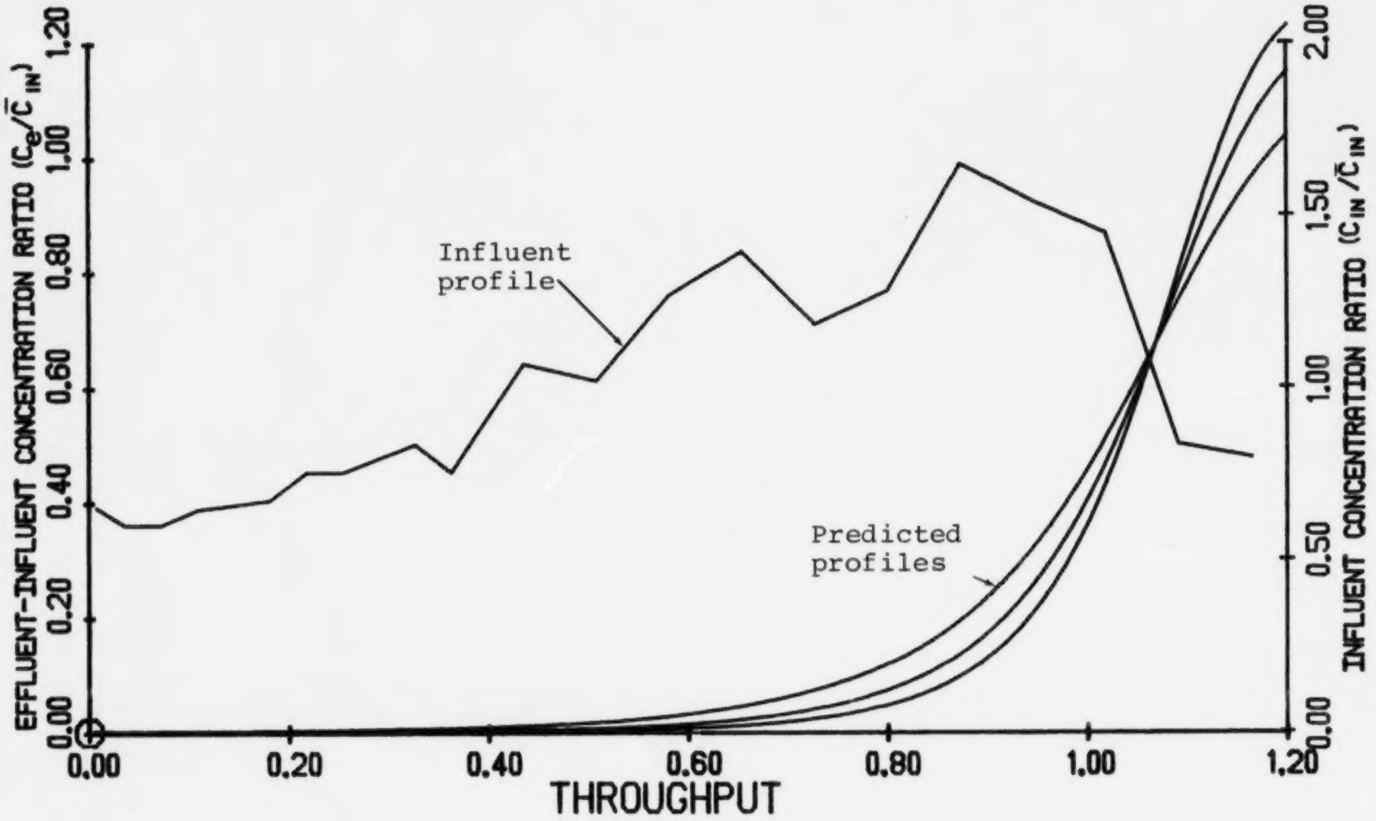

Figure 151. Sensitivity analysis of breakthrough profiles relative to the film transfer coefficient, k_f ± 25%, for PDB in OFW (fixed-bed adsorber Run I).

Desorption Studies

Dynamic desorption experiments for PDB in the fixed-bed adsorber Run II were commenced after attaining exhaustion. The column was fed with OFW and the flow rate maintained at 20 ml/min. The results, illustrated in Figure 152, indicate that a substantial quantity of PDB was desorbed.

Competitive Adsorption

As for dieldrin, two parallel mini expanded-bed systems, each containing two grams of 50/60 mesh carbon, were employed. One column was fed with PDB in OFW and the other with PDB in 5 mg/l humic acid solution. The flow rate was maintained at 15 ml/min. The experimental apparatus, arrangements and procedure were similar to those described for dieldrin. Figure 153 presents the effluent concentration ratio data for the two systems, once more confirming little if any adverse effects of the humic acids on PDB adsorption rates.

Chromatographic or displacement phenomena were investigated in the mini fixed-bed adsorber Run II after termination of the desorption sutdies. The column was fed with 5 mg/l of humic acid solution for a period of 4 days. The results, included in Figure 152, suggest no significant increase in displacement by the humic acids over amounts desorbed by the OFW alone.

Mini-adsorber column studies with virgin carbon and "humic acid pre-saturated" carbon were conducted in a manner similar to that described for dieldrin and PCB's. Each column contained 1 gram of 50/60 mesh carbon. The feed solution was dosed with 2 mg/l of Ag^+ and the flow rate was maintained at 15 ml/min. The effluent concentration data depicted in Figure 154 indicate some reduction in the capacity of the pre-saturated carbon.

SUMMARY AND CONCLUSIONS

1. Activated carbon adsorption may offer an attractive means for removal of PDB and other similar compounds in cases when more conventional treatment operations fail to accomplish the task. It was found in this research that with a load of PDB as high as 294 μg/l, an EBCT = 0.17 min, and a hydraulic loading of 3.86 gpm/ft^2, 78,700 bed volumes of water were treated before reaching a breakthrough point of ~1 μg/l.

2. The effectiveness of activated carbon for removal of PDB appears not to be adversely affected by background organic substances such as humic acids, at least under the condition tested in the current work.

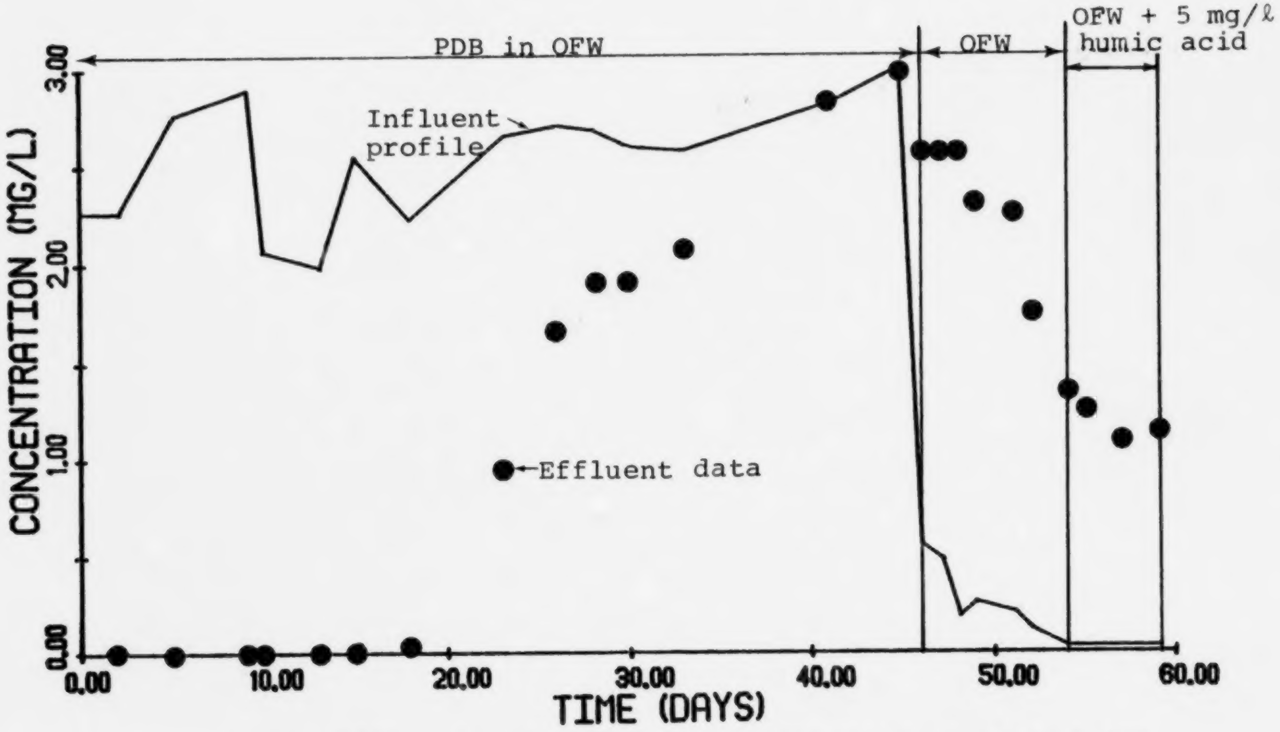

Figure 152. Effluent and influent concentration profiles for adsorption-desorption study for PDB (5 grams of 50/60 carbon, flow rate = 20 mℓ/min).

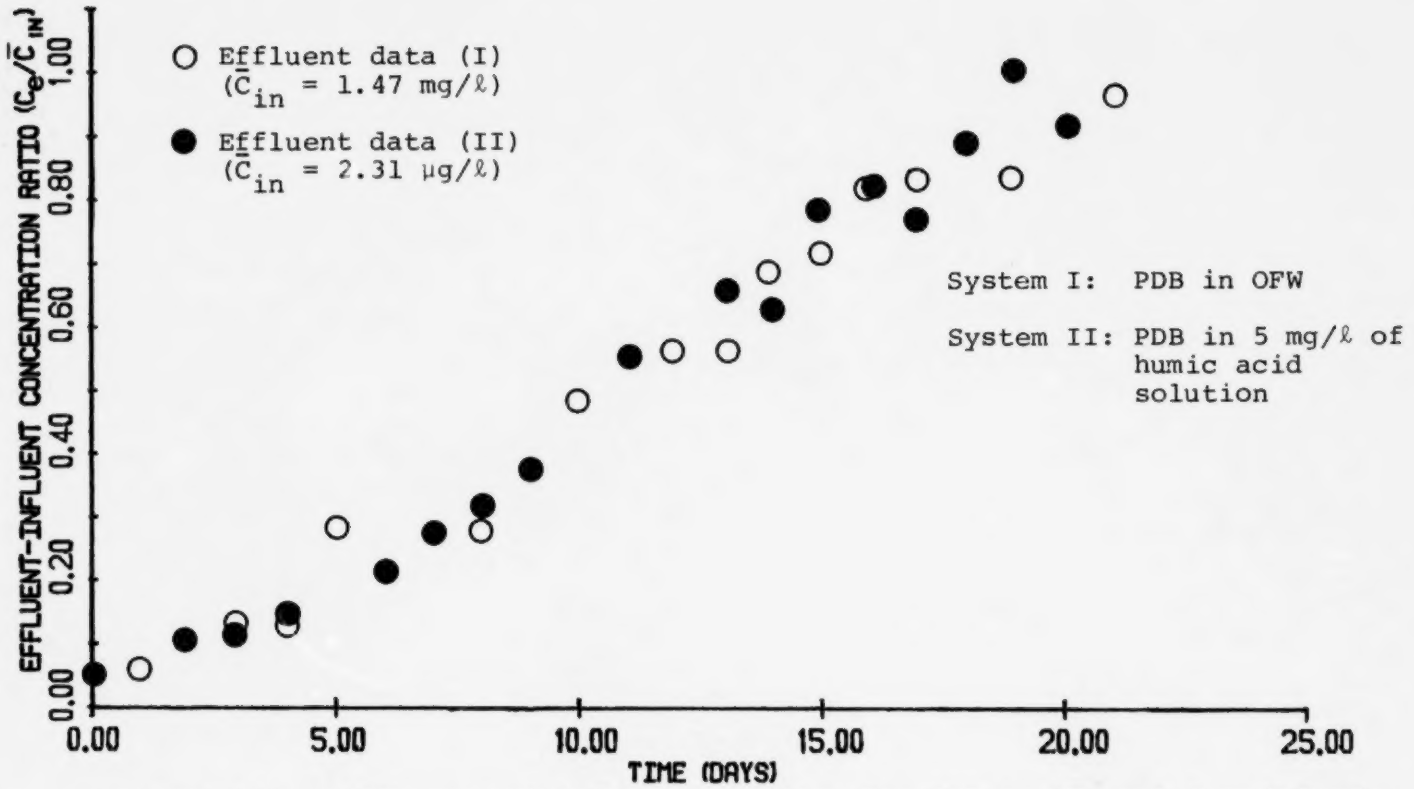

Figure 153. Effluent and influent profiles for PDB in OFW and 5 mg/ℓ humic acid solution (expanded-bed systems).

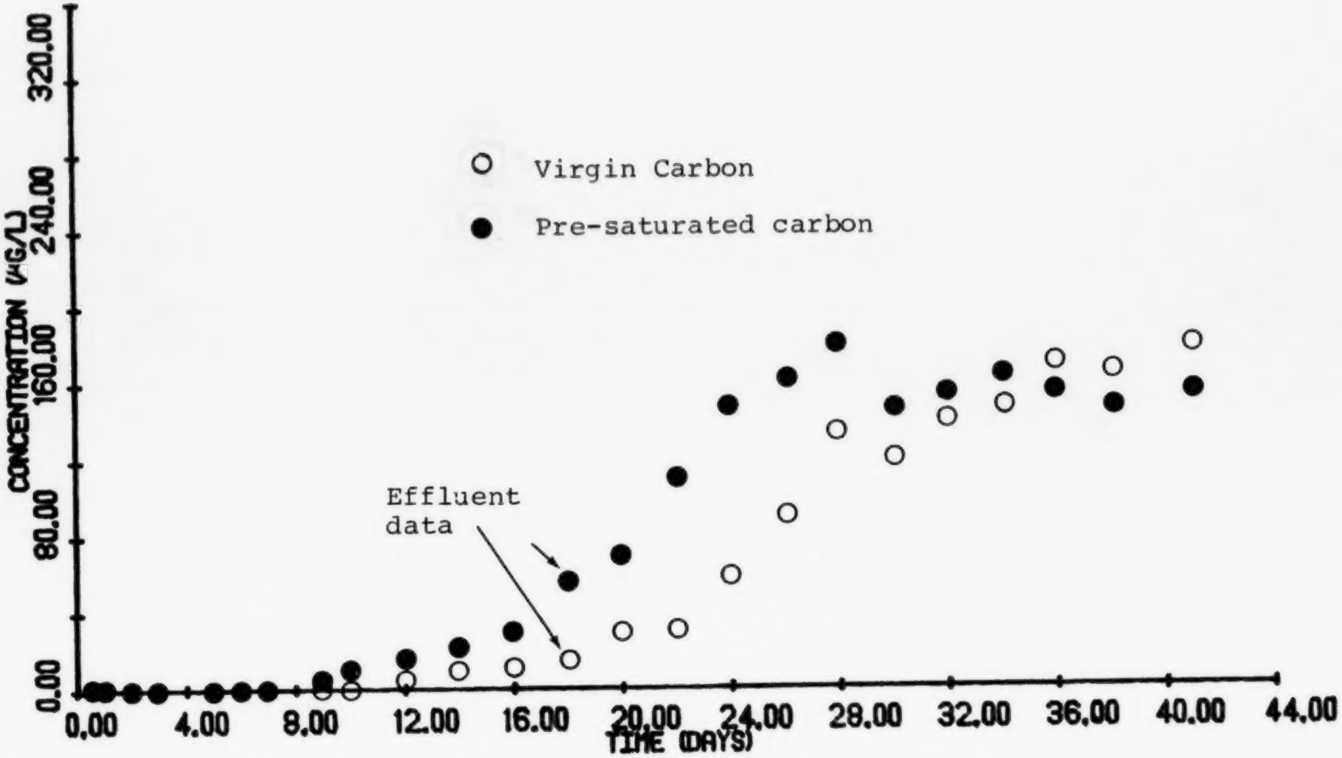

Figure 154. Effluent profiles for adsorption of PDB on virgin carbon and pre-saturated carbon ($\bar{C}_{in}$ = 185 μg/ℓ, 1 gram of 50/60 carbon, flow rate = 15 mℓ/min).

TYPING GUIDE SHEET

3. The MADAM model was generally able to simulate and predict the performance of fixed-bed adsorbers for removal of PDB.

4. The results of dynamic desorption studies suggest adsorption of PDB may predominantly occur due to weak van der Waals attracting forces (physical adsorption).

EPA-287 (Cin.)
(4-76)

BEGIN FIRST LINE OF TEXT HERE
TYPING GUIDE SHEET
CENTER OF PAGE
TOP OF IMAGE AREA
DROPPED HEAD; BEGIN SECTIONS HERE

SECTION 12

A CASE STUDY: PILOT-PLANT INVESTIGATIONS OF THE ADSORPTION OF 1,2-DICHLOROETHANE (DCE)

INTRODUCTION

To test the MADAM model for generality, simulation-prediction analyses were performed on independent pilot plant results relative to the removal of 1,2-dichloroethane (DCE) from settled river water (SRW). The Municipal Environmental Research Laboratory (MERL), USEPA, Cincinnati, Ohio, conducted the pilot studies and provided the experimental data used in these analyses. Salient features of the pilot plant investigations, as reported by MERL are summarized below.

Carbon Type

12/40 US sieve size Filtrasorb 400. Carbon particle sizes larger than 12 mesh were screened out and discarded; less than 5% of the particles were smaller than 40 mesh. For the batch experiments, the carbon was washed with organic free water, dried at 105°C, and stored in air-tight screw cap bottles.

Background Solution

Cincinnati Water Works unchlorinated effluent from a 3-day detention reservoir which is fed with "alum dosed" Ohio River water. Average total organic carbon (TOC) was reported to be 1.45 mg/l.

Analysis

Analyses were performed using a purge and trap method similar to that described by Bellar and Lichtenberg (1974); 1,2-dichloropropane was used as an internal standard. GC detector response was recorded graphically and peak height used to measure concentration.

ADSORPTION PROCEDURES

Equilibrium studies for DCE were conducted using the bottle-point technique. Different quantities of 12/40 carbon were

BOTTOM OF IMAGE AREA; OUTSIDE DIMENSION FOR TABLES AND ILLUSTRATIONS
BEGIN LAST LINE OF TEXT
3/8"

PAGE NUMBER
EPA-287 (Cin.)
(4-76)

placed in 224-ml bottles. The bottles were filled with spiked SRW, sealed, and tumbled until equilibrium was achieved. Equilibration time was two weeks.

CMB reactor rate studies were conducted in 1.7-l Biostir bottles (Wheaton) equipped with suspended magnetic stirrers. The bottles were filled, headspace free, with spiked SRW. Weighed and pre-wetted quantities of carbon were transferred to the reactors and the solutions stirred at 500 rpm. Samples of 5-ml volume were withdrawn periodically for analysis and unspiked SRW was added to reestablish a headspace-free condition.

Column studies were performed in 4-cm ID glass columns containing 400 grams of 12 x 40 carbon. The columns were fed with spiked SRW with average DCE concentration of 112, 20, and 200 μg/l and flow rates of 100 ml/min (2 gpm/ft^2 hydraulic loading), 200 ml/min (4 gpm/ft^2), and 50 ml/min (1 gpm/ft^2), respectively.

ADSORPTION EQUILIBRIUM

The Freundlich and the three parameter equations were found to provide the best statistical fits to the experimental equilibrium data for 1,2-dichloroethane. The resulting data and isotherm parameter values are presented in Figure 155 and Table 32.

ADSORPTION RATES

The CMB reactor rate data were subjected to simulation-modeling analysis for determination of appropriate mass transfer coefficients. To minimize the program search, a close control value for the film transfer coefficient, k_f, was estimated from a separate CMB rate experiment in which a large amount of carbon was employed, as discussed in Section 5. The k_f value was then calculated from the slope of the regressed line for the initial rate data presented in Figure 156. Figure 157 illustrates the results of simulaton analysis for a two-parameter search. The estimated coefficients, $k_f = 4.05 \times 10^{-3}$ cm/sec and $D_s = 1.77 \times 10^{-9}$ cm^2/sec, were used to predict the experimental profile represented by the solid line. Figures 158 and 159 represent the results of sensitivity analyses conducted for k_f and D_s, respectively, indicating that external mass transfer is a slightly more significant rate control for adsorption of 1,2-dichloroethane in the CMB reactor system.

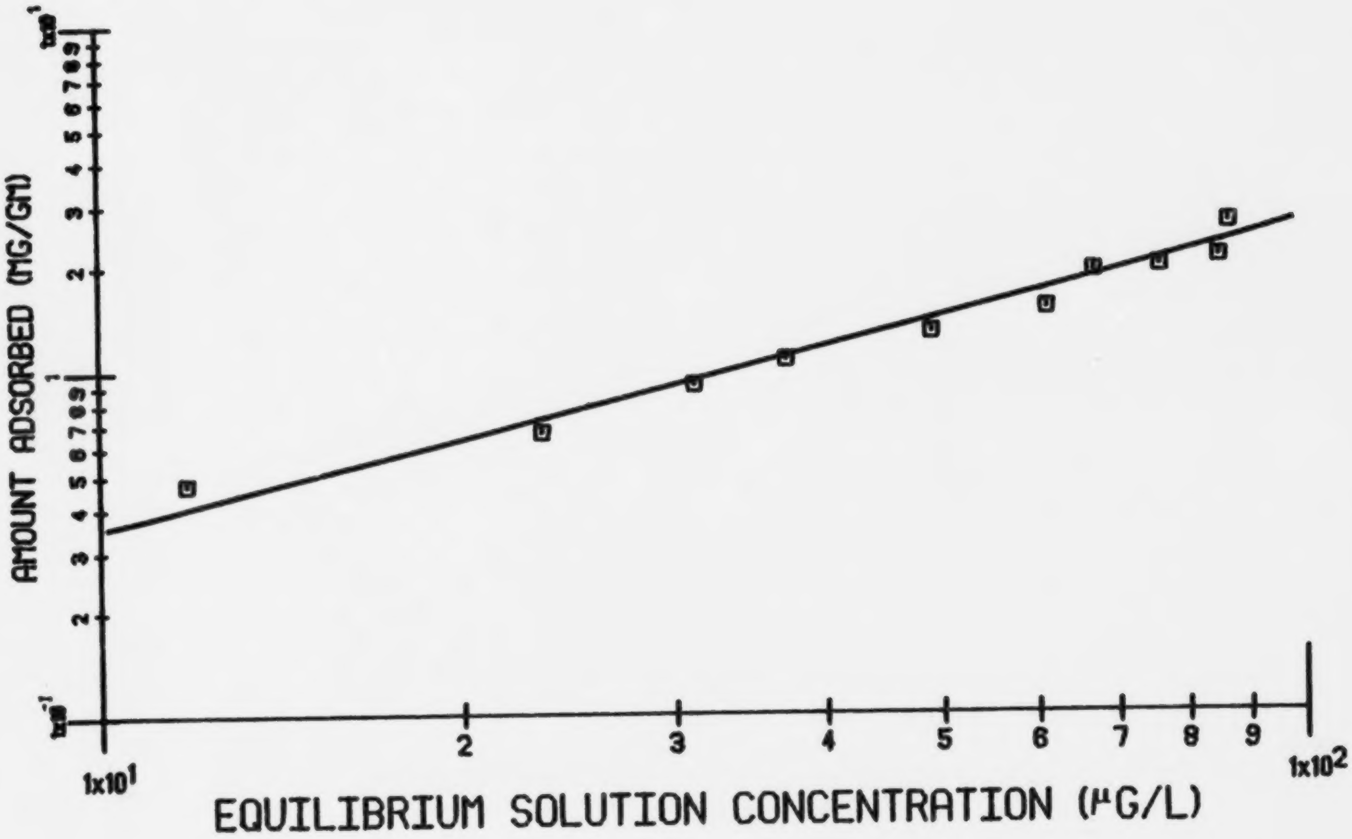

Figure 155. Adsorption isotherm for 1,2-dichloroethane in settled river water (Data provided by MERL, USEPA).

TYPING GUIDE SHEET

TABLE 32: ADSORPTION EQUILIBRIUM STUDIES FOR 1,2-DICHLOROETHANE IN COAGULATED RIVER WATER

(Data provided by MERL, USEPA)

C_e, mg/l	q_{e_1}, mg/gm	q_{e_2}, mg/gm	q_{e_3}, mg/gm
0.0118	0.47	0.42	0.41
0.0233	0.66	0.73	0.72
0.0312	0.90	0.93	0.92
0.0372	1.06	1.08	1.07
0.0491	1.27	1.36	1.35
0.0612	1.48	1.63	1.62
0.067	1.89	1.76	1.74
0.076	1.95	1.95	1.94
0.0851	2.07	2.15	2.13
0.0867	2.6	2.18	2.16

C_e, equilibrium concentration

q_{e_1}, amount adsorbed (experimental data)

q_{e_2}, amount adsorbed (calculated form the Freundlich isotherm)

q_{e_3}, amount adsorbed (calculated from the three parameter isotherm)

Freundlich isotherm: $q_{e_2} = K_f \, C_e^{1/n} = 0.0167 \, C_e^{(0.832)}$

Three parameter isotherm: $q_{e_3} = A \, C_e / (1+BC_e^{\beta}) =$

$$14740 \, C_e / [1+888C_e^{(0.167)}]$$

EPA-287 (Cin.)
(4-76)

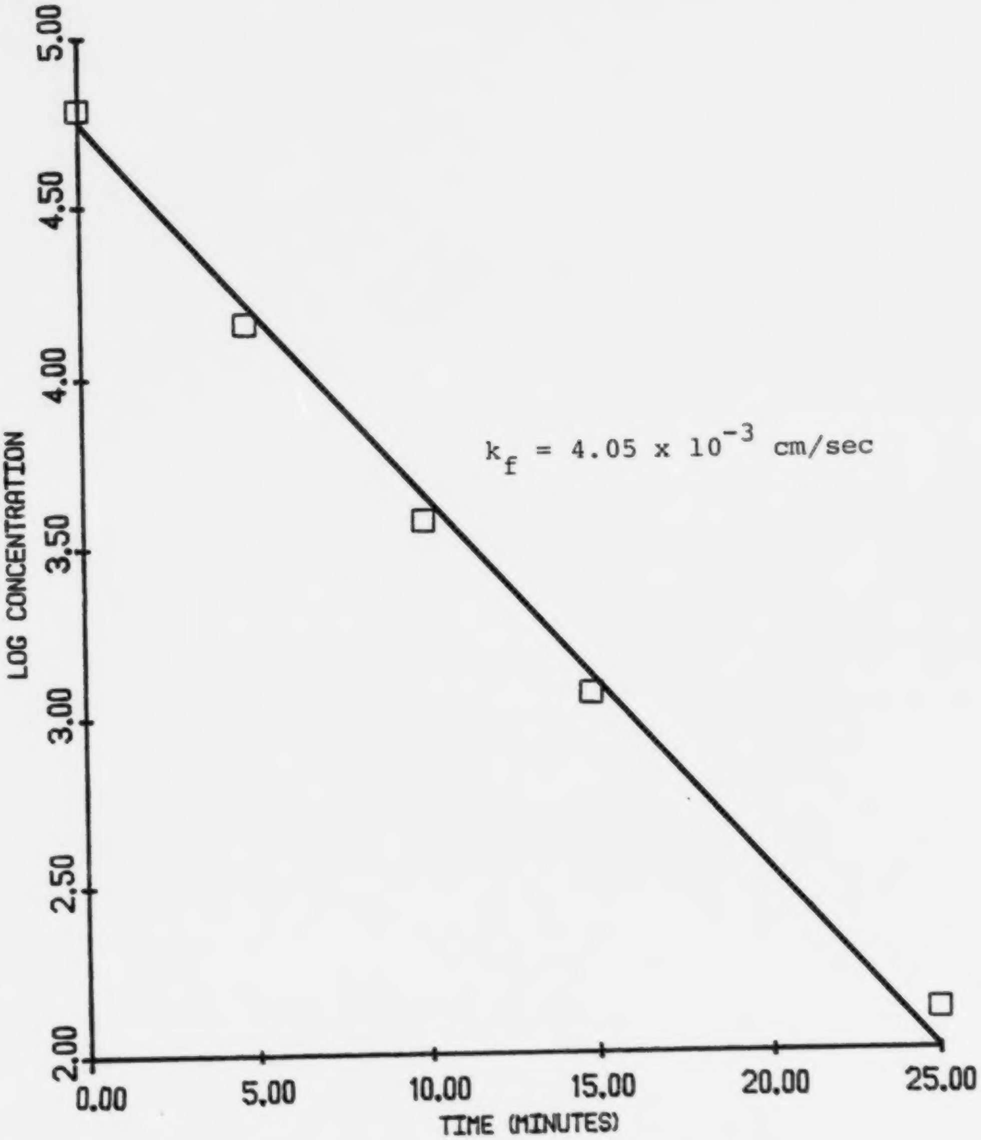

Figure 156. CMB rate study for DCE; estimation of film transfer coefficient, k_f, from the initial stages of rate curve (5.0 g/ℓ of 12/40 carbon) (Data provided by MERL, USEPA).

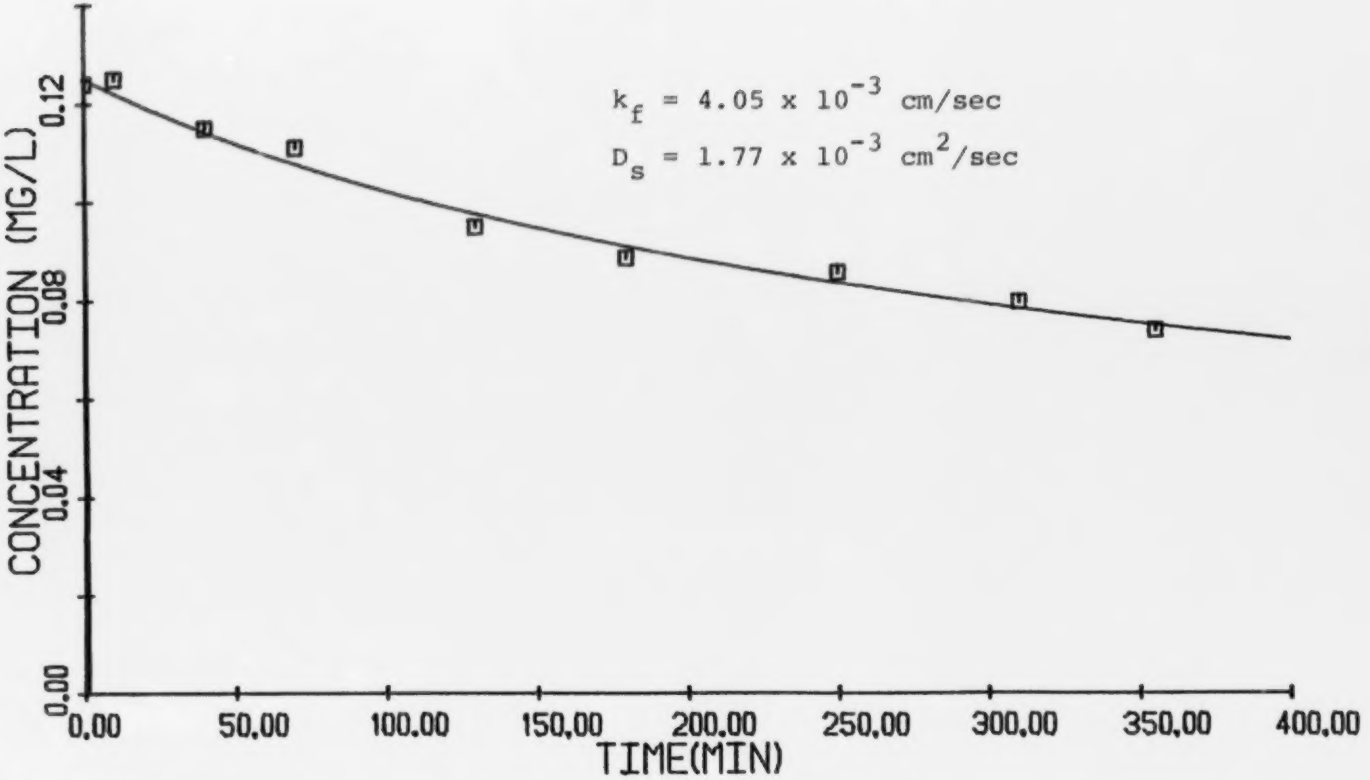

Figure 157. Experimental data and model profile for rate of adsorption of DCE from SRW in a CMB reactor (C_o = 124 μg/ℓ, 0.118 g/ℓ of 12/40 carbon). (Data provided by MERL, USEPA).

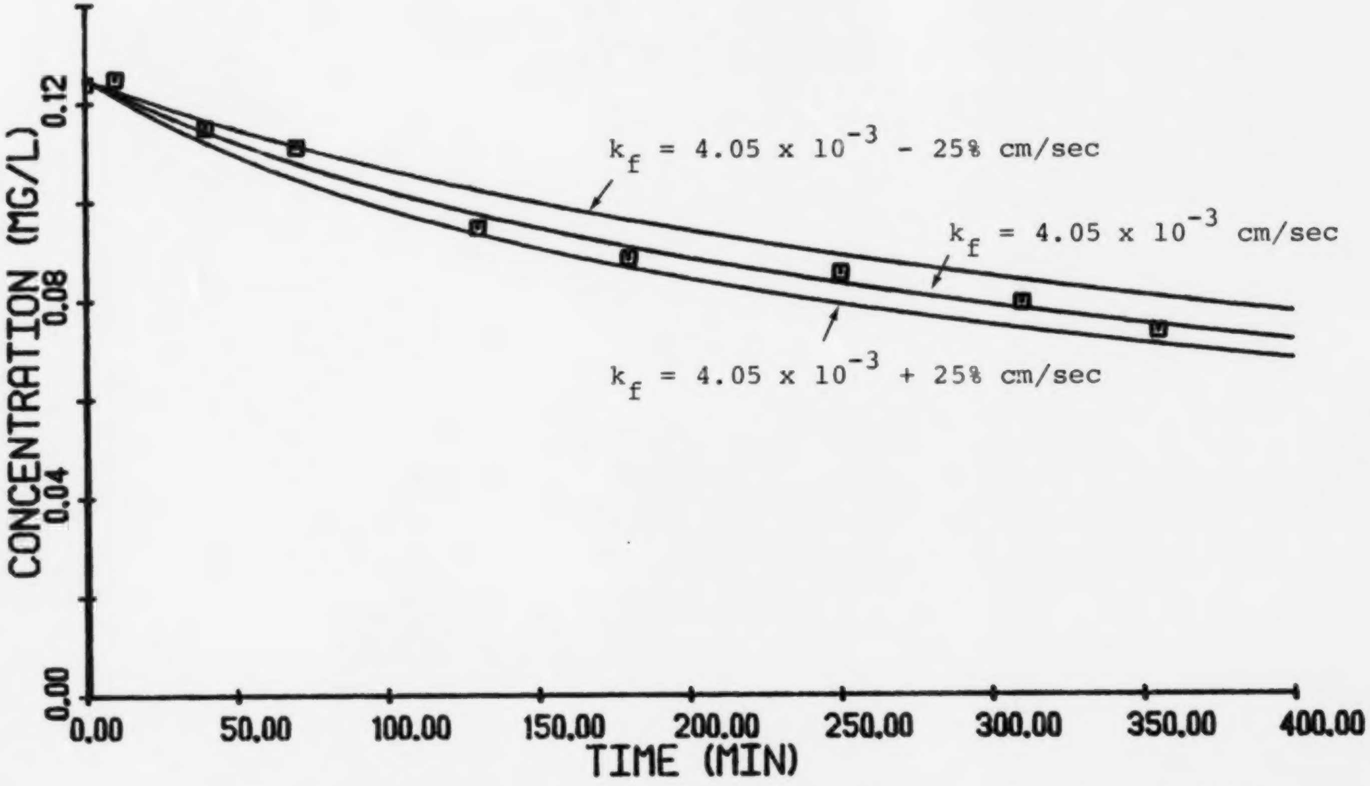

Figure 158 . Analysis of the sensitivity of model profiles to the film transfer coefficient, k_f, for DCE. (Data provided by MERL, USEPA).

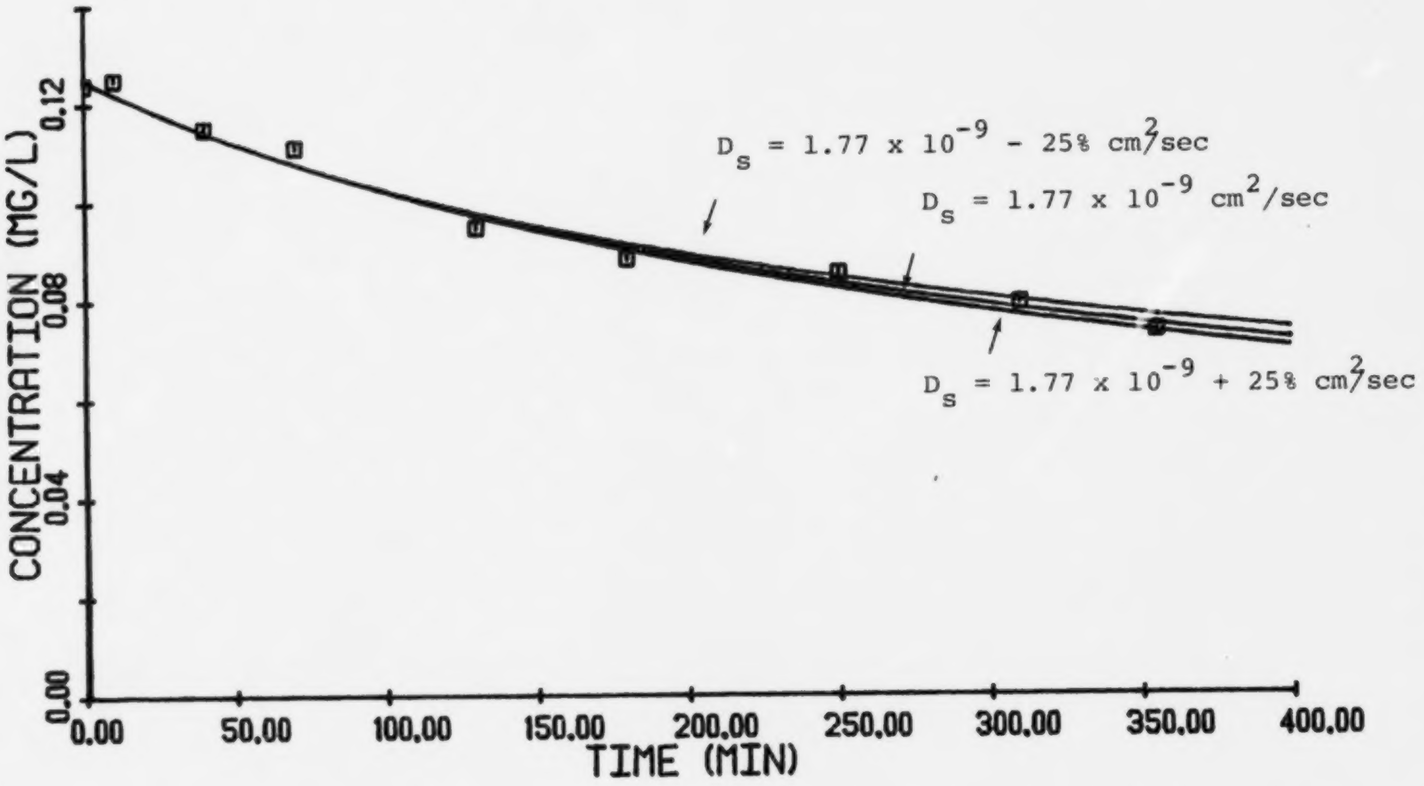

Figure 159. Analysis of the sensitivity of model to the surface diffusion coefficient, D_s, for DCE. (Data provided by MERL, USEPA).

TYPING GUIDE SHEET

ADSORPTION COLUMNS

Simulation modeling analyses were conducted for three sets of experimental conditions. Table 33 summarizes values for the physical and chemical parameters associated with these studies, including values for the surface diffusion coefficient, D_s, and the column film transfer coefficient, k_f. The surface diffusion coefficient was estimated from the CMB-reactor rate tests, and the film transfer coefficients by a correlation technique proposed by Williamson et al (1963).

Model Verification

Experimental data and predictive breakthrough profiles for the fixed-bed pilot-plant adsorbers are presented in Figures 160 through 162. Some disparity between the experimental data and the predicted breakthrough profiles is observed. This is probably in large measure to biodegradation of 1,2-dichloroethane in the carbon columns during the course of operation. MERL reported substantial loss of DCE in the adsorbers during the pilot studies. The results suggest development of a specific microorganism population in the columns different from that of the influent water. Werner et al (1979) reached a similar conclusion in studies of the activated carbon treatment of Rhine River water.

Sensitivity Analyses

Sensitivity analyses with respect to k_f and D_s were conducted for all three runs. Figures through demonstrate deviations in predicted breakthrough profiles for variations of $k_f \pm 25\%$ and $D_s \pm 25\%$. It may be observed that the predictive model displays slightly more sensitivity to D_s than to k_f suggesting that intraparticle diffusion is marginally more significant as the mass transport controlling mechanism for the adsorption of 1,2-dichloroethane in the column adsorbers .

CONCLUSION

The single-solute version of the MADAM model was generally able to simulate and predict the adsorption dynamics of 1,2-dichloroethane in the presence of naturally occurring background organics. Agreement between predicted breakthrough profiles and pilot plant verification data was slightly affected by apparent biodegradation of the DCE over the course of the pilot studies.

EPA-287 (Cin.)
(4-76)

TABLE 33. PARAMETERS USED FOR FIXED-BED ADSORBER PREDICTIVE BREAKTHROUGH PROFILES

Adsorber Run	C_{in}, µg/l	d, cm	L, cm	γ	v, cm/sec	EBCT, min	k_f, cm/sec	D_s, cm²/sec
I (Figure 160)	112	0.106	80	0.4	0.33	10	2.6×10^{-3}	1.77×10^{-9}
II (Figure 161)	20	0.106	80	0.4	0.66	5	3.29×10^{-3}	1.77×10^{-9}
III (Figure 162)	200	0.106	80	0.4	0.17	20	2.05×10^{-3}	1.77×10^{-9}

MERL Reported Parameters

$\overline{C}_{in}$: Average influent concentration;

d : Carbon particle diameter;

L : Bed length;

γ : Bed porpsity, dimensionless;

v : Interstitial velocity; and,

EBCT: Empty bed contact time.

MADAM Determined Parameters

k_f : Column film transfer coefficient; and,

D_s : Intraparticle diffusion coefficient.

TYPING GUIDE SHEET
BEGIN FIRST LINE OF TEXT HERE
DROPPED HEAD: BEGIN SECTIONS HERE
CENTER OF PAGE
TOP OF IMAGE AREA
BEGIN LAST LINE OF TEXT
BOTTOM OF IMAGE AREA: OUTSIDE DIMENSION FOR TABLES AND ILLUSTRATIONS
3/8"
9-1/8"
6-1/2"
PAGE NUMBER
EPA-287 (Cin.)
(4-76)

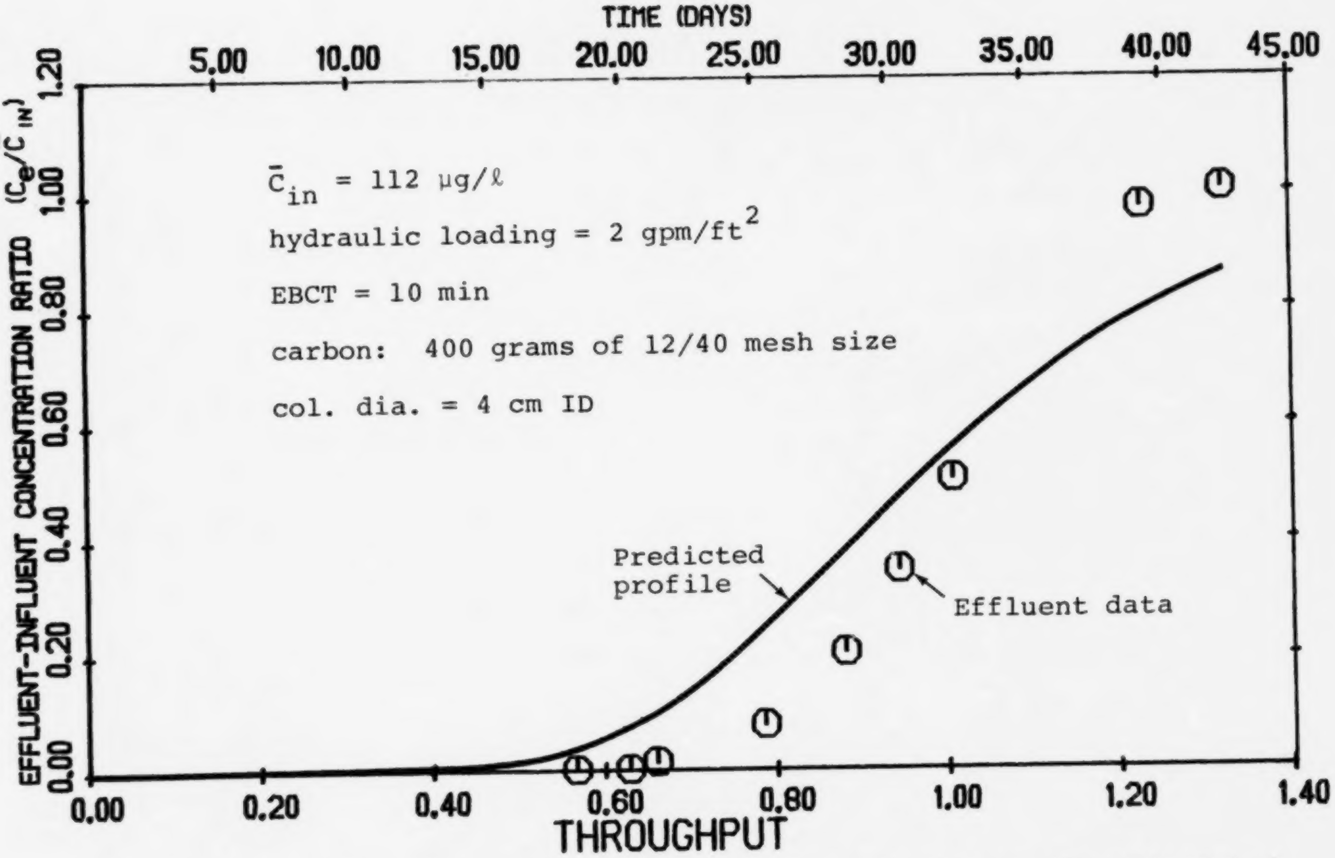

Figure 160. Effluent concentration profiles for DCE in SRW (fixed-bed adsorber Run I). (Data provided by MERL, USEPA).

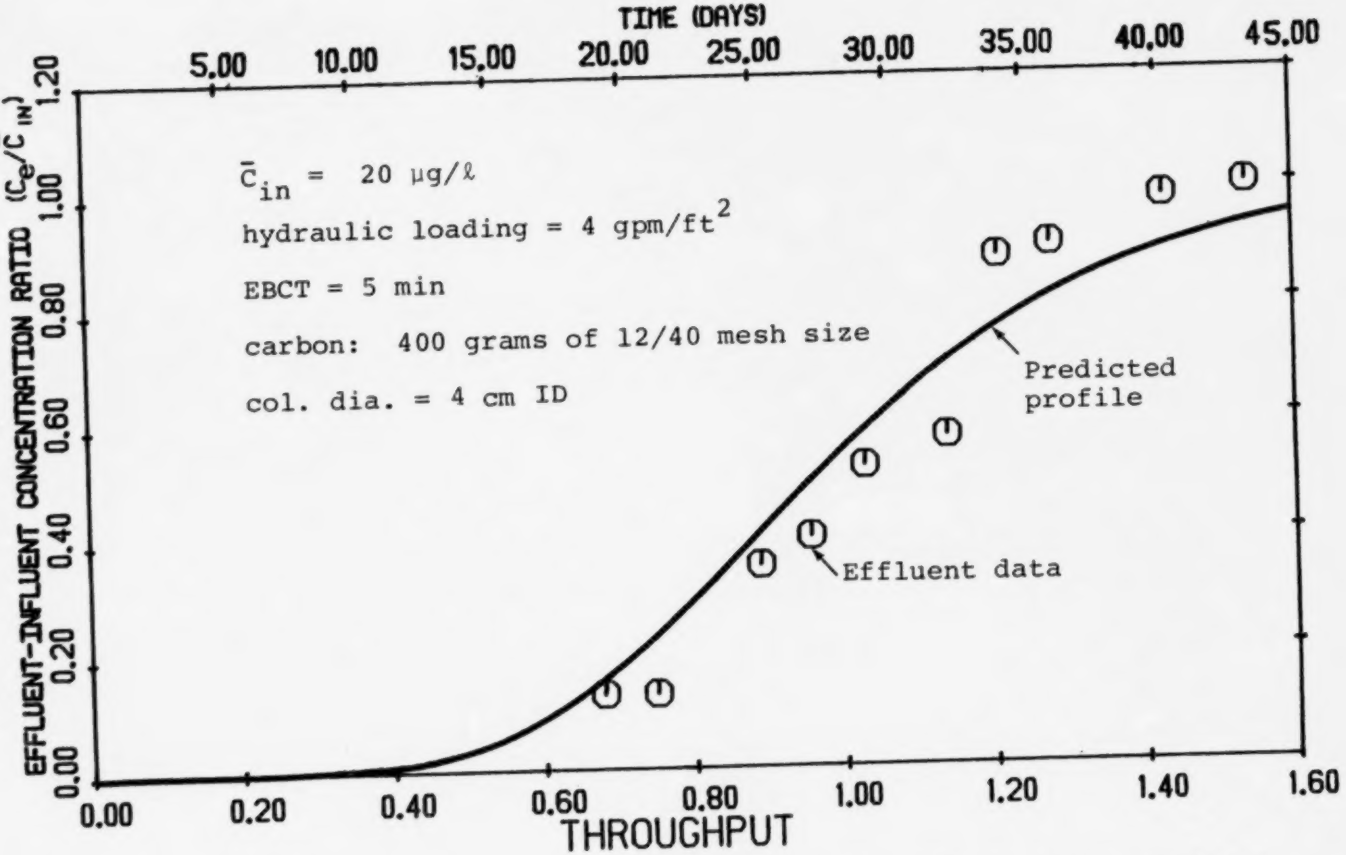

Figure 161. Effluent concentration profiles for DCE in SRW (fixed-bed adsorber Run II). (Data provided by MERL, USEPA).

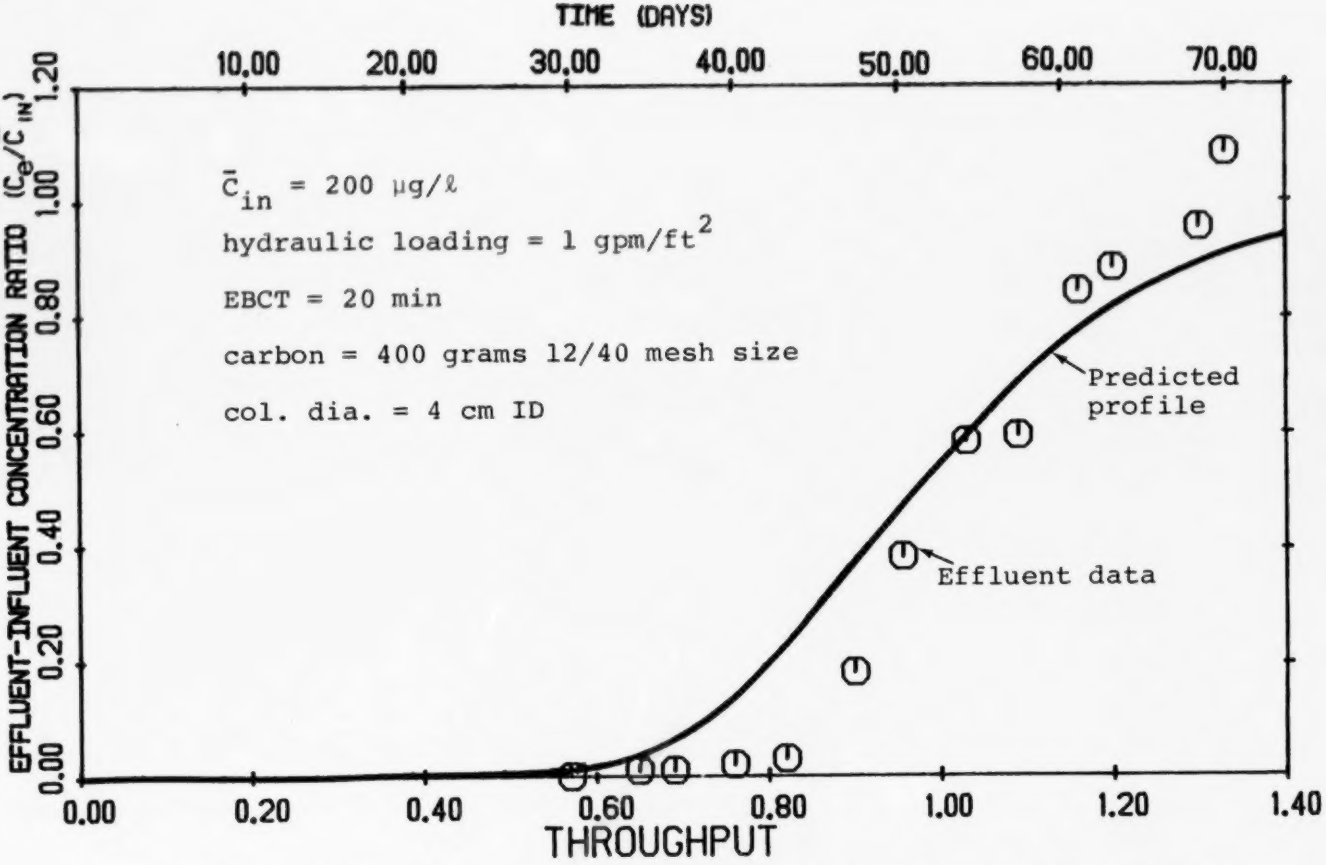

Figure 162. Effluent concentration profiles for DCE in SRW (fixed-bed adsorber Run III). (Data provided by MERL, USEPA).

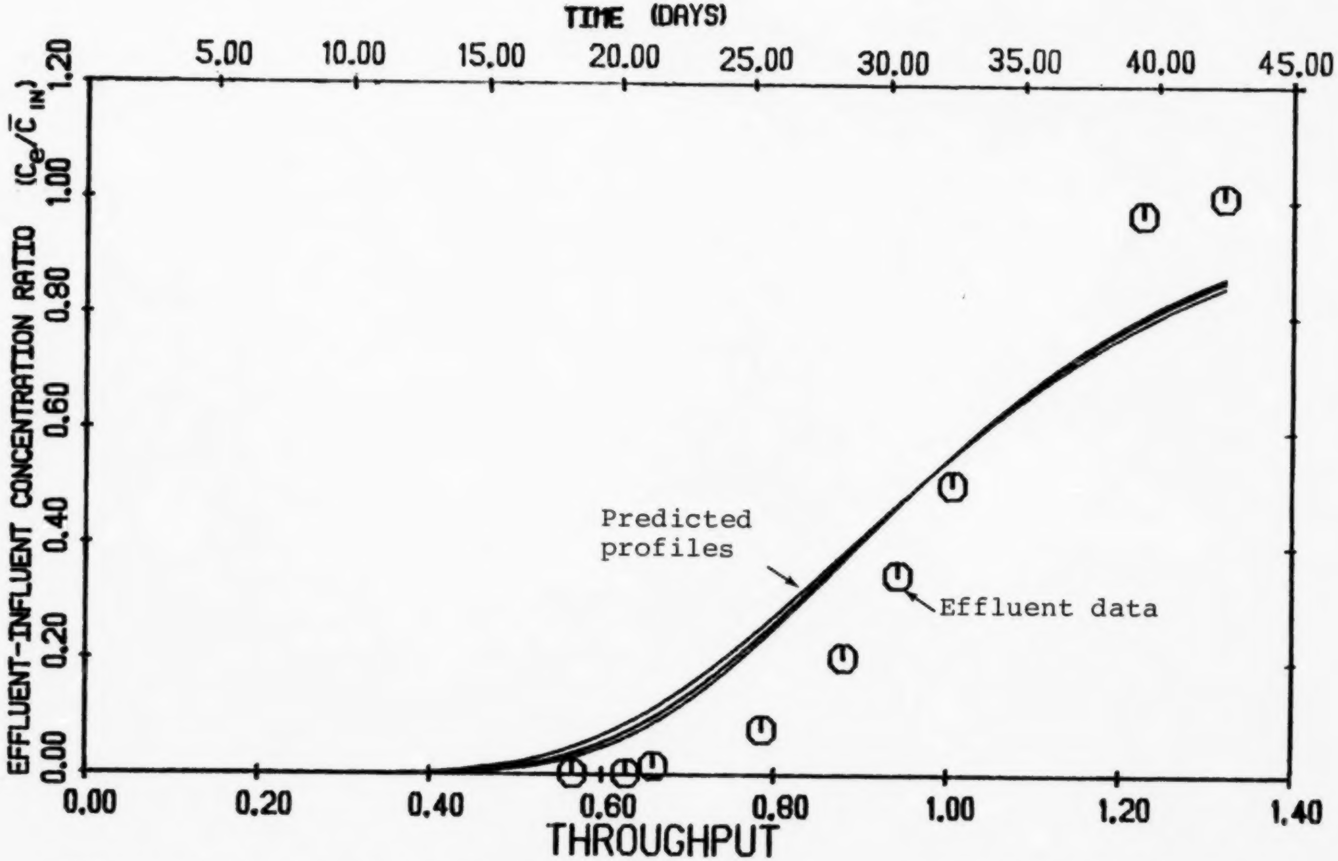

Figure 163. Sensitivity analysis of breakthrough profiles relative to the film transfer coefficient, $k_f \pm 25\%$, for DCE (fixed-bed adsorber Run I). (Data provided by MERL, USEPA).

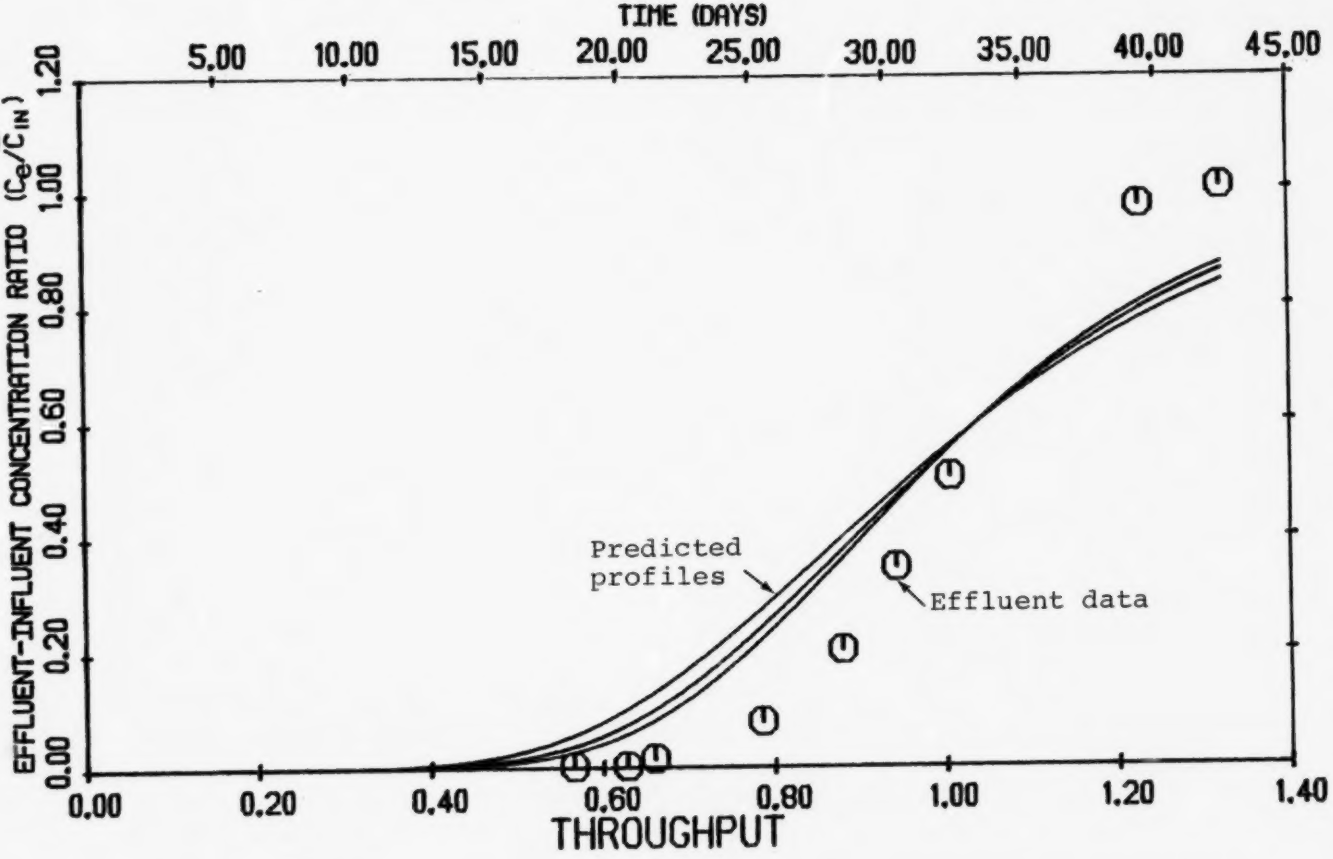

Figure 164. Sensitivity analysis of breakthrough profiles relative to the surface diffusion coefficient, D_s ±25%, for DCE (fixed-bed adsorber Run I). (Data provided by MERL, USEPA).

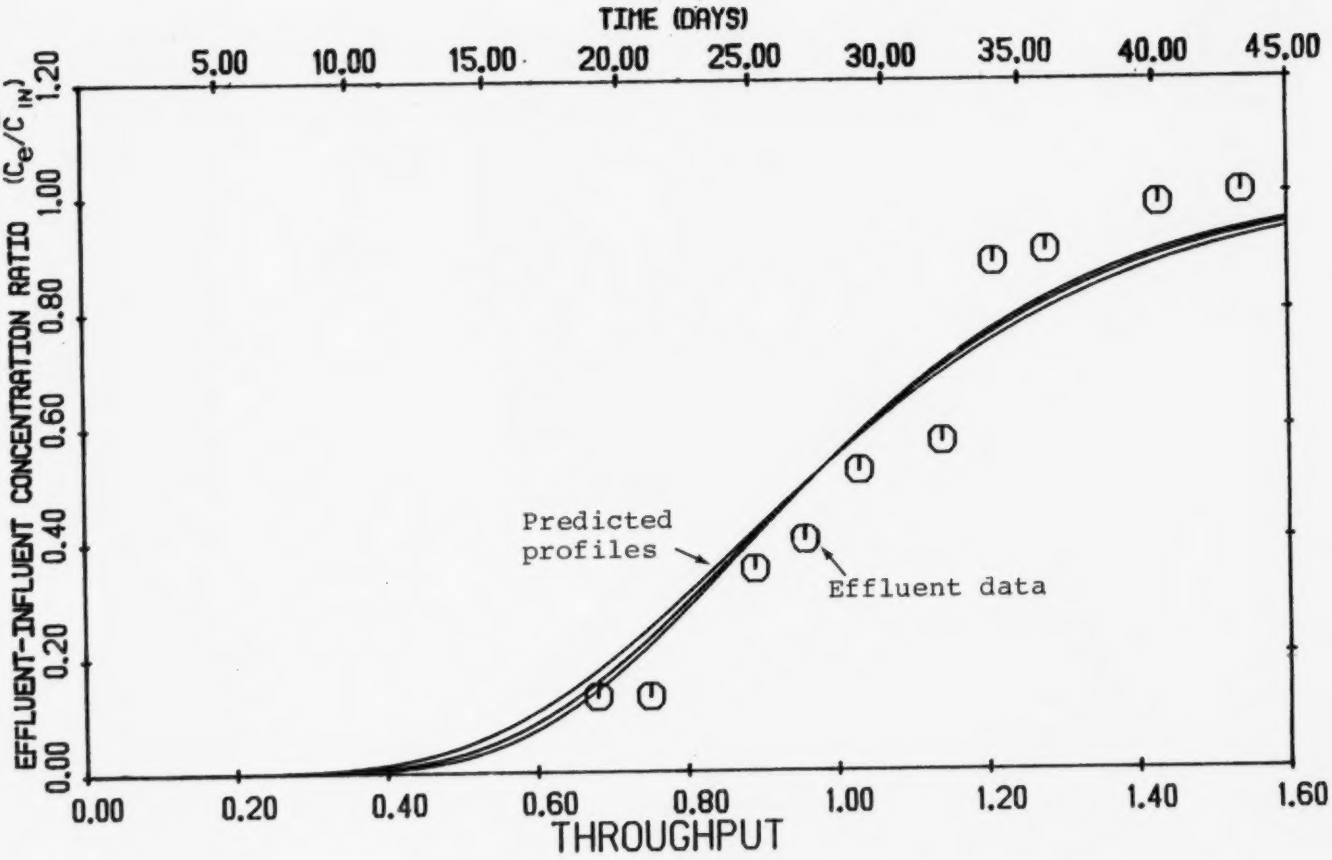

Figure 165. Sensitivity analysis of breakthrough profiles relative to the film diffusion coefficient, $k_f \pm 25\%$, for DCE (fixed-bed adsorber Run II). (Data provided by MERL, USEPA).

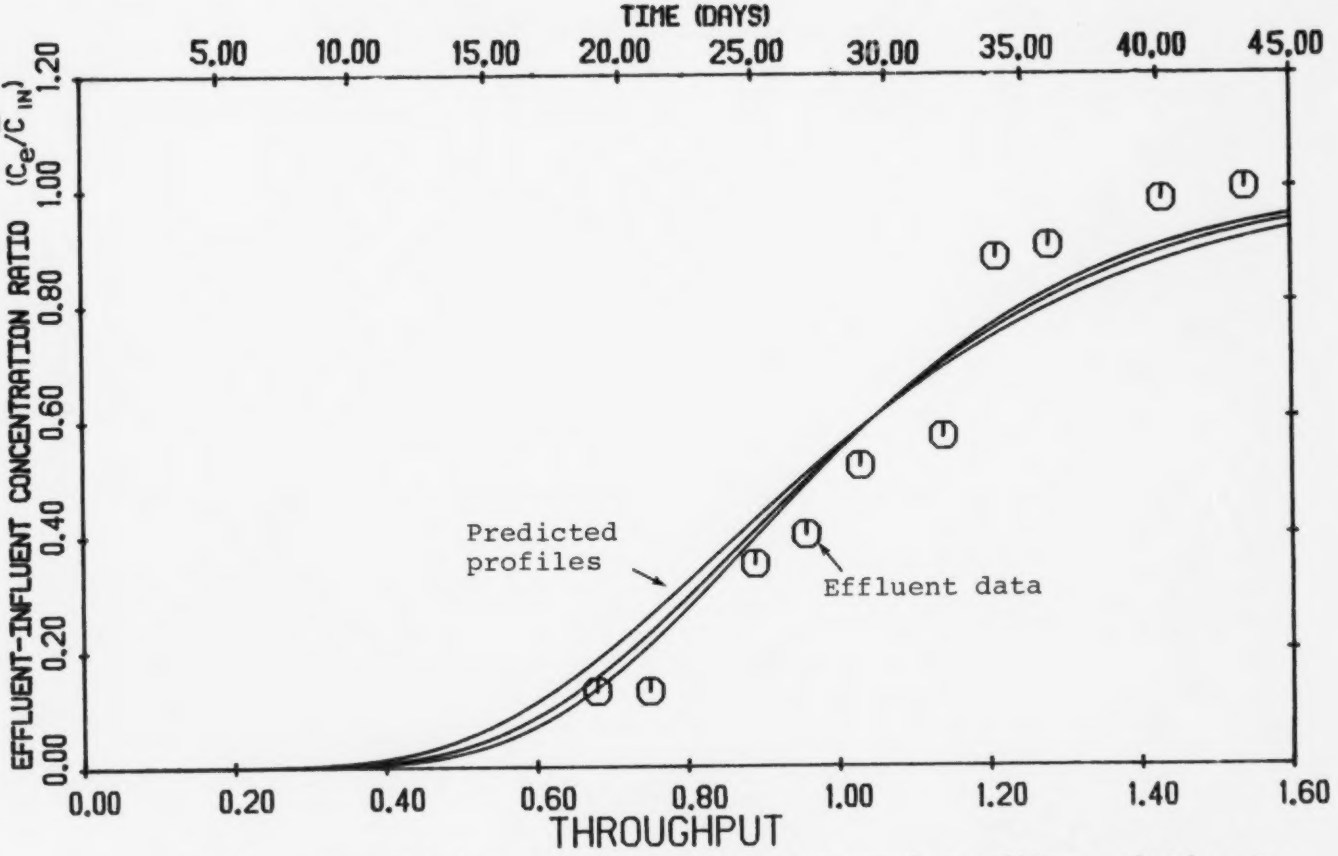

Figure 166. Sensitivity analysis of breakthrough profiles relative to the surface diffusion coefficient, $D_s \pm 25\%$, for DCE, (fixed-bed adsorber Run II). (Data provided by MERL, USEPA).

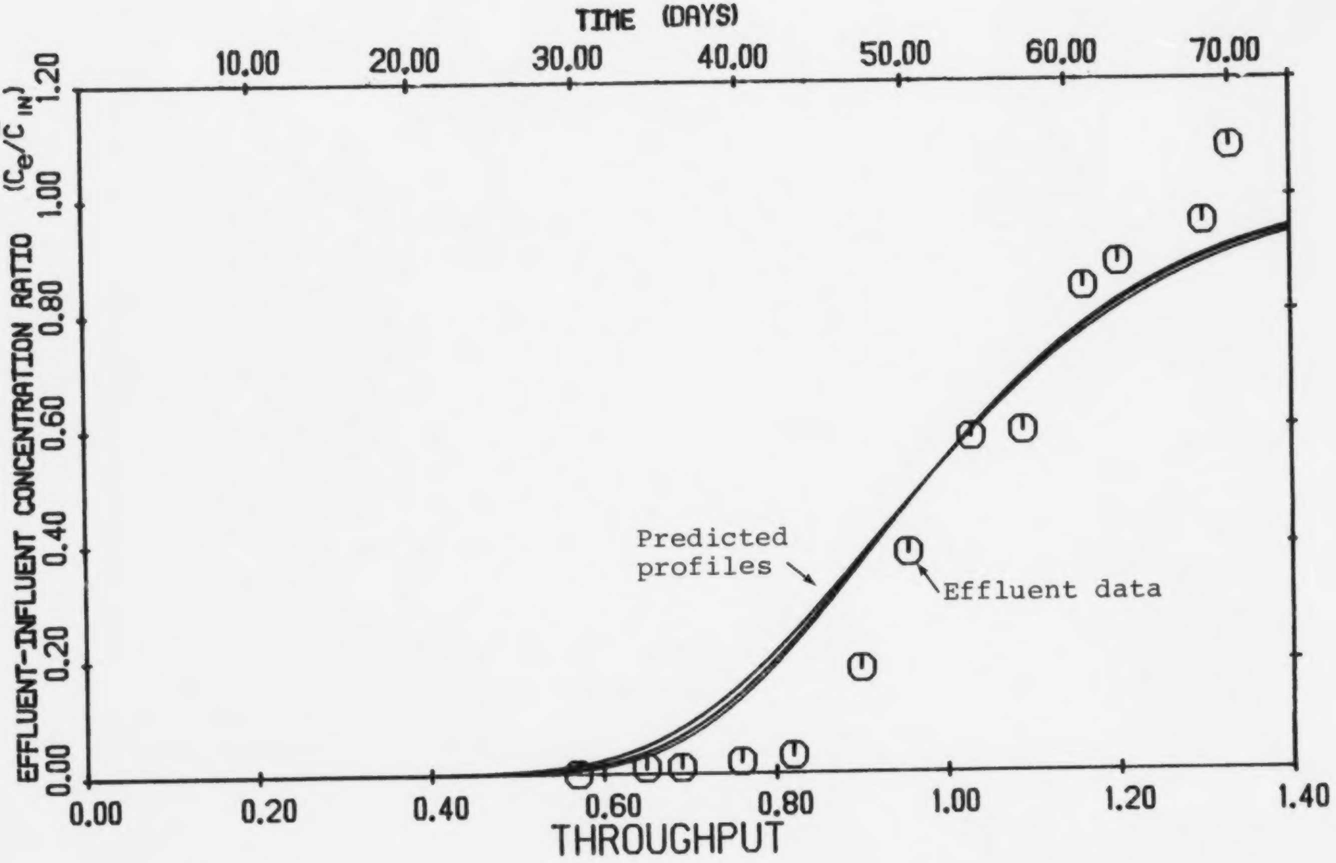

Figure 167. Sensitivity analysis of breakthrough profiles relative to the film diffusion coefficient, k_f +25%, for DCE (fixed-bed adsorber Run III). (Data provided by MERL, USEPA).

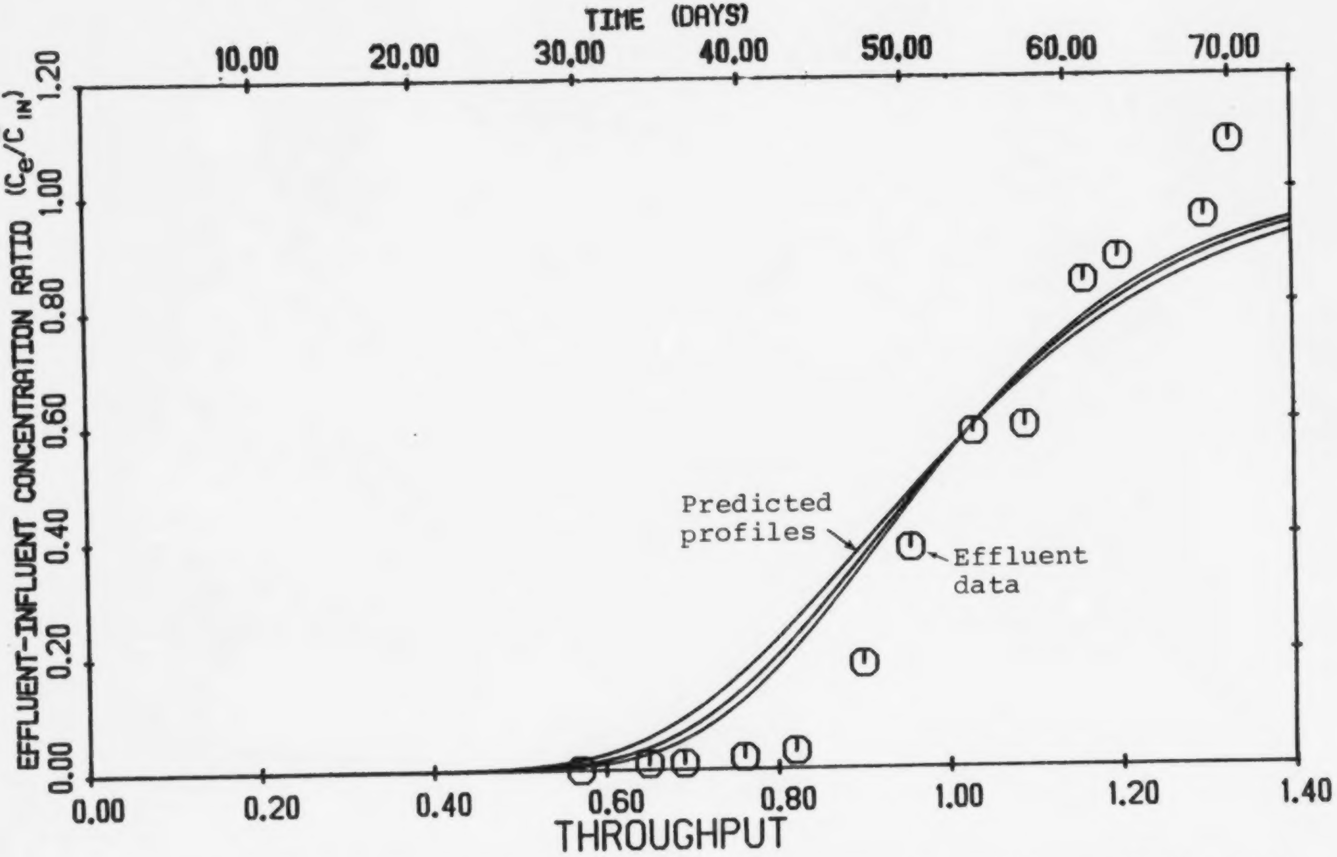

Figure 168. Sensitivity analysis of breakthrough profiles relative to the surface diffusion coefficient, $D_s \pm 25\%$, for DCE (fixed-bed adsorber Run III): (Data provided by MERL, USEPA).

TYPING GUIDE SHEET

REFERENCES

1. Ahmed, A.K., "PCB's in the Environment," *Environment*, *18*(2) (1976).

2. Ahmed, M., and D.D. Focht, "Degradation of Polychlorinated Biphenyls by Two Species of *Achromobacter*," *Can. J. Microbiol.*, *19*:47-52 (1973).

3. Altshuller, A.P., "Average Trospheric Concentration of Carbon Tetrachloride Based on Industrial Production, Usage, and Emissions," *Envi. Sci. and Tech.*, *10*(6):596-598 (1976).

4. Bartlett, A.A., and H.P. Burstyn, "A Review of the Physics of Critical Point Drying," *Proc. of 8th Annual Scanning Election Microscopy Symposium*, O. Johari and I. Corium (eds.) (1975).

5. Bellar, T.A., and J.J. Lichtenberg, "The Determination of Volatile Organic Compounds at the μg/l Level in Water by Gas Chromatography," USEPA, 670/4-74-009, Nov. 1974.

6. Birkmeier, J.L., S.A. LaRocca, and R.E. Haulsee, "Activated Carbon Removes Pesticides from Wastewater at Research Facility," *Industrial Wastes*, Sept./Oct., 1978.

7. Boucher, F.R., and F.G. Lee, "Adsorption of Lindane and Dieldrin Pesticides on Unconsolidated Aquifer Sands," *Envi. Sci. and Tech.*, *6*(6):538-543 (1972).

8. Brooks, G.T., "Chlorinated Insecticides: Retrospect and Prospect," in: *Pesticide Chemistry in the 20th Century*, J.R. Plummer, (ed.), Proceedings of 171st ACS Meeting, New York, N.Y., April 6-8, 1976; American Chemical Society, Washington, D.C. (1977).

9. Cairo, P.R., R.G. Lee, B.S. Aptowiz, and W.M. Blankenship, "Is Your Chlorine Safe to Drink?," *J.AWWA*, *71*(8):450-454, (1979).

10. Chol, W.W., and K.Y. Chen, "Association of Chlorinated Hydrocarbons with Fine particles and Humic Substances in Nearshore Superficial Sediments," *Envi. Sci. and Tech.*, *10*(8):782-786 (1976).

EPA-287 (Cin.)
(4-76)

BEGIN FIRST LINE OF TEXT HERE
TYPING GUIDE SHEET
CENTER OF PAGE
TOP OF IMAGE AREA
DROPPED HEAD: BEGIN SECTIONS HERE

11. Christman, R.F., and M. Ghassemi, "Chemical Nature of Organic Color in Water," J.AWWA, 58(6) (1966).

12. Cohen, H.S., M.L. Freedman, and B.D. Goldstein, "The Problem of Benzene in Our Environment: Clinical and Molecular Considerations," The American Journal of the Medical Sciences, 275(2):124-136 (1978).

13. Coleman, W.E., R.D. Lingg, R.G. Melton, and F.C. Kopfler, "The Occurrence of Volatile Organics in Five Drinking Water Supplies Using Gas Chromatography/Mass Spectrometer (GC/MS)," USEPA Report, June 1975.

14. The Condensed Chemical Dictionary, 8th ed., Van Nostrand Reinhold Co., New York, N.Y. (1971).

15. Coughlin, R.W., and F.S. Ezra, "Role of Surface Acidity in the Adsorption of Organic Pollutants on the Surface of Carbon," Envi. Sci. and Tech. 2(4):291-297 (1968).

16. Crank, J., The Mathematics of Diffusion, Oxford at the Calrendon Press, London, England, (1956).

17. CRC - Handbook of Chemistry and Physics, R.C. Weast (ed.), 57th edition, 1976-1977.

18. Crittenden, J.C., "Mathematic Modeling of Fixed Bed Adsorber Dynamics - Single Component and Multi-Component," Ph.D. Dissertation, The University of Michigan, Ann Arbor, MI (1976).

19. Crittenden, J.C., and W.J. Weber, Jr., "Predictive Model for Design of Fixed-Bed Adsorbers: Parameter Estimation and Model Development," J. Env. Eng. Div., ASCE, 104(EE2), (1978a).

20 Crittenden, J.C., and W.J. Weber, Jr., "Predictive Model for Design of Fixed-Bed Adsorbers: Single - Component Model Verification," J. Env. Eng. Div., ASCE, 104(EE3), (1978b).

21. Crittenden, J.C., and W.J. Weber, Jr., "Model for Design of Multicomponent Adsorption Systems," J. Env. Eng. Div., ASCE, 104(EE6), (1978c).

22. Crosby, D.G., "The Nonmetabolic Deocmpositon of Pesticides," in: Biological Effects of Pesticides in Mammalian Systems, H.F. Kraybill, (ed.), Annals of the New York Academy of Science, 82-96 (1969).

BOTTOM OF IMAGE AREA OUTSIDE DIMENSION FOR TABLES AND ILLUSTRATIONS
BEGIN LAST LINE OF TEXT

PAGE NUMBER
EPA-287 (Cin.)
(4-76)

TYPING GUIDE SHEET
BEGIN FIRST LINE OF TEXT HERE
CENTER OF PAGE
TOP OF IMAGE AREA
DROPPED HEAD. BEGIN SECTIONS HERE

23. Crosby, D.G., "The Photodecomposition of Pesticides in Water," in: Fate of Organic Pesticides in the Aquatic Environment, F.R. Gould, (ed.), Proceedings of 161st ACS Meeting, L.A., Calif., March 29-31, 1971; Advances in Chemistry Series III, Am. Chem. Soc., Washington D.C. 173-188, (1972).

24. DeFerreyra, E.C., J.A. Castro, M.I. Diaz Gomez, N. D'Acosta, C.R. Decastro, and D.M. DeFenos, "Diverse Effects of Antioxidants on Carbon Tetrachloride Hepatotoxicity," Toxicology and Applied Pharmacology, 32:504-512 (1975).

25. Dobbs, R.A., R.H. Wise, and R.B. Dean, "The Use of Ultraviolet Absorbance for Monitoring the Total Organic Carbon Content of Water and Wastewater," Water Research, 6, (1972).

26. Dowty, B., D. Carlisle, J.L. Laseter, and J. Storer, "Halogenated Hydrocarbons in New Orleans Drinking Water and Blood Plasma," Science, 187:75-77 (1975).

27. Dube, D.J., G.D. Verth, and G.F. Lee, "Polychlorinated Biphenyls in Treatment Plant Effluents," J.WPCF, 46(5): 966-972 (1974).

28. Dubinin, M.M., G.M. Plannick, and E.F. Zaternia, "Integrated Study of the Porous Structure of Activated Carbons from Carbonized Sucrose," Carbon, 2:261 (1964).

29. Duggan, R.E., "Pesticide Residues in Foods," in: Biological Effects of Pesticides in Mammalian Systems, H.F. Kraybill (ed.), Annals of the New York Academy of Science, 196-200, (1969).

30. Durham, W.F., "Body Burden of Pesticides in Man," in: Biological Effects of Pesticides in Mammalian Systems, H.F. Kraybill, (ed.), Annals of the New York Academy of Science, 183-195 (1969).

31. Dustman, E.H., and F.L. Stickel, "The Occurrence and Significance of Pesticide Residues in Wild Animals," in: Biological Effects of Pesticides in Mammalian Systems, H.F. Kraybill, (ed.), Annals of the New York Academy of Science, 162-172 (1969).

32. Eichelberger, J.W., and J. J. Lichtenberg, "Persistence of Pesticides in River Water," Envi. Sci. and Tech. 5(6): 541-544 (1971).

33. Ergun, S., "Mass Transfer Rate in Packed Columns - Its Analogy to Pressure Loss," Chemical Engineering Progress, 48(5) (1952).

BOTTOM OF IMAGE AREA; OUTSIDE DIMENSION FOR TABLES AND ILLUSTRATIONS
BEGIN LAST LINE OF TEXT
3/8"

EPA-287 (Cin.)
(4-76)

TYPING GUIDE SHEET

34. Eye, J.D., "Aqueous Transport of Dieldrin Residues in Soils," *J.WPCF*, 40(8) (1968).

35. Fukuto, T.R., and R.L. Metcalf, "Metabolism of Insecticides in Plants and Animals," in: *Biological Effects of Pesticides in Mammalian Systems*, H.F. Kraybill, (ed.), *Annals of the New York Academy of Science*, 97-111 (1969).

36. Furukawa, K., and F. Matsumura, "Microbial Metabolism of Polychlorinated Biphenyls, Studies on the Relative Degradability of Polychlorinated Biphenyl Components by *Alkaligenes* sp.," *J. Agric. Food Chem*. 24(2):251-256 (1976).

37. Furukawa, F., F. Matsumura, and K. Tonomura, "*Alcaligenes* and *Acinetobacter* Strains Capable of Degrading Polychlorinated Biphenyls," *Agric. Biol. Chem.*, 42(3): 543-548 (1978).

38. Furusawa, T., and J.M. Smith, "Fluid-Particle and Intraparticle Mass Transport Rates in Slurries," *Ind. Eng. Chem. Fund.*, 12(2) (1973).

39. Furusawa, T., and J.M. Smith, "Intraparticle Mass Transport in Slurries by Dynamic Adsorption Studies, *AIChE J.* 20(1) (1974).

40. Gaffney, P.E. "Chlorobiphenyls and PCB's: Formation During Chlorination," *J.WPCF*, 49(3):401-404 (1977).

41. Gibson, D.T. "Microbial Degradation of Aromatic Compounds," *Science*, 161:1093-1097 (1968).

42. Gingerich, W.H., L.J. Weber, and R.E. Larson, "Carbon Tetrachloride-Induced Retention of Sulfobromophthalein in the Plasma of Rainbow Trout," *Toxicology and Applied Pharmacology*, 43:147-158 (1978).

43. Gjessing, E.T., *Physical and Chemical Characteristics of Aquatic Humus*, Ann Arbor Science Publishers Inc., Ann Arbor, Mich. (1976).

44. Greene, R., "U.S. Benzene Markets to Face Slower Growth," *Chemical Engineering*, 62-66, Jan. 30, 1978.

45. Grob, K., and G. Grob, "Organic Substances in Potable Water and in its Precursor Part II. Applications in the Area of Zurich," *Journal of Chromatography*, 90:303-313 (1974).

46. Gustafson, G.G., "PCB's - Prevalent and Persistent," *Envi. Sci. and Tech.*, 4(10):814-819 (1970).

EPA-287 (Cin.)
(4-76)

TYPING GUIDE SHEET
BEGIN FIRST LINE OF TEXT HERE
CENTER OF PAGE
TOP OF IMAGE AREA
DROPPED HEAD: BEGIN SECTIONS HERE

47. Hammarstrand, K., "Chloroform in Drinking Water," Varian Instrument Applications, 10(2) (1976).

48. Harding, L.W., Jr., and J.H. Phillips, Jr., "Polychlorinated Biphenyl (PCB) Uptake by Marine Phytoplankton," Marine Biology, 49:103-111 (1978).

49. Hassler, J.W., Activated Carbon, Chemical Publishing Co., New York (1963).

50. Henderson, J. W. , G. R. Peyton, and W.H. Glaze, "A Convenient Liquid-Liquid Extraction Method for the Determination of Halomethanes in Water at the Parts-Per-Billion Level," Chapt. 7, Identification and Analysis of Organic Pollutants in Water, Ann Arbor Science, Ann Arbor, Mich. (1976).

51. Hill, D.W., and P.L. McCarty, "Anaerobic Degradation of Selected Chlorinated Hydrocarbon Pesticides," J.WPCF, 39(8):1259-1277 (1967).

52. Hiraizumi, Y., M. Takahashi, and H. Nishimura, "Adsorption of Polychlorinated Biphenyl onto Sea Bed Sediment, Marine Plankton, and Other Adsorbing Agents," Envi. Sci. and Tech., 13(5):580-584 (1979).

53. Huang, J.C., and C.S. Liao, "Adsorption of Pesticides by Clay Minerals," J. San. Eng. Div., ASCE, 90(SA5):1057-1078 (1970).

54. Hueper, W.C., and W.W. Payne, "Carcinogenic Effects of Adsorbates of Raw and Finished Water Supplies" Am. J. Clin. Path. 39(5):475-481 (1963).

55. Hutzinger, O., S. Safe, and V. Zitko, The Chemistry of PCB's, CRC Press Inc., Cleveland, Ohio (1974).

56. Jager, K.W., "Aldrin, Dieldrin, Endrin, and Telodrin," Elsevier Publishing Co., Amsterdam, Holland, (1970).

57. Jensen, S., R.G. Johnel, M. Olsson, and G. Otherlind, "DDT and PCB in Marine Animals from Swedish Waters," Nature, 224:247-250 (1969).

58. Jolley, R.L., "Chlorination Effects on Organic Constituents in Effluent from Sanitary Sewage Treatment Plants," Ph.D. Dissertation, The University of Tennessee, Knoxville, Tenn. (1973).

BEGIN LAST LINE OF TEXT
BOTTOM OF IMAGE AREA OUTSIDE DIMENSION FOR TABLES AND ILLUSTRATIONS
3/8"

PAGE NUMBER
EPA-287 (Cin.)
(4-76)

TYPING GUIDE SHEET

59. Kaiser, K.L.E., and P.T.S. Wong, "Bacterial Degradation of Polychlorinated Biphenyls I. Identification of Some Metabolic Products from Aroclor 1242," Bulletin of Environmental Contamination and Toxicology, 11:291-296 (1974).

60. Karnovsky, M.J., "A Formaldehyde-Glutaraldehyde Fixative of High Isomolarity for Use in Electron Microscopy," J. Cell. Biology, 27, 137A (1965).

61. Kavanagh, J.T., and W.J. Weber, Jr., "Effect of Adsorbed Iron on the Performance of Activated Carbon," presented at the 51st Annual Conf. of WPCF, Anaheim, Calif., Oct. 16, 1978.

62 Kavanaugh, M.C., G. Toregas, M. Chung, and E.A. Pearson, "Paritculates and Trace Pollutant Removal by Depth Filtration," Prog. Wat. Tech., Pergamon Press, 10(516): 197-215 (1978).

63. Keinath, T.M., and W.J. Weber, Jr., "A Predictive Model for the Design of Fluid Bed Adsorbers," J.WPCF, 40:743 (1968).

64. Khan, S.U., and M. Schnitzer, "The Retention of Hydrophobic Organic Compounds by Humic Acids," Geochimica et Cosmochimica Acta, 36:745-754 (1972).

65. Kinter, W.B., L.S. Merkens, R.H. Janicki, and A.M. Guarino, "Studies on the Mechanism of Toxicity of DDT and Polychlorinated Biphenyls (PCB's): Disruption of Osmoregulation in Marine Fish," Environmental Health Perspectives, 1:169 (1972).

66. Kirk-Othmer, Encyclopedia of Chemical Technology, Vol. 3, The Interscience Encyclopedia, Inc., New York, N.Y., 191-200 (1949).

67. _______, Second Edition, Vol. 5, John Wiley & Sons, Inc. New York, N.Y. (1964).

68. _______, Third Edition, Vol. 3, John Wiley & Sons Inc., New York, N.Y., 744-771 (1978).

69. Kloepfer, R.D., and B.S. Fairless, "Characterization of Organic Components in a Municipal Water Supply," Envi. Sci. and Tech. 6(12):1036 (1972).

70. Kononova, M.M., Soil Organic Matter, Pergamon Press, New York, N.Y. (1961).

EPA-287 (Cin.)
(4-76)

TYPING GUIDE SHEET

71. Kuratsune, M., T. Yoshimura, J. Matsuzaka, and A. Yamaguchi, "Epidemiological Study on Yusho, A Poisoning Caused by Ingestion of Rice Oil Contaminated With a Commercial Brand of Polychlorinated Biphenyls," Environmental Health Perspectives, 1:119 (1972).

72. Lange's Handbook of Chemistry, J.S. Dean (ed.), Twelfth edition (1979).

73. Lichtenstein, P.E., "PCB's and Interactions with Insecticides," Envi. Health Perspectives, 1:151-155 (1972).

74. Linko, R.R., R. Rantomaki, and K. Urpo. "PCB Residues in Plankton and Sediments in the Southwestern Coast of Finland," Bull. Environ. Contam. and Tox., 12(6):733-738 (1974).

75. Mathews, A.P., "Mathematical Modeling of Multicomponent Adsorption in Batch Reactors," Ph.D. Dissertation, The University of Michigan, Ann Arbor, Mich. (1975).

76. Mathews, A.P., and W.J. Weber, Jr., "Mathematical Modeling of Multicomponent Adsorption Kinetics," presented at AIChE Meeting, Los Angeles, Calif., Nov. 1975.

77. Mathews, A.P., and W.J. Weber, Jr., "Effects of External Mass Transfer and Intraparticle Diffusion on Adsorption Rates in Slurry Reactors," in: Water 1976:I Physical, Chemical Wastewater Treatment, G.F. Bennett (ed.), AIChE Symposium Series, 166(73) (1977).

78. Matsumura, F., and G.M. Boush, "Dieldrin: Degradation by Soil Microorganisms," Science, 156:959-961 (1967).

79. Mattson, J.S., and H.B. Mark, Jr., Activated Carbon, Marcel Dekker, Inc. New York (1971).

80. Middleton, F.M., "Organics in Water Supply - The Problem," Proceedings of the 15th Water Quality Conference, University of Illinois at Urbana-Champaign, Ill. (1973).

81. Mieure, J.P., "A Rapid and Sensitive Method for Determining Volatile Organohalides in Drinking Water," J.AWWA, 69(1): 60-62 (1977).

82. Miller, S.S., "Are You Drinking Bio-Refractories Too," Envi. Sci. and Tech., 1(1):14 (1973).

83. Morris, J.C., and B. Baum, "Precursors and Mechanisms of Haloform Formation in the Chlorination of Water Supplies," presented at the Second Conference on Water

EPA-287 (Cin.)
(4-76)

BEGIN FIRST LINE OF TEXT HERE
TYPING GUIDE SHEET
CENTER OF PAGE
TOP OF IMAGE AREA

Chlorination: Environmental Impact and Health Effects, Gatlinburg, Tenn., (1977).

84. Morris, R.L., and L.G. Johnson, "Agricultural Runoff as a Source of Halomethanes in Drinking Water," J.AWWA, 68(9):492-494 (1976).

85. National Cancer Institute (NCI), "Report on the Carcinogenesis Bioassay of Chloroform," Carcinogenesis Program, Division of Cancer Cause and Prevention, Bethesda, Maryland, March 1976.

86. Nicholson, A.A., and O. Meresz, "Organics in Ontario Drinking Water: Part 1. The Occurrence and Determination of Free and Total Potential Haloforms," Ontario Ministry of the Envi. Lab. Service Branch, presented at Pittsburgh Conf. of Anal. Chem. and Appl. Spect. (1976).

87. Nimmo, D.R., P.D. Wilson, R.R. Blackman, and A.J. Wilson, "Polychlorinated Biphenyl Absorbed by Fiddler Crabs and Pink Shrimp," Nature, 231:50-52 (1971).

88. Nisbet, I.C.T., and A.F. Sarafim, "Rates and Routes of Transport of PCB's in the Enviornment," Environment Health Perspectives, 1:21-38 (1972).

89. Nobuyuki, I., H. Nazasaki, A. Masayuki, S. Makura, S. Sugihara, and K. Hirae, "Istopathologic Studies on Liver Tumorigenesis Induced in Mice by Technical Polychlorinated Biphenyls and Its Promoting Effect on Liver Tumors Induced by Benzene Hexachloride," J.U.S. Natl. Cancer Inst. 51(5):1637-1642 (1973).

90. O'brien, R.D., Insecticides: Action and Metabolism, Academic Press, (1967).

91. Ongerth, H.J., D.P. Spath, J. Crook, and A.E. Greenberg, "Public Health Aspects of Organics in Water," J.AWWA 65(7):495-498 (1973).

92. Parducz, B. "Ciliary Movement and Coordination in Ciliates," Int. Rev. Cytol., 39, R70, (1967).

93. Pieffer, R., and J. Happel, "An Analytical Study of Heat and Mass Transfer in Multiparticle Systems at Low Reynolds Numbers" AIChE J. 10:605 (1964).

94. Pierce, R.H., C.E. Olney, and G.T. Felbeck, Jr., 'pp'-DDT Adsorption to Suspended Particulate Matter in Sea Water," Geochemica et Cosmochimica Acta, 38:1061-1073 (1974).

BEGIN LAST LINE OF TEXT
BOTTOM OF IMAGE AREA OUTSIDE DIMENSION FOR TABLES AND ILLUSTRATIONS
PAGE NUMBER
EPA-287 (Cin.)
(4-76)

95. Piet, G.J., and C.F. Morra, "Behavior of Micropollutants in River Water During Bank Filtration," in: *Oxidation Techniques in Drinking Water Treatment*," W. Kuhn, and H. Sontheimer (eds.), USEPA-570/9-79-020 (1979).

96. *Quality Criteria for Water*, U.S. Environmental Protection Agency, Washington D.C., EPA-440/9-76-023 (1976).

97. Radke, C.J., and J.M. Prausnitz, "Thermodynamics of Multi-Solute Adsorption from Dilute Liquid Solutions," *AIChE J.*, 18:761 (1972).

98. Resnick, W., and R.R. White, "Mass Transfer in Systems of Gas and Fluidized Solids," *Chem. Eng. Prog.*, *45*(377), (1949).

99. Risebrough, R.W., P. Rieche, and D.B. Peakall, "Polychlorinated Biphenyls in the Global Ecosystem," *Nature*, *220*:1098-1107 (1968).

100. Robeck, G.G., K.A. Dostal, J.M. Cohen, and J.F. Kreissl, "Effectiveness of Water Treatment Processes in Pesticide Removal," *J.AWWA*, 57(2):181-199 (1965).

101. Rook, J.J., "Formation of Haloforms During Chlorination of Natural Waters," *J. Water Treatment and Examination*, *23*:234-243, (1974).

102. Rook, J.J., "Haloforms in Drinking Water," *J.AWWA*, *68*(3): 168-172 (1976).

103. Rook, J.J., "Chlorination Reactions of Fulvic Acids in Natural Waters," *Envi. Sci. and Tech.*, *11*(5) (1977).

104. Rosene, M.R., R.T. Deithorn, J.R. Lutchko, and N.J. Wagner, "High Pressure Technique for Rapid Screening of Activated Carbons for Use in Potable Water," in: *Activated Carbon Adsorption of Organics from the Aqueous Phase*, I.H. Suffet and M.J. McGuire (eds.) Ann Arbor Science Publishers Inc., Ann Arbor, Mich. (1980).

105. Sayler, G.S., M. Shon, and R.R. Colwell, "Growth of an Estuarine *Pseudomonas* sp. on Polychlorinated Biphenyl," *Microbial Ecology*, *3*:241-255 (1977).

106. Schafer, M.L., J.T. Peeler, W.S. Gardner, and J.E. Campbell "Pesticides in Drinking Water: Waters from the Mississippi and Missouri Rivers," *Env. Sci. and Tech.*, *3*(12):1261-1269 (1969).

107. Schnitzer, M., and S.V. Khan, *Humic Substances in the Environment*, Marcel Dekker Inc., New York, N.Y. (1972).

TYPING GUIDE SHEET

108. Schoor, W.P., "Problems Associated with Low Solubility Compounds in Aquatic Toxicity Tests: Theoretical Model and Solubility Characteristics of A-1254 in Water," Water Research, 9:937-944 (1975)

109. Schwarzenbach, R.P., E. Molnar-Kubica, W. Giger, and S.G. Wakeham, "Distribution, Residence Time, and Fluxes of Tetrachloroethylene and 1,4-Dichlorobenzene in Lake Zurich, Switzerland," Envi. Sci. and Tech., 13(11): 1367-1373 (1979).

110. Shackelford, W.M., and L.H. Keith, "Frequency of Organic Compounds Identified in Water," USEPA, Environmental Research Laboratory, Athens, Georgia, EPA-600/4-76-062, December, 1976.

111. Singh, H.B., D.P. Fowler, and T.O. Peyton, "Atmospheric Carbon Tetrachloride: Another Man-Made Pollutant," Science, 192:1231-1234, (1976).

112. Singh, H.B., L.J. Salas, H. Shigeishi, A.J. Smith, E. Scribner, and L.A. Cavanagh, "Atmospheric Distribution, Sources and Sinks of Selected Halocarbons, Hydrocarbons, SF_6 and N_2O," USEPA, Research Triangle Park, N.C., June 1979.

113. Sissons, D., and D. Welti, "Structural Identification of Polychlorinated Biphenyls in Commercial Mixtures by Gas-Liquid Chromatography, Nuclear Magnetic Resonance and Mass Spectrometry," J. Chromatography, 60(1):15-32 (1971).

114. Smith, J.G., R.B. McCall, and P.K. Chan., "Formation of Polychlorinated Aromatic Compounds During Aqueous Chlorination," Enviornmental Pollution, 14(4) (1977).

115. Snoeyink, V.L., and W.J. Weber, Jr., "The Surface Chemistry of Active Carbon - A Discussion of Structure and Surface Functional Groups," Envi. Sci. and Tech., 1(3): 228 (1967).

116. Steelink, C., "What is Humic Acid?", Proceedings of the California Association of Chemistry Teachers, J. of Chemical Education, 40(7):380 (1963).

117. Stevens, A.A., C.J. Slocum, D.R. Seeger, and G.G. Robeck, "Chlorination of Organics in Drinking Water," J.AWWA, 68(11):615-621 (1976).

118. Stratton, C.L., and J.B. Susebee, Jr., "PCB and PCT Contamination of the Environment near Sites of Manufacture and Use," Envi. Sci. and Tech., 10(13):1229-1233 (1976).

EPA-287 (Cin.)
(4-76)

119. Tardiff, R.G., and M. Deinzer, "Toxicity of Organic Compounds in Drinking Water," *Proceedings of the 15th Water Quality Conference*, University of Illinois at Urbana-Champaign, Ill, (1973).

120. Thoenes, D., and H. Kramers, "Mass Transfer from Spheres in Various Regular Packings to a Flowing Fluid," *Chem. Eng. Sci.* *8*:271 (1958).

121. Thompson, J.F., "Manual of Analytical Methods for the Analysis of Pesticide Residues in Human and Environmental Samples," U.S. Environmental Protection Agency, Environmental Toxicology Division, Research Triangle Park, N.C. (1977).

122. Tinsley, I.J., and R.R. Lowry, "Nutritional Interactions and Organochlorine Insecticide Activity, in: *Biological Effects of Pesticides in Mammalian Systems*, H.F. Kraybill, (ed.), *Annals of the New York Academy of Science*, 291-298 (1969).

123. Thorpe, J.J., "How Much Benzene Causes Cancer?" Hydrocarbon Processing, 172-174, May 1978.

124. Tulp, M.T.M., and O. Hutzinger, "Some Thoughts on Aqueous Solubilities and Partition Coefficients of PCB, and the Mathematical Correlation Between Bioaccumulation and Physicochemical Properties," *Chemosphere*, *10*:849-860 (1978).

125. Ulanoff, D.M., "Adsorption of Polychlorinated Biphenyls by Some Species of Bacteria and Algae from the Saginaw River and Bay," Master's Thesis, Water Resources Science, The University of Michigan, Ann Arbor, Mich. (1979).

126. U.S. Enviornmental Protection Agency, "Effects of Pesticides in Water: A Report to the States," PB-222-320/BA, Washington D.C. (1972).

127. U.S. Environmental Protection Agency, "National Organics Reconnaissance Survey for Halogenated Organics," Water Supply Research Division, Municipal Environmental Research Laboratory, Cincinnati, Ohio (1975).

128. U.S. Environmental Protection Agency, "Preliminary Assessment of Suspected Carcinogens in Drinking Water," Report to Congress, Washington D.C. (1975).

129. U.S. Environmental Protection Agency, "An Ordering of the NIOSH Suspected Carcinogens List - Based Only on Data Contained in the List," EPA-560/1-76-003, Washington D.C., March 1976.

TYPING GUIDE SHEET
BEGIN FIRST LINE OF TEXT HERE
CENTER OF PAGE
TOP OF IMAGE AREA
DROPPED HEAD; BEGIN SECTIONS HERE

130. U.S. Environmental Protection Agency, "PCB's in the United States: Industrial Use and Environmental Distribution, Task I," EPA 560/6-76-005, Washington D.C. (1976).

131. Vieth, G.C., "Baseline Concentrations of Polychlorinated Biphenyls and DDT in Lake Michigan Fish - 1971," *Pest. Mon. J.* 9(1):21-29 (1975).

132. von Rumker, R., E.W. Lawless, A.F. Meiners, K.A. Lawrence, G.L. Kelso, and F. Horay, "Production, Distribution, Use and Environmental Impact Potential of Selected Pesticides," EPA 540/1-74-001, Office of Pesticide Program, USEPA, Washington, D.C. (1975).

133. Ward, P.S., "The Problems Behind the Problem of the Carbon Tet. Spill," *J.WPCF*, 49(4):529-531 (1977).

134. Webb, R.G., and A.C. McCall, "Quantitative PCB Standards for Electron Capture Gas Chromatography," *Journal of Chromatographic Science*, 11(7):366-373 (1973).

135. Weber, J.B., "Interactions of Organic Pesticides with Particulate Matter in Aquatic and Soil Systems," in: *Fate of Organic Pesticides in the Aquatic Environment*, R.F. Gould, (ed.), proceedings of 161st ACS Meeting, L.A., Calif., March 29-31, 1971; Advances in Chemistry Series III, American Chemical Society, Washington D.C. 55-120 (1972a).

136. Weber, W.J., Jr., "Competitive Interactions in Adsorption from Dilute Aqueous Bi-Solute Solutions" *J. Appl. Chem.* 14:568 (1964).

137. Weber, W.J., Jr., *Physicochemical Processes for Water Quality Control*, Wiley-Interscience, New York (1972).

138. Weber, W.J., Jr., "Adsorption Processes" *Pure and Applied Chemistry*, 37(3), (1974).

139. Weber, W.J., Jr., "Notes and Comments," *J.AWWA*, 69(10): 565-566 (1977).

140. Weber, W.J., Jr., "Purification of Industrial Effluents with Activated Carbon, "*Proceedings, NATO Advanced Study Institute: Scientific Aspects of Sorption and Filtration Methods for Water Purification*, Institute for Atomenergi, Kjeller, Norway (1974a).

141. Weber, W.J., Jr., "The Prediction of the Performance of Activated Carbon for Water Treatment," *Activated Carbon in Water Treatment*, The Water Research Association,

BEGIN LAST LINE OF TEXT
BOTTOM OF IMAGE AREA; OUTSIDE DIMENSION FOR TABLES AND ILLUSTRATIONS

PAGE NUMBER
EPA-287 (Cin.)
(4-76)

TYPING GUIDE SHEET

Medmenham, Marlow, Bucks, SL72HD, England (1974b).

142. Weber, W.J., JR., and J.C. Crittenden, "MADAM I - A Numeric Method for Design of Adsorption Systems," J.WPCF 47:5 (1975).

143. Weber, W.J., Jr., and F.A. DiGiano, "Reclamation of Water for Reuse as a Water Resource," paper presented at the International Conference on Water for Peace, Washington D.C., May 23-31, 1967.

144. Weber, W.J., Jr., G.D. Hunt, D.M. Ulanoff, and M. Pirbazari, "Equilibria and Kinetics of Adsorption/Desorption of PCB's on Suspended Solids and Bottom Sediments," presented at Sea Grant Symposium for Toxic Materials and Their Effects on Marine Resources, Madison, Wisconsin, July 11-12, 1979.

145. Weber, W.J., Jr., L.D. Friedman, and R. Bloom, Jr., "Biologically Extended Physicochemical Treatment," presented at the Sixth International Conference of Advances in Water Pollution Research, Jerusalem, Israel, June 8-23, 1972; Advances in Water Pollution Research, S.H. Jenkins (ed.), Pergamon Press, Oxford, New York, (1973).

146. Weber, W.J., Jr., and K.T. Liu, "Determination of Mass Transport Parameters for Fixed-Bed Adsorbers," accepted for publication in Chemical Engineering Communication, (in press), 1980.

147. Weber, W.J., Jr., and J.C. Morris, "Kinetics of Adsorption on Carbon from Solution," J. San. Eng. Div., ASCE, 89(SA2) (1963).

148. Weber, W.J., Jr., and J.C. Morris, "Equilibria and Capacities for Adsorption on Carbon" J. San. Eng. Div., ASCE, 90(SA3) (1964).

149. Weber, W.J., JR., M. Pirbazari, and M.D. Herbett, "Removal of Halogenated Organic and THM Precusor Compounds from Water by Activated Carbon," Proceedings of Annual AWWA Conference, Atlantic City, N.J. (1978).

150. Weber, W.J., Jr., M. Pirbazari, M.D. Herbert, and R. Thompson, "Effectiveness of Activated Carbon for Removal of Volatile Halogenated Hydrocarbons from Drinking Water," Chapter 8, in: Viruses and Trace Contaminants in Water and Wastewater, Ann Arbor Science, Ann Arbor, Mich. (1977).

EPA-287 (Cin.)
(4-76)

TYPING GUIDE SHEET

151. Weber, W.J., Jr., M. Pirbazari, and G.L. Melson, "Biological Growth on Activated Carbon: An Investigation by Scanning Electron Microscopy," Envi. Sci. and Tech., 12(7):817-819, (1978).

152. Weber, W.J., Jr., J.D. Sherrill, M. Pirbazari, C.G. Uchrin, and T.Y. Lo, "Transport and Differential Accumulation of Toxic Substances in River - Harbor - Lake Systems," in: Dynamics, Exposure and Hazard Assessment of Toxic Chemicals, R. Haque (ed.), Ann Arbor Science Publishers, Ann Arbor, Mich. (1980).

153. Weber, W.J., Jr., and P.J. Usinowicz, "Adsorption from Aqueous Solution" Proj. No. 17020 EPF, USEPA, June 1973.

154. Weber, W.J., Jr., and B.M. van Vliet, "Fundamental Concepts for Application of Activated Carbon in Water and Wastewater Treatment," in: Activated Carbon Adsorption of Organics from the Aqueous Phase, Vol. 1, I.H. Suffet, and M.I. McGuire (eds.), Ann Arbor Science, Ann Arbor, Mich. (1980).

155. Weber, W.J., Jr., and W. Ying, "Integrated Biological and Physicochemical Treatment for Reclamation of Wastewater," presented at Int. Conf. on Advanced Treatment and Reclamation of Wastewater, Johannesburg, South Africa, June 1977; Progress in Water Technology, Pergamon Press Ltd., 10(1/2) (1978).

156. Werner, P., M. Klotz, and R. Schweisfurth, "Microbiological Studies on Activated Carbon Filtration," in: Oxidation Techniques in Drinking Water Treatment, W. Kuhn and H. Sontheimer (eds.), Karlsruhe, FRG, 1978, U.S. Environmental Protection Agency, EPA-570/9-79-020, (1979).

157. Wershaw, R.L., P.J. Burcar, and M.C. Goldberg, "Interaction of Pesticides with Natural Organic Material," Envi. Sci. and Tech., 3(3):271-273 (1969).

158. Westlake, W.E., and F.A. Gunther, "Organic Pesticides in the Environment," in: Occurrence and Mode of Introduction of Pesticides in the Environment, R.F. Gould, (ed.), American Chemical Society, Washington D.C., 110-121 (1966).

159. Wheeler, W.B., "Experimental Absorption of Dieldrin by Chlorella," J. Agr. Food Chem., 18(3):416-419 (1970).

160. Wilke, C.R., and P. Chang, "Correlation of Diffusion Coefficients in Dilute Solutions, Amer. Inst. Chem.

Engr. J., 1:264 (1955).

161. William, T.C., C.C. Capen, L. Kasza, C. Carter, and R.E. Dailey, "Effects of PCB on the Thyroid Gland of Rats: Ultrastructure and Biochemical Investigation," Am. J. Path., 89(1):119-136 (1977).

162. Williamson, J.E., K.E. Bazaire, and C.J. Geankopolis, "Liquid-Phase Mass Transfer at Low Reynolds Numbers," Ind. Eng. Chem. Fund., 2(2):126 (1963).

163. Wolff, W.F., "The Structure of Gas-Adsorbent Carbons," J. Phys. Chem. 62:829 (1958).

164. Wolff, W.F., "A Model of Active Carbon," J. Phys. Chem. 63:653 (1959).

165. Ying, W., "Investigation and Modeling of Bio-Physicochemical Processes in Activated Carbon Columns," Ph.D. Dissertation, The University of Michigan, Ann Arbor, Michigan, (1978).

166. Ying, W., and W.J. Weber, Jr., "Bio-Physicochemical Adsorption Systems Model," J.WPCF, 51(11), (1979).

167. Zavon, M.R., R. Tye, and L. Latorre, "Chlorinated Hydrocarbon Insecticide Content on the Neonate," in: Biological Effects of Pesticides in Mammalian Systems, H.F. Kraybill, (ed.), Annals of the New York Academy of Science, 196-200 (1969).

168. Zettlemoyer, A.C., "Modern Techniques for Investigating Interactions with Surfaces," Chem. Rev. 59:937 (1959).

BEGIN FIRST LINE OF TEXT HERE
TYPING GUIDE SHEET
CENTER OF PAGE
TOP OF IMAGE AREA
DROPPED HEAD BEGIN SECTIONS HERE

APPENDIX A

PHYSICAL PROPERTIES OF FILTRASORB 400 ACTIVATED CARBON*

Total surface area (N_2, BET Method), m^2/gm	1050-1200
Bulk density, lbs/ft^3	25
Particle density wetted in water, g/cc	1.3 - 1.4
Pore volume, cc/g	0.94
Effective size, mm	0.55-0.65
Uniformity coefficient	1.6 - 2.1
U.S. Standard Series Sieve Size:	
Larger than No. 12	Max. 5%
Smaller than No. 40	Max. 5%
Mean particle diameter, mm	0.9 - 1.1
Iodine Number, min.	1000
Abrasion Number, min.	75
Moisture content, max.	2.0%

*SOURCE Calgon Corporation, "Filtrasorb 300 and 400 for Wastewater Treatment", Activated Carbon Product Bulletin 20-2e, 1976.

BOTTOM OF IMAGE AREA OUTSIDE DIMENSION FOR TABLES AND ILLUSTRATIONS
BEGIN LAST LINE OF TEXT
3/8"

PAGE NUMBER
EPA-287 (Cin.)
(4-76)

APPENDIX B

COMPUTER PROGRAM USED TO ESTIMATE EQUILIBRIUM CONSTANTS FOR THE THREE PARAMETER ISOTHERM MODEL

```
C      THIS PROGRAM ESTIMATES THE THREE PARAMETER
C      ISOTHERM CONSTANTS BY THE BEST STATISTICAL
C      REPRESENTATION OF THE EXPERIMENTAL DATA...
C
C
C.....MAIN PROGRAM......
       IMPLICIT REAL*8 (A-H,O-Z)
       DIMENSION X(3),Y(3),ID(18)
       COMMON C(50),Q(50),SCALE(3),PENALT,M
       EXTERNAL F
       NAMELIST / DATA / PENALT, HO, TO, IO, M, IPRIN, SCALE, C,
      1 Q, X
1      READ(5,DATA,END=999)
       N = 3
       WRITE(6,1000) ID
1000   FORMAT(18A4)
       DO 60 I=1,N
       X(I)=X(I)*SCALE(I)
 60    CONTINUE
       CALL PRAXIS(TO,HO,N,IPRIN,X,F,FMIN)
       WRITE(6,4) FMIN
 4     FORMAT(' FMIN=',E10.4)
       WRITE(6,5)
 5     FORMAT(//10X,'C',10X,'Q EXP',8X,'Q CALC')
       WRITE(6,6)
 6     FORMAT(8X,'MMOLES/L',4X,'MMOLES/GM',4X,'MMOLES/GM')
       DO 50 I=1,N
       X(I)=X(I)/SCALE(I)
 50    CONTINUE
       DO 30 I=1,M
       C2=X(1)*C(I)/(1.D0+X(2)*(C(I)**X(3)))
       WRITE(6,7) C(I),Q(I),C2
 7     FORMAT(7X,E10.4,2X,E10.4,3X,E10.4)
 30    CONTINUE
       WRITE(6,8)
8      FORMAT(' ', 9X, 'A', 12X, 'B', 12X, 'BETA')
       WRITE(6,7) X
       GO TO 1
999    CALL EXIT
       END
C
       REAL FUNCTION F(X,N)
       IMPLICIT REAL*8 (A-H,O-Z)
       DIMENSION X(3),Y(3)
       COMMON C(50),Q(50),SCALE(3),PENALT,M
C
C
C.... ESTIMATION OF ISOTHERM CONSTANTS......
       F=0.D0
       DO 12 I=1,N
       IF(X(I)) 11,12,12
 11    F=PENALT*PENALT*(1.-X(I))
```

```
      GO TO 630
12    CONTINUE
      IF(X(3)-1.D0) 15,15,16
16    F=PENALT*X(3)
      GO TO 630
15    DO 20 I=1,N
      Y(I)=X(I)/SCALE(I)
20    CONTINUE
      DO 10 I=1,M
      F=F+((Q(I)-Y(1)*C(I)/(1.D0+Y(2)*(C(I)**Y(3))))/Q(I))**2
10    CONTINUE
630   RETURN
      END
```

APPENDIX C

COMPUTER PROGRAM USED TO ESTIMATE FILM TRANSFER AND SURFACE DIFFUSION COEFFICIENTS FROM FINITE-BATH CMB RATE DATA

```
C     THIS PROGRAM ESTIMATES THE EXTERNAL MASS
C     TRANSFER COEFFICIENT, KF, AND INTERNAL MASS
C     TRANSFER COEFFICIENT, DS, USING THE IMPLICIT
C     FINITE DIFFERENCE METHOD OF CRANK-NICHOLSON.
C     THE PROGRAM SEARCHES FOR BEST VALUES OF THE
C     KF AND DS WITHIN CERTAIN SPECIFIED CONSTRAINTS
C     GIVEN BY INITIAL ESTIMATES FOR THESE VARIABLES....
C     FREUNDLICH ISOTHERM MODEL DESCRIBES THE
C     EXPERIMENTAL EQUILIBRIUM DATA....
C
C
C     IPRIN=1 PRINTS PARAMETER AND FMIN VALUES IN PRAXIS....
      IMPLICIT REAL*8(A-H,O-Z)
      DIMENSION X(2),ID(18),ETIME(50),CC(50),CE(50),XL(2),XR(2),
     *SCALE(2)
      COMMON ETIME,CC,CE,XL,XR,SCALE,PENALT,ID,L,N2,LPRIN,LO,LP
      EXTERNAL F
C
C.....READ IN EXPERIMENTAL DATA.....
C.....SPECIFY RATE DATA AT INTEGER MULTIPLES OF TIME STEP....
1     FORMAT(18A4)
2     FORMAT(I3)
      READ(5,7) PENALT
7     FORMAT(E9.4)
      READ(5,2) LPRIN
      READ(5,2) LP
      READ(5,1) ID
      READ(5,4) TO,HO,IPRIN
      READ(5,2) N2
4     FORMAT(E9.4,1X,E9.4,1X,I1)
      READ(5,6) X(1),X(2)
6     FORMAT(E9.4,1X,E9.4)
      READ(5,6) XL(1),XR(1)
      READ(5,6) XL(2),XR(2)
      READ(5,6) SCALE(1),SCALE(2)
      READ(5,3) (ETIME(I),CE(I),I=1,N2)
3     FORMAT(E10.4,1X,E9.4)
      NN=2
      L=1
      LO=1
      CC(1)=CE(1)
      DO 620 I=1,NN
      X(I)=X(I)*SCALE(I)
      XL(I)=XL(I)*SCALE(I)
      XR(I)=XR(I)*SCALE(I)
620   CONTINUE
C
      WRITE(6,104) TO,HO
```

```
104    FORMAT(//10X,'TO=',E10.4,/10X,'HO=',E10.4)
       WRITE(6,111) SCALE(1),SCALE(2)
111    FORMAT(//10X,'SCALE(1)=',E10.4,/10X,'SCALE(2)=',E10.4)
       WRITE(6,112) IPRIN, LPRIN
112    FORMAT(//10X,'IPRIN=',I1,/10X,'LPRIN=',I1)
       WRITE(5,113) XL(1),XR(1)
113    FORMAT(//10X,'XL(1)=',E10.4,/10X,'XR(1)=',E10.4)
       WRITE(6,114) XL(2),XR(2)
114    FORMAT(/10X,'XL(2)=',E10.4,/10X,'XR(2)=',E10.4)
C
C.....CALL SUBROUTINE PRAXIS FOR MINIMIZATION...
       CALL PRAXIS(TO,HO,NN,IPRIN,X,F,FMIN)
       WRITE(6,105) FMIN
105    FORMAT(1X,'FMIN=',E10.4)
C
C      PRINT CALCULATED VALUES WITH ESTIMATED COEFFICIENTS...
       WRITE(6,101)
101    FORMAT('1')
       WRITE(6,102) ID
102    FORMAT(//10X,18A4)
       X(1)=X(1)/SCALE(1)
       X(2)=X(2)/SCALE(2)
       WRITE(6,609) X(1), X(2)
609    FORMAT(//10X,'DIFFUSION COEFFICIENT=',E10.4,'     CM/SEC'/10X,'FILM
      * TRANSFER COEFFICIENT=',E10.4,' CM/SEC')
       WRITE(6,106)
106    FORMAT(//8X,'TIME',10X,'C EXP',8X,'C CALC')
       WRITE(6,107)
107    FORMAT(8X,'MIN',9X,'    MG/L',8X,'    MG/L')
       WRITE(6,108) (ETIME(I),CE(I),CC(I),I=1,M2)
108    FORMAT(4X,E10.4,6X,E10.4,3X,E10.4)
       WRITE(6,608) L
608    FORMAT(//10X,'NUMBER OF CALLS FOR SOLVE=',I3)
       STOP
       END
       REAL FUNCTION F(X,NN)
C      FUNCTION TO BE MINIMIZED IS SUM OF SQUARES OF DEVIATIONS...
C.....SUBJECT TO NON-NEGATIVE CONSTRAINTS.....
C
       IMPLICIT REAL*8(A-H,O-Z)
       DIMENSION X(2),ETIME(50),CC(50),CE(50),XL(2),XR(2),ID(18),SCALE(2)
      *,XP1(50),XP2(50),CP(50)
       COMMON ETIME,CC,CE,XL,XR,SCALE,PENALT,ID,L,M2,LPRIN,LO,LP
       IF(L .EQ. 1) GO TO 15
       DO 10 I=1,NN
       IF(X(I)) 7,7,8
7      C1=PENALT*PENALT*(1.-X(I))
       GO TO 630
8      DIF=XL(I)-X(I)
       IF(DIF) 10,10,11
11     C1=PENALT*(1.+DIF*PENALT)
       IF(I .NE. NN) GO TO 10
       GO TO 630
10     CONTINUE
       DO 30 I=1,NN
       IF(X(I)) 9,9,14
9      C1=PENALT*PENALT*(1.-X(I))
       GO TO 630
14     DIF=X(I)-XR(I)
       IF(DIF) 30,30,12
```

```
12     C1=PENALT*(1.+DIF*PENALT)
       GO TO 630
30     CONTINUE
15     CALL SOLVE(ETIME,CC,CE,X,SCALE,ID,L,M2,LPRIN)
       C1=0.0D0
       DO 20 I=1,M2
       C1=C1+((CC(I)-CE(I))/CE(I))**2
20     CONTINUE
       L1=L-L0
       XP1(L1)=X(1)/SCALE(1)
       XP2(L1)=X(2)/SCALE(2)
       CP(L1)=C1
       WRITE(6,641) XP1(L1),XP2(L1),CP(L1)
641    FORMAT(//10X,'X(1)=',E10.4,/10X,'X(2)=',E10.4,/10X,'FMIN=',E10.4)
630    F=C1
       IF(L1 .NE. LP) GO TO 640
       L0=L0+LP
       WRITE(6,631)
631    FORMAT(//10X,'X(1)',10X,'X(2)',10X,'FMIN')
       WRITE(6,632) (XP1(I),XP2(I),CP(I),I=1,LP)
632    FORMAT(5X,E10.4,4X,E10.4,4X,E10.4)
       IF(CP(LP)-CP(1)) 640,634,634
634    WRITE(6,635)
635    FORMAT(/5X,'TYPE IN 1 IF CONSTRAINTS ARE TO BE CHANGED,'/5X,'ELSE
      *TYPE IN 0 AND RETURN')
640    RETURN
       END
C
       SUBROUTINE SOLVE(ETIME,CC,CE,X,SCALE,ID,L,M2,LPRIN)
       IMPLICIT REAL*8(A-H,O-Z)
       DIMENSION X(2), Y(2),ETIME(50),CC(50),CE(50),IPERM(50),ID(50),
      1SCALE(2)
       Y(1)=X(1)/SCALE(1)
       Y(2)=X(2)/SCALE(2)
       IF(L .NE. 1) GO TO 400
C
C.....READ IN CONSTANTS......
       READ(5,1) AI,BI,RAD
1      FORMAT(E9.4,1X,E9.4,1X,E9.4)
       READ(5,2) N,M
2      FORMAT(I3,1X,I3)
       READ(5,3) CI,V1,W
3      FORMAT(E9.4,1X,E9.4,1X,E9.4)
       READ(5,4)DELX,DTIME
4      FORMAT(E9.4,1X,E9.4)
       READ(5,4) RHC, VOID
       READ(5,7) NPR,LPR
 7      FORMAT(I3,1X,I1)
C
C.....WRITE INPUT DATA .......
       WRITE(6,101)
101    FORMAT('1')
       WRITE(6,102) ID
102    FORMAT(//10X,18A4)
       WRITE(6,103) Y(1),Y(2),AI,BI,RAD
103    FORMAT(//10X,'DIFFUSION COEFFICIENT=',E10.4,'   CM/SEC',/10X,'FILM
      1 TRANSFER COEFFICIENT=',E10.4,'CM/SEC',/10X,'EQUILIBRIUM CONSTANT
      2A=',E10.4,/10X,'EQUILIBRIUM CONSTANT B=',E10.4,/10X,
      3'RADIUS OF PARTICLE=',E10.4,'CM')
       WRITE(6,104) DTIME
```

```
104   FORMAT(/10X,'TIME STEP DELT=',E10.4,'MIN')
      WRITE(6,105) CI,V1,W
105   FORMAT(//10X,'INITIAL CONCENTRATION=',E10.4,'   MG/L',/10X,'VOLUME
     *OF REACTOR=',E10.4,'LITERS',/10X,'WEIGHT OF CARBON=',E10.4,'GM')
C
 400   CONTINUE
      IF(LPR .NE. 1) GO TO 830
      NPR1=NPR+1
830   Q=0.0D0
      CS=0.0D0
      QS=0.0D0
      C=CI
      COLD=CI
      QOLD=0.0D0
      V=V1
      AP=3./RAD
      Y(1)=Y(1)*AP*60.
      Y(2)=Y(2)*AP*60./(1000.*RHO*(1.-VOID))
      TIME=0.0D0
      L1=2
      LET=ETIME(L1)
      DO 120 K=2,N
      TIME=DTIME*(K-1)
C
      Q=QOLD+Y(2)*(COLD-CS)*DTIME
      C=COLD-W*(Q-QOLD)/V
      LT=TIME
      IF((TIME-LT)-0.5) 811,811,812
812   LT=LT+1
811   IF(LT .NE. LET) GO TO 700
      CC(L1)=C
      L1=L1+1
      LET=ETIME(L1)
      IF((ETIME(L1)-LET)-0.5D0) 700,814,814
814   LET=LET+1
700   CONTINUE
C
C.....COMPUTATION OF EQUILIBRIUM SURFACE CONCENTRATION....
      QS=(Q-QOLD)/(DTIME*Y(1))+QOLD
      QS=QS/1000.
      CS=(QS/AI)**(1./BI)
C
      IF(LPR .NE. 1) GO TO 920
      IF(K .NE. 2) GO TO 820
      WRITE(6,101)
      WRITE(6,102) ID
      WRITE(6,115)
115   FORMAT(//10X,'TIME',3X,'C CALC',5X,'Q CALC',7X,'CS',9X,'QS',/
     1 10X,'MIN',8X,'  MG/L',4X,'   MG/GM',3X,'   MG/L',4X,'   GM/GM')
      WRITE(6,116) TIME,C,Q,CS,QS
820   IF(K .NE. NPR1) GO TO 920
      WRITE(6,116) TIME,C,Q,CS,QS
116   FORMAT(6X,F10.4,4X,E10.4,1X,E10.4,1X,E10.4,1X,E10.4)
      NPR1=NPR1+NPR
920   COLD=C
      QOLD=Q
120   CONTINUE
      IF(L .NE. 1) GO TO 640
      WRITE(6,101)
      WRITE(6,102) ID
      WRITE(6,206)
206   FORMAT(//8X,'TIME',10X,'C EXP',8X,'C CALC')
      WRITE(6,207)
207   FORMAT(8X,'MIN',9X,'   MG/L',8X,'   MG/L')
      WRITE(6,208) (ETIME(I),CE(I),CC(I),I=1,N2)
208   FORMAT(4X,F10.4,6X,E10.4,3X,E10.4)
640   L=L+1
      RETURN
      END
```

□

APPENDIX D

CONPUTER PROGRAM USED TO SIMULATE BREAKTHROUGH BEHAVIOR FOR SINGLE-COMPONENT SYSTEMS

```
C       THIS PROGRAM SOLVES THE PDE'S THAT DESCRIBE  THE ADSORPTION
C       IN FIXED BEDS.  THE ASSUMPTIONS INCORPORATED  IN THESE NONSTEADY-
C       STATE EQUATIONS ARE: 1.  SOLID PHASE DIFFUSION CONTROLS THE
C       INTRAPARTICLE RATE OF UPTAKE; HENCE, THE DIFFUSION COEFFICIENT
C       IS TAKEN TO BE CONCENTRATION INDEPENDENT.  2.  LAMINAR BOUNDARY
C       LAYER THEORY DESCRIBES THE LIQUID PHASE MASS TRANFER RATE.  3.
C       PLUG FLOW DESCRIBES THE FLUID MOTION IN THE FIXED BED.  4.  THE
C       THREE PARAMETER ISOTHERM DESCRIBES THE EQUILIBRIUM.  5.  EQUILI-
C       BRIUM IS INSTANTANEOUS AT THE PARTICLE SURFACE.
C            THE RESPECTIVE PDE'S ARE SOLVED BY FINITE DIFFERENCE METHODS.
C       THE USER IS LIMITED TO 25 RADIAL STEPS AND TO 100 BED STEPS.
C
C
        IMPLICIT REAL*8(A-H, O-Z)
        DIMENSION AC(25), BQ(3), CDQ(25), BETAQ(26), GAMMAQ(26),
       1 DQ(26),C(101,26), ANP1(26), THPT(201), IMAGE(1400),C(101),
       2 CDS1(201), QP1(201), CS(101), XNAME(10), CIN(100), TDATA(100),
       4 CD(100), CP1(100), TIN(100), CDS2(201), CDS3(201)
        NAMELIST / DATA / NDR, NDT, DS, TAU,AP, XKF,VOID, DG, IPRINT
       1 ,NDZ,      AR, XL, F, CO, A, B, BEXP, XNAME, DUR, PRI, ISTOP,
       2 NDATA, CIN, TDATA, CD, TIN, IMODE, NIN, DCINF
        COMMON CIN, TIN, INF, NIN
1       READ(5, DATA, END = 999)
        DS1 = DS
        XKF1 = XKF
C       WRITE(7,DATA)
C
C       UNITS AND NOTATION LIST
C
C       XNAME - HEADING FOR OUTPUT
C       A, B, BEXP, - ISOTHERM PARAMETERS
C       AP - DIAMETER OF THE PARTICLE, CM
C       AR = CROSS SECTIONAL AREA OF THE REACTOR (SQ CM)
C       CO - INLET CONCENTRATION MUST BE CONSISTANT WITH ISOTHERM
C       CIN - INFLUENT CONCENTRATION DATA
C       CINF - LINEAR INTERPOLATING INFLUENT CONCENTRATION TIME FUNCTION
C       PARAMETERS
C       DG = SOLUTE PARTITION NUMBER RHO*QINF*(1. - VOID)/(VOID*CO)
C       DS - SURFACE OR SOLID DIFFUSION, SQ CM/SEC
C       DUR - DURATION OF BREAKTHROUGH, MASS THROUGHPUT
        DO 500 NDS=1, 3
C       DS= (.75 + (NDS - 1)*.25)*DS1
        XKF= (1.25 - (NDS - 1)*.25)*XKF1
2       DR = 1./DFLOAT(NDR)
        DT = DUR/DFLOAT(NDT)
        DZ = 1./DFLOAT(NDZ)
C       F = THE FLOW RATE ML/MIN
```

```
C      FMIN - VALUE OF THER OBJECTIVE FUNCTION
C      IPRINT - NO. OF POINTS SAVED FOR PRINTING OR PLOTTING, MUST BE
C      ISTOP - STOPS EXECUTION AFTER CALCULATING F'S(ISTOP=1)
C      INTENDED TO ALLOW USER TO CHECK FOR A SINGULAR MATRIX
C      DIVISIBLE INTO NDT
C      INF - COUNTER FOR INFLUENT CONCENTRATION GENERATION FUNCTION
       INF = 1
C      NDR - NUMBER OF RADIAL STEPS, MAXIMUM ALLOWED IS 20
C      NDT - NUMBER OF TIME STEPS
C      NDZ - NO. OF BED STEPS, MAXIMUM ALLOWED  IS 20
C      OBJFUN - OBJECTIVE FUNCTION
C      PRI - PRINT INTERMEDIATE POINTS, 1 = ON,
C      TAU - RESIDENCE TIME, MIN
C      TDATA - THROUGHPUT OF THE DATA POINTS
C      VOID - VOID FRACTION OF THE BED
C      XKF - FILM TRANSFER COEFFICIENT, CM/ SEC
C      XL = LENGTH OF ADSORBER , CM
       XLC = XKF*AP/DS
       XNS = DS*TAU*DG*60./(AP*AP)
       NDR1 = NDR + 1
       NDRM1 = NDR - 1
       NDZM1 = NDZ - 1
       NDZ1 = NDZ + 1
C
C      INITIALIZE ARRYS
C
       DO 90 IZ = 1, NDZ1
       C(IZ) = 0.
       CS(IZ) = 0.
       DO 90 IR = 1, NDR1
90     Q(IZ,IR) = 0.
       DO 5 I = 1, IPRINT
5      QP1 (I) = 0.
       JPRINT = NDT/IPRINT
C
C      ARITHEMATIC ECONOMIZATION FOR SOLID PDE
C
       EQ1 = 1. + DR*DR/(XNS*DT)
       EQ2 = 1. - DR*DR/(XNS*DT)
       EQ3 = - EQ2
       EQ5 = 2.*EQ1
       EQ7 = 2.*EQ2
       EQ9 =(XKF*TAU*(1. - VOID)*DT/(AP*VOID*DR*DR*DR))*60.
       EQ10 = EQ1 - 4.
       EQ11 = 4. + EQ3
       EQ12 = DR*DR*DR
C
C      DIMENSIONLESS ISOTHERM PARAMETERS
C
       APR= A*CO/(A*CO/(1. + B*CO**BEXP))
       BP = B*CO**BEXP
C
C      ARITHEMATIC ECONOMIZATION FOR THE FLUID PDE
C
C
       XNF =(XKF*3.*(1.-VOID)*TAU/( AP*VOID))*60.
       E1 = DZ/(DT*DG)
       E2 = DZ*XNF
       E3 = 1. + E1 + E2
       WRITE(7,1012) E1, E2, E3, EQ5, EQ9
```

```
      IF(ISTOP .EQ. 1)  GO TO 3
C
C     INITIALIZE ARRAYS- SOLID PHASE PDE
C
      AQ(1) = 0.
      BQ(1) = 3.
      BQ(2) = - EQ5
      CDQ(1) = EQ10
      DO 101 I=2, NDR
      EQ4 =1./DFLOAT(I-1)
      AQ(I) = 1. - EQ4
101   CDQ(I) = 1. + EQ4
      ANR1(1) = 0.
C
C     THE MATRIX OF COEFFICIENTS FOR THE SOLID PHASE EQUATIONS ARE VALID
C     FOR AT TIME AND DISTANCE POSITIONS.
C
      BETAQ(1) = BQ(1)
      DO 102 I = 2 , NDR
102   BETAQ(I)= BQ(2) - AQ(I)*CDQ(I-1)/BETAQ(I-1)
      DO 125 I1 = 1, IPRINT
      DO 103 JPR = 1, JPRINT
C
C
C     THIS SECTION OF THE PROGRAM SOLVES THE FLUID PHASE PDES.  THE
C     PDES ARE SOLVED BY THE BACKWARD FINITE DIFFERENCE METHOD WHICH
C     RESULTS IN A DIAGONAL MATRIX AT THE NEW TIME STEP.
C
C
      IF(DOINF.NE.1.) GO TO 27
      TH = DFLOAT((I1-1)*JPRINT + JPR)*DT
      IF (TH.GT.TIN(NIN)) GO TO 27
      C(1) = CINF(TH)
      GO TO 28
27    C(1) = 1.
28    DO 10 J1 = 2, NDZ1
10    C(J1) = (C(J1-1) + E1*C(J1) + E2*CS(J1))/E3
C
C
C     THIS SECTION OF THE PROGRAM SOLVES THE SOLID PHASE PDES.  THE
C     PDES ARE SOLVED BY THE CRANK-NICHOLSON TECHNIQUE WHICH RESULTS IN
C     A TRIADIAGONAL MATRIX EXCEPT FOR THE LAST ROW - DO TO THE BOUNDARY
C     CONDITON AT THE SURFACE OF THE PARTICLE.  THE LAST ROW IS REDUCED
C     TO TWO ELEMENTS BY ROW REDUCTION AND HENCE THE MATRIX BECOMES
C     TRIDIAGONAL.  AQ, BQ, CDQ, AND DQ ARE THE SUBDIAGONAL, DIAGONAL,
C     SUPERDIAGONAL, AND THE PARTICULAR SOLUTION VECTOR, RESPECTIVELY.
C     THE SUBSCRIPTS FOR AQ, CDQ, AND DQ CORRESPOND TO ROW NUMBER.
C     BQ'S SUBSCRIPTS 1 AND 2    CORRESPOND TO THE FIRST ROW,
C     AND THE INTERMEDIATE ROWS. ANR1 CONTAINS THE ELEMENTS OF THE LAST
C     ROW AND THE SUBSCRIPTS CORRESPOND TO COLUMN NUMBER.
C
C
      DO 120 IZ = 1, NDZ1
      ANR1(2) = 1.
      ANR1(NDR1) = DFLOAT(NCP*NDR)/ 2.
      DQ(1) = - 3.*Q(IZ,1) + EQ11*Q(IZ,2)
      DQ(2) = EQ7*Q(IZ,2) - CDQ(2)*Q(IZ,3) - AQ(2)*Q(IZ,1)
      GAMMAQ(1) = DQ(1)/BQ(1)
      GAMMAQ(2) = (DQ(2) - AQ(2)*GAMMAQ(1))/BETAQ(2)
C
```

```
C      EQUATION OF EQUILIBRIUM - LINEAR C(IZ) SHOULD BE IN PLACE OF 1.
C
       DQ(NDR1) = DFLOAT(NDR*NDR)*Q(IZ,NDR1)/2. + EQ9*(C(IZ) - CS(IZ))
      1 + Q(IZ,2)
       DO 110 J=3, NDR
       ANR1(J) = DFLOAT((J-1)*(J-1))
       DQ(NDR1) = DQ(NDR1) + DFLOAT( (J-1)*(J-1))*Q(IZ,J)
C
C      THIS IS DQ/EQ4 EXCEPT FOR DQ(2)
C
       DQ(J) = - C(IZ,J-1) +EQ7*Q(IZ,J)/AQ(J) - CDQ(J)*Q(IZ,J+1)/AQ(J)
 110   GAMMAQ(J) = (DQ(J) - GAMMAQ(J-1))*AQ(J)/BETAQ(J)
C
C      ROW REDUCTION OF THE LAST ROW WHICH YEILDS A TRIDIAGONAL MATRIX
C
       DO  112 I2=2, NDRM1
       ANR1(I2) = ANR1(I2) -1.
       ANR1(I2+1) = ANR1(I2+1) + EQ5/AQ(I2+1)
       ANR1(I2+2) = ANR1(I2+2) - CDQ(I2+1) /AQ(I2+1)
       DQ(NDR1) = DQ(NDR1) - DQ(I2+1)
       I2P1 = I2 +1
       CACK1 = ANR1(I2P1)
       IF(DABS(CACK1) .LT. .1 ) GO TO 113
       DO111 I3 = I2P1, NDR1
 111   ANR1(I3) = ANR1(I3)/CACK1
 112   DQ(NDR1) = DQ(NDR1)/CACK1
       GO TO 114
 113   WRITE(7,1010)
       CALL ERROR
 114   CONTINUE
       BETAQ(NDR1) = ANR1(NDR1) - ANR1(NDR)*CDQ(NDR)/BETAQ(NDR)
       GAMMAQ(NDR1) =(DQ(NDR1) - ANR1(NDR ) * GAMMAQ(NDR) ) / BETAQ(NDR1)
       Q(IZ,NDR1) = GAMMAQ(NDR1)
       DO 120 K=1, NDR
       L = NDR1 - K
 120   Q(IZ,L) = GAMMAQ(L) - CDQ(L)*Q(IZ,L+1)/BETAQ(L)
C
C
C
C      EQUILIBRIUM CONCENTRATION  PREDICTED FROM THE ROOTS OF THE THREE
C      PARAMETER EQUATION : Q = A*C/(1. + B*C**BEXP)
C
C
       DO 51 IZ1 = 1, NDZ1
       DO 50 INST=1, 20
       IF( CS(IZ1) .GT. 0. ) GO TO 45
       IF(Q(IZ1,NDR1).LT.0.) GO TO 44
       UP = Q(IZ1,NDR1)
       IF(Q(IZ1,NDR1) .GE. 1.) UP = 2.
       DWN = 0.000
       DO 46 IHAV = 1, 20
       GUESS = (UP + DWN)/2.
       FX2 = GUESS*APP/(1. + BP*GUESS**BEXP)
       FX1 = Q(IZ1,NDR1) - FX2
       IF(FX1.EQ.0.) GO TO 47
       IF(FX1.GT.0.) GO TO 48
       UP = GUESS
       GO TO 46
 48    DWN = GUESS
 46    CONTINUE
```

```
47    CS(IZ1) = GUESS
45    FXX = (Q(IZ1,NDR1)*(1. + BP*CS(IZ1)**BEXP) -APR*CS(IZ1))/
     1(Q(IZ1,NDR1)*BP*BEXP*(CS(IZ1)**(BEXP - 1.)) - APR)
      CS(IZ1) = CS(IZ1) - FXX
      IF( DABS(FXX) .LT. 1.E-10)GO TO 51
50    CONTINUE
44    WRITE(7,1009)
      WRITE(7,1001) TH
      WRITE(7,1006) (C(IN), IN=1, NDZ1)
      WRITE(7,1008) (CS(IN), IN=1, NDZ1)
      WRITE(7,1013) (Q(IZP,NDR1),IZP=1,NDZ1)
      CALL ERROR
51    CONTINUE
      IF(PRI.NE. 1.) GO TO 103
      IF(I1.GT.1.OR.JPR.GT.5) GO TO 103
      TI = DFLOAT((I1-1)*JPRINT + JPR )*DT
      WRITE(7,1001) TI
      WRITE(7,1006) (C(IZO), IZO=1, NDZ1)
      WRITE(7,1008) (CS(IZO), IZO=1, NDZ1)
      DO 25 IZO = 1, NDZ1
25    WRITE(7,1002) IZO, (Q(IZO,IRO), IRO=1, NDR1)
103   CONTINUE
C
C     THIS SECTION SAVES OUTPUT PERIODICALLY.
C
      THPT(I1) = DFLOAT(I1*JPRINT) *DT
      IF(NDS.EQ.1) CDS1(I1) = C(NDZ1)
      IF(NDS.EQ.2) CDS2(I1) = C(NDZ1)
      IF(NDS.EQ.3) CDS3(I1) = C(NDZ1)
      DO 124 IZ= 1, NDZ1
      QP1(I1) = QP1(I1) + (EQ12*Q(IZ,NDR1)/2.)*3.*DFLOAT(NDR*NDR)
      DO 124 IAVG = 2, NDR
124   QP1(I1) = QP1(I1) + EQ12*DFLOAT((IAVG - 1)*(IAVG - 1))*3.*
     1 Q(IZ,IAVG)
      QP1(I1) = QP1(I1)/DFLOAT(NDZ1)
      IF(PRI.NE. 1.) GO TO 125
      WRITE(7,1001) THPT(I1)
      WRITE(7,1006) (C(IZO), IZO=1, NDZ1)
      WRITE(7,1008) (CS(IZO), IZO=1, NDZ1)
      DO 26 IZO = 1, NDZ1
26    WRITE(7,1002) IZO, (Q(IZO,IRO), IRO=1, NDR1)
125   CONTINUE
      WRITE(7,1000)
      WRITE(7,1011) XNAME
C     WRITE(7,1003) ( THPT(I), CP(I), QP1(I), I=1, IPRINT)
500   WRITE(7,1007) XLC, DS, DG, XKF, TAU, F, VOID, XL, AR, AP, NDT,
     1 NDR, NDZ
C     CALL OBJFUN( CD, TDATA, NDATA,CP, THPT, IPRINT,  CP1, FMIN)
C     WRITE(7,1014) FMIN
C     WRITE(6,1019) FMIN, XKF
C     WRITE(7,1015) (CD(LPR), CP1(LPR), TDATA(LPR), LPR = 1, NDATA)
C     IF(IMODE.NE.1) GO TO 1
C     WRITE(6,1020)
C     READ(5,1016) PLOT1
C     IF(PLOT1.EQ.1.) CALL PLOT(CD, TDATA, NDATA, CP, THPT, IPRINT,
C    1 TIN, CIN, NIN)
      CALL PLOT(CDS1, THPT, IPRINT, CDS2, THPT, IPRINT,
     1 CDS3, THPT, IPRINT, CIN,TIN, NIN)
3     WRITE(6,1018) NDT, NDR, NDZ, ISTOP
      READ(5,1021) NDT, NDR, NDZ, ISTOP
      GO TO 2
999   CALL EXIT
C
C     FORMATS FOR OUTPUT
C
1000  FORMAT ('1')
1001  FORMAT('0', 25X, 'THROUGHPUT =  ', F10.6, /, /)
1002  FORMAT('0 BED POSITION = ', I4, /, 'C = ', /, 101E14.6)
1003  FORMAT('0THROUGHPUT = ', F10.6, '  C(NDZ1) =  ', F10.6, ' QAVE = '
     1 , F10.6)
1004  FORMAT('0', 25X, ' REDUCED LONGITUDINAL DISTANCE')
1005  FORMAT('0', 25X, 'MASS THROUGHPUT')
1006  FORMAT('CC(IZ) = ', 101F14.6)
1007  FORMAT('0L = ', E14.6, ' DS = ', E14.6, ' SQ CM  DG = ', F14.6,
     1 ' KEF = ', F12.6, ' CM/SEC ', /,  'TAU = ', F10.6, ' MIN  F = ',
     2 F10.3, ' ML/MIN  VOID = ', F10.6, ' XL = ', F10.2,' CM  AR = ', F
     38.2,' SQ CM  AP = ', F8.6, ' CM', /, 'NDT = ', I4, ' NDR = ',I4,
     4 ' NDZ = ' , I4)
1008  FORMAT('CCS(IZ) = ', 101E14.6)
1009  FORMAT('0', 'NEWTONS METHOD FAILED FOR EQUILIBRIUM CONCENTRATION')
1010  FORMAT('0 FOR REDUCTION IS NOT GOING TO WORK')
1011  FORMAT(' ',10A8, /, /)
1012  FORMAT('0', 'E1 = ', E14.6, ' E2 = ', E14.6, ' E3 = ', E14.6,
     1 /, /, 'EQS = ', E14.6, ' FQ9 = ', E14.6, /, /, /)
1013  FORMAT('0','Q(IZ,NDR1) = ', 101E14.6)
1014  FORMAT('0', 'DATA', 6X, 'PREDICTION', 2X, 'THROUGHPUT', 4X, 'FMIN = '
     1 , E14.6)
1015  FORMAT('0', F10.6, 2X, F10.6, 2X, F10.6)
1016  FORMAT(F9.4)
1017  FORMAT('0READ IN KF',F9.4)
1018  FORMAT(' NDT = ', I4, ' NDR = ', I4, ' NDZ = ', I4,' ISTOP = ',I4,
     1 /, 'READ IN NDT, NDR, NDZ, ISTOP, I4, 1X, I4, 1X, I4, 1X, I1')
1019  FORMAT(' FMIN = ', E14.6, ' KF = ', E 14.6, ' CM/SEC ')
1020  FORMAT(' ELCT1 ?, 1. = YES, F9.4')
1021  FORMAT(I4, 1X, I4, 1X, I4, 1X, I1)
      END
      REAL FUNCTION CINF*8(T)
      IMPLICIT REAL*8(A-H,O-Z)
      DIMENSION CIN(100), TDATA(100)
      COMMON CIN, TDATA, INF, NIN
      IF(T.GT.TDATA(INF+1)) INF = INF + 1
      CINF = 1.
      IF(INF.GT.NIN) RETURN
      IF(T.LE.TDATA(INF+1)) GO TO 1
      WRITE(7,1001)
1001  FORMAT('0','TIME STEP TOO LARGE FOR INTERPOLATION')
1     CINF = CIN(INF) +(CIN(INF+1) - CIN(INF))*(T - TDATA(INF))/
     1(TDATA(INF+1) - TDATA(INF))
      RETURN
      END
      SUBROUTINE OBJFUN(CD, TD, ND, CP, TP, NP, CP1, FMIN)
      IMPLICIT REAL*8(A-H, O-Z)
      DIMENSION CD(100), TD(100), CP(201), TP(201), CP1(100)
      FMIN = 0.
      IDATA = 1
      NP1 = NP - 1
      DO 1 I =1, NP1
      IF(TD(IDATA).LT.TP(I).OR.TD(IDATA).GT.TP(I+1)) GO TO 1
      CAP = CP(I) + ((TD(IDATA) - TP(I))/(TP(I+1) - TP(I)))*(CP(I+1) -
     1 CP(I))
```

```
      CP1(IDATA) = CAP
      FMIN = FMIN + (CAP - CD(IDATA))*(CAP - CD(IDATA))
      IF(IDATA.EQ.ND) GO TO 2
      IDATA = IDATA + 1
1     CONTINUE
2     FMIN = DSQRT(FMIN/DFLOAT(ND))
      RETURN
      END
      SUBROUTINE PLOT(Y1, X1, NDATA1, Y2, X2, NDATA2, Y3, X3, NDATA3,
     1 CIN, TIN, NIN)
      IMPLICIT REAL*8(A-H,O-Z)
      DIMENSION X1(201), Y1(201), X2(201), Y2(201), X3(201), Y3(201),
     1 CIN(100), TIN(100)
C     1 = DATA, 2 = PREDICTION
C     CALL  PSCALE(9., 1., XMIN, DX, X2(1), NDATA2,1)
C     CALL PSCALE(6., 1., YMIN, DY, Y2(1), NDATA2, 1)
      XMIN = 0.
      YMIN = 0.
      DX = .20
      DY = .25
      CALL PLTOFS(XMIN,DX,YMIN, DY, 1., 1.)
      CALL PAXIS(1., 1., 10HTHROUGHPUT, -10,9., 0.0, XMIN, DX, 1.)
      CALL PAXIS(1., 1., 24HEBP CONCENTRATION (C/CC), 24, 6., 90.,
     1 YMIN, DY, 1.)
      CALL PLNSYM(.15)
      CALL PLINE(X1(1), Y1(1), NDATA1, 2, 0, 0, 1)
      CALL PLINE(X2(1), Y2(1), NDATA2, 2, 0, 0, 1)
      CALL PLINE(X3(1), Y3(1), NDATA3, 2, 0, 0, 1)
      CALL PLINE(TIN(1), CIN(1), NIN, 2, 0, 0, 1)
      CALL PLTEND
$SIGNOFF
```

TYPING GUIDE SHEET

APPENDIX E

CHN ANALYSIS

MATERIALS AND METHODS:

Carbon, hydrogen and nitrogen (CHN) analyses were performed for humic acid (Technical Grade, Aldrich Chemical), to determine percentage composition. A Hewlett Packard CHN Analyzer, Model 185B, in conjunction with a Hewlett Packard 3371B Integrator, was used for this purpose.

A standard calibration curve for each element (C, N, and H) was generated using 7 known samples of cystine; their amounts ranged from 0.3 to 2.6 milligrams. Linear regression analysis was performed on each set of data obtained (weight vs. peak area). The percent weight of each element in the unknown was calculated from the ratio of the weight of the element, determined from the calibration curve, to the total weight of the sample. Figure illustrates a typical calibration curve for the carbon analyses.

EPA-287 (Cin.)
(4-76)

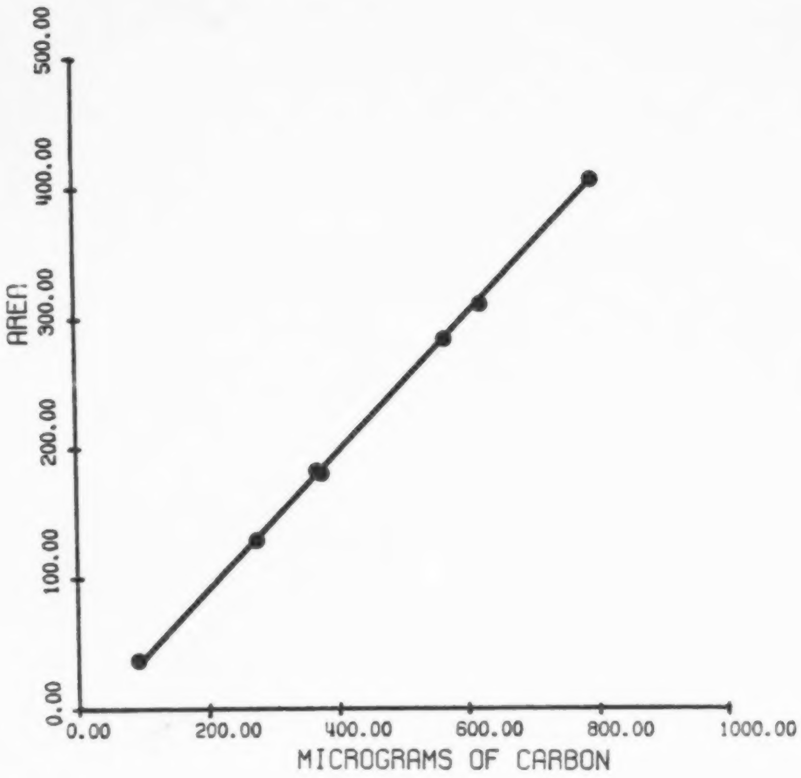

Figure E-1. Calibration curve for carbon analysis using a CHN analyzer.

TYPING GUIDE SHEET
BEGIN FIRST LINE OF TEXT HERE
CENTER OF PAGE
TOP OF IMAGE AREA
DROPPED HEAD BEGIN SECTIONS HERE

APPENDIX F

PREPARATION OF HUMIC ACID STANDARDS

MATERIALS AND METHODS:

1. An accurately weighed quantity (1 g) of humic acid was added to approximately 800 ml of deionized-distilled water in a 1-liter flask.

2. The pH was adjusted to 11 using 1.0 *N* NaOH, and the mixture shaken vigorously for 5 minutes. After re-adjusting the pH to 7 ± 0.2 with 1.0 *N* HCl, the mixture was filtered through a prewashed, dried and tared 11-cm glass-fiber filter (Reeve Angel). The filtrate was transferred to a 1-liter volumetric flask and diluted with deionized-distilled water to 1-liter.

3. The glass-fiber filter was dried at 120°C and re-weighed to determine the amount of humic acid filtered out of the solution. The weight of humic acid remaining in the solution, divided by the volume, determined the humic acid concentration of the stock solution. Solutions of desired concentration ranges for experimentation were prepared by appropriate dilution of this standard. A standard calibration curve was generated by plotting ultra-violet absorbance at 250 nm wavelength versus humic acid concentration. The instrument used was an Hitachi UV-VIS Spectrophotometer Model 181, Hitachi Ltd., Tokyo, Japan. A typical calibration curve is presented in Figure F-1.

BEGIN LAST LINE OF TEXT
BOTTOM OF IMAGE AREA OUTSIDE DIMENSION FOR TABLES AND ILLUSTRATIONS

PAGE NUMBER
EPA-287 (Cin.)
(4-76)

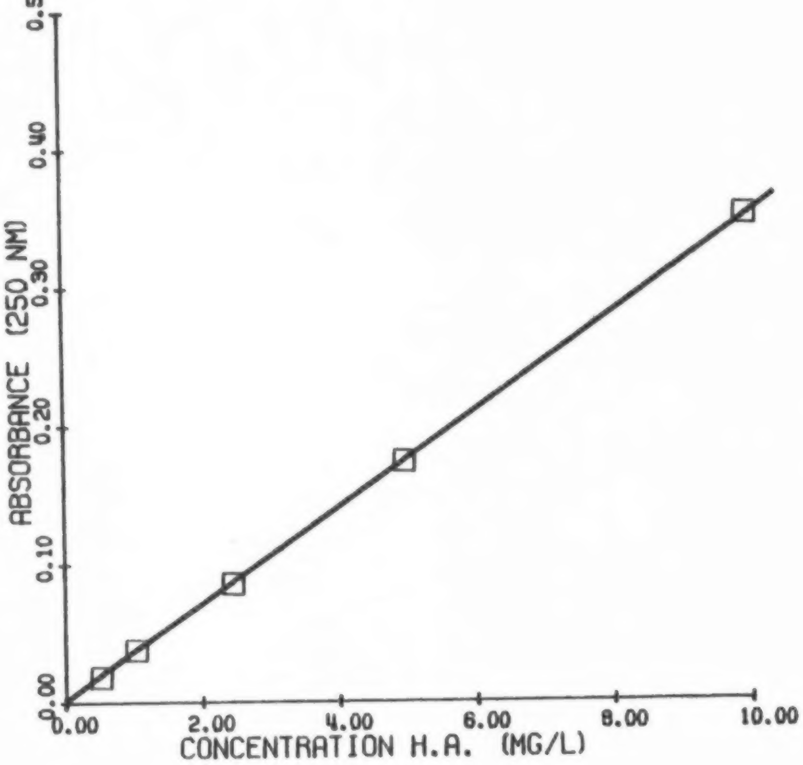

Figure F-1. Calibration curve for humic acid analysis using ultraviolet spectroscopy.

BEGIN FIRST LINE OF TEXT HERE
TYPING GUIDE SHEET
CENTER OF PAGE
TOP OF IMAGE AREA
DROPPED HEAD: BEGIN SECTIONS HERE

APPENDIX G

HUMIC ACID FRACTIONATION

MATERIALS AND METHODS:

The fractionation procedure used in this research was similar to those discussed by Schnitzer and Khan (1972)[1] and by Gaskill *et al*, (1977).[2]

A carefully weighed amount (0.2 grams) of Technical Grade humic acid (Aldrich Chemical) was dissolved in 1 liter of organic-free water, the pH of which was raised to 11 using 0.1 *N* NaOH. The non-dissolved material (humin) was separated with a washed and dried glass-fiber filter, and its dry weight was calculated. After acidifying the remaining solution to less than pH 1.0 and allowing it to remain overnight, the mixture was filtered through a washed and weighed 0.1-micron filter. This step left the fulvic acid in solution and the humic acid on the filter. The material on the filter was redissolved in NaOH and diluted, resulting in a pure humic acid solution. Dry weight calculations of the insoluble, filtered material acquired throughout the procedure allowed final concentration determinations.

[1] Schnitzer M., S.U. Khan, "*Humic Substance in the Environment*", Marcel Dekker, Inc. New York, N.Y. (1972).

[2] Gaskill, A.J., J.T. Byrd, and M.S. Schuman, "Fractionation and Trace Metal Content of a Commercial Humic Acid", *J. Environ. Sci. Health*, A(12) (3), (1977).

BEGIN LAST LINE OF TEXT
BOTTOM OF IMAGE AREA OUTSIDE DIMENSION FOR TABLES AND ILLUSTRATIONS
3/8"

PAGE NUMBER
EPA-287 (Cin.)
(4-76)

APPENDIX H

PREPARATION OF BIOGROWTH ON ACTIVATED CARBON FOR EXAMINATION BY SCANNING ELECTRON MICROSCOPY

MATERIALS AND METHODS

A modification of Karnovsky's method (1965)[1] was used to examine the physical and structural characteristics of biological growth on activated carbon by scanning electron microscopy. This fixation procedure was followed by post-fixation, dehydration, and critical point drying. The following solutions were prepared for the experiments:

1. Buffer Solutions:

   A. 27.5 g/l $NaH_2PO_4 \cdot H_2O$

   B. 28.39 g/l NaH_2PO_4

      a. 0.2 M phosphate buffer, pH 7.3:

         23 ml A + 77 ml B

      b. 0.1 M phosphate buffer with 4.5% sucrose:

         23 ml A + 77 ml B + 100 ml water + 9.0 g sucrose

2. Paraformaldehyde/Glutaraldehyde Fixative:

   One gram paraformaldehyde in 50 ml 0.2 M phosphate buffer, heat to 60°C, cool flask with tap water, add 5 ml glutaraldehyde plus 30 ml of 0.2 M phosphate buffer, and adjust the pH to 7.3.

3. OsO_4 Fixative

   50 ml 2% OsO_4 in water plus 50 ml 0.2 M buffer.

Fixation:

Method: The samples were fixed in paraformaldehyde/glutaraldehyde for 1-2 hr and rinsed in buffer/sucrose solution twice, 5 min each.

Purpose: Paraformaldehyde, a low molecular weight compound, accomplishes quick kill because of rapid cellular penetration. Glutaraldehyde forms cross-links with proteins in the cell membrane, forming a rigid network that preserves fine structures.

Post-Fixation:

Method: Following the fixation, the samples were fixed in 1% OsO_4 solution for 3 hrs and rinsed in buffer/sucrose solution.

Purpose: The liquid portion of the membrane is thus fixed (Hayat, 1970).[2]

Dehydration:

Method: After the post-fixation step, the particles were rinsed in graded ethanol (50, 70, 80, 90, and 100%) twice, 10 min each, followed by rinsing in mixtures of ethanol/amylacetate (50/50% and 10/90%) for 20 min each. Finally the samples were stored in 100% amylacetate.

Purpose: Dehydration and replacement of ethanol by a nonpolar solvent such as amylacetate further preserves the fine cell structure because nonpolar solvents freeze more like an amorphous glass than a rigid ice crystal (Boyle *et al*, 1969).[3]

Critical Point Drying:

Method: The particles were carefully transferred from the vials containing amylacetate and placed in the sample container of a DCP-1 critical point dryer. The samples were subsequently rapidly frozen by replacing the amylacetate with liquid CO_2. The temperature was then gradually increased, under pressure, to the critical pressure to equalize the densities of the vapor and liquid phases of CO_2.

Purpose: Problems associated with air drying, such as disruption of cellular structures caused by surface tension, are thus circumvented and the stability of the fixed structure is ensured (Bartlett and Burstyn, 1975).[4]

FOOTNOTES TO APPENDIX H

[1] Karnovsky, M.J., "A Formaldehyde - Glutaraldehyde Fixative of High Ismolarity for Use in Electron Microscopy", *J. Cell. Biology*, *27*, 137A (1965).

[2] Hayat, M.A., "*Principles and Techniques of Electron Microscopy*", Vol. 1, van Nostrand Reinhold Co., New York, N.Y. (1970).

[3] Boyle, A., and C. Wood, "Preparation of Animal Tissues for Surface-Scanning Electron Microscopy", *J. Microscopy*, *90*:221, (1969).

[4] Bartlett, A.A., and H.P. Burstyn, "A Review of the Physics of Critical Point Drying", *Proc. of 8th Annual Scanning Electron Microscopy Symposium*, O. Johari and I. Corium (eds.) (1975).

TYPING GUIDE SHEET
BEGIN FIRST LINE OF TEXT HERE
CENTER OF PAGE
TOP OF IMAGE AREA
DROPPED HEAD BEGIN SECTIONS HERE

APPENDIX J

BIOLOGICAL INHIBITION IN BENCH-SCALE ACTIVATED CARBON COLUMNS

MATERIALS AND METHODS:

The materials and methods used to inhibit the biological growth are carefully chosen and characterized. The inhibitor should have the following characteristics: it should be toxic to the microorganisms at low concentrations; it should not be strongly adsorbed on the carbon; it should not be reactive with either the carbon or sorbate; and, finally, it should be soluble in water at the required concentrations and pH ranges.

Copper was examined as a possible inhibitor. Copper sulfate is commonly used as a biological inhibitor in natural waters for weed control. In this study, a 3-liter solution of 50 mg/l $CuSO_4 \cdot 5H_2O$ was agitated with 500 mg Filtrasorb 400 (16/20 U.S. standard sieve size) carbon for 24 hours in a completely mixed batch (CMB) reactor. Samples were taken periodically and analyzed for copper concentration using a Varian Techtron Model 1200 Atomic Absorption Spectorphotometer (324.7 nm wavelength). Figure J-1 demonstrates that essentially no copper was adsorbed on the activated carbon.

Cupric ions were incorporated into three different column studies already in progress. The solutes for these column studies were PCB (Aroclor 1016), para-dichlorobenzene (PDB), and humic acids. For the PCB and PDB column studies the copper was added to the column influent at a concentration of approximately 20 mg/l Cu^{+2}. Prior to addition of the copper, each of the columns was air-scoured and back-washed to remove excess biological growth that had previously accumulated. After a short period of operation the accumulatin of biological film was apparent, indicating that the copper had little or no effect on the growth of the microorganisms at the concentrations used.

Experiments were conducted to evaluate the interaction of humic acids with the copper ions to determine whether any complexation (and therefore adsorption interference)

BOTTOM OF IMAGE AREA OUTSIDE DIMENSION FOR TABLES AND ILLUSTRATIONS
BEGIN LAST LINE OF TEXT
3/8"

PAGE NUMBER
EPA-287 (Cin.)
(4-76)

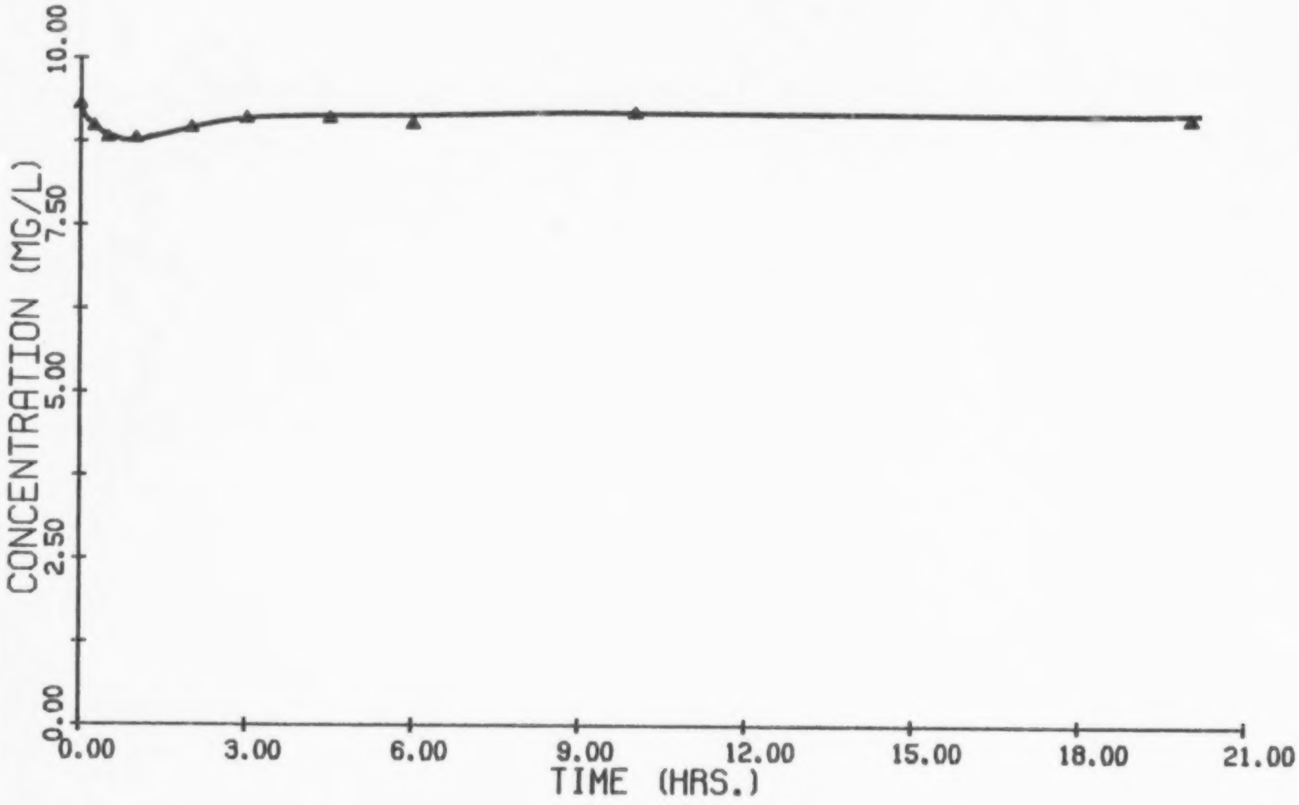

Figure J-1. Rate and extent of adsorption of Cu^{+2} from DDW by granular activated carbon in a CMB reactor (0.166 g/ℓ of 16/20 US sieve size carbon).

would occur.

To accomplish this, a 5.0-ppm humic acid solution was titrated with a 10^{-2} $\underline{M}$ Cu^{+2} solution and the Cu^{+2} activity measured potentiometrically with an Orion Cu^{+2} specific ion electrode. The results demonstrated that complexation had occurred (see Section 6, Figure 46). Further evidence of complexation was given by comparisons of the U.V. spectra of copper sulfate, humic acids, and humic acids with copper sulfate solutions, as illustrated in Figure J-2.

Alternatively, it was hypothesized that periodic backwashing with a strong copper sulfate solution might inhibit bacterial growth without complexation. A 50 mg/l copper sulfate solution was passed through the humic acid carbon column every twelve hours for a period of two hours. Again, the copper was ineffective in inhibiting bacterial growth, and was therefore eliminated as a possible inhibitory agent.

Mercury was another inhibitor considered. To determine if the mercury ions would be adsorbed on the activated carbon, a mercury adsorption rate study was performed. In this study a 3-l solution of 100 mg/l Hg^{2+} was prepared and placed in a 1.0-gallon glass CMB reactor equipped with a plastic motor-driven propeller. Three grams of 16/20 Filtrasorb 400 carbon was then added to the solution and stirring begun (550 rpm). 20-ml samples were periodically withdrawn and placed in glass sample vials for overnight storage. Mercury analysis was conducted using a Perkin Elmer 303 Atomic Absorption Spectorphotometer at a wavelength of 253.6 nm.

The results of this rate study, presented in Figure J-3, clearly demonstrate that mercury ions are strongly adsorbed on the carbon. It was therefore decided that mercury was inappropriate as a biological inhibitor.

Silver ions were also tested. The initial evaluation consisted of an adsorption rate study in which 3.0 liters of 3.7 mg/l Ag^{+} was contacted with 500 mg 16/20 Filtrasorb 400 carbon in a glass CMB reactor. Samples were periodically analyzed potentiometrically for silver ion activity with an Orion Ag^{+}/S^{2-} specific ion electrode. Figure J-4 presents the analytical results, indicating that silver ions were adsorbed rather weakly on the carbon.

As with the copper, a concentration of 3 to 5 mg/l silver was added to columns in which carbon tetrachloride, PCB's, and PDB adsorption studies were in progress. Prior to addition of the silver the columns were air-scoured and back-washed to remove excess biological floc. The film never reappeared in the column and no additional headloss was

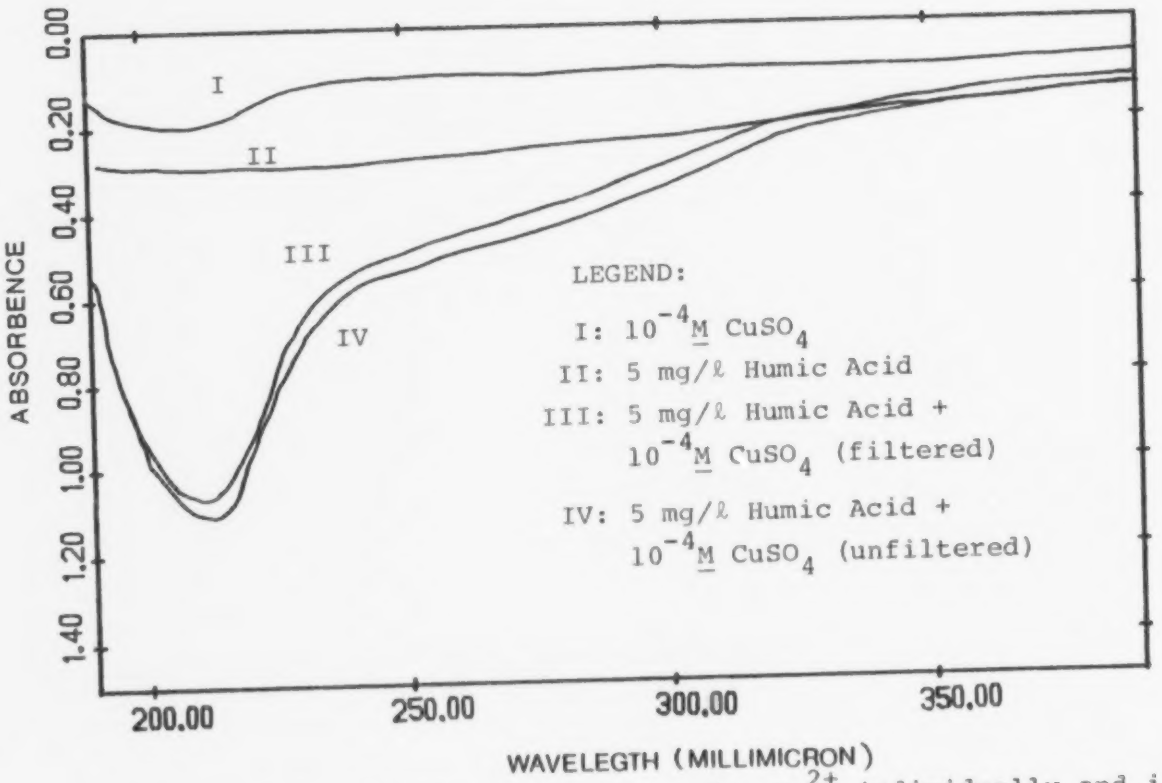

Figure J-2. Ultraviolet Spectra for Cu^{2+} individually and in the presence of humic acids.

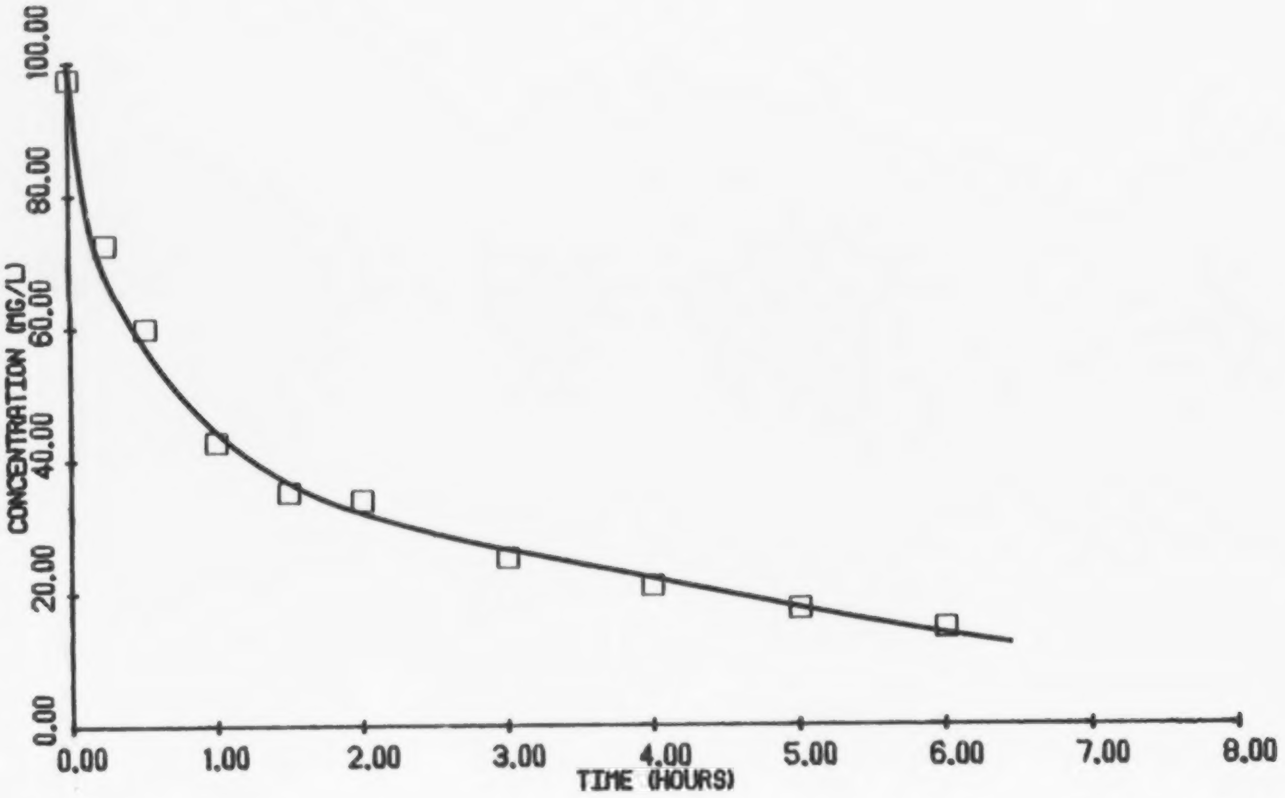

Figure J-3. Rate and extent of adsorption of Hg^{2+} from DDW by granular activated carbon in a CMB reactor (0.166 g/ℓ of 16/20 US sieve size carbon).

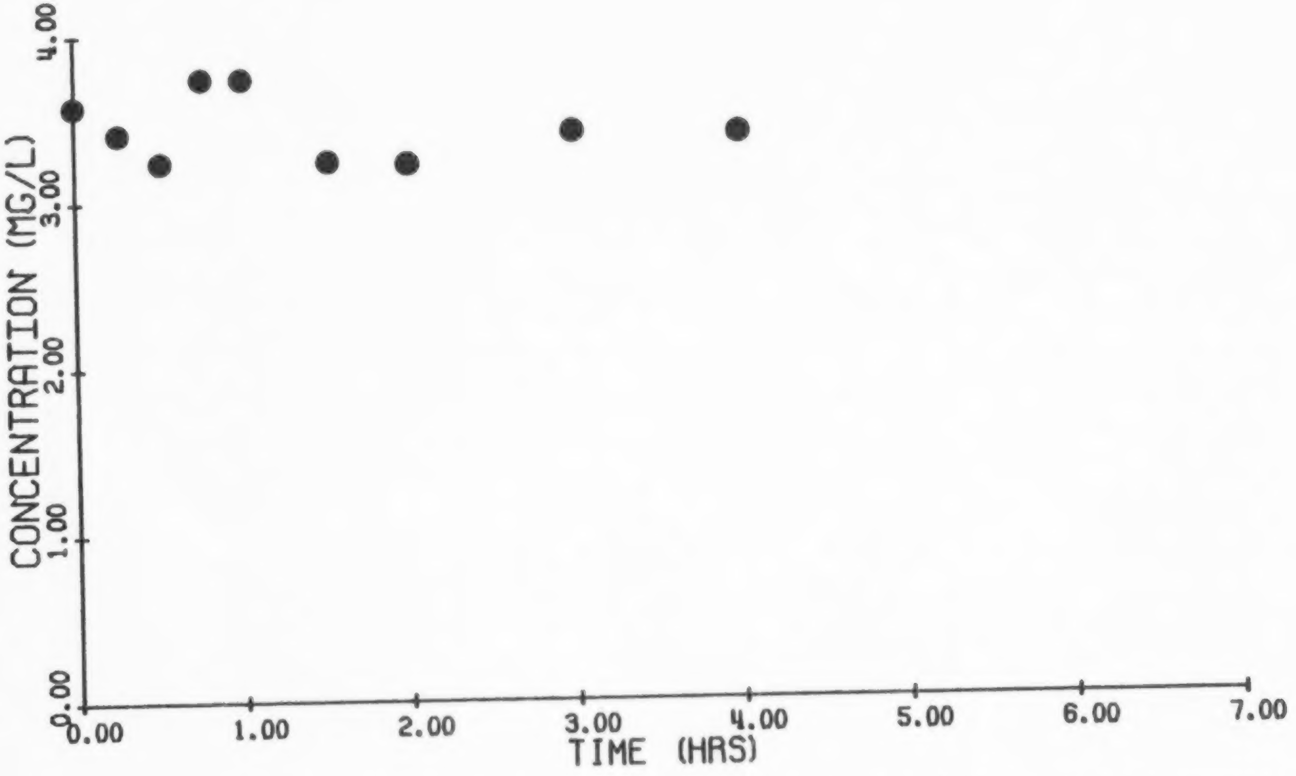

Figure J-4. Rate and extent of adsorption of Ag^+ from DDW by granular activated carbon in a CMB reactor (0.166 g/ℓ of 16/20 US sieve size carbon).

encountered, demonstrating that silver was effective in inhibiting biological growth.

Further studies were conducted to determine if silver could be used in conjunction with column studies using humic acids as a sorbate. The results indicated that silver ions also complexed with the humic acid and therefore most likely alter its adsorption characteristics. To study the complexation phenomenon, a 5.0 mg/l humic acid solution was titrated with silver ions and the silver ion activity monitored with a specific ion electrode. For comparison, the same volume of distilled water was titrated with the silver ions and silver activity monitored (Section 6, Figure 45). The complexation can also be observed by comparing the U.V. spectra of solutions of silver nitrate, humic acids, and humic acids with silver nitrate (Fig. J-5). Hence, additional studies were necessary to find an inhibitory agent that could be used in conjunction with humic acids.

Based on earlier studies, it was found that the use of Ann Arbor tap water as a solvent instead of distilled water was partially effective in inhibiting biological growth. To further evaluate this, column studies were conducted with humic acids in tap water. It was observed that much less frequent air-scouring and backwashing was needed to minimize excessive head losses caused by biological growth. It was postulated that the residual chlorine contained in the tap water was primarily responsible for the inhibitory action. It should, however, be noted that the ionic species in the tap water complex with humic acid and change its adsorption characteristics, as discussed in Section 6.

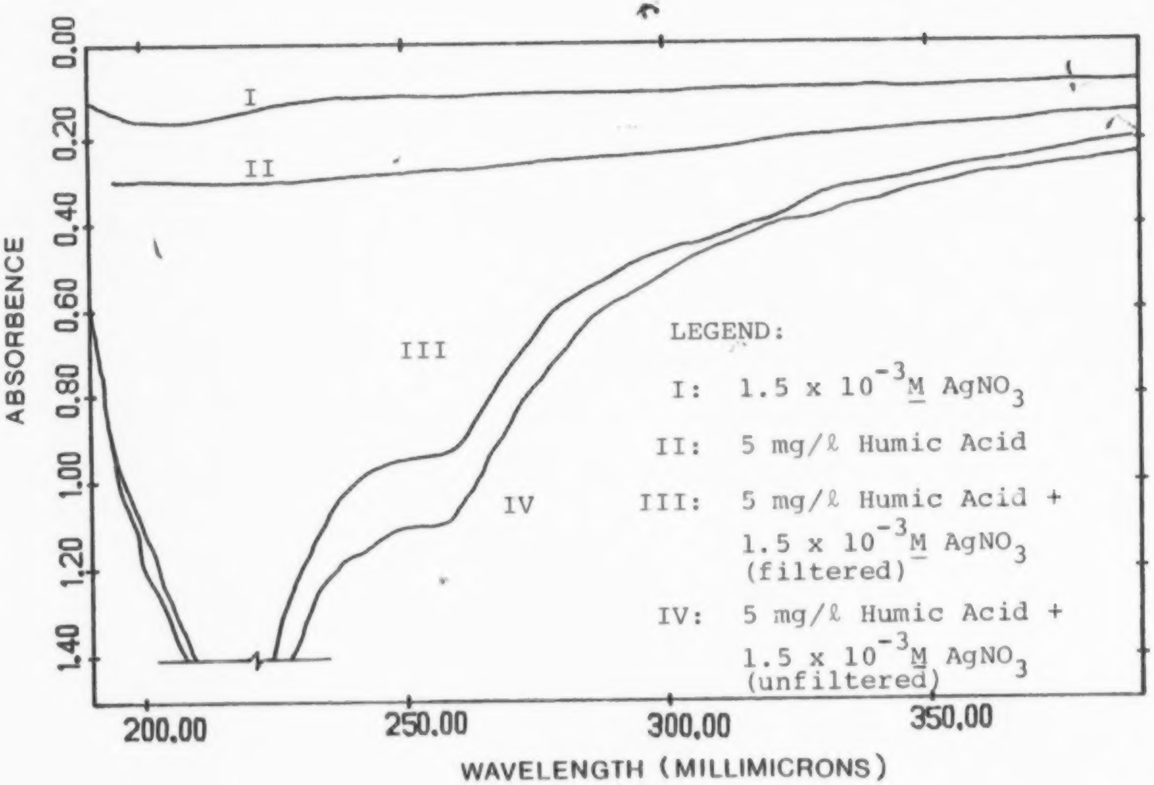

Figure J-5. Ultraviolet spectra for Ag^+ individually and in the presence of humic acids.

APPENDIX K

CCl_4 STANDARD CURVE PREPARATION

MATERIAL AND METHODS:

The CCl_4 standards were prepared by injecting a known volume of carbon tetrachloride, (Baker Instra-Analyzed), into a 100-ml volumetric flask containing Phillips 66 Pure Grade n-hexane, using a 10.0 microliter syringe. Several dilutions of this concentrated standard were made to give the concentrations needed for working standards. 2-7 μl of an appropriate working standard was then injected into a gas chromatograph (GC). The standards were analyzed in the same manner described for the analysis of CCl_4 in the "Analytical Procedures" subsection of Section 7. Figure K-1 demonstrates a typical calibration curve for CCl_4 using a scandium tritide (Sc^3H) electron capture detector (ECD).

Typical chromatograms for CCl_4 are presented in Figure K-2. Figure K-2a demonstrates a typical chromatogram using a 1700 Varian GC equipped with a Hall electrolytic conductivity detector and a 6' x 1/8" stainless steel column packed with 20% SP 2100/0.1% Carbowax 1500 on 100/120 Supelcoport. Figure K-2b represents a typical chromatogram using a 2700 Varian GC equipped with a Sc^3H ECD.

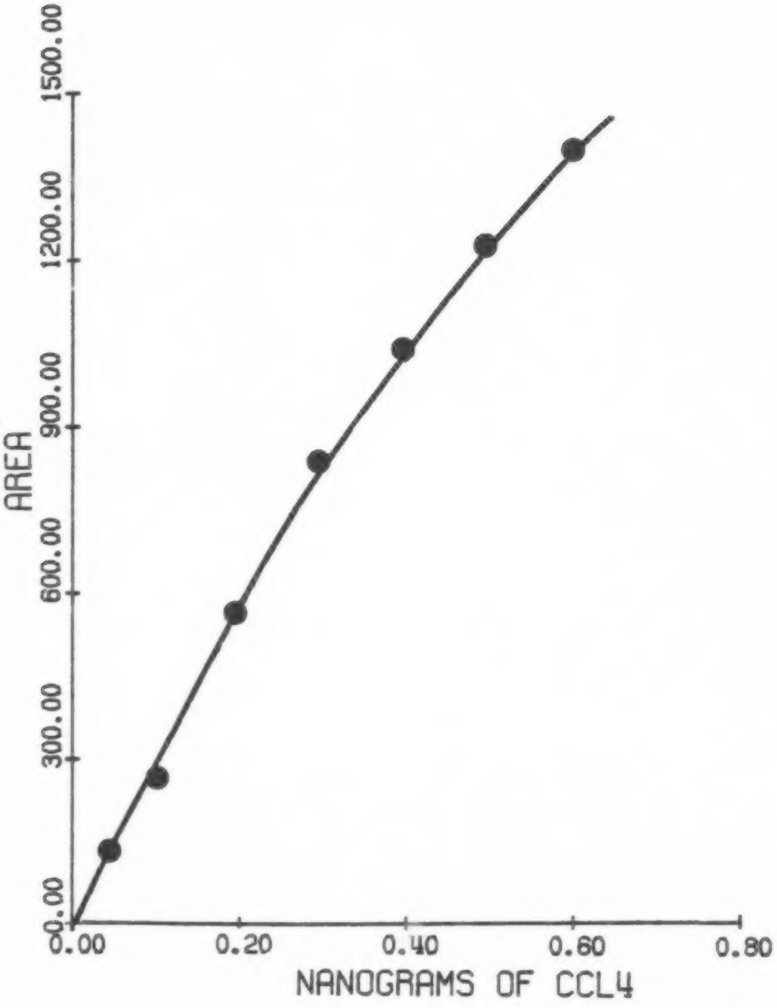

Figure K-1. Calibration curve for CCl_4 using a Sc^3H ECD.

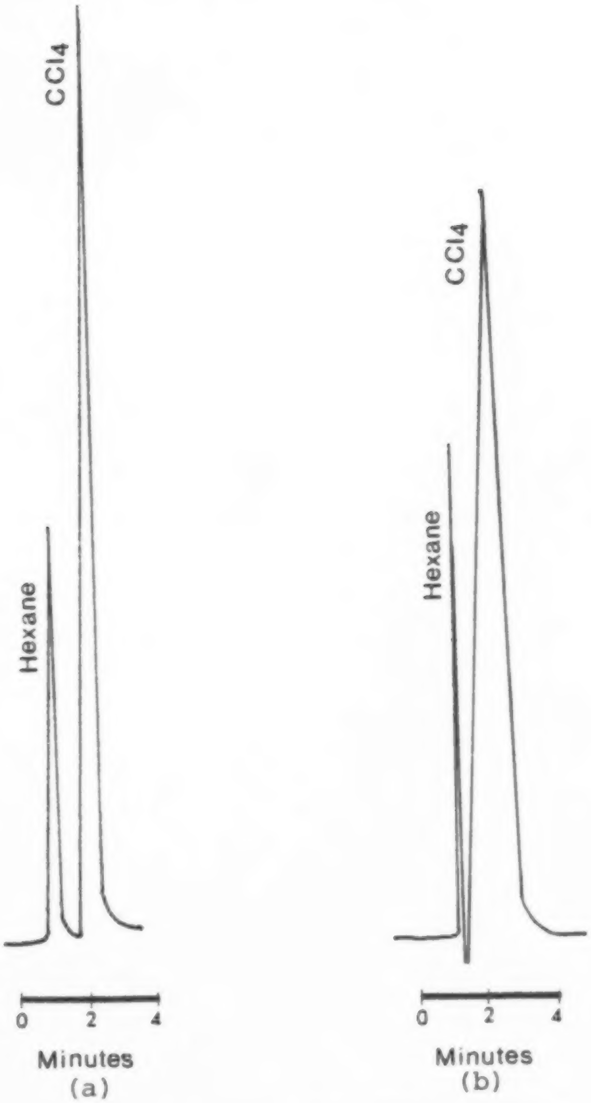

Figure K-2. Chromatograms for CCl_4 using:
a) an electrolytic conductivity detector; and,
b) a Sc^3H ECD.

APPENDIX L

BENZENE STANDARD CURVE PREPARATION

MATERIAL AND METHODS:

Benzene standards were prepared by adding 1.5 mg of benzene (Baker Instra-Analyzed) to a 150-ml Hypo-Vial containing OFW to yield a 10 mg/l stock solution. The spiking was performed by piercing the Teflon-laminated rubber spetum which was crimped onto the Hypo-Vial by an aluminum cap. The vapor-phase-free vial was vigorously agitated for 30 minutes to achieve complete dissolution, using a Teflon-coated magnetic stirrer. Desired dilutions were then made by injecting the appropriate volume of stock solution directly into a 5-ml volume of OFW contained in the purging apparatus. The standards were analyzed in the same manner described for analysis of benzene in "Analytical Procedures" subsection of Section 8 . The GC response for each standard solution was recorded by measuring the peak height. A typical calibration curve for benzene is demonstrated in Figure L-1.

Figure L-2 presents a typical chromatogram for benzene using a Varian 2700 GC equipped with flame ionization detector (FID) and a 6' x 1/8" stainless steel column packed with 10% Tri (Cyanoethoxy) Propane on 80/100 Chromosorb P AW.

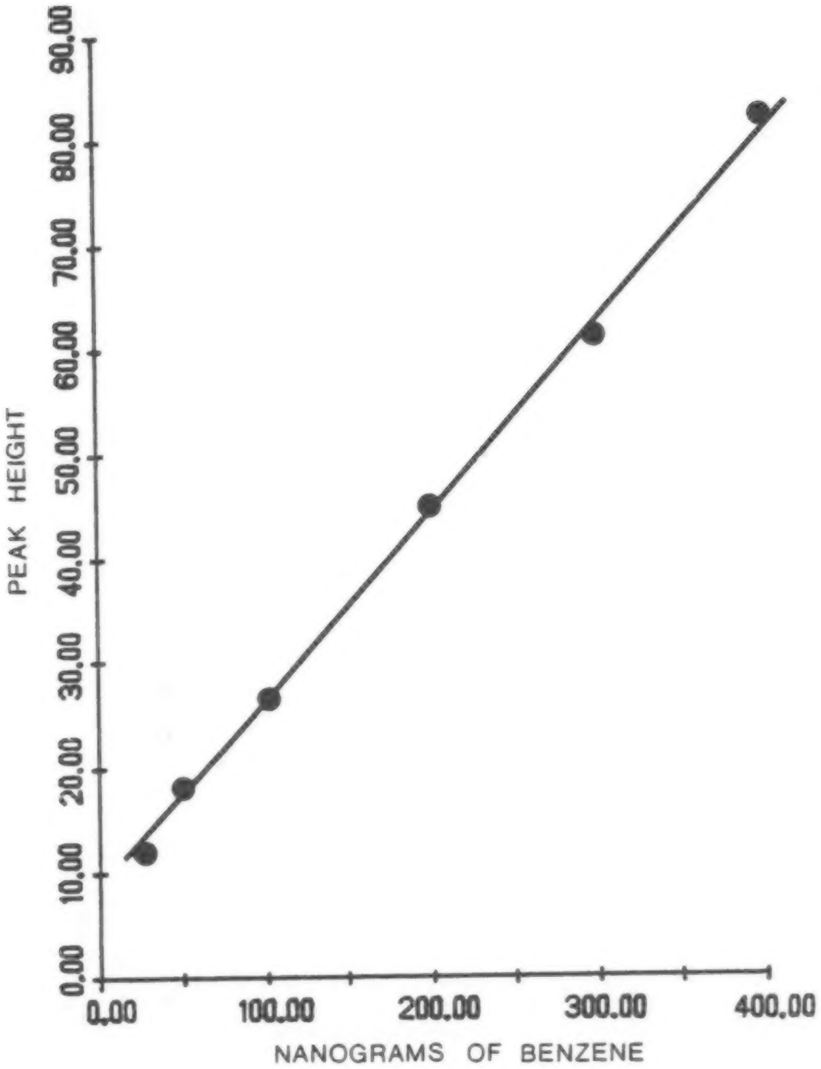

Figure L-1. Calibration curve for benzene (dynamic headspace GC analysis).

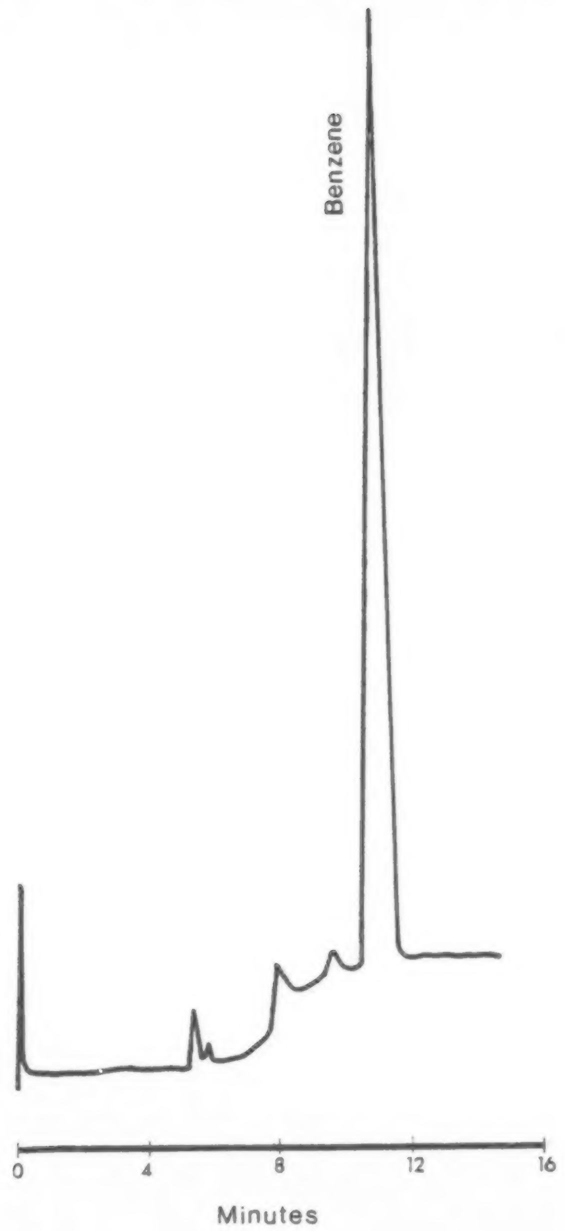

Figure L-2. Chromatogram for benzene using FID (dynamic headspace GC analysis).

APPENDIX M

PCB STANDARD CURVE PREPARATION

MATERIALS AND METHOD:

PCB stock solutions were prepared by dissolving an appropriate amount of Aroclor 1016 or Aroclor 1254 (Monsanto Chemical Co.) in 100 ml hexane (Baker Resi-Analyzed). Serial dilutions were then made in the operating range of the GC detector. A few microliters of an appropriate standard solution were injected into the GC. The standards were then analyzed in a manner similar to that described for analysis of PCB in the "Analytical Procedures" subsection of Section 9 . A typical calibration curve for A-1254 using a ^{63}Ni ECD is presented in Figure M-1.

Figure M-2 presents typical chromatograms for A-1016 and A-1254. A Varian 2700 GC fitted with a 6 ft x 2 mm ID glass column packed with 3% Silicone OV-1 on 80/100 Gas Chrom Q was used for the analysis.

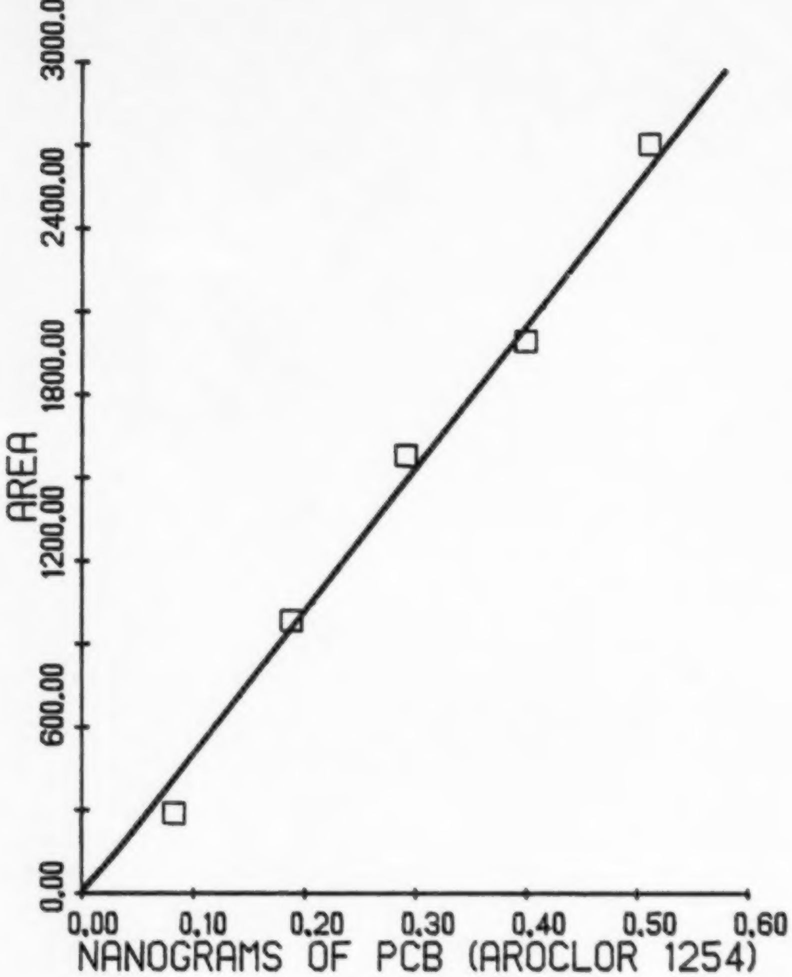

Figure M-1. Calibration curve for A-1254 using ^{63}Ni ECD.

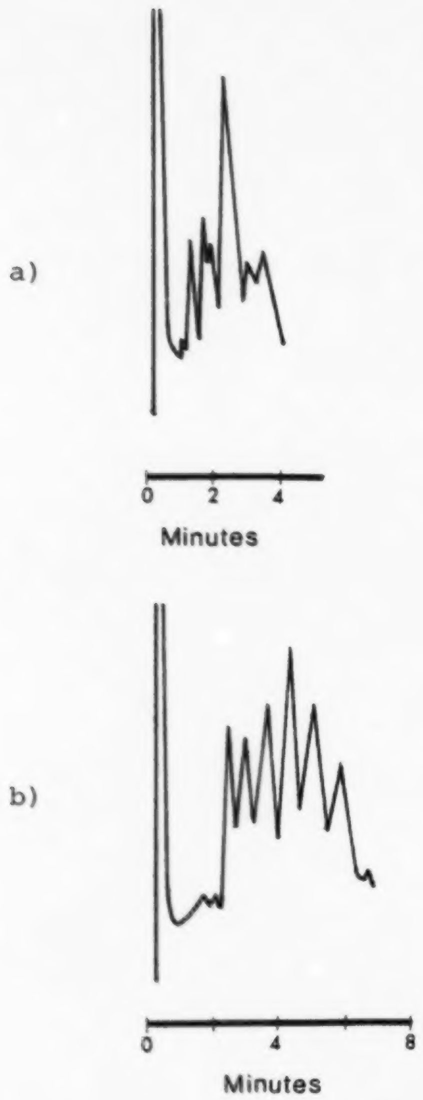

Figure M-2. Chromatograms for PCB using ^{63}Ni ECD:

a) A-1016; and, b) A-1254.

BEGIN FIRST LINE OF TEXT HERE
TYPING GUIDE SHEET
CENTER OF PAGE
TOP OF IMAGE AREA
DROPPED HEAD, BEGIN SECTIONS HERE

APPENDIX N

DIELDRIN STANDARD CURVE PREPARATION

MATERIAL AND METHODS:

Dieldrin standards were prepared by dissolving 10 mg dieldrin (Technical Grade, 99.9%) manufactured by Shell Chemical Company, in 100 ml hexane (Baker Resi-Analyzed) resulting in a 100 mg/l stock solution. Subsequent dilutions yielded standard solutions in the operating range of the GC detector. 1-8 µl of an appropriate standard solution was injected into a GC using a 10-µl syringe. The standards were then analyzed in the same manner discussed for analysis of dieldrin in the "Analytical Procedures" subsection of Section 10 . A typical calibration curve for dieldrin is presented in Figure N-1.

Figure N-2 presents a typical chromatogram for dieldrin. Figure N-2a demonstrates a typical chromatogram using a 2700 Varian GC equipped with a Sc^{3}H ECD and a 150 cm x 2 mm ID glass column packed with 3% SE-30 on Gas Chrom Q 80/100. Figure N-2b illustrates a typical chromatogram using a Varian 1700 GC equipped with a ^{63}Ni ECD and a 6' x 2mm ID glass column packed with 3% OV-1 on 100/200 Varaport 30.

BEGIN LAST LINE OF TEXT
BOTTOM OF IMAGE AREA; OUTSIDE DIMENSION FOR TABLES AND ILLUSTRATIONS
3/8"

PAGE NUMBER
EPA-287 (Cin.)
(4-76)

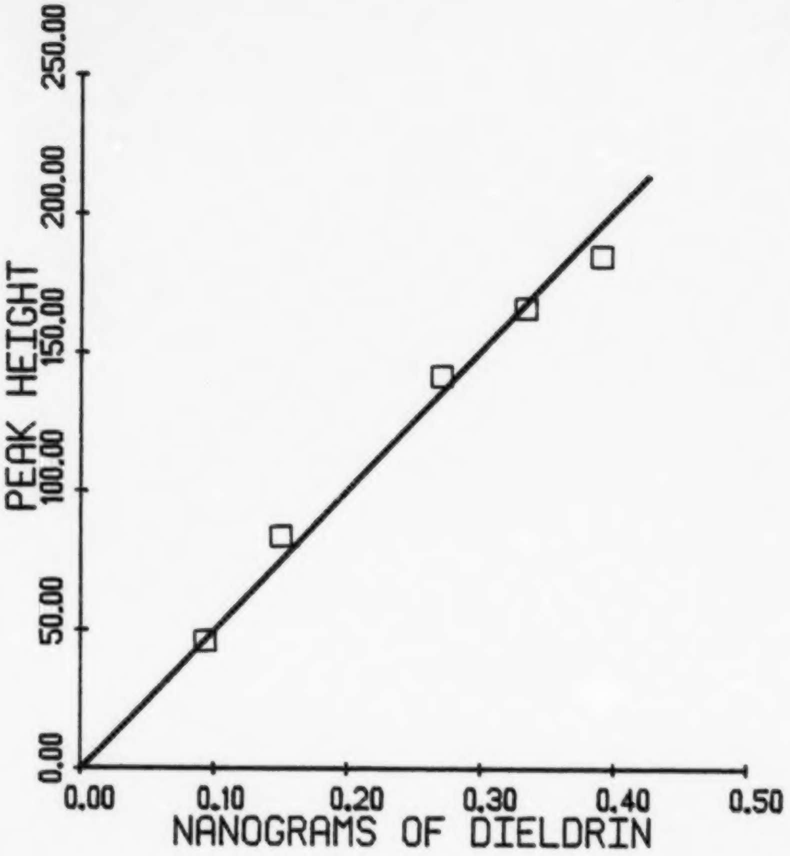

Figure N-1. Calibration curve for dieldrin using ^{63}Ni ECD.

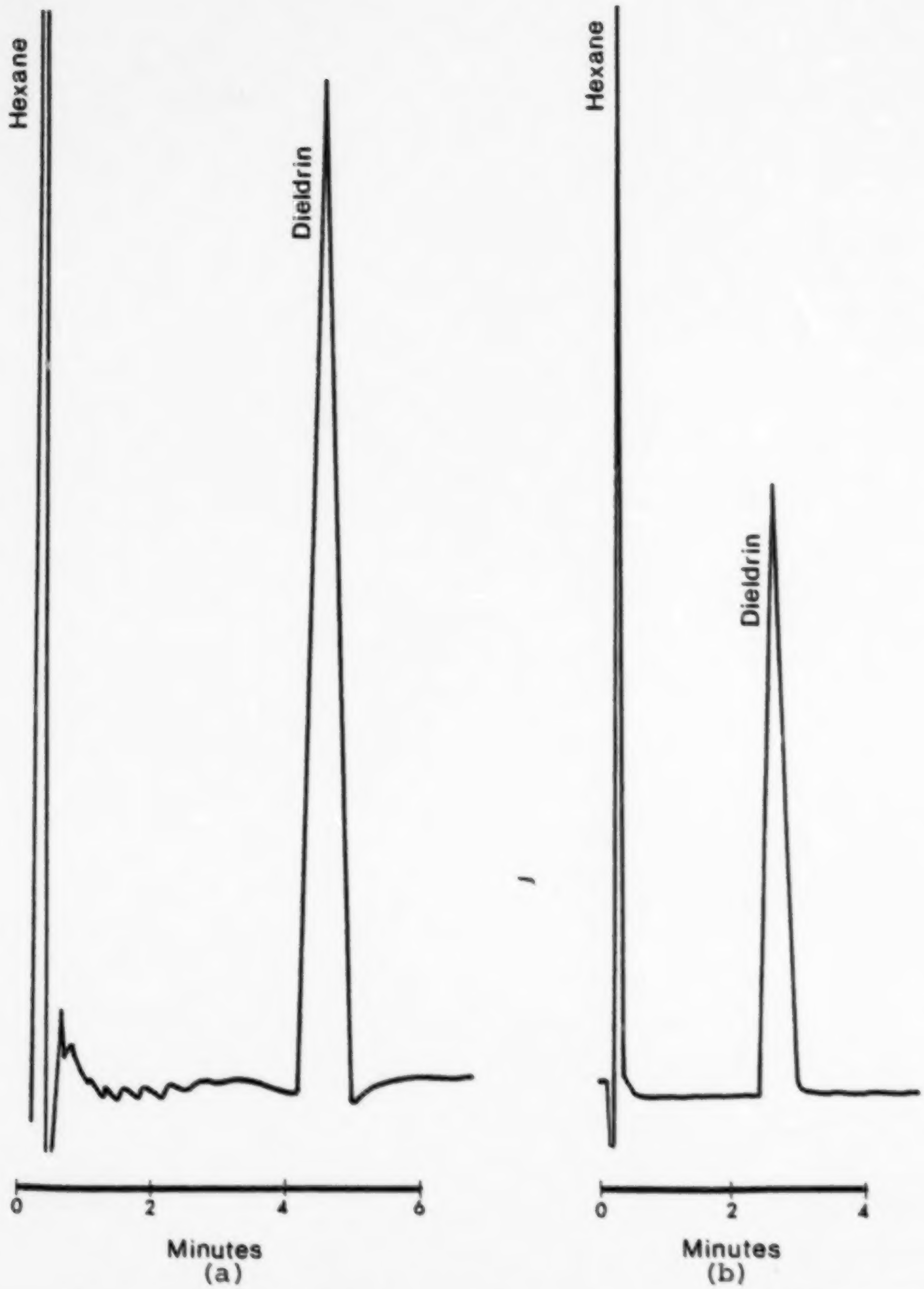

Figure N-2. Typical chromatograms for dieldrin using:
a) 3% SE-30 on Gas Chrom Q (Sc^{3}H ECD)
b) 3% OV-1 on 100/200 Varaport 30 (^{63}Ni ECD).

TYPING GUIDE SHEET
BEGIN FIRST LINE OF TEXT HERE
CENTER OF PAGE
TOP OF IMAGE AREA
DROPPED HEAD; BEGIN SECTIONS HERE

APPENDIX P

PARA-DICHLOROBENZENE (PDB) STANDARD CURVE PREPARATION

MATERIAL AND METHODS

PDB standards were prepared by dissolving 10 mg of PDB (Dow Chemical) in 100 ml hexane (Baker Resi-Analyzed), resulting in a 100-mg/l PDB stock solution. Serial dilutions were subsequently made in the operating range of the GC detector. 1-8 μl of an appropriate standard solution was injected into the GC using a 10-μl syringe. The standards were then analyzed in the manner described for analysis of PDB in the "Analtyical Procedrues" subsection of Section 11. A typical calibration curve for PDB using ^{63}Ni ECD is presented in Figure P-1.

Figure P-2 presents typical chromatograms for PDB using different detectors. Figure P-2a represents a typical chromatogram using a 1700 Varian GC equipped with a Hall electrolytic conductivity detector and a 10' x 1/8" stainless steel column packed with a 3% SE-30 on 100/200 Varaport 30. Figure P-2b demonstrates a typical chromatogram using a 1700 Varian GC equipped with a ^{63}Ni ECD.

9-1/8"
BEGIN LAST LINE OF TEXT
BOTTOM OF IMAGE AREA; OUTSIDE DIMENSION FOR TABLES AND ILLUSTRATIONS
3/8"

PAGE NUMBER
EPA-287 (Cin.)
(4-75)

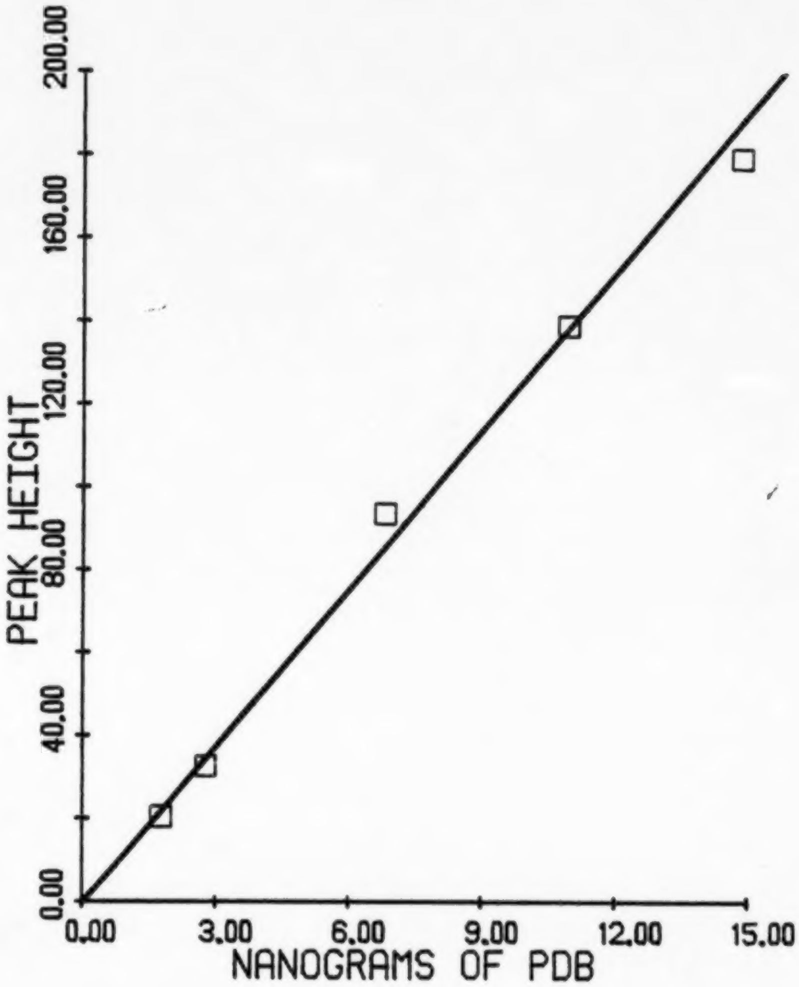

Figure P-1. Calibration curve for PDB using a ^{63}Ni ECD.

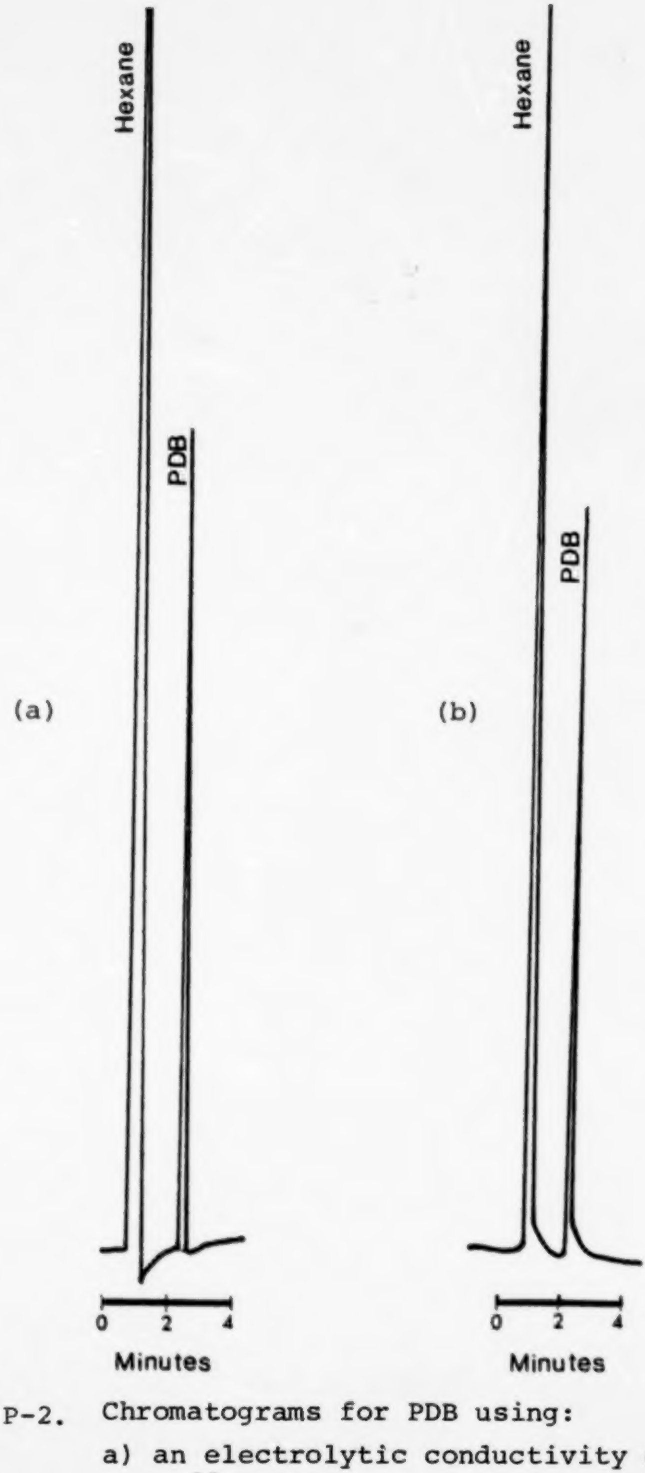

Figure P-2. Chromatograms for PDB using:
a) an electrolytic conductivity detector; and,
b) a ^{63}Ni ECD.